DATE: 12 February 1968

DOCUMENT CONTROL	
DIN____50286-154-1____PAGES__668__	
COPY NO. 64____OF____67____COPIES	

ENGINEERING ANALYSIS REPORT

ACQUISITION SUBSYSTEM

CDRL ITEM NO. 278

FEB 1 3 1968

SECRET SPECIAL HANDLING

TABLE OF CONTENTS

TABLE OF CONTENTS (Cont)

TABLE OF CONTENTS (Cont)

TABLE OF CONTENTS (Cont)

TABLE OF CONTENTS (Cont)

TABLE OF CONTENTS (Cont)

INTRODUCTION

It is the purpose of this report to support the Acquisition Subsystem PDR by documenting analysis, and descriptive material, to demonstrate the capability of subsystem design concepts to satisfy the proposed CEI requirements of ECP No. 17R5*. Most of the analysis presented represents work performed by GE. In a few cases, material has been extracted from subcontractor PDR reports to demonstrate compliance with principal requirements. In general, however, the PDR reports of Itek and Lear Siegler are considered part of the GE PDR documentation, and detailed analysis presented in these reports is not repeated here.

Section 1.0 of the report contains a table listing the requirements negotiated with the Air Force for the Acquisition Subsystem, briefly describing the design solution proposed for the requirement, and referencing the sections of the report which relate to the requirement.

A general statement of the state of compliance with the requirement is included in the table; further discussion of compliance with specific requirements is presented in Section 1.2, where required.

Section 1.3 presents a description of the Acquisition Subsystem functions and hardware.

*Issued 20 Nov 1967

SECTION 1.0

REQUIREMENTS AND SUBSYSTEM DESCRIPTION

The material in this section is subdivided as follows:

1.1 Requirements and Compliance Summary

1.2 Discussion of Compliance

1.3 Subsystem Description

1.1 REQUIREMENTS

Table 1.1-1 presents a summary of the subsystem functional requirements, briefly describes the design solution for each requirement, and references sections of the EAR report which pertain to each requirement. A yes/no statement of compliance is also included. Where further discussion is required concerning compliance, it is included in Section 1.2.

~~SECRET~~ SPECIAL HANDLING

TABLE 1.1-1. SUMMARY OF REQUIREMENTS AND DESIGN SOLUTIONS

CEI SPEC PARA.	REQUIREMENT	COMPLIANCE	DESIGN SOLUTION	EAR SECTION
3.1.1 Boresight Update ①	Provide means to boresight ATS to MO, LOS and to update target and/or ephemeris information	Yes	Separate manual sticks, and VO and AO eyepieces, are located at each crew console to permit targets to be simultaneously tracked and centered by two crewmen, one using the VO and the other the ATS. When a target is centered in each eyepiece, the computer can be directed to accept position information from each tracking mirror and calculate alignment correction parameters. It will be necessary to boresight on at least two targets.	2.6
3.1.1.1.2 Display ②	a. Provide AO display, cue display, and associated controls at each crew console.	Yes	a. An ATS and its associated eyepiece are available at each crew console. Head rests are provided to aid in viewing the exit pupil. Separate sets of crew controls are provided at each console. Separate cue screens are located to permit viewing from each head rest.	2.1 3.0 5.0 1.3.3.1
Pre-Pass Cueing	b. Provide controls for pre-pass cue review	Yes	b. Manual controls are located on each projector which permit frame call-up without computer participation.	1.3.3.3 3.0
3.1.1.1.4 Power ③	GE-AVE peak power allotment to Acquisition Subsystem is 480 watts		The operation of the magnification step change mechanism and the gyro heaters are inhibited during ATS slews to conserve peak power.	4.4
3.1.1.6.1 Decoupling ④	a. Manual Control Stick shall cause scene displacements in the ATS eyepiece which are parallel to the stick motion to within ±2°, exclusive of vehicle altitude errors.	See 1.2.8	The computer will monitor the position readouts from the gimbals, and the Pechan prism, and execute a decoupling routine to generate decoupled commands derived from the MCS inputs. The decoupled MCS commands will be summed with the computer generated tracking commands and applied to the gimbal controls.	2.7 1.3.3.1 1.2.8
Image Derotation ⑤	b. Orient the target image displayed in the ATS eyepiece so that the track vector of the track is within ±5° of vertical in the eyepiece at the end of slew.	Yes	A Pechan prism will be rotated in the ATS optical train by a closed loop control system as commanded by computer inputs. The prism will be positioned during slew and remain stationary during track.	2.2.2 1.3.3.1
3.1.1.6.3.6 Pointing Accuracy ⑥	a. The LOS shall point to a target within ±8 minutes of arc in automatic operation assuming: a. Boresighting complete b. Perfect ephemeris and target location information c. LM structural deflection does not exceed 0.5 arc minute	(See para. 1.2.d.)	Boresighting routines, control loop offsets, and alignment error apportionments have been developed to permit this requirement to be nearly met. The required alignment budget is tight, however.	2.3 1.1 1.21

~~SECRET~~ SPECIAL HANDLING

~~SECRET~~ SPECIAL HANDLING

TABLE 1.1-1. SUMMARY OF REQUIREMENTS AND DESIGN SOLUTIONS (Cont)

CEI SPEC PARA.	REQUIREMENT	COMPLIANCE	DESIGN SOLUTION	EAR SECTION
3.1.1.1.6.3.6 Pointing Accuracy (Cont) ⑦	b. The LOS shall point within ±2 minutes (2σ) after crew corrections via the stick.	Yes (See Para. 1.2.2)	The resolution of the telescope will permit this requirement to be met. The formulation of an MCS transfer function and a demonstration of the crew's ability to operate in the control loop will be accomplished in future simulation work.	1.2.2 2.2.1.9
3.1.1.1.6.3.b (2) Rate Accuracy ⑧	a. The ATS LOS shall track such that target drift is less than 540 μ rad/sec at the end of slew.	Yes	Consideration of service offsets in the rate (roll) servo loop, dynamic errors, and ephemeris uncertainties indicate that this requirement can be readily met.	2.2.1.10
⑨ Jitter	b. In automatic operation, combined drift and jitter errors shall be less than described in Figure 2.1.1 exclusive of: 1. Effects of OV motion due to non-GE equipment, ACTS operation, crew motions, main tracking mirror, and sliding mask. 2. Effects of ATS gimbal rates below 0.01 deg/sec.	Yes (See 1.2.9) No (See 1.2.3)	A position plus rate servo is utilized in pitch, and a rate system in roll. Gyros are used on both axes to increase noise rejection. Both loops can be operated in backup modes in event of gyro failure. The effects of bearing and encoder noise are relevant to this requirement and have been analyzed extensively. The design satisfies this requirement in pitch only.	2.1.1 2.1.3 2.1.5 2.1.6 1.2.9 1.2.3
⑩	c. When Main Tracking Mirror rates are 12 deg/sec (each axis) with associated sliding mask rates, the ATS LOS error shall not be more than 130 μ rad/sec over that of Figure 2.1.1.	Yes	The selection of a rate servo loop for the roll gimbal minimizes the effects of vehicle disturbances on ATS rate errors.	2.2.1.8
3.1.1.1.6.3.6 (2) Rate Accuracy ⑪	d. With OV rate increments due to ACTS thruster operation of 0.1, 0.01, and 0.01 deg/sec in roll, pitch, and yaw, respectively, the additional LOS rate error shall not exceed 750 μ rad/sec.	Yes	Same as entry ⑩	2.2.1.8

~~SECRET~~ SPECIAL HANDLING

TABLE 1.1-1. SUMMARY OF REQUIREMENTS AND DESIGN SOLUTIONS (Cont)

CEI SPEC PARA.	REQUIREMENT	COMPLIANCE	DESIGN SOLUTION	EAR SECTION
3.1.1.1.6.3.6 (3) Gyro Backup ⑫	In the event of a single gyro failure, combined LOS drift, and jitter shall be less than five times that shown in Figure 2.1.1 (with the exclusion in b) above and excluding cases where ATS gimbal rates are less than 0.05 deg/sec.	Yes	A backup loop is provided to permit operation of both pitch and roll loops as position servo systems without gyro support. It is assumed that gimbal rates to 0.05 deg/sec need be tolerated in the roll loop only.	2.2.1.6, a 2.2.1.4
3.1.1.1.6.4 Boresighting ⑬	a. Provide for boresighting both ATS LOS's to the MO LOS. After boresighting, the ATS and MO LOS's shall remain aligned to within ±6 minutes when tracking the same target (excludes errors due to LM structural deflections of more than ±0.5 arc minute after boresighting).	Yes	The crew will boresight the ATS line of sight to the MO LOS by tracking and centering the same target in both FOV's simultaneously, and initiating a software routine to calculate alignment correction parameters to be applied to subsequent targets. The software routine assumes three orthogonal parameters will define the misalignment which exists.	2.3.2 2.6
3.1.1.1.6.4.b ⑭	Provide capability to simultaneously track separate targets with the two ATS's and the MO and to accept manual control signals for any two of the three LOS's.	Yes	Separate software and control capabilities are provided for each ATS and the main optics to permit simultaneous observations of three separate targets. Two separate manual control sticks provide the capability to manually control both ATS's, or if the IVS is off, to control one ATS and the MO.	2.6
3.1.1.1.6.4.c Slave ⑮	Provide capability to slave either ATS to the MO so that ATS position, and rate corrections, are simultaneously applied to the MO	Yes	The crew can cause the main optics LOS to be slaved to either ATS LOS by actuating a panel switch to command the computer to operate the main optics in the slave mode. In this mode the ATS slews and tracks the same target as the MO. Manual stick corrections applied by the MCS for the ATS are simultaneously applied to the MO.	2.2.1.9
3.1.1.1.7.2 FOV ⑯	a. The FOV shall be at least 4.0 degrees at minimum magnification and at least 1 degree at one-half of maximum magnification.	Yes	The focal length of the telescope, and the size of the entrance pupil to the eyepiece assembly, are such as to provide the desired fields of view.	See Itek Report and 1.3.3.1
3.1.1.1.7.2 Scan Field ⑰	b. The scan field shall permit pointing between +70 degrees and -40 degrees in pitch and between +45 degrees in roll (ref to vehicle co-ordinates). There shall be no vignetting between ±35 degrees in roll and +10 to +40° in pitch.	Yes	The scanner provides sufficient gimbal freedom to satisfy the scan field requirement. The configuration of the shroud and external mirrors satisfy the vignetting requirements.	See Itek Report and 1.3.3.1

~~SECRET~~ SPECIAL HANDLING

~~SECRET~~ **SPECIAL HANDLING**

TABLE 1.1-1. SUMMARY OF REQUIREMENTS AND DESIGN SOLUTIONS (Cont)

CEI SPEC PARA.	REQUIREMENT	COM-PLIANCE	DESIGN SOLUTION	EAR SECTION
3.1.1.1.7.2.c Magnification 18	The minimum magnification shall be 16X ± 1X. The maximum power shall be 125X +5, -3. A zoom shall be provided between minimum and twice minimum magnification (low power) and between maximum magnification and one-half of maximum magnification (high power). The zoom shall respond (end to end) in less than 0.5 second. The optics shall respond from high to low power in 1 second.	Yes	A mechanically compensated zoom assembly is provided to permit continuously variable magnification over a 2:1 range. Power change lenses are inserted into the optical path to provide a 4:1 step reduction in magnification. The size of dc electrical motors required to meet the time response requirement has been determined. The drive motors are controlled by electronics in the Drive K electronics on commands from the Magnification Control Stick.	1.3.3.1 2.2.3 2.2.5

~~SECRET~~ SPECIAL HANDLING

TABLE 1.1-1. SUMMARY OF REQUIREMENTS AND DESIGN SOLUTIONS (Cont)

CEI SPEC PARA.	REQUIREMENT	COM-PLIANCE	DESIGN SOLUTION	EAR SECTION
3.1.1.1.7.2 Resolution (Static) ⑲	d. The resolving power of the acquisition optics shall be high enough to enable an observer, with vision corresponding to the flight crew standards per AFM 160-1 Flying Class I, to resolve a 3-bar target, of 1.65 feet wide white bars oriented in any direction with 1.65 feet spacing on a black background (3.3 feet per line pair). The above dimensions are projected dimensions normal to the line of sight between the target and ATS. The range from the ATS to the target is 80 nm. 1. The apparent contrast ratio of the 3-bar target, as seen by the acquisition optics aperture, is equal to 2:1. 2. The apparent scene brightness as seen by the acquisition optics aperture, is equal to 530 foot-lamberts.	Yes (See Section 1.2.4, 2.1.2, 2.1.3)	A 10-inch objective refractive telescope with a high power of 127X, will be provided to satisfy this requirement. Modulation Transfer function analysis by Itek is provided to demonstrate conformance with this requirement. Backup GE analysis is also presented which indicates that an extreme worst-case buildup of tolerances could result in a slight out-of-spec condition.	1.2.4 2.1.2 2.1.3
⑳	3. The LOS between target and ATS is static (no jitter). 4. The 1.65 feet wide (pro-jected) bars are at the center of the apparent field of view.			
㉑	Within 10 degrees of the center of the apparent field-of-view, the observer shall be able to resolve lines of TBD feet width and spacing (projected) under the above (except 4) conditions. At the edge of the real field-of-view in the areas not obscured by the peripheral display, the observer shall be able to resolve lines of TBD feet width and spacing (projected) under the above (except 4) condition.		Analytical predictions of off-axis performance are included in this report. These predictions have been made by GE. The subcon-tractor has not yet submitted his estimates of off-axis performance.	2.1.2

~~SECRET~~ SPECIAL HANDLING

TABLE 1.1-1. SUMMARY OF REQUIREMENTS AND DESIGN SOLUTIONS (Cont)

CEI SPEC PARA.	REQUIREMENT	COMPLIANCE	DESIGN SOLUTION	EAR SECTION
3.1.1.1.7.2, e Brightness (22)	The image brightness at the edge of the FOV shall be at least one-half of that at the center when no vignetting occurs and for targets of uniform brightness.	Yes	The vignetting and transmission of the telescope are controlled to satisfy this requirement.	See Itek PDR Report 2.1.4.4
3.1.1.1.7.2, f Focus (23)	Means shall be provided to insure that ground scenes are properly focused when the MOL altitude is between 75 and 230 nm. At any given altitude, the scene shall remain in focus throughout the scan field without manual focusing. The eyepiece shall permit focusing from -2.5 to +3.5 diopters.	Yes	The telescope will be slightly defocused on the ground so that it will be properly focused in an orbit, 5 psi, environment. The focal length is short enough, (73 inches at high power) to permit ground scenes to be accommodated without refocusing as a function of slant range. The eyepiece will permit manual focusing to accommodate eye dissimilarities.	See Itek Report and 2.1.4.5 1.3.3.1
3.1.1.1.7.2, g Display (24)	a. The ATS shall provide a monocular eyepiece. The eyepiece shall incorporate a peripheral display. The PD shall not obscure the target scene within 25 degrees of the in-track vector.	Yes	35 lights are mounted at the periphery of the eyepiece FOV. The lamps are controlled by computer commands via the console controller. Pin lights are utilized to conserve power and space. The display has been mocked up for crew review of its effectiveness. Priority and timing information to the crew. The display conforms with the obscuration requirements.	1.3.3.1 5.0
	b. The eye relief shall be at least 0.4 inch and shall not vary by more than 0.06 inch.	Yes	The eye relief is 0.77 inch. Eye relief varies less than 0.02 inch during zoom and magnification step changes.	1.3.3.1 and Itek Report
	c. A single circle reticle which indicates the real FOV at maximum zoom position shall be provided. The reticle shall include cross hairs for centering.	Yes	An optical flat is located in the optical train at the entrance pupil of the zoom eyepiece. This element is inscribed with a circle equal in diameter to the FOV of the eyepiece at high zoom.	1.3.3 and Itek Report
3.1.1.1.7.2, h Cue Displays (27)	A pictorial screen-projected cue and a six character alphanumeric shall be displayed at each crew station.	Yes	A Visual Display Projector with a 6.5 inch circular, rear projection screen will be located at each crew station in a position to permit viewing from the ATS headrest. The alphanumeric display will be placed over the screen.	1.3.3.3 3.0
3.1.1.1.7.2, i Cue Storage (28)	Storage for 16 film modules shall be provided.	Yes	A single storage rack is planned for all 16 modules on console 8A.	1.3.3.4

~~SECRET~~ SPECIAL HANDLING

TABLE 1.1-1. SUMMARY OF REQUIREMENTS AND DESIGN SOLUTIONS (Cont)

CEI SPEC PARA.	REQUIREMENT	COM-PLIANCE	DESIGN SOLUTION	EAR SECTION
3.1.1.1.7.2, j Cue Display Time (29)	a. The cue frame shall be displayed and held automatically for K seconds after beginning of slew to target. The target shall be automatically released when a target vote button is actuated.	Yes	The computer will output a binary, serial callup command, which will be held in the console controller and presented to the VDP or a continuous, parallel signal. The computer will change the cue after K seconds by sending a new callup command.	1.3.3.3
Cue Hold (30)	b. A cue hold control shall be provided to permit longer viewing of the cue desired.	Yes	The crew can hold a cue beyond K seconds by twisting the handle of the magnification stick to signal the computer to hold the cue.	1.2.5 1.3.3.5
Retrieval Time (31)	c. The cue frame for a target shall be displayed within $0.45 + \frac{N}{100}$ seconds after the release of the previous cue.	Yes	The cue projector provides a two-speed film transport system to slew the film. Each film frame is read during retrieval by silicon photo transistors which detect binary descriptor bits on the film. A velocity track on the film is also optically monitored during slew to control film slew speed. Proper motor sizing and break design permit compliance with the requirement.	1.3.3.3 and Lear Report
(32)	d. The alphanumerics shall be displayed within 0.3 seconds after the start of ATS slew.	Yes	The alphanumerics shall display information received from the computer within 0.3 seconds. The information is decoded for display in the VDP. The AN display will not have the capability of displaying information from the cue film.	1.3.3.3
3.1.1.1.7.2, k	Controls shall be provided to permit the crew to manually command the display of any cue frame without computer processing.	Yes	Manual selection dials calibrated in decimal numbers will be located on each VDP. The VDP will be designed to accept octal numbers from these dials and call up the commanded frame.	1.3.3.3
3.1.1.1.7.2, l Headrests (34)	Adjustable headrests shall be provided to facilitate viewing of the ATS display.	Yes	Headrests have not been designed at this time. Trial headrests have been installed in the console mockup for crew review.	1.3.3.6
3.1.1.1.7.2, m Protective Covers (35)	Protection shall be provided for external ATS components against ACTS and waste product contamination. Protection shall be provided as necessary to adequate thermal stability.	Yes	A hinged protective shroud will cover and protect all external components when the ATS is not in use. The shroud door will be controlled by redundant motors commanded by either the computer or a panel switch. The shroud provides passive thermal control for external ATS components, protects against Orbit Adjust thruster impingement, and protects against contaminants with a sealing gasket. A final shroud design concept has not been accepted.	2.4 2.4.1 1.2.6 2.5.3 1.3.3.1

~~SECRET~~ SPECIAL HANDLING

~~SECRET~~ SPECIAL HANDLING

TABLE 1.1-1. SUMMARY OF REQUIREMENTS AND DESIGN SOLUTIONS (Cont)

CEI SPEC PARA.	REQUIREMENT	COM-PLIANCE	DESIGN SOLUTION	EAR SECTION
3.1.1.1.7.2, n Magnification Control Stick ㊱	a. A magnification control stick shall be provided to control ATS magnification, VO magnification, target voting, and cue hold.	Yes	The magnification control stick has not been designed. It will be designed to permit the crew to effect the required controls with the left hand. A "slew" signal will be derived from the computer gimbal commands in the Drive K electronics and used to inhibit step magnification changes during ATS slew.	1.3.3.5 4.2
	b. The stick shall be inhibited from commanding step changes during ATS slew.	Yes		

TABLE 1.1-1. SUMMARY OF REQUIREMENTS AND DESIGN SOLUTIONS (Cont)

CEI SPEC PARA.	REQUIREMENT	COMPLIANCE	DESIGN SOLUTION	EAR SECTION
3.1.1.1.7.2,n Magnification Control Stick (37)	The stick shall generate signals which vary the gains of the manual control stick.	Yes	c. The magnification stick will provide signals to the computer to indicate which of four magnification ranges are in effect. The computer will apply suitable corrections to the manual control stick transfer function to reduce apparent rate and sensitivity changes when the ATS magnification is changed. The magnification stick will generate signals used by the computer to vary the gain of the MCS.	1.3.3.5
	When the magnification stick is in the ATS position, the manual control stick shall control only ATS pointing. When in the VO position, the manual control stick will control only main optics pointing.	Yes	d. The magnification stick will actuate a microswitch to indicate to the computer whether the crew wants the MCS to control the ATS or the VO. The crewman will be allowed to control the main optics with the stick only if the IVS is off and the LEFT-RIGHT AUTO switch is in the proper non-AUTO position, or if the MO target was assigned to his ATS. Tentative design will permit the MCS to control the VO only when: 1. The magnification stick is in the VO position. 2. The IVS is off. 3. The main optics target was assigned to the crew console requesting MCS control.	
3.1.1.1.7.2,o ATS Cant Angle (38)	The roll axis of each ATS shall be canted outboard (from the +X axis of the OV) 9±0.5 degrees. The optical axis between the centers of the fixed and tracking mirrors shall be parallel to the X-axis of the OV within 0.5 degree. The roll axis of each ATS shall be parallel to the X-Y plane of the OV within 0.5 degree.	Yes	The components will be nominally aligned as described to minimize the occurrence of zero roll rates. The tolerances will be considerably tighter than the 0.5 degrees specified in order to meet pointing requirements.	2.3
3.1.1.1.7.2,p Blanking (39)	Automatic blanking provisions shall be incorporated to prevent crew injury resulting from inadvertent sun viewing through the acquisition optics. The blanking mechanism shall be reset manually.	Yes	An automatically triggered blanking shutter will be provided whose response and sun sensor FOV are such that the sun can not enter the FOV at maximum slew speeds. It is planned that the shutter will be manually cocked though this feature has not negotiated with the sub contractor.	2.2.4 6.4
3.1.1.2.6.3.5 Slave (40)	The main optics LOS shall track within 100 μrad/sec of the desired rate when operating in the slave mode in the track period.	Yes	Two techniques have been considered for slaving. One causes the main optics and the ATS to track the same target independantly with MCS corrections applied to both subsystems simultaneously. The other causes the position information from the two subsystem's encoders to be compared and the difference nulled.	2.2.19

~~SECRET~~ SPECIAL HANDLING

TABLE 1.1-1. SUMMARY OF REQUIREMENTS AND DESIGN SOLUTIONS (Cont)

CEI SPEC PARA.	REQUIREMENTS	COM-PLIANCE	DESIGN SOLUTION	EAR SECTION
3.1.1.2.7.2.1 Slew Requirements ㊶	The slew capability of the acquisition scopes shall satisfy the following requirements: Slew Time ≤ $\frac{\Delta\theta}{30}$ + 1 seconds, where $\Delta\theta$ is the LOS angle (degrees) between the current target and the subsequent target at the start of slew.	Yes	The ATS gimbal drive motors are sized and controlled to permit compliance. The dynamic range of the servo loop amplifier gains are dictated by the slew requirements.	Itek Report 2.2.1.6 2.3
	Mechanical stops shall be incorporated on each ATS scanner to prevent damage to the ATS tracking mirror in the event of a worst-case slew signal failure.	Yes	Energy absorbing stops are provided, to permit compliance.	See Itek Report
3.1.1.2.7.2.2 Filters ㊷	Means shall be provided for a crew member to select and insert any one of four spectral or neutral density filters into the image path in the acquisition optics within 5 seconds.	Yes	A "wheel" containing four filters will be inserted in the ATS optical train in the eyepiece. The crew will select filters manually.	1.3.3.1 2.1.1.4.2
3.1.1.2.7.2.3.1 Cue Resolution ㊸	The visual display projector (VDP) with the associated VDP film module, shall project a 6.5 inch (minimum) diameter image onto a backlighted screen from a 0.500 ± 0.005 inch diameter target image on the cue film in the VDP film module. The projector, when projecting a medium contrast ratio (6:1) Standard Resolving Target, per MIL-STD-150A, within 2 inches of the center of the screen, shall permit a viewer, with vision corresponding to the flight crew standards per AFM 160-1 Flying Class I, with a 10X (maximum) magnifier to resolve up to and including 228 line pairs/mm (Group 7-6) as referenced to the source material.	Yes	The optical system of the VDP employs a cook triplet projection system and a high-resolution high-gain screen capable of providing the required resolution. GE and Lear analysis is presented to demonstrate compliance.	3.2

1-11

~~SECRET~~ SPECIAL HANDLING

~~SECRET~~ SPECIAL HANDLING

TABLE 1.1-1. SUMMARY OF REQUIREMENTS AND DESIGN SOLUTIONS (Cont)

CEI SPEC PARA.	REQUIREMENT	COM-PLIANCE	DESIGN SOLUTION	EAR SECTION
3.1.1.2.7.2.3.1 Cue Resolution (Cont) ㊸	With the same target projected within 1/4 inch of the edge of the screen, the viewer with a 10 10X (max) magnifier shall be capable of resolving up to and including 204.5 line pairs/mm (Group 7-5) as referenced to the source material. The modulation transfer function of the VDP at one line pair/mm, as referenced to the source material, shall be no less than 0.83.	Yes	(Same as previous page)	
3.1.1.2.7.2.3.2 Cue Brightness ㊹	The display shall be optimized for viewing from the crew head position dictated by the acquisition optics eyepiece. The brightness of the cue screen shall be adjustable, continuously, from 0 to 15 foot-lamberts as measured within 1 inch of the center of the screen. At the maximum screen brightness setting, the brightness within 1/4 inch of the edge of the screen shall be no less than half of that at the center.	Yes	The projector will permit viewing from the ATS headrests. A knob on the VDP will permit adjustment from 0 to 25 foot-lamberts. An incandescent projection lamp will provide the necessary illumination. Projection lamps will be interchangeable on orbit. The projection lamp will be turned off during frame retrieval (slew). A blue filter will permit the lamp intensity to be varied with a minimum shift in apparent color on the screen.	Lear Report
3.1.1.2.7.2.3.3 Cue Retrieval ㊺	a. The VDP shall be capable of automatically displaying any of 4094 cue frames per film module. b. The crew shall be capable of exchanging film modules within 10 seconds. c. The VDP shall satisfy retrieval requirements with 6:1 minimum contrast ratio between 1's and 0's on the film.	Yes Yes Yes	a. Cue modules will have capacity for 4094 useful frames. Sufficient leader film on either end will be provided to permit any of the 4094 frames to be retrieved and displayed. b. The projector will permit module change in about four seconds. Provisions will be made to store modules near each crew station to assure compliance with the overall ten second requirement. c. The film reader circuitry has not been finalized. GE belives that a design can be developed which will permit compliance.	1.3.3.3 3.2
3.3.1 Weight ㊻	Weights have not been negotiated for the aquisition optics hardware. This weight is based upon a weight of 329 lb for the subcontracted optical assembly (Spec. No. EC331), not including gyros and gyro electronics. The GE-AVE weight will be adjusted at PDR to reflect the prime contractor/Air Force weight agreement for the subcontracted optical assembly.	See 1.2.7 No	Weight problems exist in the Drive K electronics. A weight figure for the shroud has not been negotiated with Itek.	1.2.7 4.4 2.5.3 2.5.8

~~SECRET~~ SPECIAL HANDLING

1.2 COMMENTS CONCERNING GE COMPLIANCE WITH SPECIFICATIONS

Table 1.1-1 indicates that most of the negotiated requirements are being complied with at the preliminary design stage. This section presents a brief discussion of those areas where a flat statement of compliance can not be made in the table.

1.2.1 POINTING ACCURACY - Refer to entry ⑥ in Table 1.1-1

A detailed error analysis is presented in Section 2.3 of this report which demonstrates that the eight-minute pointing accuracy is generally met. A worst case set of alignment errors and error buildup is shown to produce 8.2 minutes of pointing error, however.

The analysis shows that pointing error is a function of over twenty independent error parameters, most of which are alignment uncertainties prior to boresighting and time fluctuating errors after boresighting. It is shown that static misalignments between the various ATS components do influence pointing accuracy despite boresighting.

The determination of an attainable set of on-orbit alignment tolerance requirements depends to a large extent on the degree to which the structure preserves ground established alignment in the presence of pressurization changes, launch loads, and gravity field relief. Analysis is planned to further investigate the capability of the structure and to establish realistic alignment error apportionments based on this capability. A precise estimate of status relative to the 8-minute pointing requirement can not be made until this work is performed. In the meantime, it is felt that the analysis presented herein indicates that the pointing accuracy requirement will be difficult to comply with.

GE is presently studying several approaches to improving pointing performance, including;

   a. Increasing boresighting capability to desensitize ATS pointing to misalignments between the folding mirror and the scanner.

   b. Analytically predicting on-orbit alignment, and pre-biasing the ground alignment accordingly (either in the hardware or the software).

   c. Stiffening the structure between the folding mirror and the scanner to minimize alignment changes.

The effectiveness of increasing boresighting capability will be available prior to P.D.R.

1.2.2 MCS POINTING CORRECTIONS (Refer to entry ⑦ in Table 1.1-1)

It is required that the crew be able to correct ATS pointing accuracy to within two minutes of arc with the Manual Control Stick. The accuracy and speed with which a man can control the pointing of the ATS will depend on, among other things, the transfer function of the Manual Control Stick and the characteristic response of the man as a servo loop component. The necessary simulation has not been performed to determine either the MCS transfer functions or the characteristics of the man at this time, and it is thus not possible to present relevant analysis to demonstrate compliance with this requirement.

Preliminary simulation and servo analysis, however, has not revealed any difficulties which will prevent compliance with this requirement.

1.2.3 JITTER PERFORMANCE (See entry ⑨ Table 1.1-1)

Present analysis shows that the design will meet the jitter requirement as specified in roll.

The design will not meet the specified performance with pitch gimbal rates as low as 0.01 deg/sec. Since these rates will not occur during the mission it is assumed that intent of this requirement applies only to the roll gimbal at gimbal rates of 0.01 deg/sec. The jitter requirement will be met in pitch for the gimbal rates to be experienced during the mission.

1.2.4 ATS RESOLUTION (Refer to Item ⑲ in Table 1.1-1)

The optical resolution predicted for the telescope is dependent on the magnitude of the various manufacturing errors assumed and, to some extent, the analytical methods utilized. Itek has presented analysis as part of their PDR report which shows that the required resolution of 3.3 feet can be achieved with the present design if the combination of manufacturing error sources does not produce more than 0.152λ of wavefront deformation. They feel that this represents a tight, but achievable tolerance budget for the system, and that they will meet the requirement.

In view of the critical nature of this requirement GE has performed extensive independent analysis of the system using the optical prescription curve supplied by Itek. The results of this analysis are comparable to, but not identical with the Itek analysis. GE analysis of the prescription optical system, with no allowance made for errors, yields somewhat better resolution than the Itek analysis. With a worst case tolerance buildup, however, GE has produced one case where the predicted on-axis resolution was 3.4 feet.

On the basis of the analysis performed to date it is concluded that the specified resolution can be met, but that considerable effort will have to be expended in establishing and maintaining a realistic error budget for the system.

Visual Threshold Curve

Uncertainties concerning the exact nature of the eye's modulation threshold characteristic introduces a significant element of uncertainty in the prediction of ATS performance. The curve determined by Otto Shade has been used in all Itek and GE analyses. Itek is preparing an experiment designed to gain some verification of the Shade curve and to determine the effects of dynamic jitter on resolution.

Dynamic Resolution

In order to better understand the degrading effects of jitter, GE has derived an analytical method of predicting the effects of monotonic, high frequency jitter (above 6 cps) on resolution. This work is presented in Section 2.1.3 and yields results which are similar to those obtained using a method applied by Itek. The analysis indicates that a dynamic resolution of no worse than 3.6 ft. will be achieved.

1.2.5 CUE RETRIEVAL TIME (Refer to entry (31) in Table 1.1-1)

Lear presented an analysis and demonstrated on a breadboard that the required retrieval time can be met if at least three consecutively numbered frames precede the commanded frame. In the event that three such frames do not exist, the projector may require an

~~SECRET~~ **SPECIAL HANDLING**

additional 0.1 second for retrieval. GE interprets the negotiated requirement to apply
only when the commanded frame is preceded by the three consecutively numbered frames.

1.2.6 PROTECTIVE SHROUD (Refer to entry (35) in Table 1.1-1)

The design concept proposed by the subcontractor at their PDR was not accepted by GE
due to excessive weight, unacceptable mechanism design, and an excessive reliance on
pyrotechnic caging devices. At the time of this publication both Itek and GE are indepen-
dently establishing new design concepts. A review of the structural aspects of the GE
design is included in Section 2.5. The Itek new design has not been presented to GE
at this time.

1.2.7 WEIGHT

Weight figures have been negotiated for all elements of the subsystem except the Acquisition
Optics. At time of this publication GE has not yet established an acceptable weight bogey for
the A.O. subcontractor (Itek), and the weight bogey established for the prime K electronics
is being exceeded.

1.2.8. DECOUPLING - (See Entry (4) in Table 1.1-1.)

While the two degree decoupling requirement can be met, GE proposes increasing the per-
missable decoupling to 5 degrees to relieve hardware and equipment alignment constraints.
At present a 1 degree error allotment is required by the position readout potentiometer on
the pechan prism, and a 1/2 degree allotment is required by the A/D converter. Thus less
than 1/2 degree remains for errors in the alignment of the Manual Control Stick and the
ATS. Considering the relative motion between the consoles and LM structure during powered
flight, this would dictate the need for on-orbit alignment of the stick to the ATS.

~~SECRET~~ **SPECIAL HANDLING**

1.2.9 JITTER PERFORMANCE - (See Table 1-1, entry ⑨).

The best data available from the gimbal encoder vendor (Wayne George) indicates that encoder noise from the 18 bit pitch encoder will exceed the level required to meet the jitter specification in the CEI specification. A 20 bit pitch encoder will permit the specification to be met, but will exceed the space envelope available for the encoder with the current scanner design. GE is continuing to evaluate the use of a 19 or 20 bit encoder to meet the requirement. Consideration is also being given to switching to a straight rate loop in pitch which does not depend on the encoders in the track mode.

GE intends to comply with the present CEI jitter requirement and will discuss the alternate design changes which are necessary to meet the requirement with the Airforce.

G.E.'s interpretation of the jitter requirement is discussed in section 2.2.1.1 of this report. It is believed that this interpretation is in agreement with Airforce/Aerospace intent.

1.3 SUBSYSTEM DESCRIPTION

This section presents a brief description of the subsystem hardware and functions. The material is subdivided as follows:

1.3.1 Purpose of the Acquisition Subsystem

1.3.2 Operational Modes

1.3.3 Description of Subsystem Hardware

1.3.4 Description of ATS Controls

1.3.1 PURPOSE OF THE ACQUISITION SUBSYSTEM

The Acquisition Subsystem provides the crew with high-resolution telescopes whose LOS's are computer-controlled in the same manner as the main tracking mirror. With these devices the crew can observe weather and activity at the selected target areas and can select the most desirable targets for photographic operations. By manually correcting computer commands, the crew can minimize pointing and tracking errors due to target location information, ephemeris prediction, attitude reference, computation, and servo errors. Therefore, the crew and an effective Acquisition Subsystem will eliminate most of those factors which limit performance in the Automatic Mode of operation, and increase the quantity and quality of intelligence data acquired in the manned-automatic mode.

Specifically, the Acquisition Subsystem - crew combination permits the following:

a.   Target appraisal for activity

b.   Target weather evaluation

c.   Selection of optimum targets for photography

d.   Target centering and rate nulling

e.   Stored target position parameters to be updated by crew observations.

A schematic showing the relationships between the various elements of the Acquisition Subsystem and related Subsystems is shown in Figure 1.3-1.   Reference to panel controls shown on this Figure can be found in Section 5.

1-20

Figure 1.3-1. Acquisition Subsystem
and Related Hardware

1.3.2 OPERATIONAL MODES

Detailed operational modes are still being refined. The modes described here are intended to summarize, in general terms, some of the ways the ATS's may be utilized.

A. <u>Activity Mode</u> - The activity mode represents the primary mode of ATS operation. In this mode, each crewman observes pre-programmed targets for activity. The selected targets will be identified in target "groups", where each group will contain one primary target and up to six secondary targets. One target in each group will be selected by the computer for photography by the main optics at a predetermined time designated "decision time". The main optics will photograph selected targets without direct crew support. In selecting the target to be photographed, the computer will consider stored information concerning the targets importance and the crews inputs concerning current target activity and weather conditions.

The crew will be able to indicate three levels of target visibility and activity by depressing one of three "voting" buttons. The ACTIVITY button will tell the computer that the target is visible and that an unusual level of activity exists (such as the loading of a missile in a silo, etc.). The INACTIVITY button will tell the computer that the target is visible but that no unusual level of activity exists. The REJECT button will indicate that the target is cloud covered or too hazy to be photographed. The activation of any of these voting buttons will cause the ATS to slew to the next programmed ATS target. The computer will select the primary target if a reject vote is not entered for this target, and if no active votes are entered for the secondary targets in the group.

Each target will be assigned a weighted number in the computer to provide the basis for the computer to select the most desirable target when one or more ACTIVE votes are entered for secondary targets or when the primary target is rejected.

~~SECRET~~ **SPECIAL HANDLING**

In some cases the computer logic might be such that an INACTIVE primary target will take precedence even over certain ACTIVE secondary targets. If the crew observes a level of activity at a given target which he feels makes photography mandatory, he can override the computer selection logic by actuating the PRIMARY OPTICS OVERRIDE button to cause the primary optics to immediately slew to the target under observation by the ATS.

In addition to appraising activity and weather conditions, the crew will have the capability of updating the computer stored target position parameters. When the crew observes a primary or an active secondary target which is not positioned near the center of the FOV, he may center the target with the Manual Control Stick and actuate the POSITION UPDATE switch to cause the actual target position as recorded by the ATS gimbal encoders to update the target location in the computer.

B. <u>Single Operator</u> - In this mode, one crewman performs a complete target operation, using first the ATS to acquire the target for weather assessment and to null rates and center the target (if required). The crewman then switches his attention to the visual (main) optics and nulls rates (if required). If the IVS is operating within spec., the crew involvement with the visual optics would only be occasional to check on IVS performance. The crewman would then revert to the ATS and repeat the above process with another target.

C. <u>Specialist</u> - In this mode, one crewman acquires all targets with the ATS, performing the same ATS operations as described for the single operator mode. The second crewman works only with the visual (main) optics, taking over control of the target after the main optics slew to the target. If the IVS is operating, visual optics operations would not be necessary.

D. <u>Leap-Frog</u> - This mode consists of two crewmen, each operating in the single operator mode. Since only one crewman can use the visual optics at a time, the operations of the two crewmen are programmed such that while one crewman is using an ATS, the other is using the visual optics. If the IVS is operating, visual optics operations would not be necessary.

1-24

Although the Acquisition Subsystem can be operated in any of the four primary modes as described above, it is most likely to be used in the Activity Mode.

1.3.3 LIST OF PRINCIPAL COMPONENTS COMPRISING THE ACQUISITION SUBSYSTEM

The acquisition subsystem is comprised of the following elements;

a. Acquisition Optics (on ATS) – Includes;

- Telescope
- Window
- Scanner
- Folding Mirror
- Peripheral Display
- Shroud and Shroud Door

b. Cue Projector and Alpha Numerics Display

c. Drive K Electronics

d. Cue Module Storage Rack

e. Magnification Control Stick

f. Head Rest

g. Gyroscopes

The manual control stick is considered part of the N&C subsystem.

1.3.3 DESCRIPTION OF SUBSYSTEM HARDWARE

1.3.3.1 Acquisition Optics

The Acquisition Optics (or ATS) consists of the optical elements of the subsystem and their supporting hardware. All elements of the Acquisition Optics are supplied by Itek under subcontract to GE, and are shown schematically in Figure 1.3-2.

1.3.3.1.1 Telescope Assembly and Optical Performance Description

The heart of the acquisition subsystem is the Acquisition Telescope whose size and elements are shown schematically in Figure 1.3-3. This component consists of a 10-inch objective, refractive, high power, telescope mounted within the pressurized Lab Module of the spacecraft. It presents a magnified ground scene to the crew through an eye piece with a 60-degree apparent FOV and a 2 mm (minimum) exit pupil. Two such telescopes are included in each spacecraft as shown in Figure 1.3-4.

The peak magnification of the telescope is 127 power. At this power, the telescope will have a field of view of 0.5 degree and will view approximately 0.7 nautical miles on the earth at a slant range of 80 nautical miles (nadir).

The on-axis resolution of the telescope from 80 nm is predicted to be about 3.6 feet when operating in orbit in the presence of a low level of predictable "jitter" caused by servo noise. The static resolution of the telescope is about 3.3 feet.

The scanner (to be discussed later) is designed to permit the LOS of the telescope to be directed through a scan field from 70 degrees forward to 40 degrees aft in pitch, and from -45 degrees to +45 degrees in roll. In operation it will be possible to lock on and track a target at something less than a full 70 degrees forward in pitch.

OPTICAL SCHEMATIC

FOLDING MIRROR

CUE MIRROR (BLANKING)

DEROTATION PRISM

FIELD FLATTENER

RETICLE

ZOOM LENS

FILTERS

EYEPIECE

LOW POWER GROUP

OBJECTIVE LENS

WINDOW

FIXED MIRROR

TRACKING MIRROR

IMAGE PLANE

IMAGE PLANE
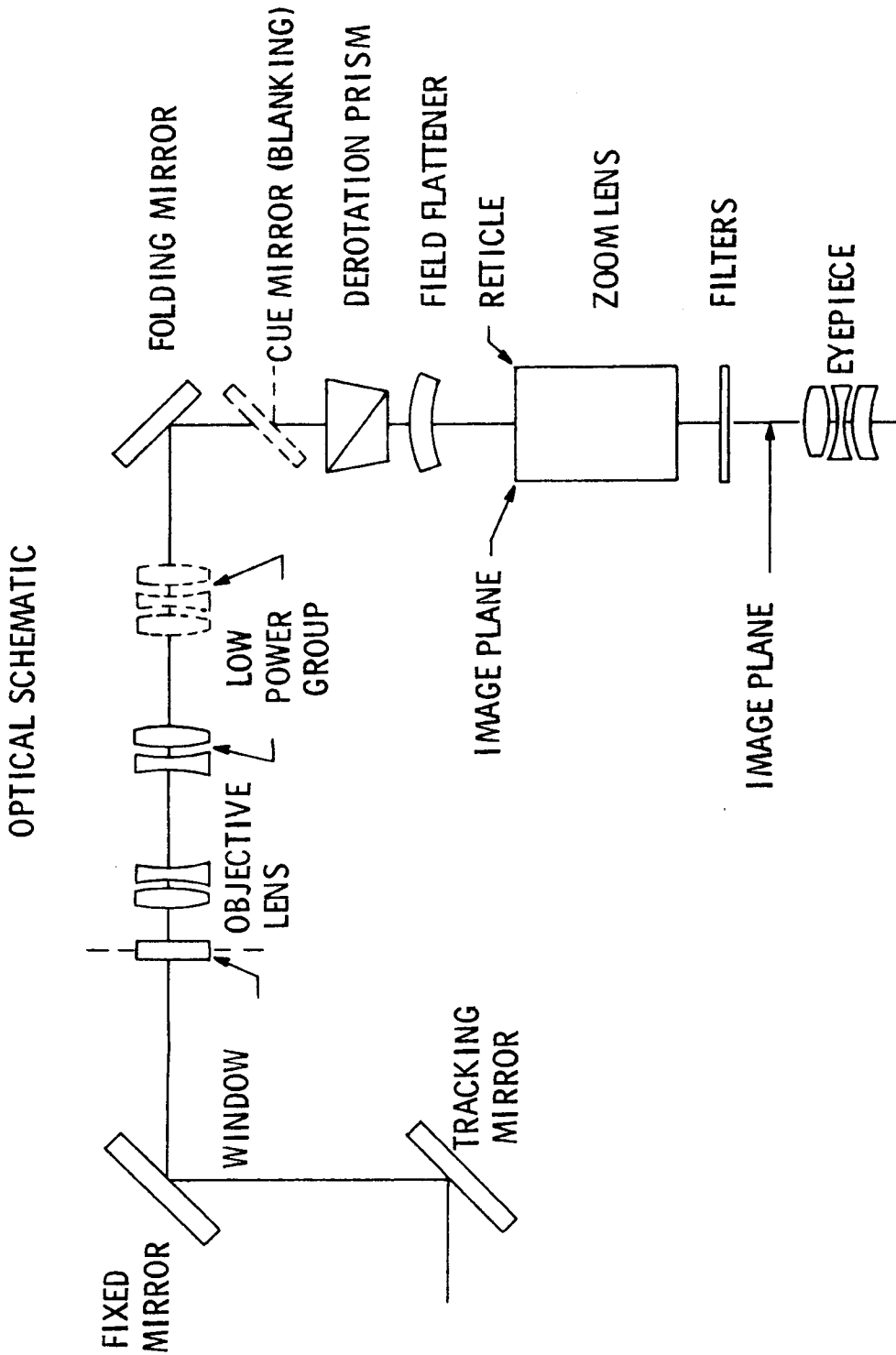
Figure 1.3-2. Acquisition Optical Schematic

Figure 1.3-3. Acquisition Telescope
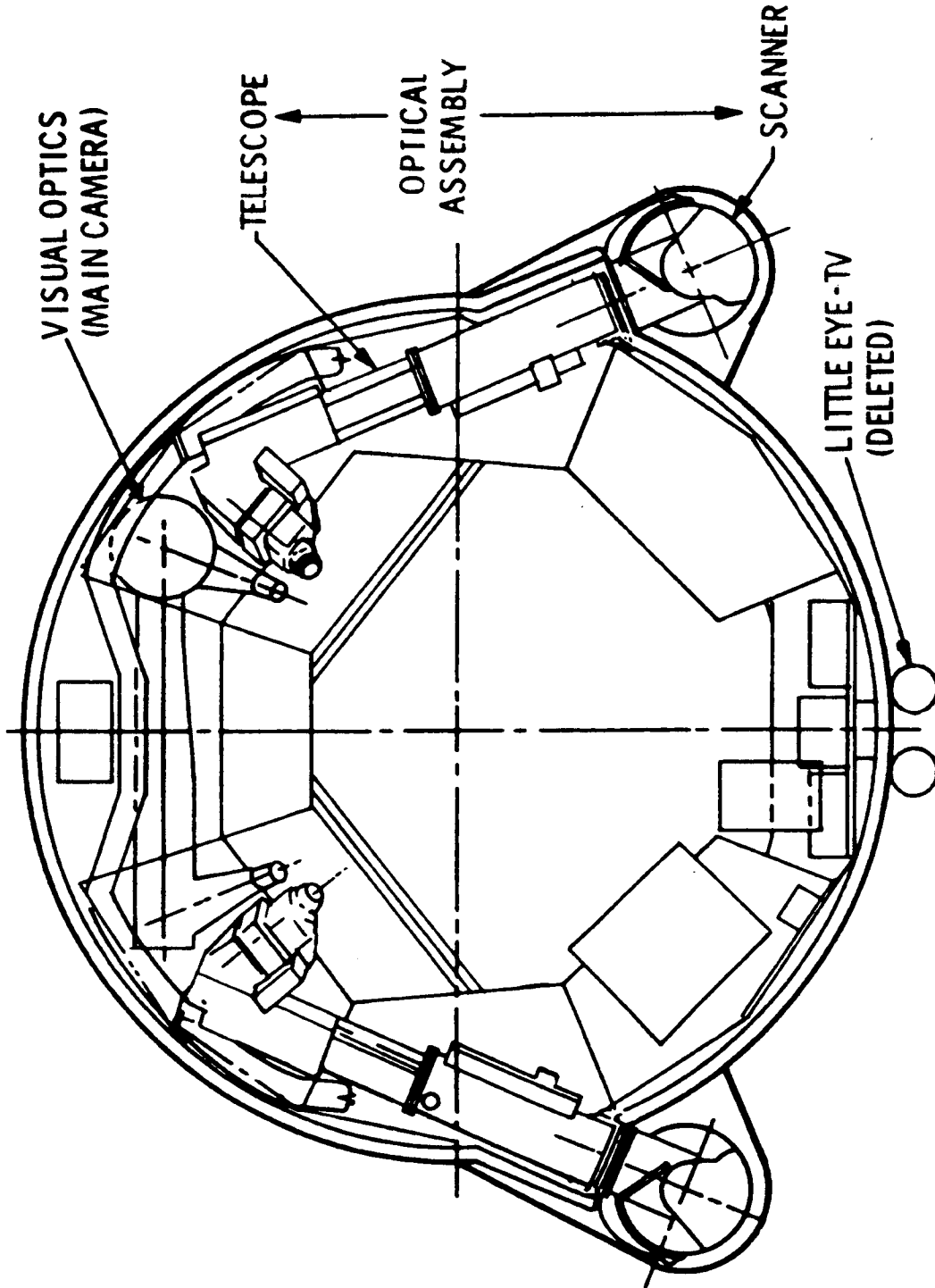
Figure 1.3-4. LM Installation of ATS

There will be no vignetting in the optical system of the acquisition optics from +10 degrees to +60 degrees in pitch and from -35 degrees to +35 degrees in roll. Outside of this region, vignetting will occur in the external optical elements.

The magnification of the telescope can be continuously varied from 16 to 32 power, and from 63 to 127 power, by means of two independent mechanisms as described below.

The magnification of the telescope can be reduced by a factor of four by inserting a set of low power lenses into the optical train. These lenses reduce the effective entrance aperture to 2.5 inches; they do not change the exit pupil diameter. The lenses are inserted and removed by an electric motor on command from the flight crew via the Magnification Control Stick and the Drive K Electronics. A manual override exists to permit operation of the power lenses in the event of control system failure.

The magnification of the telescope can vary continuously over a two-to-one range by means of a zoom mechanism. This 2:1 change can be obtained with the low-power lenses either in or out of the optical train. The zoom is part of the eye piece optical train and its operation affects the exit pupil size, causing it to increase to 4 mm at one-half maximum power. The zoom magnification changes are effected by two sets of lenses which are axially positioned in the telescope by an electric motor. The relative movement of the two sets of lenses is controlled by a cylindrical cam which in turn is driven by an electric motor. The commands for the zoom mechanism are originated by the crew at the Magnification Control Stick. Electronic controls for the zoom are contained in the Drive K electronics. A manual backup is provided to permit control of the zoom mechanism in the event of automatic control failure.

A pechan prism is contained in the optical train to permit the target scene to be rotated to present the crew with a scene whose in-track component is always vertical in eyepiece FOV at the end of slew. The prism is prevented from rotating during the tracking of a

target so as not to introduce jitter into the scene. The scene will thus rotate slightly in the eyepiece as the target is tracked. Commands generated by the manual control stick will be decoupled in the software to remove the effects of this scene rotation such that vertical displacements of the stick always cause vertical scene displacements.

The pechan prism is driven by a control system in the Drive K electronics in accordance with commands generated in the computer. A manual backup will permit setting the prism to a zero reference position in the event of mechanism failure.

A <u>solar blanking</u> shutter and associated sun sensor are included to protect the crew from inadvertant viewing of the sun. This mechanism will be controlled by the Drive K Electronics in such a manner as to prevent any portion of the solar disk from entering the FOV of the ATS when the gimbals are slewing at any speed up to the maximum gimbal rate. After closing, the shutter will be re-cocked (opened) manually by the crew.

A <u>filter wheel</u> is included in the telescope to permit the crew to insert any one of four filters into the optical train to improve optical performance.

The telescope will not require any <u>refocusing</u> when the target range lies anywhere within the scan field for spacecraft altitudes from 75 to 230 nm. The eyepiece of the telescope will be focusable over a range from -2.5 to +3.5 diopters to permit individual crewmen to adapt the telescope to their eyes.

The telescope eyepiece includes a <u>reticle</u> with cross hair references to locate the center of the FOV, and a circle to reference the size of the real field of view attainable at maximum zoom magnification.

The telescope eyepiece also includes a peripheral display to be described later in this section.

~~SECRET~~ **SPECIAL HANDLING**

The telescopes are mounted in the spacecraft by a rigid mount to the pressure shell at the objective end. The objective lens serves as a backup for the window which provides the primary optical feedthrough in the pressure shell. A shear mount near the elbow in the telescope provides additional mounting restraint. The eyepieces for the two telescopes are brought through consoles 2 and 8 for crew observations. The telescope can be broken down into three pieces at "field breaks" to facilitate installation in the Lab Module. Precise alignment of the telescope will not be required; the external folding mirror will provide the necessary alignment adjustment.

Peripheral Display

The Acquisition Telescope contains a set of peripheral display lights arranged in the eyepiece as shown in Figure 1.3-5. The brightness of the lights in the display can be controlled from a single panel control.

The operation and function of the display groups is presently planned as described below.

a. Group I - Time Reference Display - This group of 25 lights will convey information to the crew concerning:

   1. The number of seconds remaining to the next decision time (up to 25 seconds).

   2. The number of targets remaining to be evaluated in the group.

   3. The ground estimate of the point in time at which the crew should have released each target (by voting).

   At the beginning of a new target group, a light will be lit in the display at a position indicative of the time remaining to decision time (that is if 24 seconds remain, the 24th light will be activated). The position of the activated light ("bouncing ball") will be advanced one position in the display each second. In addition the first light in the display will remain lit during the countdown to serve as a zero reference point.

   In addition to the time reference countdown described above, one light will be activated in Group 1 for each target which remains to be evaluated in the group. The position of each "marker" light in the group will be indicative of the time by

~~SECRET~~ **SPECIAL HANDLING**

~~SECRET~~ **SPECIAL HANDLING**
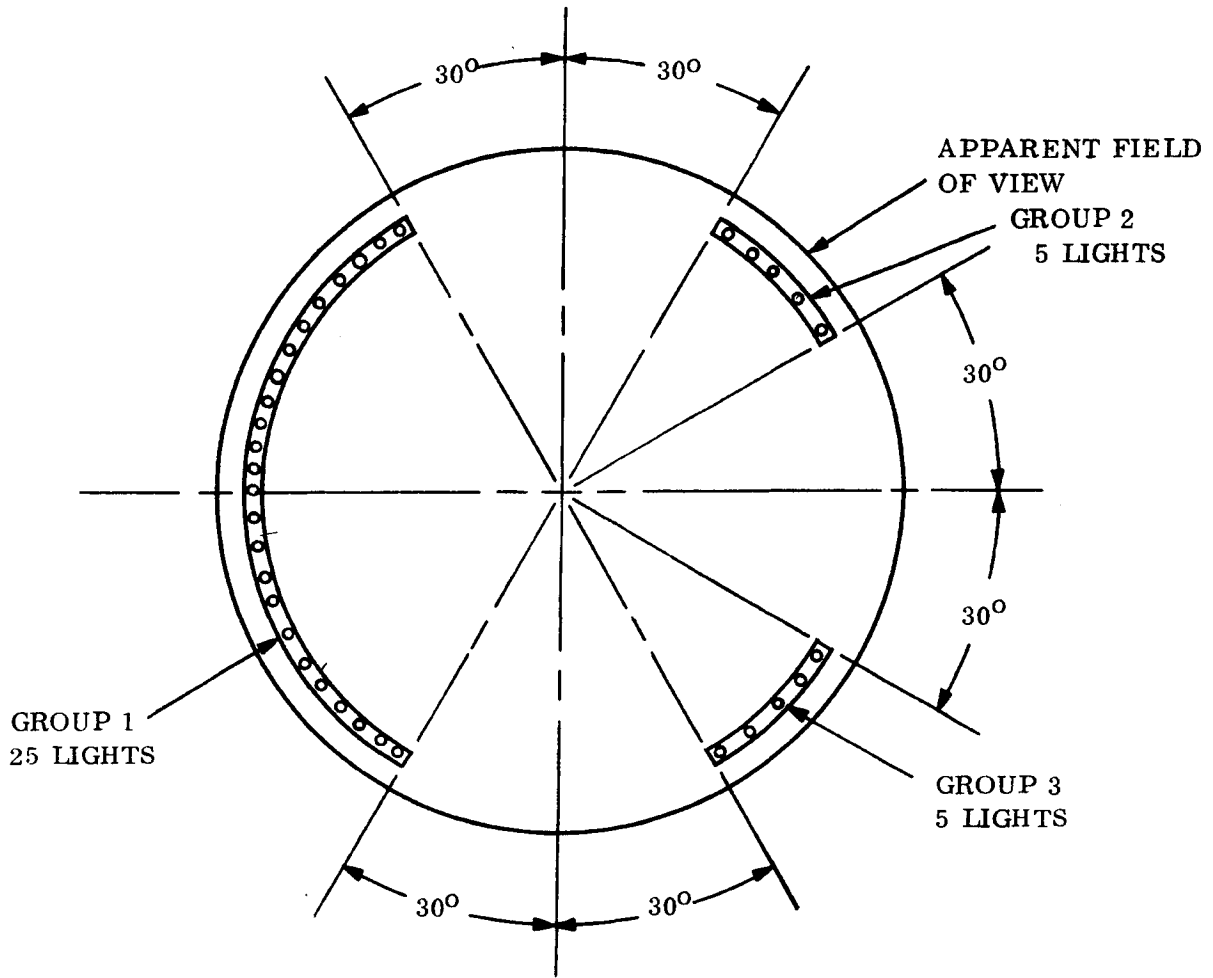
Figure 1.3-5. Peripheral Display Pattern

~~SECRET~~ **SPECIAL HANDLING**

which ground personnel recommend that a vote be entered to release the target. As each target is released, its marker light in the display will be extinguished, while the time wipeout countdown continues.

b. <u>Group II and III</u> - These two 5-light groups will be controlled by the computer to convey information on target priorities, voting instructions, etc. Final determination of the precise information to be conveyed will be made later. The switching control for these lights will permit them to be individually controlled.

The lamp drivers for the peripheral display lights are located in the console controller.

1.3.3.1.2 <u>Window</u> - The window provides the optical feedthrough through the Lab Module pressure shell. It is mounted in the pressure shell in a DAC-supplied penetration fitting which controls the temperature of the circumference of the window within ±2 degrees.

1.3.3.1.3 <u>Folding Mirror (Fixed)</u> - The folding mirror is located external to the spacecraft and functions to fold the telescope LOS parallel with the roll axis. The mirror provides alignment adjustments in its mount to permit accurate alignment of the LOS between the folding mirror and the scanner. The folding mirror is mounted to the same penetration fitting which supports the window and the telescope to minimize relative alignment changes between these components.

1.3.3.1.4 <u>Scanner</u> - The scanner provides the gimballed flat mirror which permits the telescope line of sight to be directed within the prescribed scan field. It consists of the scanner mirror, supported on two orthogonal gimbals, and associated gyros, bearings, encoders, and alignment references.

The outer axis of the gimbal is the roll axis of the scanner and is mounted such that it is canted 9 degrees from the spacecraft roll axis in the horizontal (X-Y) plane. This gimbal cant minimizes the occurrence of zero roll rate conditions during target tracking and thus minimizes jitter due to bearing stiction.

Incremental shaft encoders are mounted on both gimbal shafts. The incremental pulses are accumulated in the Drive K to generate shaft position signals for the computer and the Drive K servo loop.

The gimbals are driven by brushless dc torquers which are controlled by servo electronics in the Drive K in response to computer-generated commands. Gyros, mounted on each gimbal, are an integral part of the rate loops in each servo control system. Energy-absorbing stops limit the gimbals' movement.

The bearings supporting the gimbals are the object of a continuing development program to insure smooth jitter-free tracking by the gimbals.

The scanner is mounted to the pressure shell on a three-point mount. Alignment references will be provided to permit accurate installation.

1.3.3.1.5   Shroud and Shroud Door - The external components of the ATS are enclosed in a hinged shroud which provides thermal control and protection from contaminants when the ATS is not in use. When closed, the shroud will compress a seal to insure that contaminants from the thrusters and the waste management system do not degrade the optical quality of the mirrors.

Thermal control of the shroud and its internal components is achieved passively. The shroud is opened and closed by redundant electric motors, controlled via the Drive K electronics in accordance with commands generated either by the computer or the flight crew. The shroud door drive will be interlocked to prevent closing when the scanner is not in its stow position.

1.3.3.2 Drive K Electronics

Most electronics associated with AO operation will be in a single package called the Drive K Electronics. The functions of the Drive K Electronics are categorized in ten groups, designated K1 through K10, and are described briefly here. The K designations are utilized in non-classified documents to refer to the functions listed. A more detailed description of the controls is presented in paragraph 1.3.4.

K0 - Digital Processor - Processes digital signals from the MDAU for the Drive K.

K1 - Gimbal Control - The K1 electronics receive inputs from the MDAU and the MCSA (in backup mode) and provides drive signals to gimbal gyro torquers.

K2 - Gimbal Control - The K2 electronics receive gyro rate signals from the gimbal gyros and process them for application to the gimbal torquers.

K3 - Derotation - The K3 electronics receive derotation signals from the MDAU/computer, and the analog prism position pickoff, and generates the drive signals for the derotation prism in the AO.

K4 - Zoom - The K4 electronics receive inputs from the Magnification Control Stick and the analog zoom position transducers and generate the drive signals for the zoom motor in the AO.

K5   – <u>Power Change</u> – The K5 electronics receive signals from the Magnification Control Stick and generate signals to control the power change lens in the ATS.

K6   – <u>Solar Blanking</u> – The K6 electronics receive analog signals from the AO sun sensor, provide threshold detection, and generate the necessary signals to actuate the solar blanking mechanism.

K7   – <u>Door Control</u> – The K7 electronics receive signals from the control console door switch and the door limit switches, and generate a signal to drive the external AO door.

K8   – <u>Power</u> Supply – The K8 electronics receive unregulated power from the OV power system, and generates necessary regulated DC voltage.

K9   – <u>Telemetry</u> – The K9 electronics perform signal conditioning necessary for telemetry.

K10 – <u>Monitor and Failure Switching</u> –

1.3.3.3 <u>Visual Display Projector – Design and Description</u>

The Visual Display Projector is primarily intended to aid the crewman in locating targets in the ATS field of view by cueing him with high-resolution pictures of the scene. It is intended that the crew review the cues for the targets assigned before each target pass (prepass briefing), and that he be briefly presented a cue for each target during the pass while the ATS is slewing to the target. A secondary function of the VDP is to provide maintenance or instructional material to the crew.

In order to satisfy the mission requirement the VDP will be capable of rapidly retrieving and displaying cue frames from 16mm strip film. The retrieval time will be less than $0.45 + N/100$ seconds where N is the number of frames traversed in retrieving the cue (provided that at least three consecutively numbered frames precede the desired cue).

The resolution of the VDP will permit 228 lp/mm material on the film, with a 6:1 contrast ratio, to be visible on the screen with the aid of a 10-power loupe.

During target pass operations, cues will be called up by computer commands which are held in the console controller and presented to the VDP as parallel binary words. Each cue frame so retrieved will be held for a short fixed duration and then released to permit the projector to retrieve the next cue. The operation will be planned so that the cue is being retrieved during the periods when the astronaut is viewing an ATS scene, and displayed during the slew period (perhaps with some overlap into the track period). The cue will be released automatically if the crew votes on the target while it is still being displayed. The crew can retain a cue frame beyond the planned release time by actuating a cue hold control on the magnification control stick.

The VDP is located on the console in a position to permit the crew to view the projected scene from the ATS head rest position to maximize usefulness during the target pass. The 6 1/2-inch rear projection screen has a high gain to provide minimum screen resolution degradation and maximum illumination efficiency.

During prepass briefing periods, it is intended that the computer automatically command each frame retrieval as in the target pass operation. The cue would be released and the next cue displayed, however, by the crew by operating a manual control (probably the REJECT button on the magnification control stick).

Cue frames can be called up manually by dialing the desired frame number, in octal form, on the manual selector control on the face of the VDP panel.

Film for the VDP is stored in special modules which can be quickly inserted or removed in the VDP front panel. Schematics of the projector and film module are shown in Figures 1.3-6 and 1.3-7.

Alpha-Numeric Display

A six-character alpha-numeric display is included on the VDP to project cue words relating to each ATS target. The information for these frames is stored in the computer, not on the film.

LOOK PROJECTION SYSTEM

FILM MODULE

FLAT MIRROR

SCREEN

MANUAL SELECTOR
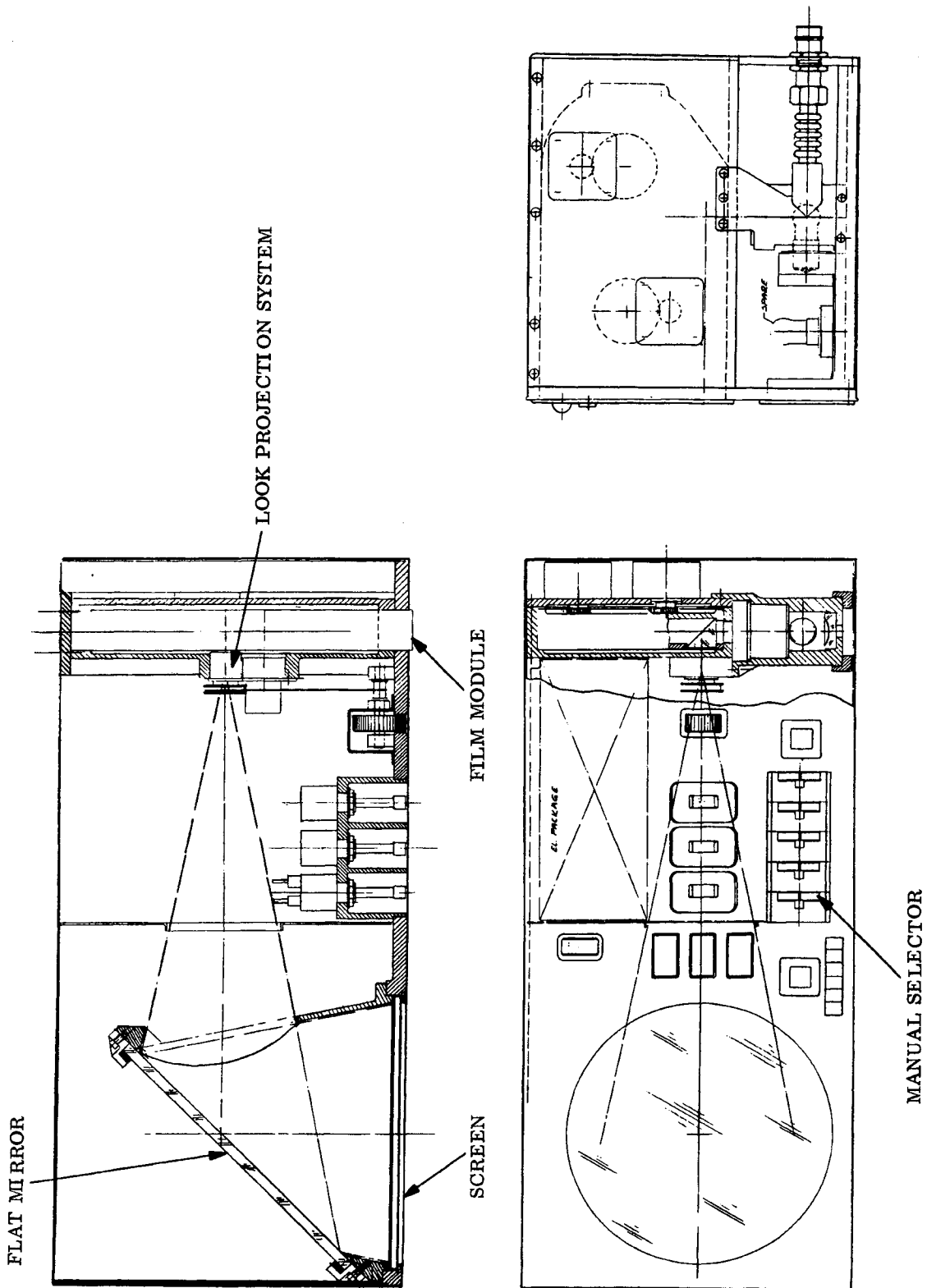
Figure 1.3-6. Visual Display Projector Layout
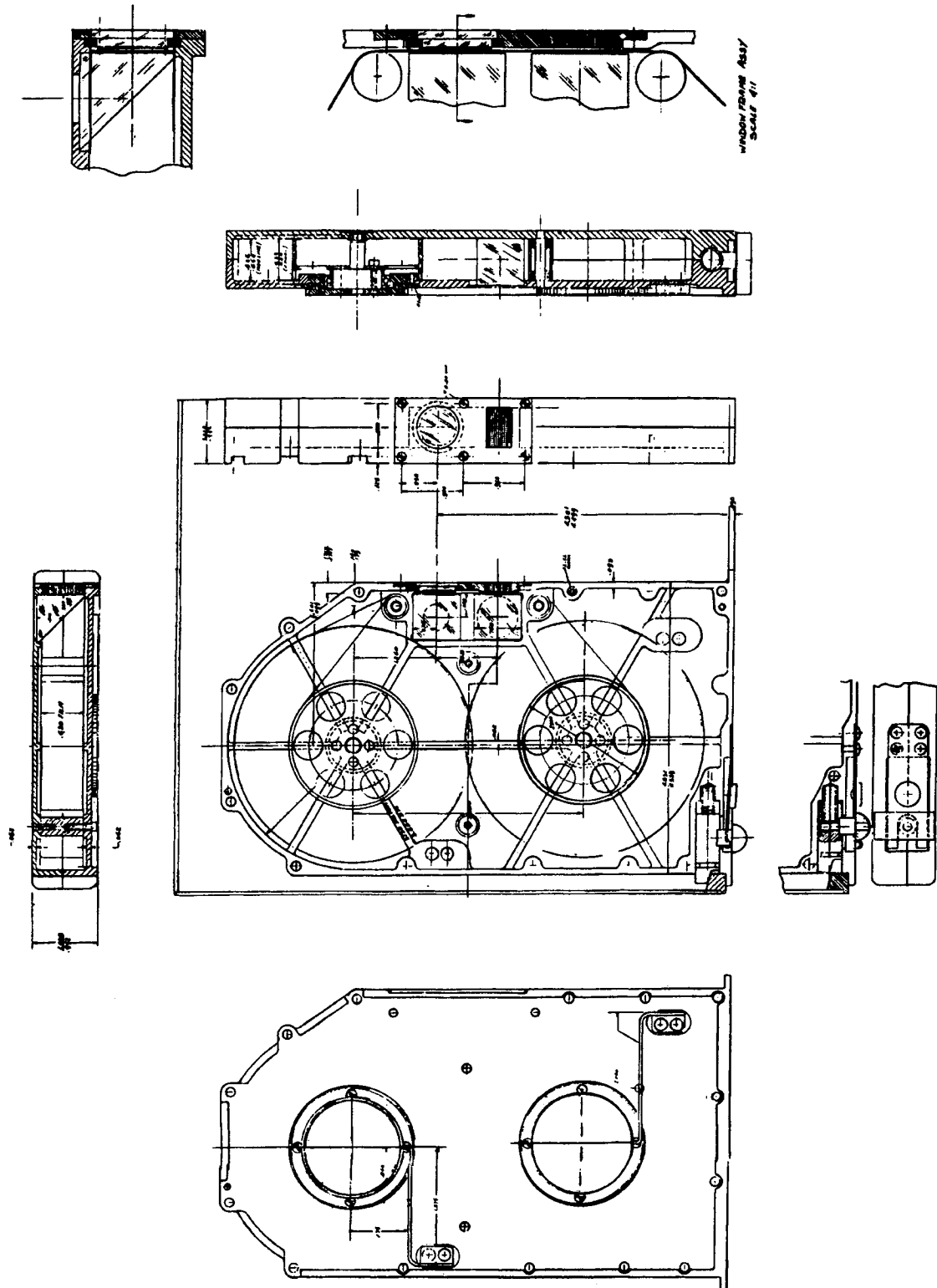
Figure 1.3-7. Film Module Layout

Operational Description

The Visual Display Projector has the capability of displaying any cue frame in a library of 32,752 frames. These cue frames will be stored in 8 film modules, each containing 4,094 frames. Each frame is uniquely identified by a binary code which is printed on the film.

When the frame called for is not on the film, the servo will recognize this and stop to prevent damage to the film.

The beginning of the film reel is identified by a series of frames identified by all zeros, and the end of the film is identified by all ones. In the event that the frame called for appears to be off the end of the reel, the servo will recognize the end of the reel and stop to prevent damage to the film.

Drawing 47D405106 (Figure 1.3-8) is the schematic arrangement for the Visual Display Projector.

When the Off-Auto-On switch is in the Auto position, the projector is in the automatic mode. In this mode, the projector will accept binary commands from the computer via the console controller, and in the absence of commands from the console controller it will accept octal commands from the manual frame selector.

When the Off-Auto-On switch is in the On position, the projector is in the manual mode and will accept commands from the manual frame selector only. The console controller input is inhibited.
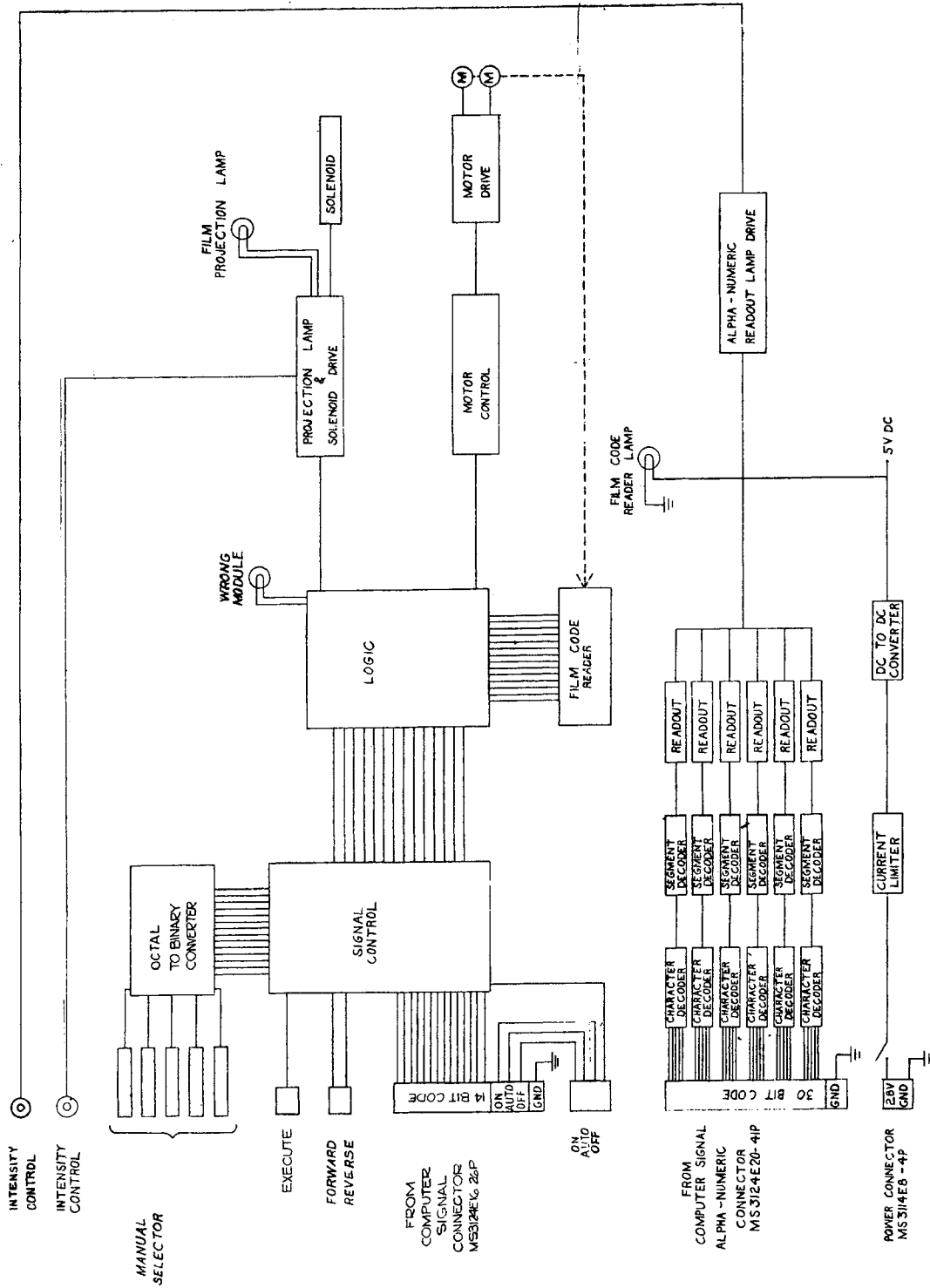
Figure 1.3-8. Visual Display Projector

In the Automatic mode, inputs from the console controller will command a particular cue to be displayed. Upon receipt of this command, the projector will read the code of the cue frame in the film gate and compare it to the new input code. As a result of comparison, the logic will determine the direction the film should be moved and the speed. If the command frame is more than three frames away from the frame in the film gate, the servo drives the film at 100 frames per second, until the frame which is three frames prior to the commanded frame is reached. At this time, the servo dynamically brakes until a speed of approximately 10 frames per second is reached. The film travels at this speed until the binary code of the frame in the film gate corresponds to the commanded binary code. When this occurs, the servo switches to fine position and centers the frame in the film gate. The motors are de-energized, the platen presses the film against the prism face to insure flatness, and the projection lamp is turned on. If the commanded frame is three frames or less away from the frame in the film gate, the servo drives the film at the low speed until the commanded frame is in the film gate. The sequence is then the same as above.

In the manual mode, the thumbwheel switch is set to the octal number that describes the frame to be displayed. The octal-to-binary converter converts this signal to binary code. The execute button injects the binary code into the signal control and the servo handles this input in the same manner as an input from the console controller.

In either the manual mode or the automatic mode, the astronaut may select the frame immediately ahead or behind the projected frame by depressing the forward-reverse switch in the proper direction. This command is overridden by a new input from either the manual frame selector or the console controller, depending on the mode of operation.

When the VDP is energized, the alpha-numeric circuitry will accept binary commands.

Each readout segment is controlled by a 5-bit binary code and is capable of displaying any number, 1 through 9, or any letter, A through Y, with the following letters missing: O I S Q. The display remains illuminated as long as the command is present.

The outline of the Visual Display Projector is shown in Drawing 47D405104 (Figure 1.3-9).
The screen size and location, the controls provided, and their description are shown on the
drawing and need no further description. The test switch, the 2X/1X switch, frame missing
light, and end of reel light have been deleted since the preparation of this drawing. In addi-
tion, the location of the Visual Display Projector is being changed in the console, and the
change in relocation will require a complete repackaging of the Visual Display Projector.
The outline drawing presented here represents the previously defined baseline design with
the Visual Display Projector subcontractor.

1.3.3.4 Cue Module Storage Rack

16-cue modules will be stored in a single-cue module storage rack in the Lab Module.
Detailed design of this rack is not complete. It is presently intended that this rack be
located in console 8A. During the launch phase, the cues will be stored in the Gemini.

1.3.3.5 Magnification Control Stick

The Magnification Control Stick will be designed for operation by each crewman's left hand.
Its functions will be to:

a. Provide the means to electrically select any of four incremental magnification
   levels for the visual optics.

b. Provide a signal to switch the manual control stick between the Main Optics and
   the Acquisition Subsystem.

c. Provide two separate continuous control ranges for controlling ATS zoom magnifi-
   cation in the high-and the low-magnification ranges, respectively (63 to 127X, 16
   to 32X).

d. Provide a switch for commanding magnification step changes to the ATS.

e. Provide three finger-operated voting switches for target REJECT, ACTIVE, and
   INACTIVE votes on the stick handle.

f. Provide a control for commanding CUE HOLD by twisting the stick handle.

~~SECRET~~ **SPECIAL HANDLING**
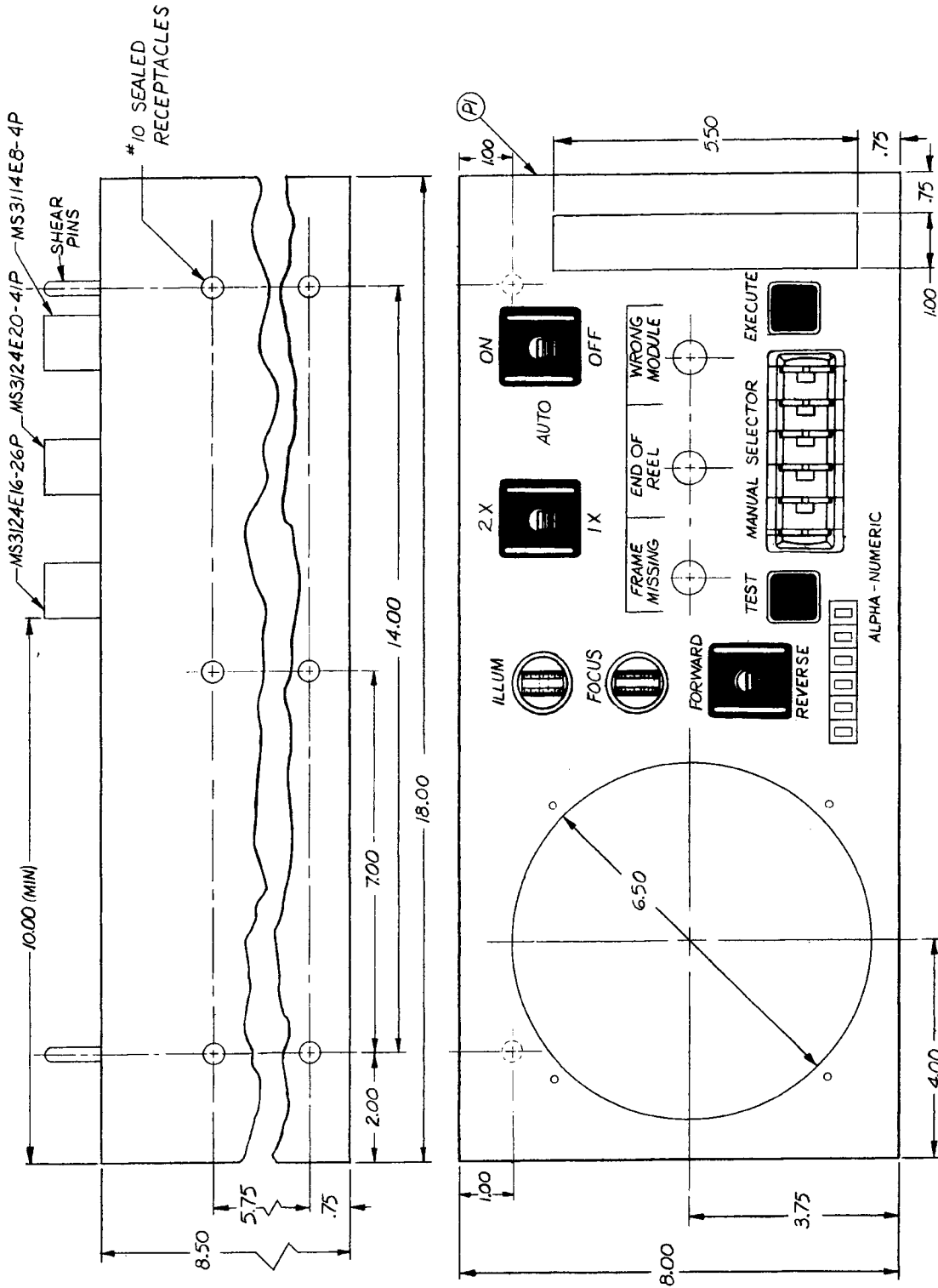
Figure 1.3-9. Outline Drawing, Visual Display Projector

~~SECRET~~ **SPECIAL HANDLING**

The Magnification Control Stick will move in a two-range track on the console as shown in Figure 1.3-10. One range will provide four discrete positions corresponding to four discrete VO magnification levels. The other range shall provide two continuous ATS zoom concontrol ranges separated by a detent corresponding to the position at which a magnification step change is commanded. The two ranges (ATS and VO) are separated by a switch to signal the computer which subsystem the manual control stick controls (Acquisition or Main Optics).

Visual Optics Control

It will be possible for the crew to select any of the four visual optic magnification levels without commanding intermediate power levels (i.e., it will be possible to switch from 1000X to 125X without going through the intermediate steps of 250 and 500 power). Detents or other means shall be provided to permit the crew to position the stick by "feel".

A functional block diagram of the magnification stick is shown in Figure 1.3-11. A detailed design of the stick has not been completed.

1.3.3.6 Head Rests

Head rests will be provided at each console to aid in stabilizing the observer's head in the head rests. Detailed design of the head rests has not begun and will ultimately be constrained by simulation results and flight crew preference. The following general guidelines are considered relevant:

a. The head rest will provide maximum crew comfort over the duration of full target pass.

b. It will provide stable, comfortable positioning of the crewman's head to allow viewing through a 2-mm AO exit pupil in a zero-g environment.

~~SECRET~~ SPECIAL HANDLING

MAGNIFICATION
CONTROL
STICK

CREW
INPUT

PROVIDES

1) V.O. MAG. SELECTION

2) ATS ZOOM CONTROL

3) ATS MAG. CONTROL

4) CUE HOLD

5) TARGET VOTING

6) DIRECTION OF MCSA
   TO ATS OR M.O.

TO TLM

● CUE HOLD STATUS

● MCS STATUS

TO DRIVE K

● DISCRETE MAG.
  STEP COMMAND

● ZOOM CONTROL
  SIGNAL

TO CONSOLE
CONTROLLER

● V.O. MAG. LEVEL
  SIGNAL

● TARGET VOTING
  SIGNALS

● ATS MAGNIFICATION
  STATUS SIGNAL
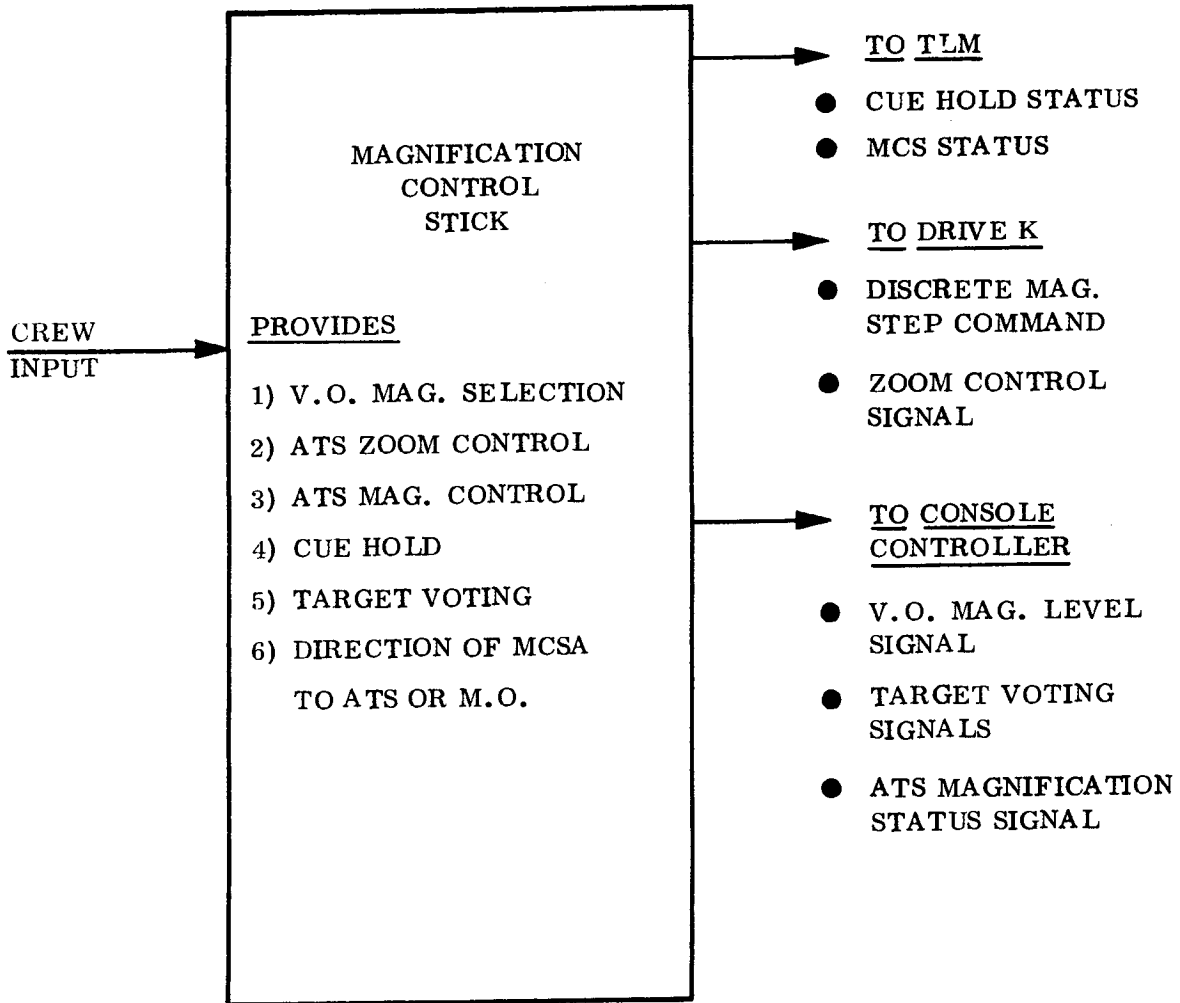
Figure 1.3-11. Functional Block Diagram,
Magnification Control Stick

~~SECRET~~ SPECIAL HANDLING

~~SECRET~~ **SPECIAL HANDLING**

1000X

500X

**V.O. CONTROL
RANGE**

250X

125X   127X

**SWITCH TO SIGNAL
COMPUTER WHICH
RANGE THE STICK
IS IN**

63X
32X   **ATS CONTROL
RANGE**

16X
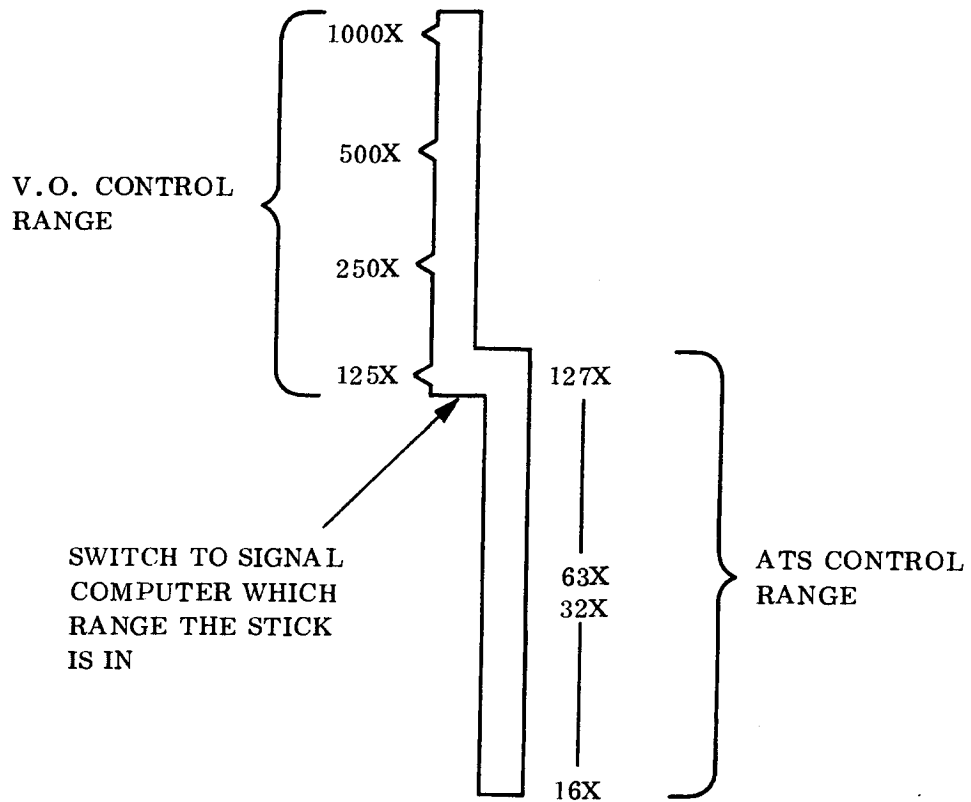
Figure 1.3-10. Magnification Control Stick Slot Configuration

~~SECRET~~ **SPECIAL HANDLING**

c. It will maximize the crew's ability to scan the FOV at all magnification and pupil sizes produced by the AO.

d. It will provide sufficient adjustment to allow either eye to be used and to allow each crewman to position his head in accordance with the AO eye relief. It shall be adjustable with a gloved hand.

e. It will prevent contact of crew head with ATS eyepiece.

f. It will not interfere with the crew's ability to move quickly from the ATS to the VO eyepiece.

1.3.4 ATS CONTROLS DESCRIPTION

1.3.4.1 General Functional Description

The functions of S/S Alpha Controls will be described with reference to Figure 1.3.4-1.

The primary functions of S/S Alpha controls are to provide:

  a.   Proportional control of the ATS two axis gimballed LOS scanner mirror in response to computer generated digital steering commands (Functions K0, K1, and K2)

  b.   Bi-valued position control of an environmental protective shroud door in response to computer controlled (primary) or manually initiated commands originating on the control console (Function K7)

  c.   Proportional position control of an image orientation prism in the ATS telescope in response to a computer digital command (Function K3)

  d.   Proportional position control of a zoom lens assembly on the ATS telescope in response to signals originating from a manually operated zoom/magnification controller. (Function K4)

  e.   Bi-valued position control of a magnification lens assembly on the ATS telescope to select a high or low range of magnification in response to a command from the zoom/magnification controller (Function K5)

  f.   An ATS telescope solar blanking mechanism which will protect the astronaut against viewing the sun through the telescope (Function K6a)

1.3.4.2 Detailed Functional Description

The detailed functional description of the S/S Alpha controls is presented in the following paragraphs:

1.3.4.2.1 Scanner Control

The functional block diagram of the scanner controller is presented in the top portion of Figure 1.3.4-1 and, in greater detail, in Figure 1.3.4-2. The scanner control operates on separate inner and outer axis digital rate command signals received from either MDAU No. 1 or No. 2.
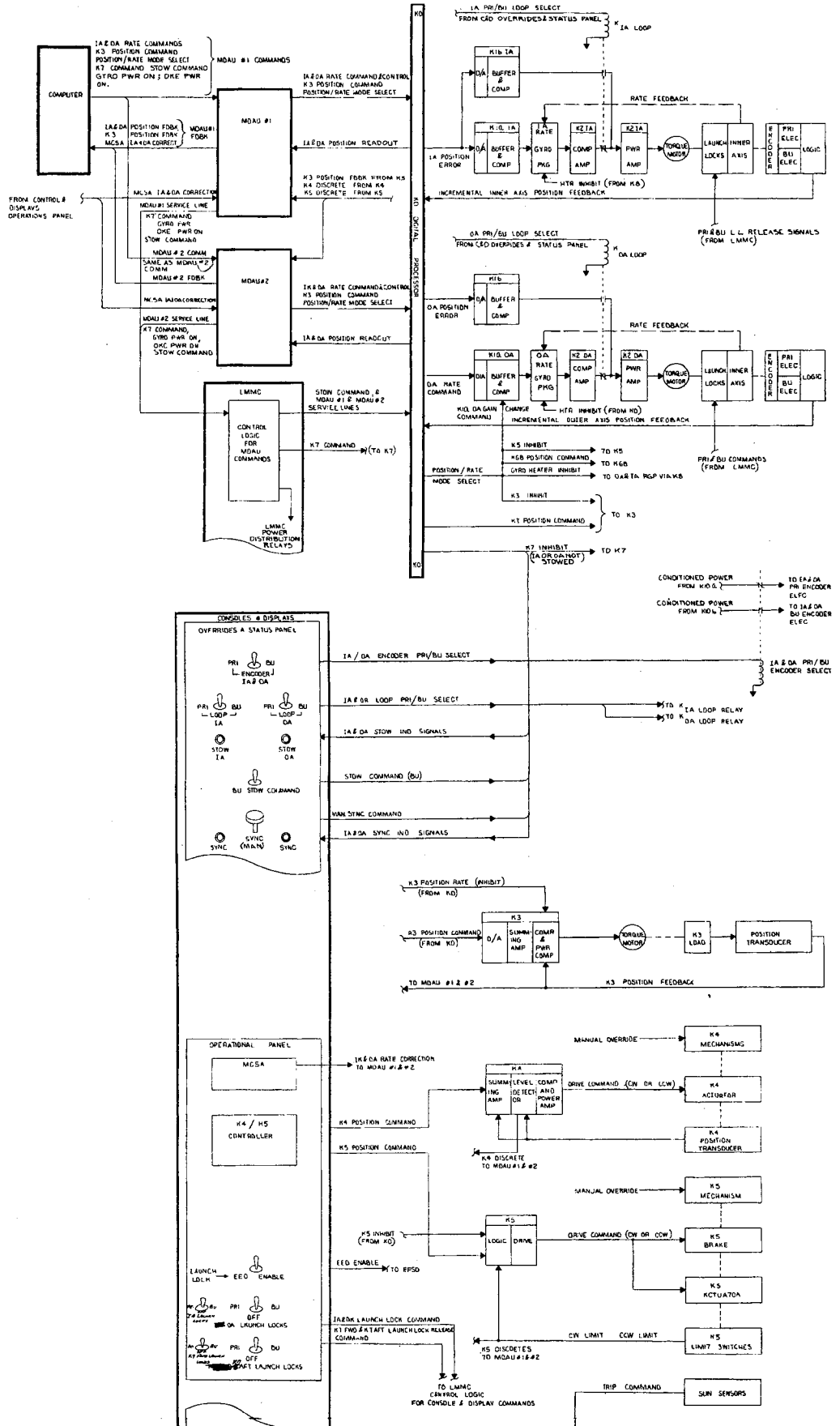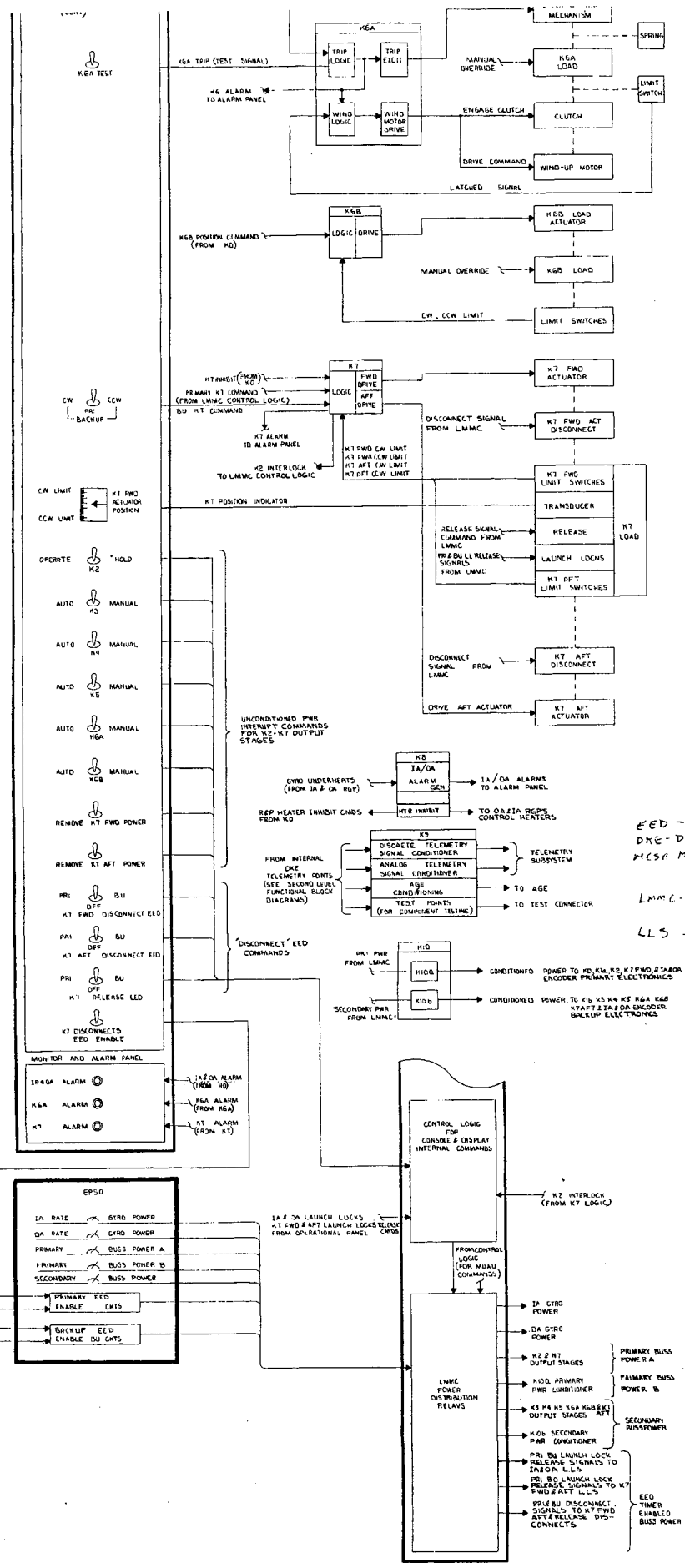
Figure 1.3.4-1. Drive "K" Control
Functional Block Diagram,
First Level
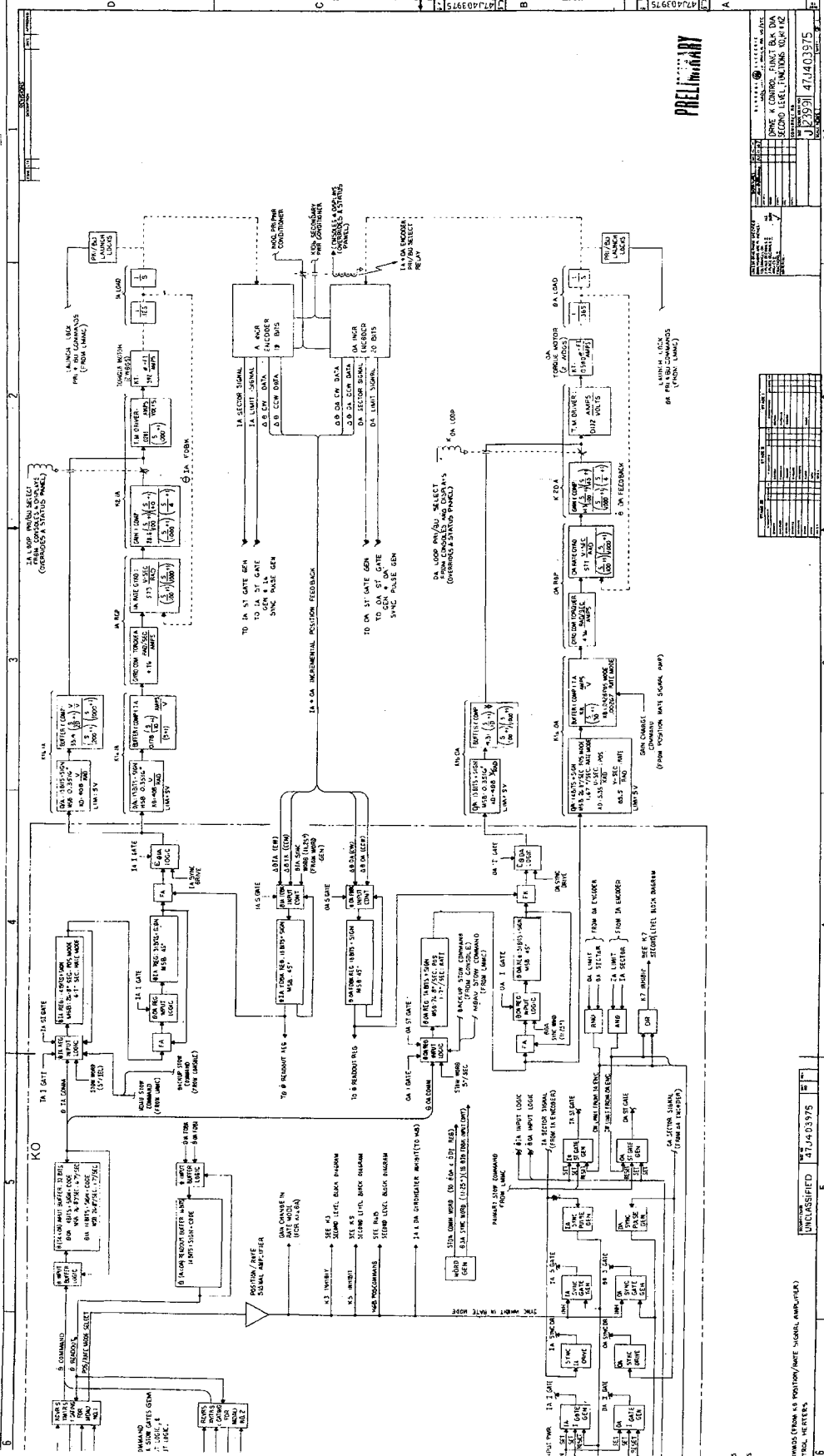
Figure 1.3.4-2. Drive "K" Control,
Functional Block Diagram,
Second Level, Functions
K0, K1 and K2

1.3.4.2.2 Inner Axis (IA)

For the Inner axis, control is provided by either of two configurations. In both modes the IA rate command is integrated at a 19.5 KC rate and stored in the θ_{IA} command register. The contents of this register is compared to the "whole-word" gimbal feedback information formed in the θ_{IA} feedback register from the incremental data generated by the IA gimbal encoder. The error signal, $\epsilon_{\theta_{IA}}$ is sent to the K1 D/A converters.

In the primary mode the error signal is used as the input to a rate minor loop formed around the IA Rate Gyro Package (RGP) mounted on the IA gimbal. Functional block K1aIA provides the D/A conversion, compensation and gyro command torquer drive.

Functional block K2 IA operates on the gyro output signal and provides the compensation and the torquer motor drive capability.

In the back-up configuration, the rate minor loop is not required and the digital error signal is converted and compensation is supplied by functional block K1bIA. The compensated signal directly drives the IA torque motor power amplifier. In both primary and back-up configurations, the position feedback data is read out to the computer (via the MDAU) from the θ_{IA} readout buffer.

1.3.4.2.3 OUTER AXIS (OA)

Two control loops are also available in the OA. The primary configuration operates directly on the rate command word from the $\dot{\theta}_{OA}$ register. This rate command is converted to an analog signal, compensated and conditioned to drive the OA rate gyro torquer in functional block K1aOA.

The gyro output signal is then compensated and applied to the OA torquer motor driver in functional block K2OA. In the back-up mode the integrated rate command in the θ_{OA} register is compared with θ_{OA} feedback register to produce a position error, $\epsilon_{\theta_{OA}}$, as in

the IA loops. As in the back-up IA loop the OA position error is converted, compensated (in K1bOA), and applied directly to its torque motor amplifier (via K2OA).

Also as in the IA loop, the θ_{OA} feedback data is read out to the computer via the MDAU's, in both primary and back-up modes, from the $\theta_{IA \& OA}$ readout buffer.

1.3.4.2.4 Operational Control

On orbit, during normal operation, certain scanner functions are automatically carried. These include power turn on and off, initialization and synchronization of digital registers, in K0 and stowing of the scanner. In addition, an interlock with the shroud door (K7) is provided to prevent either moving the scanner from its stowed position while the shroud door is closed (by interrupting unregulated power to K2 until door is fully open), or closing the shroud door with the scanner not in its stowed position (by K2 interlock signal to K7 input logic). The signal flow for these functions can be seen in Figure 1.3.4-1.

Launch lock release is manually actuated from the Operational Panel. In the present baseline design the scanner and environmental launch lock employ electro-explosive devices (EED's) to supply the force to remove locking pins. (Studies are under way to eliminate EED's.)

Both scanner and environmental door are released by operation of switches on the Operational Panel, employing the primary and backup actuation circuits in sequence. An EED circuit enable switch (also on the Operational Panel) must be actuated in conjunction with the release switches, as a safety precaution.

Contingency control, by redundant command signal paths, can be initiated by manually actuated switches on the Overrides and Status Panel to perform the following functions:

    a.   Stow the scanner

    b.   Synchronize the position feedback registers

c. Remove power manually from torque motor amplifiers (to hold scanner position while switching configuration)

d. Perform an operational check of the scanner

e. Select the backup loop configuration

f. Select backup encoder electronics

A description of the Initialization and Synchronization, Stow Procedure and the Scanner Operational Check is given in the following paragraphs:

Initialization and Synchronization (See Figure 1.3.4-2)
These functions serve to minimize the "turn-on" transient (initialization) and force agreement (synchronization) between the feedback registers and the gimbal positions (IA and OA) initially, and periodically throughout the active period.

Initialization begins immediately after power turn-on or when commanded manually from the control console and results in blocking the normal rate commands; and setting the rate command registers ($\dot{\theta}_{IA}$ REG and $\dot{\theta}_{OA}$ REG) to zero; the OA position register (θ_{OA} REG) to zero; the IA position register (θ_{IA} REG) to approximately 11.25 degrees; and the application of a constant rate command (via the IA and OA D/A converters) to drive the IA and OA axes toward their respective "synch" positions, (0° for OA, and 11.25° for IA). As each gimbal reaches its "synch" position the constant rate drive in that axis is removed, and when both gimbals have reached their respective "synch" positions the normal rate commands are again admitted.

Synchronization takes place in each axis independently, and occurs not only as part of the initialization process but whenever the gimbals pass through their respective synch positions during the periodic slews. Synch is inhibited from occurring during the "rate" mode.

1-61

Synchronization is accomplished by resetting the position feedback registers (θ_{OA} and θ_{IA} FDBK REG) to 0° and 11.25°, respectively, as the associated gimbal passes through its synch position.

For manual initizalization, which is employed in a contingency mode, the synch pulse in each axis is stretched out to approximately one second duration and used to momentarily light indicators on the Overrides and Status Panel as an indication that initialization was successful. The initialization and synchronization function described above are implemented by the various gate, pulse, drive and word generators and register input logic shown in Figure 1.3.4-2, operating on the sector signals generated by the OA and IA shift position encoders.

1.3.4.2.5 Stow Procedure

The stow operation consists of commanding the scanner gimbals to a position which will permit the environmental shroud door to be closed. The scanner will be maintained in this position, with power off, until the shroud door is opened at the commencement of the next operating period. A non-power consuming latching device will be supplied, if necessary, to hold the scanner in the stowed position. As shown in Figure 1.3.4-2, the present baseline selection for this holding device is a permanent magnet.

Stowing is initiated by the computer, via the MDAU's, at the end of an active period, or by the manual actuation of a switch on the Override and Status Panel. On the receipt of a stow command the normal rate commands are blocked and a 5°/sec rate is introduced in both rate command registers ($\dot{\theta}_{OA}$ and $\dot{\theta}_{IA}$ REG's). As each gimbal reaches its stow position, the stow rate command to that axis is terminated. The normal rate commands, however, remain blocked, and effectively zero rates are commanded, as long as the stow command is continued.

Stowing is implemented by employing the stow commands to the rate register input logic to block the normal commands and to set up to IA and OA "ST" Gates. These gates are reset

by the stow position signals (CW Limits) from the encoders. The "ST" gates go to their respective rate command registers to gate in the stow rate command until the stow positions are reached. An indication of stow for each gimbal is provided on the Override and Status Panel.

1.3.4.2.6 Scanner Operational Check

An operational check of the scanner can be quickly performed with the controls and displays available on the Override and Status Panel, and a stop watch. The first step is to manually initiate synch by means of the manual synch switch. Completion of manual initialization is signaled by the synch indicators.

The next step is to manually initiate the stow procedure and time the period elapsed before the stow lamps are lit in each axis. Knowledge of the stow rate and the gimbal displacement between the synch and stow locations in each axis provides the astronaut with the nominal reference times, for a properly operating system, with which to compare his measured values.

1.3.4.2.7 Image Orientation Control (Function K3)

The functional features of the Image Orientation Control is shown in Figure 1.3.4-3. The control consists of a proportional position servo loop operating on a digital step position command received from the computer through the MDAU's. The input is converted to an analogue command signal and lagged by the shaper transfer function before being compared to analogue position feedback signal. The shaper function limits rate of build-up of a step command to reduce the tendency to saturate the following amplifier stages. (Saturation would reduce the loop response time.) The Summer and Power amplifier generates the error signal, provides compensation and drives a pechan prism to orient the image.

Image orientation is made to some angle predetermined by the computer for each slew, and executed during the slew period. In the tracking mode the control loop is opened to immobilize the prism. This function is performed by solid state switching in the power amplifier

SECRET—SPECIAL HANDLING

NOTES:
1. INTERPRETATION OF ELECTRICAL OR ELECTRONIC SYMBOLS AND REFERENCE DESIGNATIONS PER MIL-STD-15-1 AND MIL-STD-16.

ACTUATOR+LOAD REFERRED TO MOTOR
FRICTION = 1.5 O3 - IN

$\frac{2500}{5}$

.0339 #Ft AMP

.0384 AMPS $\overline{(.0008S+1)VOLT}$

$KV = \frac{.006 \text{ VOLT-SEC}}{RAD}$

SUMMER COMP&PA $\frac{60(\frac{5}{5}+1) \frac{V}{V}}{\frac{5}{100}+1}$

COMMAND SHAPER $\frac{131 V}{(\frac{V}{2}+1)}$

DA CONVERTER 10 bits + Sgn MSB 22.5° $K_D = .766 \frac{V}{RAD}$

SIGNAL CONDITIONER 1 $\frac{V}{V}$

POSITION XDCR 3.8 V V/RAD

LIMIT = I

DIFF

2 / 1

MANUAL OVERRIDE

LOAD

STOPS ±1

K0
K0 RECEIVER & GATING FOR MDAU #1 DATA

K0 RECEIVER & GATING FOR MDAU #2 DATA

K3 POSITION COMMAND&CONTROL
POSITION/RATE MODE SELECT
K3 POSITION
SERVICE LINE MDAU #1

MDAU #2
SERVICE LINE
K3 POSITION COMMAND CONTROL
POSITION/RATE MODE SELECT
K3 POSITION

K3 COMMAND
TELEMETRY GATING
LIMIT 0 +5V
TO TELEM

MDAU NO. 1

LMMC

MDAU NO. 2

CONSOLES & DISPLAYS
OVERIDES AND STATUS PANEL
AUTO
K3
MANUAL

LMMC
K3
UNCONDIT POWER
CONTACTS IN NORMAL OPERATING CONDITION
K3 POWER STAGE

SECRET—SPECIAL HANDLING

STAGE II
NOT FOR PROCUREMENT OR FABRICATION OF PRIME HARDWARE

PRELIMINARY

Figure 1.3.4-3. Drive "K" Control, Functional Block Diagram, Second Level, Function K3

1-65/1-66

stage responding to the position/rate synch from K0. The position feedback signal is read out to the computer, to be used in conditioning the MCSA transfer function with respect to prism position.

The pechan prism can be manually positioned in case of failure of the electrical control loop. The electrical drive can be disabled by a switch provided on the Override and Status Panel if it becomes necessary to use the manual back-up. The electrical disable control operates through the LMMC to cut-off unregulated power to the output stage.

1.3.4.2.8 Zoom Control (Function K4)

The Zoom control is functionally depicted in Figure 1.3.4-4. The zoom function employs a proportional control loop with an analogue command signal derived from the zoom/mag stick on the Operational Panel and an analogue position feedback signal. Shaping is provided on the command signal to minimize saturation and resulting loss in response time, in the event of a steep-sloped input.

A signal indicating high or low zoom magnification setting is generated from the position feedback signal to be used by the computer in adjusting MCSA sensitivity. This signal is transmitted through the MDAU's.

Manual zoom positioning is provided as a back-up to the servo loop control.

A manually operated switch, located on the Override and Status Panel is used to disconnect the unregulated power to the output stage to disable the motor drive during manual operation.

1.3.4.2.9 Magnification Control (Function K5)

The K5 functional block diagram is shown as part of Figure 1.3.4-1. In operation, a constant voltage is applied to the load actuator, to drive the lens assembly to the commanded position. A limit switch removes the drive when the attained position agrees with the command. The command is bi-valued, corresponding to lens assembly "out" (for high

1-67/1-68

SECRET SPECIAL HANDLING

SECRET SPECIAL HANDLING
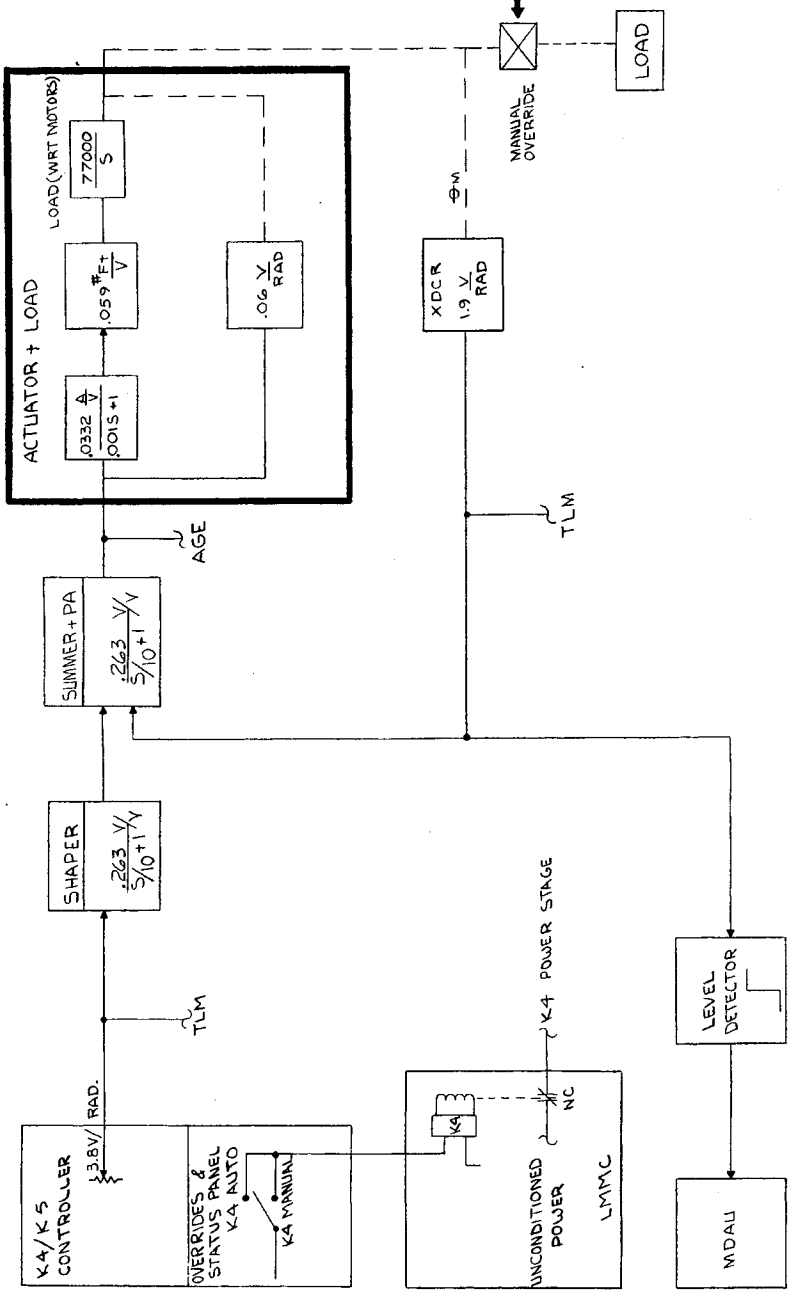
NOTES

1. INTERPRETATION OF ELECTRICAL OR ELECTRONIC SYMBOLS & REFERENCE DESIGNATIONS PER MIL-STD-15-1 & MIL-STD-16

STAGE II

NOT FOR PROCUREMENT OR FABRICATION

PRELIMINARY

Figure 1.3.4-4. Drive "K" Control,
Functional Block Diagram,
Second Level, Function K4

1-69/1-70

ACTUATOR + LOAD

LOAD (WRT MOTORS)

$\dfrac{7700}{S}$

$.059 \dfrac{\#F+}{V}$

$.0332 \dfrac{A}{V}$ $\dfrac{1}{.0015 + 1}$

$.06 \dfrac{V}{RAD}$

AGE

SUMMER + PA $\dfrac{.263}{5/10 + 1} \dfrac{V}{V}$

SHAPER $\dfrac{.263}{5/10 + 1} \dfrac{V}{V}$

TLM

XDCR $1.9 \dfrac{V}{RAD}$

θ_M

MANUAL OVERRIDE

LOAD

TLM

K4 POWER STAGE

K4/K5 CONTROLLER

3.8V / RAD.

OVERRIDES & STATUS PANEL

K4 AUTO

K4 MANUAL

UNCONDITIONED POWER

K4

NC

LMMC

LEVEL DETECTOR

MDALI

magnification power) or "in" (for low power) of the optical path. Position accuracy in the optical path is established by a cam configuration that assures the lens is firmly positioned against its precisely located stops before a limit switch signal is generated, and the incorporation of a brake that is applied when power is removed. The state of the limit switches is also sent to the computer (via the MDAU's) for adjusting sensitivity of the MCSA.

Commands to the lens assembly are inhibited during scanner slew. Manual positioning of the lens assembly is employed as a backup. Disconnection of power to the power switch during manual operation is accomplished by actuating a switch on the Override and Status Panel.

1.3.4.2.10 Solar Blanking (Function K6a)

The solar blanking control functional block diagram is shown as part of Figure 1.3.4-1. The solar blanking mechanism is a lightweight shutter that is removed from the optical path when an actuation spring is wound up and latched. The shutter will be manually cocked (reset) by the crew. A "sun-presence" will light an alarm indicator on the Monitor Alarm Panel

1.3.4.2.11 Cue Insertion (Function K6b)

Space provisions are included in the telescope for a cue insertion mechanism in the event such a feature is desired. The cue insertion mechanism would drive a mirror into the optical path to allow cue information to be presented to the astronaut in place of the ground image. The functional block diagram of K6b shown in Figure 1.3.4-1, represents a possible configuration for this control if it is added to the subsystem. This function is not a part of the baseline design.

1.3.4.2.12 Shroud Door Drive and Launch Lock Release Actuation (Function K7)

The functional characteristics of the shroud door control is shown as part of Figure 1.3.4-1.

a. <u>Shroud Door Control</u> – The Shroud door is driven by two motors, one placed on each end of the door (forward and aft). In the primary mode of operation the command to open or close the door is received from the LMMC (shown as the K7 command) and is applied to the drive logic of both aft and forward motors. A separate set of limit switches is associated with each end of the door and is used to cut off the associated motor drive when its end is positioned as commanded.

The input logic also incorporates an interlock signal which prevents the door from being closed unless the scanner is stowed (K2 interlock). The scanner stowed signal is derived from the scanner encoder position limit and sector signal. (Shroud door launch locks are also provided and are released as described in paragraph 1.3.4.2.4.)

For back-up to the primary mode of operation, the following functions are provided:

1. A manually initiated switch signal from the Override and Status Panel can operate the doors in place of the normal command from the LMMC.

2. Power can be removed from either motor by switches on the Override and Status Panel in case of an electrical control loop failure, permitting control through the remaining motor and control loop.

3. Either motor can be mechanically disconnected from the drive shaft by manually actuating a switch on the Override and Status Panel, in case of binding of one of the motor shafts.

4. A spring incorporated on the door drive mechanism can be released to open the door after mechanically disconnecting both motors. (Note that in the current baseline configuration the disconnects and door release function of (3) and (4) are accomplished by EED actuated pins, and for safety reasons an EED circuit enable switch is also provided. Currently a study is being made to reduce the number of/or eliminate completely, these EED's.)

5. A continuous position indicator is also provided on the control console to aid in determining which motor must be mechanically disconnected in case of a binding shaft. The position signal is derived from one end of the door so that the response, or lack of response of the position indicator to a door drive command determines which side is binding.

1.3.4.2.13 Power Conditioning and Distribution

A functional diagram of the power conditioning and distribution is shown in Figure 1.3.4-5.

The general features of the arrangement shown are dictated by the following considerations:

a. Power turn on will be accomplished on computer commands to the LMMC via the MDAU's.

b. Flexibility to turn on gyros separately for peak power management.

c. Two separate power paths. Primary and Secondary Power Generation and Routing.

   1. Primary power for primary scanner, shroud door and launch lock control

   2. Secondary power for all remaining functions.

   This separation will prevent propagation of electrical failures through a common power path, from the functions in path (2) to function in path (1).

   This is advantageous since all functions in (2) can either be performed without electrical power, in a back-up mode, or are part of back-up provisions for the path (1) functions.

d. Separate control of unregulated power to individual functions to allow overload, isolation, failure mode switching, and interlocking on an individual function basis.

   An additional feature which is shown in Figure 1.3.4-5, but is still tentative, is the inclusion of fuses on the regulated power inputs to the functions of path (2). A possible reliability penalty may be tolerable for these functions since they have function manual back-up.

   The advantage lies in the ability to operate in a normal mode with the remaining functions after one function fails in a manner which overloads its conditioned power lines.

   The functions of path (1) will not be fused, since reliability of these functions cannot be compromised.
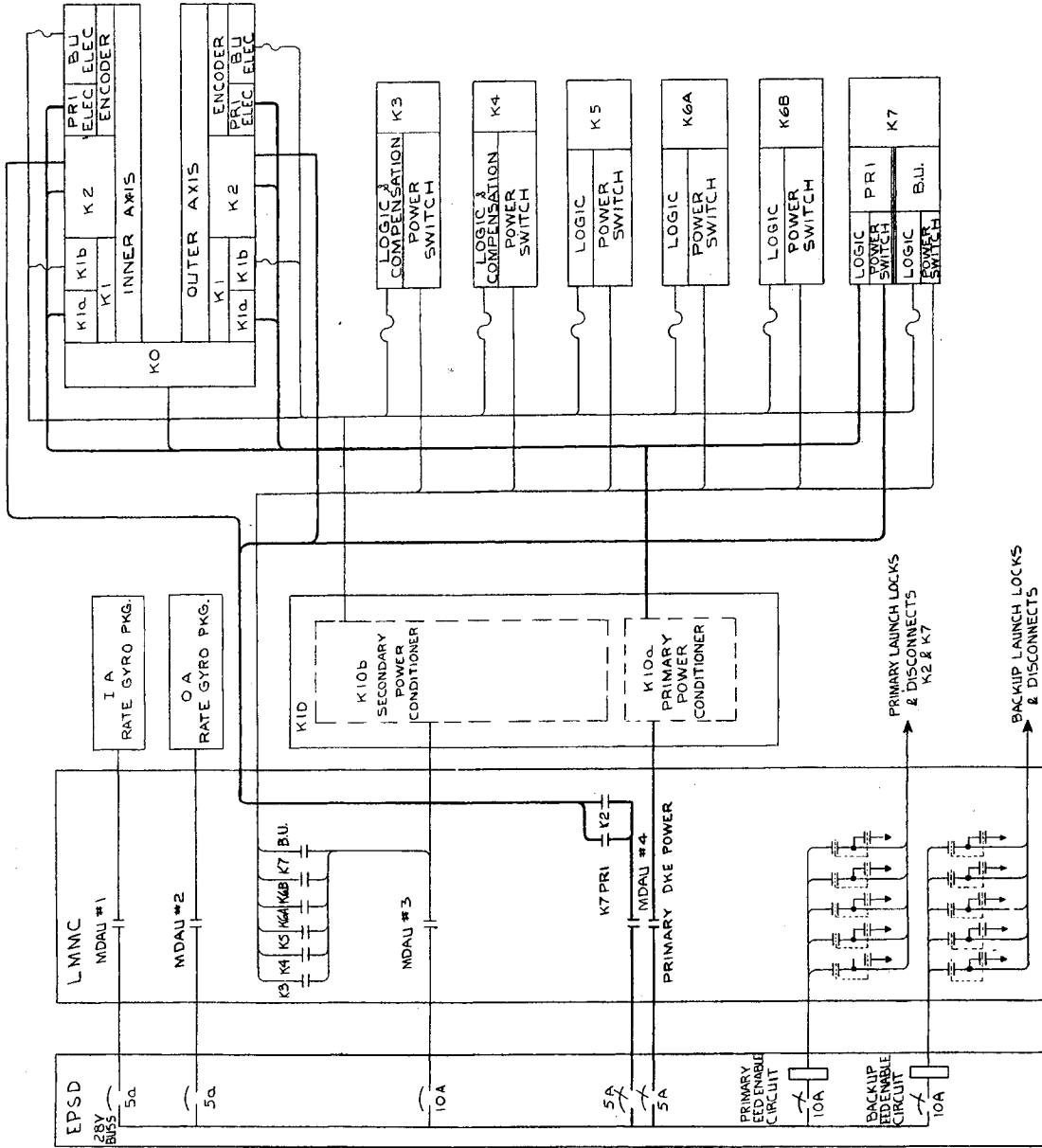
NOTES:
1- INTERPRETATION OF ELECTRICAL OR
   ELECTRONIC SYMBOLS AND
   REFERENCE DESIGNATIONS PER
   MIL-STD-15-1 AND MIL-STD-16.

STAGE II
NOT FOR PROCUREMENT OR FABRICATION
PRELIMINARY

Figure 1.3.4-5. Drive "K" Control
Subsystem Power Distribution

1-75/1-76

SECTION 2.0

ATS ANALYSIS

This section contains analysis relative to the design and performance of the acquisition optics components. The material is subdivided as follows:

2.1 ATS Optics Analysis

2.2 ATS Controls Analysis

2.3 ATS Performance Error Analysis

2.4 ATS Temperature Control Analysis

2.5 ATS Structure Analysis

2.6 Boresighting

2.7 Image Rerotation and Decoupling

2.1 ATS OPTICS ANALYSIS

This section presents material related to the optical design and performance of the ATS. The material is subdivided as follows:

2.1.1 Design Description

2.1.2 GE Performance Analysis

2.1.3 GE Analysis of Optical Performance Under Dynamic Conditions

2.1.4 Secondary Design and Performance Information

2.1.1 DESIGN DESCRIPTION

This section defines the optical design as it exists for preliminary design review.

2.1.1.1 Optical Prescription

The optical prescription for the ATS is given in Table 2.1-1. The prescription is not expected to change further. Minor adjustments will be made based on melt and manufacturing tolerances. Column headings are as follows:

1. Surface Number – The outside surface of the telescope objective is Surface No. 1 The exit pupil is surface No. 53. Surface Nos. 5 through 15 inclusive are contained only in the power changer mechanism.

2. Radius – Radius of curvature at each surface

3. Radius tolerance

4. Thickness

5. Thickness tolerances

6. Air Space

7. Air Space tolerance

8. Clear Aperture

~~SECRET~~ SPECIAL HANDLING

TABLE 2.1-1. OPTICAL PRESCRIPTION FOR ATS

1 SURFACE NO.	2 RADIUS (INCHES)	3 RADIUS TOL. (INCHES)	4 THICKNESS (INCHES)	5 THICKNESS TOL. (INCHES)	6 AIR SPACE (INCHES)	7 AIR SPACE TOL. (INCHES)	8 CLEAR APRTR (INCHES)	9 n*	10 v**	11 GLASS TYPE AND MELT
29	- 1.6161	± 0.002	0.3996	±0.005	0.3342	±0.005	0.66	1.62004	36.37	F-2
30	- 0.8979	± 0.005			1.1384	High / Mid. / Low	0.67			
31	1.7353	± 0.015	0.3246	±0.005	1.3933		0.75	1.51680	64.17	BK-7
32	0.8258	± 0.003			0.0500		0.79			
33	- 0.7985	± 0.003	0.3933	±0.005	1.8578	±0.005	0.78	1.62004	36.37	F-2
34	- 3.4038	± 0.041			0.7597	High / Mid. / Low	0.91			
35	1.7311	± 0.009	0.2072	±0.005	0.0266		0.98	1.62004	36.37	F-2
36	1.0715	± 0.004			0.3178	±0.005	0.98			
37	1.2965	± 0.004	0.3000	±0.005			1.18	1.62041	60.33	SK-16
38	5.4668	± 0.069			0.1500	±0.005	1.18	1.51680	64.17	BK-7
39	∞ Filter		0.1700				1.18			
40	∞				0.1500	±0.005	1.18			
41	- 1.9993	± 0.009	0.2001	±0.005		±0.005	1.18	1.51680	64.17	BK-7
42	- 4.1623	± 0.035			1.0426	±0.005	1.24			
43	∞				0.2000	±0.005	1.50			Image Plane
44	- 7.4978	± 0.084	0.1670	±0.005			1.54	1.68893	31.18	SF-8
45	1.1851	± 0.002	0.7560	±0.005			1.67	1.62041	60.33	SK-16
46	- 1.7750	± 0.004			0.7504	±0.005	1.74			
47	2.1978	± 0.006	0.2100	±0.005			1.78	1.64831	33.84	SF-12
48	1.1552	± 0.002	0.5880	±0.005			1.67	1.62041	60.33	SK-16
49	- 30.2177	± 1.253			0.0150	±0.005	1.61			
50	0.9348	± 0.002	0.500	±0.005			1.44	1.62041	60.33	SK-16
51	- 11.9989	± 0.300	0.1490	±0.005			1.29	1.68893	31.18	SF-8
52	1.3461	± 0.006			0.7716	±0.005	1.02			
53										Eye Point

*n Refractive index measured at 5876 Angstrom units
** Dispersion

~~SECRET~~ SPECIAL HANDLING

~~SECRET~~ SPECIAL HANDLING

TABLE 2.1-1. OPTICAL PRESCRIPTION FOR ATS (Cont)

1 SURFACE NO.	2 RADIUS (INCHES)	3 RADIUS TOL. (INCHES)	4 THICKNESS (INCHES)	5 THICKNESS TOL. (INCHES)	6 AIR SPACE (INCHES)	7 AIR SPACE TOL. (INCHES)	8 CLEAR APRTR (INCHES)	9 n*	10 v**	11 GLASS TYPE AND MELT
1	40.1302	± 0.080	1.3544	+0.000 −0.005			10.00	1.62041	60.33	SK-16
2	− 18.4179	+ 0.005			0.2656	+0.002	9.98			
3	− 17.8183	± 0.005	0.6000	+0.000 −0.005			9.84	1.61340	44.30	KzFSN-4
4	273.6105	+ 3.000			28.8180	+0.030	9.73			
5	− 8.9940	+ 0.036	0.3613	+0.005			2.79	1.62041	60.33	SK-16
6	10.7028	+ 0.050			0.0200	+0.005	2.79			
7	7.6130	+ 0.026	0.2934	+0.005			2.80	1.62004	36.37	F-2
8	486.4318	±105.000			13.9069	±0.010	2.79			
9	∞				10.0873	±0.010	2.06			Aperture
10	− 5.4627	± 0.010	0.4468	+0.005			3.28	1.62041	60.33	SK-16
11	− 3.1057	± 0.003			0.1337	±0.005	3.35			
12	− 3.0157	± 0.003	0.4516	±0.005			3.32	1.62004	36.37	F-2
13	− 6.7970	± 0.013			0.0220	±0.005	3.55			
14	11.9795	± 0.038	0.5711	±0.005			3.63	1.62041	60.33	SK-16
15	− 18.5349	± 0.090			12.0696	±0.010	3.63			
16	∞		9.1391	Unfolded			2.22	1.51680	64.17	BK-7
17	∞				0.1017	±0.005	1.55			
18	2.2310	± 0.008	0.2391	±0.005			1.53	1.51680	64.17	BK-7
19	2.2002	± 0.008			0.7916	+0.005	1.46			
20	∞		0.200	±0.005			1.36	1.51680	64.17	BK-7
21	∞				0.3229	±0.005	1.37			Reticle
22	2.5493	± 0.011	0.3959	±0.005			1.39	1.62041	60.33	SK-16
23	− 1.8689	± 0.006			0.0837	±0.005	1.36			
24	− 1.3669	± 0.004	0.2310	+0.005			1.33	1.68893	31.18	SF-8
25	1.3808	± 0.004	0.4500	±0.005	0.2274	±0.005	1.35	1.62041	60.33	SK-16
26	− 2.2523	± 0.009			0.5215	{ High Mid Low	1.37			
27	2.9031	± 0.022	0.3200	±0.005	0.9993		1.09	1.51680	64.17	BK-7
28	− 1.4431	± 0.006			0.3750		1.05			

*n Refractive index measured at 5876 Angstrom units
** Dispersion

~~SECRET~~ SPECIAL HANDLING

9. Refractive Index measured at 5876 Angstroms

10. Dispersion

11. Glass Type

2.1.1.2 Optical Design – Low Power

The optical design of the telescope design at low magnification is shown in Figure 2.1-1. Optical elements 5 through 16 are part of a power change mechanism inserted into a basic telescope design to reduce the magnification and to increase the field of view. Optical elements 1 through 4 make up the objective lens assembly. Optical elements 20 through 52 are part of the eyepiece assembly. These parts will be described in more detail in paragraph 2.1.1.3.

2.1.1.3 Optical Design – High Power

The optical schematic of the telescope design at a magnification of 127 times is shown in Figure 2.1-2. Optical elements 5 through 15 have been removed to increase the magnification of the telescope. The optical element between surface 16 and 17 is the Pechan Prism used for image rotation. The optical element between surface 18 and 19 is a field flatner. The reticle is contained on surface 21 of an optical flat represented by surface 20 and 21. Optical elements between surface 22 to 46 are part of a zoom mechanism. The peripheral display will be located between surface 46 and surface 47.

2.1.1.4 Eyepiece Assembly

The eyepiece assembly consists of the following subassemblies:

a. Eyepiece

b. Peripheral Display

c. Filter Assembly

d. Zoom

e. Reticle

ZOOM RELAY & EYEPIECE
67-0075

PECHAN PRISM
(UNFOLDED)

22.8816 WITH UNFOLDED PRISM
16.1297 WITH FOLDED PRISM
16.00 ± 1.00 IS SPEC.

34.9512 WITH UNFOLDED PRISM
28.1993 WITH FOLDED PRISM
27.90 +2.00 IS SPEC.
     -0.00

POWER CHANGER 4:1
67-0064

APERTURE
STOP

94.2813 WITH UNFOLDED PRISM
85.5294 WITH FOLDED PRISM
85.64 ± 1.00 IS SPEC

OBJECTIVE LENS
67-015

ALL DIMENSIONS ARE IN INCHES
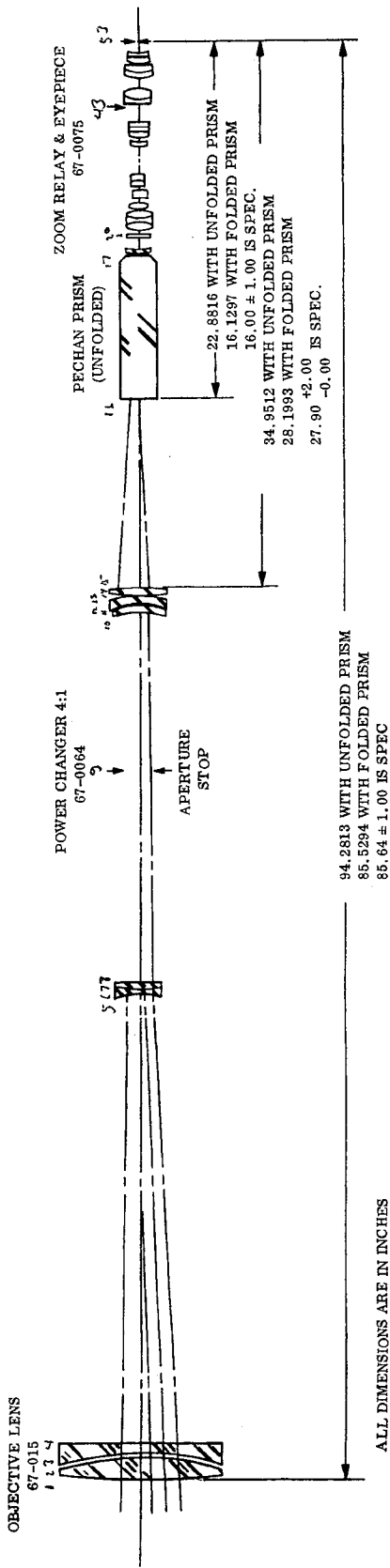
Figure 2.1-1. Optical Design –
Low Power
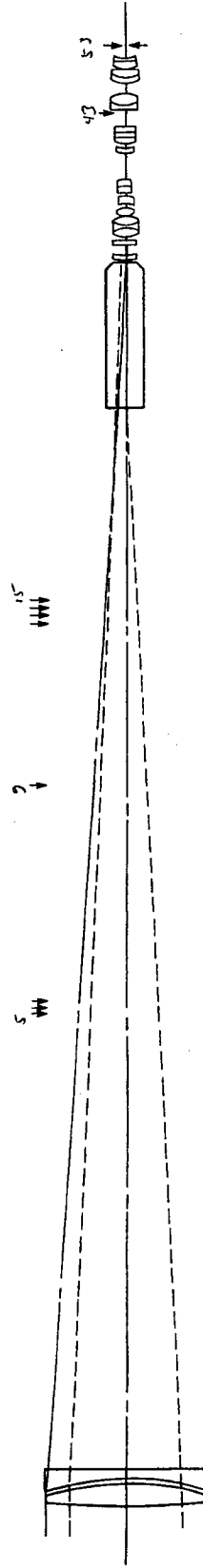
Figure 2.1-2. Optical Design –
High Power

In addition to supporting the optical elements, the eyepiece mechanical design must allow a focusing adjustment to be made. This adjustment is to compensate for the eye differences between various observers.

The eyepiece of the AO Telescope is specially designed to compensate for residual aberrations of the zoom relay assembly. Because of this, the alignment tolerances are considerably tighter than the standard eyepieces found in military instruments. These tighter tolerances impose a restraint on the design of the focusing mechanism.

The individual lenses are kept in optical alignment via accurate fabrication of the glass, tube bore and spacers. Decenter and tilt errors are kept small by manufacturing tolerances and can only be built up by the operational clearances between the tube and the outer housing. The final scheme will reflect the final allowable optical design tolerance on tilt and decenter.

Weight is minimized by using the smallest elements optically allowable thus producing a minimum eyepiece envelope. A weight reduction study on the eyepiece housing and tube will be performed as soon as final tolerances are established.

2.1.1.4.1 Peripheral Display

Another design restriction imposed upon the eyepiece focusing mechanism is the space required for incorporation of the peripheral display.

Three types of light sources for the peripheral display have been considered: solid state, electro-illuminance, and incandescent.

For any type of light source, it may be viewed directly or the light transmitted to the image plane by an optical means. While direct viewing is more efficient and possibly lighter weight, it does present packaging problems.

During the course of display evolution the pattern as seen in the apparent field has gone from two complete annular rings of possible sources to the present arrangement of three groups, each being a single row.

The lamps will be epoxied into recesses machined in the circuit board. Multi-colored lamps will be visible from the front side through clear viewing ports. The wiring side of the board will be epoxied over to provide both structural integrity and electrical protection.

The present approach using the printed circuit board is geared toward quickly getting a workable system to prove out the optical design problems through simulation. Full attention will be given to developing a minimum size, reliable, minimum weight system that will provide optimum display information while allowing minimum degradation of the optical system. It is intended that this approach be developed further through evaluations of such techniques as flexible printed circuits and complete encapsulation.

The design will minimize package size to allow for the - 2.5 to + 3.5 eyepiece dioptric adjustment. The optical design of the peripheral display will provide patterns visible in the eyepiece field of view while at the same time providing for minimal degradation of system performance. Optical design objectives include minimizing random reflections, minimizing obscuration of the apparent field of view, and minimizing the undesirable effects cuased by moving the eyepiece through its diopter range. The display luminosity level is yet to be determined. The display does not encroach upon the eyepiece field within ± 30 degrees of the in-track vector thus meeting the requirement of ± 27 degrees.

2.1.1.4.2 Filter Assembly

Various methods of inserting a filter into position on the optical axis were studied. One method evaluated has four individual filters mounted in arms that pivoted on a common shaft but were inserted into position separately. This design used at a minimum four to five filter thickness of space on the axis. As the optical design became firmer the space available

for filter insertion became smaller until only one filter and its mount could fit into position. This requirement led to the bar approach whereby all four filters in a rectangular plate were racked into and out of position. This scheme made for a large bulky envelope requirement. The wheel or disc filter was studied in order to minimize space. Compacting the filters as close together as possible led to the final filter design.

Several drive mechanisms for the filter wheel were studied and refined until a minimum space requirement was achieved.

The filter wheel drive mechanism consists of a single pass, 4 : 1 ratio gear drive. This system provides filter-to-filter indexing with only a 22-1/2 degree motion of the filter control knob. Total knob motion is 90 degrees. Sealed ball bearings are used to support the control knob shaft. A sector gear transmits knob motion to the pinion gear which also serves as a shaft bearing for the filter wheel. A stub shaft extending from the zoom housing supports and retains the filter wheel pinion gear assembly. The filter wheel is firmly positioned by a spring loaded roller into a local groove detenting on the wheel periphery. There are four grooves, one corresponding to each filter position.

The filter wheel design was limited by the spacer envelope remaining after adjacent glass elements were mounted in their respective positions. The most compact approach of mounting the lenses was used so as to provide maximum space for the filter wheel. Even so, the filter glass must be bonded into place because of lack of room for a retaining ring. However, optical tolerances on the filter glass are looser than on other elements; therefore bonding and staking the filter into place is satisfactory for all load conditions.

The filter wheel assembly, as now designed, permits the use of four selectable spectral or neutral density filters. Additional study is required before the characteristics of these filters can be specified. Based upon current knowledge of atmosphere haze, human eye response and chromatic characteristics of the AO Assembly, it is expected that two yellow

2-11

filters, plus one neutral density filter will be specified, plus a clear optical window in the fourth filter slot. The two yellow filters will be a deep yellow filter for very hazy viewing conditions and a light yellow filter for normal viewing. The neutral density filter will permit more comfortable viewing of very bright scenes; and the clear window may be used for viewing targets at night and for viewing poorly illuminated targets (e.g. high latitude targets).

2.1.1.4.3 Zoom

The optical design tradeoffs between mechanically compensated zoom configurations are discussed in this section.

The three major zoom types are:

a. Mechanical Compensation - Two or more lens groups move with respect to the focal plane and each other.

b. Linear Compensation - A mechanically compensated lens with the added restriction that the motions of the moving groups are linearly related.

c. Optical Compensation - A linearly compensated lens with the added restriction that the moving groups move as a unit with one stationary group between each pair of moving groups.

Optically compensated zooms are a small subset of mechanically compensated zoom lenses. They are used based on mechanical considerations, provided satisfactory optical performance can be achieved. The mechanical tradeoff is not straight forward. In the mechanically compensated AO Zoom, only two groups move with no stationary elements in between. In optically compensated zooms, two or more groups move with mechanical means required to keep a lens group stationary, between each pair of moving groups. In addition, the defocusing as a function of zoom position is exactly zero for mechanically compensated zoom lenses but a non-zero value for optically compensated zoom lenses, reaching a small value as the number of moving groups is increased.

The practical question arises of whether two conjugate pairs (in this case the objective image pair and the entrance/exit pupil pair) can be kept stationary in an optically compensated zoom. This has been shown to be possible paraxially by Silvertooth (Wooters and Silvertooth, Josa 55, 347-1965) and is thus clearly achievable with mechanically compensated zooms. However, the ability to control the real exit pupil position to ±0.02 inch over a 2 : 1 zoom range and 60-degree apparent field is not as easily proven and in fact is a property of the higher order aspects of the design. No optically or mechanically compensated zoom in the open literature has been found with these properties. For this and other reasons, the AO Telescope zoom was designed to achieve these specifications without the added restriction of optical compensation. The resulting zoom relay eyepiece has less than 0.2 wave spherical aberration and chromatic aberration throughout the zoom range on axis. The variations of field aberrations with zoom position is very small and the actual field correction is limited by the eyepiece portion rather than the zoom portion of the system.

2.1.1.4.4 Reticle

A single circle reticle which indicates the real field of view at maximum zoom position is provided. The reticle includes cross hairs for centering.

The reticle material has been selected as BK-7 glass with a clear aperture of 1.36 inches and is 0.200 inch thick. The reticle pattern described above will be deposited on the glass by a method yet to be determined.

Prime consideration has been given to the reticle mounting requirements because of the need for adjustment to set focus and because of the critical cleanliness problems associated with reticles. The reticle is mounted as an integral part of the zoom lens assembly. This allows us to fix the position of the reticle at the front focal point of the zoom lens while still isolating it from the mechanism, thus maintaining its tilt and decenter requirements.

The compensating adjustments, at assembly, are accomplished by shimming the entire zoom reticle assembly at the field break behind the Pechan Prism, after the reticle zoom relationship is established.

~~SECRET~~ **SPECIAL HANDLING**

To control the cleanliness of the reticle surface the optical design has been modified to place the reticle surface inside the zoom lens (i. e. , second surface of the reticle lens). If the telescope tube is separated at this field break the critical surface will not be contaminated or damaged.

2-14

~~SECRET~~ **SPECIAL HANDLING**

2.1.2 ANALYSIS OF PROPOSED ATS OPTICAL DESIGN

2.1.2.1 Introduction

In the analysis that follows, the static physical frequency response of the ATS optical design has been computed. Physical frequency response curves have been generated at six magnification powers for the proposed design subject to manufacturing tolerance and for the nominal (pristine) design. The resolution generated for the design subject to manufacturing tolerance represents a realistic performance level while the resolution level of the nominal design is over-optimistic since every manufacturing and alignment tolerance is zero. The estimate achievable ground resolutions have been obtained by superimposing the Schade Visual Resolution Threshold curve on the physical frequency response curves and determining the points of intersection.

The effect of element curvature and air space/glass thickness on total system performance was also investigated. To accomplish this, the partial derivative of the total system performance relative to each curvature and air space/glass thickness was determined. These partial derivatives, given the same sensitivity coefficients, revealed that the first two elements of the objective have a more significant relative effect on the total system performance than the relative effect of the remaining elements combined.

The following conditions were used in the analysis:

a. Target Definition - A white bar, on a black background, separated by an equal distance from a similar bar.

b. Orbital Altitude - 80 nautical miles

c. Apparent Contrast - 2:1 at aperture

d. Illumination at target - 530 foot lamberts

e. Vibration Level - Static

~~SECRET~~ **SPECIAL HANDLING**

2.1.2.2 Conclusions

a. The zero degree (in-axis) field physical frequency response of the optical pre-
    scription computed for the high power 127X indicates a ground resolution capa-
    bility of 2.4 feet. The value determined from Itek data is 2.8 feet. Both values,
    although considerably better than the 3.3-feet requirement, are very optimistic
    since manufacturing tolerances have not been considered.

b. The estimated worst case achievable ground resolution, determined by applying
    a tolerance budget to the nominal design prescription is 3.4 feet. The value sub-
    mitted by Itek is 3.3 feet. The static requirement is 3.3 feet. The GE estimate
    is the worst case resolution found after applying eight different tolerance budgets.
    Six of the eight tolerance budgets resulted in an estimated ground resolution of
    2.7 feet or better.

c. A level of confidence that the proposed design can be improved upon if tolerance
    budgets bring the system performance below an acceptable level has been estab-
    lished. Of eight different tolerance budgets applied five immediately resulted in
    an acceptable performance level; three did not. A further analysis demonstrated
    that the performance level of the three could be significantly improved by tweak-
    ing the doublet airspace and applying an appropriate reticle refocusing.

d. The analysis demonstrated that the doublet is the most sensitive portion of the de-
    sign. Assigned manufacturing tolerances to the doublet have a more significant
    effect on total performance than the effect of manufacturing tolerances assigned
    over the remainder of the design. This result has been predicted by the sensitivity
    coefficients which had the doublet account for 89.64% of the total sensitivity co-
    efficients.

e. The analysis demonstrated that assigned manufacturing tolerances to the doublet
    radii of curvatures which alternate in sign have a significant degrading effect on
    ground resolution. Such tolerances even after a doublet airspace adjustment is
    made, result in the worst case estimated ground resolution of 3.4 feet. Toler-
    ances in the doublet radii of curvature which are of one sign also have a degrading
    but less significant effect to the resolution capabilities. Such tolerances, when
    accompanied by a doublet airspace adjustment, result in an estimated 2.7 feet.

f. The analysis demonstrated that the resolution is considerably degraded as the
    apparent field is transversed from 0° to 30°. For the high power design – 127X,
    the estimated achievable ground resolution at 0° is 3.4 feet; at 10° it is 5.5 feet;
    at 21° it is 8.4 feet; at 27° it is 8.8; and at 30° it is 9.3 feet. A resolution degra-
    dation across the field for the other zoom powers is also apparent. For the lower
    power design – 15.88X, the estimated achievable ground resolution at 0° is 18.8
    feet; at 10° it is 35.0 feet; at 21° it is 171.9 feet; at 27° it is 244.8 feet; at 30° it
    is 266.1 feet. (Note: The system resolution figure for off axis performance are

the result of very preliminary General Electric analysis and have neither been substantiated or disproved by Subcontractor analyses. Off-axis performance is an area where additional analysis is required to predict system capability).

2.1.2.3 Recommendations

a. Manufacturing tolerances of the doublet radii of curvatures should be reassigned to values which do not alternate in sign. Two alternate procedures would be to either minimize the tolerances or fabricate duplicate elements which could then be subject to selection.

b. The use of a triplet design in place of a doublet design should be re-evaluated to determine if the sensitivity coefficients of the objectives lens can be reduced. Itek has completed an optical prescription using a triplet objective lens, but discarded this design based on weight considerations when the doublet objective lens met performance requirements. The triplet objective lens weighs 2 to 3 pounds more than the doublet design; however, the use of a triplet design may result in a total system weight saving by reducing environmental control requirements in the area of the objective lens. The use of a triplet design will also permit a further reduction in chromatic aberration and may result in improved ground resolution better than 3.4 feet.

2.1.2.4 Discussion of Results

The primary objective of this analysis was to determine if the proposed design can meet or surpass the specified performance level and if so, with what level of confidence. To carry out this result the physical frequency response of the nominal design was determined, the level of confidence of the design was investigated, a realistic performance estimate was established and the effect of tolerances was determined.

A. Nominal Design Capabilities - The physical frequency response of the nominal prescription was computed for six magnification powers. This was done for the on-axis - 0° field since the specified CEI requirements are given in terms of on-axis resolution. The response curves generated are given in Figures 2.1-3 to 2.1-8. Also included in each figure is the corresponding Itek supplied curve and the Schade Visual Resolution Threshold

~~SECRET~~ **SPECIAL HANDLING**
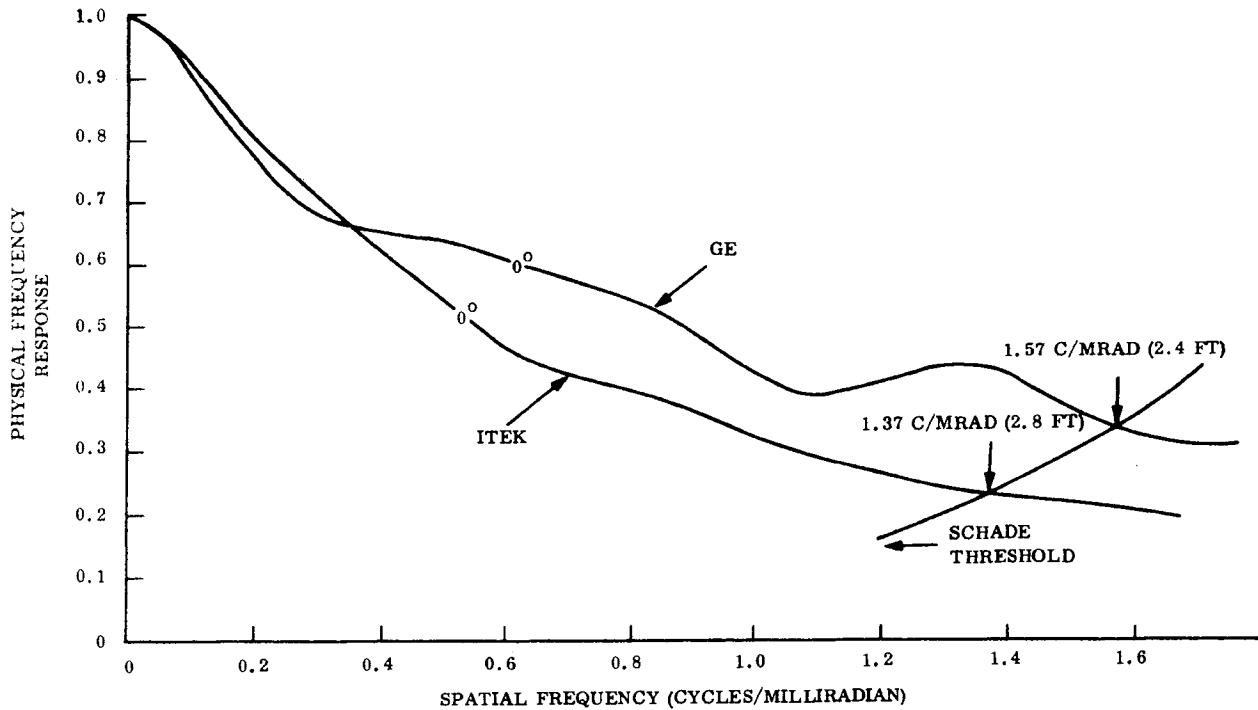
Figure 2.1-3. Nominal Design – Physical
Frequency Response – 127X
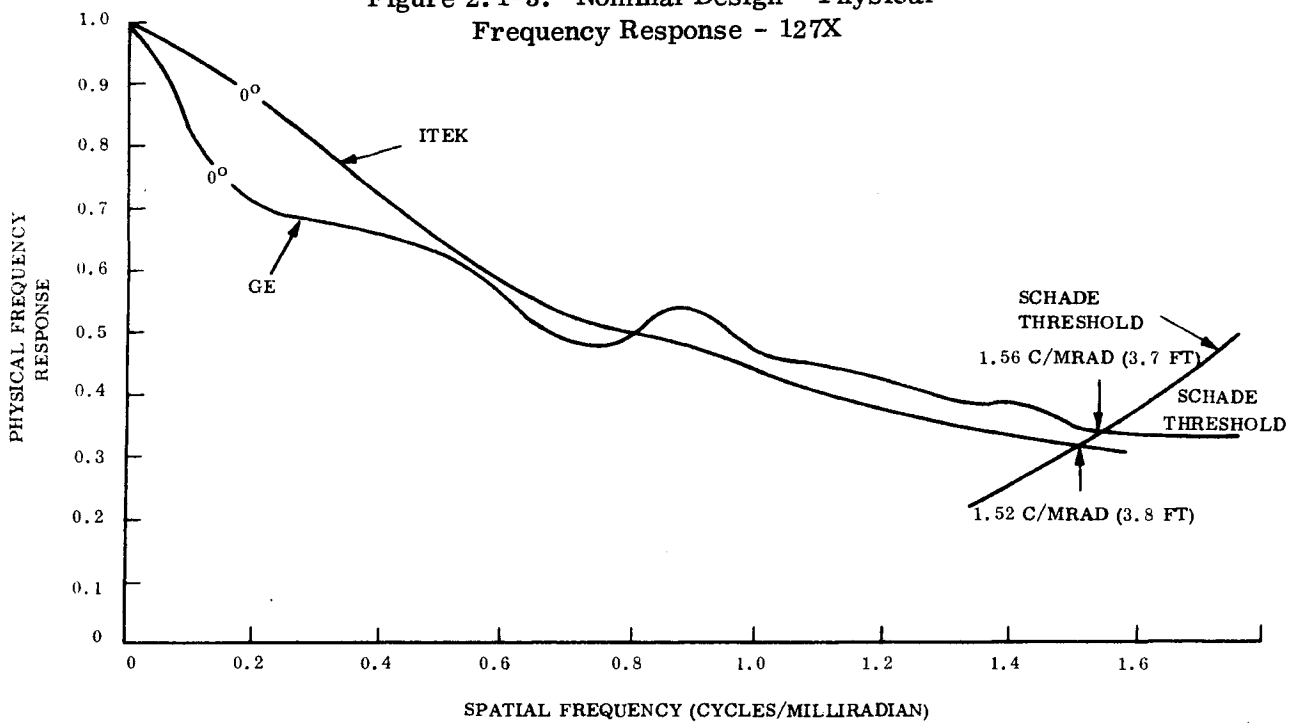
Figure 2.1-4. Nominal Design – Physical
Frequency Response – 84.67X

2-18

~~SECRET~~ **SPECIAL HANDLING**

~~SECRET~~ **SPECIAL HANDLING**
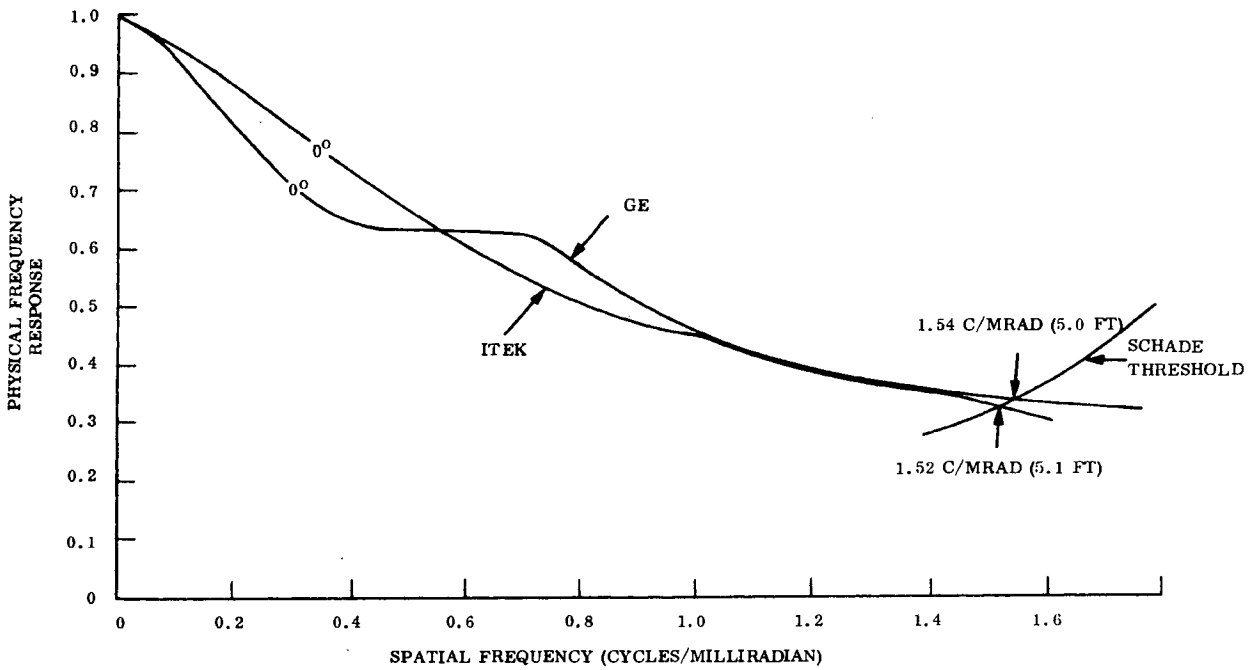
Figure 2.1-5. Nominal Design – Physical
Frequency Response – 63.5X
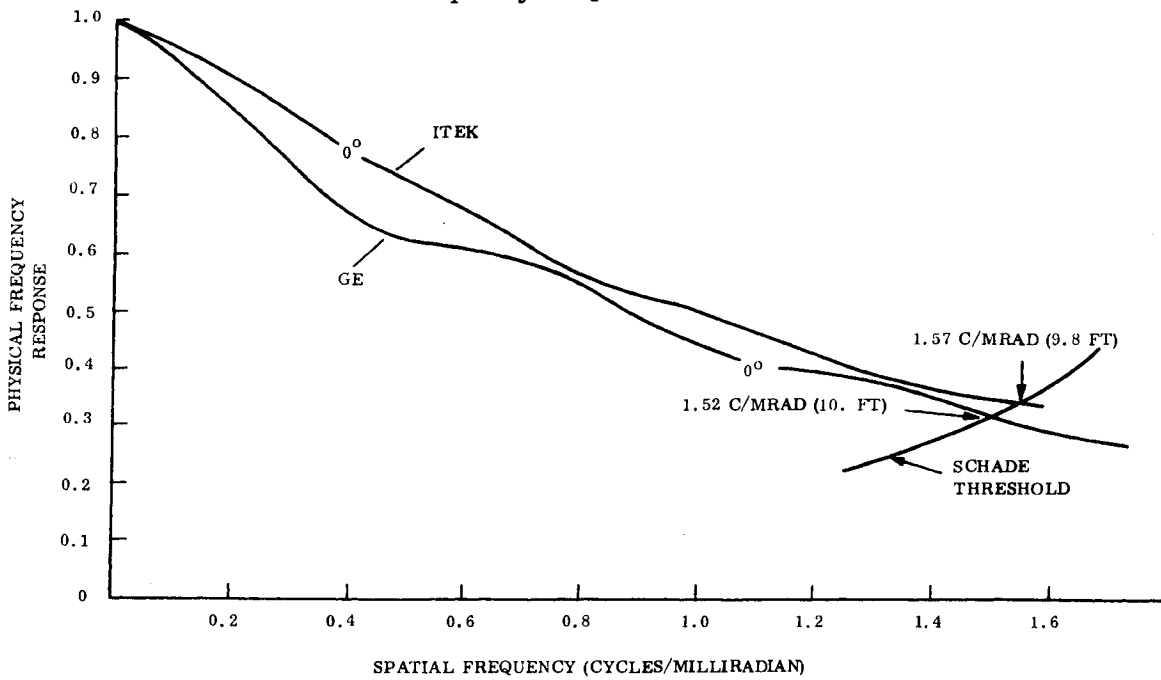
Figure 2.1-6. Nominal Design – Physical
Frequency Responses – 31.75X

~~SECRET~~ **SPECIAL HANDLING**

~~SECRET~~ **SPECIAL HANDLING**
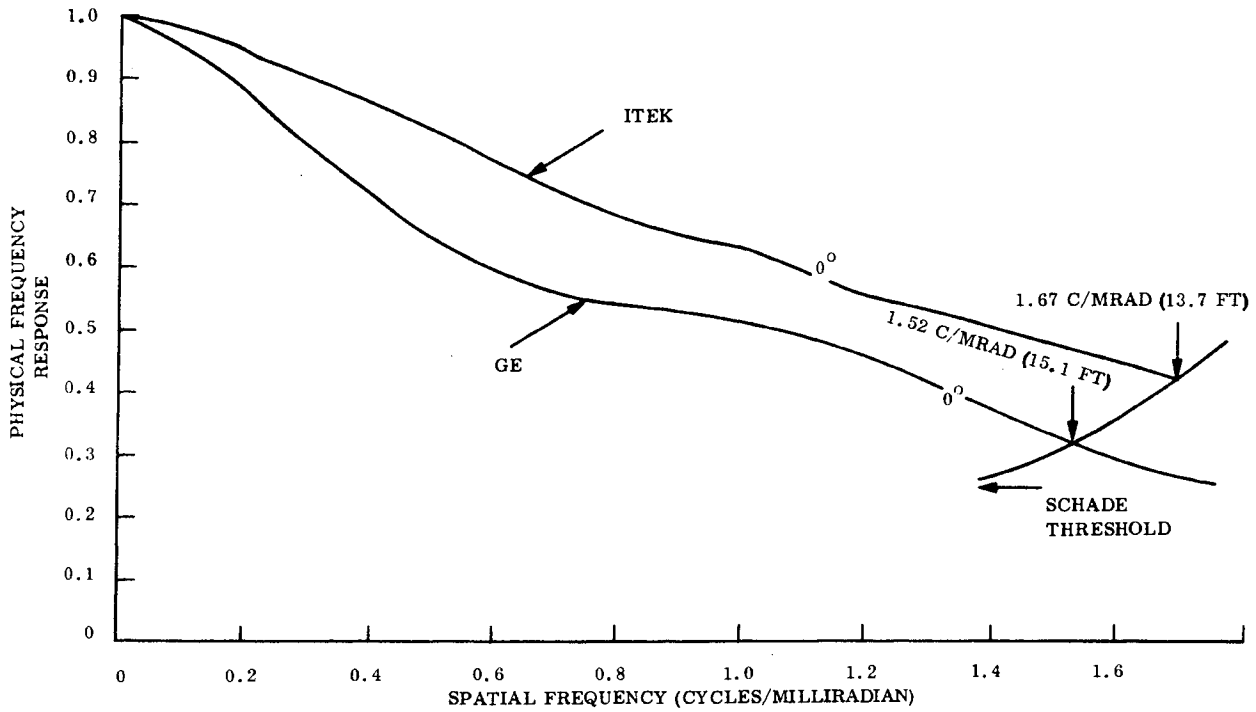
Figure 2.1-7. Nominal Design - Physical
Frequency Response - 21.17X
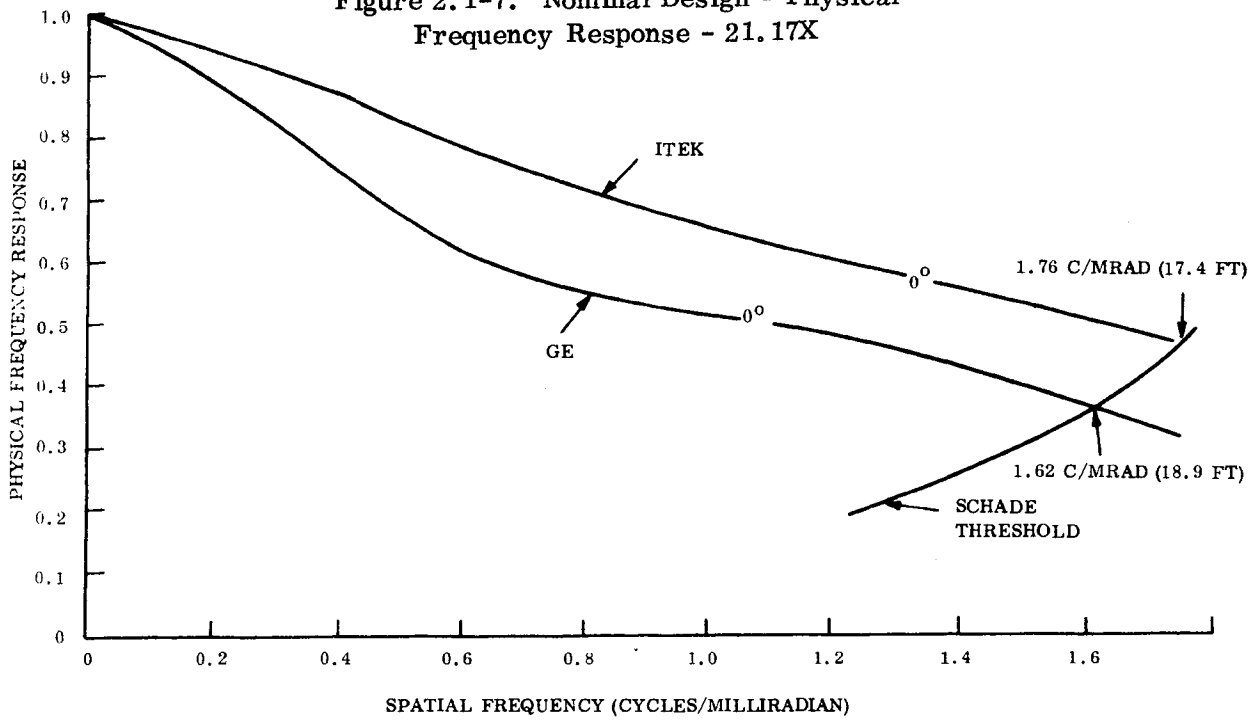
Figure 2.1-8. Nominal Design - Physical
Frequency Response - 15.88X

2-20

~~SECRET~~ **SPECIAL HANDLING**

Curve. The intersections of the physical frequency response curves and the Threshold curve are denoted by an arrow with the frequency of intersection and the corresponding ground resolved distance written above.

In general, the GE computed curve and the Itek Curve are in good agreement. Any differences between the curves may have resulted from the fact that Itek used nine spectral wavelengths to compute their curves while the computer program used to generate the GE Curves is capable of incorporating only three spectral wavelengths.

At the high power design - 127X, the GE curve indicates a theoretical ground resolution of 2.4 feet and the Itek curve indicates a theoretical ground resolution of 2.8 feet. Both are better than the static requirement of 3.3 feet. However, they are overoptimistic, since manufacturing tolerances have not been considered in the computations. (Unless otherwise specified, system performance curves have been calculated by tracing 75 rays through the system. An explanation of the computation techniques is included in Section 2.1.4.)

B. <u>Design Level of Confidence</u> - After the nominal prescription performance as a function of magnification was established, the level of confidence of the design was investigated. The purpose of this level of confidence investigation was to determine if tolerance budgets would bring the system performance below an acceptable level. If so, could anything be done to improve the performance level?

In this section each computation was made for the 127 power at 0° field. The manufacturing tolerance budgets specified in Table 2.1-2 were applied to the doublet, zoom relay, eyepiece, and over the complete design. In each case, the physical frequency response of the high power 127X system was computed. The curves are plotted in Figures 2.1-9 through 2.1-13. In Figure 2.1-9, curve 1 is the system physical frequency response when case "e" tolerances are given to the zoom relay; curve 2, the response when case "f"

2-21

~~SECRET~~ **SPECIAL HANDLING**

TABLE 2.1-2. TOLERANCE BUDGETS

TYPE AND NUMBER	a	b	c	d	e	f	a_T	d_T
R1	+0.08	−0.08	+0.08	−0.08			+0.08	−0.08
T1	0	−0.005	−0.005	−0.005			0	−0.005
R2	−0.005	+0.005	+0.005	−0.005			−0.005	−0.005
T2	−0.002	+0.002	+0.002	+0.002			−0.002	+0.002
R3	+0.005	−0.005	+0.005	−0.005			+0.005	−0.005
T3	0	−0.005	−0.005	−0.005			0	−0.005
R4	−3.00	+3.00	+3.00	−3.00			−3.00	−3.00
T4	−0.03	+0.03	+0.03	+0.03			−0.03	+0.03
R16								
T16	NOMINAL DESIGN	NOMINAL DESIGN	NOMINAL DESIGN	NOMINAL DESIGN	NOMINAL DESIGN	NOMINAL DESIGN		
R17								
T17								
R18							−0.008	−0.008
T18							−0.005	−0.005
R19							−0.008	−0.008
T19							−0.005	−0.005
R20								
T20							e TOLERANCES	e TOLERANCES
R21								
T21								
R22					−0.011			
T22					−0.005			
R23					−0.006			
T23					−0.005			
R24					−0.004			
T24					−0.005			
R25					−0.004			
T25					−0.005			

~~SECRET~~ **SPECIAL HANDLING**

~~SECRET~~ SPECIAL HANDLING

TABLE 2.1-2. TOLERANCE BUDGETS (CONT)

TYPE AND NUMBER	a	b	c	d	e	f	a_T	d_T
R26					-0.009			
T26					-0.005			
R27					-0.022			
T27					-0.005			
R28					-0.006			
T28					-0.005			
R29					-0.002			
T29					-0.005			
R30					-0.005			
T30					-0.005			
R31	NOMINAL DESIGN	NOMINAL DESIGN	NOMINAL DESIGN	NOMINAL DESIGN	-0.015	NOMINAL DESIGN	e TOLERANCES	e TOLERANCES
T31					-0.005			
R32					-0.003			
T32					-0.005			
R33					-0.003			
T33					-0.005			
R34					-0.041			
T34					-0.005			
R35					-0.009			
T35					-0.005			
R36					-0.004			
T36					-0.005			
R37					-0.004			
T37					-0.005			
R38					-0.069			
T38					-0.005			
R39								
T39					-0.005			

2-23

~~SECRET~~ SPECIAL HANDLING

~~SECRET~~ **SPECIAL HANDLING**

TABLE 2.1-2. TOLERANCE BUDGETS (CONT)

TYPE AND NUMBER	a	b	c	d	e	f	a_T	d_T
R40								
T40					-0.005			
R41					-0.009			
T41					-0.005			
R42					-0.035			
T42								
R43								
T43								
R44						-0.084		
T44	NOMINAL DESIGN	NOMINAL DESIGN	NOMINAL DESIGN	NOMINAL DESIGN	NOMINAL DESIGN	-0.005	f TOLERANCES	f TOLERANCES
R45						-0.002		
T45						-0.005		
R46						-0.004		
T46						-0.005		
R47						-0.006		
T47						-0.005		
R48						-0.002		
T48						-0.005		
R49						-1.253		
T49						-0.005		
R50						-0.002		
T50						-0.005		
R51						-0.300		
T51						-0.005		
R52						-0.006		
T52								

~~SECRET~~ **SPECIAL HANDLING**

~~SECRET~~ SPECIAL HANDLING
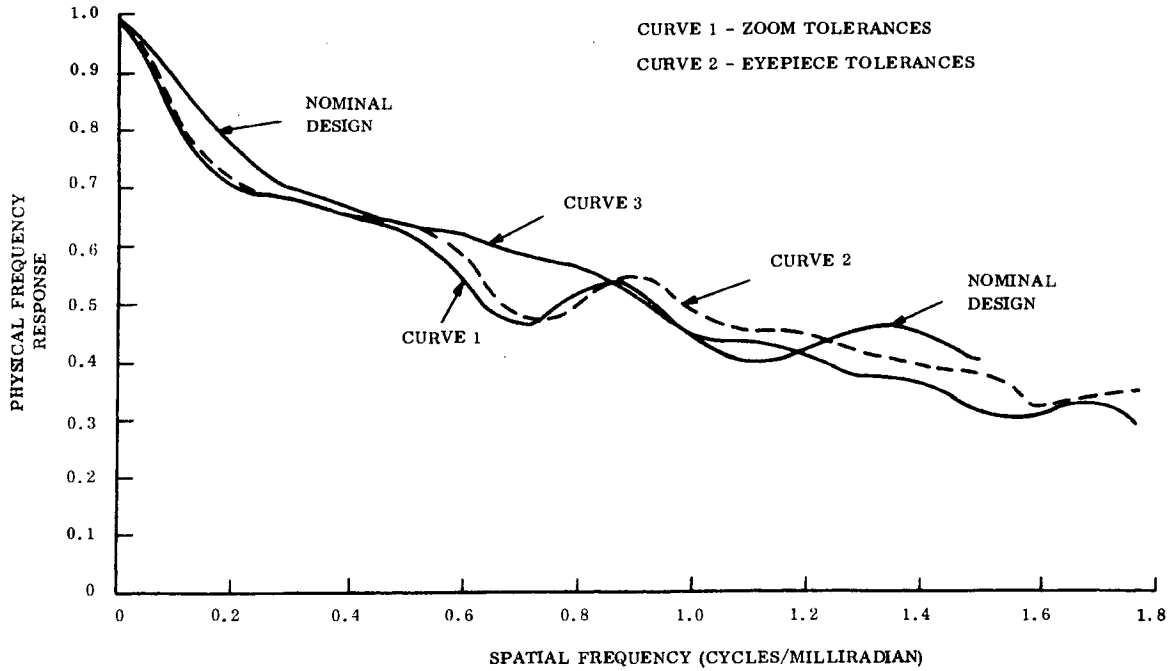
Figure 2.1-9. Physical Frequency Response - 127X
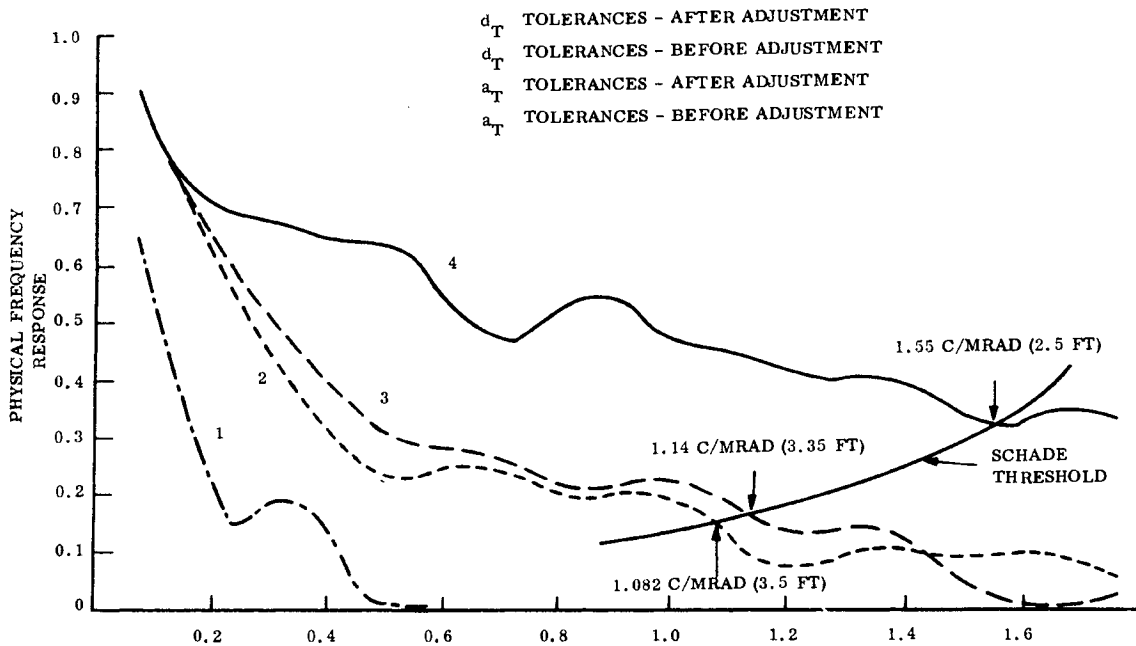
Figure 2.1-10. Physical Frequency Response - 127X

2-25

~~SECRET~~ SPECIAL HANDLING

~~SECRET~~ **SPECIAL HANDLING**
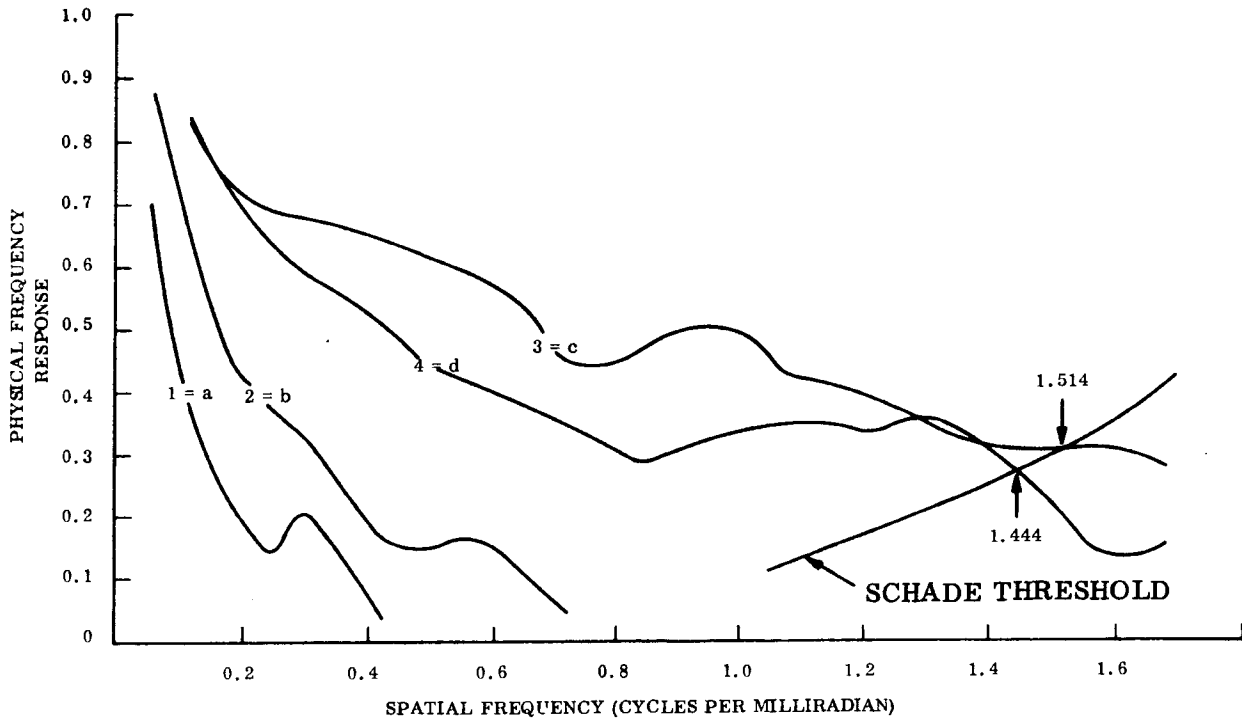
Figure 2.1-11. Comparison of a, b, c, d Tolerance
Budget-Physical Frequency Response-127X
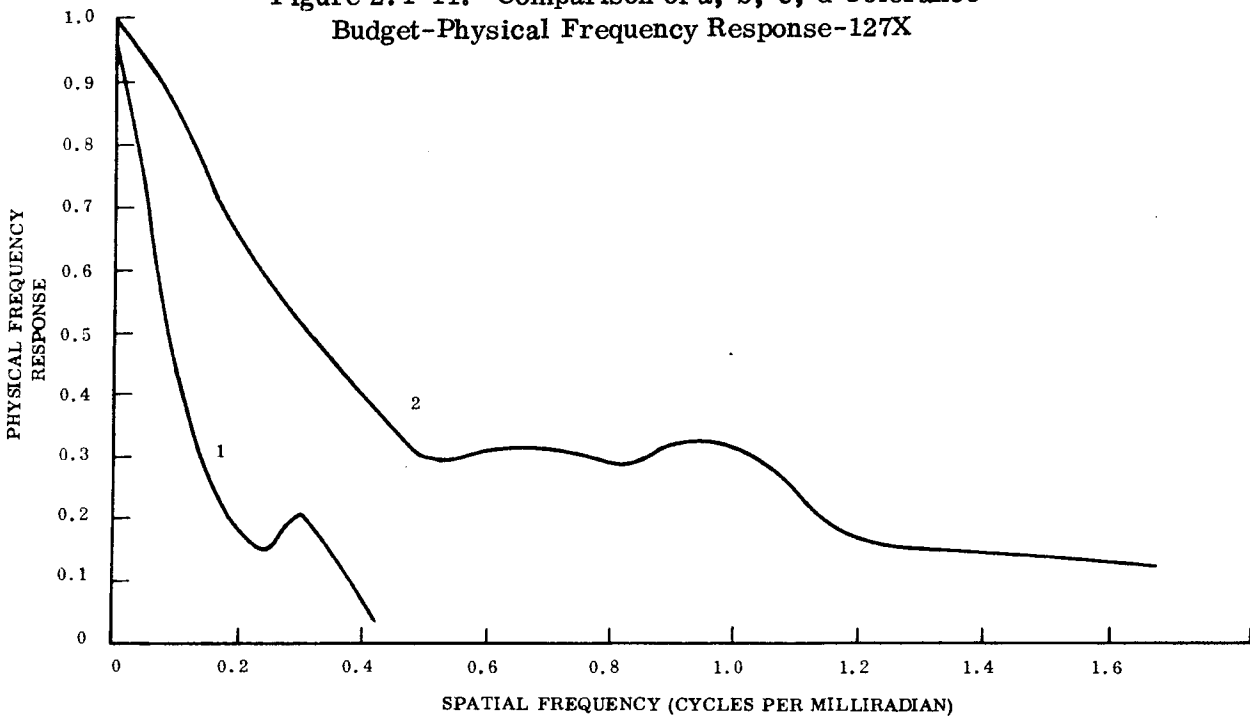
Figure 2.1-12. Effect of Tolerance Budget a
Before and After Adjustment-127X

~~SECRET~~ **SPECIAL HANDLING**
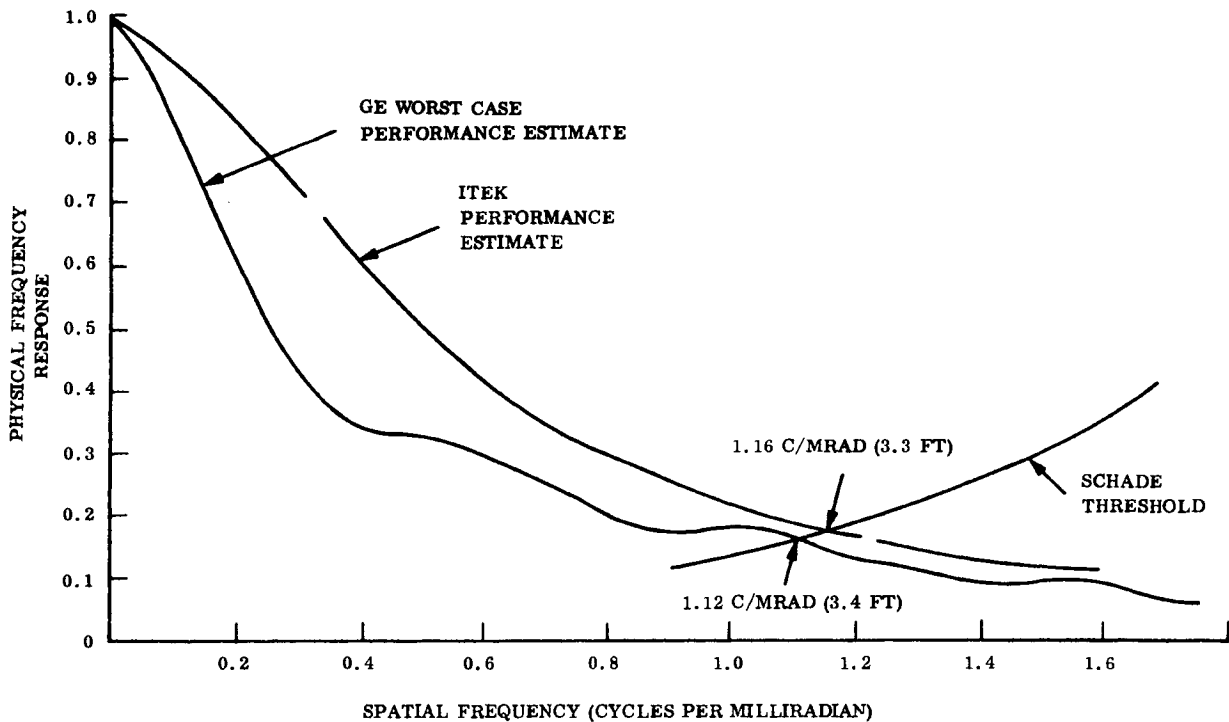
Figure 2.1-13. Comparison of Performance
Estimate - Zero Degree Field 127X

tolerances are given to the eyepiece; curve 3, the response of the prescription design. In-cluded in this figure is the threshold curve. For an estimated ground resolution of 3.3 feet, the physical frequency response curve and the threshold curve must interset at 1,160 cycles/radian. Each case intersects at a frequency better than the limiting frequency, 1,160 cycles/radian. By inspection, it is apparent that the zoom relay or eyepiece tolerances have little effect on the physical frequency response.

Figure 2.1-10 contains the physical frequency responses generated for two different toler-ance budgets distributed over the complete design before an element adjustment is made (curves 1 and 3). These responses are significantely improved by applying an adjustment to the doublet airspace (curves 2 and 4). The fact that the performance level was significantly improved by an element adjustment increases the level of confidence of the design.

The level of confidence was further investigated by applying tolerances only to the doublet. Four combinations of doublet tolerances were formulated and added to the nominal design.

The physical frequency response curve was computed for each combination. (A more detailed account of this treatment is given in Section 2.1.4.4 of the analysis). The results are given in Figure 2.1-11 along with the threshold curve. Curves 1 and 2 indicate a degraded performance while 3 and 4 prove acceptable. An element adjustment was given to case "a". The response was vastly improved. The improved response is shown compared to the original response in Figure 2.1-12.

From this discussion, it is apparent that for each tolerance grouping applied, the system performance either immediately surpassed the minimum required or was significantly improved to an acceptable level by an element adjustment.

C. Performance Estimate and Estimated Ground Resolution - To arrive at a realistic performance estimate, tolerance budgets were applied to the nominal design. A performance estimate, to be realistic, would have to be generated by distributing tolerances over the complete design. The physical frequency response curve selected would then have to represent a worst case level, and yet be generated after an element adjustment is made to simulate a worst case in the laboratory. Such a worst case tolerance performance estimate is represented by curve 1, of Figure 2.1-13. This curve was calculated by tracing 750 rays through the system to obtain a more accurate prediction of system performance. Comparing this curve to the Itek performance estimate curve (curve 2), curve 1 runs about 30% lower than the Itek curve at the lower frequencies; however, the curves tend to approach each other in the frequency range 1000-1200 cycles/radian. The Itek curve intersects at 1,160 cycles/radian, which results in an estimated achievable ground resolution of 3.3 feet. The GE performance estimate curve intersects at 1,082 cycles/radian, which results in an estimated achievable ground resolution of 3.4 feet. The difference in the curves can not be explained since the Itek tolerance budget was not available. The tolerance budget used to generate the GE worst-case performance estimate curve has then been used to compute the

0° field physical frequency response performance estimates for each zoom power. Further-more, with the same tolerance budget applied, it was then possible to compute the off-axis resolutions as well, and be confident that they correspond to a realistic performance level. The off-axis physical frequency response curves for each zoom power was thus computed. The generated curves are given in Figures 2.1-14 through 2.1-19. Included in these figures is the Itek-supplied 127X Performance estimate curve, which is for on-axis only, and the Schade Visual Resolution Threshold curve. All GE-calculated curves in these six figures were produced by tracing 75 rays through the system due to the large amount of computer computation time required to generate each curve using 750 rays. However, it is felt that the error introduced by using the smaller number of rays is quite small since the dif-ference in performance between the 750-ray case (Figure 2.1-13) and the 75-ray case (Figure 2.1-14) is only 0.1 foot.

The intersections of the physical frequency response curves and the Threshold curves are the frequencies from which the estimated achievable ground resolutions are obtained. Es-timated achievable ground resolutions at five points in the apparent field of view have been tabulated for each zoom power and is given in Table 2.1-3. The results show a significant resolution degradation that the viewer will experience as he transverses the field: 3.4 feet ground resolution at 0° compared to 9.3 feet at 30° for the 127 power (worst-case).

Another result demonstrated by the on-axis performance estimate curves is that the 127X curves are inferior to the curves obtained for the other magnifications. Thus, the 127 power should be used as the worst case power in the tolerance analysis.

~~SECRET~~ **SPECIAL HANDLING**

$k/4017$?

TABLE 2.1-3. TABULATION OF ESTIMATED WORST CASE
ACHIEVABLE GROUND RESOLUTIONS (FEET)

FIELD ANGLE	MAGNIFICATIONS					
	127X	84.67X	63.5X	31.75X	21.17X	15.88X
0°	3.5	4.74	5.7	11.5	15.3	18.8
10°	5.2	7.3	9.6	18.9	26.8	33.5
21°	7.8	7.6	41.4	18.6	104	185
27°	8.1	27.9	61.2	53.4	163	306
30°	8.5	54.0	69.5	72.9	201	340

D. Sensitivity Coefficients and Tolerances - The sensitivity coefficients indicate the relative effect of each curvature and airspace/glass thickness on total system performance. Parameters with larger sensitivity coefficients have a more pronounced effect on total system performance than those with smaller sensitivity coefficients.

The sensitivity coefficients obtained for the high-power case (127X) have been tabulated and are given in Table 2.1-4. These coefficients represented by an algebraic sign and magnitude were determined using the General Electric Auto-Spryte computer program.

In order to express the sensitivity in a numerical manner, the sensitivity coefficients were all added together and each sensitivity coefficient was expressed as a percentage of the total. These Relative sensitivity coefficients are also included in Table 2.1-4. In this table, surface number pertains to the surface place in the total collection of surfaces that comprise the design (i.e., Surfaces 1 through 4 comprise the four surfaces of the doublet). The letter "C" designates the sensitivity coefficient related to curvature (equal to reciprocal of radius of curvature). The letter "T" designates the sensitivity coefficients with respect to airspace or glass thickness, whichever applies.

~~SECRET~~ **SPECIAL HANDLING**
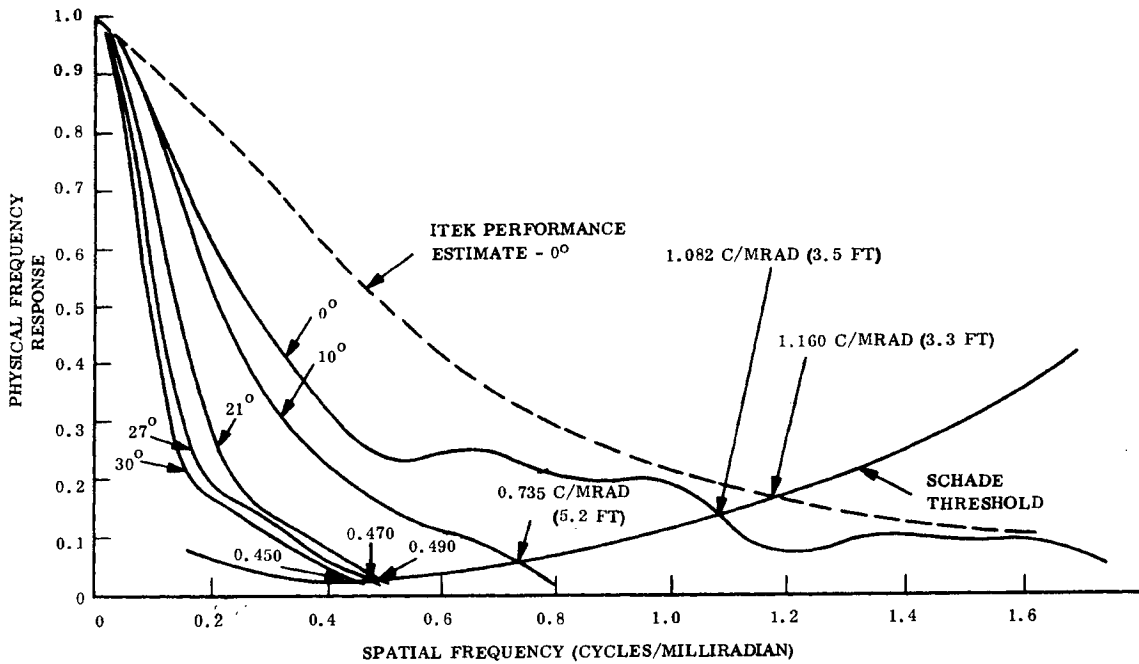
Figure 2.1-14. System Performance Estimates-127X
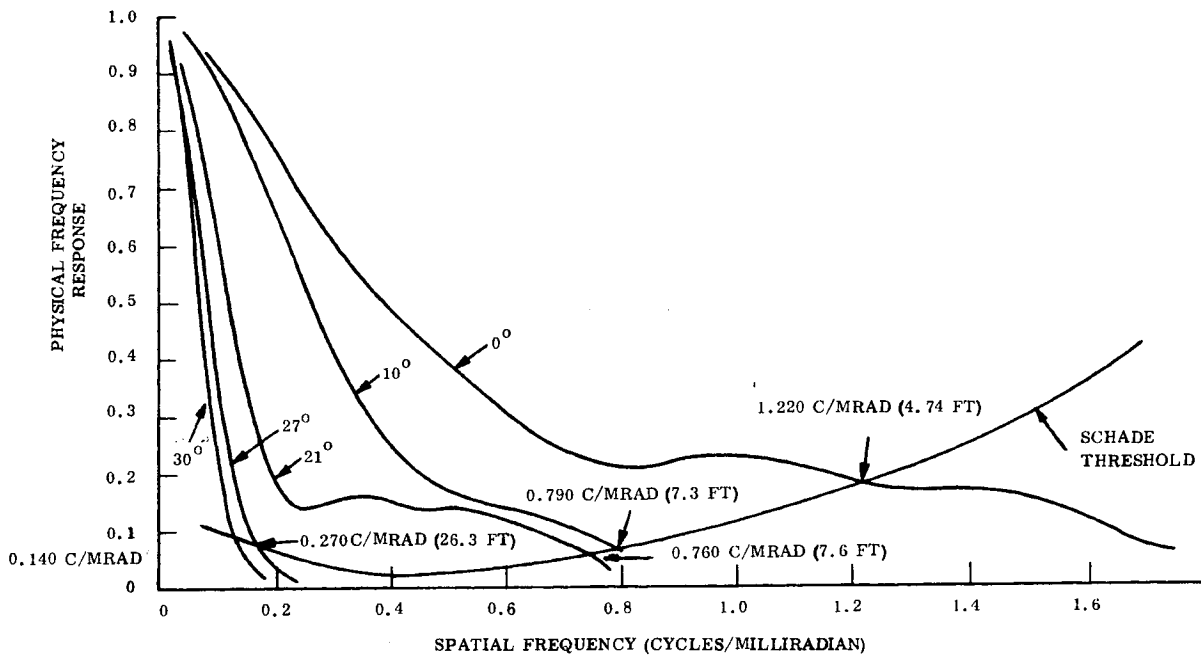
Figure 2.1-15. System Performance Estimates - 84.67X

2-31

~~SECRET~~ **SPECIAL HANDLING**
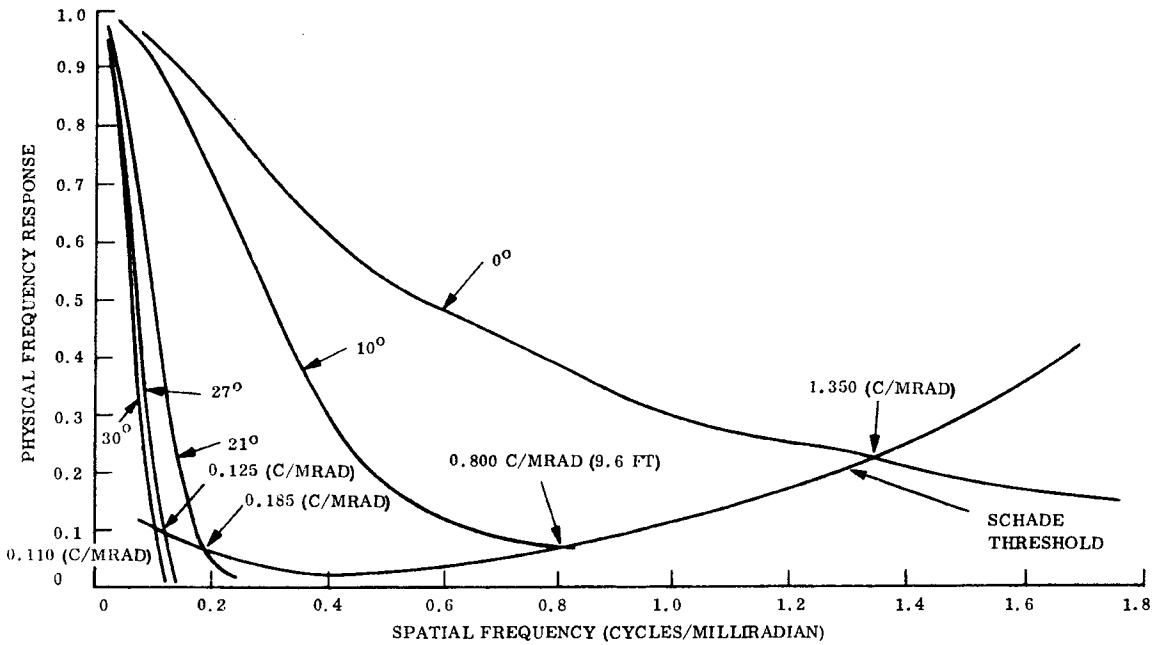
Figure 2.1-16. System Performance Estimates - 63.5X
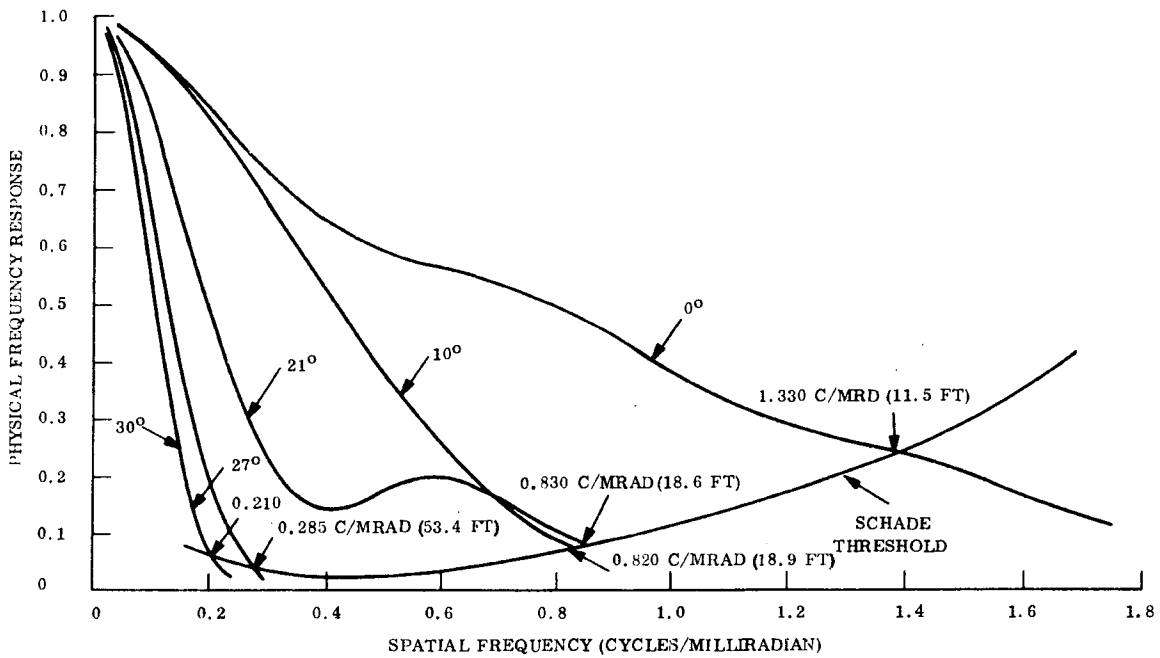
Figure 2.1-17. System Performance Estimates - 31.75X

~~SECRET~~ **SPECIAL HANDLING**
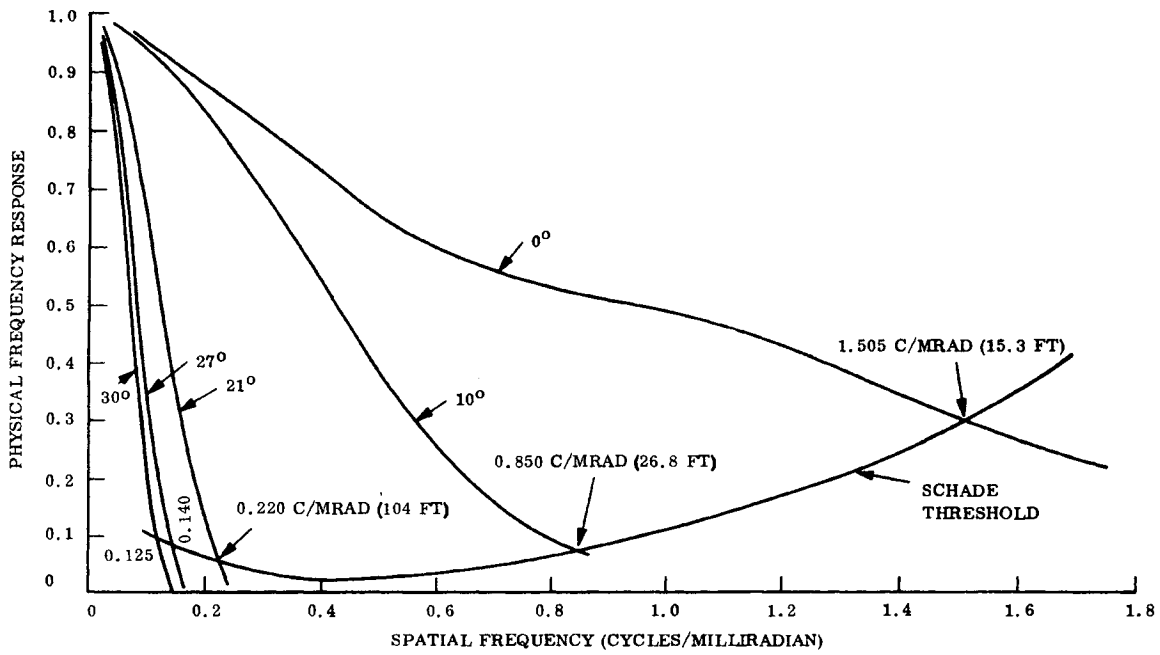
Figure 2.1-18. System Performance Estimates - 21.17X
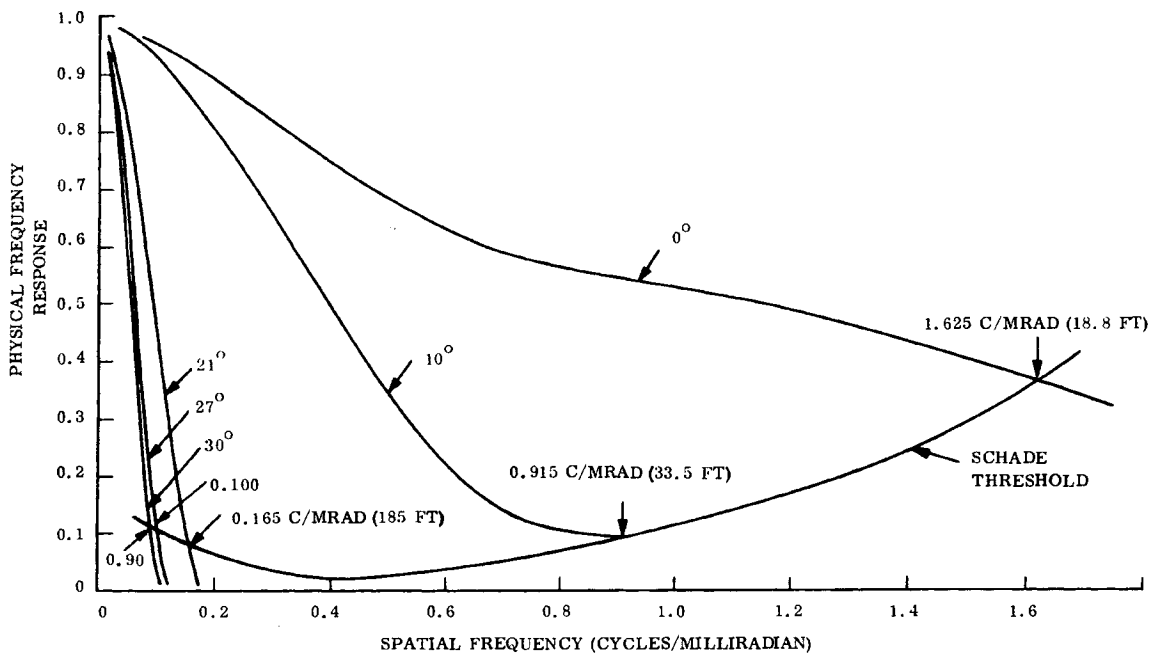
Figure 2.1-19. System Performance Estimates - 15.88X

2-33

~~SECRET~~ SPECIAL HANDLING

TABLE 2.1-4. ABSOLUTE AND RELATIVE SENSITIVITY COEFFICIENTS

SURFACE	ABSOLUTE	RELATIVE	SURFACE	ABSOLUTE	RELATIVE	SURFACE	ABSOLUTE	RELATIVE
1,C	-0.461489	0.18411	26,C	-0.007289	0.002908	40,C	-	--
1,T	-0.040055	0.015950	26,T	-0.001998	0.000797	40,T	0.002495	0.000995
2,C	-0.518593	0.206892	27,C	-0.006490	0.002589	41,C	0.002194	0.000875
2,T	-0.212488	0.084772	27,T	-0.001031	0.000411	41,T	0.002555	0.001019
3,C	-0.545727	0.217718	28,C	-0.007377	0.003182	42,C	-0.002615	0.001043
3,T	-0.038295	0.015278	28,T	-	-	42,T	0.002653	0.001058
4,C	-0.397200	0.158463	29,C	0.010264	0.004095	43,C	-	-
4,T	-0.033166	0.015232	29,T	-0.002962	0.001142	43,T	0.003221	0.001285
16,C	-	-	30,C	-0.011479	0.004580	44,C	0.007204	0.002874
16,T	-	-	30,T	-0.000244	0.000097	44,T	0.003696	0.001475
17,C	-	-	31,C	0.007790	0.003108	45,C	-0.004139	0.001651
17,T	-	-	31,T	0.000858	0.000342	45,T	0.006027	0.002404
18,C	-0.002499	0.000997	32,C	-0.009322	0.003799	46,C	-0.009110	0.003634
18,T	-0.003686	0.001471	32,T	-	-	46,T	-0.003203	0.001278
19,C	0.001572	0.000627	33,C	0.009853	0.003931	47,C	0.010930	0.004361
19,T	-0.002727	0.001128	33,T	-	-	47,T	0.00873	0.000348
20,C	-	-	34,C	0.008877	0.003541	48,C	-0.000908	0.000386
20,T	-0.002322	0.000926	34,T	0.000644	0.000257	48,T	-0.000318	0.000127
21,C	-	-	35,C	-0.002966	0.000824	49,C	-0.009112	0.003635
21,T	-0.002411	0.000962	35,T	0.002428	0.000985	49,T	0.000576	0.000230
22,C	0.004436	0.001790	36,C	0.001940	0.000774	50,C	0.012859	0.005130
22,T	-0.002249	0.000897	36,T	0.002874	0.001147	50,T	0.008373	0.003340
23,C	-0.005251	0.002095	37,C	0.003010	0.001201	51,C	0.001362	0.000543
23,T	-0.001290	0.000515	37,T	0.002255	0.000891	51,T	0.007016	0.002798
24,C	0.002217	0.002480	38,C	-0.002127	0.000849	52,C	-0.008217	0.003278
24,T	0.002667	0.001064	38,T	0.002463	0.000979	52,T	-	-
25,C	0.000791	0.000316	39,C	-	-			
25,T	0.002859	0.001141	39,T	0.002375	0.000948			

~~SECRET~~ SPECIAL HANDLING

The sensitivity coefficients with respect to curvature and airspace/glass thickness of the first four surfaces which comprise the doublet are overwhelmingly greater than the coefficients of the remaining surfaces. The relative sensitivity coefficient of the first four surfaces is 89.64 percent of the total. It can be stated that departures from nominal of these parameters affects total performance more significantly than the departures from nominal in the zoom relay or eyepiece.

This is apparent when the curves in Figure 2.1-9 are compared to the curves in Figure 2.1-11. The curves computed for tolerance budgets applied to the zoom relay and eyepiece (shown in Figure 2.1-9) run consistently better than the curves generated for doublet tolerance budgets shown in Figure 2.1-11. The percentage of the total sensitivity coefficients contained by the zoom relay is 5.96 percent. That of the eyepiece is 3.87 percent. That Case 3 is betten than Case 2 confirms the prediction of the sensitivity coefficients.

Since the doublet tolerances have such a strong bearing on the total performance, it is highly probable that a poor performance level of the adjusted system will be caused by misalignment, poor adjustment, or excessive manufacturing tolerance in the doublet portion of the design. Furthermore, any adjustment of the doublet elements will have to be accompanied by an appropriate shift of the reticle plane.

Another result is apparent when the on-axis performance estimate curves (shown in Figures 2.1-14 through 2.1-19) are compared to the physical frequency response of the nominal designs (shown in Figures 2.1-3 through 2.1-8). The high power magnifications (127X - 63.5X) curves show a considerable difference between the nominal design and the performance estimate curves, but in the low power magnifications (31.75X - 15.88X) the curves are in close agreement. In the analysis, it will be pointed out that the entrance pupil diameter of the high-power magnifications is 10.0 inches compared to 2.54 inches in the low-power magnifications. With more lens surface being used, tolerances are seen to have much greater effect on the system performance, as is expected.

2.1.2.5 Discussion of Analysis Techniques

A. Method of Determination of Physical Frequency Response – Image evaluation computer programs have been used to determine the physical frequency responses of the proposed design. The following procedure was taken to obtain the final curves:

B. Determination of Entrance Pupil and Relative Aperture (F/Number) – The entrance pupil is obtained by determining the limiting aperture of the design and finding the Gaussian image and magnification of this aperture formed by the elements which precede it. In the high-power mode, the limiting aperture is the first surface of the doublet. The entrance pupil thus coincides with this surface and has a radius of 5 inches. In the low-power mode, the aperture stop is surface 9. The image of this stop, formed by the forward elements, has a radius of 1.27 inches. This is, then, the entrance pupil radius for the low-power mode.

The relative aperture of the design is the effective focal length divided by the entrance pupil diameter. The effective focal length, which is the distance from the second principle plane of the objective grouping to the image at the reticle of an infinitely located point object, has been determined. Focal lengths are shown below with the corresponding relative apertures:

	Eff. Focal Length (Inches)	Relative Aperture
High Power (127X – 63.5X)	111.87	11.18
Low Power (31.75X – 15.88X)	28.00	11.0

C. Computation of Geometric Frequency Response – The IBM Program for Optical System Design has been used to compute the geometrical frequency response of the proposed design. In making the computations, a selected number of rays from a single object point at infinity

2-36

~~SECRET~~ **SPECIAL HANDLING**

are traced through the entire system and emerge through the exit pupil having close degree of parallelism. The total number of rays traced are divided into three portions, each portion for a selected wavelength of the visible spectrum. The number of rays in each wavelength portion is governed by the standard eye luminosity curve published in the MIL-141 Handbook[1]. In this way, the spectral distribution of the ATS optical system is given the eye spectral response. The wavelengths and number of rays in each portion is given in the table below:

Spectral Wavelength (Microns)	Number of Rays
0.56	57
0.47	12
0.65	6

The Program for Optical Systems Design (POSD) computes the geometrical frequency response by doing a computer analysis of the spot diagram traced from a point object. The computation technique is standard and is described in several up-to-date references[2]. The response at a given frequency is obtained from the summations:

$$A_C(\nu) = \frac{\sum_j A(x) \cos 2\pi \nu X_j \Delta X}{\sum_j A(x) \Delta x}$$

$$A_S(\nu) = \frac{\sum_j A(x) \sin 2\pi \nu X_j \Delta X}{\sum_j A(x) \Delta x}$$

[1]. "Handbook of Optical Design," MIL-HDBK-141.

[2]. Smith, "Modern Optical Engineering," McGraw Hill, 1966

2-37

Geometrical Frequency

$$\text{Response} = \sqrt{\left[A_C(\nu)\right]^2 + \left[A_S(\nu)\right]^2}$$

where:

ν =   Spatial frequency of the image

x_j = j^{th} coordinate of ray intercept in image plane.

$A(x)$ =   Line spread function in image space

The POSD computes the geometrical frequency response by performing the above summations over the spot diagram that is formed by tracing rays through the system from a point object.

Since the emerging rays of the proposed system are nearly parallel, a special technique pertaining to afocal systems was required to form a spot diagram. This was done without introducing any additional aberrations. Such a technique is described in the MIL-141[1] Handbook, paragraph 8.8.

Once the spot diagram is formed, the geometrical frequency response is computed by making the summations that have been written above. Off-axis as well as on-axis spot diagrams may be formed from which off-axis and on-axis geometrical frequency responses are obtained.

D. <u>Determination of Physical Frequency Response</u> - The POSD forms the spot diagram which is then analyzed using a ray trace that is governed by a strictly geomatrical theory. To account for diffraction effects, the geometrical response is multiplied by the physical response of a diffraction-limited optical system of the same relative aperture. This product tends to err toward the low side, thus resulting in a conservative or safe performance estimate.

2-38

The physical frequency response of diffraction-limited systems have been computed for the low-and high-power relative apertures of the design. This was done by using a computer to evaluate the physical frequency response expression:

$$\text{PFR } (\nu) \;=\; \frac{2}{\pi}(\wp - \cos \wp \sin \wp)(\cos \theta)^K$$

where:

ν = Spatial frequency

$\wp$ = $\cos^{-1}(\lambda \nu F^{\#})$

θ = half-field angle

λ = Spectral wavelength (taken to be the mean wavelength), 0.56 microns

k = 1 and $F^{\#}$ = relative aperture

The product of this evaluated expression and the geometrical frequency response has been obtained using computer methods on a frequency-by-frequency basis. The products are the physical frequency response which are shown plotted in the results section.

It should be pointed out that the diffraction effects result in a limiting frequency beyond which the system can not resolve. This limiting frequency is obtained by setting the physical frequency response (PFR) expression to zero:

$$\text{PFR } (\nu) \;=\frac{2}{\pi}(\wp - \cos \wp \sin \wp)(\cos \theta) \;=\; 0$$

The solution of this equation is

$$\wp \;=\; 0$$

~~SECRET~~ **SPECIAL HANDLING**

or

$$\varphi = \cos^{-1}(\lambda \nu oF\#)$$

This occurs when

$$\lambda \nu oF^{\#} = 1$$

or

$$\nu o = \frac{1}{\lambda F^{\#}}$$

Assuming λ to equal 0.22×10^{-4} inches and the $F^{\#}$ value taken for the high-power design 11.18, 4150 cycles/radian is then the cutoff spatial frequency.

E. Formation of Sensitivity Coefficients – Sensitivity coefficients are computed but usually stored internally by optical automatic design programs, such as the General Electric Auto-Spryte Program. In solving an automatic design problem, the program seeks to find a solution or something approaching a solution of an equation of the form.

$$F_k P_1, P_2, ----- P_j) = S_k$$

The P_1, P_2 ----- P_j are the j-designated variables of the system. In this case, they are the curvatures and air spaces/glass thickness of the system. The S_k is some designated target value, representing the desired system performance. $F_k(P_1, P_2, ----- P_j) = S_k$ says that the target value S_k is a function, F_k, of the system parameters, P_1, P_2 ----- P_j. To solve this equation, the program employs an iteration technique which, as a method of solution, computes the partial derivarives.

~~SECRET~~ **SPECIAL HANDLING**

$$\frac{\partial F_k}{\partial P_1}, \quad \frac{\partial F_k}{\partial P_2}, \quad ---- \quad \frac{\partial F_k}{\partial P_j}$$

These partial derivatives are the sensitivity coefficients.

For this determination, the target value was the slope angle at the exit pupil of the 30-degree chief ray. The chief ray was chosen since it is the mean ray of the bundle, and ideally the other emerging rays of the bundle should have an identical slope angle. The sensitivity coefficients resulting from this analysis were tabulated in Table 2.1-4.

F. Treatment of Manufacturing Tolerances - Manufacturing tolerances have been assigned by Itek as shown in Section 2.1.1.1. In assigning these tolerances, Itek has been careful to emphasize that the assigned tolerances are tentative, and that the problem of tolerances will be given more serious consideration prior to the critical design review. The resolution level obtained for nominal designs is, in general, overoptimistic since all the tolerances are zero and the elements are assumed to be perfectly aligned. The performance level obtained when manufacturing tolerances are included in a design is the realistic level and was the one used to determine the estimated ground resolutions reported in Section 2.1.2.4.C. The difficulty in making a tolerance analysis is knowing how to combine the tolerances to compute the physical frequency response. There is a multitude of combinations over the 53 surfaces of this design which are possible. What is required to simplify the problem is to determine if there is a grouping of elements in the design which most significantly affects the total system performance. If so, the emphasis of the analysis should be placed on them. It was pointed out in Section 2.1.2.4.D that the first four surfaces which comprise the doublet contain 89.64 percent of the relative sensitivity coefficients, compared to 5.96 percent contained by the zoom relay, and 3.87 percent contained by the eyepiece. This says that the effect of the doublet tolerances should be the most significant on the total system performance level. To substantiate this prediction, the total system physical frequency response of the high power 127K design was computed for the following three cases.

~~SECRET~~ **SPECIAL HANDLING**

a. Tolerance budgets a, b, c, d applied to the doublet portion of the design.

b. Tolerance budget "e" applied to the zoom relay portion of the design.

c. Tolerance budget "f" applied to the eyepiece.

In applying these tolerances, it became necessary to adjust the three focal distances in the design to obtain optimum imagery. The adjustments are given in the following table (refer to Table 2.1-1 for surface notation):

Tolerance Budget	Adjusted Airspace	New Value
a	AS-8	1.237
b	AS-8	0.354
c	AS-8	0.788
d	AS-8	0.701
e	AS-31	1.256
f	AS-32	0.216

The generated physical frequency responses are shown plotted in Figure 2.1-9 and Figure 2.1-11. A comparison of the curves demonstrates that doublet tolerances have a more significant degrading effect on system performance, as predicted by the sensitivity coefficients. It then follows that the performance level of the proposed design can be investigated with a high degree of confidence by applying the assigned manufacturing tolerance just to the doublet portion of the design. This is a significant simplification to the tolerance analysis.

The assigned manufacturing tolerances of the first four surfaces which comprise the doublet are given in Table 2.1-1.

~~SECRET~~ **SPECIAL HANDLING**

The four tolerance budgets, a, b, c, d, have been arbitrarily formulated as typical group-ings of tolerances which could be distributed over the doublet. Two combinations (a, b) have the radii of curvature tolerances alternating in sign while two (c, d) have tolerances all of the same sign. The physical frequency responses for the four cases were computed, for the high power design 127X and plotted in Figure 2.1-11. Budgets c and d which do not alternate in sign (shown as curves 3 and 4) have a less degrading effect than budgets a and b (shown as curves 1 and 2) which do alternate in sign.

By inspection, tolerance budget "a" is the worst case. It then follows that a worst-case tolerance budget for the complete system would have to include tolerance budget "a". To determine this worst-case performance level, tolerances were applied over the entire de-sign. The physical response function was computed, after focal adjustments were made for optimum imagery, for the a, e and f budgets combined with tolerances of the remaining surfaces of the objective assembly. This combined budget is denoted a_T. The result is shown in Figure 2.1-10 as curve 1. If such degraded resolution ocurred in the laboratory, it would be normal procedure to tweak the doublet airspace. To simulate this procedure, tolerance budget "a" was treated again. A significant improvement was found for a doublet airspace of 0.2755 inch and reticle separation of 0.725 inch. The improved response, compared to the original response, is given in Figure 2.1-12. The zoom-relay and eye-piece tolerances were then combined to this modified budget. The resulting response is curve 1 of Figure 2.1-13. This curve represents the worst case found and was the budget used to generate the performance estimate curves for each magnification.

2.1.3 GE ANALYSIS OF OPTICAL PERFORMANCE UNDER DYNAMIC CONDITIONS

Introduction

This section documents the results of a GE study to analytically predict ATS optical resolution under dynamic (jitter) conditions. The study presents a method of treating the degrading effects of jitter on image modulation curves presented, demonstrating ground resolution as a function of jitter amplitude. A curve is also included showing the maximum jitter amplitude as a function of frequency which will permit 3.6-foot ground resolution to be achieved.

The method employed has been derived by GE and is not the same as that previously employed by Itek. The results are similar, however.

An interesting secondary conclusion of the analysis is that the static resolution can not be rigorously obtained from the intersection of the MTF curve and the eye threshold curve. It is shown that the actual resolution is somewhat better than predicted by the intersection of the curves thus providing a safety margin in the analysis presented in the previous section.

The Itek MTF curve is used as the analytical model for the telescope.

The specific objectives of this performance study were:

    a.   Analytically determine the dynamic performance of the acquisition telescope and relate the dynamic performance to that obtained under static conditions.

    b.   To specify the magnitude of half-amplitude jitter, as a function of jitter frequency, below which resolution of a three bar, 3.6 feet per cycle, 2 to 1 contrast target (viewed from 80 nautical miles, at nadir) is possible. (Note: Unless otherwise specified, all jitter amplitudes referred to in this report will be half-amplitude values).

    c.   To verify the methods and results from the Acquisition Subsystem Subcontractor, Itek Corporation, in the areas of static and dynamic performance analysis.

The analysis was conducted using the final lens design Modulation Transfer Function (MTF) provided by Itek Corporation in their Acquisition Optics Subsystem PDR Report dated 25 September 1967. (See Figure 2.1-20.)

The Schade visual resolution threshold characteristic specified by Itek in the same report was also adopted for use in this analysis. (See Figure 2.1-21.) A literature search was conducted to determine if experimental data was available to establish a more reliable eye resolution threshold characteristic; however, no data was found which appeared to be more reliable. It is imperative that a reliable eye resolution threshold characteristic be generated in order to accurately predict both static and dynamic performance of the Acquisition Subsystem. Itek Corporation is presently engaged in the design of an experiment that will yield the necessary data on eye modulation and contrast threshold.

ANALYTICAL MTF - $e^{-\alpha/f/}$

ACTUAL SYSTEM MTF - $A(\omega)$

SPATIAL FREQUENCY (CYCLES/FT GND)
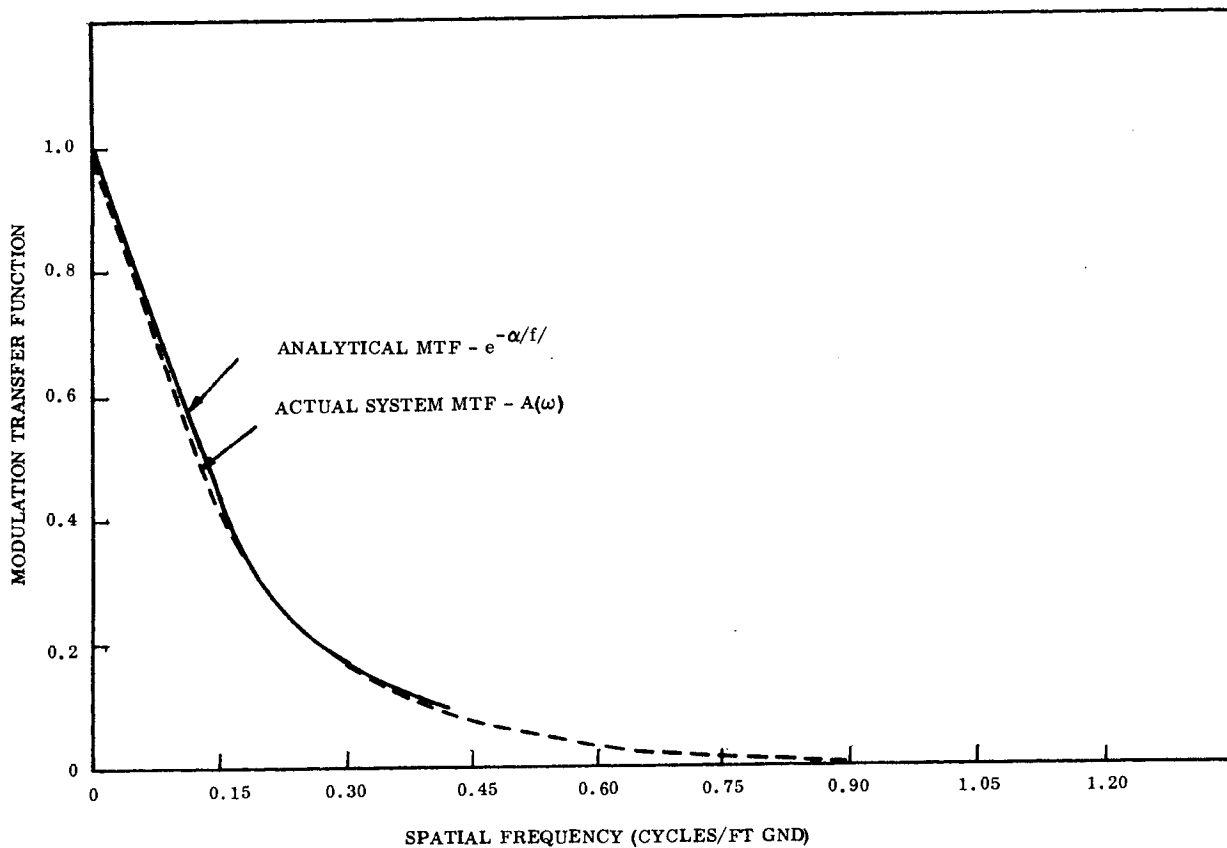
Figure 2.1-20. Acquisition Telescope Transfer Function

SECRET SPECIAL HANDLING
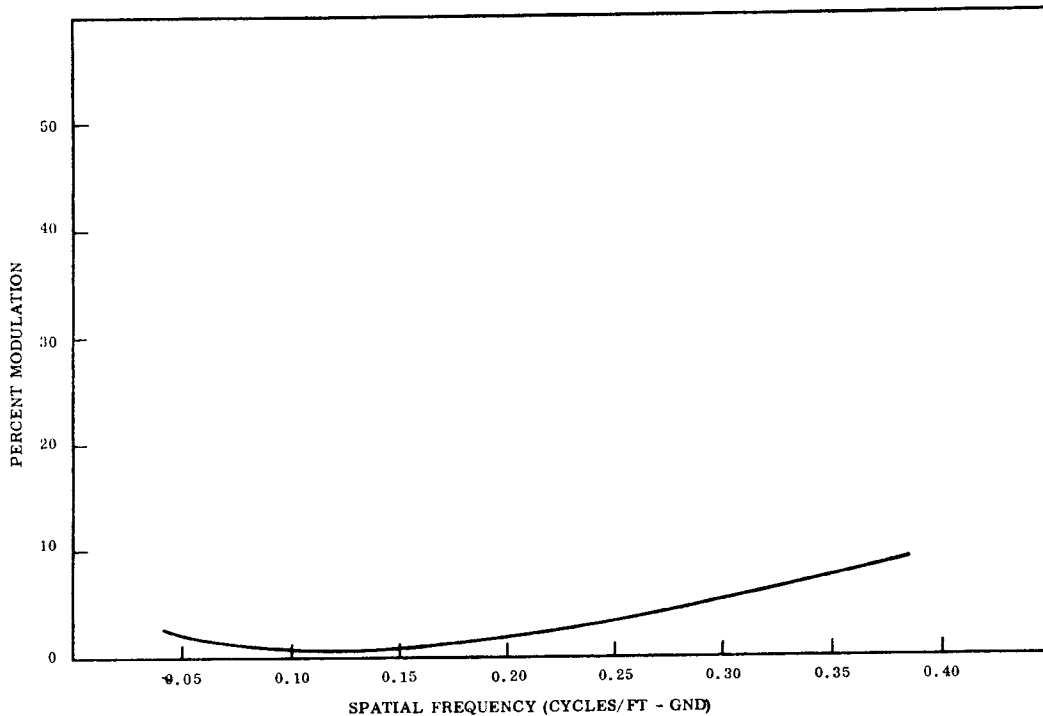
Figure 2.1-21. Low Contrast Visual Threshold (Schade 1964; MDM = 0.015)

It should be clearly understood that the intent of this study is only to verify that the Acquisition Subsystem meets the system performance requirements as contained in the GE-AVE CEI Specification. No attempt was made to predict system performance under actual on-orbit operating conditions.

For example, in reality, jitter imposed on the system will have a random spectrum (i.e., at any given time will be composed of many frequencies with definite phase and amplitude relationships) and will be two dimensional in nature.

For purposes of this analysis, only the degradation in resolution due to discrete frequencies was considered. Also, motion of the line-of-sight (LOS) was reduced to motion in a plane perpendicular to the axis of the bars being viewed. These assumptions are valid for purposes of verifying that the system design meets the specification requirements, but they are

SECRET SPECIAL HANDLING

not valid when predicting system performance on-orbit. Consideration of these additional factors will further reduce system resolution. It is felt that work in the area of system performance prediction should be continued to further define system resolution under actual operating conditions. However, a more realistic eye threshold characteristic must be established before this can be done.

2.1.3.1 Target Characteristics

The analytical results obtained for the Acquisition Telescope static and dynamic performance were derived for a target with the characteristics specified below:

    a.   Three light bars on a dark background

    b.   Contrast ratio of 2 to 1 at the input to the optical system

    c.   Apparent average brightness of 530 ft.-lamberts at the input to the optical system

For purposes of this analysis, it was assumed that the target is being viewed from 80 nautical miles (at nadir) with a magnification of 127X. Figure 2.1-22 is a graphic representation of a target with a spatial period of 3.6 feet per line pair on the ground (τ = 0.9 feet).

2.1.3.2 Summary of Static Performance Analysis

Results obtained from analysis of the Acquisition Telescope performance under static conditions show that for a tri bar target input (square wave brightness distribution) with a spatial period between 3.0 and 4.2 feet per cycle, the image formed by the telescope has a sinusoidal brightness distribution. For a given ground spatial period in this region the output image contrast and modulation may be determined from Figure 2.1-23. This is based on three bar target input with characteristics as described above. Using the Schade threshold specified in Figure 2.1-22, the static resolution of the Acquisition Telescope is 3.12 feet per cycle on the ground. This result is considerably lower than that calculated by Itek. They obtained a minimum resolution of 3.3 feet per cycle from the direct intersection of the telescope Modulation Transfer Function and the Schade Threshold multiplied by a

~~SECRET~~ SPECIAL HANDLING

$$\tau = 0.9 \ \text{FT}$$
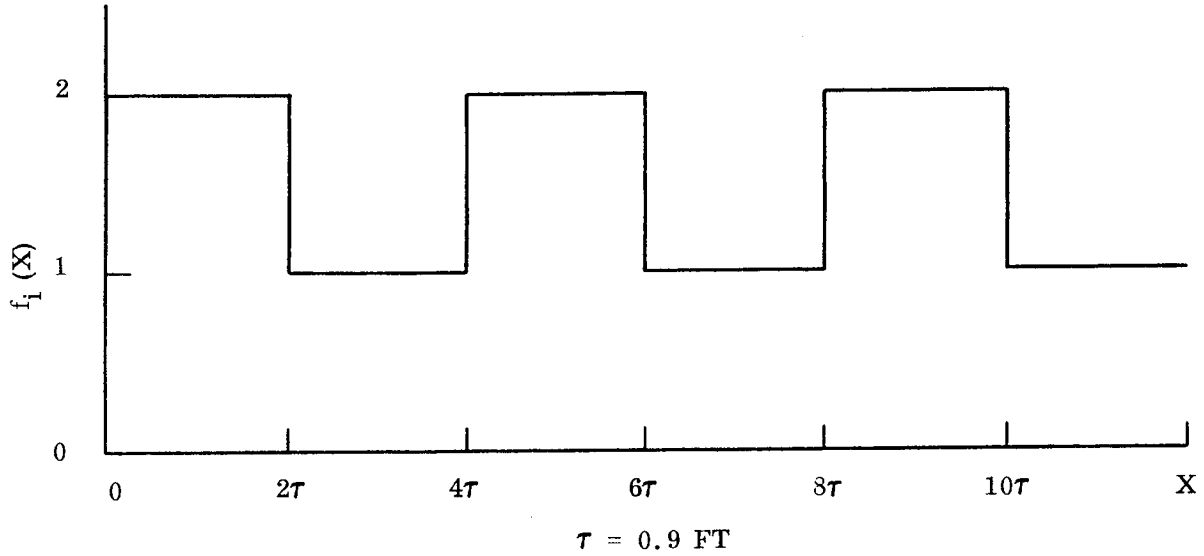
Figure 2.1-22. Graphic Representation
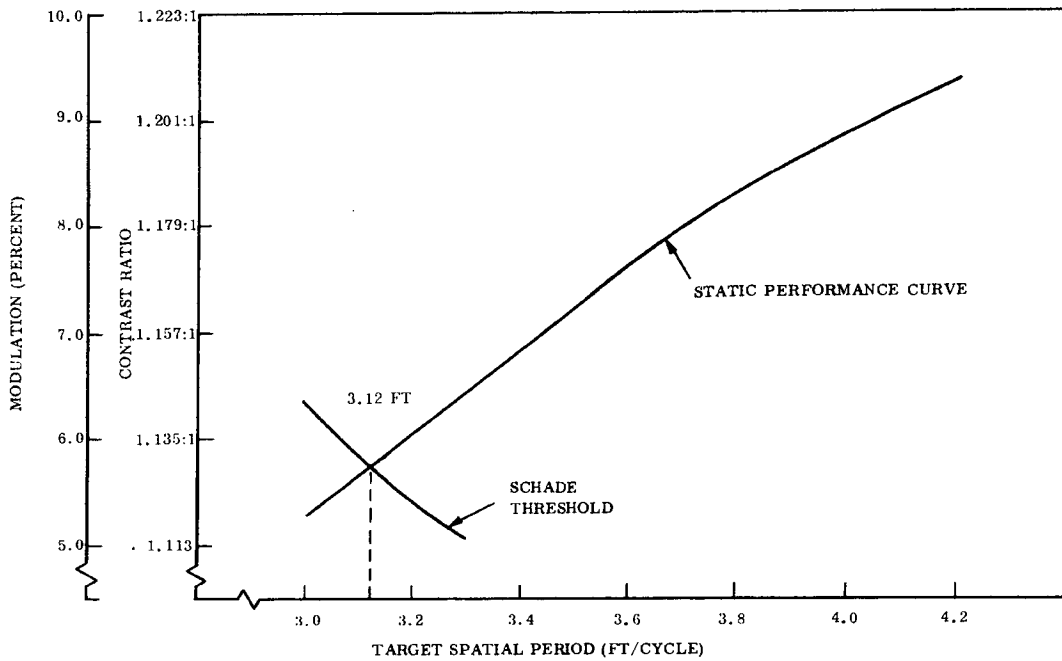
Figure 2.1-23. Acquisition Telescope Static Performance

~~SECRET~~ SPECIAL HANDLING

factor of three (multiplication by three is necessary since the MTF is normalized to 1.0, thus representing a high contrast input). A direct intersection of these two curves is not possible unless the input and output brightness waveforms are considered.

The increase in system resolution can be most easily understood by analyzing the static system performance using a target with an infinite number of bars. In this case, a 2 to 1 contrast square wave input to the Acquisition Telescope produces an output waveform equivalent to that obtained for a 2.5 to 1 contrast sinusoidal input. In other words, the first harmonic of the square wave brightness distribution has a greater contrast ratio than 2 to 1. The result is a higher output modulation at the specified threshold frequency than computed in the Itek analysis.

2.1.3.3 Summary of Dynamic Performance Analysis

ECP Number 17 to the GE-AVE CEI Specification contains a curve of acceptable half amplitudes of oscillation of the LOS as a function of frequency. This is reproduced in Figure 2.1-24 (solid curve). Analysis in this report shows that a system designed to meet this allowable jitter characteristic will have the capability of resolving a 3.38 feet per cycle three bar target on the ground.

Also included in Figure 2.1-24 (dashed curve) is the half amplitude jitter as a function of frequency that will produce a minimum resolution of 3.6 feet per cycle on the ground. The allowable jitter specified by the broken curve between 0.001 and 1.0 Hz is conservative since it is based on the value of jitter which begins to produce resolution degradation. The shape of the characteristic between 1.0 and 6.0 Hz has been estimated. Degradation in resolution due to jitter in this region is a function of both amplitude and frequency. Therefore, it is not possible at this time to analytically predict system performance.

Figure 2.1-25 (solid curve) shows the minimum system resolution as a function of jitter half amplitude (above 6.0 Hz). Due to the numerical integration techniques used to generate this curve, accuracy below five-foot minimum resolution is approximately three percent.
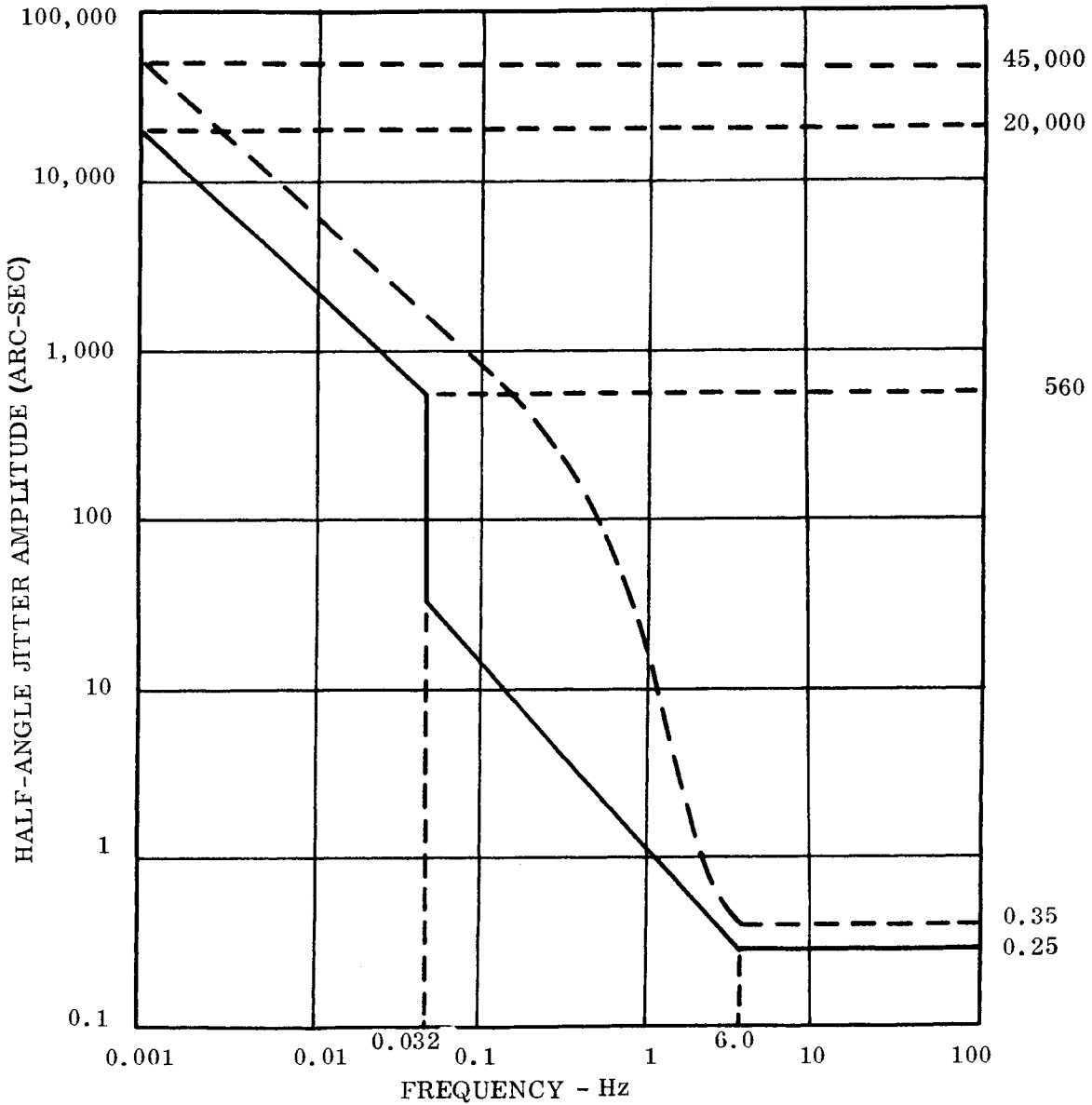
Figure 2.1-24. Acceptable Half Amplitudes of Oscillation

~~SECRET~~ SPECIAL HANDLING
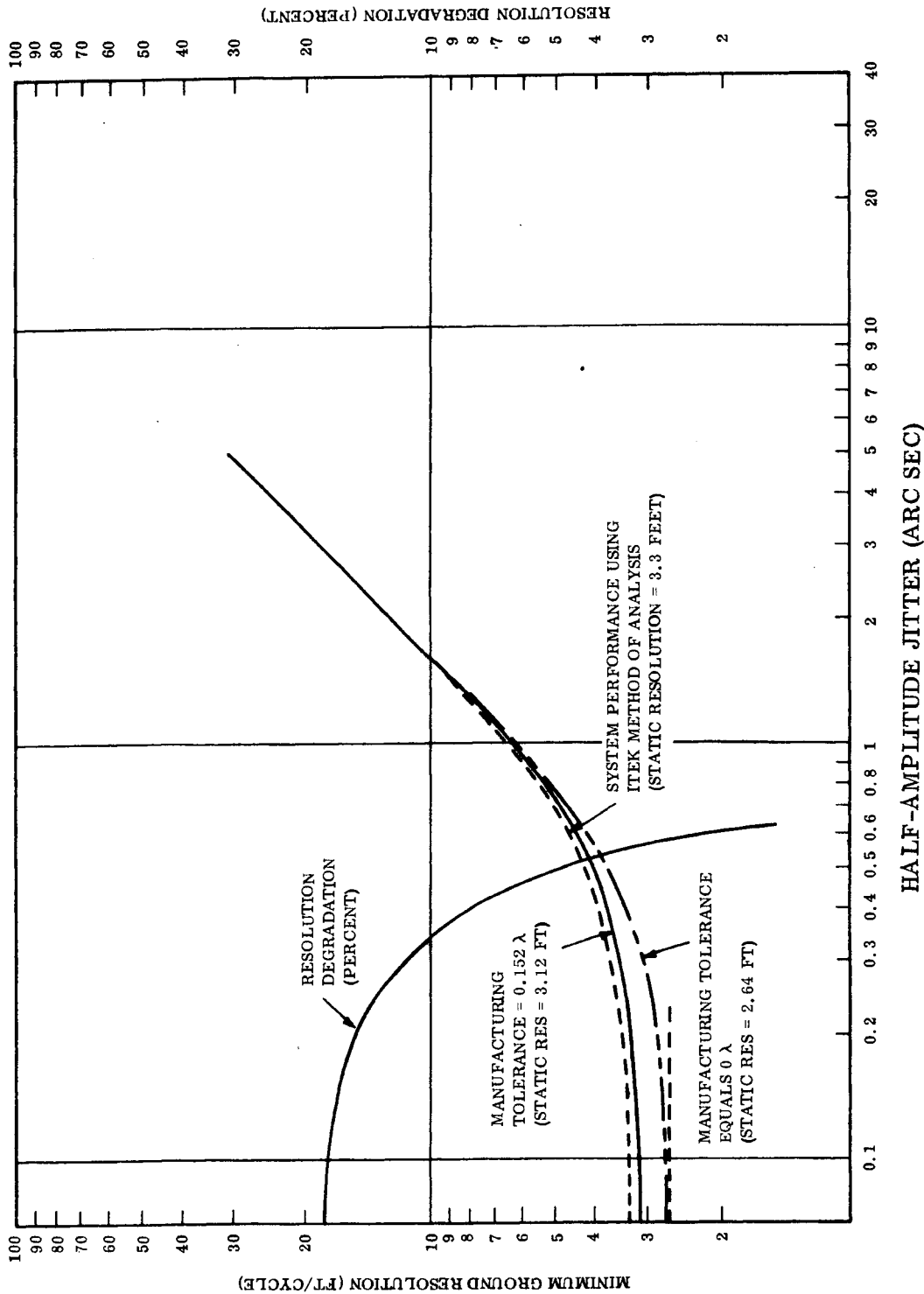
Figure 2.1-25. Acquisition Telescope Dynamic Performance Curve for Final System Design

2-51

~~SECRET~~ SPECIAL HANDLING

Above five-foot, accuracy, is approximately seven percent. From this curve it may be seen that as the maximum allowable jitter half amplitude increases above the 0.35-to 0.45- arc second region, a sharp decrease in system resolution occurs.

The System MTF used to generate the solid curve contains a manufacturing tolerance of 0.152 λ. The broken curve in Figure 2.1-25 shows the minimum system resolution with a manufacturing tolerance of 0 λ.

A comparison of the two curves shows that under static conditions, the minimum resolution is degraded 19 percent by a manufacturing error equivalent to 0.152 λ. However, as the maximum allowable jitter is increased, the effect of the manufacturing error becomes less. The system degradation in percent as a function of maximum allowable jitter amplitude is also shown in Figure 2.1-25. For example, a system with a maximum allowable jitter of 0.6 arc seconds will show a 2.3 percent decrease in resolution as the manufacturing and alignment errors increase from zero to 0.152 λ.

Also shown in Figure 2.1-25 (dash curve), is the minimum system resolution as a function of jitter obtained using the Itek Corporation method of analysis.

2.1.3.4 Static Performance Analysis

E.L. O'Neill[1] demonstrates an analogy between linear time filters and optical spatial filters (conventional optical systems with lenses, prisms, etc.). Using this analogy, it is possible to specify an optical system in terms of its spatial frequency characteristic or transfer function $G(\omega)$. The output of such a system at any frequency ω_0 may be represented as $G(\omega_0)$ times the input. The output wave form may then be found by use of the inverse Fourier Transform.

[1] O'Neill, E.L., Introduction to Statistical Optics; Addison-Wesley Publishing Co., Inc., 1963

$$F_o(\omega) = G(\omega)\, F_i(\omega)$$

$$R_o(\omega)e^{j\varphi_o(\omega)} = A(\omega)\, e^{j\theta(\omega)} \cdot R_i(\omega)\, e^{j\varphi_i(\omega)}$$

$$f_o(X) = F^{-1}\left[F_o(\omega)\right]$$

$$f_o(X) = F^{-1}\left[A(\omega) \cdot R_i(\omega) \cdot e^{j\left[\theta(\omega) + \varphi_i(\omega)\right]}\right]$$

The three bar target of Figure 2.1-22 has a continuous frequency spectrum described by:

$$F_i(\omega) = 2A\tau \left(\frac{SIN\ \omega\tau}{\omega\tau}\right)\left[e^{-j\omega\tau} + e^{-j5\omega\tau} + e^{-j9\omega\tau}\right]$$

$$= \frac{2A\tau}{\omega\tau}\left[\frac{e^{j\omega\tau} - e^{-j\omega\tau}}{2j}\right]\left[e^{-j\omega\tau} + e^{-j5\omega\tau} + e^{-j9\omega\tau}\right]$$

$$= A\left[\frac{e^{-j0\omega\tau}}{j\omega} - \frac{e^{-j2\omega\tau}}{j\omega} + \frac{e^{-j4\omega\tau}}{j\omega} - \frac{e^{-j6\omega\tau}}{j\omega}\right.$$

$$\left. + \frac{e^{-j8\omega\tau}}{j\omega} + \frac{e^{-j10\omega\tau}}{j\omega}\right]$$

An attempt was made to find an analytical function to represent the magnitude $A(\omega)$ of the Acquisition Telescope transfer function specified by Itek Corporation with no regard for the phase characteristic. Due to the nature of the analyses, neglecting the phase of $G(\omega)$ will have a negligible effect on the results. A Fourier Spectrum with a magnitude equal to an exponential decay $e^{-\alpha/f/}$ and $\alpha = 6$ provides a good fit for $A(\omega)$ over the spatial frequency region defined in the PDR report. A comparison of $e^{-\alpha/f/}$ and $A(\omega)$ is shown in Figure 2.1-20.

Now

$$F_o(\omega) = G(\omega) \ F_i(\omega)$$

$$= A \ e^{-\frac{\alpha}{2\pi}} \ |P| \left[\frac{e^{-0P\tau}}{P} - \frac{e^{-2P\tau}}{P} + \frac{e^{-4P\tau}}{P} - \frac{e^{-6P\tau}}{P} \right.$$

$$\left. + \frac{e^{-8P\tau}}{P} - \frac{e^{-10P\tau}}{P} \right]$$

where

$$P = j\omega$$

The output function $f_o(X)$ can be obtained by taking the inverse transform of the above equation. The analytical expression for the resultant is an extremely complex equation and is difficult to interpret. A graphical interpretation is much more meaningful and is obtained as follows:

$$g(X) = F^{-1} \left[G(\omega) \right]$$

$$f_i(X) = F^{-1} \left[F_i(\omega) \right]$$

$$\therefore \ f_o(X) = g(X) * f_i(X)$$

The graphic interpretation of the convolution of $g(X)$ and $f_i(X)$ is shown in Figures 2.1-26a through e.

2-54

~~SECRET~~ **SPECIAL HANDLING**

$$\frac{1}{\pi\alpha} - \qquad g(\lambda) = \frac{\alpha}{\pi(\lambda^2 + \alpha^2)} \quad \mu(\lambda)$$

a.

$$\frac{1}{\pi\alpha} \qquad g(X, -\lambda) = \frac{\alpha}{\pi\left[(X, -\lambda)^2 + \alpha^2\right]} \mu(X_1 - \lambda)$$

b.

$f_i(\lambda)$
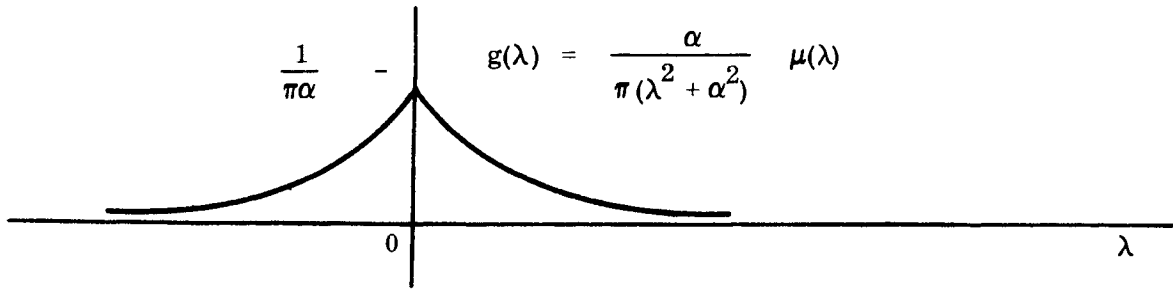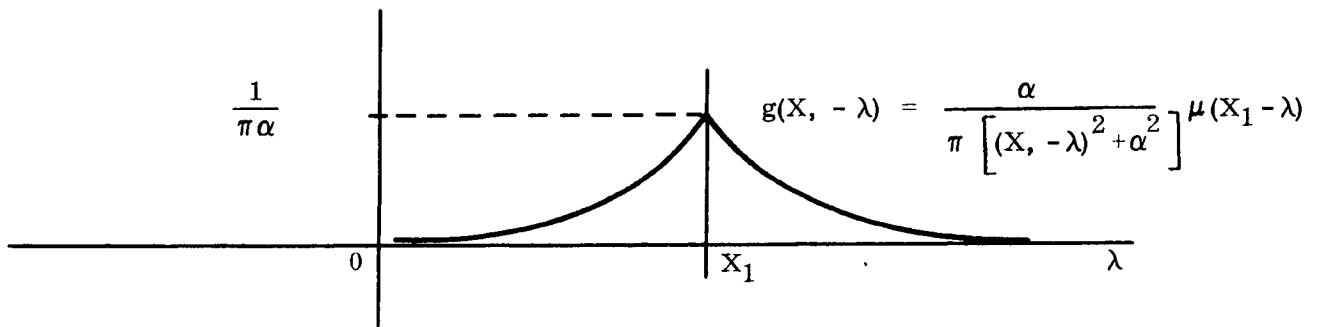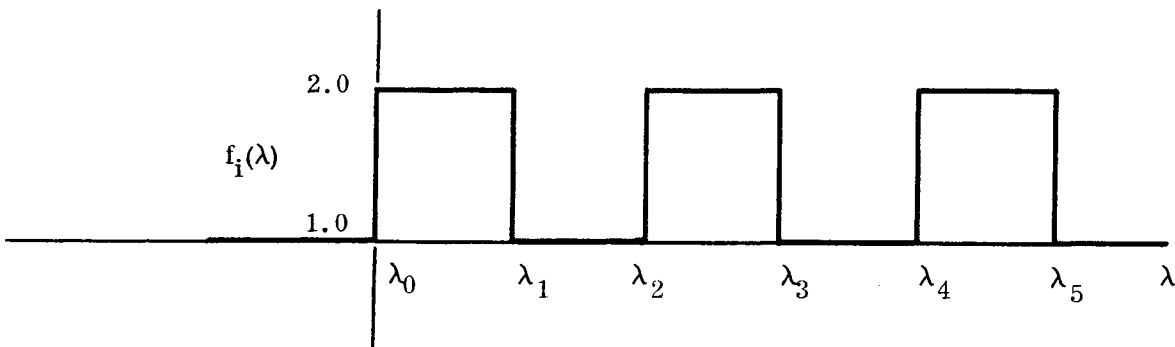
c.

Figure 2.1-26. Graphic Interpretations

~~SECRET~~ **SPECIAL HANDLING**

The product of $g(X, -\lambda)$ and $f_i(\lambda)$ is:
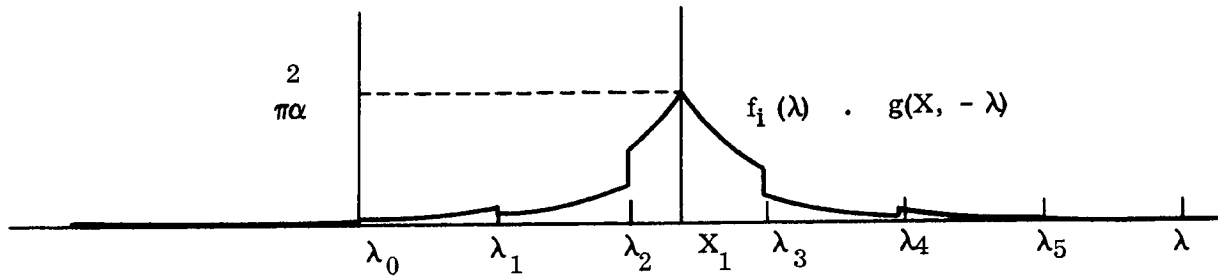
Figure 2.1-26d. Graphic Interpretations

The ordinate of the output waveform $f_o(X)$ at $X = X_1$ is the product of the two functions with $\lambda = X$. For an input square wave with a period of 3.6 feet per line pair ($\tau = 0.9$ feet) the resultant output waveform is:
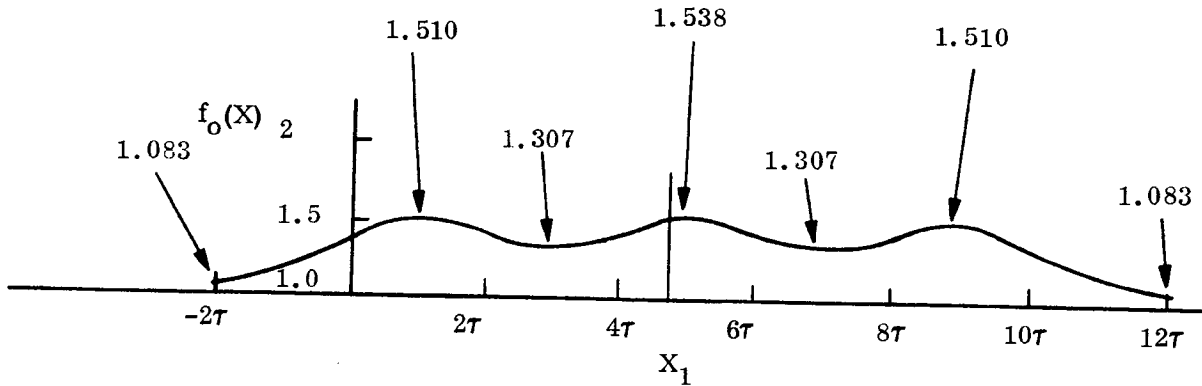
Figure 2.1-26e. Graphic Interpretations

SECRET SPECIAL HANDLING

Figure 2.1-26e shows that under static conditions, the acquisition telescope degrades a 3.6 feet per cycle three bar target input with 2 to 1 contrast and 33 percent modulation to a low contrast three cycle sinusoidal waveform with an average contrast of 1.17 to 1 and average modulation of 7.6 percent.

Figure 2.1-23 is a curve which shows output waveform modulation and contrast, for a 2 to 1 contrast three-bar target input, as a function of spatial frequency on the ground. When the Schade modulation Threshold characteristic is superimposed, the two curves intersect at 3.12 feet which means that under static conditions the smallest three-bar target that can be resolved is 3.12 feet per cycle. This contradicts the 3.3-foot result presented by Itek Corporation in their PDR report. The reason for this discrepancy is most easily explained by performing a similar image waveform analysis for a bar target consisting of an infinite number of light and dark bars (instead of three). This is a much simpler problem since a periodic function consisting of an infinite number of pulses may be represented by the following series:

$$f_i(X) = 2A_{av} \left(\frac{1}{2} + \frac{2}{\pi} \cos y - \frac{2}{3\pi} \cos 3y + \frac{2}{5\pi} \cos 5y \ldots \right)$$

where

$$y = \frac{2\pi X}{\tau} \quad \text{and } A_{av} \text{ is a function of average brightness.}$$

This function has a discrete Fourier spectrum of the form:

$$F_i(\omega) = A \frac{\sin \omega \tau}{\omega \tau} \; \delta (\omega - \omega g)$$

SECRET SPECIAL HANDLING

where

$$\omega g = 2\pi n f_i$$

$$n = 1, 2, 3, 4, \ldots\ldots$$

f_i = Frequency components of the Fourier series representation

A plot of this $F_i(\omega)$ is shown in Figure 2.1-27.

Operating on this discrete frequency spectrum with the transfer function $A(\omega)$ of the tele-scope shows that each frequency component is multiplied by the ordinate of the transfer function at that particular value of spatial frequency. The resultant is a brigthness distri-bution represented by the equation:
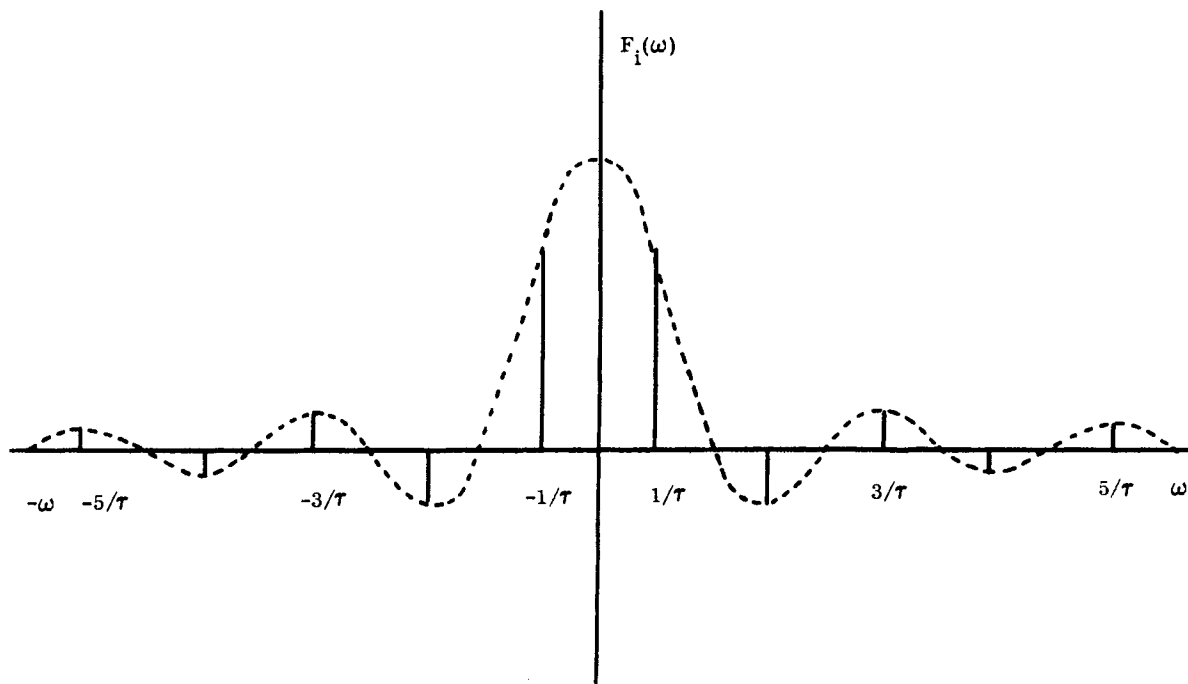
Figure 2.1-27. Plot

$$f_0(X) = 2 A_{av} \left[(1) \frac{1}{2} + (0.190) \frac{2}{\pi} \cos y \right.$$

$$\left. - (0.006) \frac{2}{3\pi} \cos 3y + \ldots \right]$$

The amplitude of the fundamental frequency term is a factor of 80 times the amplitude of the third harmonic term. Therefore, all higher order terms may be neglected and

$$f_0(X) = 2 A_{av} \left[(1) \frac{1}{2} + (0.190) \frac{2}{\pi} \cos \frac{2\pi X}{\tau} \right]$$

This shows that a 2 to 1 contrast infinite bar target input produces an output waveform equal to the output produced by infinite sinusoidal target input with 2.5 to 1 contrast. Therefore, the direct superposition of a threshold curve on a modulation transfer function to yield system resolution is not valid unless the type of input and output waveforms are considered.

2.1.3.5 Dynamic Performance Analysis

Oscillation of the acquisition telescope LOS with respect to a point in the object plane produces a point in the image plane which appears to oscillate at the same frequency as the LOS oscillation but with an angular amplitude of 127 times that of the LOS oscillation amplitude. The same image motion result is obtained with a static LOS and an oscillating target. Therefore, for purposes of analysis, all jitter will be introduced as oscillation of the target with respect to a static LOS.

To analyze the effects of jitter on system resolution, jitter frequencies in the range 0.001 to 100 Hz were considered. ECP number 17 to the GE-AVE CEI Specification contains a curve of acceptable amplitudes of oscillation of the LOS as a function of frequency. This characteristic was shown in Figure 2.1-24 (solid curve). This spectrum was broken into four regions (0.001 to 0.032, 0.032 to 1.0, 1.0 to 6.0, and 6.0 to 100 Hz) and the allowable jitter amplitude determined in each region.

~~SECRET~~ **SPECIAL HANDLING**

Low frequency, large amplitude jitter (in the 0.001 to 0.032 Hz range) makes the image appear to move across the field-of-view at a constant rate. Therefore, the factor affecting resolution due to jitter in the 0.001 to 0.032 Hz range is the linear velocity at which the eye must tract the image. The maximum linear image velocity with respect to the eye for the allowable jitter specified of Figure 2.1-24 was calculated and found to be 4.5 degrees per second. Data presented in the Bioastronautics Data Book (1964) indicates that very little degradation in resolution is introduced for velocity up to 10 degrees per second. This corresponds to a jitter half amplitude of approximately 45,000 arc-seconds at 0.001 Hz and 1,400 arc-seconds at 0.032 Hz.

Jitter in the frequency range 0.032 to 1.0 Hz will produce small sinusoidal oscillations of the image with respect to the eye. Again, this motion will not produce a significant resolution degradation around 0.032 Hz if the angular rate of image motion is less than 10 degrees per second. Experimentation done by Jones & Draxin and Guignard & Irving show that for frequencies around 1 Hz, the eye can track sinusoidal motion with half amplitudes up to 0.5 degree with respect to the eye. This corresponds to a jitter amplitude of approximately 14 arc-seconds.

The next range of jitter frequencies to be considered is the 1.0 Hz to 6.0 Hz range. Figure 2.1-28 is a plot showing the ratio between actual motion of the eye when viewing an oscillating target and the motion of the target with respect to the eye. This characteristic shows that in the 1 to 6 Hz region, degradation of the image resolution is a function of both jitter amplitude and frequency. Because the degradation is a function of both variables, an analytical performance prediction cannot be obtained.

When the frequency of oscillation of a point in the object plane is above 6 Hz, the point in the image plane viewed by an observer appears to be a continuous line. Therefore, image degradation of a point oscillating above 6 Hz is independent of the frequency of oscillation. The primary factors that contribute to the degradation are oscillation amplitude and wave-shape (i.e., sinusoidal, linear, random, etc.). For this analysis, the degradation effects of both linear and sinusoidal jitter were investigated.

~~SECRET~~ **SPECIAL HANDLING**
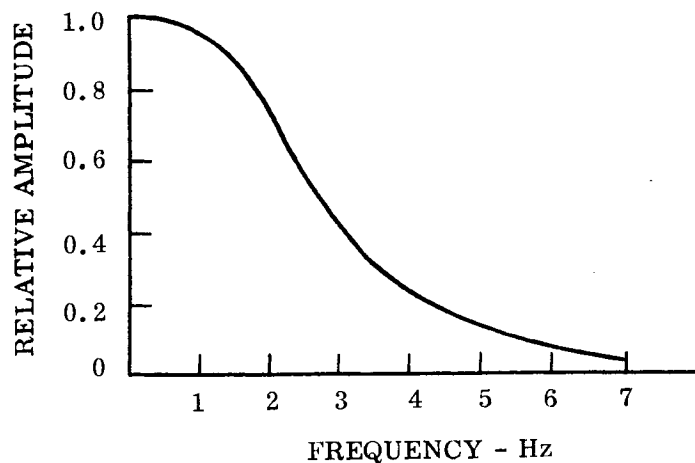
FIGURE 2.1-28. Ratio Plot

The brightness distribution characteristic for a three-bar target (the object) as a function of half amplitude linear and sinusoidal jitter is shown in Figures 2.1-29 and 2.1-30, respectively. The object waveform contrast ratio as a function of jitter amplitude is shown for linear and sinusoidal jitter in Figure 2.1-31. This shows that the contrast of the object remains constant up to and including amplitudes of jitter which produce peak-to-peak LOS excursions on the ground equal to half the spatial period of one target cycle. The object contrast then decreases to 1 to 1 as the p-p LOS excursion increases above this value. The contrast of the image formed at the output of the telescope begins to degrade immediately as jitter is introduced. This is due to the fact that the Fourier components of the object brightness characteristic (shown in Figures 2.1-29 and 2.1-30) change as target motion is introduced. For example, when the linear half amplitude jitter is such that the brightness distribution of the object is a triangular wave (half-amplitude jitter (a) equals τ), the Fourier expansion of this brightness distribution (assuming an infinite target) may be represented as:

$$f_i(X) = 1.5 \; \frac{4}{\pi^2} \; \left(\cos y + \frac{1}{9} \cos 3y + \frac{1}{25} \cos 5y + \dots \right)$$

where

$$y = \frac{2\pi X}{\tau}$$

2-61
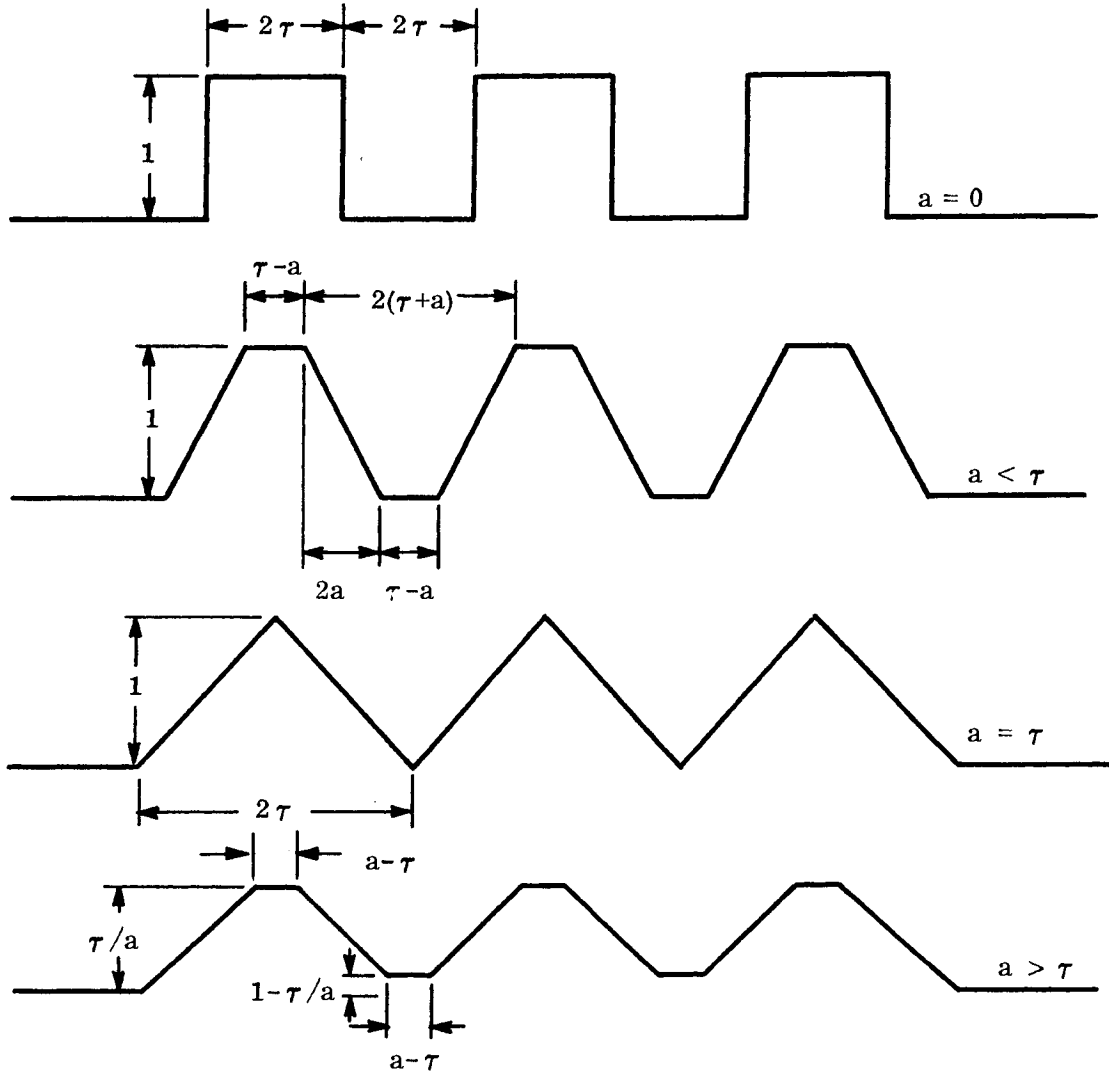
Figure 2.1-29. Target Brightness Characteristics as a Function
of Linear Jitter Amplitude

~~SECRET~~ **SPECIAL HANDLING**
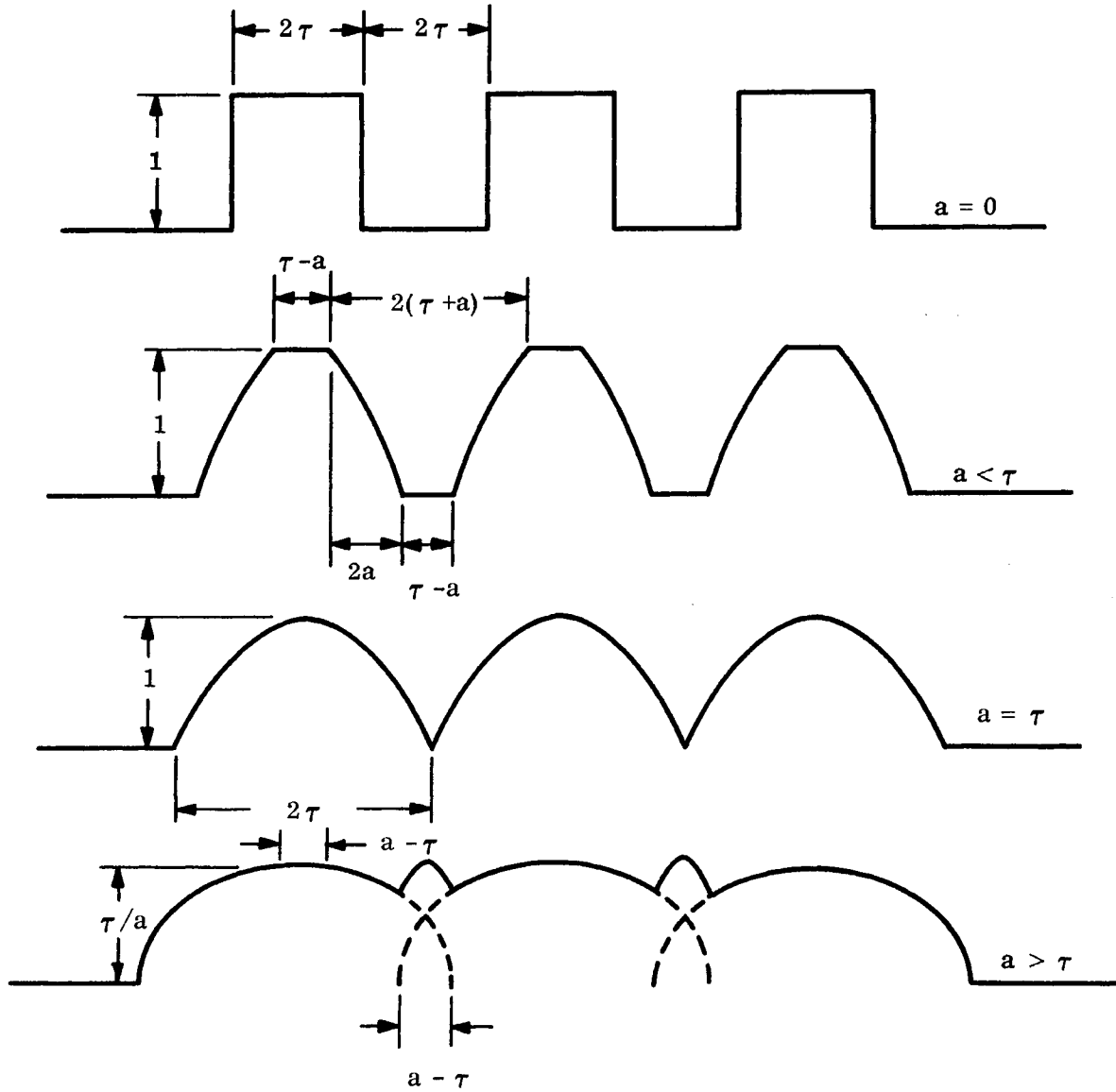
Figure 2.1-30. Target Brightness Characteristics as a Function
of Sinusoidal Jitter Amplitude

~~SECRET~~ **SPECIAL HANDLING**
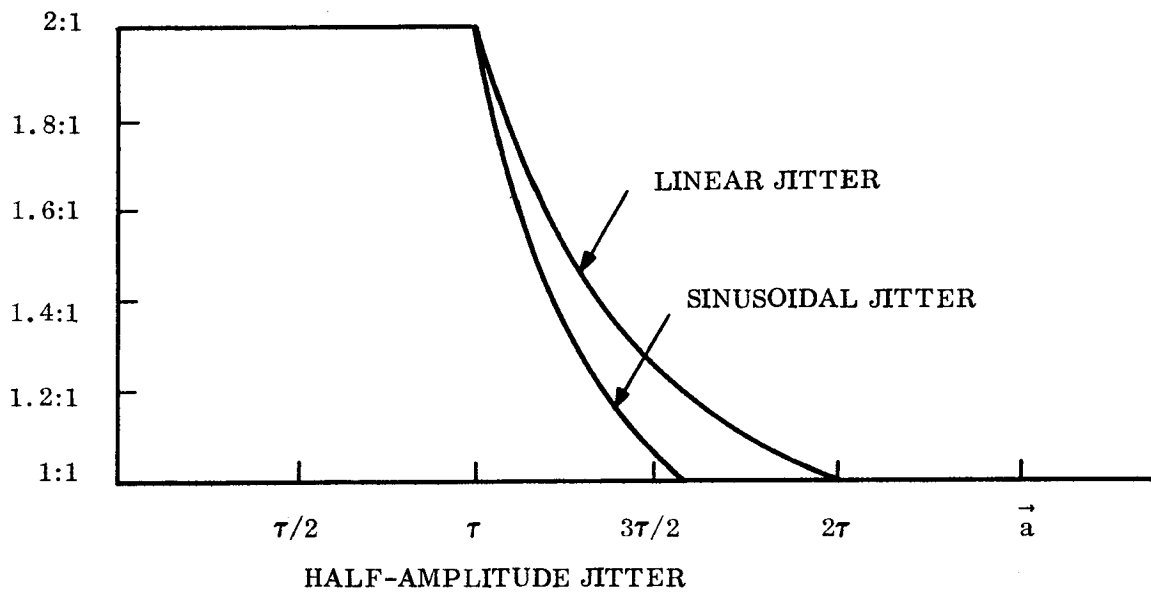
Figure 2.1-31.   Object Waveform Contrast as a
Function of Jitter Amplitude

As was the case for the square wave brightness distribution (zero jitter), harmonics above the fundamental frequency may be neglected. Therefore, with linear jitter of $a = \tau$, the image at the output of the telescope (for a spatial period of 3.6 feet per cycle) has a sinusoidal brightness distribution with contrast and modulation reduced from 1.18 to 1 and 8.0 percent (at zero jitter) to 1.10 to 1 and 5.1 percent.

Figure 2.1-32 shows the effect of half amplitude jitter (both sinusoidal and linear) on a 2 to 1 contrast 3.6 feet per cycle three-bar target. This figure demonstrates that 0.35 arc-second half amplitude sinusoidal jitter will yield a sinusoidal brightness distribution with 1.10 to 1 contrast and 4.3 percent modulation. This corresponds to visual threshold as defined by the Schade Threshold characteristic.

This analysis was extended to include spatial periods from 3.0 to 4.2 feet per cycles on the ground. The result of this analysis for the sinusoidal jitter is shown in Figure 2.1-33.
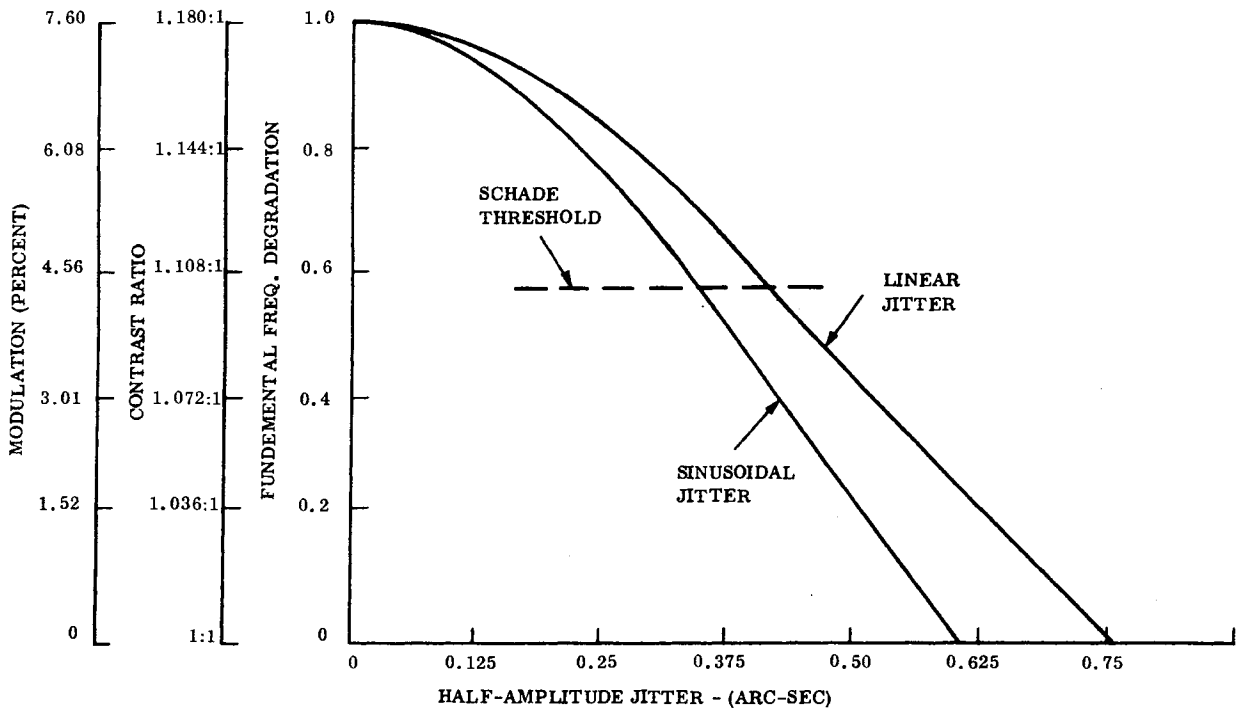
Figure 2.1-32. Image Modulation and Contrast as a Function of Jitter
(3.6 Ft/Cycle Tri-Bar Target)
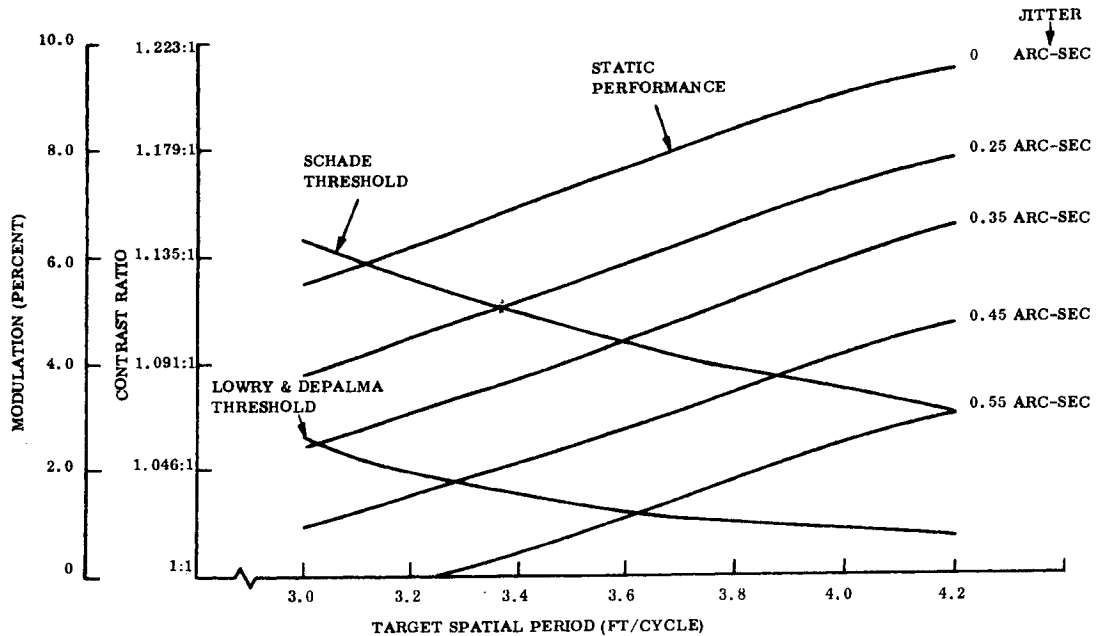
Figure 2.1-33. Acquisition Telescope Dynamic Performance
Curves for Sinusoidal Jitter

The curves depicted were calculated using a numerical integration technique to convolve the three-bar brightness distribution waveforms shown in Figure 2.1-30 with the transfer function of the Acquisition Telescope in the spatial frequency domain. Comparing the results obtained using the numerical integration techniques with an analytical solution of zero jitter and for an infinite target indicated an accuracy of three percent.

Figure 2.1-33 shows the degradation in system performance from the static performance (both image contrast and modulation) as a function of target period on the ground for discrete half amplitudes of jitter (0.25, 0.35, 0.45, and 0.55 arc-seconds). Also drawn on this graph are two eye threshold curves, the Schade Threshold previously discussed and a more optimistic curve by Lowry and DePalma[2]. Using the Schade curve, a three-bar target

[2]DePalma, J.J. and Lowry, E.M.; Journal of the Optical Society of America, Volume 52, March 1962, Page 328.

with a spatial period of 3.38 feet per cycle is the minimum size that can be resolved if the system is acted upon by half-amplitude jitter of 0.25 arc-second. The maximum jitter that can be experienced to allow a resolution of a 3.6 feet per cycle target is 0.35 arc-second. It is felt that the data obtained by Lowry and DePalma to generate their threshold curve is optimistic. However, if this curve is used, 0.53 arc-second of jitter can be tolerated to obtain a minimum resolution of 3.6 feet per cycle.

~~SECRET~~ **SPECIAL HANDLING**

2.1.4 SECONDARY DESIGN PERFORMANCE INFORMATION

2.1.4.1 Vignetting

This subsection describes analysis performed to determine the amount of vignetting present in the design. The description is presented in two parts.

A. Internal Telescope Vignetting - To determine if there is any internal vignetting in the telescope, the following analysis was performed by Itek.

The vignetting in the telescope was calculated at the peak wavelength (0.56 microns) and also throughout the visible (0.47 to 0.65 micron) spectral region. At the peak wavelength, 253 rays were traced at normalized field positions of 0.0, 0.5, and 1.0, since the transmission specifications are given at these field positions. To calculate the vignetting over the visible spectral region, 70 rays were traced at each of the following wavelength, 0.65, 0.605, 0.56, 0.515, and 0.47 microns. In both the monochromatic and polychromatic cases, the rays were traced at six magnifying powers; namely, 127X, 84.67X, 63.5X, 31.75X, 21.17X, and 15.88X.

The percent vignetting for all these different cases is given in Table 2.1-4 where percent

$$\text{vignetting} = \frac{\text{Rays in} - \text{Rays out}}{\text{Rays in}} \times 100.$$

This shows that only at the condition of low zoom power is there any internal vignetting and this is not expected to significantly effect resolution.

B. External Component Vignetting - A complete study of vignetting (including the effects of external components) is in progress.

~~SECRET~~ **SPECIAL HANDLING**

~~SECRET~~ SPECIAL HANDLING

TABLE 2.1-4. PERCENT VIGNETTING

MAGNIFYING POWER	MONOCHROMATIC = 0.0	= 0.5	PERCENT VIGNETTING = 1.0	POLYCHROMATIC = 0.0	PERCENT VIGNETTING = 0.5	= 1.0
127X	0.0	0.0	0.0	0.0	0.0	0.0
84.67X	0.0	0.0	0.0	0.0	0.0	0.0
63.50X	0.0	0.0	20.2	0.0	0.0	19.2
31.75X	0.0	0.0	0.0	0.0	0.0	0.0
21.17X	0.0	0.0	0.0	0.0	0.0	0.0
15.88X	0.0	0.0	19.0	0.0	0.0	20.3

~~SECRET~~ SPECIAL HANDLING

2.1.4.2 Gimbal Angles Versus Scan Field Position

Line of sight and gimbal angles required for the scan field coverage were derived by Itek for the nine-degree total cant configuration and are presented in tabular form.

The results are listed in Tables 2.1-5 and 2.1-6. The tables give either the LOS or gimbal angles for the nine-degree cant angle. The top chart shows the extreme or worst case angles alone with the corresponding LOS angles with respect to vehicle axes. This gives the pitch and roll ranges required to cover the entire + 70 degrees to - 40 degrees in pitch and ±45 degrees in roll. The lower chart shows the angles corresponding to various points of interest within the total range. Reference to Dwg. 905842 shows that the required (and computed) gimbal angles were used in the design of the scanner gimbal assembly. However, further analysis is needed to determine if the LOS intersects the Lab Module contour.

2.1.4.3 Exit Pupil Shift

The exit pupil shift as a function of zoom position, or magnification, is shown in Figure 2.1-34. The specification limits are also shown on this figure. The curve shown in Figure 2.1-34 clearly indicates that the specification requirements on exit pupil shift have been met. A more detailed discussion of this topic can be found in the Itek PDR Report.

2.1.4.4 Total Transmittance Summary

The total transmittance of the complete AO Telescope system has been calculated by Itek (see Table 2.1-7) and found to be 35.4 percent for the 127X (high power) mode and 31.2 percent for the 31.75X (low power) mode. The following assumptions were made: single layer magnesium fluoride anti-reflection coatings on all refracting surfaces, both external mirrors are aluminized and have a silver oxide protective coating (87 percent reflection each). The internal folding mirror aluminized with a two-layer enhancement coating (93 percent reflectance), and multilayer coatings (98.5 percent reflection) on two surfaces of the Pechan Prism. The transmittance calculation takes into account the expected reflection

~~SECRET~~ **SPECIAL HANDLING**

TABLE 2.1-5. LOS ANGLES FOR PLUS NINE-DEGREE CANT

EXTREME ANGLES		CORRESPONDING LOS ANGLES (WITH RESPECT TO VEHICLE AXES)	
ROLL	PITCH	ROLL	PITCH
-48.21		-45	-40
	-40.83	+18	-40
	+70.26	-26	+70
+54.80		+45	+70

PITCH (LOS Angles with respect to vehicle axes)

PITCH \ ROLL	+45	0	-45
+70	+55.85 / +54.80	+68.14 / +23.26	+68.25 / -29.16
+40	+24.13 / +48.21	+39.41 / +7.48	+36.81 / -40.58
+10	+0.71 / +45.43	+9.88 / +1.58	+13.41 / -43.83
0	-6.35 / +44.65	±0 / ±0	+6.35 / -44.65
-40	-36.81 / +40.58	-39.41 / -7.48	-24.13 / -48.21

ROLL (LOS angles with respect to vehicle axes)

~~SECRET~~ **SPECIAL HANDLING**

~~SECRET~~ **SPECIAL HANDLING**

TABLE 2.1-6. GIMBAL ANGLES FOR PLUS NINE-DEGREE CANT

EXTREME ANGLES		CORRESPONDING LOS ANGLES (WITH RESPECT TO VEHICLE AXES)	
ROLL	PITCH	ROLL	PITCH
-40.75		-45	-40
	+22.25	+29	-40
	+80.39	-45	+70
+62.26		+45	+70

PITCH
(LOS Angles with respect to vehicle axes)

PITCH \ ROLL	+45	0	-45
+70	+69.05 / +62.25	+76.58 / +41.58	+80.39 / -4.26
+40	+53.47 / +54.00	+63.53 / +18.55	+65.93 / -30.93
+10	+41.85 / +51.08	+49.17 / +10.56	+54.45 / -36.40
0	+38.33 / +50.40	+44.30 / +8.89	+50.95 / -37.47
-40	+23.12 / +48.08	+24.67 / +4.17	+35.79 / -40.75

ROLL
(LOS Angles with respect to vehicle axes)

~~SECRET~~ **SPECIAL HANDLING**

Figure 2.1-34. Exit Pupil Shift as a Function of 200 M Position

TABLE 2.1-7. TRANSMISSION OF COMPLETE SYSTEM

	HIGH POWER MODE 0.56 μ (PERCENT)	LOW POWER MODE 0.56 μ (PERCENT)
Transmission due to reflection losses alone	39.2	34.8
Transmission due to absorption losses alone	90.2	89.6
Transmission due to combined effects	34.4	31.2

and absorption losses of each element, rather than the theoretically predicted values. The performance assumed for the single layer magnesium fluoride coatings, for example, is based on actual measurements made on coatings on different index glasses. Although the variation of reflection with glass index and angle of incidence of the light are considered, the effects of vignetting and filters (aside from surface reflections) has been ignored.

All values are given for 5600 $\overset{o}{A}$ light. The theoretical data is obtained from a CDC 3300 computer using the MULTIFILM program. The practical data are measured values for the anti-reflecting films and estimates for the reflectors. The estimated values are based upon prior knowledge of typical performance.

2.1.4.5 Focus

Means have been provided to insure that ground scenes are properly focused when the MOL altitude is between 75 and 230 nautical miles. At any given altitude the scene remains in focus throughout the scan field without manual refocussing. The eyepiece has a focusing range (manual) from – 2-1/2 to + 3-1/2 diopters to compensate for individual eye differences

between various observers. With linear defocus (moving the image plane off the reticle) the reticle may appear to lose some of its definition, causing the observer's eye to have to re-focus as he concentrates on either the reticle, or the scene. This will be a cause for concern only if the reticle to scene defocus exceeds the depth of field of the eye. The eye has a depth allowance of one-half diopter so that any lesser depth will be within the focusing tolerance.

Defocus errors were calculated by Itek for altitudes of 70 to 230 nautical miles, pitch angles from zero degrees to 70 degrees and roll angles from zero degrees to 45 degrees.

The greatest error of any altitude will be for the maximum pitch and roll.

ALTITUDE	WORST CASE (INCHES)
70	0.0008
80	0.0007
100	0.00056
150	0.00038
230	0.00025

At 80 nautical miles (at high power), the worst case slant range defocus is 0.0007 inch at the objective lens focal plane, corresponding to 0.003 inch at the eyepiece object plane. At 230 nautical miles (at high power), the defocus is 0.00025 inch at the objective or 0.00107 inch at the object plane.

The effects of the curvature of the earth has been calculated on the slant range with the following equation:

$$d = \frac{h + R (1 - \cos \gamma)}{\cos \beta}$$

h = altitude

R = Radius of earth

γ = Geocentric angle to intercept pt.

β = Vehicle centered angle

Beta (β) includes obliquity and stereo factors as well as roll and pitch angles and is measured on a plane through vehicle, earth center and intercept point. Gamma (γ) is on the same plane and is measured as follows:

$$\gamma = \cos^{-1} \frac{A^2 B \pm \sqrt{A^4 B^2 - (A^2 + 1)(A^2 B^2 - 1)}}{A^2 + 1}$$

where

$$A = \tan \beta$$

$$B = \frac{h}{R} + 1$$

The slant range at 70 degrees goes from 215 for a flat earth to 238 on a curved earth, a 10 percent increase. The slant range at 230 nautical miles is 706.5 nautical miles for a flat earth and 708 nautical miles on a curved earth, less than one percent. The 10 percent increase will increase the defocus error by approximately 10 percent and the defocus will then amount to 0.0033.

The defocus is less at higher altitudes, so we need only consider the 80 nautical miles worst case, i.e., 0.0033 at the eyepiece object (reticle) plane.

The defocus effect on the eye of a 0.0033 difference between reticle and image corresponds to a 0.14 diopter error. The depth of field of the eye is 0.5 diopter which is four times as large as the image distance, so no visible effect is predicted.

The requirement for a manual focussing range from - 2-1/2 to + 3-1/2 diopters is met by the mechanical eyepiece design as follows:

The eyepiece of the AO Telescope is specially designed to compensate for residual aberrations of the zoom relay assembly. Because of this, the alignment tolerances are considerably tighter than the standard eyepieces found in military instruments. These tighter tolerances impose a restraint on the design of the focusing mechanism.

SECTION 2.2

ATS CONTROLS

This section presents servo-analysis pertinent to the ATS controls. A description of the operation of the controls is included in Section 1.3.4. The material in this section is sub-divided as follows;

2.2.1   Scanner Controls

2.2.2   Image Orientation Controls

2.2.3   Zoom Control

2.2.4   Blanking Servo

2.2.5   Power Change Servo

2.2.1 SCANNER CONTROLS

2.2.1.1 Requirements Interpretation

The LOS of the acquisition optics shall be driven such that the nominal rate error (drift) is less than 540 microradians/sec at the end of slew. The LOS displacement (jitter) requirement about the nominal LOS is defined in Figure (2.2-1). This requirement must be met when the roll tracking rate is 0.1 degrees/sec or greater and when no vehicle transients are being induced into the vehicle by the Main Tracking Mirror or the ACTS operation.

The interpretation of the jitter requirement is that gimbal displacements at frequencies below 0.032 cps are considered D.C. drifts and above 0.032 cps the gimbal displacements are weighted by the inverse of curve shown in Figure 2.2-1.

The gimbal displacements are determined by relating the noise input (where the noise is defined in terms of its PSD signature) to gimbal displacements. This relationship makes use of a weighting function $F(\omega)$ which normalizes the specified jitter amplitude over the frequency spectrum above 0.2 radians per second and the control loop transfer function $\dfrac{\theta(\omega)}{N(\omega)}$ where $\theta(\omega)$ is the gimbal displacement and $N(\omega)$ is the noise input.

The Power Spectral Density is defined as

$$\varphi(\omega) = \lim_{T \to \infty} \frac{1}{T} \left| \int_{-\frac{T}{2}}^{\frac{T}{2}} f(t)\, e^{-j\omega t}\, dt \right|^2$$

where $f(t)$ is the noise to be analyzed.
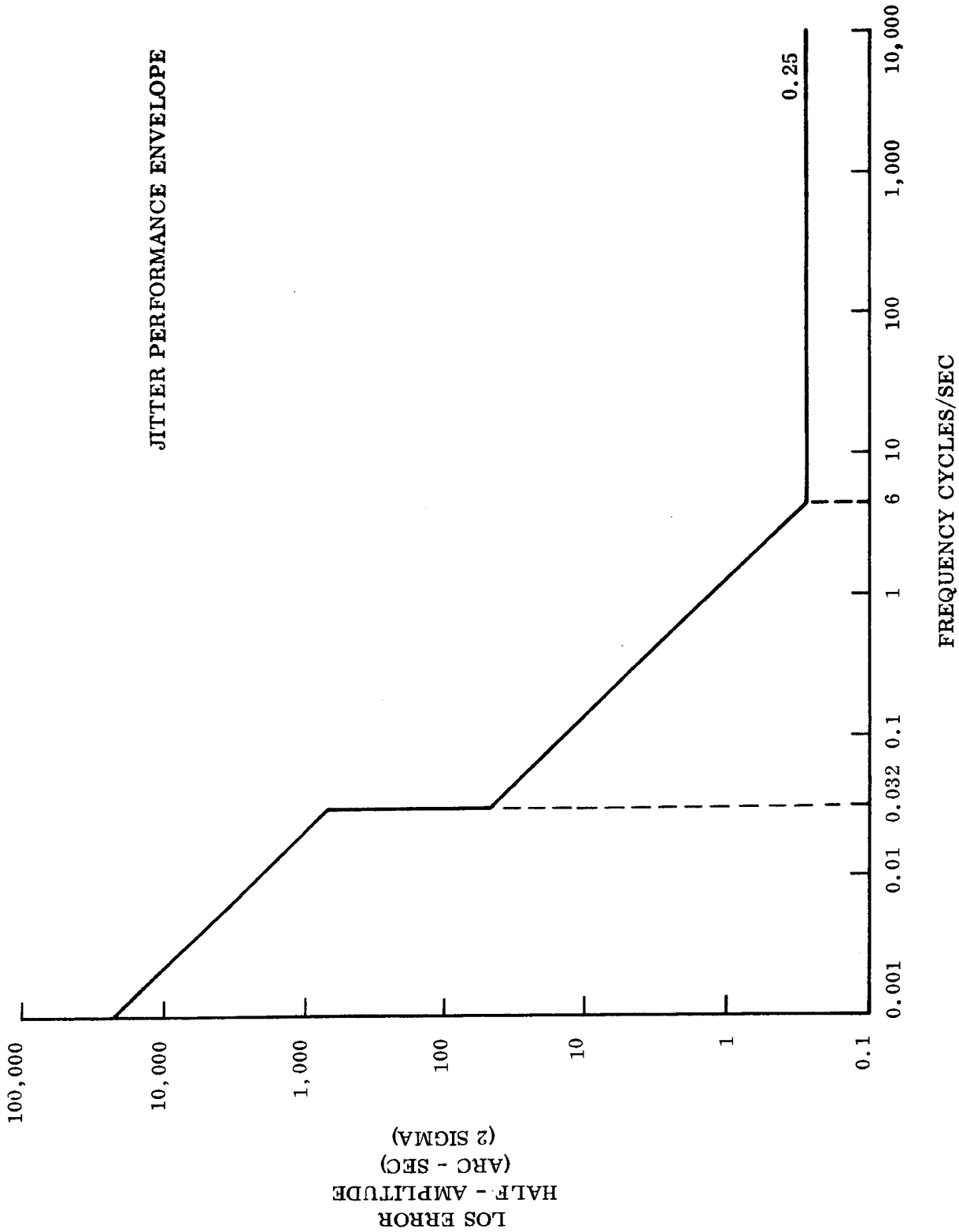
Figure 2.2-1. Jitter Performance Envelope

The weighting function $F(\omega)$ is defined as

$$F(\omega) = \frac{0.027S}{(S/37 + 1)}$$

The closed loop transfer function for the gimbal displacement as a function of noise at a specific input point is defined as

$$G(\omega) = \frac{\theta(\omega)}{N(\omega)}$$

The RMS gimbal displacement weighted with respect to the curve of Figure 2.2-1 is determined using the following relationship

$$\theta_{RMS} = \sqrt{\int_{0.2}^{\infty} 2 \left(\Phi(\omega)\right) \cdot \left(F(\omega)\right)^2 \cdot \left(G(\omega)\right)^2 \, d\omega}$$

where

θ = radians of displacement

$$\Phi(\omega) = \frac{(ft\ lbs)^2}{Radian\ per\ second}$$

$$G(\omega) = \frac{Radians}{ft\ lb}$$

$F(\omega)$ = is dimensionless

In determining the optimum servo configuration a "hand off" position was assumed for the crewman. This assumes no noise rejection or D.C. offset removal by the crewman.

2.2.1.2 Discussion of Approaches

In attempting to design the scanner control loop to meet the stated requirements, three servo configurations are synthesized and evaluated. The three configurations are:

    a.   Rate control loop

    b.   Position control loop

    c.   Combination position and rate control loop

The rate loop configuration utilizes a gyro on the gimbal to sum the command and gimbal rates. The input to this loop is a rate command.

The position loop which is the least complex of the three considered, utilizes position feed-back via a position encoder. The same encoder is used in the slew configuration. The gimbal rate commands are integrated by digital techniques and the input to this loop is a position command.

The position and rate configuration consists of a position loop with feedback via a position encoder on the gimbal. This configuration has a rate minor loop with feedback via a rate gyro on the gimbal. This configuration is the most complex of the three configurations considered, but offers the greatest flexibility with respect to minimizing extraneous inputs.

The bandwidths of the configurations considered allow only one of the tracking configurations to be made part of the slew configuration during the slew mode of operation.

The following three sections discuss the performance of each of the configurations in detail with respect to the scanner tracking mode requirements.

As a result of the studies of the three servo configurations it is concluded that a position plus rate servo configuration for the pitch axis and a rate servo configuration for the roll axis allows the following:

a. The jitter requirement to be met (see Table 2.2-1).

b. Provides flexibility for changing gains and bandwidths to minimize noise inputs as these become defined.

c. Low sensitivity to errors in the command signal resulting from vehicle disturbances.

The following three sections discuss the performance of each of the configurations in detail with respect to scanner tracking mode requirements.

2.2.1.3 Rate Control Servo Configuration

The rate control configuration is shown in Figure 2.2-2 and ultilizes a rate gyro to make the summation of the command rate $(\dot{\theta}i)$ and the gimbal rate $(\dot{\theta}G)$ to develop the rate error signal $(\dot{\theta}e)$ where $\dot{\theta}e = \dot{\theta}i - \dot{\theta}G$.

The open loop GH has a crossover frequency of 150 radians per second and allows the command signal to be followed with a dynamic error of less than 5 microradians per second. The crossover frequency was selected using the curves of Figures 2.2-2 and 2.2-3.

The following analysis was used to determine the dynamic error.

2.2.1.3.1 Rate Loop Dynamic Error

The dynamic servo error will be less than 10 μ radians per second during the rate mode. This is determined from an analysis of the input function generated during the rate mode. The equivalent inputs are determined considering the derivatives of a sinusoidal input.

~~SECRET~~ **SPECIAL HANDLING**
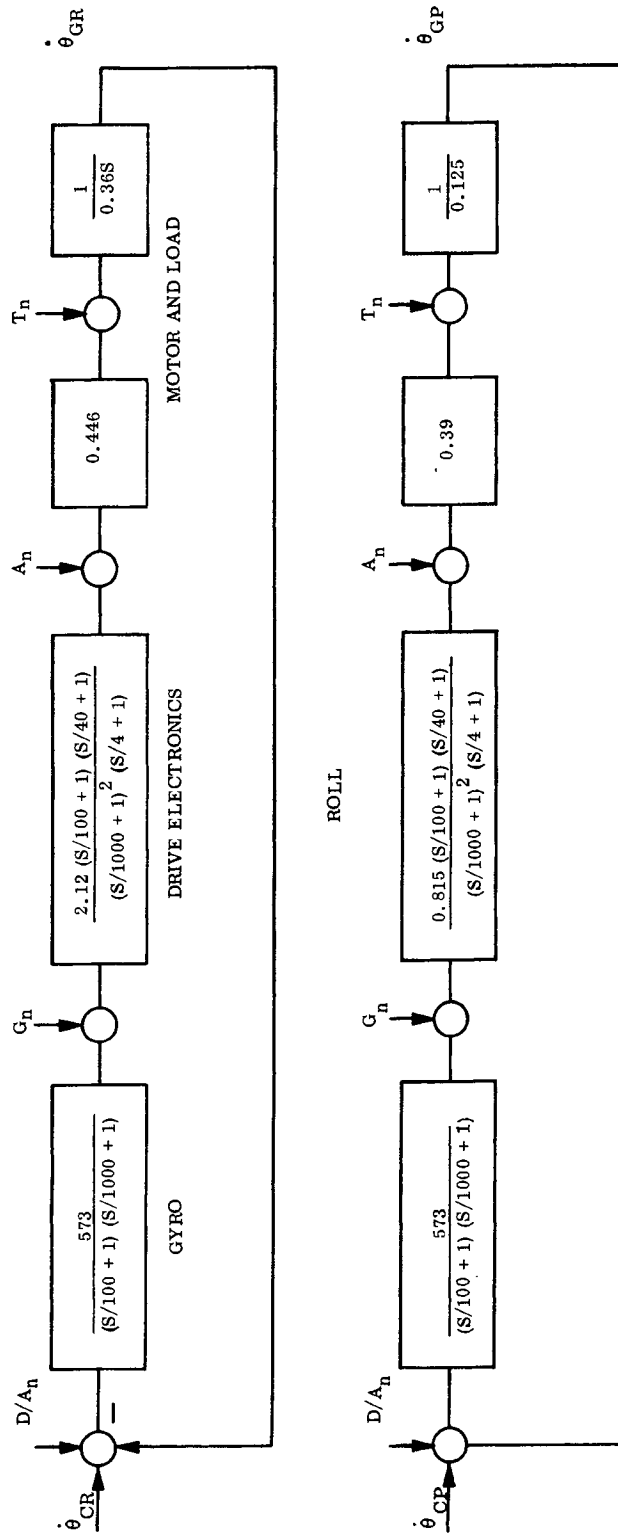
Figure 2.2-2. Rate Servo Configuration
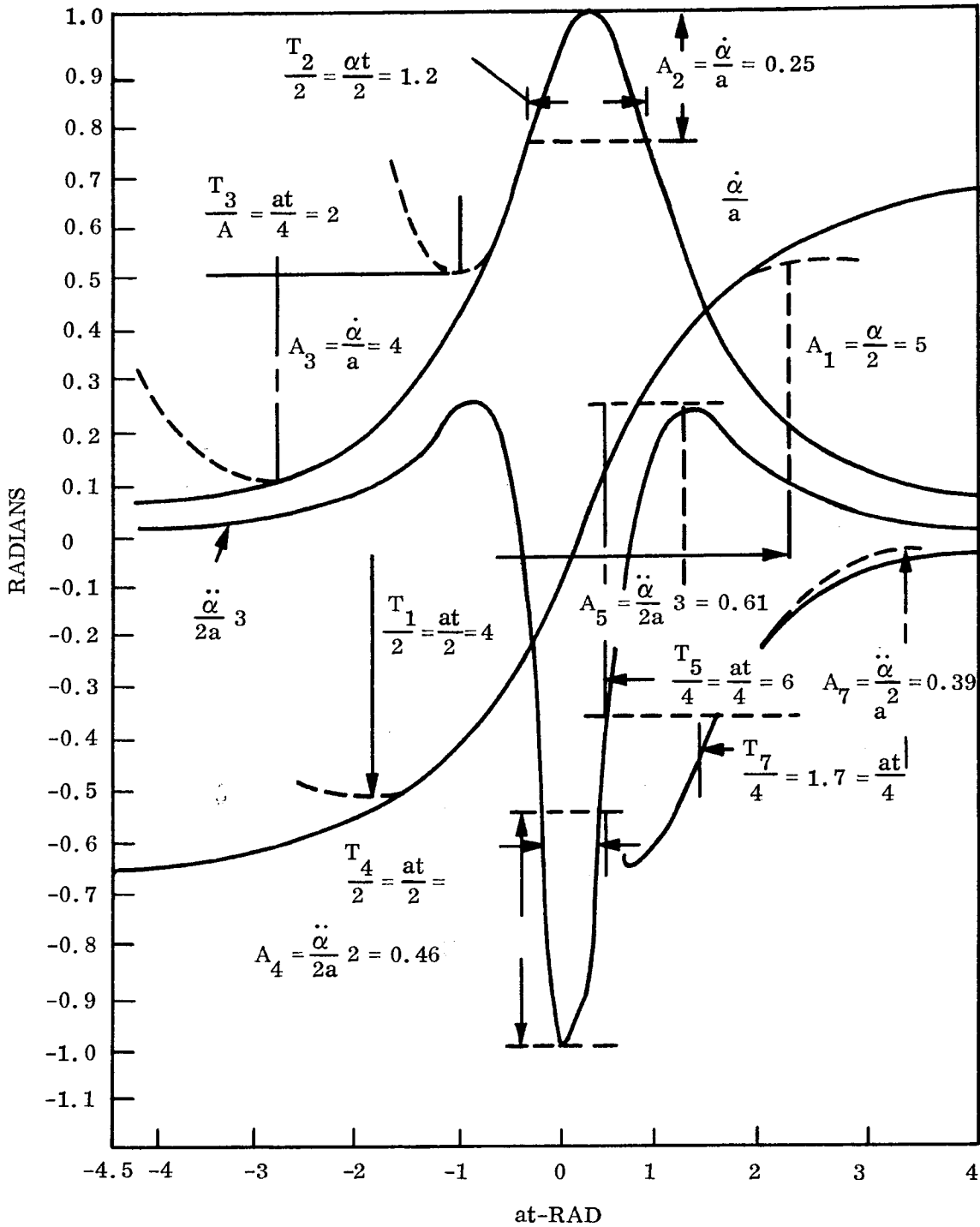
~~SECRET~~ **SPECIAL HANDLING**

Figure 2.2.-3. Plot of $\frac{\alpha}{2}$, $\frac{\dot{\alpha}}{2}$, $\frac{\ddot{\alpha}}{2}$, $\frac{\dddot{\alpha}}{2a^3}$

If

$$\dddot{\theta} = \overset{M}{\dddot{\theta}} \sin \omega t$$

$$\ddot{\theta} = \frac{\overset{M}{\dddot{\theta}}}{\omega} \cos \omega t$$

$$\dot{\theta} = \frac{\overset{M}{\dddot{\theta}}}{\omega^2} \sin \omega t$$

$$\theta = \frac{\overset{M}{\dddot{\theta}}}{\omega^3} \cos \omega t$$

Therefore the equivalent position amplitudes of the derivatives are

$$\theta_s = \frac{\overset{M}{\dddot{\theta}}}{\omega^3}$$

$$\theta_A = \frac{\overset{M}{\ddot{\theta}}}{\omega^2}$$

$$\theta_R = \frac{\overset{M}{\dot{\theta}}}{\omega^3}$$

Where $\overset{M}{\dot{\theta}}$, $\overset{M}{\ddot{\theta}}$, $\overset{M}{\dddot{\theta}}$ are the half amplitudes of the sinusoidal portions of those derivatives and $\omega = \frac{2\pi}{T}$ where T is the period of the equivalent sinusoid. If the fundamental position signal and the derivatives occur at the same time the equivalent sinusoid must be considered to be impressed on the system at the same time and hence the error are additive also. The split should be made so that the total error at that time, t, does

~~SECRET~~ **SPECIAL HANDLING**

not exceed the allowable error, but the error split should be balanced to a slope that is realizable (i.e., 0 db/dec, -20 db/dec, -40 db/dec, etc.). If E/R for the system is known the required value of $\frac{C}{E}$ can be determined.
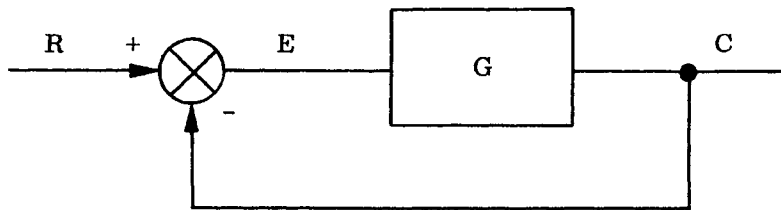
$$R - C = E$$
$$R - E = C$$

For most systems $R \gg E$, therefore $R = C$, and

$$\frac{R}{C} = \frac{C}{E}$$

$$R = M \sin \omega t$$

at max value $R = M$

and $\frac{M}{E} = \frac{C}{E}$

If the input is of such a form that the rate, acceleration, and jerk are not sinusoidal derivates of the position input, the input can be represented by equivalent position inputs

~~SECRET~~ **SPECIAL HANDLING**

which have the characteristics of the several components. The middle range of frequencies of C/E can then be determined so that the error will be within the constraints dictated. When the requirements are written in terms of rate of change of output and input the several components of the actual input can be converted to equivalent rate inputs.

If $\dfrac{SE}{SR}$ = K is required and SE is known, the value of K can be determined by the allowable value of Se and the macimum value of SR.

Since the input is a sum of sinusoidal inputs,

$$\frac{E}{R} = \frac{E_1}{R_1} + \frac{E_2}{R_2} + \frac{E_3}{R_3} \qquad .$$

For sinusoidal inputs of rate are considered and the allowable input is considered to be 1/4 of each component. Figure 2.2-3 shows the curves of $\dfrac{\dot{\alpha}}{2}$, $\dfrac{\ddot{\alpha}}{a}$ and $\dfrac{\ddot{\alpha}}{a^2}$ and $\dfrac{\dddot{\alpha}}{2a^3}$ which were used to determine the following relationships:

Position:

$$A_\omega 1 \quad = \quad 0.0412 \sin 0.0412 \, t \text{ (equivalent rate input)}$$

Rate:

$$A_\omega 2 \quad = \quad 0.013 \sin 0.1372t \text{ (from } \alpha/a)$$

$$A_\omega 3 \quad = \quad 0.021 \sin 0.412t \text{ (from } \dot{\alpha}/a)$$

Acceleration:

$$A_\omega 6 \quad = \quad 0.013 \sin 0.1372t \text{ (from } \ddot{\alpha}/a^2\text{)}$$

$$A_\omega 7 \quad = \quad 0.443 \sin 0.0485t \text{ (from } \ddot{\alpha}/2a^3\text{)}$$

Jerk:

$$A_\omega 4 \quad = \quad 0.00176 \sin 0.275t \text{ (from } \dddot{\alpha}/2a^3\text{)}$$

$$A_\omega 5 \quad = \quad 0.000935 \sin 0.1372t \text{ (from } \dddot{\alpha}/2a^3\text{)}$$

These relations are used to develop the error locus shown in Figure 2.2-4.

The locus indicates a maximum error of 1.6μ rad at 0.137 radians for an unconditionally stable loop with an open loop gain of 10,000 at 0.137 radians and LOS rate inputs. Allowing a line-of-sight error of 5μ radians, the necessary gain at 0.137 radians can be determined. Since the scanner error is equal to 2 x LOS error, the gain (K) required at 0.137 radians is

$$\frac{10}{1.6} = \frac{10,000}{K}$$

$$K = 625$$

Therefore, designing the scanner pitch and roll servos such that the gain at 0.137 radians is a minimum of 1000 insures that a servo dynamic error requirement of 45 μ rad/sec will be met.

~~SECRET~~ **SPECIAL HANDLING**

At - RADIANS ~

$\dot{u}$ RAD/SEC
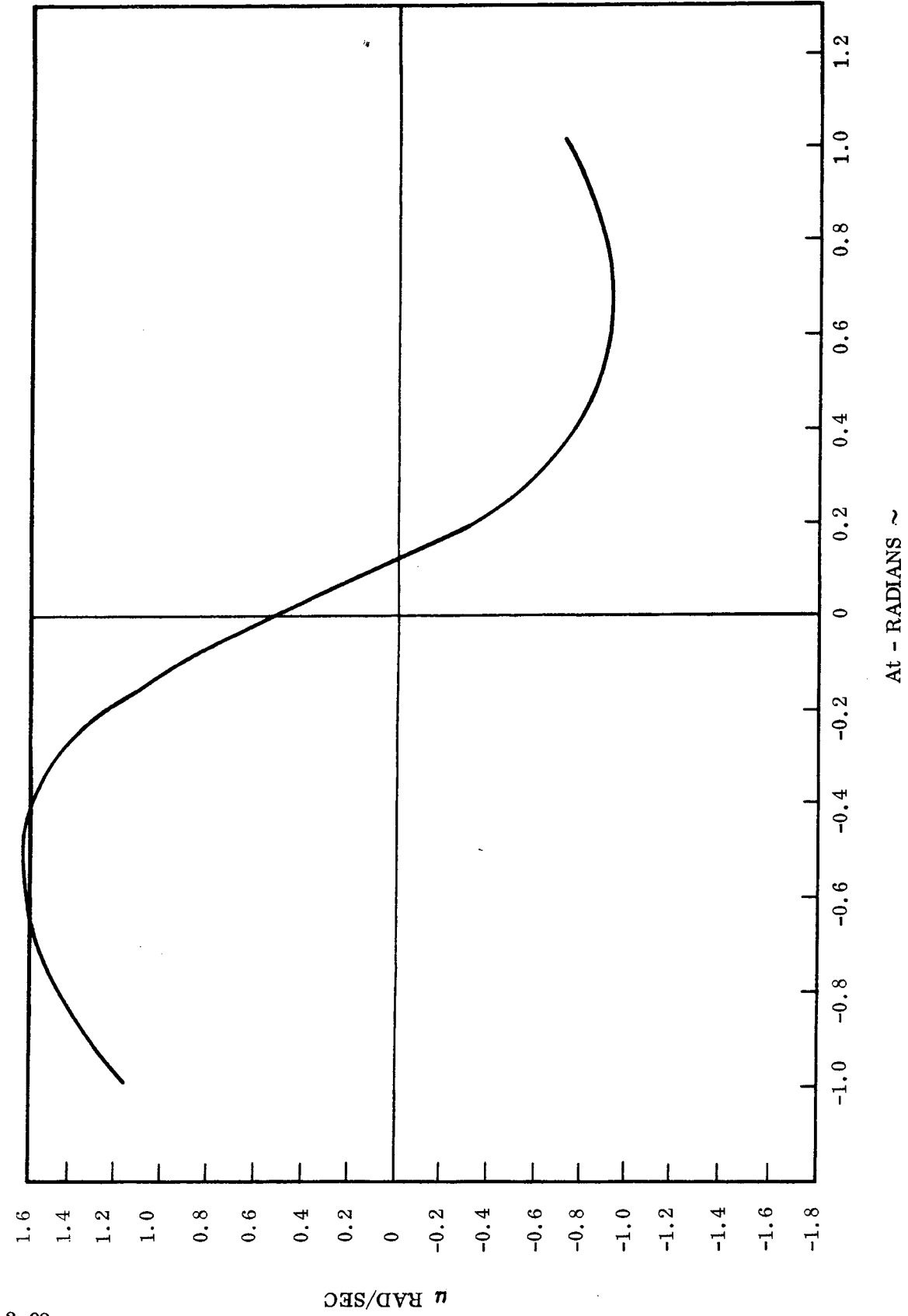
Figure 2.2-4. Error Focus

~~SECRET~~ **SPECIAL HANDLING**

2.2.1.3.2 Jitter Performance

The performance with respect to the requirements of Figure 2.2-1 is evaluated by determining the LOS jitter resulting from the following extraneous inputs.

Bearing Noise (Tn)

Electronic Noise (An)

Gyro Noise (Gn)

Input Noise (D/An)

The contributions of these sources to the total line-of-sight (LOS) jitter error are calculated using their respective Power Spectral Density ($\Phi(\omega)$) characteristics and closed loop transfer function $G(\omega) = \dfrac{\theta(\omega)}{N(\omega)}$ weighted by the function $F(\omega)$.

For the rate configurations of Figure 2.2-2 the error resulting from gyro noise (Gn) is

$$E_{Gn} = 0.206 \times 10^6 \sqrt{2 \int_{0.2}^{2000} \Phi(\omega) \cdot (F(\omega))^2 \cdot \left(\frac{\theta(\omega)}{Gn(\omega)}\right)^2 d\omega} \quad \text{sec}$$

$$= 0.206 \times 10^6 \sqrt{2 \int_{0.2}^{2000} \left(\frac{-162 \text{ db S}}{(S/100+1)(S/300+1)}\right)\left(\frac{-31 \text{ db S}}{(S/37+1)}\right)^2 \left(\frac{-56 \text{ db }(S/100+1)}{S(S/150+1)(S/100+1)}\right)^2 d\omega}$$

$$E_{Gn} = 0.023 \text{ second of arc}$$

The transfer function of the PSD of the gyro noise was taken from a PSD measurement made by Honeywell on a gyro similar to the one selected for the ATS scanner control system.

2-93

The noise at the input due to electronic noise generated in the D/A convertor and buffer amplifier is not known. To make the necessary configuration tradeoffs it was assumed this noise source would not cause an RMS gimbal error of greater than 0.016 arc seconds.

Using this error allotment the allowable RMS value of D/A converter and buffer amplifier noise can be determined as follows:

$$E_{D/A} = \sqrt{2 \int_{0.2}^{2000} \Phi_{D/A}(\omega) \cdot \left(\frac{-31 \text{ db } S}{(S/37+1)}\right)^2 \left(\frac{1}{(S/150+1)(S/1000+1)^3}\right)^2 d\omega}$$

assuming $E_{D/A} = 0.016 \; \widehat{\text{sec}}$

$0.016 \; \widehat{\text{sec}} = 0.0775 \times 10^{-6}$ radians

$$E_{D/A} = \sqrt{\int_{0.2}^{2000} \Phi_{D/A}(\omega) \; d\omega} \quad (2.95)$$

$$(0.0262 \times 10^{-6})^2 = \sqrt{\int_{0.2}^{2000} \Phi_{D/A}(\omega) \; dw}$$

with gyro scale factor of 0.00436 rad/sec/ma and torque resistance of 100 ohms

$$6.8 \times 10^{-16} = \int_{0.2}^{2000} \Phi_{D/A}(\omega) \; d\omega$$

$$6.8 \times 10^{-16} \; rad^2/sec^2 \; x \left(\frac{1}{0.0436}\right)^2 \; volt^2/rad^2/sec^2 = 1.56 \times 10^{-14} \; volts^2$$

$$1.56 \times 10^{-14} \; volts^2 = \int_{0.2}^{2000} \Phi_{D/A}(\omega) \; d\omega$$

If the noise is assumed to be bandwidth limited white noise, where the bandwidth is equal to 2000 radians per second, then the level of the noise is equal to

$$\frac{1.56 \times 10^{-14} \; volts^2}{2000 \; rad/sec} = 0.78 \times 10^{-17} = \frac{0.078 \times 10^{-16} \; volts^2}{rad/sec}$$

This is then the level of noise that will produce a position error of 0.016 arc seconds RMS gimbal error. It should be noted that a roll-off of 30 radians per second at the buffer amplifier could be implemented without affecting loop dynamics in track or slew modes. This will increase the allowable noise at the D/A convertor output and make it much easier to implement.

The allowable noise at the input of the compensating amplifer in the Main Tracking Mirror control loop was assumed to be representative of that which would be present in a rate servo configuration. This noise in terms of bandwidth limited white noise (4.5×10^{-8} volts^2/rad/sec to 2000 rad/sec) was used to determine the position error resulting from electronic noise within the control loop.

The position error resulting from this noise source is:

$$E_{An} = 0.206 \times 10^6 \sqrt{2 \int_{0.2}^{2000} (-147 \text{ db}) \left(\frac{-31 \text{ db } S}{(S/37+1)} \right)^2 \left(\frac{-51 \text{ db } (S/100+1)}{S(S/150+1)(S/1000+1)^2} \right)^2 d\omega}$$

$$E_{An} = 0.022 \text{ sec}$$

This error can be decreased by decreasing the allowable amplifier noise. It should be noted that the allowable noise requirements are much more severe on the buffer amplifier electronics than on the amplifier within the control loop. This is due to the noise rejection, provided by the high gain gyro, to amplifier noise within the control loop.

The bearing noise information on the tracking mirror drive indicates the bearing noise PSD for the Main Tracking Mirror is approximately equal to $\dfrac{-6 \text{ db}}{(S/0.1+1)^2} \dfrac{(\text{ft} - \text{lb})^2}{\text{rad/sec}}$ Assuming the pre-load on the ATS Scanner gimbal bearings is approximately equal to 50 times less than that of the tracking mirror bearings and the bearings are 1/3 as large, the ATS scanner bearing noise PSD signature is assumed to be

$$\Phi(\omega) = \frac{-86 \text{ db}}{(S/0.1+1)^2} \frac{(\text{ft} - \text{lb})^2}{\text{rad/sec}}$$

For the roll servo configuration the error resulting from this bearing noise (E_{Tn}) is equal to

$$\text{Roll } E_{Tn} = 0.206 \times 10^6 \sqrt{2 \int_{0.2}^{2000} \left(\frac{-86 \text{ db}}{(S/0.1+1)^2}\right) \left(\frac{-31 \text{ db } S}{(S/37+1)}\right)^2 \cdot \left(\frac{-75 \ (S/0.4+1)}{S(S/40+1)(S/150+1)}\right)^2 d\omega}$$

$$= 0.014 \ \widehat{sec}$$

$$\text{Pitch } E_{Tn} = 0.206 \times 10^6 \sqrt{2 \int_{0.2}^{2000} \left(\frac{-86 \text{ db}}{(S/0.1+1)^2}\right) \left(\frac{-31 \text{ db } S}{(S/37+1)}\right)^2 \left(\frac{-65 \text{ db } (S/0.4+1)}{(S/40+1)(S/150+1)}\right)^2 d\omega}$$

$$= 0.042 \ \widehat{sec}$$

Figures 2.2-2 and 2.2-3 show the pitch and roll RMS gimbal errors as a function of the bandwidth for lag-lead ratios of 10 to 1 and 100 to 1. It should be noted that the error resulting from the assumed bearing noise PSD can be reduced by a factor of approximately 2 to 1 by increasing the gain and using a 100 to 1 lag-lead network rather than a 10 to 1 lag-lead network.

The error values shown in Table 2.2-1 are based on a 100 to 1 lag-lead ratio. The electronic noise error shown in Figures 2.2-5 and 2.2-6 is based on a white noise input to the electronics in the loop and the bandwidth is changed by changing the amplifier gain.

Figure 2.2-6a shows the open loop frequency response and Figure 2.2-6b shows the slew loop frequency response with the rate loop incorporated.

The rate loop configuration has the advantage of being able to control the gimbal rates down to the structure level of the drive. It also is the least sensitive, of the three configurations considered, to errors in the rate commands induced by vehicle transient disturbances.

The rate loop configuration has the disadvantage of providing less bearing noise rejection than either of the other configurations studied. It also requires that the D/A convertor noise be less than the configurations with the D/A convertor inside the servo loop.

~~SECRET~~ **SPECIAL HANDLING**

TABLE 2.2-1. RATE SERVO CONFIGURATION ERROR SUMMARY
(JITTER PERFORMANCE)

ERROR SOURCE	PITCH AXIS	ROLL AXIS
Bearing Noise	0.043 sec	0.0143 sec
Gyro Noise	0.023 sec	0.023 sec
Loop Electronic Noise	0.016 sec	0.016 sec
Input Noise (D/A)	0.022 sec	0.022 sec

RMS Gimbal Error 0.054 sec 0.0375 sec

RMS LOS 0.1105 sec

2σ LOS 0.221 sec

I_p = 0.12, 0.36, 0.08

100:1 lag-lead

150 rad/sec ω_e

~~SECRET~~ **SPECIAL HANDLING**

$$GH = \frac{K\,(S/40 + 1)}{S(S/4 + 1)\,(S/1000 + 1)^3}$$
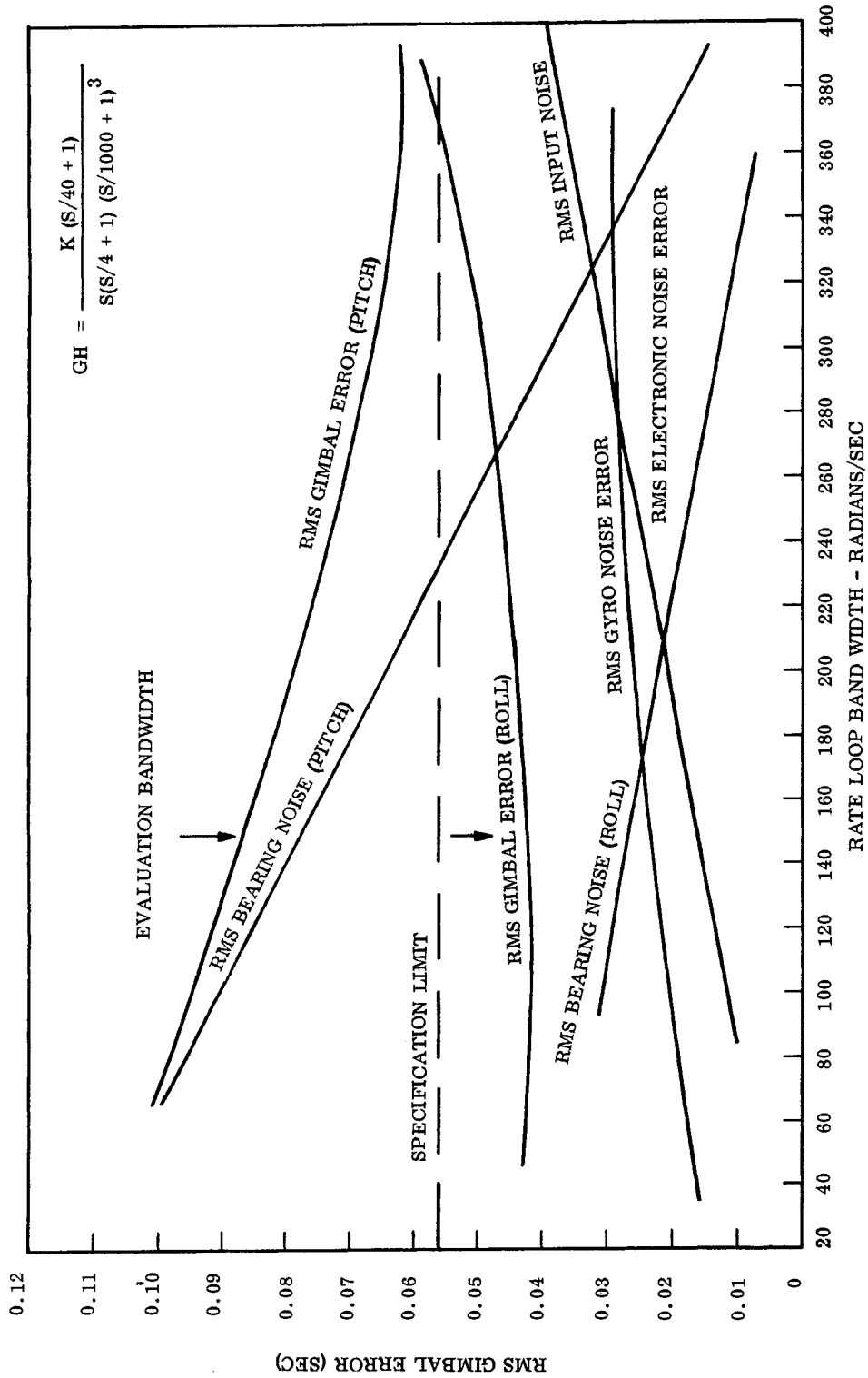
Figure 2.2-5. Rate Configuration (Jitter Performance)
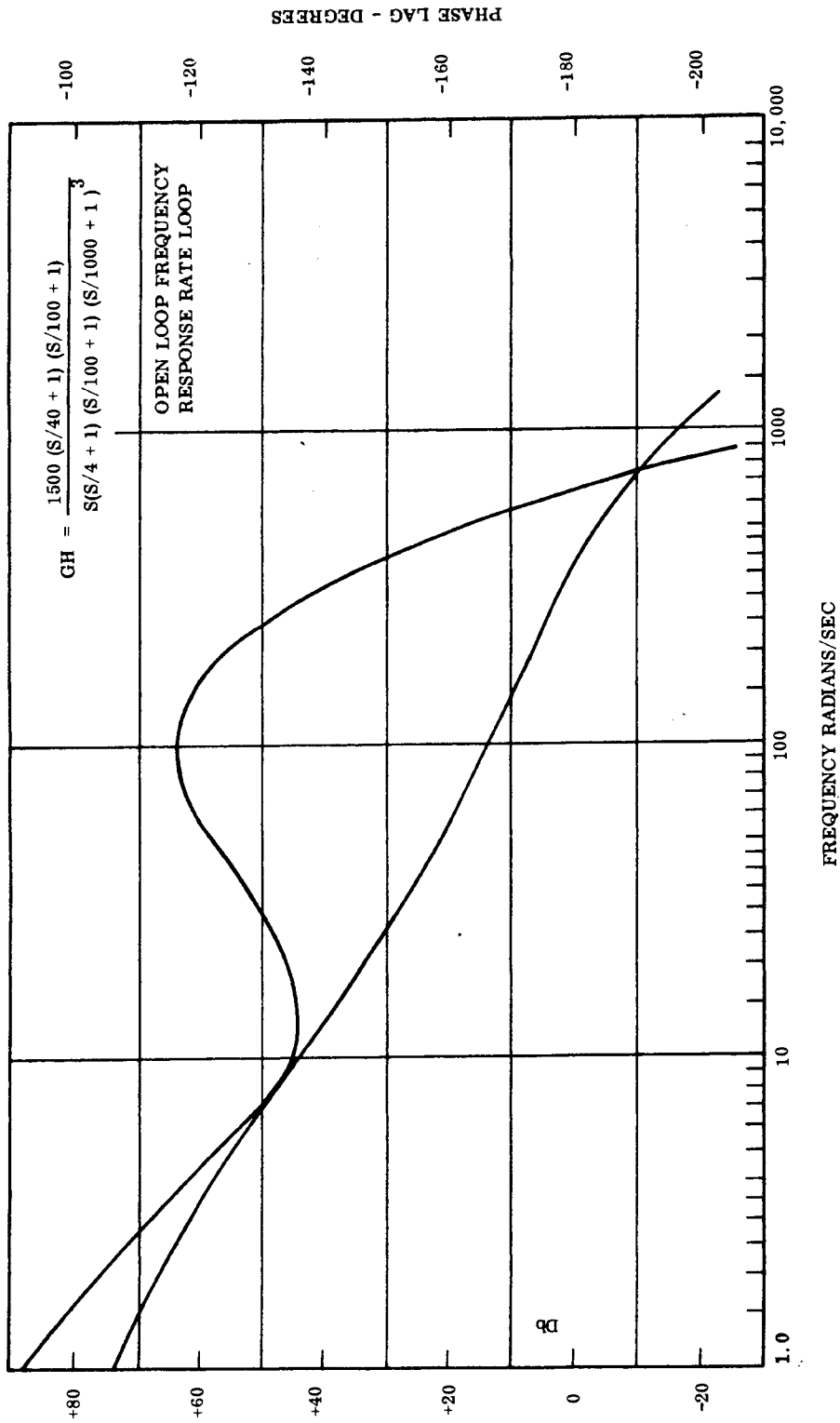
Figure 2.2-6. Rate Configuration (Jitter Performance)

$$GH = \frac{1500 \, (S/40 + 1) \, (S/100 + 1)}{S(S/4 + 1) \, (S/100 + 1) \, (S/1000 + 1)^3}$$

OPEN LOOP FREQUENCY
RESPONSE RATE LOOP

$$GH = \frac{K(S/40 + 1)}{S(S/0.4 + 1)(S/1000 + 1)^3}$$
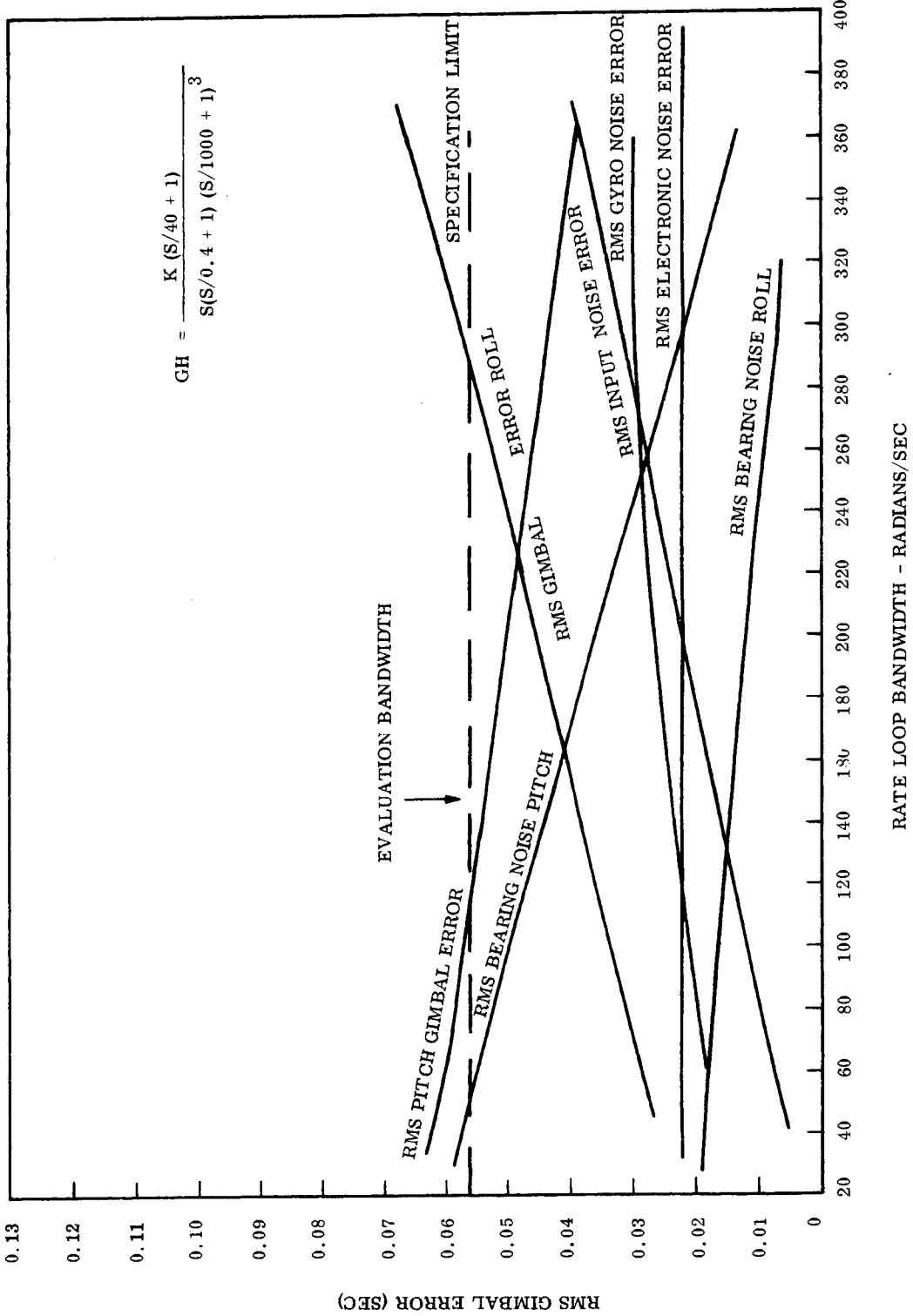
Figure 2.2-6a. Open Loop Frequency Response Rate Loop (10 to 1 Lag-Lead)

2-101

~~SECRET~~ **SPECIAL HANDLING**
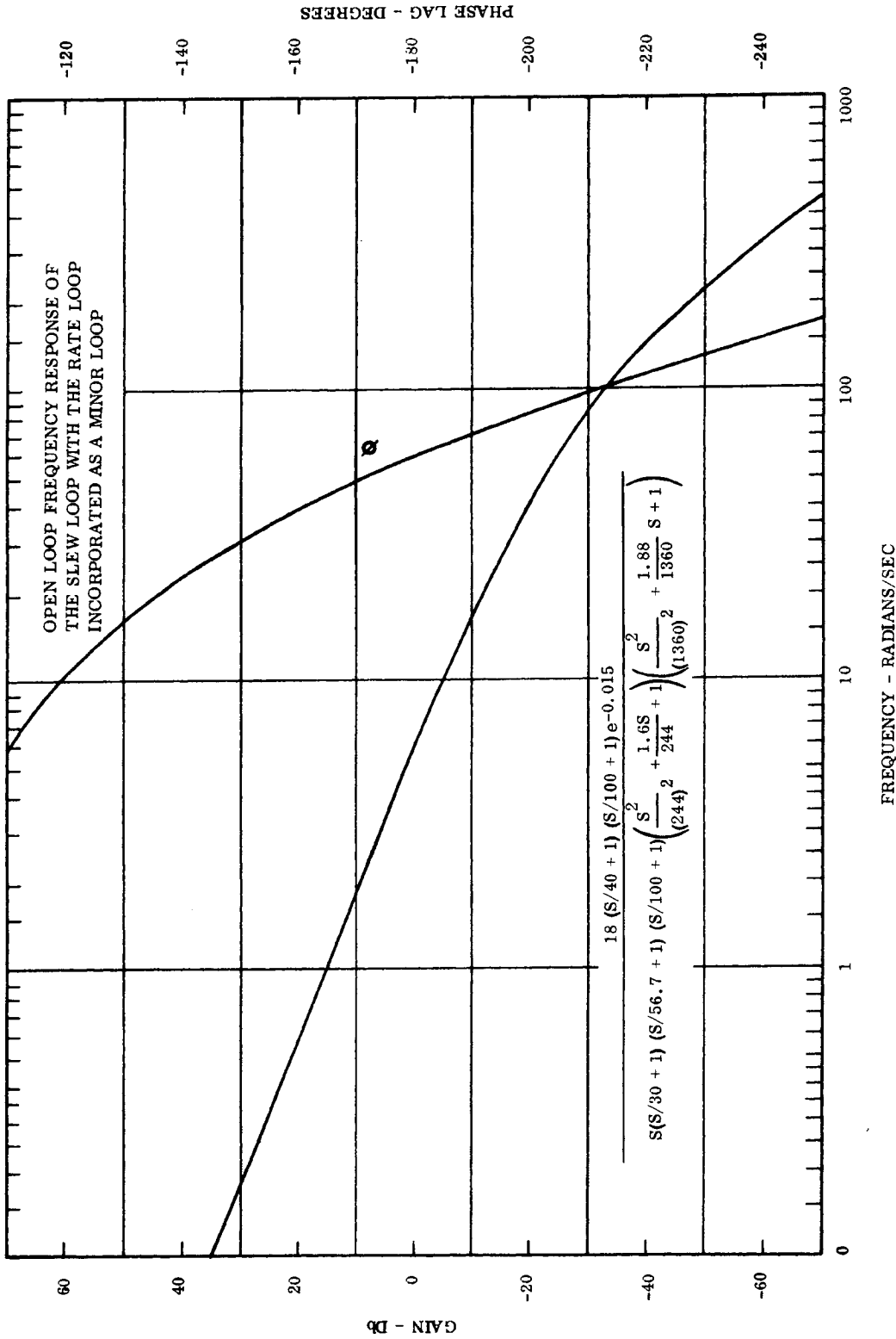
Figure 2.2-6b. Rate Configuration (Jitter Performance)

OPEN LOOP FREQUENCY RESPONSE OF
THE SLEW LOOP WITH THE RATE LOOP
INCORPORATED AS A MINOR LOOP

$$\frac{18\,(S/40 + 1)\,(S/100 + 1)e^{-0.015}}{S(S/30 + 1)\,(S/56.7 + 1)\,(S/100 + 1)\left(\dfrac{S^2}{(244)^2} + \dfrac{1.6S}{244} + 1\right)\left(\dfrac{S^2}{(1360)^2} + \dfrac{1.88}{1360}\,S + 1\right)}$$

~~SECRET~~ **SPECIAL HANDLING**

2.2.1.4 Position Servo Configuration

The position servo configurations are shown in Figure 2.2-7. A bandwidth of 60 radians per second in pitch and 30 radians per second in roll was selected for the position servo configurations.

The selected bandwidths allow the scanner tracking control loop to be incorporated into the slew servo configuration as a minor servo loop. This allows the transistion from slew to track mode to be made with a minimum servo transient.

Figures 2.2-8 and 2.2-9 show the RMS gimbal error in pitch and roll as a function of the position configuration bandwidth. The open loop frequency response of the servo loops is shown in Figures 2.2-10 and 2.2-11. The loops have an approximate gain of 50,000 and 13,000 at 0.15 radians per second in pitch and roll respectively

Figures 2.2-12 and 2.2-13 show the open loop frequency response of pitch and roll slew servo loops with the position servo configuration of the tracking loops incorporated as minor loops.

For the position configurations of Figure 2.2-7, the error resulting from the assumed bearing noise PSD is:

$$\text{Pitch (ETn)} = 0.206 \times 10^{6} \sqrt{2 \int_{0.2}^{2000} \frac{-86 \text{ db}}{(S/0.1+1)^{2}} \left(\frac{-31 \text{ dbs}}{(S/37+1)} \right)^{2} \cdot \left(\frac{-43 \text{ db}}{(S/20+1)(S/60+1)} \right)^{2} dw}$$

$$\text{Roll (ETn)} = 0.206 \times 10^{6} \sqrt{2 \int_{0.2}^{2000} \frac{-86 \text{ db}}{(S/0.1+1)^{2}} \left(\frac{-31 \text{ dbs}}{(S/37+1)} \right)^{2} \left(\frac{-41 \text{ db}}{(S/10+1)(S/30+1)} \right)^{2} dw}$$

2-103

~~SECRET~~ SPECIAL HANDLING
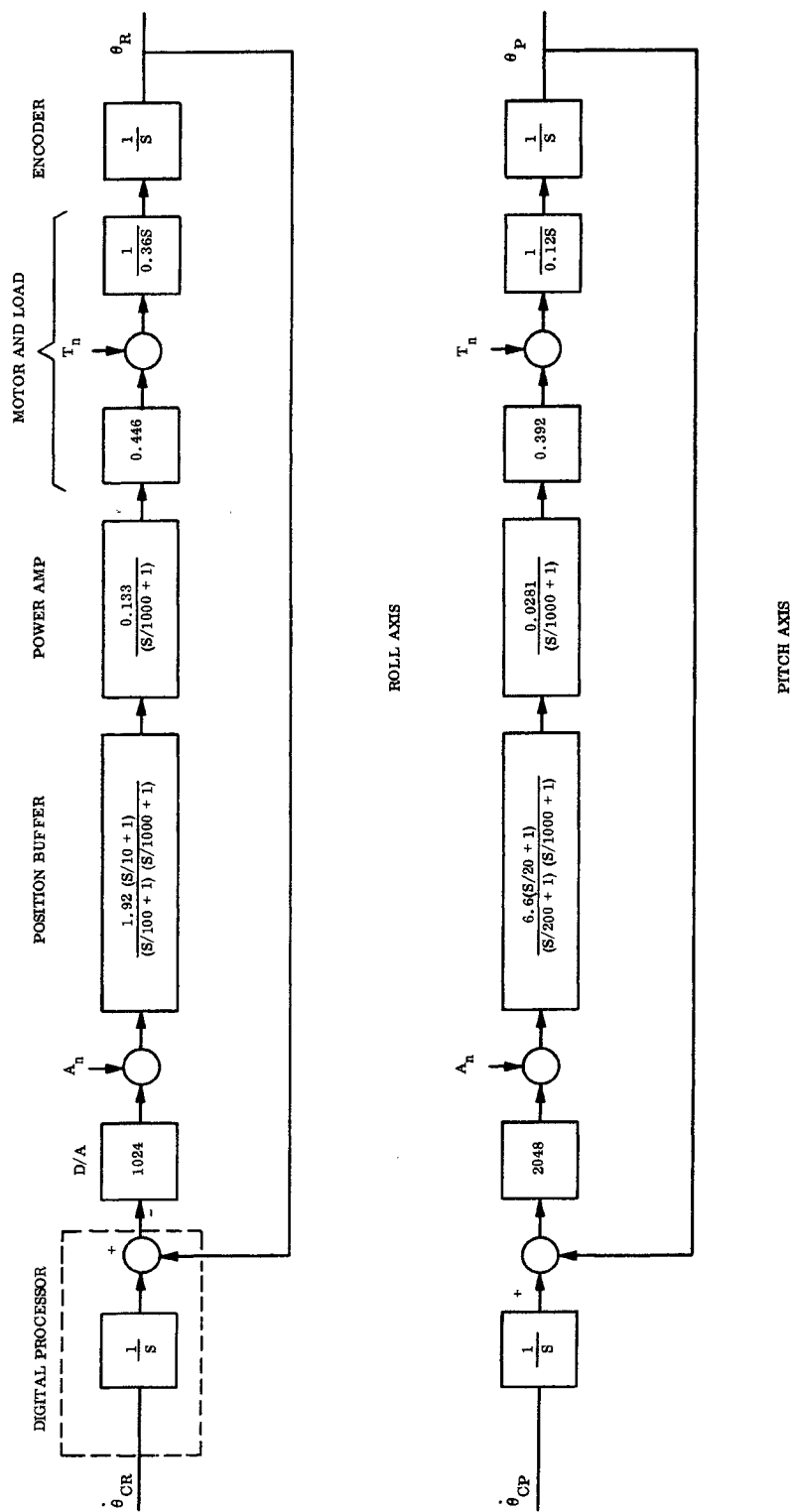
Figure 2.2-7. Position Servo Configurations

~~SECRET~~ SPECIAL HANDLING

~~SECRET~~ SPECIAL HANDLING
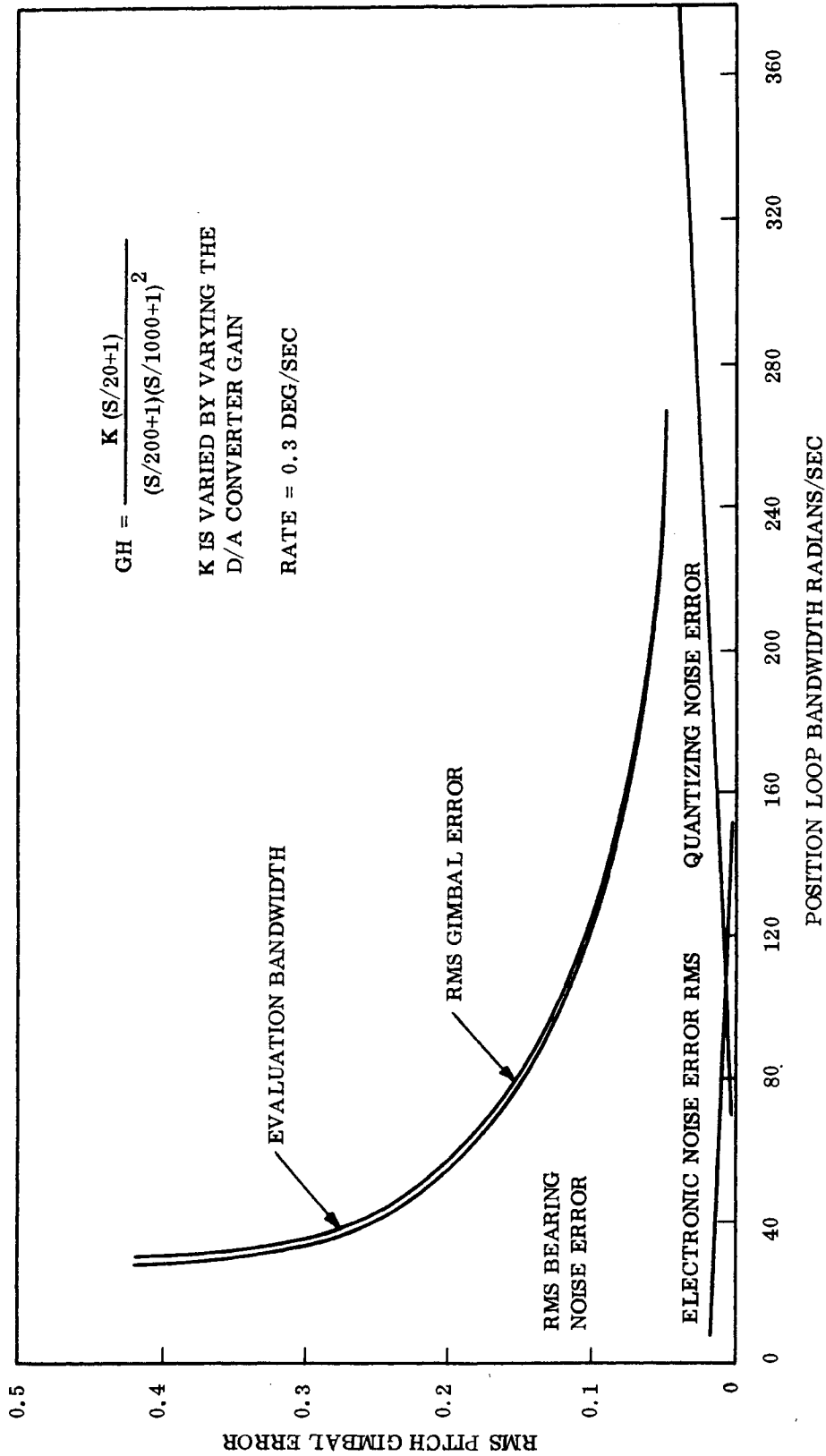
Figure 2.2-8. Pitch Position Servo

~~SECRET~~ SPECIAL HANDLING

$$GH = \frac{K\,(S/10+1)}{(S/100+1)(S/1000+1)^2}$$

RATE = 0.5 DEGREE/SEC
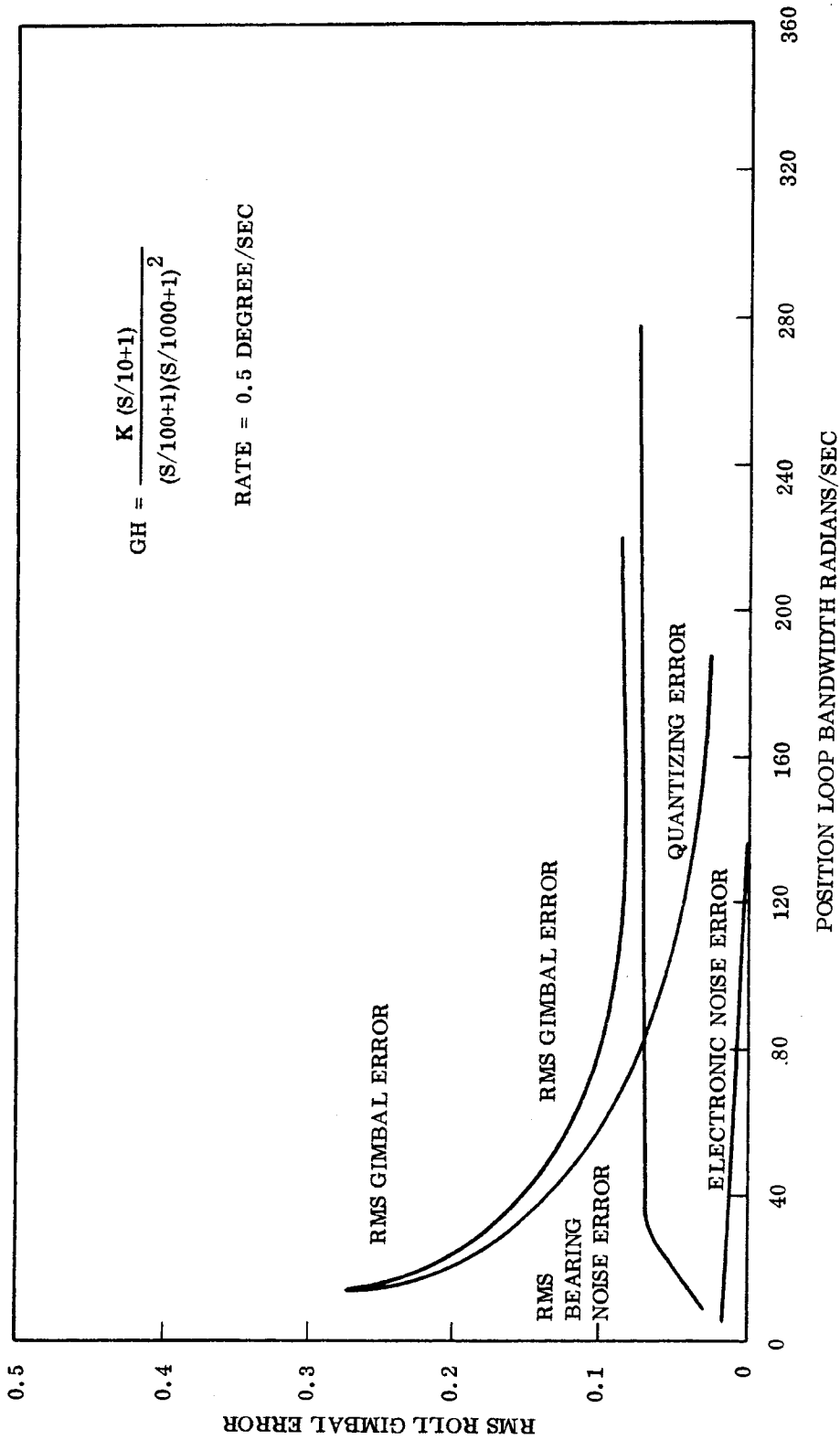
Figure 2.2-9. Roll Position Servo

2-106

$$GH = \frac{1270 \ (S/20+1)}{S^2 \ (S/200+1)(S/1000+1)^2}$$
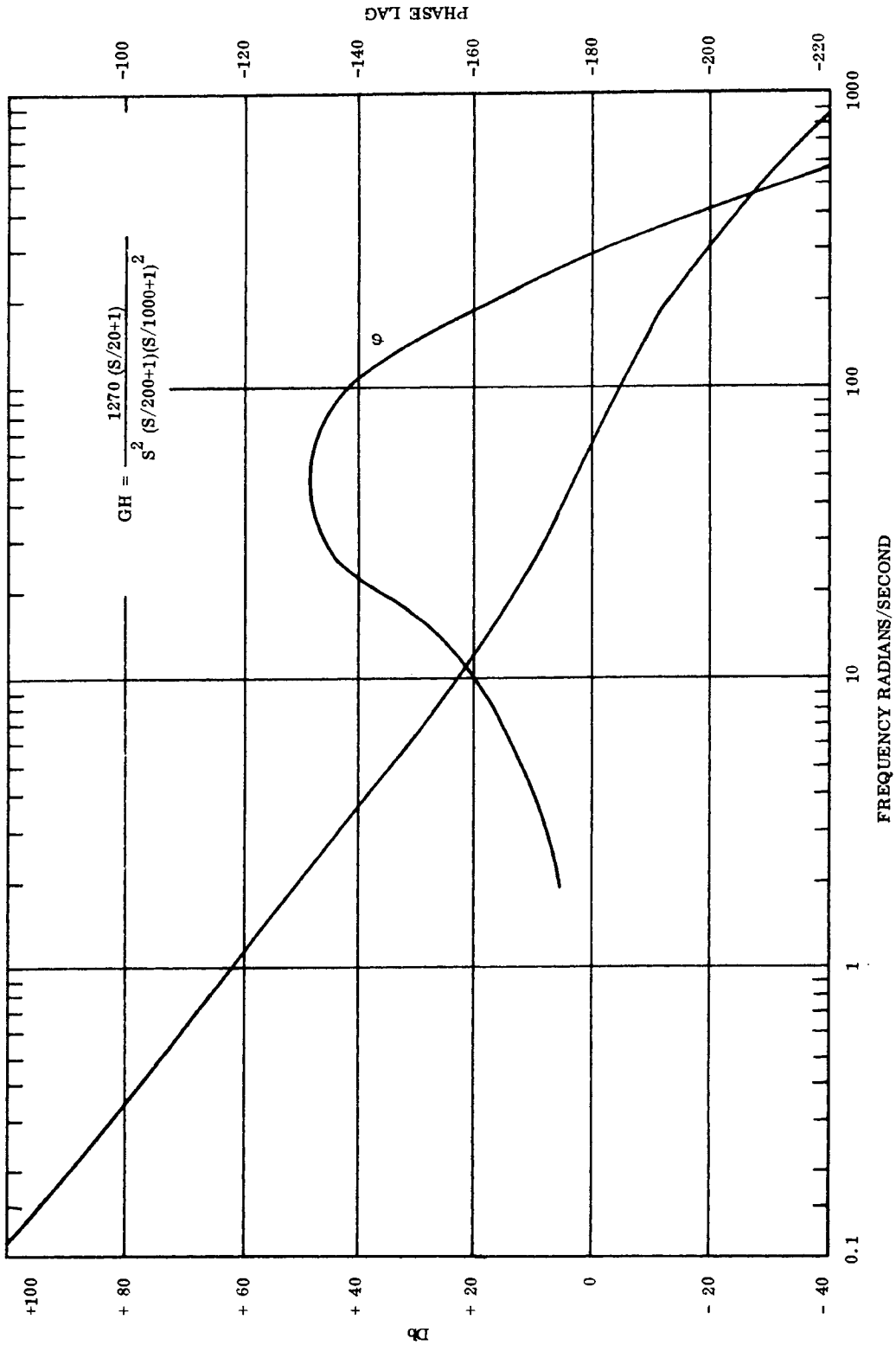
Figure 2.2-10. Open Loop Frequency Response – Pitch Backup Servo

2-107

~~SECRET~~ **SPECIAL HANDLING**

$$GH = \frac{316 \, (S/10+1)}{S^2 \, (S/100+1)(S/1000+1)^2}$$

Figure 2.2-11. Open Loop Frequency Response – Roll Backup Servo

~~SECRET~~ **SPECIAL HANDLING**

$$GH = \frac{18\,(S/20+1)\;e^{-.01s}}{S(S/34.3+1)\left(\dfrac{S^2}{(86.5)^2}+\dfrac{2(0.8)}{86.5}S+1\right)\left(\dfrac{S^2}{(1111)^2}+\dfrac{2(0.92)}{1111}S+1\right)}$$
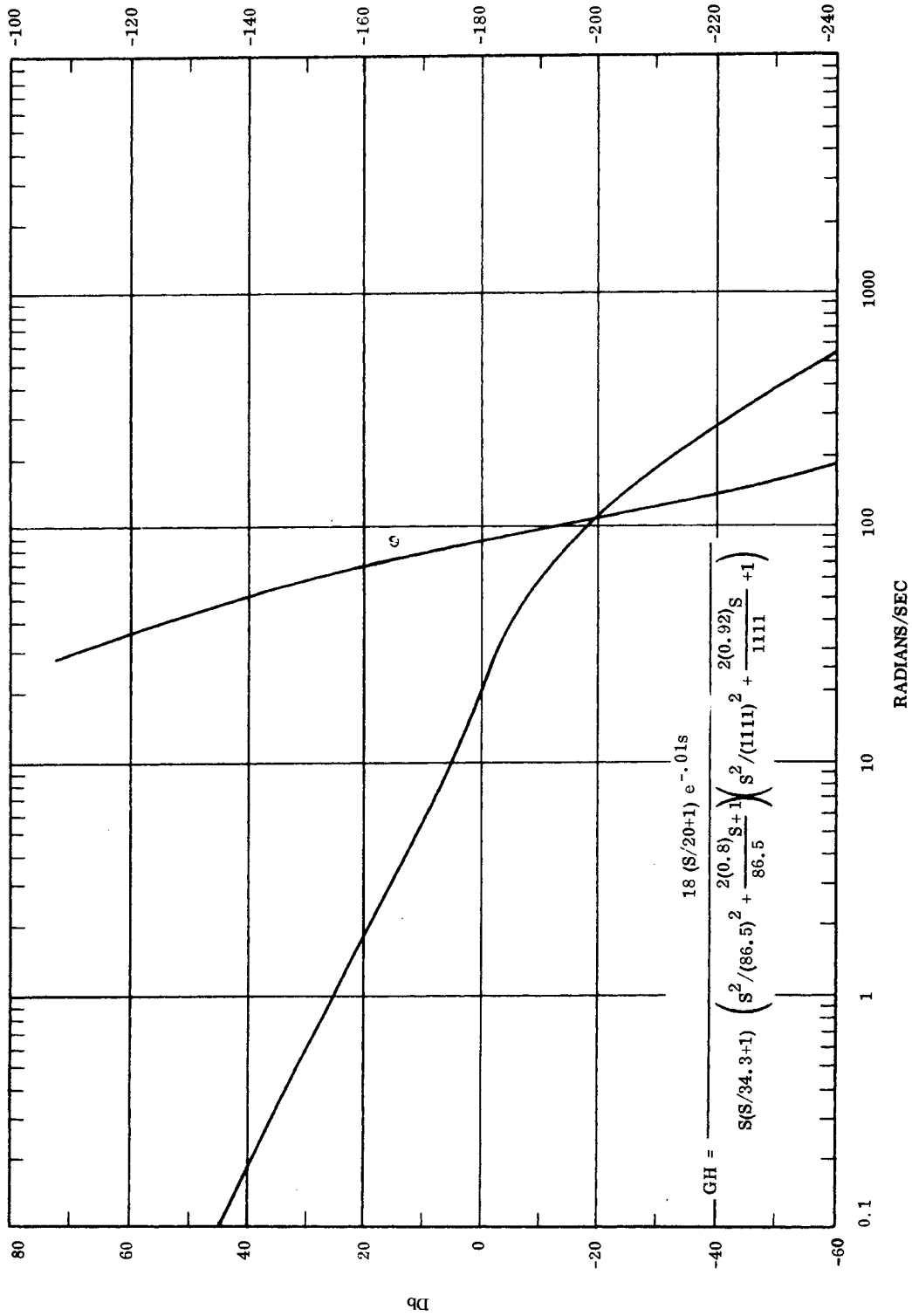
Figure 2.2-12. Pitch Open Loop Frequency Response of Slew Loop with Position Minor Loop
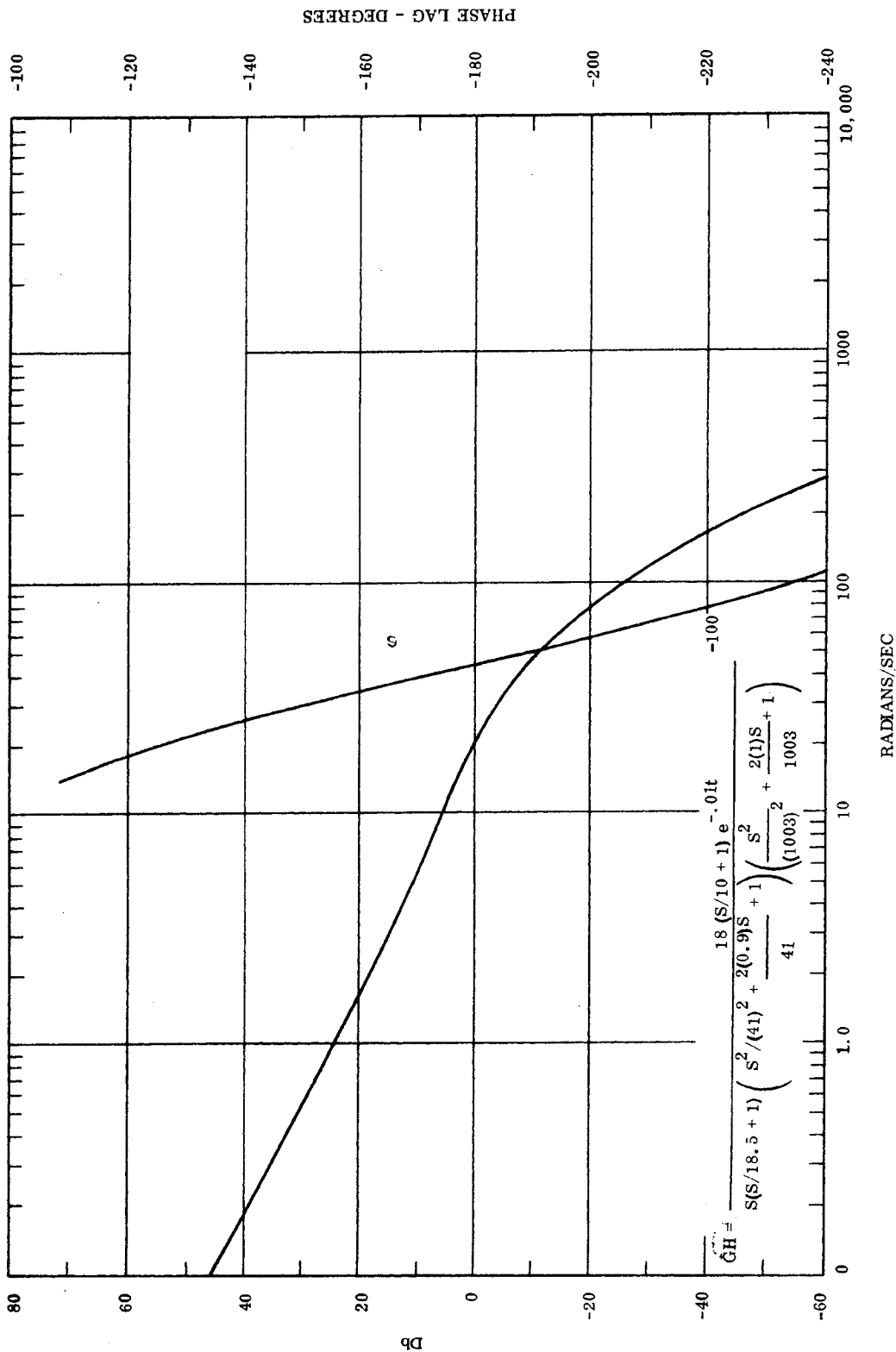
Figure 2.2-13. Roll Open Loop Frequency Response of Slew Loop with Position Minor Loop

Assuming electronic noise in the loop is represented as bandwidth limited white noise at the input to the position buffer amplifier and the allowable position error resulting from this noise is 0.016 seconds of arc. The value of the input noise is

$$\text{Roll (An)} = 0.16 \times 4.85 \times 10^{-6} = \sqrt{2 \int_{0.2}^{2000} \Phi_{An}(\omega) \left(\frac{-31 \text{ dbs}}{S/37+1}\right)^2 \cdot \left(\frac{-60 \text{ db}}{(S/30+1)(S/100+1)}\right)^2 dw}$$

$$0.0775 \times 10^{-6} = \sqrt{\int_{0.2}^{2000} \Phi_{An}(\omega) \, dw \cdot (0.00506)}$$

$$1.52 \times 10^{-5} = \sqrt{\int_{0.2}^{2000} \Phi_{AN}(\omega) \, dw}$$

$$\Phi_{An} = \frac{2.30 \times 10^{-10}}{2000} = 1.15 \times 10^{-13} \frac{\text{Volts}^2}{\text{Radian/Sec}}$$

$$\text{Pitch (An)} = 0.0775 \times 10^{-6} = \sqrt{2 \int_{0.2}^{2000} \Phi_{An}(\omega) \left(\frac{-31 \text{ dbs}}{(S/37+1)}\right)^2 \left(\frac{-66 \text{ db}}{(S/60+1)(S/200+1)}\right)^2 dw}$$

$$0.0775 \times 10^{-6} = \sqrt{\int_{0.2}^{2000} \Phi_{An}(\omega) \, dw \ (0.00454)}$$

$$17.6 \times 10^{-6} = \sqrt{\int_{0.2}^{2000} \Phi_{An}(\omega) \, dw}$$

$$\Phi_{An} = \frac{3.1 \times 10^{-10}}{2000} = 1.51 \times 10^{-13} \frac{\text{Volt}^2}{\text{Radian/Sec}}$$

2-111

It should be noted that the position configuration provides a higher rejection to D/A buffer amplifier noise than does the rate configuration; this permits the design of the buffer amplifier in the position configuration to be less complex than in the rate configuration.

An additional source of jitter in the position configuration that is not present in the rate configuration is the jitter generated by digital summation of the encoder output and position command signal. (See Figures 2.2-13 and 2.2-14.)

The jitter resulting from the generation of the quantized error signal can be calculated by determining the amplitude of the fundamental of the square wave and operating on this with the response of the servo at the error signal quantizing frequency.

For the case of the pitch axis with a 2^{20th} encoder quantum level on the gimbal the quantizing is equal to:

$$\theta_G = \frac{2A}{\pi} \sin \omega \, (D) \; \left[G \right]$$

where G is the attenuation of the control loop at the quantizing frequency.

Assuming (D) = 0.5 (worst case) and the gimbal rate is 0.3 degrees per second, the loop roll off will attenuate the quantizing error by a factor of approximately -100 dg

$$\therefore \; \theta_{GE} = \frac{2 \times 1.25}{3.14} \times 1 \times 0.00001 = 0.00008 \; \text{sec}$$

This error can further be reduced if the input command has a quantum level which is $\leq 1/4$ of the position encoder quantum level. This allows the quantized error signal to approach a triangular wave, the fundamental of which is equal to 0.5 times the fundamental of a square wave.

2-112
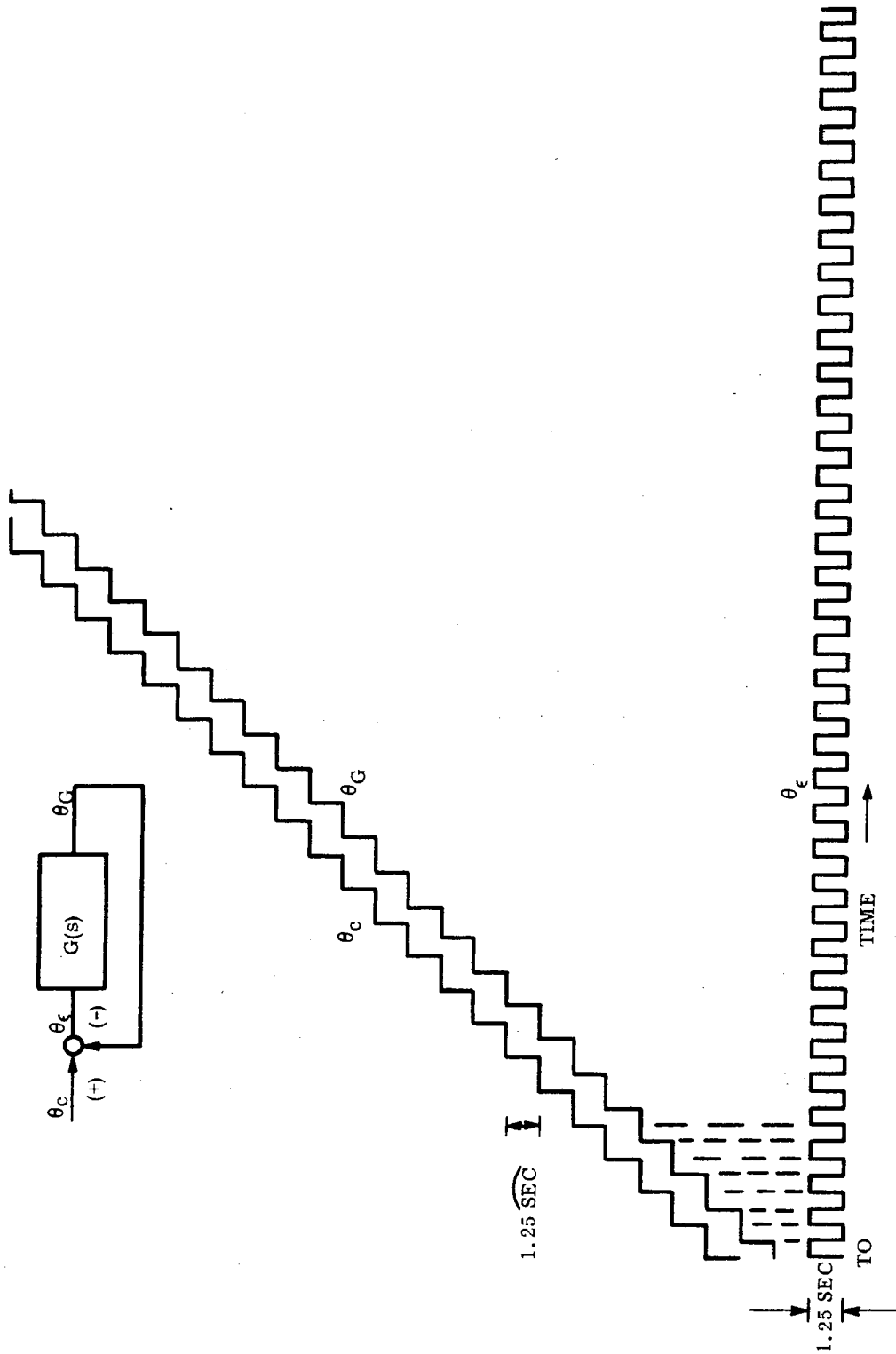
Figure 2.2-14. Generation of Quantized Error Signal

2-113

20 BIT
INPUT

22 BIT
INPUTS
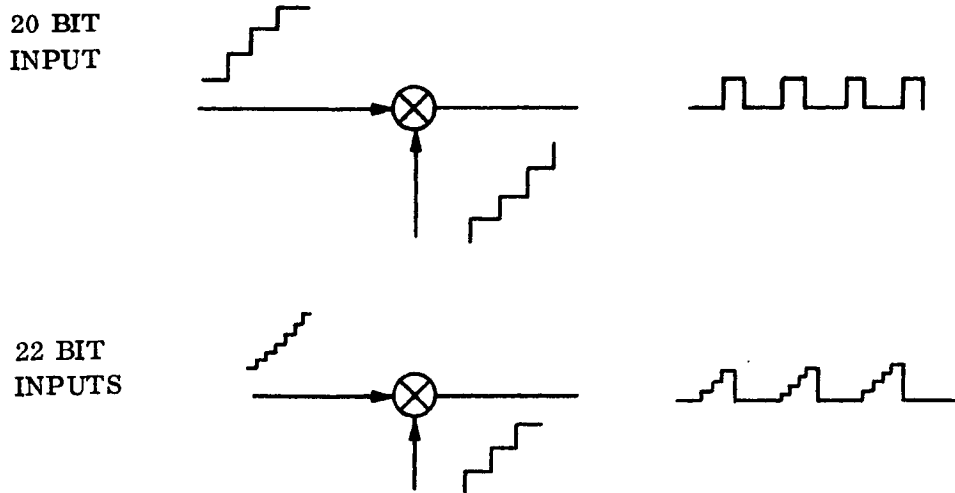
An additional source of error results because the encoder quantum level varies about the nominal value. A digital simulation was run to determine the effects of this bit to bit variation. Figure 2.2-15 shows the servo configuration used in the simulation and the encoder bit distribution which was simulated.

The error resulting from the bit to bit variations can be controlled by controlling the allowable bit variations of the encoder with respect to the nominal quantum level. Using an allowable variation of ±0.1 arc seconds per quantum level with the restriction that the maximum accumulative error never exceeds 0.2 arc second at any time nor 0.1 arc second over any 5 bit interval it is possible to restrict the gimbal jitter to less than 0.0125 second of arc at a gimbal rate of 0.3 degree per second with a 30 radian per second servo bandwidth.

Figure 2.2-16 is a plot of quantizing error as a function of gimbal rate for a 2^{20th} encoder and a 30 radian per second bandwidth. Figure 2.2-17 shows the same error information for a 60 radian per second bandwidth.

~~SECRET~~ **SPECIAL HANDLING**
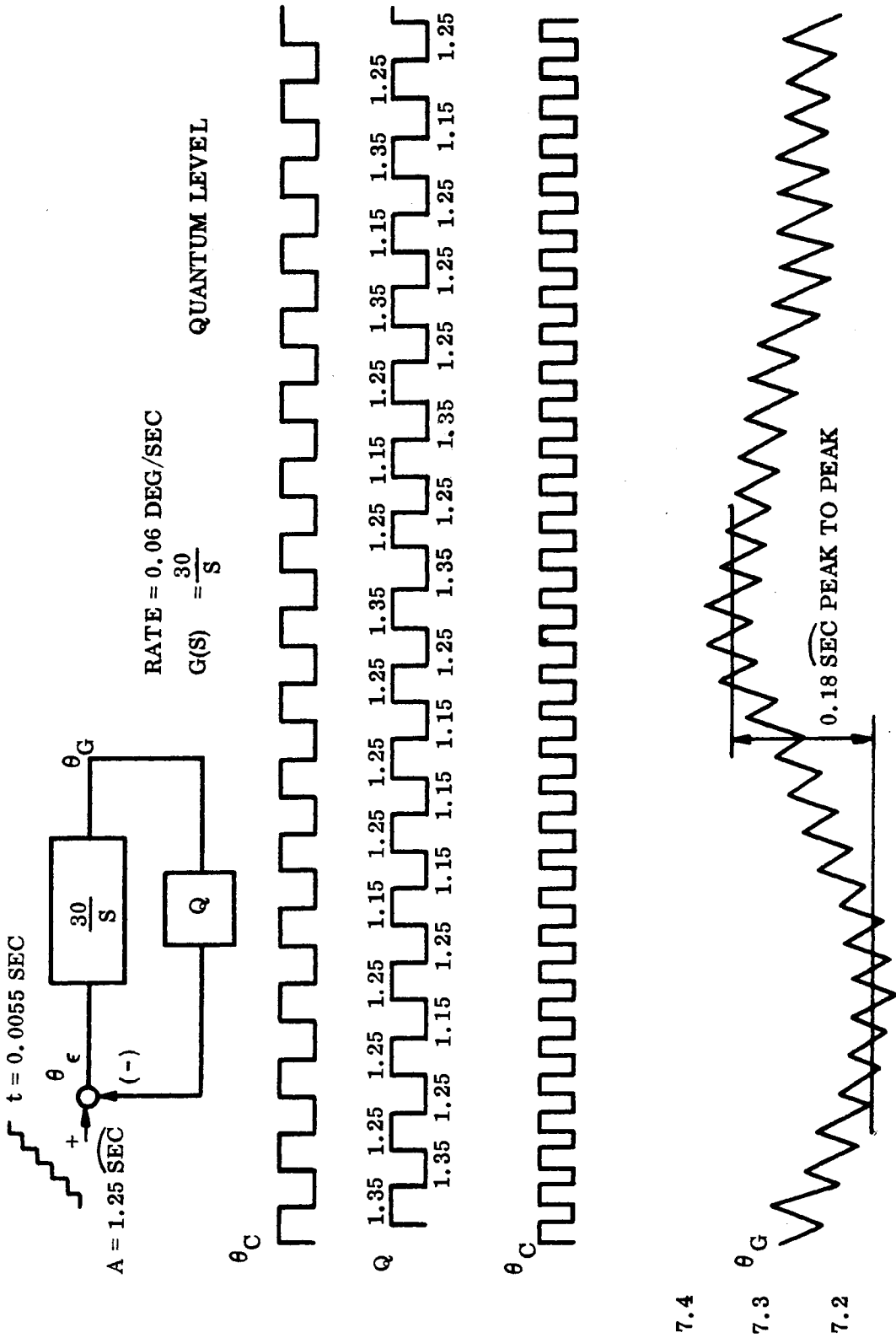
Figure 2.2-15. Simulation of Digital Position Central Loop

~~SECRET~~ **SPECIAL HANDLING**

$$GH = \frac{316\ (S/10+1)}{S^2\ (S/100+1)(S/1000+1)^2}$$
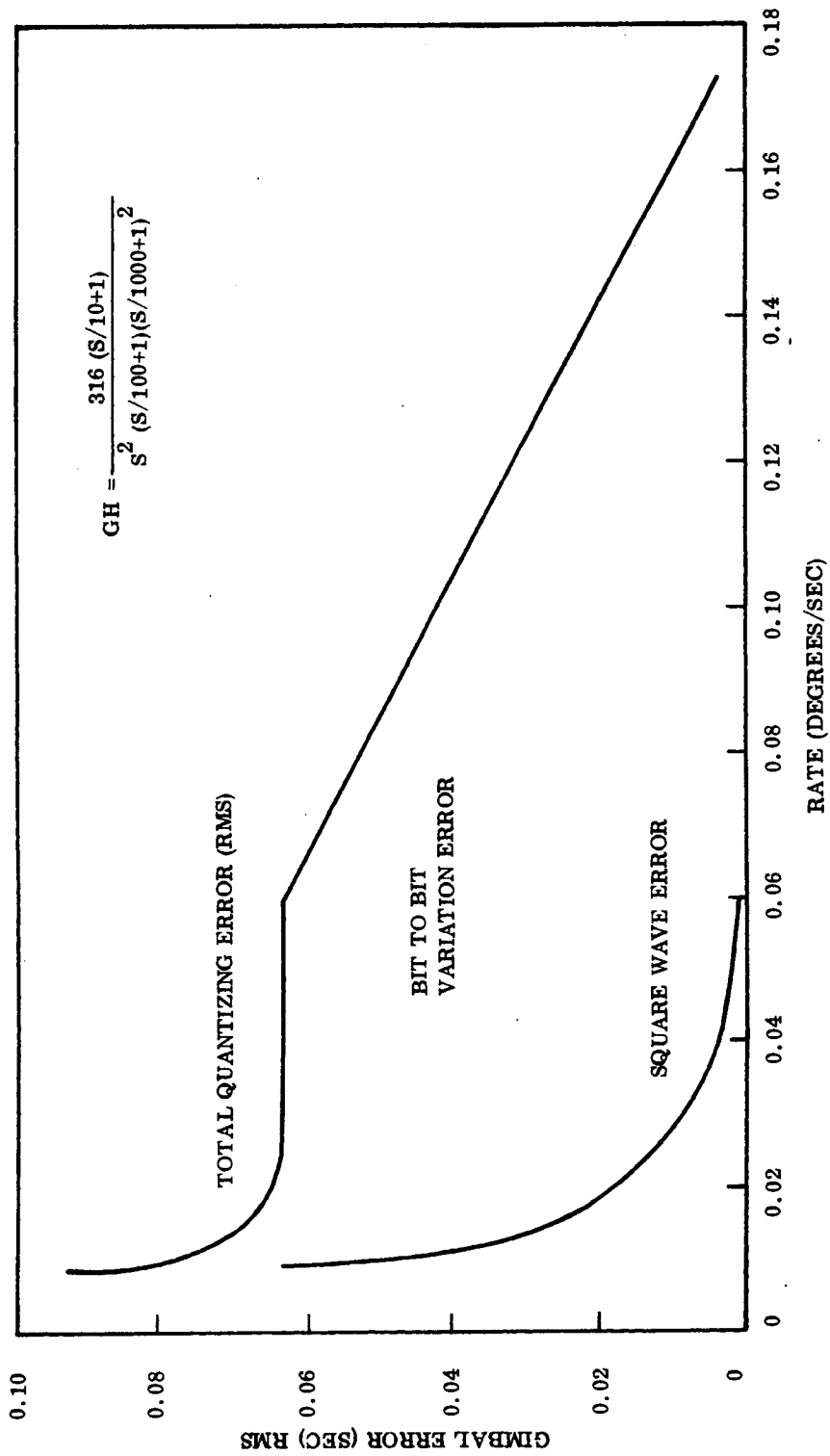
Figure 2.2-16. Roll Quantizing Error -- 2^{20th} Encoder

2-116

$$GH = \frac{1270\ (S/20 + 1)}{S^2 (S/200 + 1)\ (S/1000 + 1)}$$

Figure 2.2-17. Pitch Quantizing Error -2^{20th} Encoder

~~SECRET~~ **SPECIAL HANDLING**

The position servo configuration is the least complex of the three configurations considered and does not require a rate gyro as a sensor. Thus it also uses less power and weighs less than the other two configurations. Position feedback is via the gimbal encoder which is also used in the slew configuration, thus an additional sensor is not required.

The bearing noise rejection characteristic of the position configuration is approximately equal to that of the rate configuration for the bearing noise profile assumed for the trade-off studies:

$$\left(\Phi = \frac{-86 \text{ db}}{(S/0.1+1)^2} \frac{\text{volts}^2}{\text{rad/sec}} \qquad \text{where } 0.1 = 20 \log \text{db} \right)$$

The sensitivity of the position control loops to errors in the rate commands induced by vehicle transient disturbance is the highest of the three configurations considered. Table 2.2-2 shows the tabulated error inputs for the position configurations.

TABLE 2.2-2. POSITION SERVO CONFIGURATION ERROR SUMMARY

ERROR SOURCE	PITCH	ROLL
Bearing Noise	0.18 sec	0.165 sec
Electronic Noise	0.016 sec	0.016 sec
Quantizing Error	0.025 sec	0.062 sec
	RMS Gimbal = 0.182 sec	0.172 sec
	RMS = 0.403 sec	
	2σ = 0.806 sec	

~~SECRET~~ **SPECIAL HANDLING**

2.2.1.5 Position and Rate Servo Configuration

This configuration is shown in Figure 2.2-18. The inner loop is a rate loop with feedback via the gyro and the outer loop is a position loop with feedback from a position encoder. The dynamic error of this configuration with respect to the tracking input command is less than one microradian per second (see Section 2.2.1.3.1).

The performance with respect to the requirements of Figure 2.2-1 is evaluated by considering the following noise error sources:

Bearing Noise (Tn)

Electronic Noise (An)

Gyro Noise (Gn)

Quantizing Noise (Q)

Using the same noise profiles as in the evaluation of the rate and position servo configurations, performance of the rate plus position configuration was determined as follows:

$$EGn = 0.206 \times 10^6 \sqrt{2 \int_{0.2}^{2000} \left(\frac{-162 \text{ db s}}{(S/100+1)(S/300+1)}\right)\left(\frac{-31 \text{ db s}}{(S/37+1)}\right)^2 \left(\frac{-105 \text{ db }(S/1+1)(S/100+1)}{(S/10+1)(S/40+1)(S/150+1)(S/1000+1)^2}\right)^2 dw}$$

$$= 0.022 \text{ sec}$$

$$\text{Pitch } ETn = 0.206 \times 10^6 \sqrt{2 \int_{0.2}^{2000} \left(\frac{-86 \text{ db}}{(S/0.1+1)^2}\right)\left(\frac{-31 \text{ db s}}{(S/37+1)}\right)^2 \left(\frac{-96 \text{ db }(S/4+1)(S/1+1)}{(S/10+1)(S/37+1)(S/30+1)(S/40+1)(S/150+1)}\right)^2 dw}$$

$$= 0.02 \text{ sec}$$

$$\text{Roll } ETn = 0.206 \times 10^6 \sqrt{2 \int_{0.2}^{2000} \left(\frac{-86 \text{ db}}{(S/0.1+1)^2}\right)\left(\frac{-31 \text{ d(s)}}{(S/37+1)}\right)^2 \left(\frac{-106 \text{ db }(S/4+1)(S/1+1)}{(S/10+1)(S/37+1)(S/30+1)(S/40+1)(S/150+1)}\right)^2 dw}$$

2-119

~~SECRET~~ **SPECIAL HANDLING**
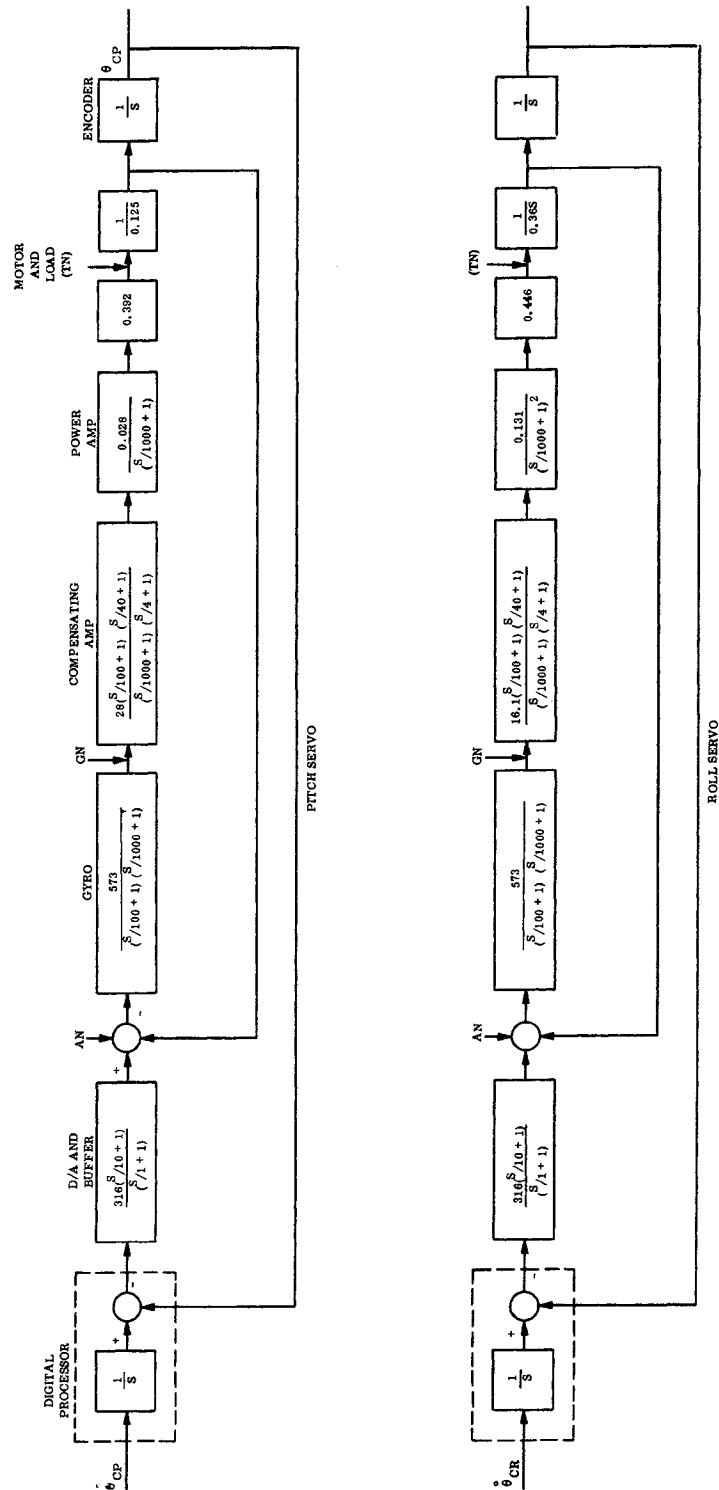
Figure 2.2-18. Position and Rate Servo Configuration

~~SECRET~~ **SPECIAL HANDLING**

Quantizing Noise:

$$\text{Roll} = \sqrt{\left(\frac{0.18}{2.828}\right)^2 + (0.004)^2} = 0.0635 \text{ sec at } 0.05^\circ/\text{sec with a } 2^{20\text{th}} \text{ encoder}$$

$$\text{Pitch} = \sqrt{\left(\frac{0.18}{2.828 \times 5}\right)^2 + (0.00008)} = 0.0125 \text{ sec at } 0.3^\circ/\text{sec with a } 2^{20\text{th}} \text{ encoder}$$

The error due to electronic noise has been assumed to be less than 0.016 seconds of arc for the configurations shown in Figure 2.2-18. This is consistent with the assumed electronic noise error used in the evaluation of the rate and position configurations. To meet this error allotment the electronic noise also is budgeted such that the D/A buffer noise contributes 15/16 of the allowable noise error. This is a reasonable allotment in that the gimbal position is approximately 30 times more sensitive to this noise source than to the noise within the rate minor loop.

Figures 2.2-19 through 2.2-21 show the RMS gimbal error for the pitch and roll control loop with the position plus rate configurations. Table 2.2-3 gives an error tabulation for this servo configuration.
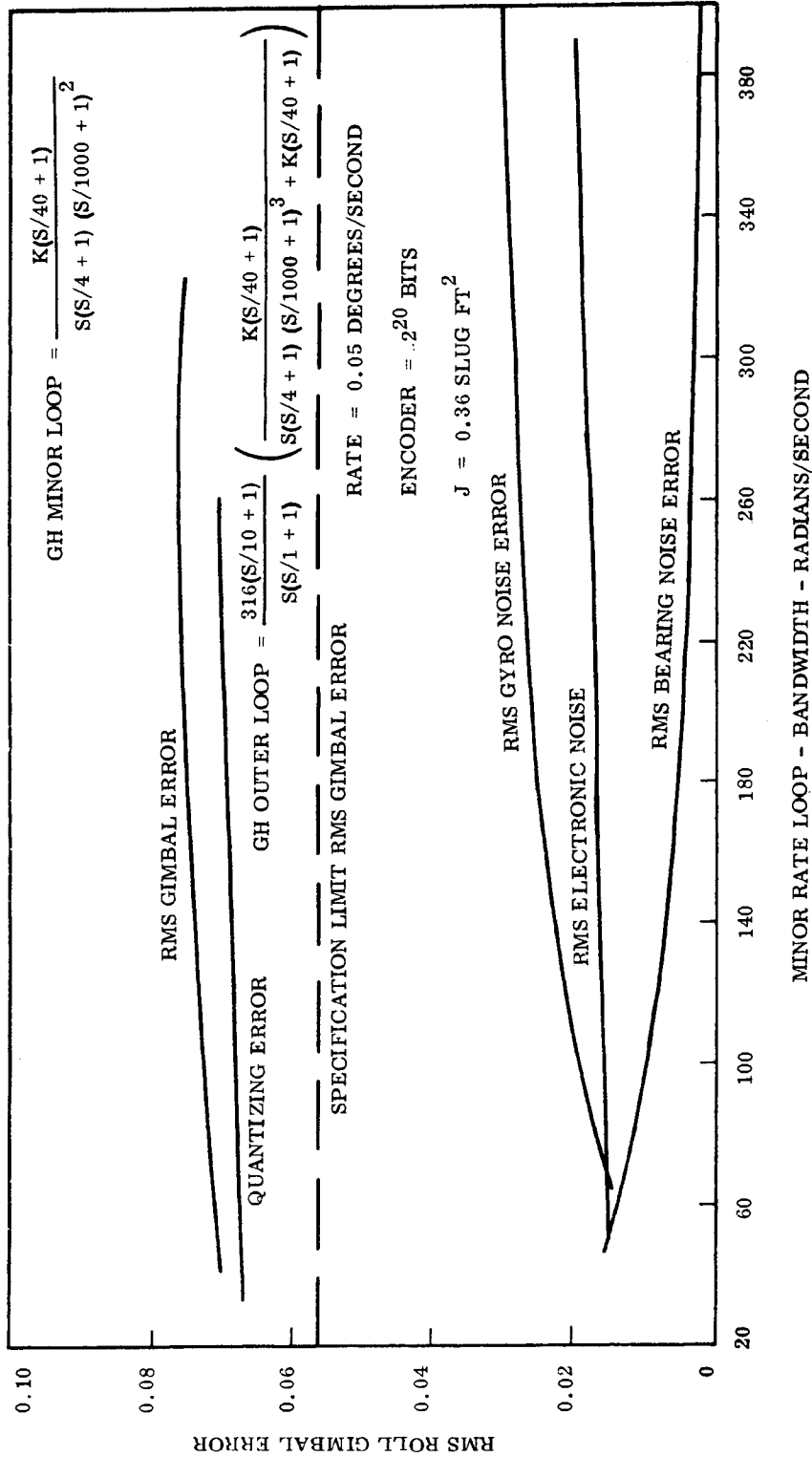
Figure 2.2-19. Position and Rate Configuration (Jitter equals 0.36 slug ft^2)

$$\text{GH MINOR LOOP} = \frac{K\,(S/40 + 1)}{S(S/4 + 1)\,(S/1000 + 1)^3}$$

$$\text{GH OUTER LOOP} = \frac{316\,(S/10 + 1)}{S(S/1 + 1)} \left(\frac{K\,(S/40 + 1)}{S(S/4 + 1)\,(S/1000 + 1)^3 + K\,(S/40 + 1)} \right)$$

RATE = 0.30 DEGREES/SECOND

ENCODER = 2^{20} BITS

$J = 0.08$ SLUG FT^2

SPECIFICATION LIMIT RMS GIMBAL ERROR

RMS GIMBAL ERROR

RMS QUANTIZING ERROR

RMS BEARING NOISE ERROR

RMS GYRO NOISE ERROR

RMS ELECTRONICS NOISE ERROR

MINOR RATE LOOP – BANDWIDTH – RADIANS/SECONDS

RMS PITCH GIMBAL ERROR

Figure 2.2-20. Position and Rate Configuration (Jitter equals 0.08 slug ft^2)

2-123

~~SECRET~~ SPECIAL HANDLING

$$\text{GH MINOR LOOP} = \frac{K \, (S/40+1)}{S(S/4+1)(S/1000+1)^3}$$

$$\text{GH OUTER LOOP} = \frac{316 \, (S/10+1)}{S(S/1+1)} \left(\frac{K \, (S/40+1)}{S(S/4+1)(S/1000+1)^3 + K(S/40+1)} \right)$$

RATE = 0.30 DEGREE/SECOND

ENCODER = 2^{20} BITS

J = 0.12 SLUG FT^2

SPECIFICATION LIMIT RMS GIMBAL ERROR

RMS GIMBAL ERROR

RMS GYRO NOISE ERROR

RMS ELECTRONIC NOISE ERROR

RMS QUANTIZING ERROR

RMS BEARING NOISE ERROR

MINOR RATE LOOP - BANDWIDTH - RADIANS/SECONDS

RMS PITCH GIMBAL ERROR (SEC)

Figure 2.2-21. Position and Rate Configuration (Jitter equals 0.12 slug ft^2)

~~SECRET~~ SPECIAL HANDLING

TABLE 2.2-3.   POSITION PLUS RATE SERVO CONFIGURATION ERROR SUMMARY

ERROR SOURCE	PITCH	ROLL
Bearing Noise	0.02 sec	0.0066 sec
Electronic Noise	0.016 sec	0.016 sec
Gyro Noise	0.023 sec	0.023 sec
Quantizing Error	0.0125 sec	0.068 sec
RMS Gimbal	0.037 sec	0.074 sec
1σ LOS	0.105 sec	
2σ LOS	0.21 sec	

Figure 2.2-22 shows the open loop frequency response of the position plus rate configuration.

Figure 2.2-23 shows the open loop frequency response of the slew loop with the position and rate configuration incorporated as minor loops.

The 30-radian position loop allows the tracking requirements to be met by the servo while allowing it also to be incorporated into the slew configuration.

The 150-radian per second minor loop is used to develop a high rejection of bearing noise (Tn). The 150-radian bandwidth requires the scanner structural frequency be greater than 150 radians and the allowable frequency ratio and damping are functions of the exact structural frequency.

An advantage of the rate and position configuration is that it has flexibility such that the minor loop bandwidth and gain can be increased for maximum rejection of bearing noise or gyro and amplifier noise depending on which becomes the more significant as the noise characteristics of the individual components become better defined.

$$GH = \frac{18\,(S/40+1)\,(S/100+1)\,(S/10+1)\,e^{-.01s}}{S(S/100+1)\,(S/479+1)\,(S/1327+1)} \cdot \frac{\left(\dfrac{S^2}{(16.7)^2} + \dfrac{1.845}{16.7} + 1\right)}{\left(\dfrac{S^2}{(103)^2} + \dfrac{1.65}{103} + 1\right)}$$

PHASE LAG - DEGREES

RADIANS/SECOND
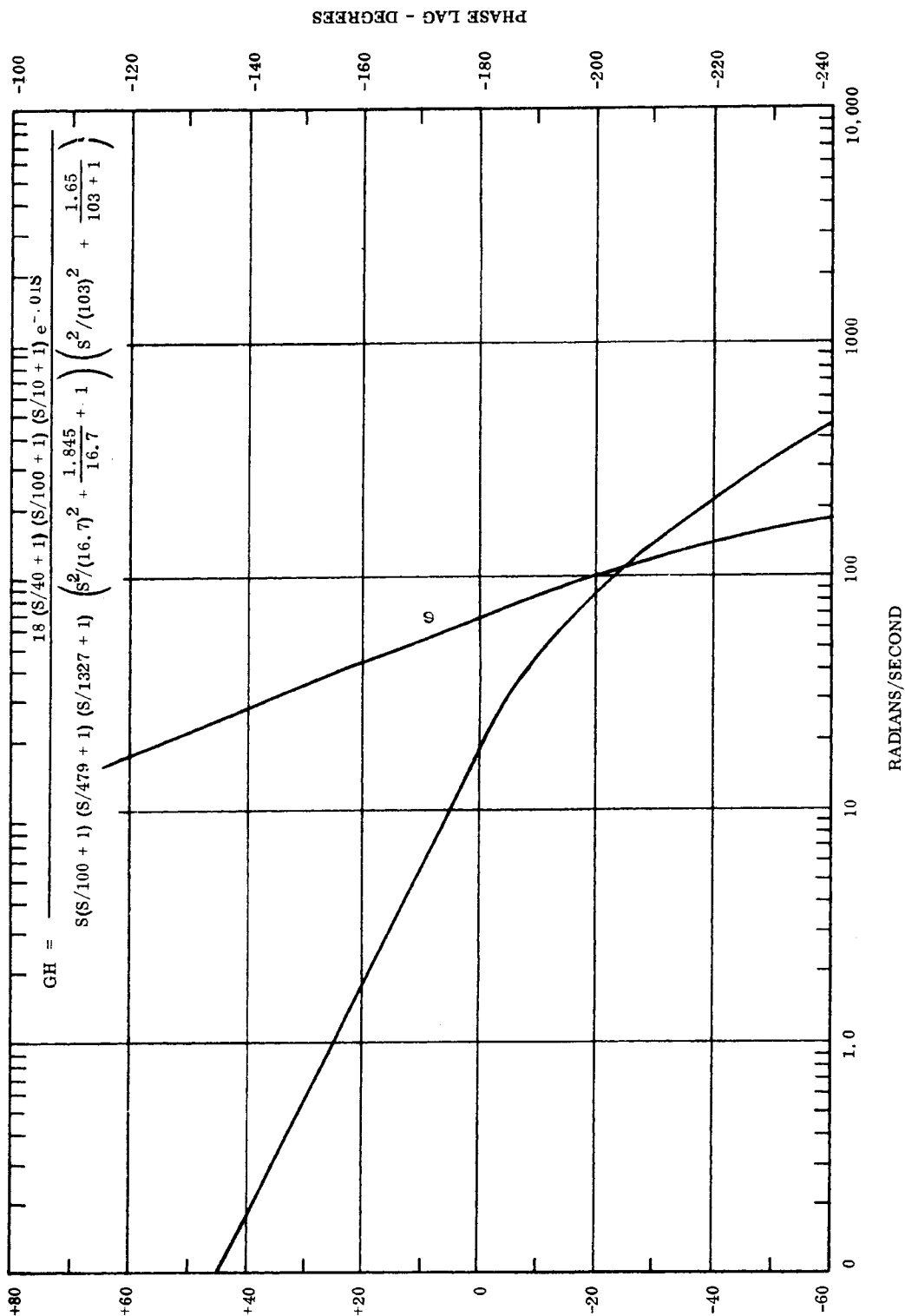
Figure 2.2-22. Open Loop Frequency Response of Pitch Slew Servo

$$GH = \frac{316 \ (S/10 + 1) \ (S/40 + 1) \ (S/100 + 1)}{S(S + 1) \ (S/59 + 1) \ (S/100 + 1) \ (S/171+1) \ (S/441+1) \ (S/1331 + 1)}$$

RADIANS/SEC
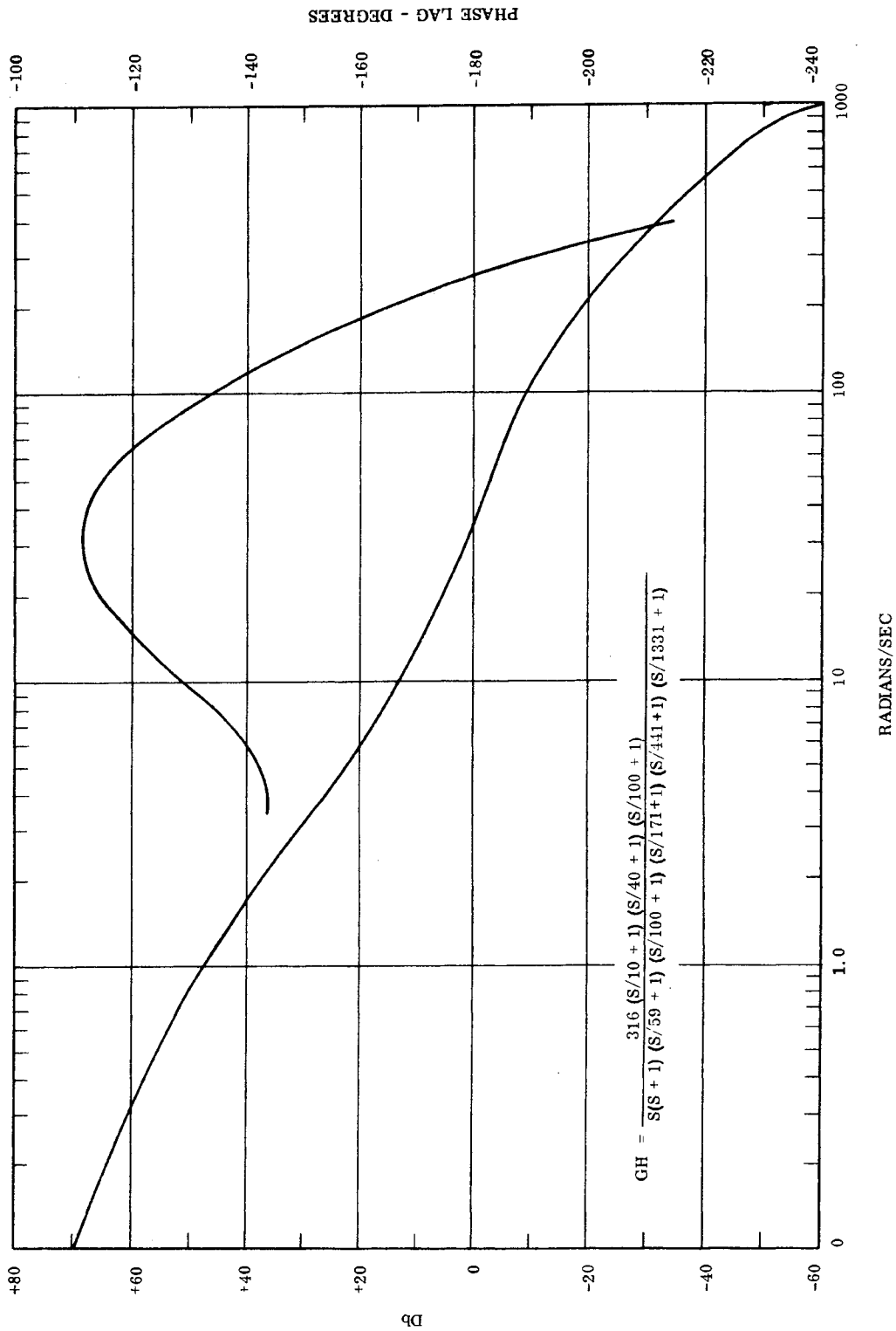
Figure 2. 2~23.   Closed Loop Frequency Response Rate Loop

2-127

2.2.1.6 Baseline Configuration - Description, Requirements and Design Margins

2.2.1.6.1 General

The baseline configuration incorporates the three servo configurations previously discussed. It consists of a primary mode and secondary mode of operation. The primary mode utilizes a position plus rate servo configuration for pitch axis control and a rate servo configuration for roll axis control. The bandwidths of these servos are as discussed in Paragraphs 2.1.3.1 and 2.1.2.5. These are a 30 radian per second position loop with a 150-radian per second rate minor loop in pitch.

The primary configuration has the following advantages:

a. Increased bearing noise rejection in the pitch axis. This is required due to the higher sensitivity of the LOS to pitch jitter and the lower inertia of the pitch gimbal.

b. Increased flexibility, in that the bandwidths and gains can be varied to minimize specific unwanted disturbances.

c. Bandwidths can be reduced to accommodate lower structural natural frequencies if this should become necessary while still being capable of meeting the jitter performance requirements.

d. Inherent capability of tracking at the minimum rates of 0.3 degree per second in pitch and 0.01 degree per second in roll (requirement). The use of a rate loop in roll allows the lower tracking rate, while the pitch encoder quantum level limits the minimum pitch tracking rate to 0.3 degree/second.

The primary pitch axis servo configuration provides increased bearing noise rejection and reduced noise requirements on the D/A converter at the expense of added complexity and encoder uncertainty. The increased complexity also allows a backup mode to be incorporated.

The primary roll axis servo configuration provides sufficient bearing noise rejection with relative simplicity while decreasing the ATS error sensitivity to vehicle transient disturbances. It requires tighter control on the D/A converter and buffer amplifier noise and does not provide as large a design margin with respect to bearing noise increases as does the pitch servo configuration.

The backup configuration utilizes a 60-radian per second position loop in pitch and a 30-radian per second position loop in roll. The characteristics of these servos are the same as those discussed in Paragraph 2.2.1.4.

The backup configuration provides redundancy should a gyro or compensating amplifier fail in the primary servos at the expense of a decrease in pitch performance.

The baseline servo configurations are shown in Figure 2.2-24 and the tabulated error date is listed in Table 2.2-4.

The baseline configuration has the advantage of being able to be converted to any one of the three configurations discussed by the use of a few switching points in the primary and backup servo loops.

2.2.1.6.2 Dynamic Requirements for the Baseline Scanner Control System.
The scanner pitch and roll configurations contain the primary mode (switch number 1 in the one position) and the backup configuration (switch number 1 in the two position).

In operation all components would be energized and the Digital Processor would always have the current position stored. This would allow the switch to be closed and the change made from the primary mode to backup mode with a minimum transient in the loop.

~~SECRET~~ **SPECIAL HANDLING**
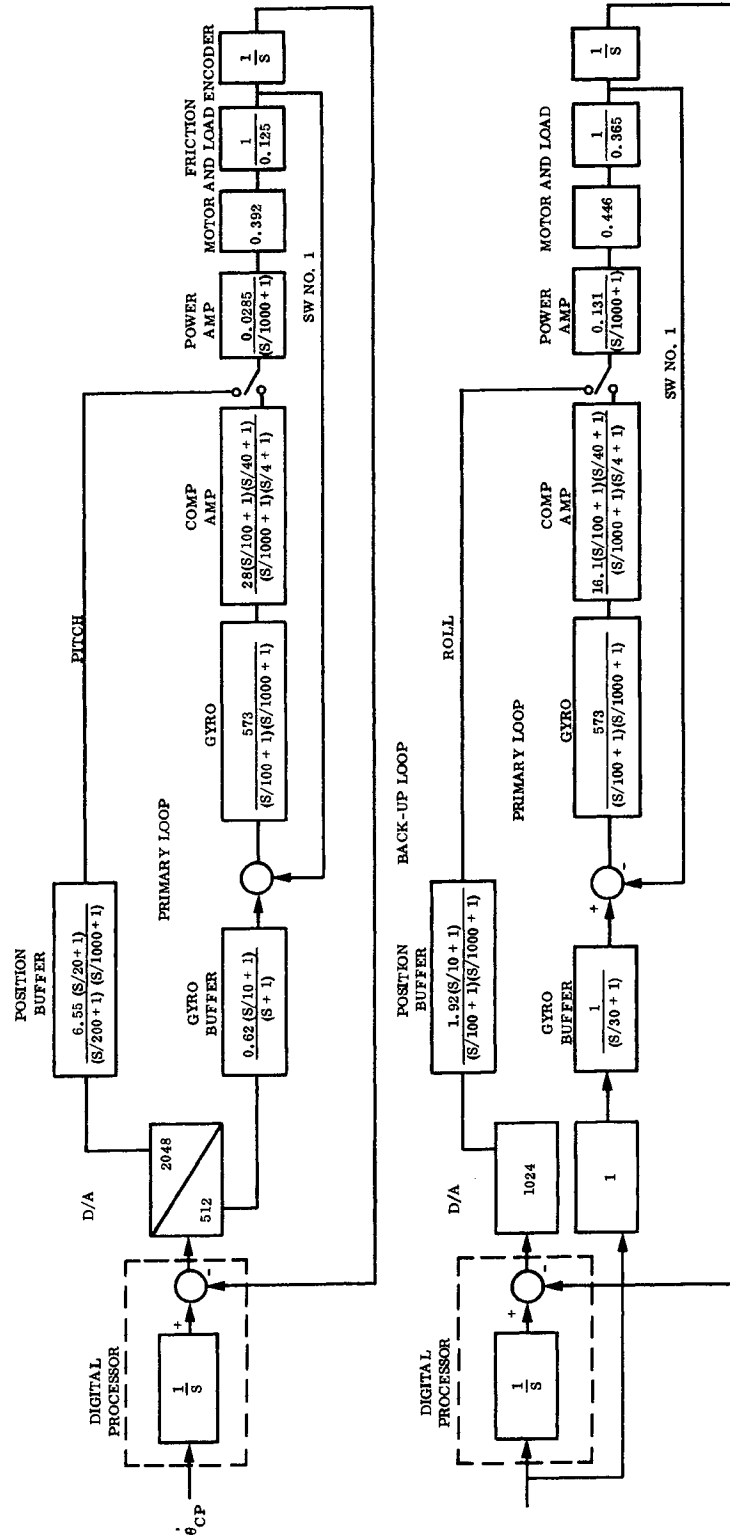
Figure 2.2-24. Pitch and Roll Servo Configurations – Backup Mode Loop

~~SECRET~~ **SPECIAL HANDLING**

TABLE 2.2-4. PRIMARY MODE ERROR SUMMARY

	PITCH	ROLL
Bearing Noise	0.02 sec	0.026 sec
Electronic Noise	0.016 sec	0.022 sec
Gyro Noise	0.022 sec	0.023 sec
Input Noise		0.016 sec
Quantizing Noise	0.0125 sec	
RMS Gimbal error −	0.037 sec	0.0434 sec
RMS LOS −	0.086 sec	
2σ LOS −	0.172 sec	

BACKUP MODE ERROR SUMMARY

	PITCH	ROLL
Bearing Noise	0.180 sec	0.165 sec
Electronic Noise	0.016 sec	0.016 sec
Quantizing Noise	0.0125 sec	0.062 sec
RMS Gimbal −	0.182 sec	0.172 sec
RMS LOS −	0.403 sec	
2σ LOS −	0.806 sec	

The dynamic requirements for the D/A converter and buffer amplifier have been combined and are given as requirements for each combination. This will allow the electronic designer to determine the optimum gain distribution between the two components with respect to noise and other design parameters. The gain distribution selected must allow the dynamic requirements specified for the combination of the D/A and buffer to be met.

A. Scanner Pitch Loop - Digital Processor (Pitch) - The Digital Processor shall receive the pitch command ($\dot{\theta}_{pc}$) from MDAU and integrate this command ($\dot{\theta}_{pc}$) by digital summation techniques. It shall receive the pitch incremental encoder output and convert this to a position reference (θ_p). The integrated rate command signal and the position reference shall be summed and the resultant shall be the output of the Digital Processor.

$$(\theta_{p\epsilon} = \int \dot{\theta}_{pc} - \theta_p)$$

The integrated rate command ($\dot{\theta}_{pc}$) shall have a maximum quantum level of 0.32 $\widehat{sec}$ and the position reference (θ_p) a maximum quantum level of 1.25 $\widehat{sec}$.

Timing reference inaccuracies in the Digital Processor shall not cause an error at the output of greater than 1μ radian for any one second period. This error shall not vary at a frequency between 0.2 radian per second and 1000 radians per second.

B. D/A Converter and Gyro Buffer (Pitch) - The D/A converter in pitch receives its inputs from the Digital Processor in both the primary and backup modes of operation. The D/A converter and Gyro Buffer combination shall process the pitch position command signal from the Digital Processor and develop a signal to command the pitch rate gyro.

The dynamic requirements of the D/A converter-Gyro Buffer combination are:

Gain - 72.5 ± 10 percent amperes per radian into a 100-ohm load ± 10 percent with a stability of ± 1 percent. The gain shall be linear for inputs from -0.0105 to +0.0105 radian.

Frequency Response - The frequency response of the Buffer amplifier shall have the following characteristics:

$$\frac{(\tau_1 S+1)}{(\tau_2 S+1)} \quad \text{where} \quad \begin{array}{l} \tau_1 = 0.1 \text{ sec} \\ \tau_2 = 1 \text{ sec} \end{array}$$

~~SECRET~~ **SPECIAL HANDLING**

Additional breaks shall not contribute more than 6 degrees of phase shift below 1000 radians per second.

Offset - The dc offset and long term drift shall not exceed 1 ma. Long term drift shall include all noise components below 0.2 radian per second.

Noise - The noise at the output of the D/A Converter - Gyro Buffer shall not cause an rms position error of greater than 0.016 units when the pitch gimbal position with respect to noise at the Buffer output is expressed as:

$$\frac{\theta_G}{N_{GB}} \quad \frac{4.1 \times 10 \ (S/0.2+1) \ (S/1+1)}{(S/10+1)(S/30+1)(S/37+1)(S/150+1)(S/1000+1)^3} \quad \frac{sec}{rad/sec}$$

for frequencies above 0.2 radian per second.

C. D/A Converter and Position Buffer (Pitch) - The D/A Converter and Position Buffer combination is used in the backup mode. It shall process the position error signal from the digital processor for input to the power amplifier. The dynamic requirements of the D/A converter and Gyro Buffer combination are:

Gain - 13,600 volts per radian ± 5 percent
The gain shall be linear for inputs from -0.003 to +0.003 radian.

Frequency Response - The frequency response of the D/A Converter-Position Buffer combination shall have the following characteristics.

$$\frac{(\tau_1 S+1)}{(\tau_2 S+1)(\tau_3+1)} \quad \text{where} \qquad
\begin{aligned}
\tau_1 &= 0.05 \text{ sec} \pm 10 \text{ percent} \\
\tau_2 &= 0.005 \text{ sec} \pm 10 \text{ percent} \\
\tau_3 &= 0.001 \text{ sec} \pm 10 \text{ percent}
\end{aligned}$$

Additional breaks shall contribute no more than six degrees of phase shift below 1000 radians per second.

Offset - The dc offset and long term drift shall not exceed 40 millivolts. Long-term drift shall include all noise components below 0.2 radian per second.

2-133

~~SECRET~~ **SPECIAL HANDLING**

Noise - The noise at the output of the Pitch Position Buffer shall not cause an RMS pitch gimbal error of greater than 0.016 unit when the pitch gimbal position with respect to noise at the Position Buffer output is expressed as:

$$\frac{\theta_G}{N_{PB}} = \frac{0.6 \times 10^{-1} (S/0.2+1)}{(S/20+1)(S/37+1)(S/60+1)(S/1000+1)^2} \frac{\widehat{sec}}{volt}$$

for frequencies above 0.2 rad/sec.

D. Gyro Pitch - Gyro shall be as presently specified in TR-1717.

E. Compensating Amplifier (Pitch) - The pitch compensating amplifier receives the output from the gyro and processes this signal for input to the power amplifier. The dynamic requirements of the compensating amplifier are:

Gain - 28 volts/volt ± 10 percent
The gain shall be linear for inputs from -4 to +4 volts.

Frequency Response - The frequency response of the compensating amplifier shall have the following characteristics.

$$\frac{(\tau_1 S+1)(\tau_3 S+1)}{(\tau_2 S+1)(\tau_4 S+1)} \quad \text{where} \quad \begin{aligned} \tau_1 &= 0.025 \text{ sec} \pm 10 \text{ percent} \\ \tau_2 &= 0.250 \text{ sec} \pm 10 \text{ percent} \\ \tau_3 &= 0.010 \text{ sec} \pm 10 \text{ percent} \\ \tau_4 &= 0.001 \text{ sec} \pm 10 \text{ percent} \end{aligned}$$

Additional breaks shall contribute no more than 6 degrees of phase shift below 2000 radians per second.

Offset - The dc offset and long term drift shall not exceed 100 millivolts. Long term drift shall include all noise components below 0.2 radian per second.

Noise - The noise at the output of the compensating amplifier shall not cause an rms gimbal position error of greater than 0.004 unit when the pitch gimbal position with respect to noise at the output of the compensating amplifier is expressed as:

$$\frac{\theta}{N_{CA}} = \frac{1.50 \times 10^{-4}\ (S/2+1)(S/1+1)(S/4+1)}{(S/10+1)(S/30+1)(S/37+1)(S/40+1)(S/510+1)(S/1000+1)}\ \frac{\overset{\frown}{sec}}{volt}$$

for frequencies above 0.2 radian per second.

F. __Power Amplifier (Pitch)__ - The power amplifier receives the output of the compensating amplifier in the primary mode and the output of the position buffer in the backup mode.

The dynamic requirements of the pitch power amplifier are:

__Gain__ - In the current feedback configuration the gain shall be 0.0224 amp per volt ± 5 percent into a load of 64 ohms and a back emf of 0.31 emf of 0.31 volt max.

The gain shall be linear to ± 0.4 amp output.

__Frequency Response__ - The frequency response of the Pitch Power amplifier shall have the following characteristics

$$\frac{K}{(\tau_1 S+1)} \qquad \text{where} \qquad \begin{array}{l} \tau_1 = 0.001 \text{ sec max.} \\ K = \text{gain} \end{array}$$

Additional breaks shall contribute no more than 6 degrees of phase shift below 2000 radians per second.

__Offset__ - The dc offset and long term drift shall not exceed 2 ma. Long term drift shall include all noise components below 0.2 radian per second.

__Noise__ - The noise at the output of the power amplifier shall not cause an rms gimbal position error of greater than 0.004 unit when the relationship between noise at the power amplifier output and the gimbal position is expressed as

$$\frac{\theta_G}{N_{PA}} = \frac{3.34 \times 10^{-3}\ (S/0.2+1)(S/1+1)(S/4+1)}{(S/10+1)(S/30+1)(S/37+1)(S/40+1)(S/150+1)}\ \frac{\overset{\frown}{sec}}{volt}$$

frequencies above 0.2 radian per second.

2-135

G. <u>Torquer (Pitch)</u> - The following characteristics were given by Subcontractor "A" for the pitch axis torquer:

Rated Torque = 37.6 oz - in with 16 volts across both windings

Resistance of each winding = 155 ohms

Time Constant = 0.001 second (both windings)

KV = 0.31 volt/radian/second

These characteristics were used to determine the pitch loop component dynamic requirements.

Tolerances which should be applied to the torquer parameters are

Torque = Level given should be the minimum allowable level

Resistance of windings ± 10 percent

Time constant ± 10 percent

Back Emf constant (K_N) ± 5 percent

H. <u>Encoder (Pitch)</u> - The pitch gimbal encoder is a 2^{18} incremental encoder.

<u>Accuracy</u> - Each quantum of encoder output shall be equal to 1.25 ± 0.1 sec of shaft position angle.

<u>Noise</u> - The Power Spectral Density of the components of the encoder position readout error resulting from bit variations with respect to the nominal quantum level shall be within the envelope of Figure 2.2-25 when the encoder shaft is rotated at a constant rate of 0.065 degree per second.

<u>Response</u> - The accuracy requirements shall be met for all shaft rotation rates from 0.3 to 4.5 degrees per second.

Note: The test information presently available from the encoder vendor indicates that they can not meet the noise specification detailed above with an 18 bit encloder and that the CEI jitter requirement could not thus be met. Studies are in progress evaluating the expected noise from a 2^{19} and a 2^{20} bit encoder.

Analysis of the latter, (page 2-112), demonstrates that a 2^{20} bit encoder adequately meets the design objective. This device, however, is larger than the 2^{18} bit encoder space envelope designed into the scanner. Recent information from the Wayne-George vendor, indicates that a 2^{19} bit encoder can be manufactured in the same disk size, and consequently same space envelope, as the 2^{18} bit encoder. Studies are continuing to evaluate its noise characteristics and packaging requirements.
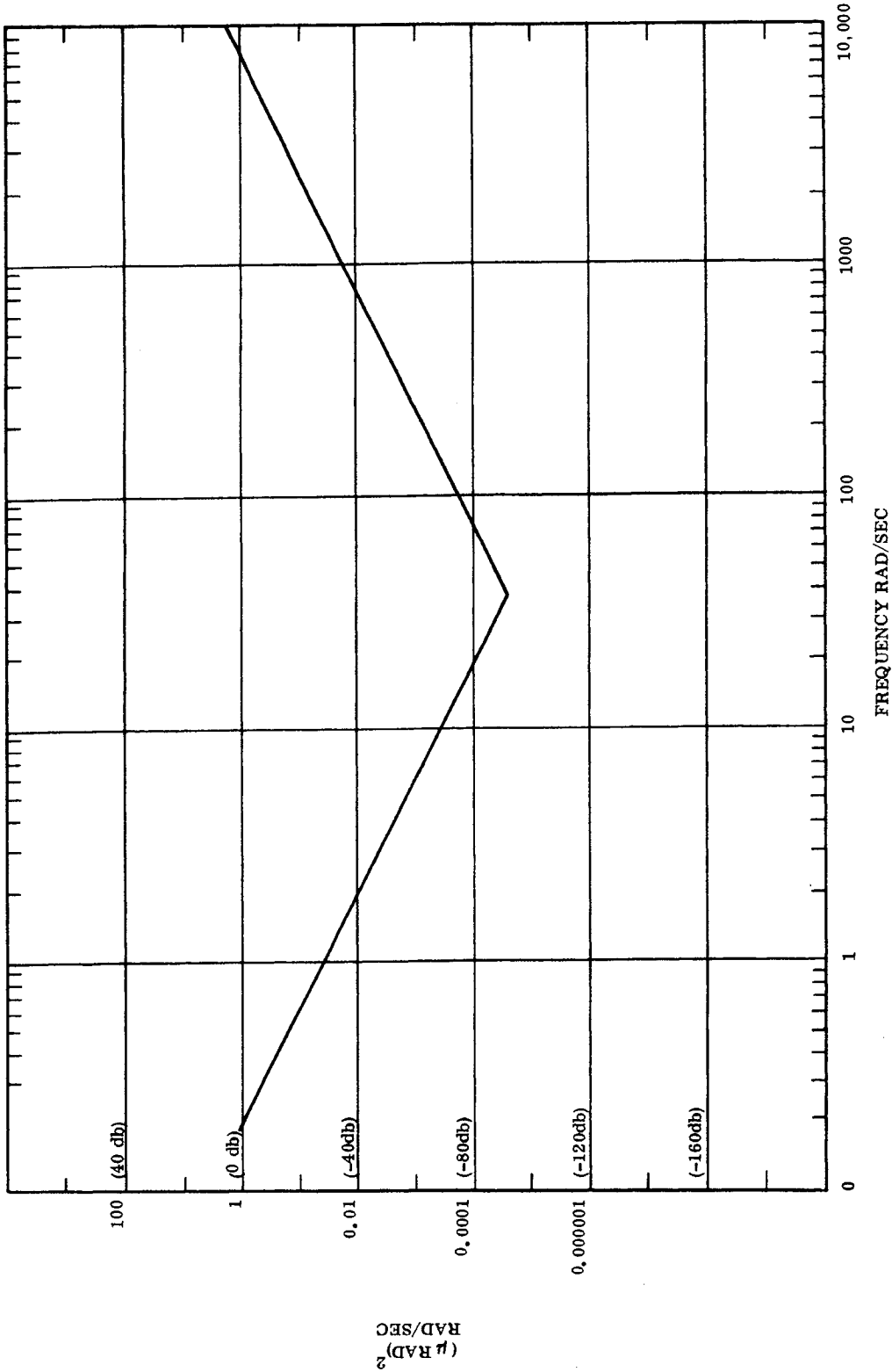
Figure 2.2-25. Allowable Encoder PSD Envelope

I. **Mass Properties (Pitch)** - The pitch axis inertia shall be no less than 0.12 slug foot squared.

Structural Dynamics (Pitch) - The Structural dynamics of the pitch gimbal assembly gyro assembly and mount location shall be such that the frequency response of the gyro output signal to motor excitation normalized to the response at one radian per second and compensated for the motor electrical time constant and the gyro transfer function shall have no amplitude above the profile of Figure 2.2-26.

J. **Mechanical Noise (Pitch)** - Power Spectral Density of the torque variations resulting from mechanical noise input such as Bearing noise and cable noise shall be within the envelope shown in Figure 2.2-25 for all gimbal rates from 0.1 to 1.8 degrees per second.

K. **Friction (Pitch)** - The mean value of running friction torque for the pitch gimbal shall be no greater than 2 in.-oz. Starting friction torque shall be no greater than 1.5 times the mean value of running friction torque.

SCANNER ROLL LOOP

L. **Digital Processor (Roll)** - The Digital Processor shall receive the roll rate command signal from the MDAU. It shall integrate this command signal by digital summation techniques. It shall receive the roll incremental encoder output and convert this to a position reference, (θ_R). The integrated rate command signal and the position reference shall be summed and the resultant shall be the output of the Digital Processor.

The integrated rate command shall have a maximum quantum level of 0.32 unit.

The position reference (θ_R) shall have maximum quantum level of 1.25 units.
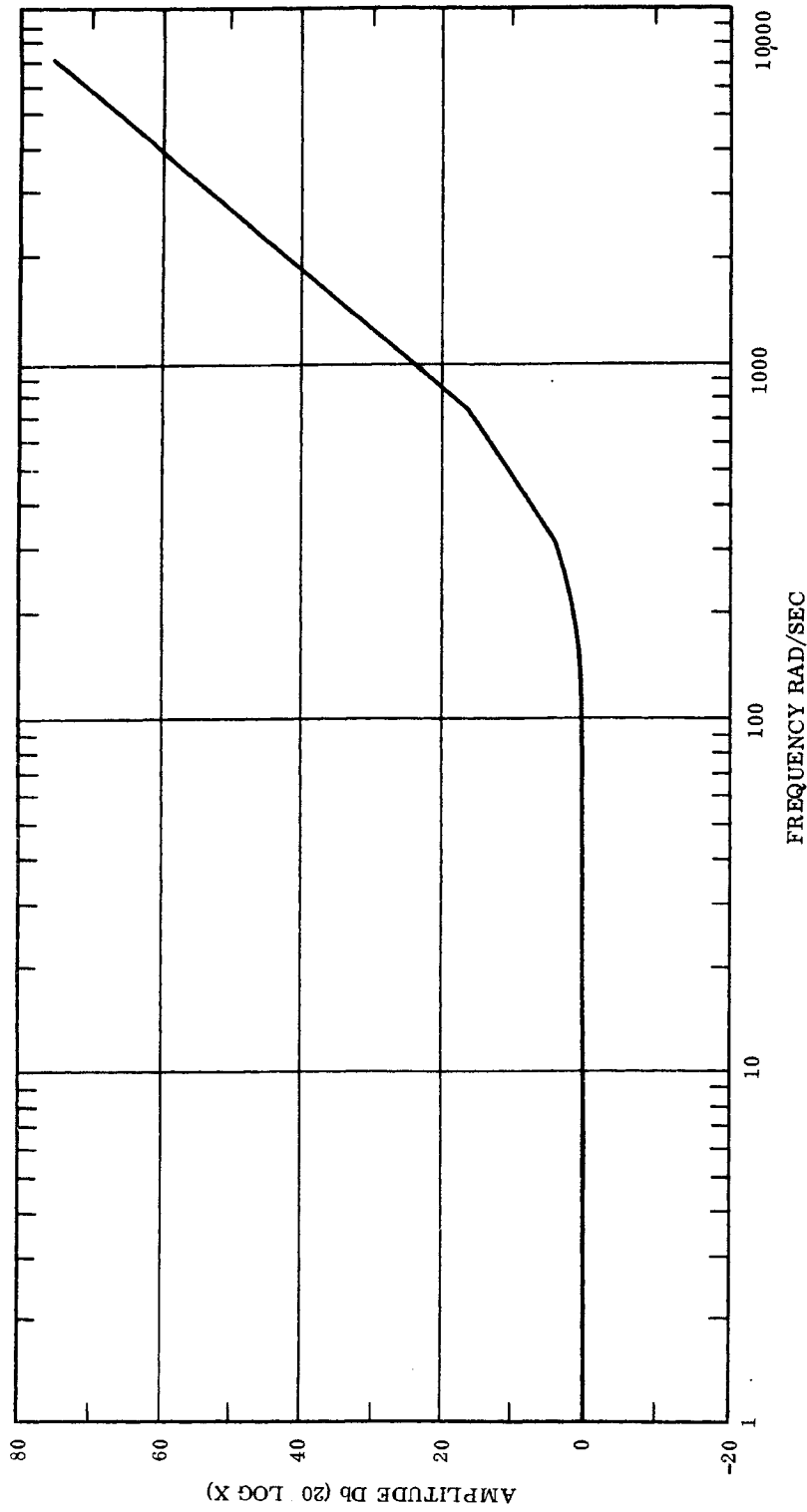
Figure 2. 2-26. Normalized Gimbal Rate Response Envelope for Structural Dynamics Specification

Timing reference inaccuracies in the digital process shall not cause an error at the output of greater than 1 un radian for any one second period. This error shall not vary at a frequency greater than 0.2 radian per second or less than 1000 radians per second.

M. **D/A Converter and Gyro Buffer (Roll)** – The D/A Converter in roll receives its inputs from the MDAU in the primary mode of operation and from the Digital Processor in the backup mode. The D/A Converter and Gyro Buffer combination shall process the roll rate command signal from the MDAU and develop a command to the roll rate gyro.

The dynamic requirements of the D/A Converter and Gyro Buffer combination are:

Gain = 0.25 ma/deg/sec into a 100 ohm load ± 10 percent with a stability of ± 1 percent. The gain shall be linear for inputs from ± 0.005 deg/sec to ± 45 degrees/sec.

The D/A gain shall be equal to 0.1 times the buffer gain in the position mode and equal to 10 times the buffer gain in the rate mode.

Offset – The dc offset and long term drift shall not exceed $10\,\mu$ amperes. Long term drift shall include all noise components below 0.2 radian per second.

Frequency Response – The frequency response of the D/A Converter and Gyro Buffer shall have the following characteristics:

$$\frac{K}{(\tau_1 S+1)} \qquad \text{where} \qquad \tau_1 = 0.033 \text{ sec} \pm 10 \text{ percent}$$

$$K = \text{gain}$$

Noise – The noise at the output of the D/A Converter – Gyro Buffer shall not cause an rms gimbal position error of greater than 0.016 unit when the roll gimbal position with respect to noise at the Gyro Buffer output is expressed as

$$\frac{\theta}{N}_{GS} = \frac{5.55 \times 10^{+3}}{(S/37+1)(S/150+1)(S/1000+1)^3} \frac{\text{sec}}{\text{volt}}$$

for frequencies above 0.2 radian per second.

N. D/A Converter and Position Buffer (Roll) - The D/A Converter and Position Buffer combination is used in the backup mode. It shall process the position error signal from the digital processor, and the output shall go to the power amplifier. The dynamic requirements of the D/A Converter and Gyro Buffer combination are

Gain (K) - 1976 volts per radian ± 5 percent
The gain shall be linear for inputs from -0.005 to +0.005 radian

Frequency Response - The frequency response of the Buffer amplifier shall have the following characteristics

$$\frac{(\tau_1 S+1)}{(\tau_2 S+1)(\tau_3 S+1)} \quad \text{where} \quad \begin{array}{l} \tau_1 = 0.1 \text{ sec} \pm 10 \text{ percent} \\ \tau_2 = 0.01 \text{ sec} \pm 10 \text{ percent} \\ \tau_3 = 0.001 \text{ sec} \pm 10 \text{ percent} \end{array}$$

Additional breaks shall contribute no more than 6 degrees of phase shift below 1000 radians/sec.

Offset - The dc offset and long term drift shall not exceed 20 millivolts. Long term drift shall include all noise components below 0.2 rad/sec.

Noise - The noise at the output of the output of the Roll Position Buffer shall not cause an RMS roll gimbal error of greater than 0.016 units when the roll gimbal position with respect to noise at the Position Buffer output is expressed as

$$\frac{\theta}{N_{PB}} = \frac{6.5 \times 10^{-1} (S/0.2+1)}{(S/10+1)(S/30+1)(S/37+1)(S/1000+1)} \quad \frac{\text{sec}}{\text{volt}}$$

frequencies above 0.2 radian per second.

Gyro (Roll) - Gyro shall be as presently specified in TR - 1717.

O. Compensating Amplifier (Roll) - The roll compensating amplifier receives the output from the gyro and processes this signal for input to the power amplifier.

~~SECRET~~ **SPECIAL HANDLING**

The dynamic requirements of the compensating amplifier are:

Gain (K) - 16 volts/volt ± 10 percent
The gain shall be linear for inputs from -4 to +4 volts.

Frequency Response - The frequency response of the compensating amplifier shall have the following characteristics:

$$\frac{(\tau_1 S+1)(\tau_3 S+1)}{(\tau_2 S+1)(\tau_4 S+1)} \quad \text{where} \quad$$

$\tau_1 = 0.025 \text{ sec} \pm 10 \text{ percent}$

$\tau_2 = 0.250 \text{ sec} \pm 10 \text{ percent}$

$\tau_3 = 0.010 \text{ sec} \pm 10 \text{ percent}$

$\tau_4 = 0.001 \text{ sec} \pm 10 \text{ percent}$

Additional breaks shall contribute no more than 6 degrees of phase shift below 2000 radians/sec.

Offset - The dc offset and long term drift shall not exceed 20 mv rms. Long term drift shall include all noise components below 0.2 rad/sec.

Noise - The noise at the output of the compensating amplifier shall not cause an rms gimbal position error of greater than 0.004 unit when the relationship between the noise at the compensating output and the gimbal position is expressed as

$$\frac{\theta}{N_{CA}} = \frac{6.5 \times 10^{-1} (S/4+1)}{(S/37+1)(S/40+1)(S/150+1)(S/1000+1)} \quad \frac{\text{sec}}{\text{volts}}$$

frequencies above 0.2 rad/sec.

P. Power Amplifier (Roll) - The power amplifier receives the output of the compensating amplifier in the primary mode and the output of the position buffer in the backup mode. The dynamic requirements of the roll power amplifier are:

Gain - In the current feedback configuration the gain shall be 0.133 amp per volt ± 5 percent into a load of 6.5 ohms and a back-emf of 0.87 volt max. The gain shall be linear to ± 2.5 amps output.

~~SECRET~~ **SPECIAL HANDLING**

Frequency Response - The frequency response of the Roll Power amplifier shall have the following characteristics

$$\frac{K}{(\tau_1 S+1)} \qquad \text{where} \qquad \tau_1 = 0.001 \text{ sec max.}$$

$$K = \text{gain}$$

Additional breaks shall contribute no more than 6 degrees of phase shift below 2000 radians per second.

Offset - The dc offset and long term drift shall not exceed 4.0 milliamps. Long term drift shall include all noise components below 0.2 rad/sec.

Noise - The noise at the output of the power amplifier shall not cause an rms gimbal position error of greater than 0.004 unit when the relationship between the noise at the power amplifier output gimbal position is expressed as

$$\frac{\theta}{N_{PA}} = \frac{4.5 \times 10 \, (S/4+1)}{(S/40+1)(S/150+1)(S/37+1)} \quad \frac{\text{sec}}{\text{volt}}$$

above 0.2 radian/sec.

Q. Torquer (Roll) - The following characteristics were given by subcontractor "A" for the roll axis torquer:

Rated Torque = 210 - with 16 volts across both windings

Resistance of each winding = 13 ohms

Time constant = 0.028 second (both windings)

K_v = 0.87 volt/radian/second

These characteristics were used to determine the roll loop component dynamic requirements. Tolerances which should be applied to the torquer parameters are:

Torque – Level given should be the minimum allowable level

Resistance of windings ± 10 percent

Time constant ± 10 percent

Back Emf constant (K_v) ± 5 percent

R. Encoder (Roll) – The Roll gimbal encoder shall be a 2^{20} incremental encoder.

S. Accuracy – Each quantum of encoder output shall be equal to 1.25 ± 0.1 sec of shaft position angle.

T. Noise – The Power Spectral Density of the components of encoder position readout error resulting from bit variations with respect to the nominal quantum level shall be within the envelope of Figure 2.2-25 when the encoder shaft is rated at a constant rate of 0.065 degree per second.

U. Response – The accuracy requirements shall be met for all shaft rotation rates from 0.01 to 45 degrees per second.

V. Mass Properties – The roll axis inertial shall be no less than 0.36 slug foot squared.

W. Structural Dynamics (Roll) – The structural dynamics of the roll gimbal assembly, gyro assembly and mount location shall be such that the frequency response of the gyro output signal to motor excitation, normalized to the response at one radian per second and compensated for the motor electrical time constant and the gyro transfer function shall have no amplitude excursions above the profile of Figure 2.2-26.

X. Mechanical Noise (Roll) – Power Spectral Density of the torque variations resulting from mechanical noise inputs such as bearing noise and cable noise shall be within the

envelope shown in Figure 2.2-25 for all gimbal rates from 0.01 to 0.04 degree per second.

Y. <u>Friction (Roll)</u> - The mean value of running friction torque for the roll gimbal shall be no greater than 2 in.-oz. Starting friction torque shall be no greater than 1.5 times the mean value of running friction torque.

DESIGN MARGINS

The selected configuration for the primary mode of operation has the highest design margin with respect to meeting the jitter requirement based on the present assumed noise input. The Design Margins for the possible servo configurations are:

Pitch	Roll	Jitter Amplitude	Design Margin
Rate	Rate	0.221	1.14
Position	Position	0.806	----
Position and Rate	Position and Rate	0.21	1.19
Rate	Position	0.406	----
Position	Rate	0.76	----
Position and Rate	Rate	0.166	1.51
Rate	Position and Rate	0.23	1.09

All of the servo configurations considered have sufficient phase and gain margins for operation in both the slew and track modes of operation.

~~SECRET~~ **SPECIAL HANDLING**

SLEW MODE

Requirements

The slew maneuver shall be completed in $\left(\dfrac{\Delta\theta}{30}+1\right)$ and $\left(\dfrac{\Delta\theta}{15}+1\right)$ seconds for the roll and pitch axes respectively. The end of the slew maneuver is defined as that time at which the gimbal position error is less than 1 arc minute and the rate error is less than 0.01 degree per second per axis.

Servo Configuration

Figure 2.2-27 shows the pitch and roll slew loop configurations. Advantages of the slew servo configuration are:

a.   Software is similar to that required for the Main Tracking Mirror.

b.   It allows the tracking servo configuration to be an integral part of the slew servo (minimum transient at completion of slew).

c.   Generates shaped torque pulses (minimum structural excitation)

d.   Allows dead beat operation

e.   There are no saturations – linear operation

f.   Limits command rates

The pitch and roll baseline slew loop servo configurations are position loops with a band-width of 18 radians per second. Figures 2.2-28 and 2.2-29 show the open loop frequency response of the slew loops with the baseline tracking mode servos incorporated as minor loops.

2-146

~~SECRET~~ **SPECIAL HANDLING**
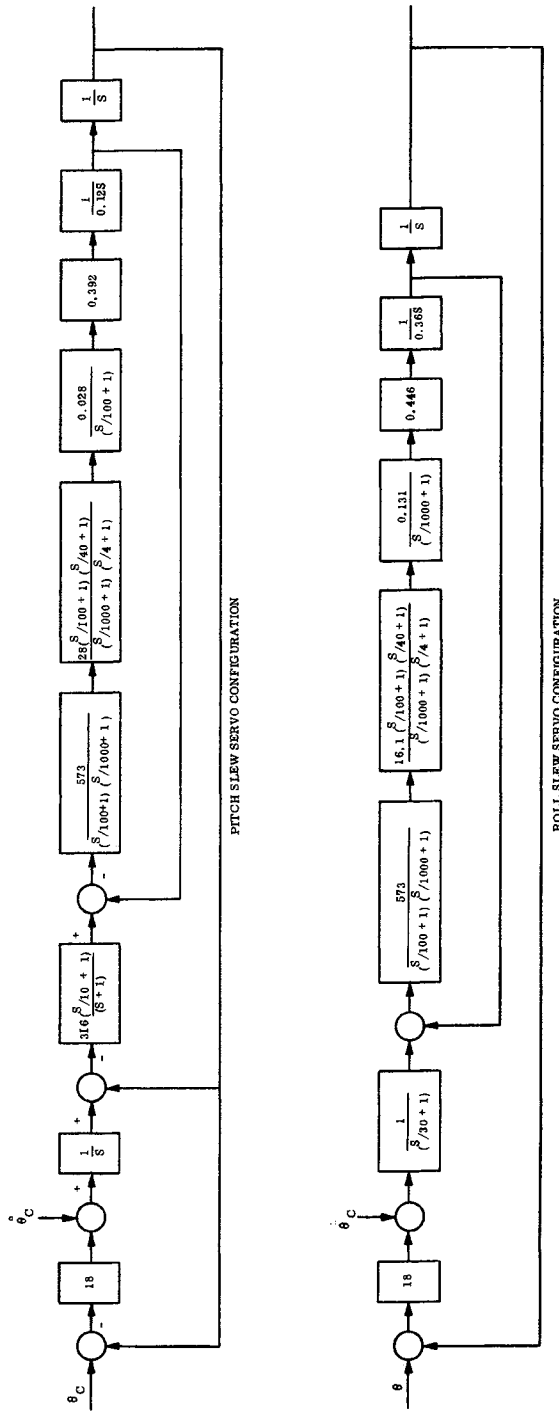
Figure 2.2-27. Pitch and Roll Slew Servo Configurations

~~SECRET~~ **SPECIAL HANDLING**

$$GH = \frac{18 \left(\frac{S}{90}+1\right)\left(\frac{S}{100}+1\right)e^{-.01S}}{S\left(\frac{S}{30}+1\right)\left(\frac{S}{100}+1\right)\left(\frac{S}{51}+1\right)\left(\frac{S}{171}+1\right)\left(\frac{S}{441}+1\right)\left(\frac{S}{153}+1\right)}$$
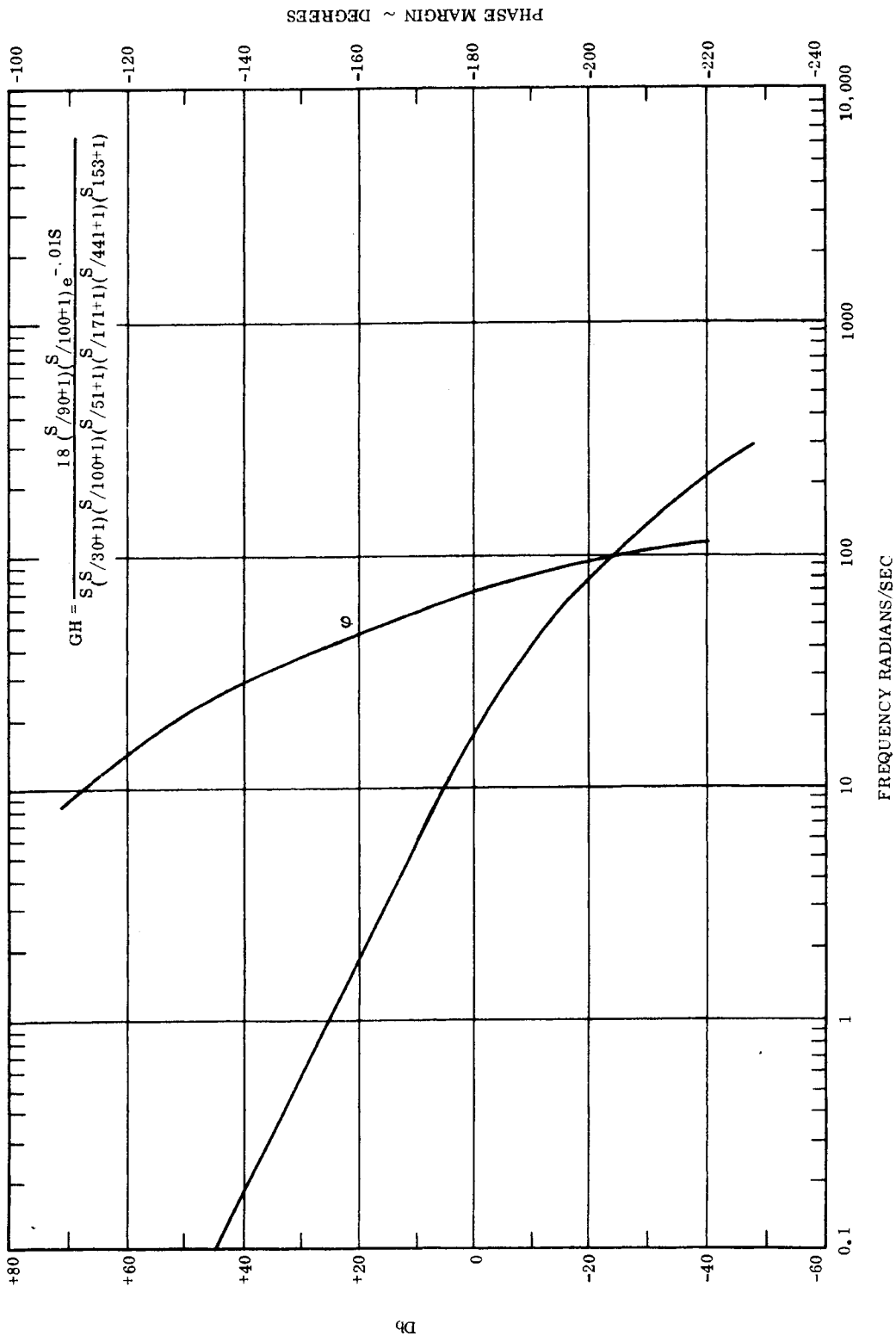
Figure 2.2-28. Open Loop Frequency Response Roll

~~SECRET~~ **SPECIAL HANDLING**

$$GH = \frac{18\ (S/40+1)(S/100+1)(S/1041)\ e^{-.01S}}{S(S/100+1)(S/479+1)(S/1327+1)(S^2/(167)^2 + \frac{1.95}{167} + 1)(S^2/153+1.6)}$$
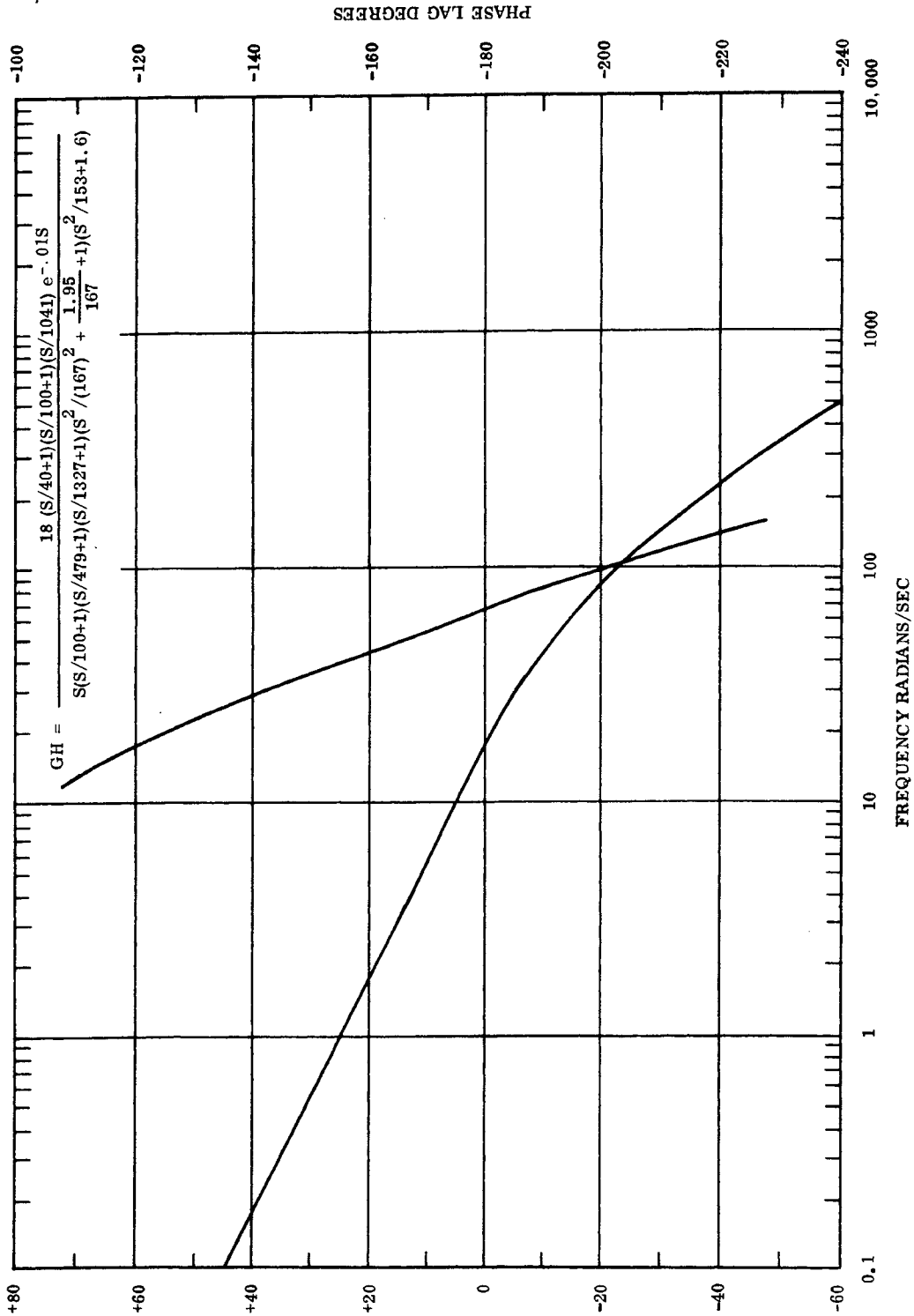
Figure 2.2-29. Open Loop Frequency Response of Pitch Slew Servo

2-149

Digital simulations were made using both 12-radian and 18-radian position loops. The results indicate that the slew time requirements can be met with the 12-radian slew loops, however the baseline configuration of 18 radians provides some margin in meeting the time requirements. Figures 2.2-30 and 2.2-31 show the slew performance in pitch and roll as a function of $\Delta\theta$. Figure 2.2-32 shows the shape of the slew command signal for two different $\Delta\theta$'s. Figures 2.2-33 and 2.2-34 show analog representations of the slew command generation equations.
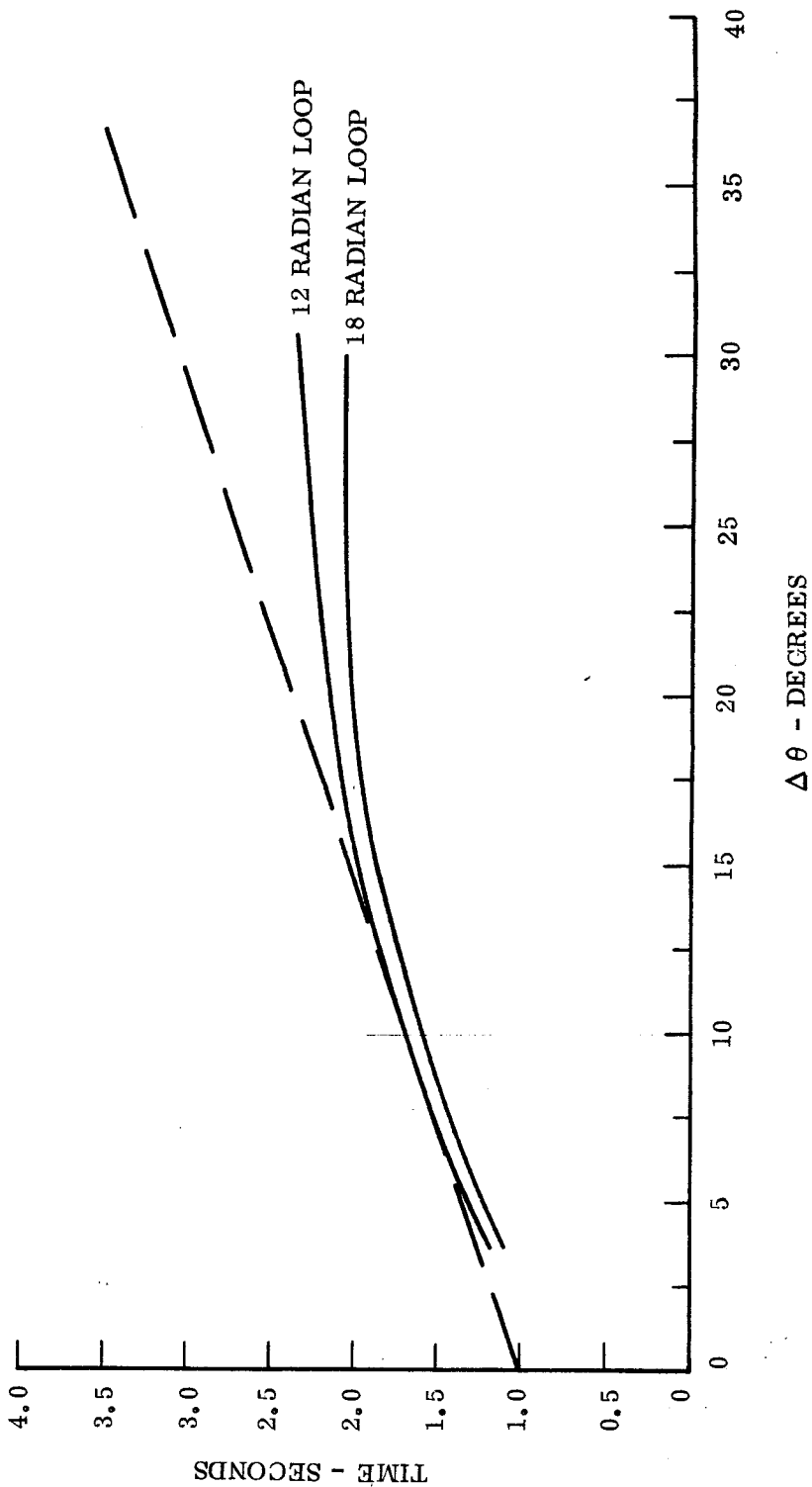
Figure 2.2-30. Pitch Slew Performance

~~SECRET~~ SPECIAL HANDLING
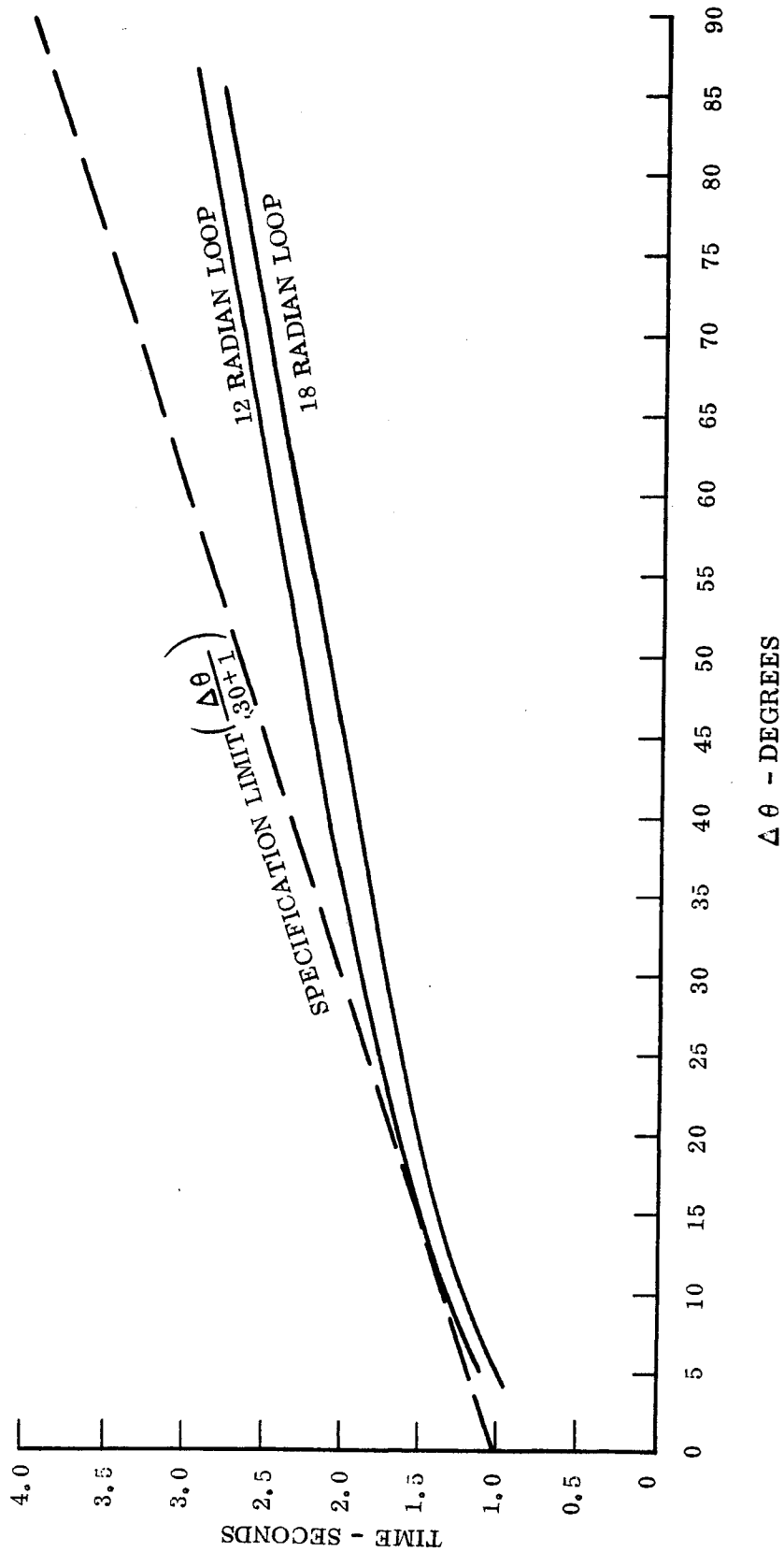
Figure 2.2-31. Roll Slew Performance

~~SECRET~~ SPECIAL HANDLING

~~SECRET~~ **SPECIAL HANDLING**
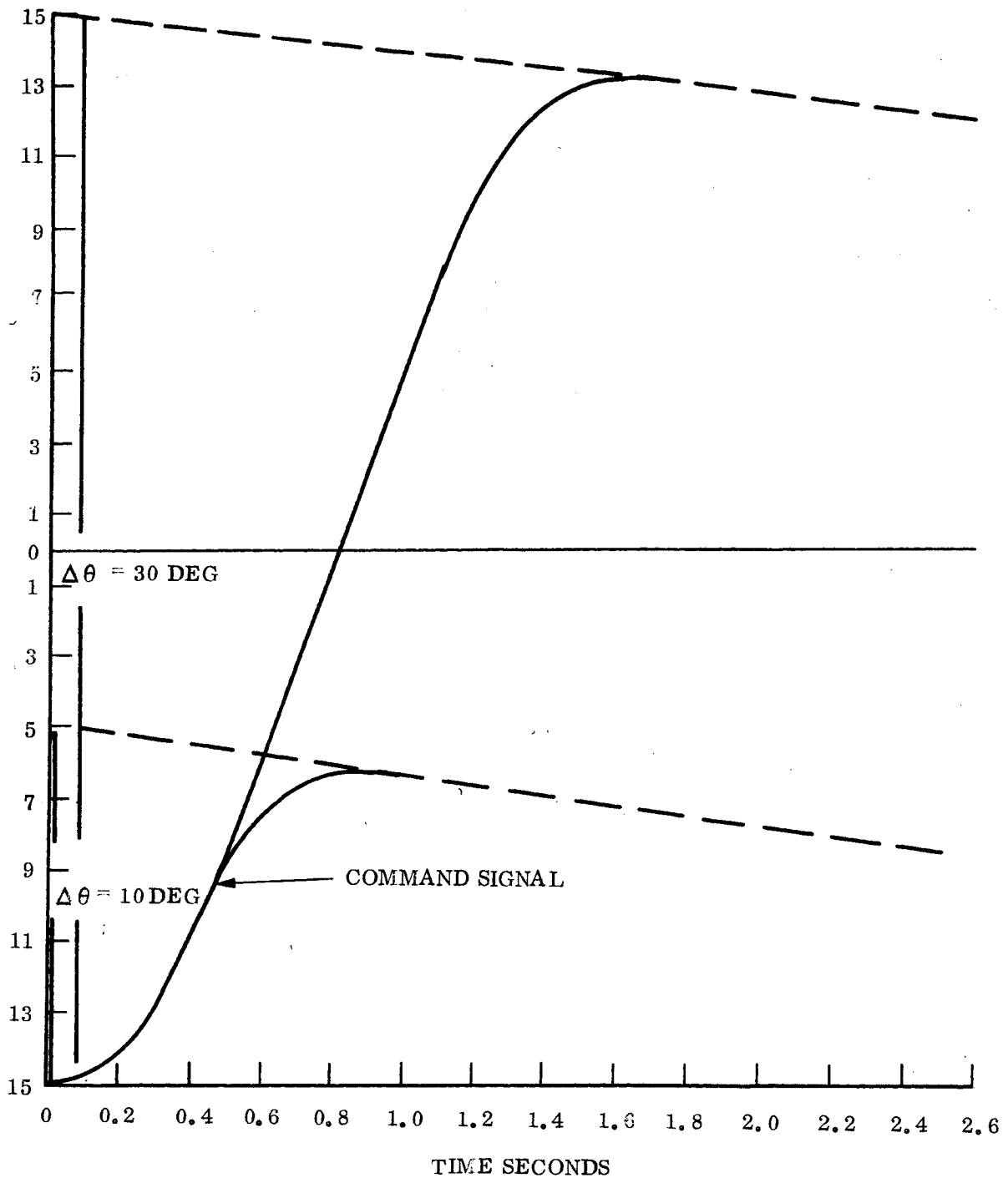
Figure 2.2-32. Pitch Slew Command

2-153

~~SECRET~~ **SPECIAL HANDLING**

~~SECRET~~ **SPECIAL HANDLING**
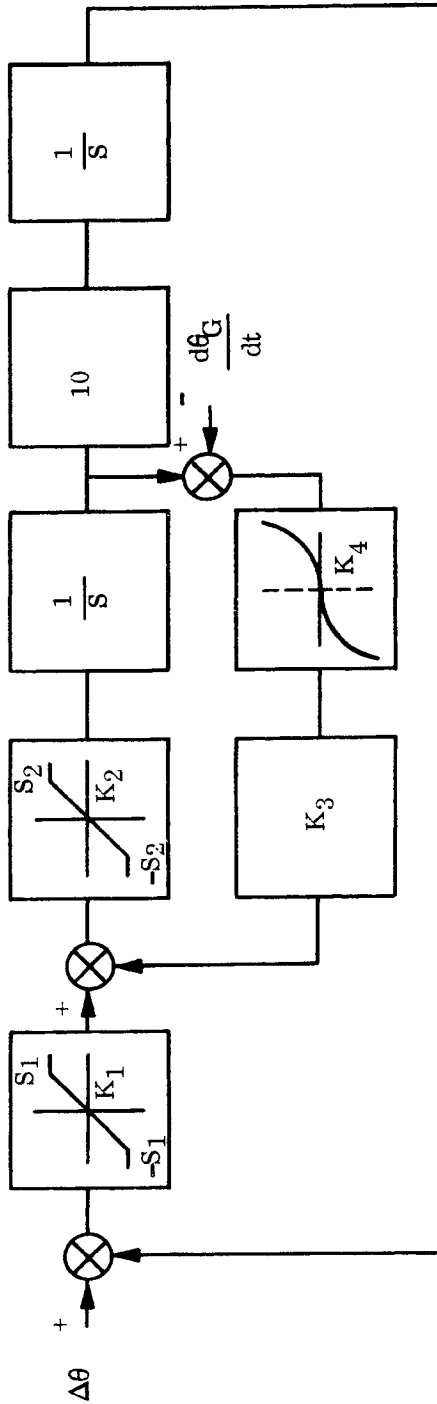
$$K_1 = 1$$

$$S_1 = \pm 2.52$$

$$K_2 = 850$$

$$S_2 = \pm 11.5$$

$$K_3 = 0.125$$

$$K_4 = \begin{cases} 1 & -1 < \dot\theta < 1 \\ \dot\theta & \dot\theta \\ -1 & \dot\theta > \dot\theta < 1 \end{cases}$$

Figure 2.2-33. Roll Axis Slew Command Generator

~~SECRET~~ **SPECIAL HANDLING**

~~SECRET~~ SPECIAL HANDLING
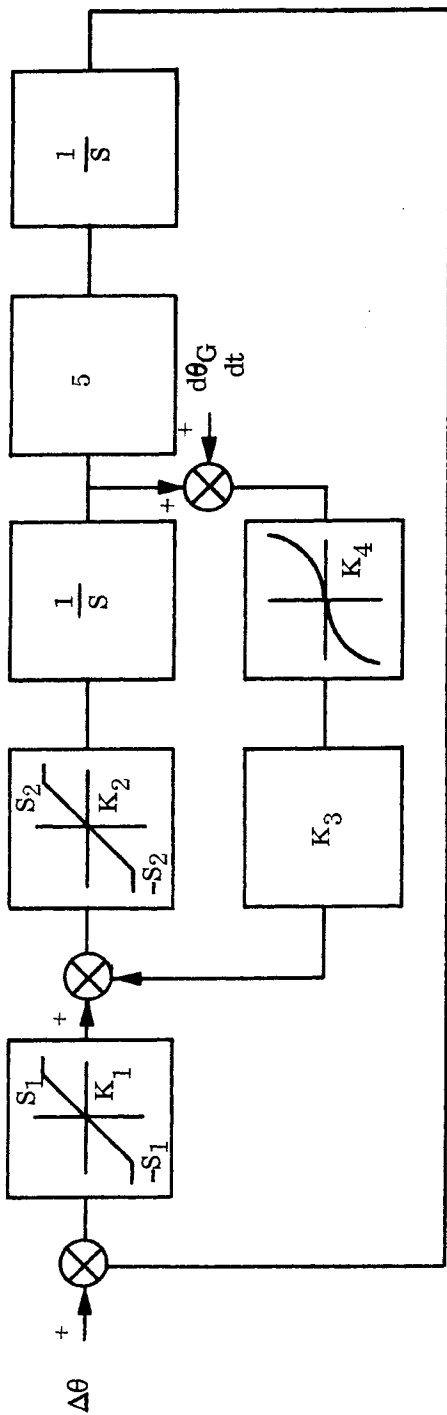
$K_1 = 1$

$S_1 = \pm 10.5$

$K_2 = 850$

$S_2 = \pm 11.5$

$K_3 = 0.125$

$$K_4 = \begin{cases} 1 & -1 < \dot{\theta} < 1 \\ |\dot{\theta}| & |\dot{\theta}| \ -1 > \theta > 1 \end{cases}$$

Figure 2.2-34. Pitch Axis Slew Command Generator

2.2.1.7 Command Generation

The slew command is generated in such a manner as to command the servo to have a dead-beat response, generate shaped torque pulses, and limit the gimbal rates to ± 45 degrees per second.

The slew command is shaped to command the servo to the desired response characteristics. The command signal (θc) generation equations can be represented by the analog configuration of Figures 2.2-33 and 2.2-34.

For values of $\Delta\theta$ greater than 8.8 in roll and 17.6 in pitch the inner loop of the slew command generator will go to zero and the output of the generator will become a ramp with a slope of 45. This limits the maximum gimbal rates to 45 degrees per second for any $\Delta\theta$ input.

Figures 2.2-35 through 2.2-39 show the variations of torque, gimbal rate, gimbal position, and gimbal position and rate errors as a function of time for a 10 degree roll slew.

Digital simulations have been made of the slew manuever using the backup servo configurations. A slew performance requirements are met with this servo configuration.

D/A Gain Switching – To reduce the noise present at the output of the position electronics, A_{np}, the gain of the D/A convertor can be increased. This increase is accomplished by changing the inputs to the D/A ladder network and does not cause a corresponding increase in noise at the D/A output. Thus the signal to noise ratio of A_{np} can be increased if the D/A gain is increased. An increase of D/A gain must be accomplished by a reduction in the dynamic range of the D/A.

~~SECRET~~ **SPECIAL HANDLING**
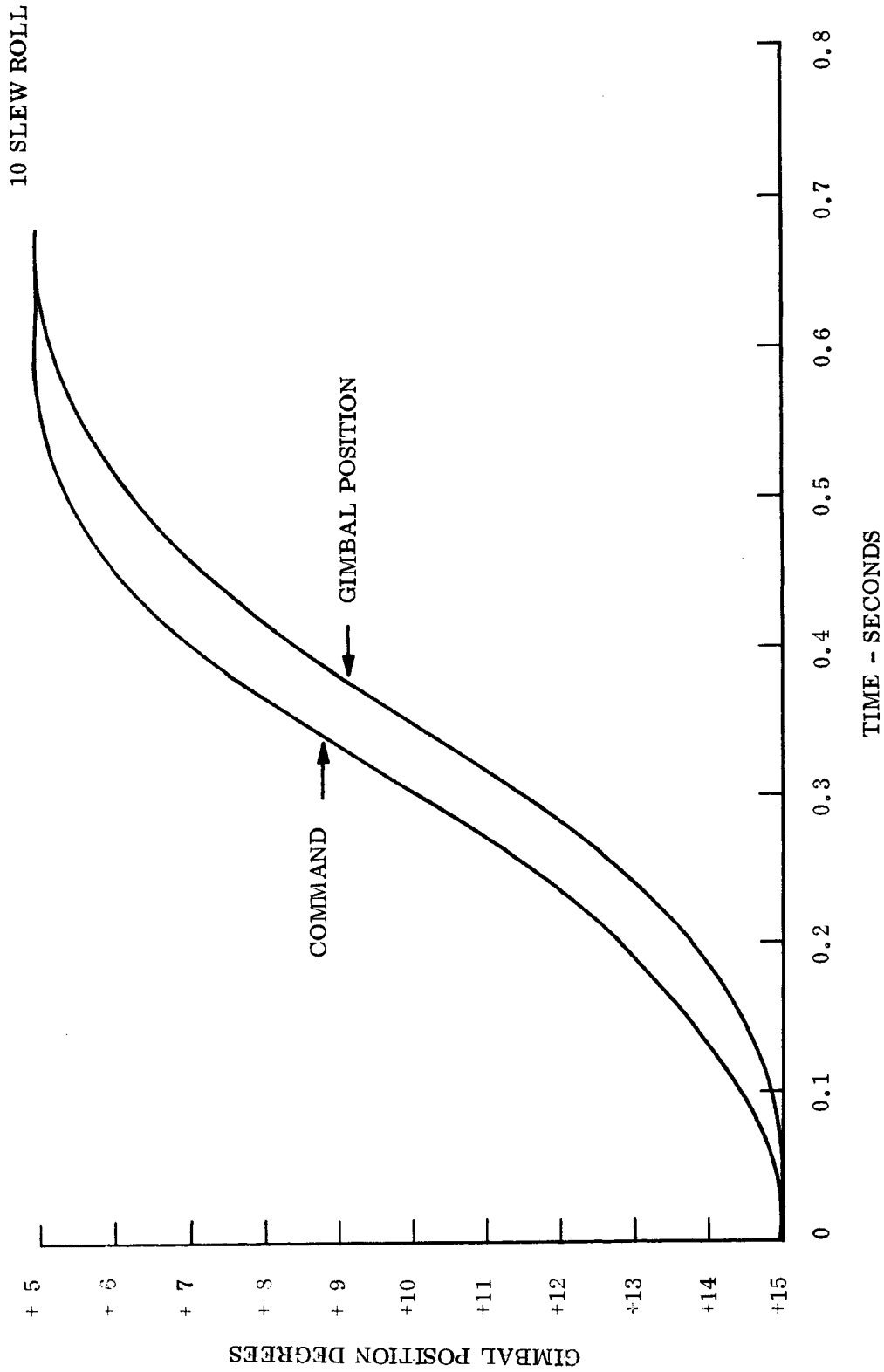
Figure 2.2-35. Ten Degree Slew Roll

2-157

~~SECRET~~ **SPECIAL HANDLING**

~~SECRET~~ **SPECIAL HANDLING**

10 DEGREE SLEW ROLL

POSITION ERROR PROFILE

TIME – SECONDS
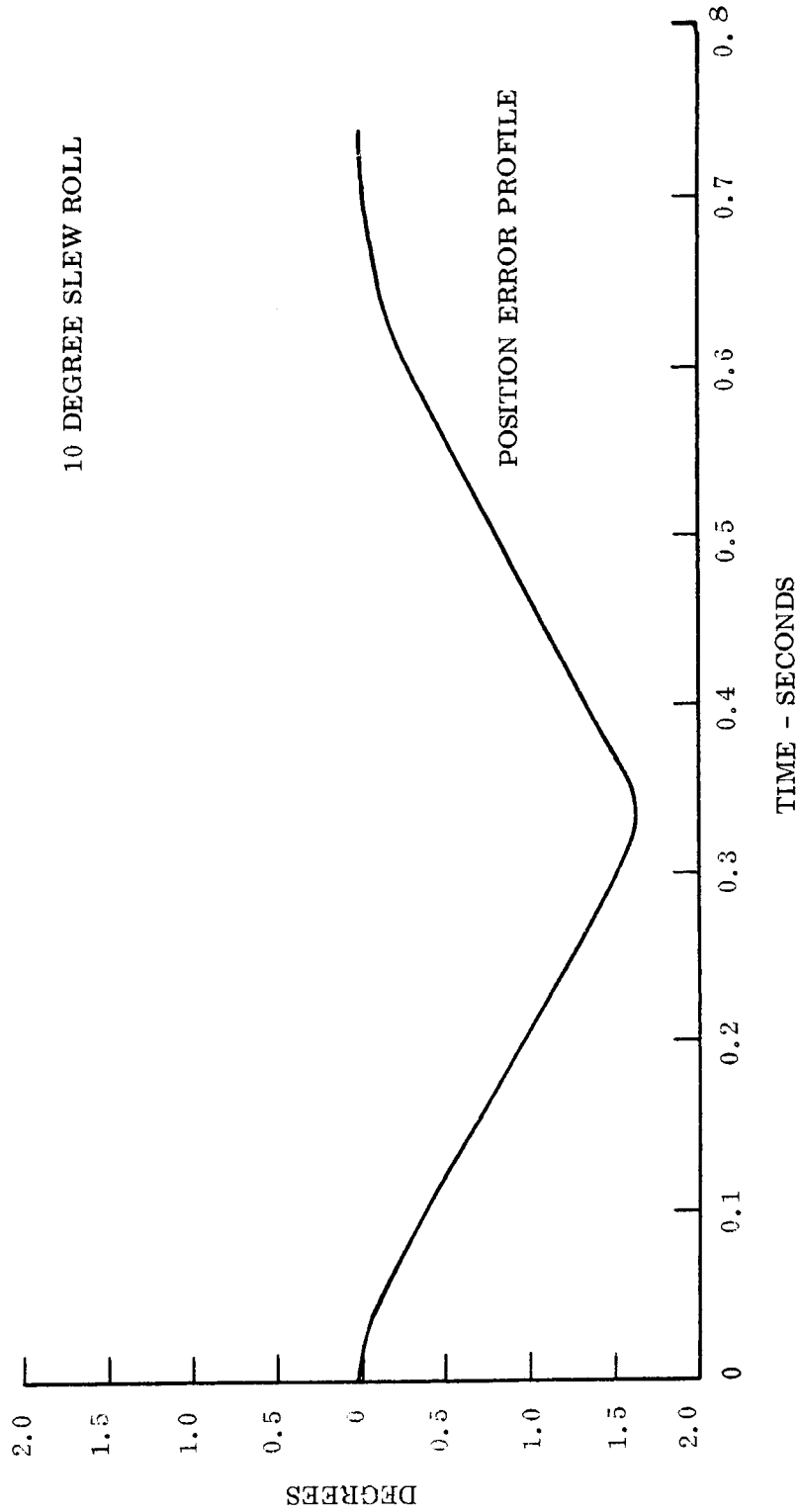
DEGREES

Figure 2.2-36. Ten Degree Slew Roll

~~SECRET~~ **SPECIAL HANDLING**
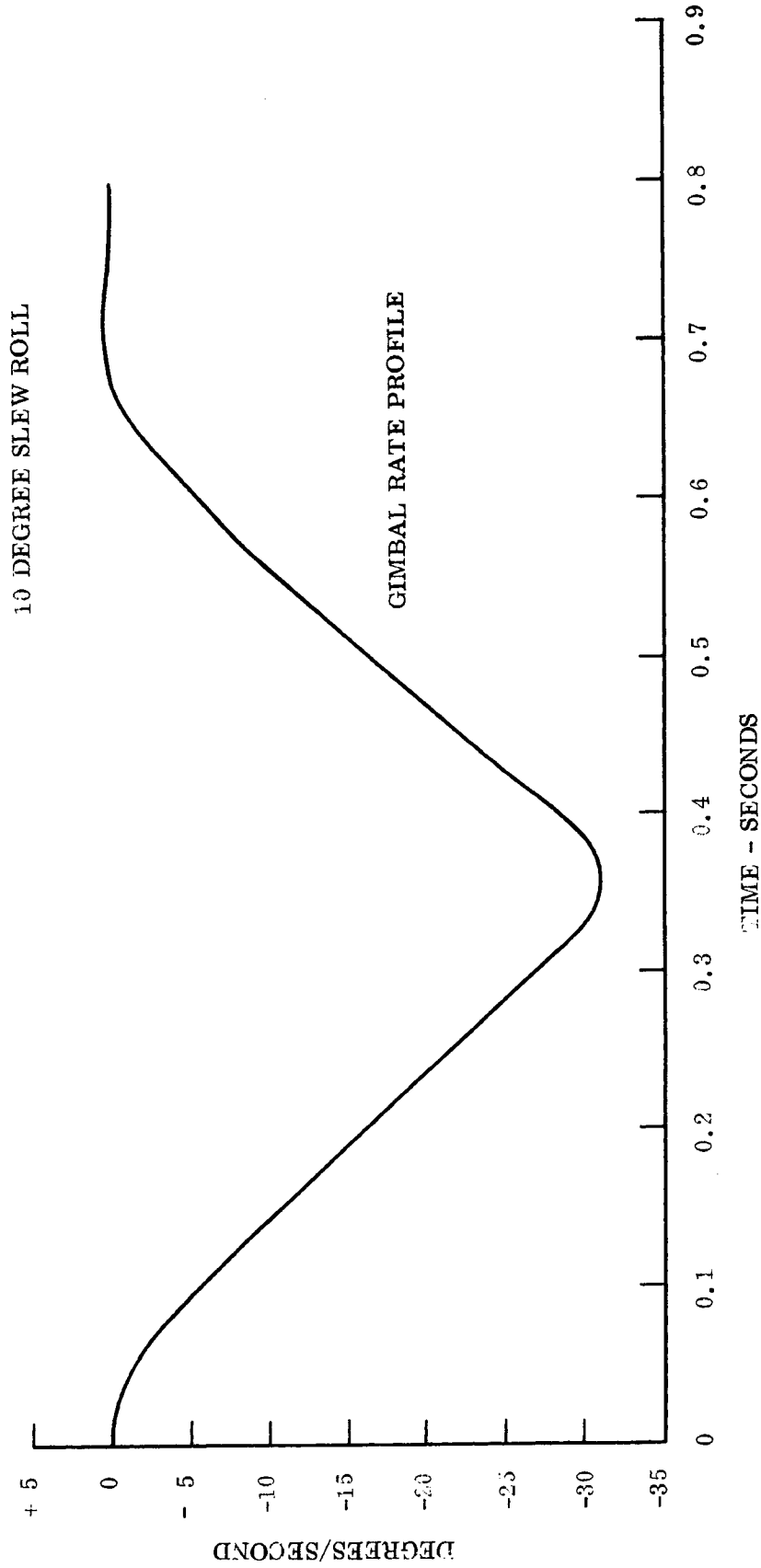
Figure 2.2-37. Ten Degree Slew Roll

2-159

~~SECRET~~ **SPECIAL HANDLING**
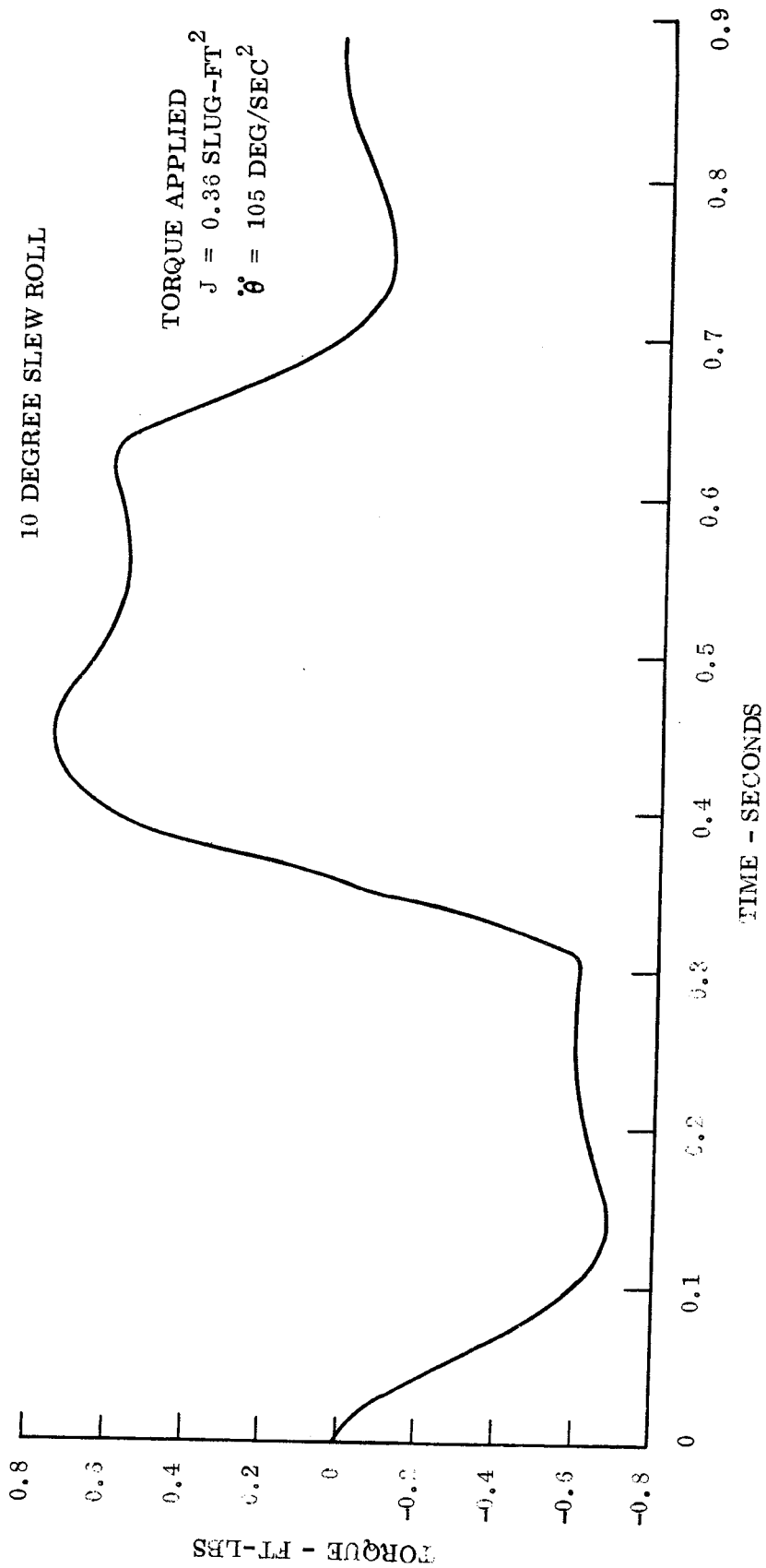
Figure 2.2-38. Ten Degree Slew Roll

~~SECRET~~ **SPECIAL HANDLING**

~~SECRET~~ SPECIAL HANDLING

10 DEGREE SLEW ROLL

POSITION AND RATE ERRORS

RATE ERROR
LIMIT
(0.010 DEG/SEC)

TIME LIMIT

$$\left(\frac{\Delta\theta}{30} + 1\right) \text{ SEC}$$

RATE
ERROR

POSITION ERROR
LIMIT
(0.014 DEG/SEC)

POSITION
ERROR

TIME – SEC
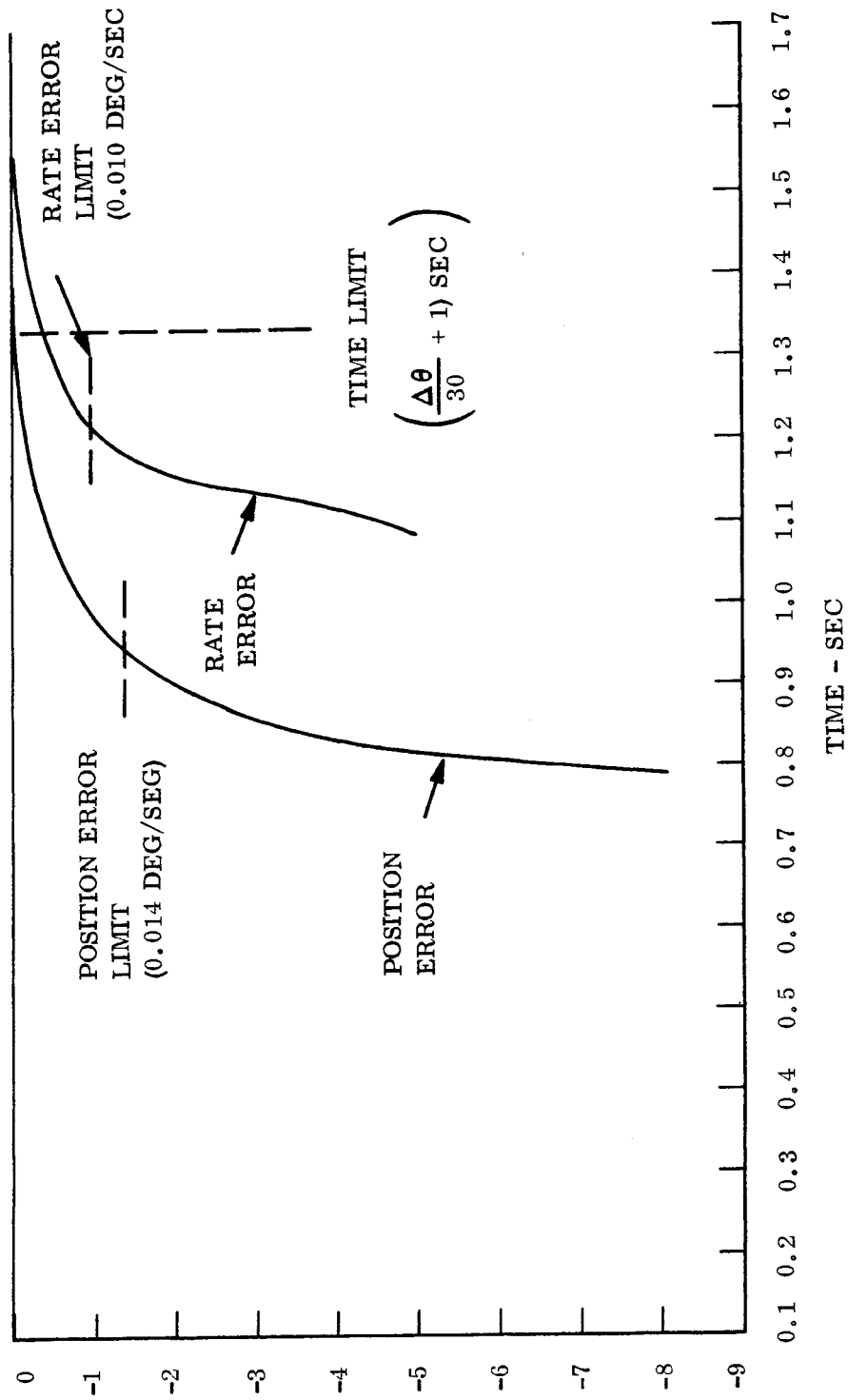
Figure 2.2-39. Ten Degree Slew–Roll Position and Rate Errors

~~SECRET~~ SPECIAL HANDLING

2-161

~~SECRET~~ **SPECIAL HANDLING**
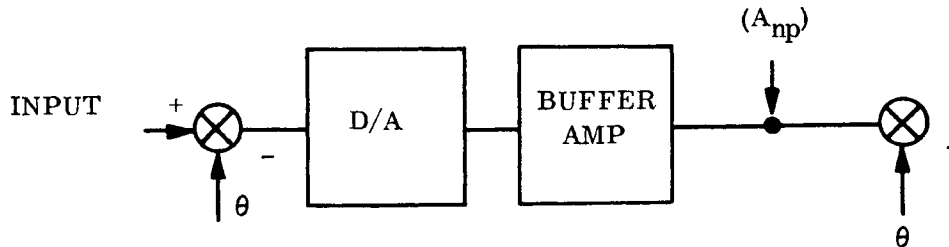
To optimize the gain-dynamic range relationship it is necessary to change the gain and range when switching from the slew mode to the track mode. Thus, if the noise requirements of the tracking mode configuration require a high D/A gain it is possible to accomplish this by incorporating gain switch logic in the electronics.

This condition can be simulated on a digital computer. The effects of a gain change equal to 30 are shown in Figure 2.2-40. This change is made in the roll channel at 2.8 seconds after the start of a 60 degree slew. The buffer amplifier gain is reduced by a factor of 30 and then 0.1 second later the D/A gain is increased by a factor of 30. The results indicate that this gain change can be made just prior to the end of a slew and the effects on the acceleration and rate error will be minimum when the gain change in the buffer amplifier precedes the change in the convertor. The 0.1 second delay used in this simulation is a severe case and it is assumed that this delay will be much smaller in most cases.

~~SECRET~~ **SPECIAL HANDLING**
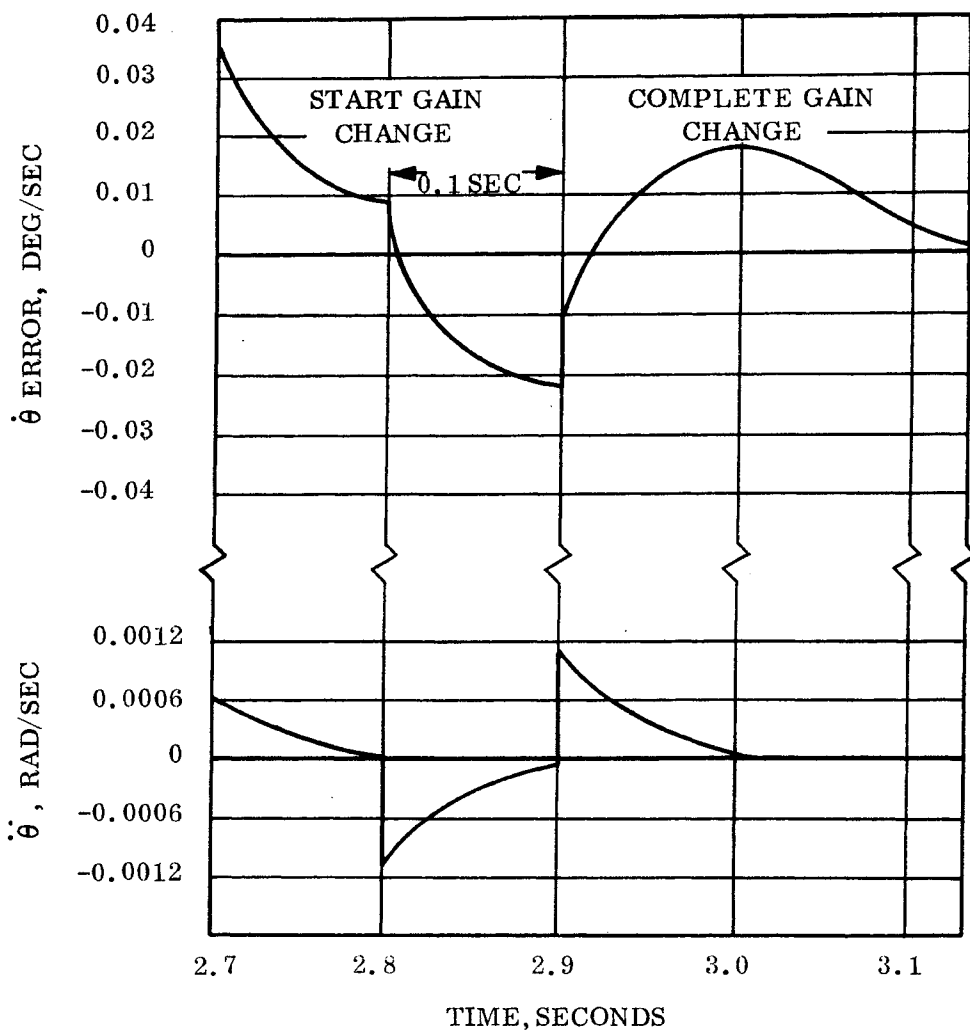
Figure 2.2-40. Effects of a $\dfrac{D}{A}$ gain change at End of Slew

2.2.1.8 Slaving Mode

The requirement for slaving the Main Tracking Mirror to the ATS exists, and methods of accomplishing this were investigated.

The configuration shown in Figure 2.2-41 appears to be the optimum in that the closed loop configuration causes the gimbals of both systems to be driven to the same position. The rate input to both systems is then updated by the crewman in the ATS control loop.

Both loops would be slewed to the same target and switch no. 1 would be closed. The crewman would reduce the rate error in the ATS. The change in rate needed to accomplish this would also be summed into the Tracking Mirror control loop.

When the rate was reduced switch no. 1 would be opened and the value present would be clamped to prevent the generation of a transient due to rate biases in the tracking mirror control loop.

Figure 2.2-42 shows that the two drives could be slaved together to a rate accuracy of less than 1 microradian per second and a position accuracy of less than 30 seconds of arc. This could be accomplished in less than three seconds starting from the normal end of slew position and rate error values.

The method referred to above involves the actual comparison of the ATS and main optics gimbal positions as well as the application of the man's rate corrections to both subsystems. A method of slaving which does not provide position coupling between the two subsystems, but simply provides the man's rate corrections to both subsystems is also under consideration. This approach would simplify the software needed to implement slaving.

The table below shows the error allocation assumed to determine the rate error in the slave mode. The numbers are considered conservative and demonstrate that the 100 μrad/sec requirement is met.

<div align="center">

Tracking Mirror LOS Error – Slaving

</div>

Structural Vibration	26 μ rad/sec
TM Servo Noise	26 μ rad/sec
ATS Servo Noise	45 μ rad/sec
Crew Error	17 μ rad/sec
Slaving Error	20 μ rad/sec
Misalignment Error	50 μ rad/sec
RSS Total	81 μ rad/sec

Figure 2.2-41. Slaving Mode Configuration
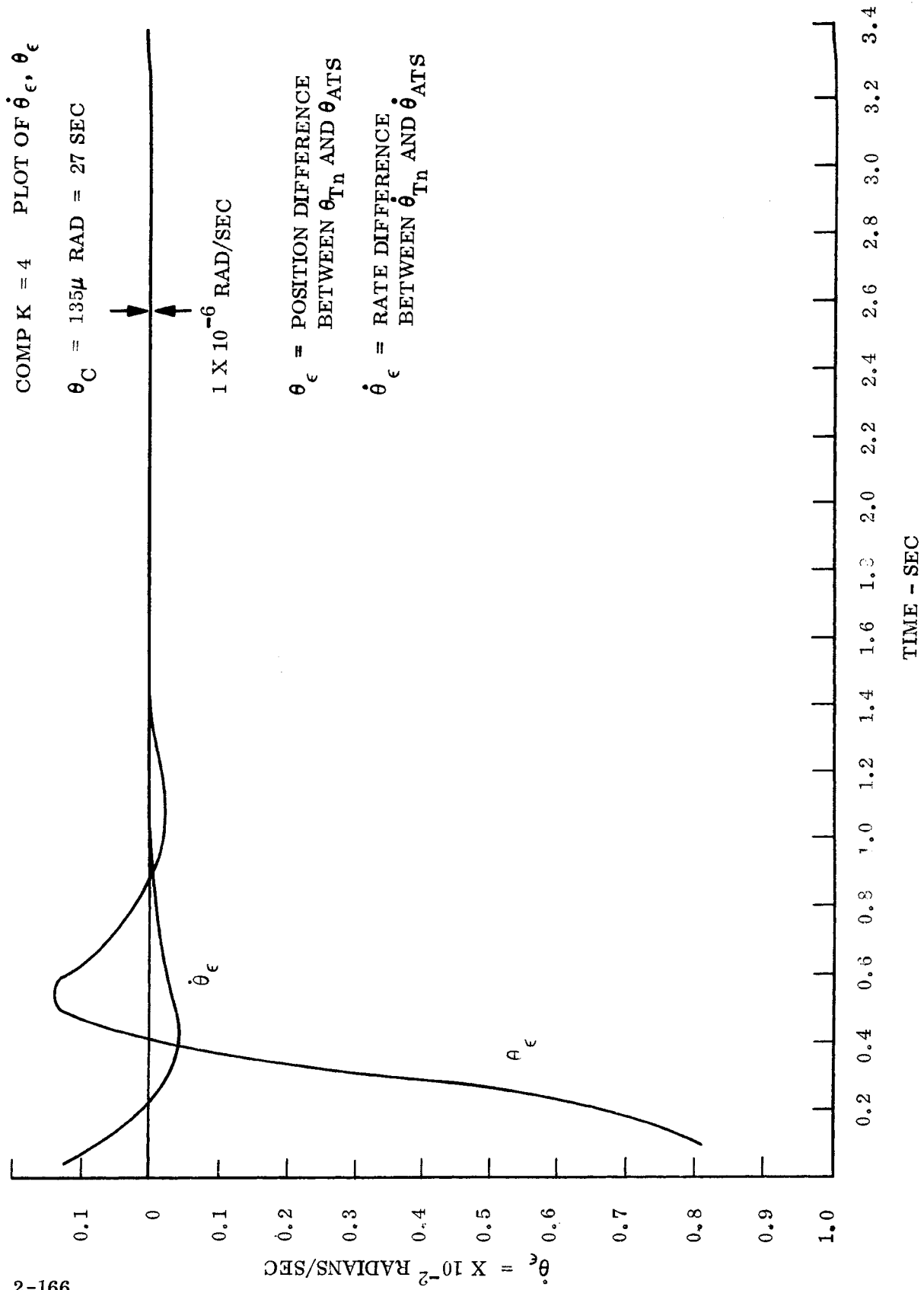
~~SECRET~~ SPECIAL HANDLING

Figure 2.2-42. Slaving Transient Profile

~~SECRET~~ SPECIAL HANDLING

2.2.1.9 ATS Performance with the Man in the Loop

Only very preliminary analysis has been performed relative to the performance of the ATS with the man in the loop via the MCS. A few comments are included here describing the general philosophy being applied to man's role and performance in the control loop. Man's performance in the loop will be optimized by simulation experiments to determine optimum manual stick transfer functions.

It has been shown that operators in manual control systems exhibit a type of behavior analogous to the behavior of compensating elements which have been inserted to improve the overall dynamic performance. When tested, it was found that the human control performance characteristics depended on the dynamic nature of the controlled element as well as the forcing function. This characteristic can be obscured in testing; but for averaged data taken with trained subjects, it is possible to show (McKruer and Kreudel, "The Human Operator as a Servo System Element," Journal of the Franklin Institute vol 267 (1959), pp 381-403 and 511-536) that an analytical describing function form is adequate to describe human behavior for a given controlled element and forcing function. When these describing functions are generalized, a servo model of human operation and adaptation (in compensatory tasks with random-appearing forcing functions) is obtained. This model is a dynamic description of human capabilities in such situations. The model consists of two elements:

a. A generalized describing function form

b. A series of "adjustment rules" which specify how to "set" the parameters in the generalized describing function.

The generalized describing function form for one- and two-dimensional compensatory control tasks is

$$N = \frac{K_p e^{-tS} (T_L S + 1)}{(T_N S + 1)(T_e S + 1)}$$

where

t is the reaction time delay.

T_N is the neuromuscular time constant.

T_L and T_e are the compensation characteristic time constants.

The gain K_p and the compensation time constants are the only parameters subject to control by the operator.

When in a task, the human operator adjusts these parameters to achieve the following objectives:

a. To achieve stable control

b. To achieve good low-frequency closed-loop response to the forcing function, where "good" means something like minimum rms error.

c. To achieve a phase margin of between 60 and 110 degrees based on the operator-generated criteria of b, above.

This describing function, with the parameters adjusted by the rules, applies quite well to all situations where the system crossover frequency, estimated by the application of the describing function model, is greater than the cutoff frequency of the system forcing function; that is, when the operator can make the controlled element follow the fastest fluctuations of the input.

The ATS design has incorporated the philosophy described above, including the time response requirements of the mission function, in the following fashion:

a. The describing function used in the synthesis of the tracking loop is the generalized describing function described above, but does not depend on the compensation

2-168

characteristic. This approach has been recommended by Kreudel and McRuer
in their WADC report as "The best performance is achieved when the describing
function required of the operator is as simple as possible."

b. The bandwidth (equivalent) of the tracking loop, including the human operator,
has been set by the response time requirements. (The response of the main
optics has been used as a requirement in the ATS because of the similarity of the
two tasks. The concept of limited slew or search has not been included as it is
not part of the SPDR requirements.) This approach far exceeds the bandwidth
criteria discussed earlier in this section for the validity of the describing function.

The philosophy was also tested in the Interim Simulation, which was a compensatory
tracking problem with the AVE forcing function (less noise) and the baseline controlled
element. The results showed that no major discrepancies existed in this area. One of the
aspects of AVE characteristic that has not been verified (except analytically) are the effects
of sampling, quantizing, and extrapolation on human performance in this problem.

2.2.1.10 Initial Tracking Error

At the end of slew the LOS error must be less than 540 μ rad/sec (See Table 1.1-1 entry 8).
In addition 2 minutes of position error are alloted in the pointing error analysis (See
Section 2.3). It is the purpose of this section to briefly summarize the calculations which
demonstrate compliance with these requirements.

Rate errors are introduced by off sets in the roll servo loop, a dynamic rate error of 0.01
deg/sec which can exist at the end of slew, and ephemeris errors which are principally
due to altitude uncertainties.

The ephemeris error is taken here as 130 μ rad/sec. This value is undoubtably high in
that it reflects an altitude error of 0.2 nm, considerably more than is now expected with
or without the low "g" accelerometer. The off set error in roll is calculated in Table 2.2-5,
to be 52 μ rad/sec. The position loop in pitch does not contribute to the rate "off-set"
error. The 0.01 deg/sec (174 μ rad/sec) dynamic error exists for both axes. The total
error is thus,

$$\sqrt{(52)^2 + (130)^2 + 5(174)^2} = 400 \; \mu \; \text{rad/sec}$$

Thus the 540 μ rad/sec requirement is satisfied.

The two minute position error allotment is used in the pointing error analysis in section 2, 3. The pitch axes contribution to this error is derived and compiled in Table 2.2-6 and is found to be virtually negligible.

The effect of the 9$^{\text{o}}$ cant has not been considered in this analysis. The effect of ephemeris errors is being revised downward. The results of this re-analysis will be documented in the next issue of CDRL 100.

TABLE 2.2-5.

COMPONENT	OFFSET	LOOP ERROR
Roll D/A Convertor	10^{-6} Amp	43.6 μ rad/sec
Roll Gyro	4×10^{-5} Rad/Sec	0.7 μ rad/sec
Roll Compensating Amp	2×10^{-2} Volts	22.0 μ rad/sec
Roll Power Amp	4×10^{-3} Amps	33.0 μ rad/sec
Roll Gimbal Friction	1×10^{-2} ft-lbs	18.5 μ rad/sec

Roll Off-Set Error = 52.5 μ rad/sec

LOS Rate Error = 52.5 μ rad/sec

~~SECRET~~ SPECIAL HANDLING

TABLE 2.2-6.

COMPONENT	OFFSET	LOOP ERROR
Pitch D/A Convertor	0.001 Amp	0.043 Min
Pitch Gyro	4×10^{-5} Rad/Sec	0.0000 Min
Compensating Amp	1×10^{-2} Volts	0.0012 Min
Power Amp	4×10^{-3} Amps	0.0018 Min
Friction	1×10^{-2} ft-lbs	0.0001 Min

Pitch Off-Set Error = 0.043 Min

LOS Position Error = 0.096 Min

~~SECRET~~ SPECIAL HANDLING

2.2.2 IMAGE ORIENTATION (DEROTATION) CONTROL SYSTEM

The image orientation control system is used to orient the target image that is displayed to the crewman. The target image is oriented in such a way that the in-track component of the target coordinate vector is aligned vertically at the completion of a scanner slew. Subsequent to the slew, the system is not driven to "track" the angular alignment. In the absolute worst case situation the initial alignment of the in-track vector will deviate by 16 degrees.

2.2.2.1 Requirements - System Level

a. Slew time - The prism slew shall be accomplished in $\left(\dfrac{\Delta\theta}{30}\right) + 1$ seconds where $\Delta\theta$ is the LOS angle in degrees between the correct pointing angle and the target when the slew command is applied.

b. Position accuracy - The position accuracy of the control system shall be within $+2.0$ degree of the command at $\left(\dfrac{\Delta\theta}{30}\right) + 1$ seconds after command initiation.

c. Position Feedback to MDAU - The decoupling computation requires that the prism position be known to within ± 1.0 degree and be available to the MDAU in digital form.

2.2.2.2 Servo Configuration

The servo was configured to meet the dynamic requirements while minimizing software, power, and weight.

The software is minimized by requiring that the input command be a step output from the computer. This type of input command avoids updating as a function of time until the start of the next slew.

The motor was sized for this application to minimize weight and power. The rated torque available from the motor is 4 inch-ounces for a 16 volt input.

The servo configuration for the Image Orientation drive is shown in Figure 2.2-43. This configuration allows the control loop to meet the performance requirements with a minimum of software, power, and weight.

A step input is applied to the command filter. The filter shapes the input to the servo loop such that the overshoot which results due to amplifier saturation is minimized. Amplifier saturation is a result of the high gain necessary to reduce the offset, caused by motor and load friction, to less than 1 degree. The open loop frequency response of the control loop is shown in Figure 2.2-44. Figure 2.2-45 shows the image rate and position as a function of time for step commands of 0.5 and 1.0 radian. Figure 2.2-46 illustrates the torque applied to the load as a function of time for input steps of 0.5 and 1.0 radian.

2.2.2.3 Error Analysis

The following error apportionment has been established

Servo Static Error	± 1.0 degree
Position Transducer Error	± 1.0 degree
A/O Conversion Error	± 0.5 degree
Command Equation Error*	± 0.5 degree

The RMS prism error is thus 1.6 degrees, considerably better than the allowed ±5 degrees. This apportionment does not consider misalignments between the ARS and the OV. It is possible that approximations may be made in the drive equations which will increase the command error above 0.5 degree.

---

*Conservative Estimate

~~SECRET~~ **SPECIAL HANDLING**
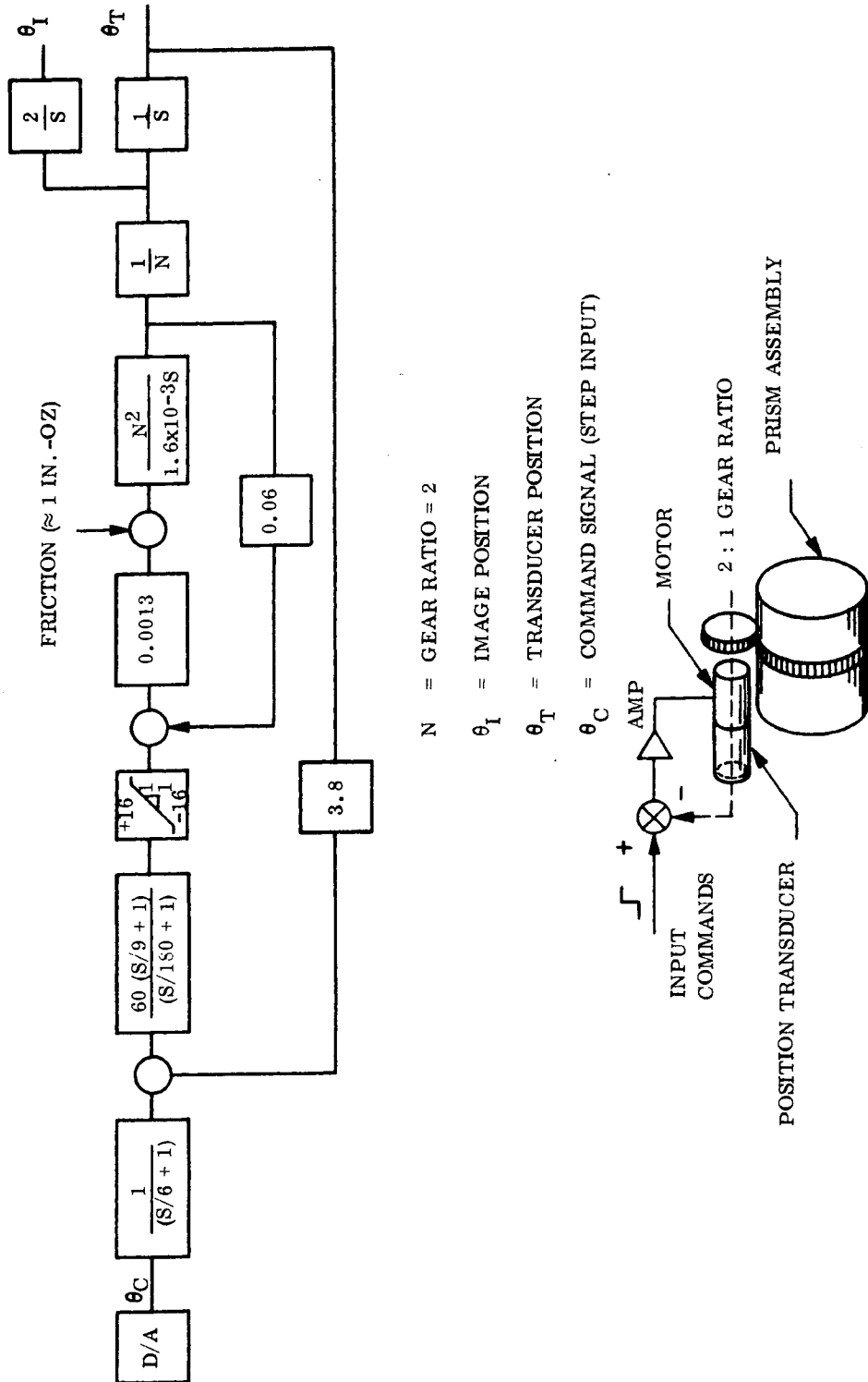
Figure 2.2-43. Image Orientation Control Loop

N = GEAR RATIO = 2

θ_I = IMAGE POSITION

θ_T = TRANSDUCER POSITION

θ_C = COMMAND SIGNAL (STEP INPUT)

~~SECRET~~ **SPECIAL HANDLING**

~~SECRET~~ **SPECIAL HANDLING**
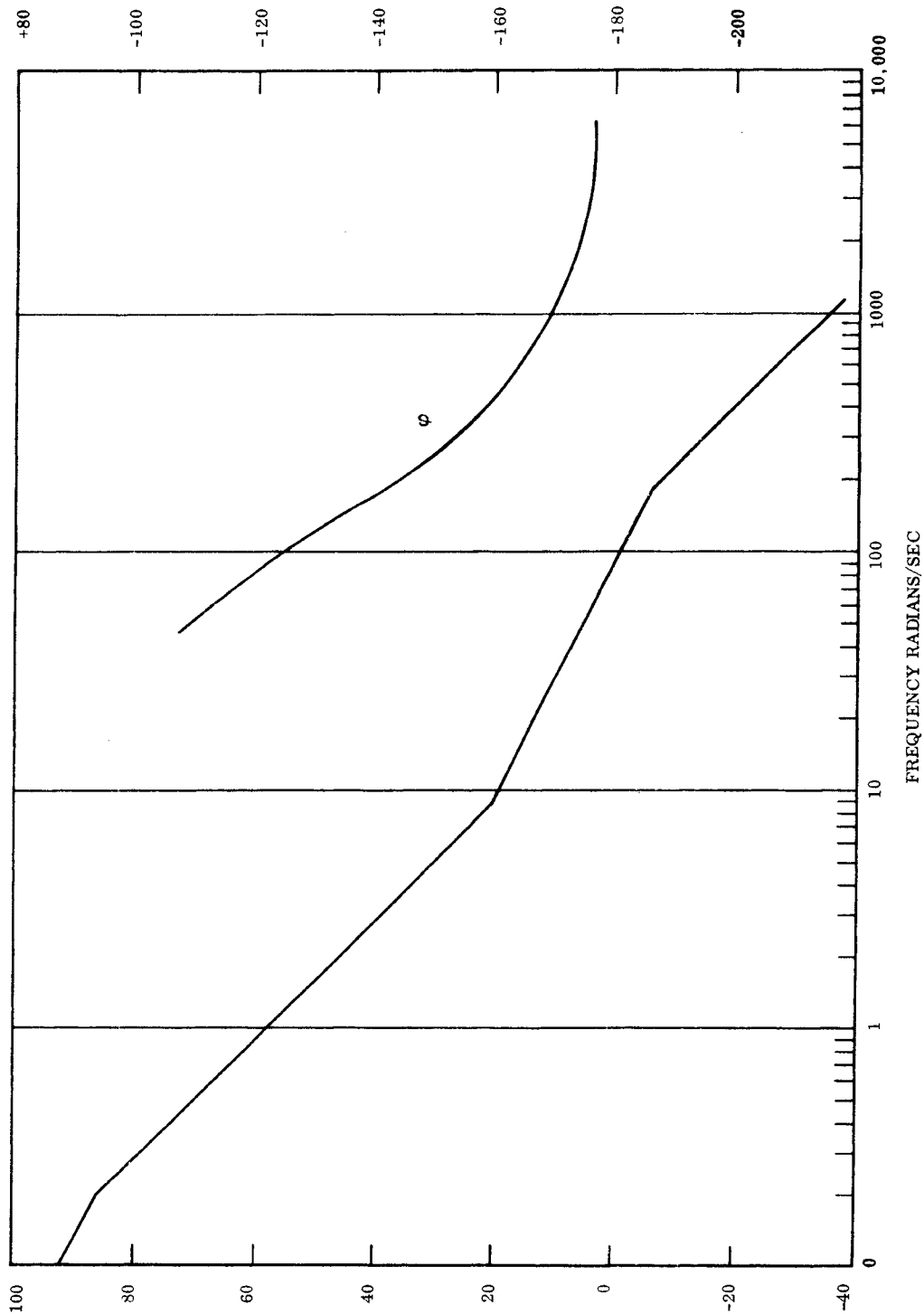
Figure 2.2-44. Open Loop Frequency Response of the Image Orientation Servo

2-175

~~SECRET~~ **SPECIAL HANDLING**

~~SECRET~~ **SPECIAL HANDLING**
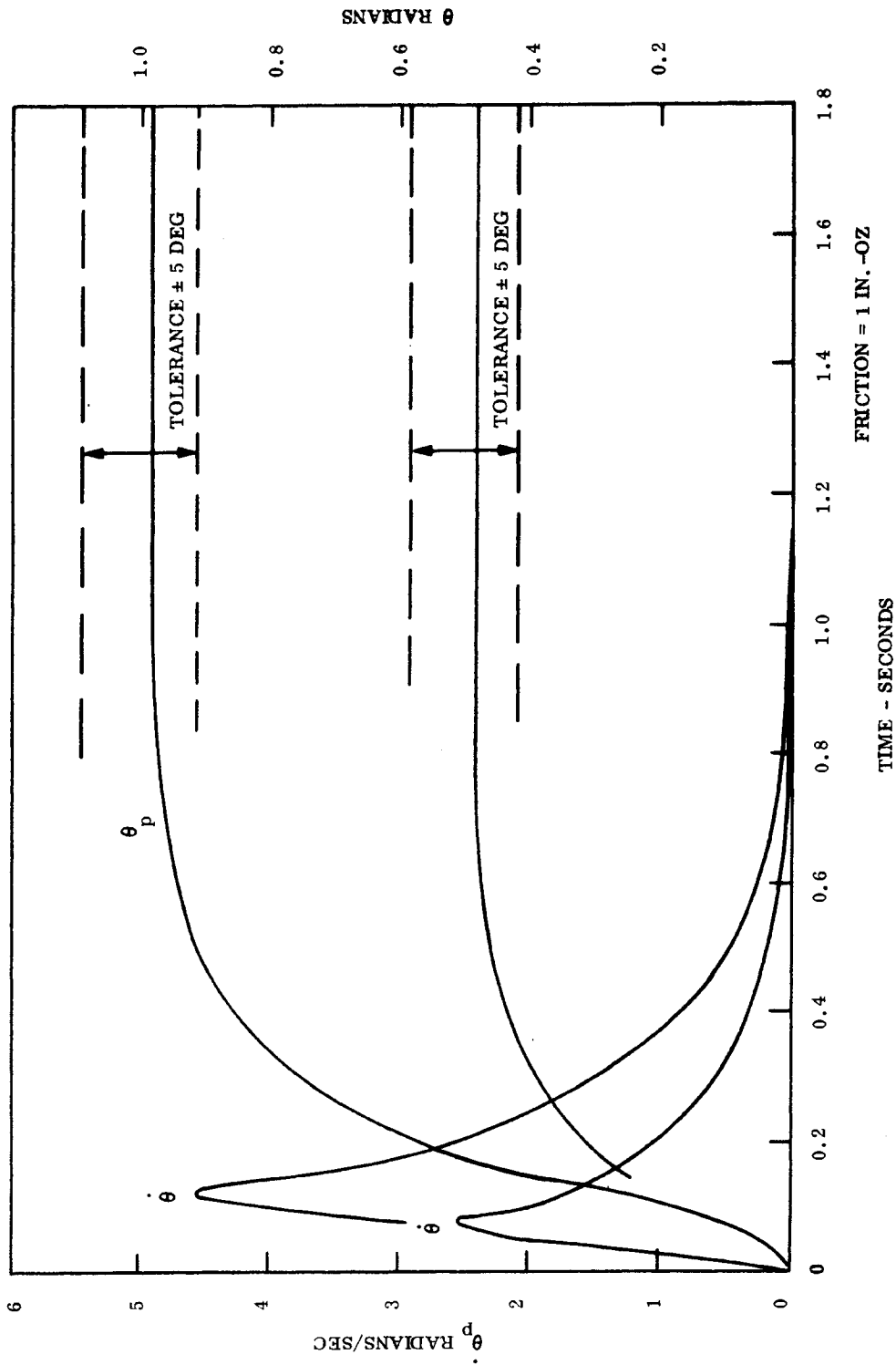
Figure 2.2-45. Prism θ and $\dot{\theta}$ as a Function of Time
for Input Steps of 0.5 and 1 Radian

~~SECRET~~ **SPECIAL HANDLING**
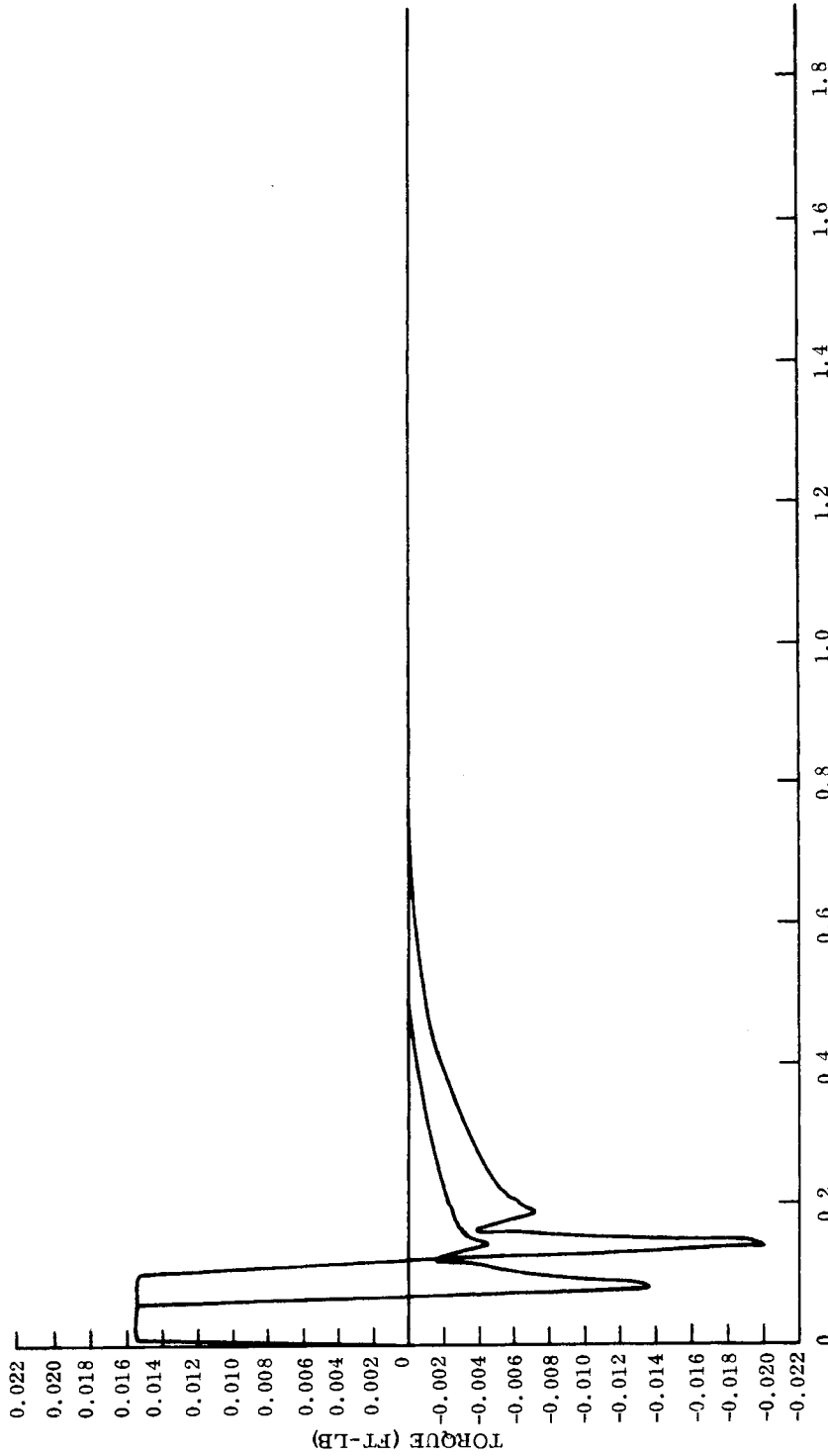
Figure 2.2-46. Torque Applied to the Load as a Function
of Time for Input Steps of 0.5 and 1.0 Radian

2-177

2.2.3 DYNAMIC COMPONENT REQUIREMENTS

2.2.3.1 Command Filter

The command filter receives a step command from the MDAU and processes this signal for input to the K – 3 amplifier. The gain of the command filter is equal to 1 volt per volt ± 2 percent. The gain shall be linear for inputs from +4 to –4 volts.

The frequency response of the command filter shall have the following characteristics:

$$\frac{K}{(\tau_1 S + 1)}$$

where

τ_1 = 0.166 second ± 5 percent

K = gain

Additional breaks shall not contribute more than 6 degrees of phase shift below 100 radians per second.

2.2.3.2 Amplifier

The K – 3 amplifier shall sum the input signal from the command filter and the feedback signal from the position transducer. It shall process this signal and output it to the motor winding. The gain of the K – 3 amplifier is equal to 60 volts per volt ± 10 percent. The output shall be linear from + 16 to – 16 volts.

The frequency response of the K – 3 amplifier shall have the following characteristics:

$$\frac{(\tau_1 S + 1)}{(\tau_2 S + 1)}$$

2-178

~~SECRET~~ **SPECIAL HANDLING**

where

$$\tau_1 = 0.111 \text{ second} \pm 10 \text{ percent}$$

$$\tau_2 = 0.0055 \text{ second} \pm 10 \text{ percent}$$

Additional breaks shall not contribute more than 6 degrees of phase shift below 1000 radians per second.

2.2.3.3 Motor

The following characteristics were submitted by Subcontractor "A" for the K - 3 motor.

    a.   Rated Torque = 4 inch-ounces

    b.   Resistance of winding = 26 ohms

    c.   Time constant = 0.0008 second

    d. $K_v = 0.06$ volt/radian/second

The characteristics were used to determine the K - 3 servo loop dynamic requirements.

2.2.3.4 Position Transducer

The position transducer converts the motor shaft angular position to an analog voltage for feedback to the K - 3 amplifier. The gain of the position transducer is equal to 3.8 volts per radian $\pm$ 2 percent. The gain shall be linear for inputs from +1 to -1 radian. The position transducer shall contribute no more than 6 degrees of phase shift below 1000 radians per second.

~~SECRET~~ SPECIAL HANDLING

2.2.4 ZOOM CONTROL SERVO

The zoom control system functions identically in the two zoom magnification ranges: 15 to 30 power and 63-1/2 to 127 power. The difference being the insertion of the power change lenses into the system when the zoom control is operating in the high range.

a. Requirements - The servo response to a step input shall be such that the position error is less than 5 percent of the step amplitude in 0.5 second.

   The zoom assembly position shall be monitored and fed to the MDAU to modify the gain of the scanner control loops with the crewman in the loop.

b. Servo Configuration - The servo was configured to meet the dynamic requirements while minimizing weight and power.

   Figure 2.2-47 shows the servo configuration of the zoom servo assembly and Figure 2.2-48 shows the open loop frequency response. The servo was designed to get as much gain as possible in front of the point of motor and load friction while still minimizing the servo overshoot to transient inputs.

   Figure 2.2-49 shows zoom assembly rate and position as a function of time for a step input equal to the total zoom range.
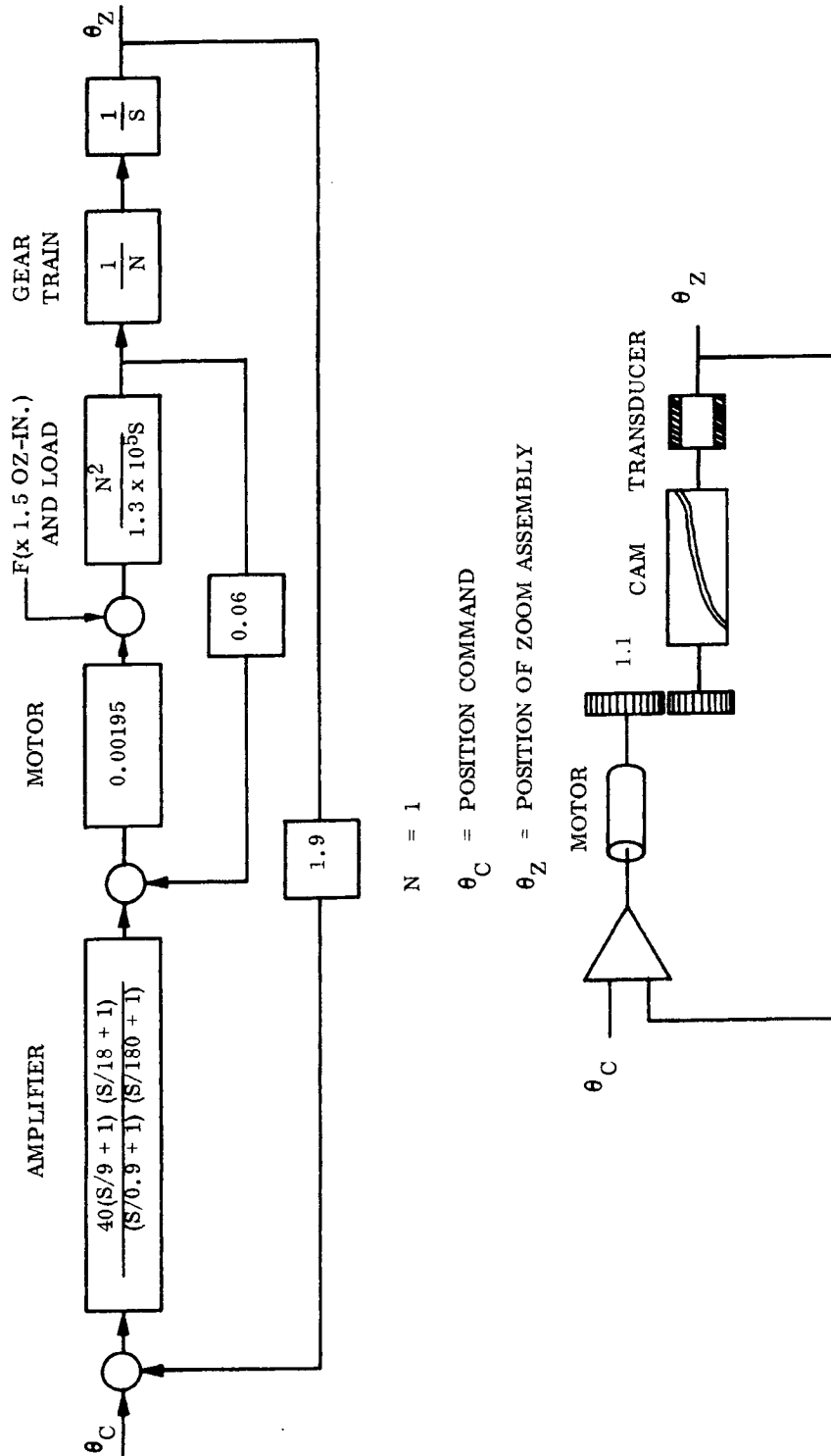
Figure 2.2-47. Zoom Assembly

~~SECRET~~ **SPECIAL HANDLING**

$$GH = \frac{1250 \ (S/9 + 1) \ (S/18 + 1)}{S(S/19 + 1) \ (S/9 + 1) \ (S/180 + 1)}$$

FREQUENCY RADIANS/SEC
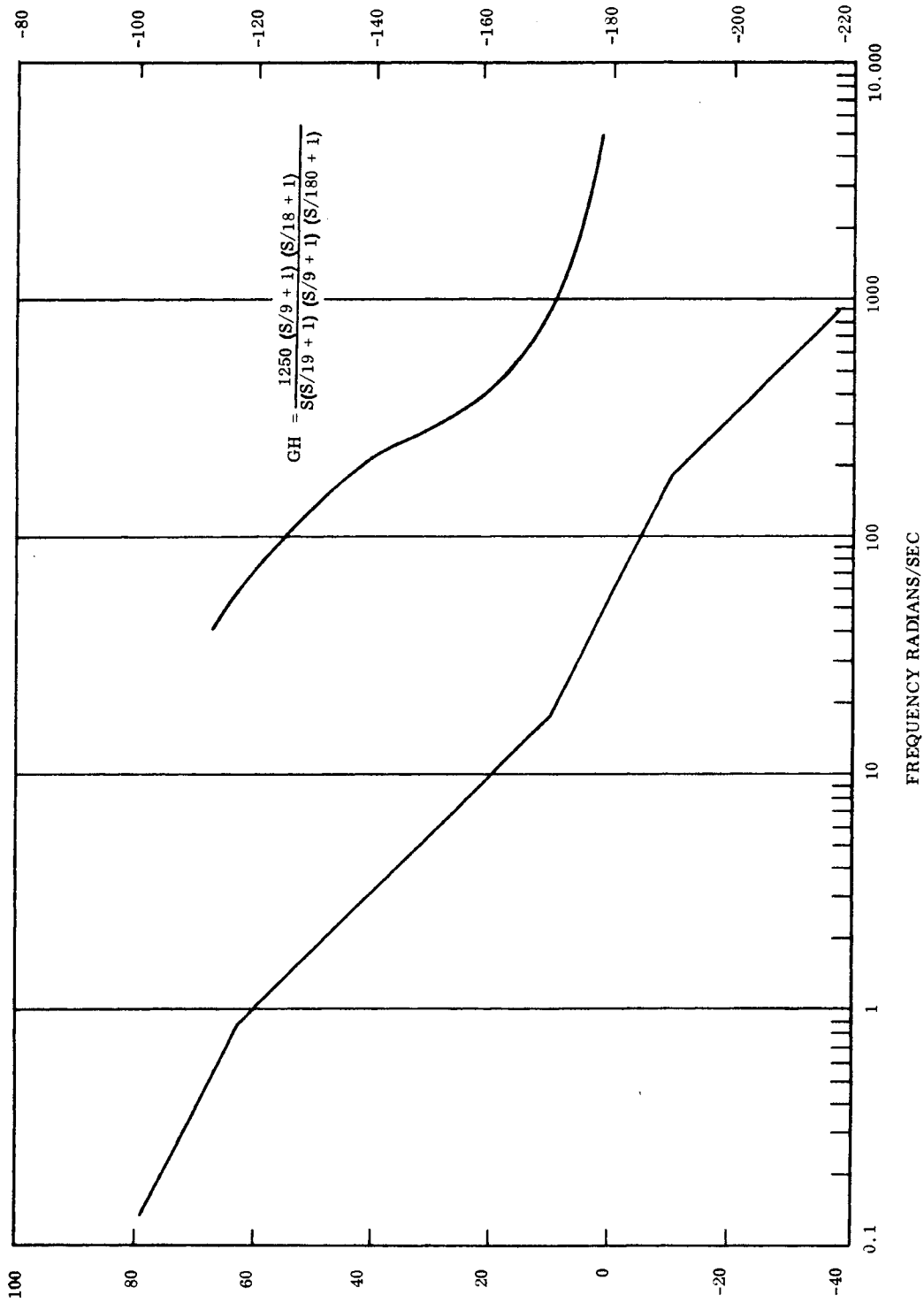
Figure 2.2-48. Open Loop Frequency Response of the Zoom Control Loop

~~SECRET~~ **SPECIAL HANDLING**
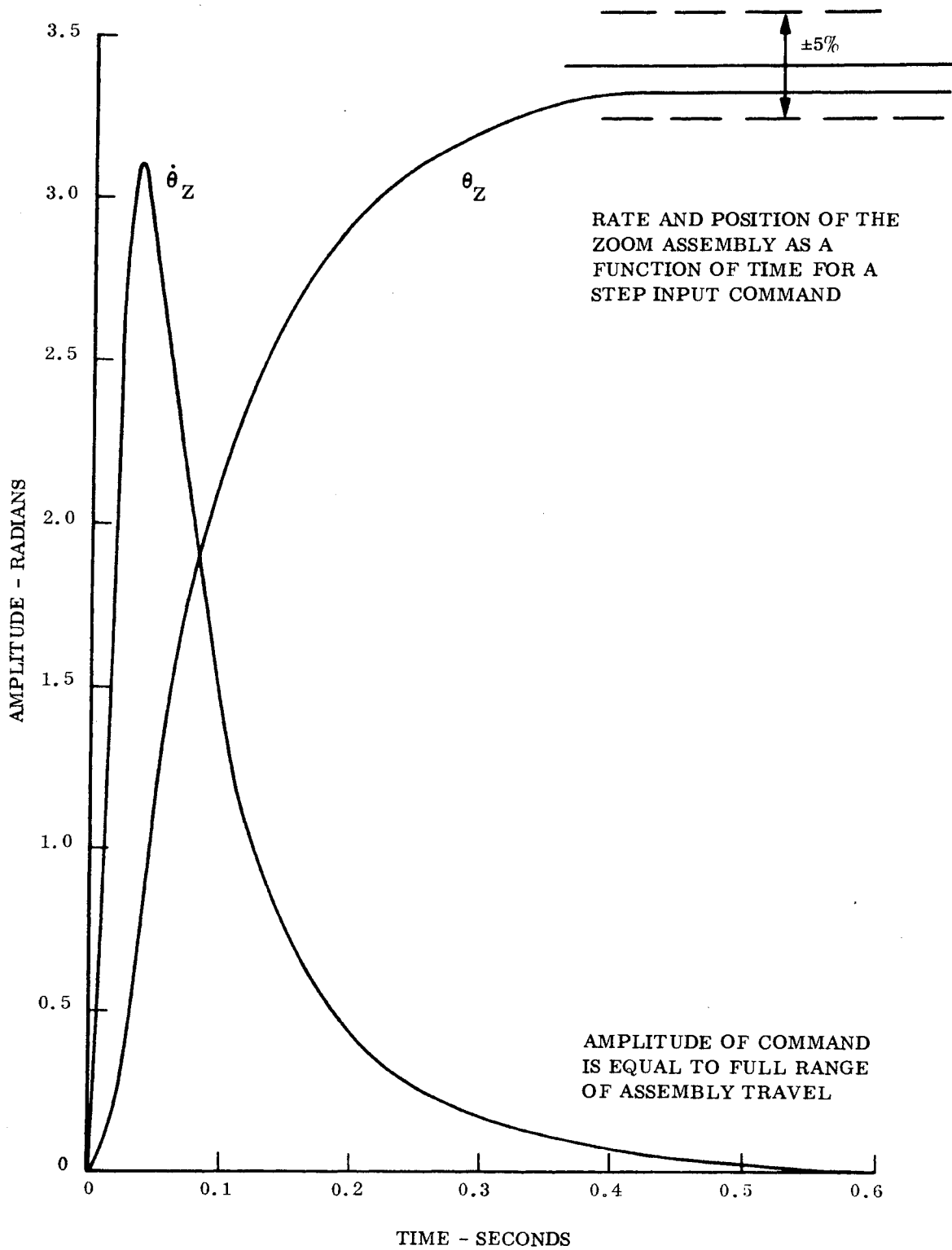
Figure 2.2-49. Rate and Position of the Zoom Assembly as a
Function of Time for a Step Input Command

2.2.5 BLANKING CONTROL SERVO

This blanking control servo serves to protect the ATS optics and the flight crew from a direct view of the sun. The blanking control unit drives the shutter into the optical path when the sun sensor detects illumination above a preset level. The shutter has two discretes positions. A signal from the sun sensor to the control electronics will allow the shutter to be driven to the closed position by a mechanical spring.

2.2.6 POWER CHANGE SERVO

The magnification controller provides the command signal to the power change control.
Either of two signals are provided, depending upon whether the magnification controller
is in the low or high zoom ranges. The power change control system drives a set of two
lenses into or out of the optical path. Functionally, the power change lenses are inserted
to provide the lower range of magnification as the magnification control stick passes from
the high to low range. The lenses shall be able to move from one position to the other in
1.0 second. The power change drive shall be provided with a manual backup in the event
of drive failure.

The power change servo is an open loop control which drives the lenses into position when
the magnification controller passes from low to high power range. The lenses have two
discrete positions. Figure 2.2-50 illustrates the control servo. It shows a discrete signal
feedback from the lens assembly to indicate its arrival at either extreme of the travel with
this signal being used to terminate the drive excitation.

COMMAND
FROM
MAGNIFICATION ⟶ LOGIC ⟶ DRIVE ELECTRONICS ⟶ MOTOR AND LOAD
CONTROL
STICK

DISCRETE POSITION TRANSDUCER
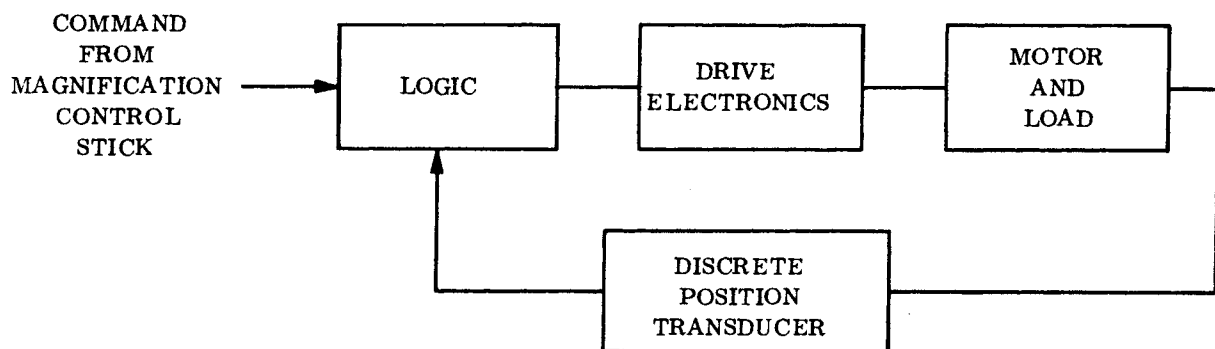
Figure 2.2-50. Control Servo

2-185/2-186

2.3 ATS POINTING ERROR ANALYSIS

This section presents an error analysis which identifies all major contributors to ATS
pointing error in the automatic and slave modes and demonstrates a general capability
to meet the CEI requirements. The alignment error apportionment considered does per-
mit the pointing requirements to be slightly exceeded in the event of a worst case tolerance
buildup.

The material is subdivided as follows:

2.3.1   Discussion of Results

2.3.2   Description of Error Sources and Errors Removed by Boresighting

2.3.3   Procedure for Determining Errors

2.3.4   Statistical Treatment of Error Sources and the Total Pointing Error

2.3.5   Results of Monte Carlo Computer Programs

2.3.6   Procedure Required to Determine Allowable Misalignments

2.3.1 DISCUSSION OF RESULTS

Table 2.3-1 presents a list of the sources of pointing error for the main optics and ATS,
a brief description of each, the current allocated value, and describes the type of each
error for any given vehicle (i.e., random, time varying, or constant error.) It is ex-
pected that all of the alignment tolerances listed in Table 2.3-1 can not be met during on-
orbit operation. As a result, more realistic misalignments were assumed in some of the
error sources and are shown in Table 2.3-2.

Table 2.3-3 summarizes the pointing errors that result from the error values in Tables
2.3-1 and 2.3.2. The errors in Table 2.3-3 correspond to the targets "2 sigma" pointing
errors that occur over the scan field of:

~~SECRET~~ **SPECIAL HANDLING**

TABLE 2.3-1

ATS/MAIN OPTICS ERROR SOURCES		VALUE ARC MIN. (2σ) (ON-ORBIT)	TYPE OF ERROR (GIVEN A PARTICULAR VEHICLE)
ATS	δby_a — Optical Axis	1.2	Constant
	δbz_a — Errors	1.2	Constant
	$\delta \theta_{1a}$ — Roll Gimbal Direction	0.5	Constant
	$\delta \psi_{1a}$ — Errors	0.5	Constant
	$\delta \psi_{2a}$ — Mirror Mounting Error	0.5	Constant
	$\delta \psi_{3a}$ — Gimbal Non-Orthogonality	0.5	Constant
	$\delta \theta_a^m$ — Gimbal Angle	0.333	Random
	$\delta \Omega_a^m$ — Measurement Error	0.333	Random
	$\delta \theta_a^{cs}$ — Control System	0.894	Random
	$\delta \Omega_a^{cs}$ — Pointing Error	0.894	Random
Prime Optics	δby — Optical Axis Measurement	0.667	Random
	δbz — Errors	0.667	Random
	$\delta \theta_1$ — Roll Gimbal Direction	0.5	Constant
	$\delta \psi_1$ — Errors	0.5	Constant
	$\delta \psi_2$ — Mirror Mounting	0.5	Constant
	$\delta \psi_3$ — Gimbal Non-Orthogonality	1.5	Constant
	$\delta \theta^m$ — Gimbal Angle	0.333	Random
	$\delta \Omega^m$ — Measurement Error	0.333	Random
	$\delta \theta^{cs}$ — Control System	0.447	Random
	$\delta \Omega^{cs}$ — Pointing Error	0.447	Random

~~SECRET~~ **SPECIAL HANDLING**

Table 2.3-1 (Cont)

ATS/MAIN OPTICS ERROR SOURCES	VALUE ARC MIN. (2σ) (ON-ORBIT)	TYPE OF ERROR (GIVEN A PARTICULAR VEHICLE)
Vehicle Attitude $\left\{ \begin{array}{l} \delta g_x \\ \delta g_y \text{,} \\ \delta g_z \\ \rho_{xy} \\ \rho_{yz} \\ \rho_{xz} \end{array} \right.$ Vehicle Attitude Error (Referenced to TM Reference) / Correlation in Attitude Error	2.311 / 1.477 / 1.477 / * 0.873 / *-0.8395 / *-0.7467	Random + time variant component / N.A. / N.A. / N.A.
δby^T_a } ATS Tracking	0.667	Random
δbz^T_a } Error	0.667	Random
δby^T_a { Prime Optics	0.667	Random
δbz^T_a } Tracking Error	0.667	Random
$\left. \begin{array}{l} \delta\alpha_x \\ \delta\alpha_y \\ \delta\alpha_z \end{array} \right\}$ ATS/Prime Optics Alignment	1.0 degree (total)	
$\left. \begin{array}{l} \delta\alpha_{x_1} \\ \delta\alpha_{y_1} \\ \delta\alpha_{z_1} \end{array} \right\}$ Increase in Attitude Error Due to DACO Rate Gyro Error	1.36 **2 / 1.025 **2	Increases with time from last star tracker update
$\left. \begin{array}{l} \delta R_x \\ \delta R_y \\ \delta R_z \end{array} \right\}$ Target Location Error	500 ft / 500 ft / 100 ft	Random / Random / Random

* Correlation Coefficients are dimensionless.
**2This value corresponds to 44 seconds after the last star tracker update.

TABLE 2.3-1 (Cont)

ATS/MAIN OPTICS ERROR SOURCES		VALUE ARC MIN (2σ) (ON-ORBIT)	TYPE OF ERROR (GIVEN A PARTICULAR VEHICLE)
δr_x δr_y δr_z	Vehicle position error without low "g" accel.	3200 ft 370 ft 210 ft	Random with bias component
δr_X δr_Y δr_Z	Vehicle position error with low "g" accel.	1300 ft 145 ft 210 ft	Random with bias component

TABLE 2.3-2

ERROR SOURCE		VALUE AND TYPE OF ERROR GIVEN A PARTICULAR VEHICLE (ARC MIN.) "2 SIGMA"			
ATS	δby_a	(2.4)	Constant	(0.707)	Time Varying
	δbz_a	(2.4)	Constant	(0.707)	Time Varying
	$\delta \theta_{1a}$	(1.224)	Constant	(0.52)	Time Varying
	$\delta \psi_{1a}$	(1.224)	Constant	(0.52)	Time Varying
	$\delta \psi_{2a}$	0.5	Constant		
	$\delta \psi_{3a}$	0.5	Constant		
	$\delta \theta_a^m$	0.333	Random		
	$\delta \Omega_a^m$	0.333	Random		
	$\delta \theta_a^{cs}$	0.894	Random		
	$\delta \Omega_a^{cs}$	0.894	Random		

( )----Numbers in parentheses indicate changes from Table 3.2-1.

~~SECRET~~ **SPECIAL HANDLING**

TABLE 2.3-2 (Cont)

ERROR SOURCE		VALUE AND TYPE OF ERROR GIVEN A PARTICULAR VEHICLE (ARC MIN.) "2 SIGMA"	
Prime Optics	δby	0.667	Random
	δbz	0.667	Random
	$\delta \theta_1$	0.5	Constant
	$\delta \psi_1$	0.5	Constant
	$\delta \psi_2$	0.5	Constant
	$\delta \psi_3$	1.5	Constant
	$\delta \theta^m$	0.333	Random
	$\delta \Omega^m$	0.333	Random
	$\delta \theta^{cs}$	0.447	Random
	$\delta \Omega^{cs}$	0.447	Random
Vehicle Attitude	δg_x	2.311	
	δg_y	1.477	
	δg_z	1.477	
	ρ_{xy}	0.873 *	
	ρ_{yz}	-0.8397 *	
	ρ_{xz}	-0.7467 *	
	δby^T_a	0.667	Random
	δb^T_{za}	0.667	Random
	δb^T_y	0.667	Random
	δb^T_z	0.667	Random
	$\delta \alpha_x$ $\delta \alpha_y$ $\delta \alpha_z$	Less than 40 min. each axis constant error plus 0.707 arc min. each axis time varying	

*Correlation Coefficients are Dimensionless.

~~SECRET~~ **SPECIAL HANDLING**

TABLE 2.3-2. (Cont)

ERROR SOURCE	VALUE AND TYPE OF ERROR GIVEN A PARTICULAR VEHICLE (ARC MIN.) "2 SIGMA"	
$\delta\alpha_{x1}$	1.36 **	Time Varying
$\delta\alpha_{y1}$	1.025 **	Time Varying
$\delta\alpha_{z1}$	1.025 **	Time Varying

**Corresponds to 44 seconds after the last star tracker update.

TABLE 2.3-3. SUMMARY OF POINTING ERRORS "2 SIGMA"

	BASED UPON ERRORS IN TABLE 2.3-1	BASED UPON ERRORS IN TABLE 2.3-2
Primary Optics Pointing Error (Automatic Mode)		
Including all errors, after 2.5 rev. (without low "g" accelerometer)	23.7 arc min.	23.7 arc min.
Including all errors, after 2.5 rev. (with low "g" accelerometer)	11.3 arc min.	11.3 arc min.
Neglecting ephemeris and target location errors--2 axis alignment monitor on star tracker and at time of star tracker update	4.2 arc min.	4.2 arc min.
Neglecting ephemeris and target location errors, and with perfect knowledge of attitude	3.2 arc min.	3.2 arc min.

TABLE 2.3-3. SUMMARY OF POINTING ERRORS "2 SIGMA" (Cont)

	BASED UPON ERRORS IN TABLE 2.3-1	BASED UPON ERRORS IN TABLE 2.3-2
Primary Optics Pointing Error (Pointing angles derived from the ATS, or Slave Mode) Boresighting Angles $\Omega_1 = 20^\circ;\ \Sigma_1 = -20^\circ$ $\Omega_2 = -20^\circ;\ \Sigma_2 = -20^\circ$	4.0 arc min.	5.3 arc min.
ATS Pointing Error (Automatic Mode and After ATS Boresighting)		
Neglecting ephemeris and target location errors but including 2 axis alignment monitor on star tracker and at time of star tracker update	4.58 arc min.	5.65 arc min.
Same as above, but 44 seconds after star tracker update	5.0 arc min.	6.0 arc min.

$$-30^\circ < \Sigma \le 15^\circ \qquad \text{for the primary optics}$$

$$|\Omega| < 40^\circ$$

$$-30^\circ < \Sigma \le 60^\circ \qquad \text{for the ATS}$$

$$|\Omega| < 45^\circ$$

(In the discussion section of this report, it can be seen that the pointing error varies with the pointing angles.)

These "2 sigma" error values mean that given a large number of vehicles, 95.4 percent of them will always have pointing errors less than the value shown in Table 2.3-3. (For the remaining 4.6 percent of the vehicles, the pointing error can be always greater than the values shown in Table 2.3-3.)

It is required that, given any vehicle, the ATS and primary optic pointing error be respectively less than 8 arc min. and 6 arc min. for 95.4 percent of the times that these systems are automatically pointed at a target. (This is neglecting target location and vehicle ephemeric errors.) In addition, in a slave mode, the primary optics must point to within 6 arc min. of the ATS line of sight for 95.4 percent of the time.

Sections 2.3.3 and 2.3.5 of the discussion show that even though the pointing errors summarized in Table 2.3-3 are less than 6 arc min. -- "two sigma" -- the overall pointing requirements are not met for any given vehicle.

This analysis assumes time varying errors from the PAC structure which exceed 0.5 degrees of LOS error, however, and are thus in violation of our CEI spec guarantees.

2.3.2 DESCRIPTION OF ERROR SOURCES AND ERRORS REMOVED BY BORESIGHTING.*
Figure 2.3-1 and 2.3-2 show sketches of the ATS and primary optical systems. To physically describe each error source, it is helpful to consider that only one error exists at any one time. To define optical axis errors, assume that the image of a spot on the center of the tracking mirror could be observed on the display screen, (see Figure 2.3-3) and that only optical axis errors, δby_a, δbz_a, exist. The angle between the actual and the desired optical axes (i.e., the angle between the lines $a\sigma$ and $d\sigma$ in Figure 2.3-3) is defined as the optical axis error. δby_a and δbz_a are the pitch and yaw components of this error.

The roll gimbal direction errors, $\delta\theta_{1a}$ and $\delta\psi_{1a}$ are defined in Figure 2.3-4 with respect to a set of ATS references axes, x_a, y_a, z_a.

The mirror mounting error, $\delta\psi_{2a}$, is defined as the acute angle between a line on the mission surface and the mirror pitch axis. The gimbal orthogonality error, $\delta\psi_{3a}$, is defined as the angular deviation from 90° between the gimbal pitch and roll axes. A similar set of errors is defined for the primary optical system. Next, the errors removed by ATS to primary optics boresighting will be discussed.

When the ATS and primary optical systems are installed within the vehicle, they are aligned to a reference system located at the Laboratory Module bulkhead, x_b, y_b, z_b. The boresighting procedure assumes that each element of the ATS and primary optics is perfectly aligned to coordinate systems, x_a, y_a, z_a, and x_p, y_p, z_p. The boresighting procedure is then used to find the angular rotation between the $\vec{x}_a$ and $\vec{x}_p$ coordinate systems. (Or equivalently, the angular rotation between the $\vec{x}_a$ and $\vec{x}_b$ and $\vec{x}_b$, $\vec{x}_p$ coordinate systems.)

Now, if any ATS or primary optic components shift in alignment with respect to the $\vec{x}_a$ or $\vec{x}_p$ coordinate system (see Figure 2.3-4) the boresighting procedure will equate the effect of these misalignments to motions of the entire ATS with respect to the primary

*See also Section 2.6, Boresighting.
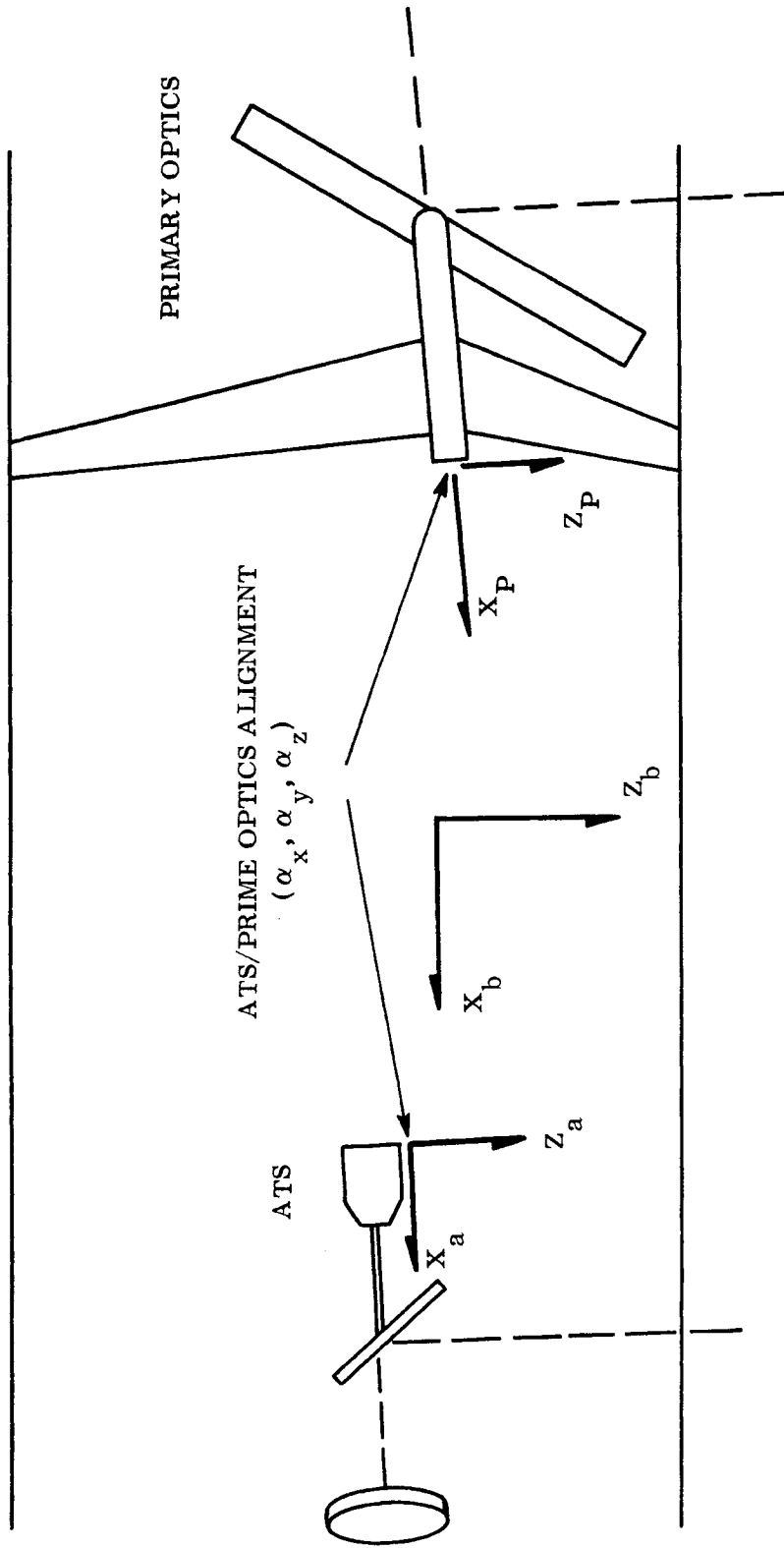
Figure 2.3-1. ATS and Primary Optics Configuration (Side View)

~~SECRET~~ **SPECIAL HANDLING**

PRIMARY OPTICS

$\dot{Y}_P, Y_b$

x_b, x_P

$\alpha_x, \alpha_y, \alpha_z$

Y_a

ATS

x_a
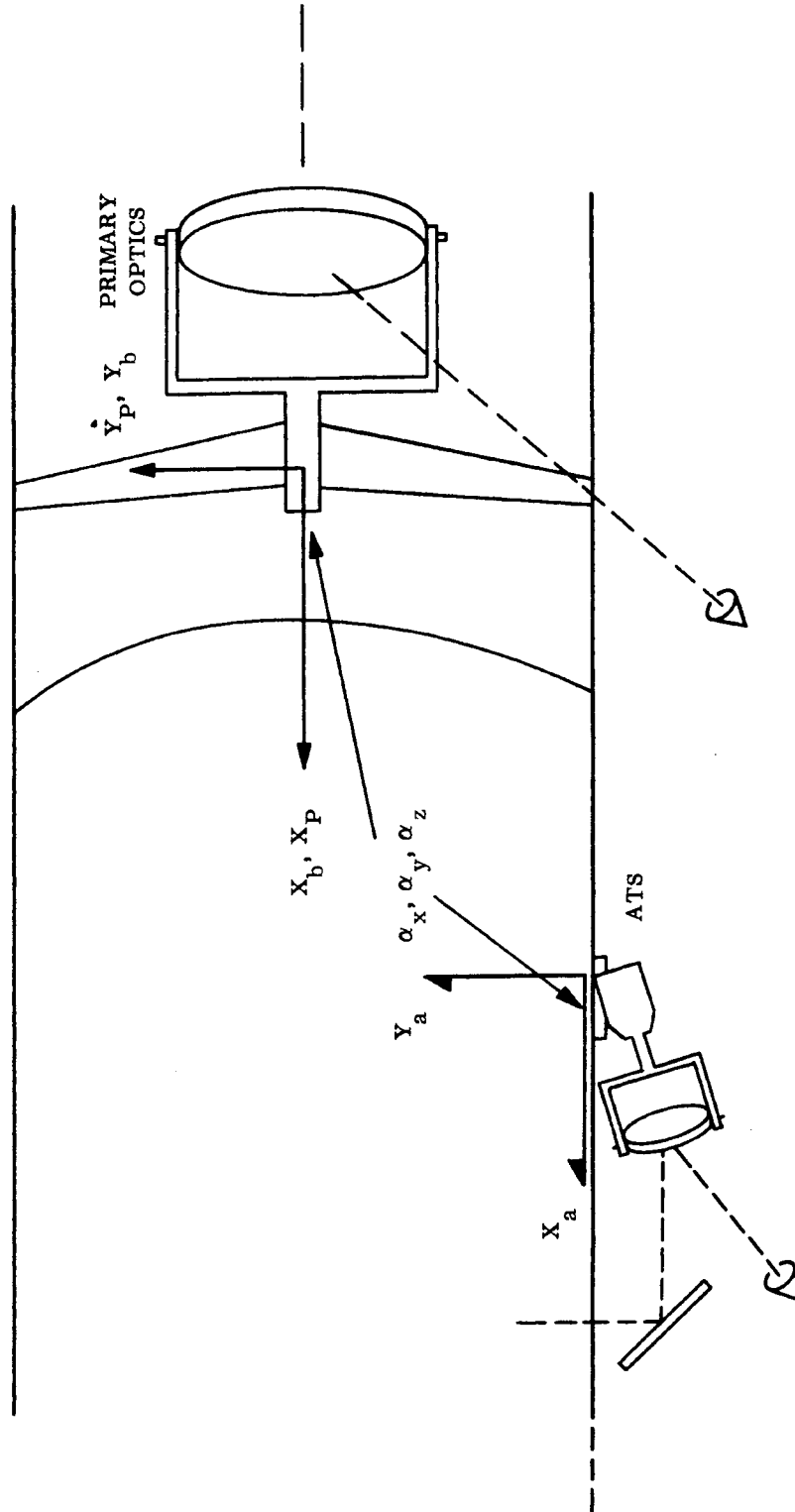
Figure 2.3-2. ATS and Main Optics Configuration (Top View)

~~SECRET~~ **SPECIAL HANDLING**

OPTICAL AXIS ERROR

Y

Z

"TARGET" IMAGE

DESIRED OPTICAL AXIS

d

a

σ

"TARGET"

ACTUAL OPTICAL AXIS
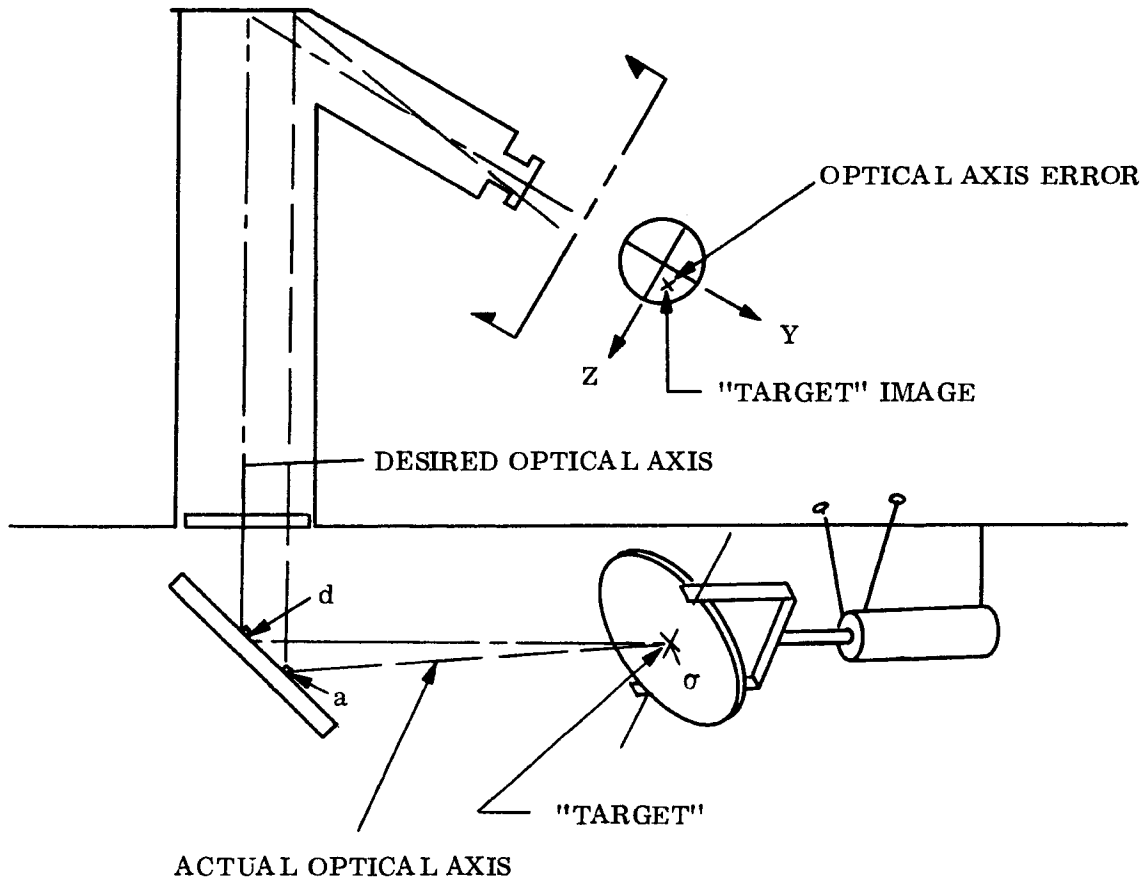
Figure 2.3-3. ATS Configuration

~~SECRET~~ **SPECIAL HANDLING**

OPTICAL AXIS

X_a

$\delta \theta_{1a}$

δbz_a

Z_a

LOS
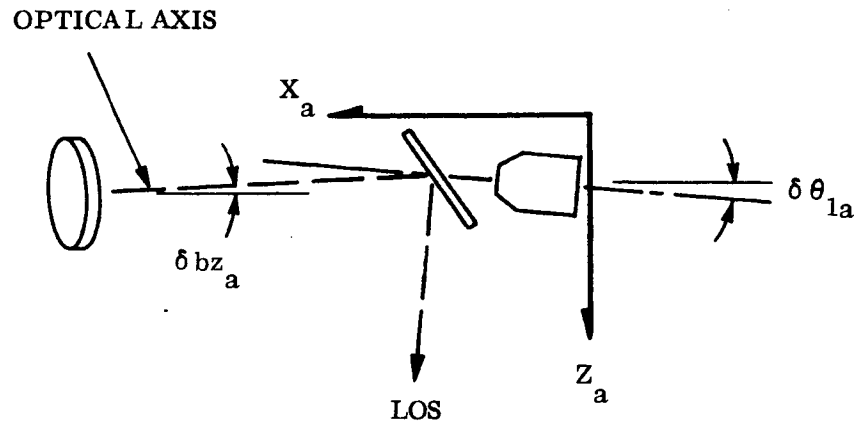
δby_a, δbz_a - OPTICAL AXIS ERRORS

$\delta \theta_{1A}$, $\delta \psi_{ia}$ - ROLL GIMBAL DIRECTION ERRORS

Y_a

$\delta \psi_{1a}$

OPTICAL AXIS

X_a

90°

δby_a
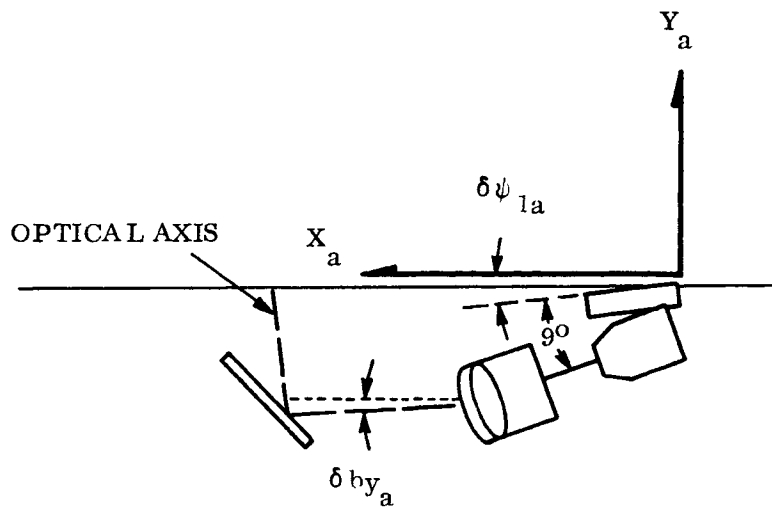
Figure 2.3-4. ATS Errors

optics. This causes an error in the computed value of the alignment α_x, α_y, α_z and also in the primary optics pointing when in the slave mode or in ATS pointing for the automatic mode.

Even though the boresighting procedure does not determine the misalignments of all of the ATS and primary optic elements, it does tend to reduce the effects of the static and random error. Table 2.3-4 shows the absolute value of the sensitivity of the primary optic and ATS pointing error (at nadir) to some of the sources of error for the case with no bore-sighting and the case with boresighting. It is important to note that even though the bore-sighting at $\Omega_1 = 20^o$, $\Sigma_1 = -20^o$ and $\Omega_2 = -20^o$, $\Sigma_2 = -20^o$ decreased the sensitivity of the pointing error to most of the error sources for nadir pointing, the error sensitivities can increase for other pointing angles.

For example, at pointing angles of $\Sigma = -30$, $\Omega = 45$ the sensitivity of the main optic or ATS pointing error to the ATS optical axis error in the pitch direction is:

$$\frac{\partial \text{ (Los Error)}}{\partial \text{ by}_a} = 1.0 \quad \text{without boresighting}$$

and;

$$\frac{\partial \text{ (Los Error)}}{\partial \text{ by}_a} = 1.06 \quad \text{without boresighting.}$$

In conclusion, the boresighting procedure tends to reduce the sensitivity of the pointing error to the static or random type errors. (Static errors are misalignments that do not change during the time interval from the start of a boresighting operation until the next boresighting operation.) Also the best reduction in sensitivity of the pointing error can be expected to occur for pointing angles close to the boresighting angles.

~~SECRET~~ **SPECIAL HANDLING**

TABLE 2.3-4. SENSITIVITY OF POINTING ERROR AT NADIR

ERROR SOURCE	PRIME OPTICS (SLAVED)		ATS AUTOMATIC	
	WITH BORESIGHTING	WITHOUT BORESIGHTING	WITH BORESIGHTING	WITHOUT BORESIGHTING
$\delta \theta_{1A}$	0	2.0	0	2.0
$\delta \psi_{1A}$	0.28	1.0	0.28	1.0
$\delta \psi_{2a}$	0.19	1.414	0.19	1.414
$\delta \psi_{3a}$	0.3	1.0	0.3	1.0
δby_a	0	1.0	0	1.0
δbz_a	0.34	1.0	0.34	1.0
$\delta \theta_{1p}$	0	2.0	2.0	0
$\delta \psi_{1p}$	0.34	1.0	0.657	0
$\delta \psi_{2p}$	0.392	1.414	1.81	0
$\delta \psi_{3p}$	0.43	1.0	1.43	0
α_x	0	1.0	0	1.0
α_y	0	1.0	0	1.0
α_z	0	0	0	0

Boresighting performed for targets at:

$$\Omega_1 = 20^o, \quad \Sigma_1 = -20^o$$

$$\Omega_2 = -20^o, \quad \Sigma_2 = -20^o$$

~~SECRET~~ **SPECIAL HANDLING**

2.3.3 PROCEDURE FOR DETERMINING POINTING ERRORS

To obtain the pointing errors that result from the sources of error in Tables 2.3-1 and 2.3-2, a computer program using Monte Carlo techniques was written. (The Monte Carlo technique was used to allow appropriate probability distributions to be used for each error source and to correctly combine the effects of the error sources to obtain the total pointing error probability distribution.) Figure 2.3-5 shows the procedure for obtaining pointing errors after ATS boresighting. (To obtain pointing errors for the automatic mode without boresighting, the same program is used but the part enclosed by the dashed line is omitted.) In this technique, values of all errors are initially selected from appropriate probability distributions, normal, uniform, etc. -- and gimbal angles are computed for the first boresighting target. New error values are then found for randomly varying errors, and the ATS and primary optic gimbal angles are computed for the second boresighting target. The error in computed ATS/Primary Optics alignment is then found. Finally, new error values are found for the random and time varying errors and the ATS or primary optic pointing errors are found for several different pointing angles. This process is then repeated several hundred times to gain confidence in the probability distributions obtained for the pointing error. The sources of error that are considered to be constant, randomly varying or time varying given any particular vehicle were shown in Tables 2.3-1 and 2.3-2.

The method used in obtaining the ATS/TM alignment involves a least squares solution. (There are three unknowns and four independent equation.) Computer results have indicated that the accuracy of the boresignting procedure is degraded if one of the independent equations is dropped and ATS/TM alignment found by standard matrix inversion.

2.3.4 STATISTICAL TREATMENT OF ERROR SOURCES AND THE TOTAL POINTING ERROR.

Tables 2.3-1 and 2.3-2 show whether each error sources is constant, randomly varying, or time varying given a particular vehicle, and show the two sigma values for each error source. For the present, it is assumed that the value of each error is normally distributed

~~SECRET~~ **SPECIAL HANDLING**

```
┌──────────────────────────┐        ┌──────────────────────┐
│ INPUT ERROR CHARACTERISTICS│───▶   │      INITIALIZE      │
│ AND BORESIGHTING ANGLES    │       │     PROBABILITY      │
│   Σ_i, Ω_i; Σ_2, Ω_2       │       │  DENSITY FUNCTIONS   │
└──────────────────────────┘        └──────────────────────┘
```

$$\Sigma_i, \Omega_i; \Sigma_2, \Omega_2$$

SELECT VALUES FOR ALL ERRORS ◀── RANDOM NO. GENERATOR

COMPUTE GIMBAL ANGLES FOR FIRST BORESIGHTING TARGET Σ_1, Ω_1 ──▶ SELECT NEW VALUES FOR RANDOM ERRORS

COMPUTE GIMBAL ANGLES FOR SECOND BORESIGHTING TARGET Σ_2, Ω_2 ──▶ OBTAIN SOLUTION FOR ERROR IN COMPUTED ATS/PRIME OPTICS ALIGNMENT, $\alpha_x, \alpha_y, \alpha_z$

PLACE $\alpha_x, \alpha_y, \alpha_z$ IN PROBABILITY DENSITY

REPEAT FOR 1000 TRIALS

SELECT NEW VALUES FOR RANDOM AND TIME VARYING ERRORS ◀── RANDOM NO. GENERATOR

COMPUTE LOS POINTING ERROR FOR POINTING ANGLES $-30^\circ < \Sigma < 15^\circ$ $|\Omega| < 40^\circ$ ──▶ PLACE EACH LOS POINTING ERROR IN PROBABILITY IN DENSITY

PRINT OUT PROBABILITY DISTRIBUTIONS

Figure 2.3-5. Boresighting Error Analysis Computer Program

~~SECRET~~ **SPECIAL HANDLING**

and has a zero mean value. Then, for example, if 1,000 vehicles were constructed, the "2 sigma" value of 0.5 arc min. for allowable mirror mounting error requires that 954 of the vehicles must have mirror mounting errors less than 0.5 arc min. and 46 of the vehicles can have mirror mounting errors greater than 0.5 arc min. Also, since the mirror mounting error is considered to be constant, its value must remain constant during the time interval between boresighting. Random and time varying errors are also considered to vary randomly from one vehicle to the next. However, given a particular vehicle, it is assumed that the time varying errors remain constant only during the boresighting operation, while the randomly varying errors can change even during the boresighting procedure. Then to properly interpret the total pointing error obtained, one must consider a large number of vehicles. For example, the "2 sigma" pointing error of 4 arc min. for the main optics in the automatic mode at the viewing angles of $\Sigma = -30^O$ and $\Omega = 40^O$ means that 954 out of 1000 vehicles will have pointing errors less than 4 arc min. when pointing to a target located at $\Sigma = -30^O$ and $\Omega = 40^O$. Now, if a vehicle is constructed with the alignment tolerances in Table 2.3-1 or 2.3-2, the pointing error observed with this particular vehicle may always be greater than 6 arc min. for some particular stereo and obliquity angle. This indicates that it was one of the 46 out of 1000 "bad vehicles".

Now if the requirement is that for any vehicle the pointing error must be less than 6 arc min. at least 95.4 percent of the time ("2 sigma"), then the alignment tolerances in Tables 2.3-1 or 2.3-3 are not acceptable and additional work is required to define an acceptable set of alignment tolerances. (This is discussed in Section 2.3.) If the requirements mean that pointing errors must be less than 6 arc min. for 95.4 percent of the vehicles, then the tolerances in Table 2.3-3 are acceptable.

Finally, some discussion of the use of the words "2 sigma" is warranted. "Two sigma" as used in describing the pointing error, means that given a large number of vehicles, 95.4 percent of the vehicles will have pointing errors less than the value shown, and does not refer to twice the standard deviation of the pointing error. Twice the standard deviation of an error only gives the value that is greater than the actual error 95.4 percent of the

time if that error is distributed normally and has a zero mean value. From Figure 2.3-6, showing the distribution of pointing error, it can be seen that the error is not distributed normally -- in fact it closely resembles a Rayleigh distribution. Thus, "2 sigma" value used in describing the pointing error refers only to the 95.4 percent level and not to twice the value of the standard deviation of the pointing error.

If all errors are RSS'd to give the pointing error, the difference between the 95.4 percent confidence level pointing errors for an assumed normal distribution and the actual distribution for the pointing error becomes even more noticeable.

If we assume for simplicity that only optical axis errors exist, the primary optics pointing error, $\Delta\theta$, for the automatic mode can be written as;

$$\Delta\theta = \sqrt{\delta bz^2 + \delta by^2}$$

If RSS techniques are assumed, and the "2 sigma" value of optical axis errors, δ by and δbz are 0.667 arc min., Figure 2.3-7 shows the assumed distribution for the total pointing error. For this simple case an exact combination of errors shows the pointing error distribution to be a Rayleigh distribution. Comparing the exact and the RSS'd summation of errors in Figure 2.3-7, one can see that overly large errors are indicated if only the RSS'd technique is used.

2.3.5 RESULTS OF MONTE CARLO COMPUTER PROGRAMS.

Figures 2.3-8 through 2.3-12 show the cumulative probability distributions of ATS and Primary Optics Pointing errors based upon the error values in Tables 2.3-1 and 2.3-3 and for selected stereo and obliquity angles. Figure 2.3-13 and 2.3-14 show the error in computed value of ATS/Primary Optics alignment. (However, in Section 2.3.1 it was noted that the error in the computed value of ATS/TM alignment does not necessarily increase pointing error. Constant errors, such as gimbal non-orthogonality, will cause error in

~~SECRET~~ SPECIAL HANDLING
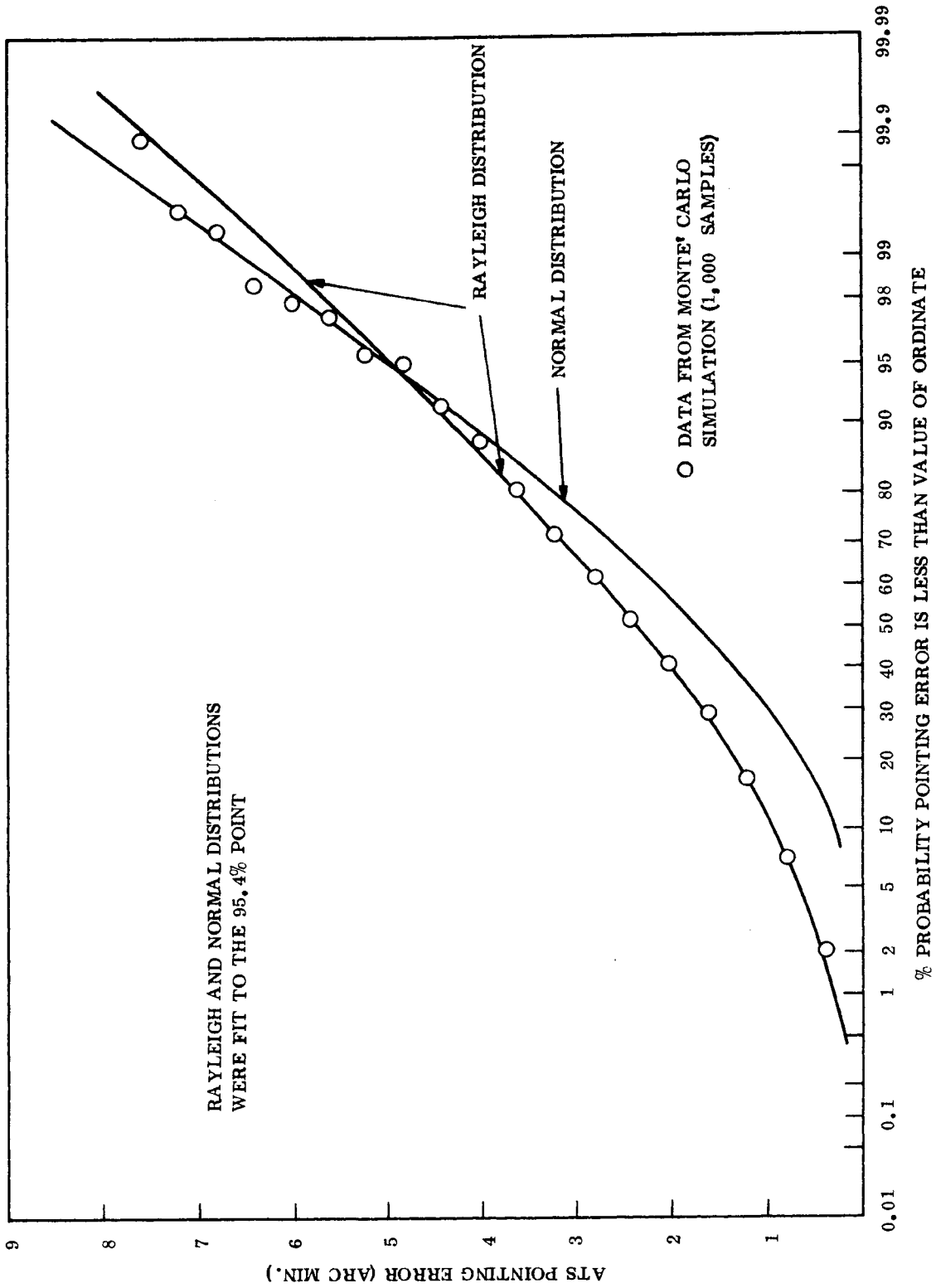
Figure 2.3-6. Comparison of Pointing Error Distributions

~~SECRET~~ SPECIAL HANDLING
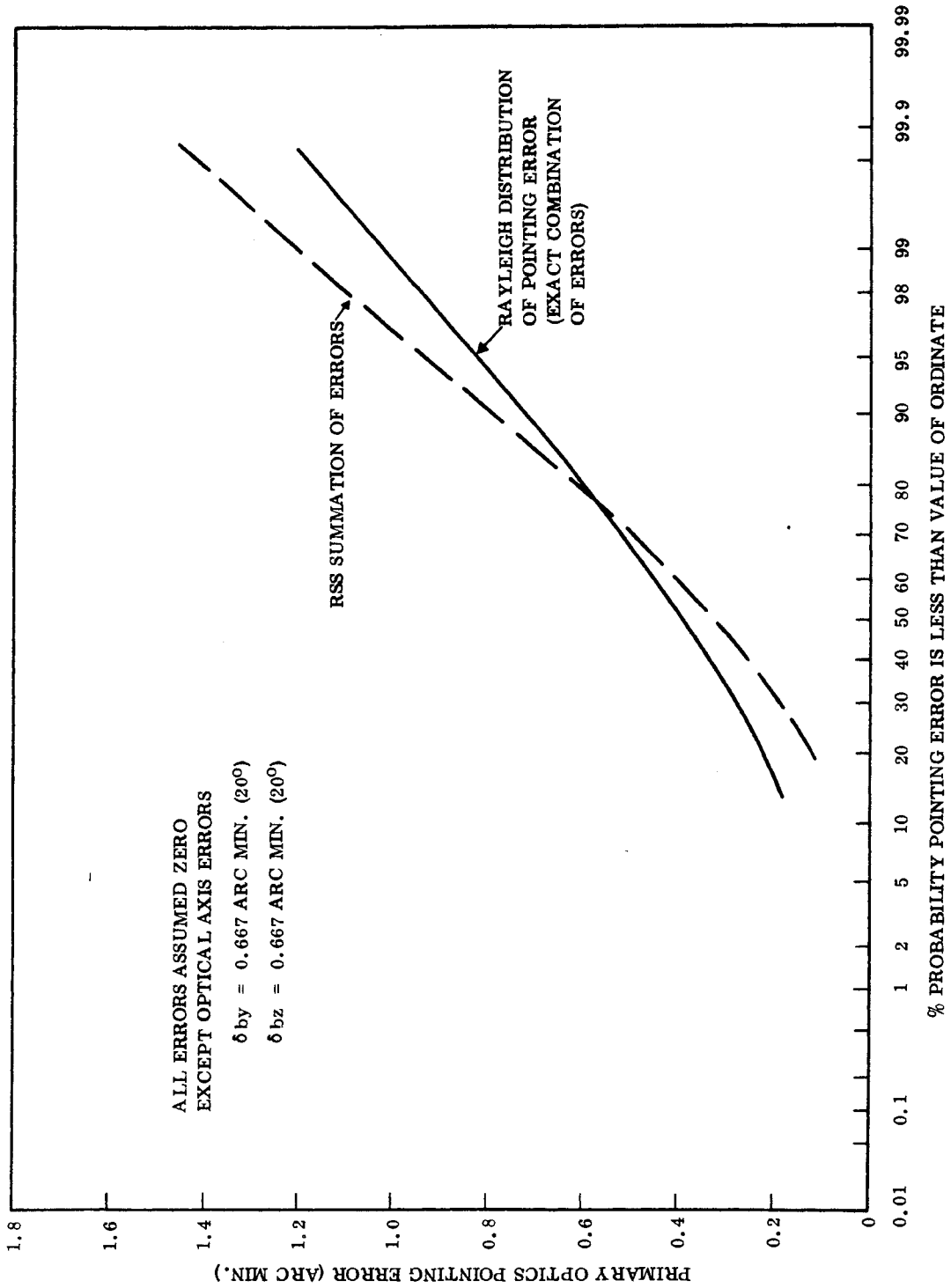
Figure 2.3-7. Comparison of RSS'd and Exact Summation of Errors

~~SECRET~~ **SPECIAL HANDLING**
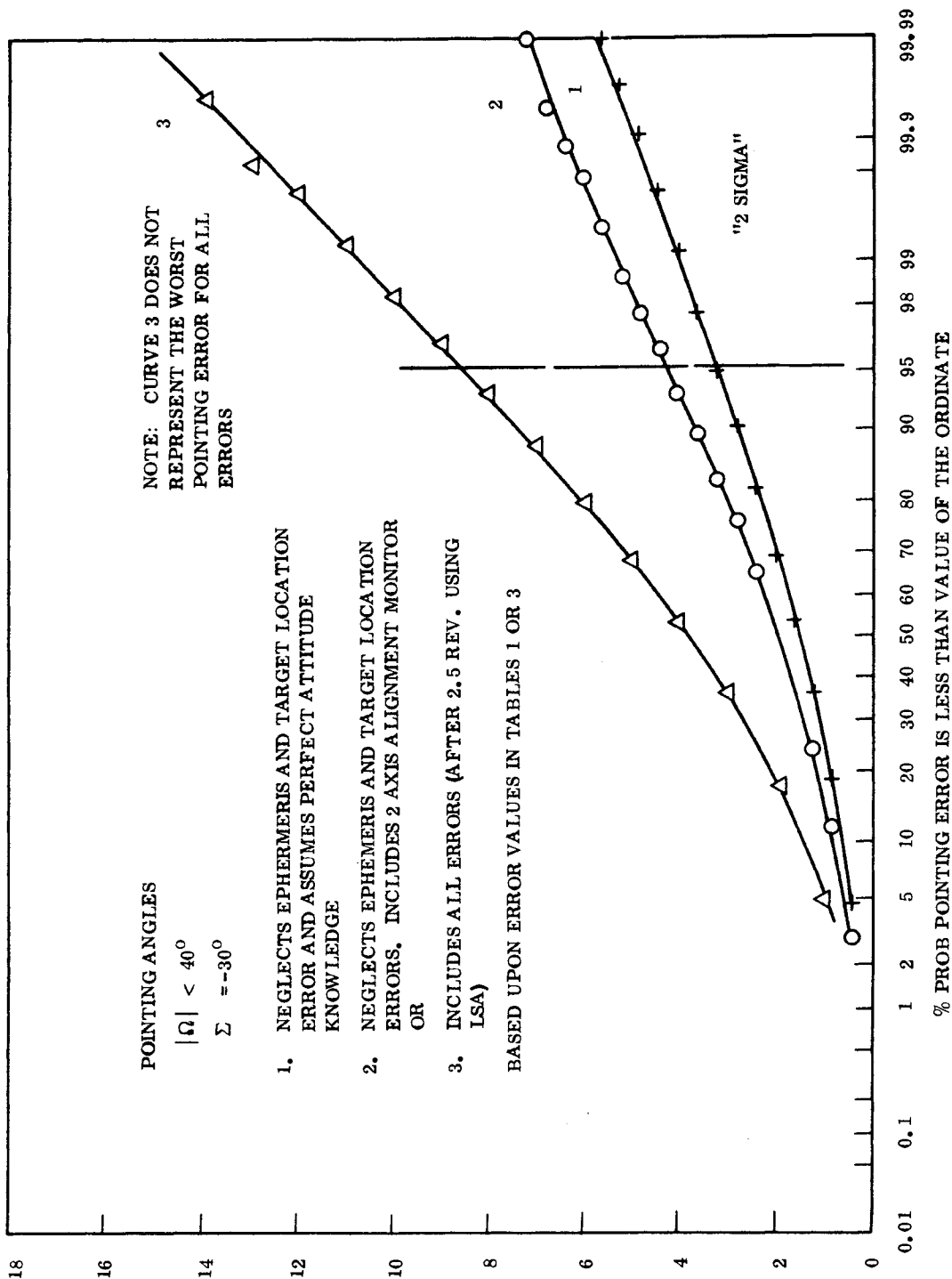
Figure 2.3-8. Primary Optics Pointing Error (Automatic Mode)

~~SECRET~~ **SPECIAL HANDLING**
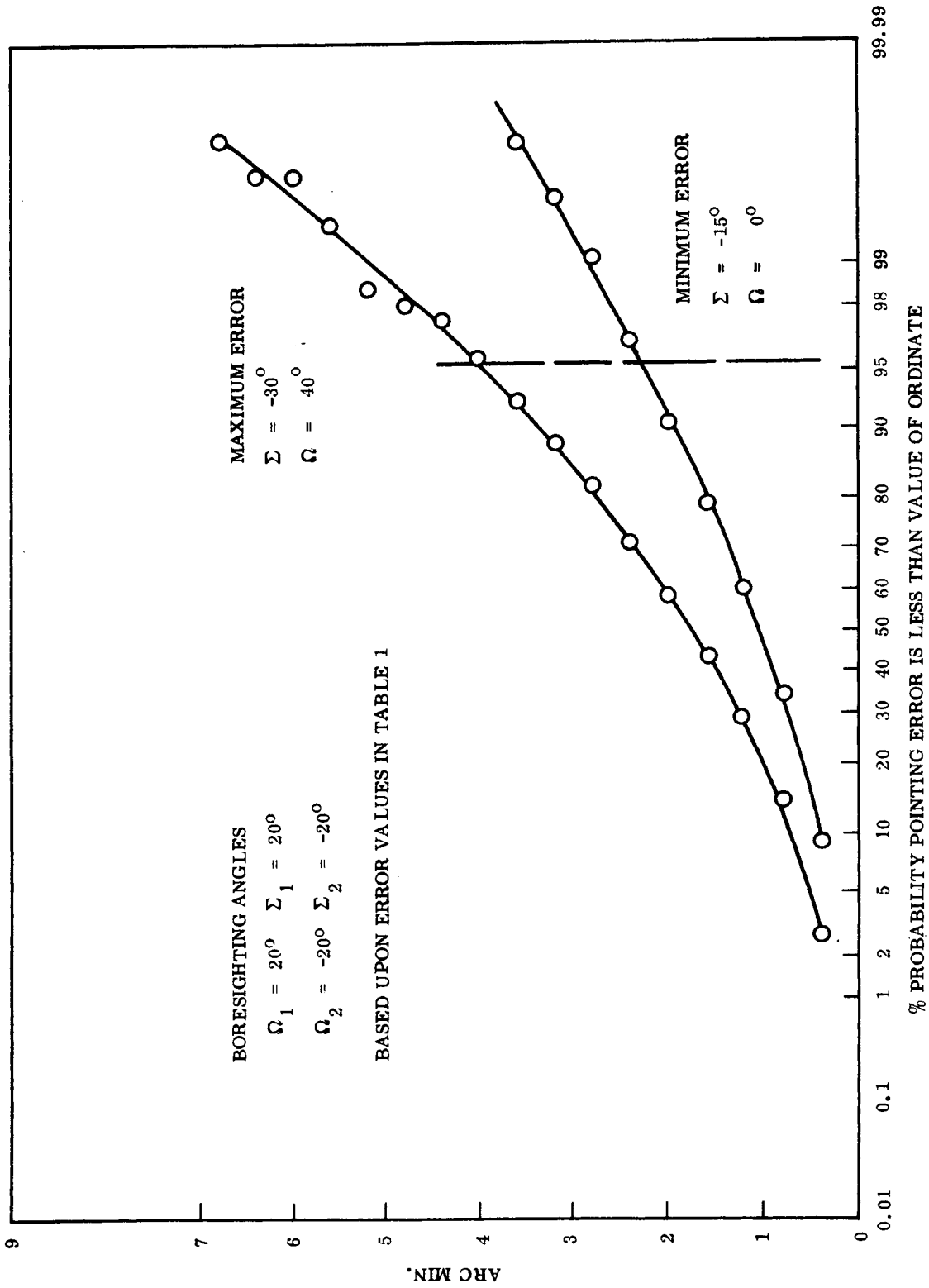
Figure 2.3-9. Primary Optics Pointing Error (Slave Mode)

SECRET SPECIAL HANDLING
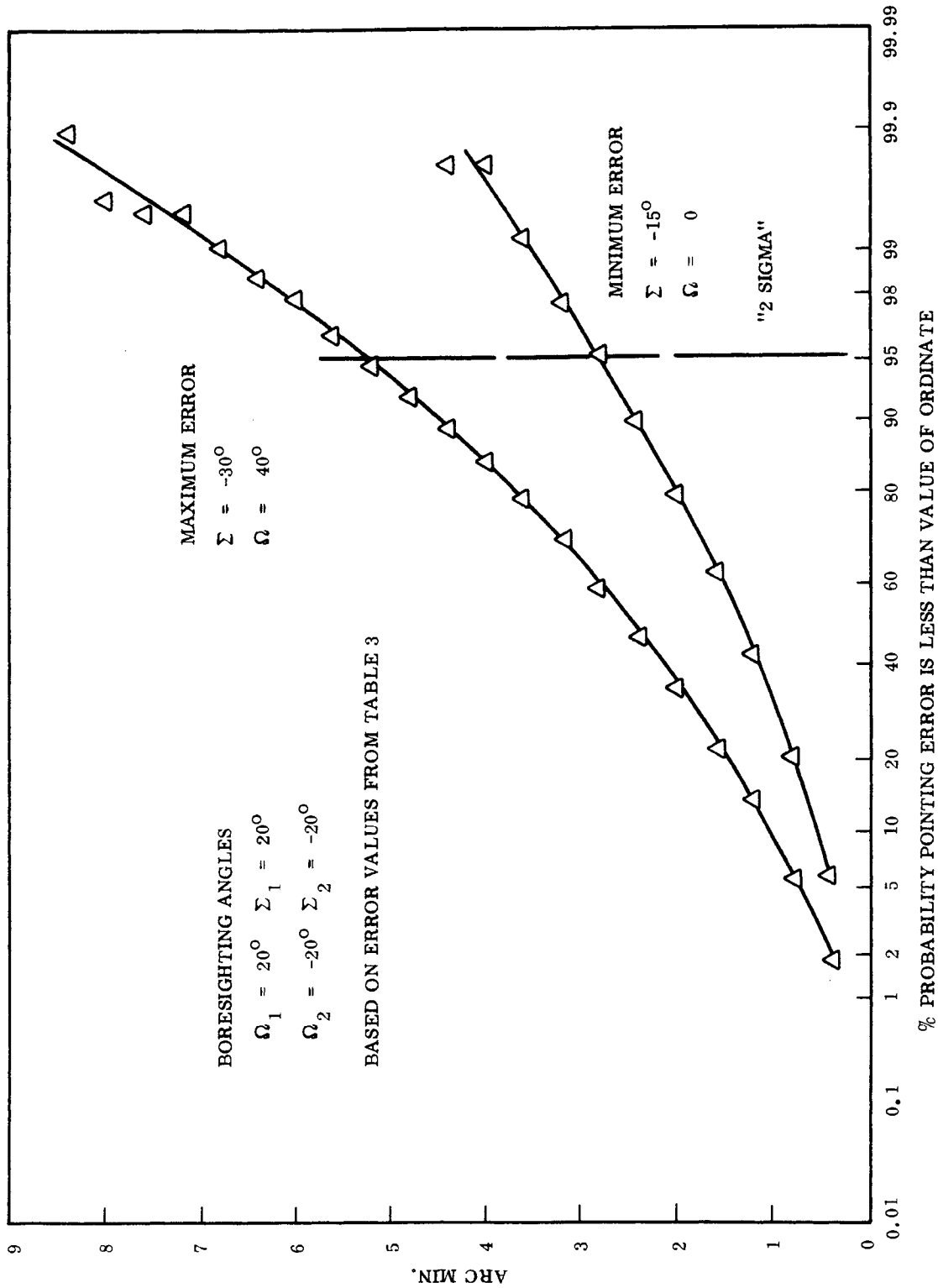
Figure 2.3-10. Primary Optics Pointing Error (Slave Mode)

SECRET SPECIAL HANDLING

~~SECRET~~ **SPECIAL HANDLING**
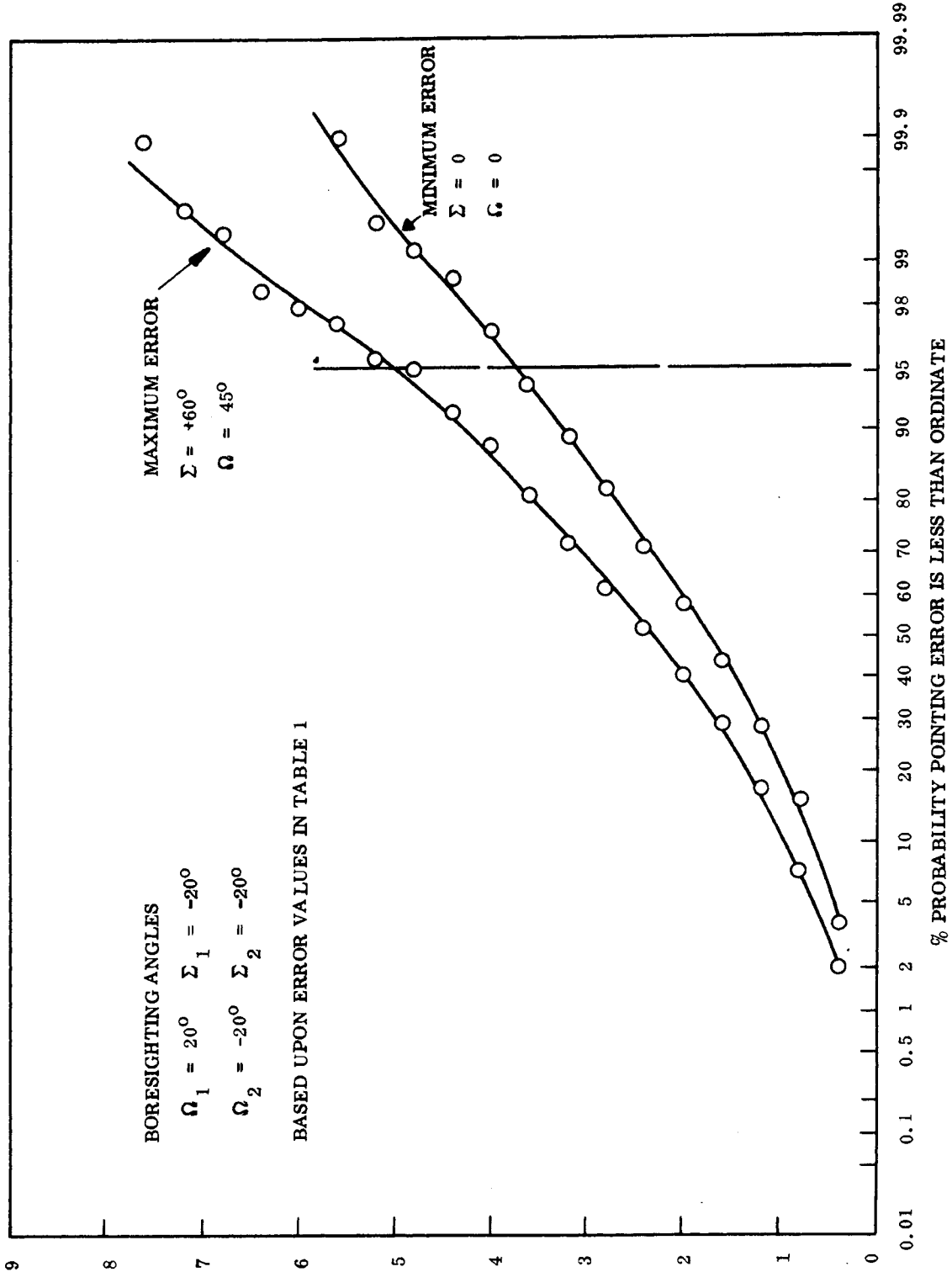
Figure 2.3-11. ATS Pointing Error (Arc Min.) (Automatic Mode – After Boresighting)

~~SECRET~~ **SPECIAL HANDLING**

~~SECRET~~ **SPECIAL HANDLING**
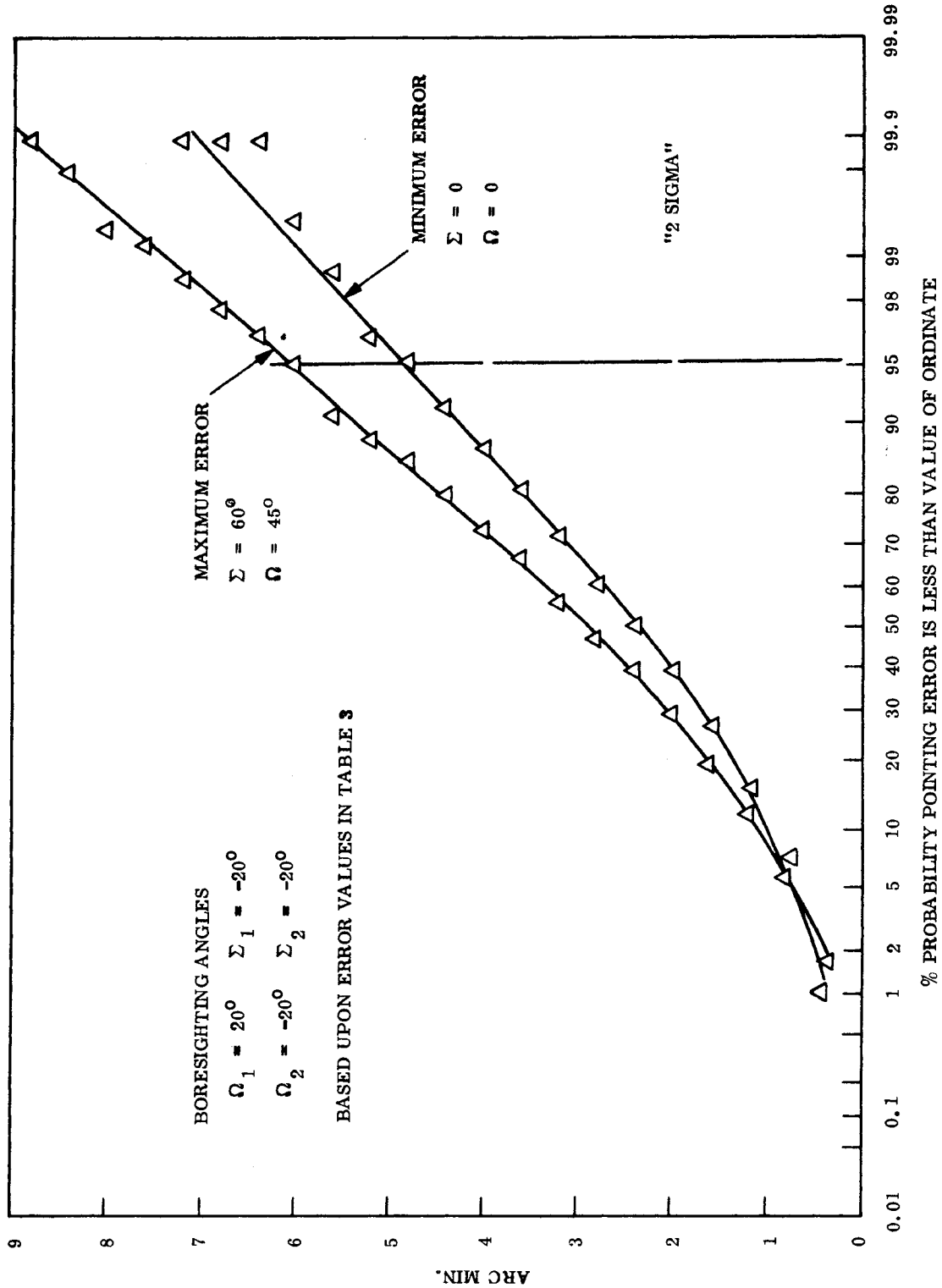
Figure 2.3-12. ATS Pointing Error (After Boresighting)

~~SECRET~~ **SPECIAL HANDLING**
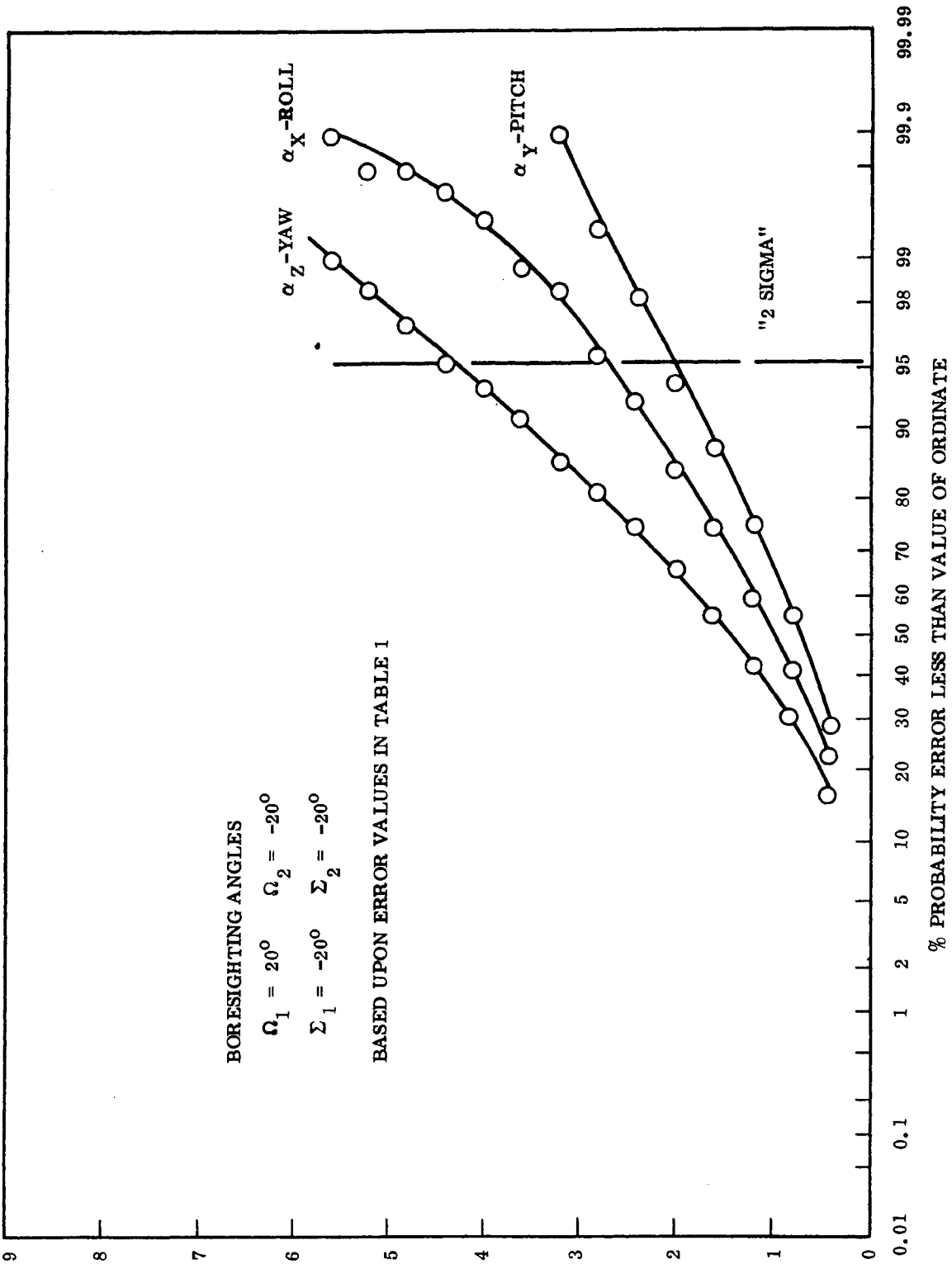
Figure 2.3-13. Error In Computed Value of ATS/Primary Optics Alignment (Arc Min.)

2-213

~~SECRET~~ **SPECIAL HANDLING**

Figure 2.3-14.   Error In Computed Value of ATS/Primary Optics Alignment (Arc Min.)

~~SECRET~~ **SPECIAL HANDLING**

the computed value of ATS/TM alignment, but since the computed alignment does contain
information on the constant error, the total effect is to improve the ATS or primary optics
pointing when using the ATS/TM alignment.

2.3.6 PROCEDURE REQUIRED TO DETERMINE ALLOWABLE MISALIGNMENTS.

In Section 2.3.1, it was stated that if the pointing requirements mean that for any MOL vehicle,
the on-orbit pointing errors must be less than 6 arc min. (8 arc min. for the ATS) at least
95.4 percent of the time, then the alignment tolerances in Tables 2.3-1 and 2.3-3 are not
acceptable. Assuming this to be the case, additional work is required to determine correct
alignment tolerances.

One approach is to select tolerances from Table 2.3-1 or 2.3-2 and accept the risk of
having any particular vehicle always show excessive pointing errors for some particular
pointing angles. The magnitude of this risk will depend upon the probability distribution of
the pointing angles as well as the values of allocated errors. Based upon the curves shown
in Figures 2.3-8 to 2.3-12, Table 2.3-5 shows the limiting values of the risk involved in
accepting either Table 2.3-1 or 2.3-3 as being acceptable error tolerances. The actual
value of the risk involved can be obtained by using the Monte Carlo computer programs with
appropriate probability distributions of ATS and primary optics pointing angles.

Another approach is to: use the worst possible combination for the constance errors, allow
random and time varying errors to vary, and use target pointing angle probability distribu-
tions to obtain the probability of having pointing errors be less than 6 or 8 arc min. 95.4
percent of the time.

If the targets are assumed to be uniformly situated on the ground, and the ATS or Primary
Optics is assumed to randomly point at a target, the probability density distributions of the
pointing obliquity and stereo angles are:

$$f_\Omega(\Omega) = \frac{1}{2 \tan \Omega_o \cos^2 \Omega} \qquad\qquad |\Omega| \leq \Omega_o$$

and

$$f_\Sigma(\Sigma) = \frac{1}{\Sigma_2 - \Sigma_1} \qquad\qquad \Sigma_1 < \Sigma \leq \Sigma_2$$

where

Ω_o is the maximum obliquity angle.

Σ_1 is the maximum aft stereo angle.

Σ_2 is the maximum forward stereo angle.

Using these probability distributions, and assuming that all constant errors have the worst case and sign, the Monte Carlo program was used to obtain the preliminary on-orbit error apportionment shown in Table 2.3-6. The pointing errors obtained from this error apportionment are shown in Figure 2.3-13.

From Figure 2.3-15, the primary optics pointing error is less than the required 6 arc min. for the 95.4 percent of the time that any particular vehicle points at a target. The ATS pointing error is 8.2 arc min. as compared to the required 8 arc min. However, since the probability is very small that all constant errors would have the worst case magnitude and sign the probability of having the actual pointing error observed for any ATS exceed 8.0 arc min. 95.4 percent of the time is small.

Future efforts will refine the apportionment of allowable system errors.

TABLE 2.3-5

	PROBABLE RISK USING ERROR VALUES FROM:	
	TABLE 2.3-1	TABLE 2.3-3
Prob. Prime Optics Pointing Error is always greater than 6 arc min.	< 0.002	< 0.002
● Automatic mode*	> 0.0001	> 0.0001
● Slave mode	< 0.003	< 0.02
(after boresighting)	> 0	> 0.0001
Prob. ATS Pointing Error is always greater than 8 arc min.		
● Automatic mode*	< 0.001	< 0.004
(after boresighting)	> 0	> 0.0001

*Neglecting vehicle ephemeris and target location errors

TABLE 2.3-6. APPORTIONMENT OF SYSTEM ERROR

	MAXIMUM VALUE	REMARKS
Constant Errors		
δby_a } ATS Optical Axis	1.2 arc min.	apportionment
δbz_a	1.2 arc min.	apportionment
$\delta \theta_{1a}$ } ATS Roll Gimbal Direction	0.5 arc min.	apportionment
$\delta \psi_{1a}$	0.5 arc min.	apportionment
$\delta \psi_{2A}$ ATS Mirror Mounting	0.5 arc min.	ITEK Spec. EC-331B
$\delta \psi_{3A}$ ATS Gimbal Orthogonality	0.5 arc min.	ITEK Spec. EC-331B
$\delta \alpha_x$ } ATS/Prime Optics Align	15 arc min. (total)	apportionment
$\delta \alpha_y$		
$\delta \alpha_z$		

~~SECRET~~ **SPECIAL HANDLING**

TABLE 2.3-6. APPORTIONMENT OF SYSTEM ERROR (Cont)

		MAXIMUM VALUE	REMARKS
Constant Errors (Cont)			
$\delta\theta_1$	Prime TM Roll Gimbal Dir.	0.5 arc min.	Apportionment
$\delta\psi_1$		0.5 arc min.	Apportionment
$\delta\psi_2$	TM Mirror Mounting	0.5 arc min.	EK Spec 101.2
$\delta\psi_3$	Gimbal Orthogonality	1.5 arc min.	EC-1204
Time Varying Errors		2 Sigma Value (arc min.)	
δby_a	ATS Optical Axis	0.707	Apportionment
δbz_a		0.707	Apportionment
$\delta\theta_{1a}$	ATS Roll Gimbal Dir.	0.52	±.75 min. total due to pressure variations
$\delta\psi_{1a}$		0.52	
$\delta\alpha_x$		0.707	
$\delta\alpha_y$	ATS/Prime Optics Align	0.707	Estimate--includes pressure and thermal variations
$\delta\alpha_z$		0.707	
$\delta\theta_1$	Prime TM Roll Gimbal Dir.	0.3535	0.5 min. total due to thermal effects
$\delta\psi_1$		0.3535	
Random Errors		2 Sigma Value (arc min.)	
$\delta\omega_a^m$	ATS Gimbal Angle Meas.	±.33 *1	16 bit shaft encoder
$\delta\theta_a^m$		±.33 *1	
$\delta\Omega_a^{cs}$	Control System		Estimated error after settling
$\delta\theta_a^{cs}$	Pointing of TM	2.0 (total)	

*1 This error has a uniform distribution. ±.33 arc min is the absolute maximum value.

~~SECRET~~ **SPECIAL HANDLING**

TABLE 2.3-6. APPORTIONMENT OF SYSTEM ERROR (Cont)

	MAXIMUM VALUE	REMARKS
Random Errors (Cont)		
δby } Primary Optical Axis	0.667	Estimate of alignment
δbz } Alignment and Monitor Error	0.667	monitor error
$\delta \Omega^m$ } Gimbal Angle Meas.	±0.33 *1	16 bit shaft encoder
$\delta \theta^m$ }	±0.33 *1	
$\delta \Omega^{cs}$ } Control System	1.0 (total)	Estimated error after
$\delta \theta^{cs}$ } Pointing of TM		settling
δby^T } ATS or Prime Optics	0.667	Corresponds to 95 ft.
δbz^T } Tracking Error	0.667	each axis at nadir

*1 This error has a uniform distribution. ±0.33 arc min is the absolute maximum value.

~~SECRET~~ SPECIAL HANDLING
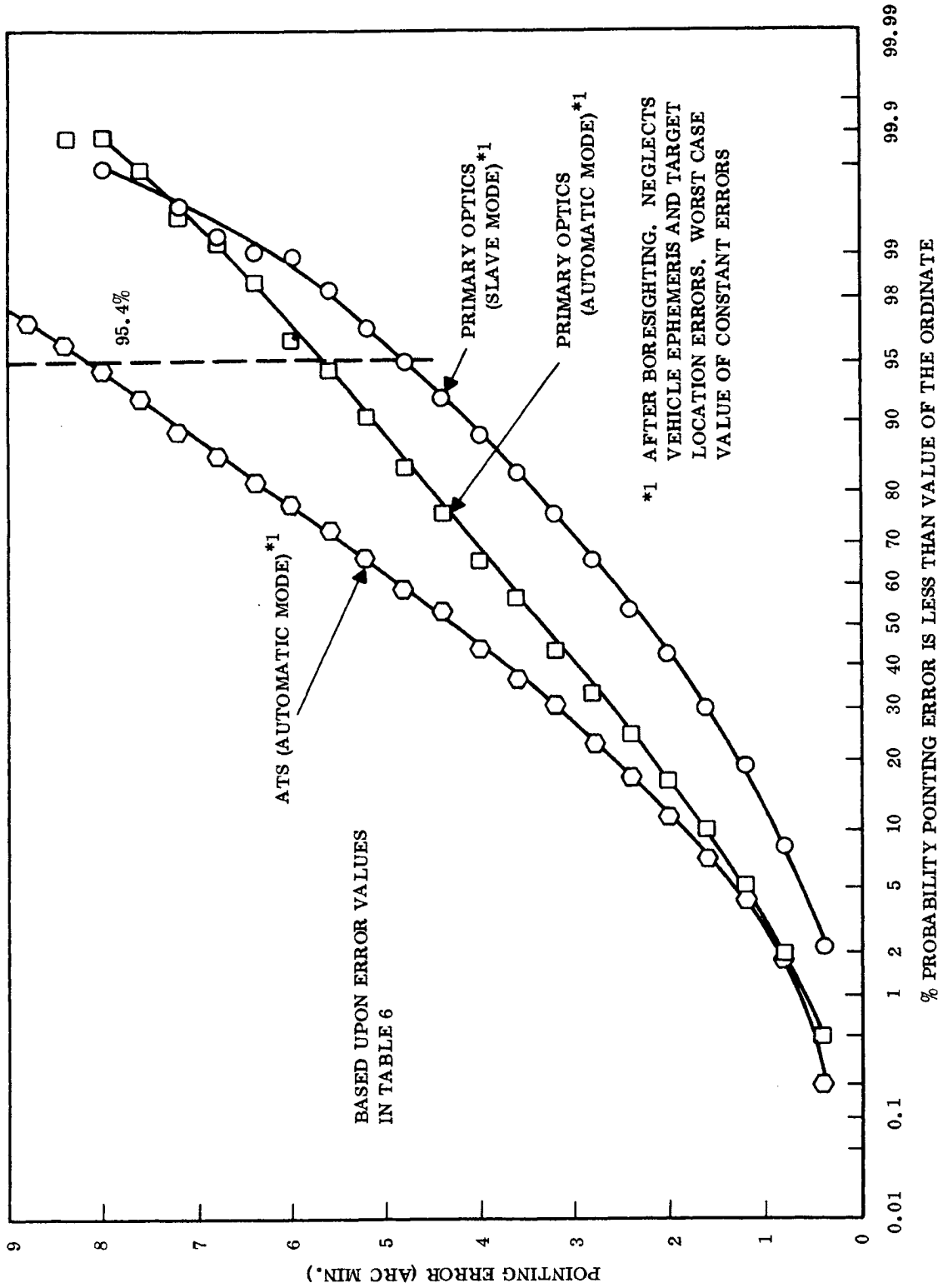
Figure 2.3-15. Line of Sight Pointing Error

~~SECRET~~ SPECIAL HANDLING

2.4 ATS THERMAL ANALYSIS

The material in this section pertains to the thermal design of the Acquisition Optics Components. The material is subdivided as follows:

2.4.1   External Optics Assembly

2.4.2   Telescope Assembly

2.4.3   Thermal Development Test Plans.

2.4 ATS THERMAL ANALYSIS

2.4.1 EXTERNAL OPTICS ASSEMBLY

2.4.1.1 General External Component Design Philosophy

2.4.1.1.1 Passive Versus Active Thermal Control

Both active and passive thermal control systems have been investigated in developing a design concept. An active control system was discarded very early in the analysis on the basis of the additional weight and reliability penalty associated with such a system. Two of the active control systems considered were:

a. Thermostatically actuated heaters

b. Movable louvers

A passive system is one employing coatings, component thermal inertia, internal conductance, and insulation to maintain a system within a given temperature range.

2.4.1.1.2 Design Concepts and Configurations

The basic configuration consists of a shroud with a hinged panel which totally encloses the tracking mirror and fixed fold assembly. During a target pass, the hinged panel opens up to provide a viewing slot approximately 24 in. x 44 in. This shroud serves four purposes:

a. Provides an accurately controlled temperature enclosure.

b. Protects the optical system from direct insolation.

c. Protects the external optics from contamination by the orbital maintenance thrusters and the output of the waste management system.

d. Protects the external optics from the heating effects resulting from firing of the orbital maintenance thrusters.

Very early in the program, the concept of a single shroud was proposed. This shroud would serve two functions:

    a.   Serve as an aerodynamic fairing during ascent.

    b.   Function as an orbital protective shroud once orbit has been achieved.

This concept was discarded by Aerospace as representing potentially too large a weight penalty plus an extremely complex interface. In lieu of this, a dual shroud concept has evolved. The outer shroud serves solely for protection against ascent heating and pressure loading effects. The outer shroud is ejected prior to orbit injection. The inner shroud or on-orbit shroud functions as a protective cover during all orbital operations. The following design concepts for the protective shroud have been identified along with their relative advantages and disadvantages.

    a.   Single wall shroud
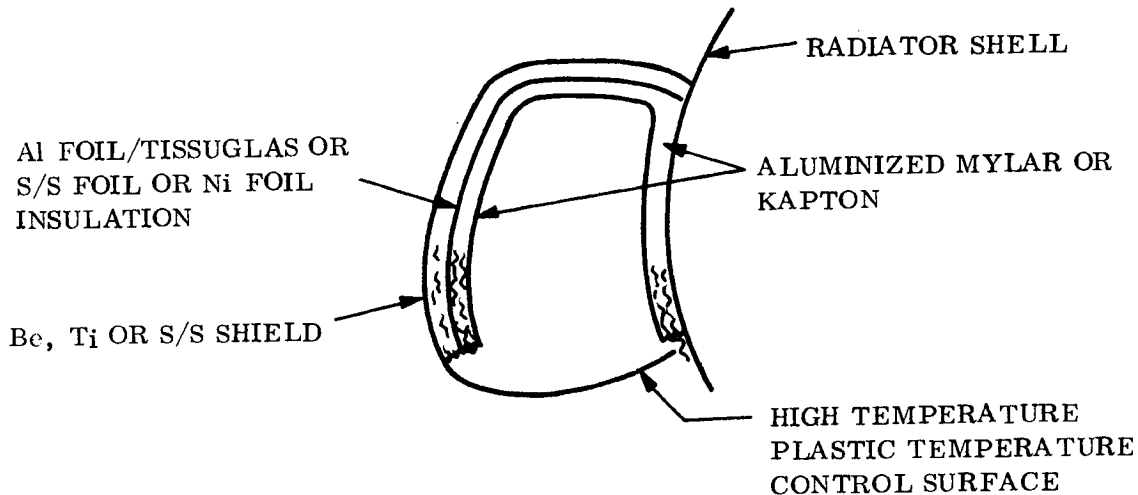
Advantages:

1. Composite insulation layup optimizes insulation weight.

2. High temperature plastic temperature control surface helps isolate control surface from hot surfaces.

Disadvantages:

1. Design fairly sensitive to accuracy with which one can analytically predict transient characteristics of composite insulation.

2. S/S or Ni foil, if required from temperature standpoint, represent a significant weight penalty.

b. Double wall shroud

RADIATOR SHELL

AL OR Be INNER SHELL

Ti, Be OR S/S SHIELD
(GOLD PLATED INSIDE)

ALUMINIZED MYLAR OR
KAPTON INSULATION

INSULATING STANDOFF

HIGH TEMPERATURE PLASTIC
SUCH AS IMIDITE 1850 OR
TEXTOLITE GRADE 11617B
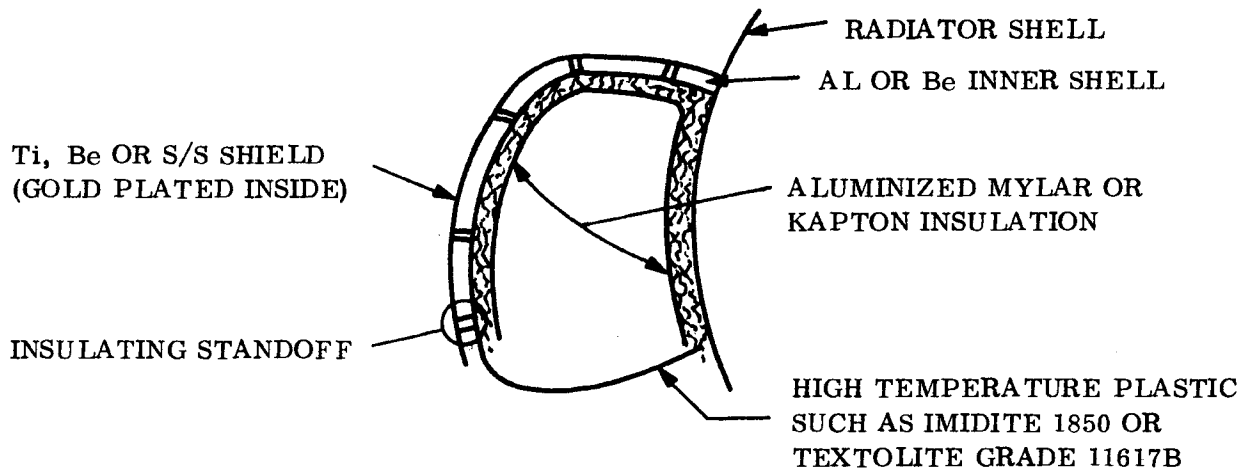
Advantages:

1. Somewhat easier to analytically predict characteristics than configuration a.

2. High temperature plastic surface tends to help isloate temperature control surface from the higher temperature structure. This should help to lessen impact of heating effects from the on-orbit thruster plume.

3.   The shield or shields could be optimized to cover just the most critical areas.

Disadvantages:

1.   Possibly higher weight than configuration a.

c.   Heat of fusion shroud
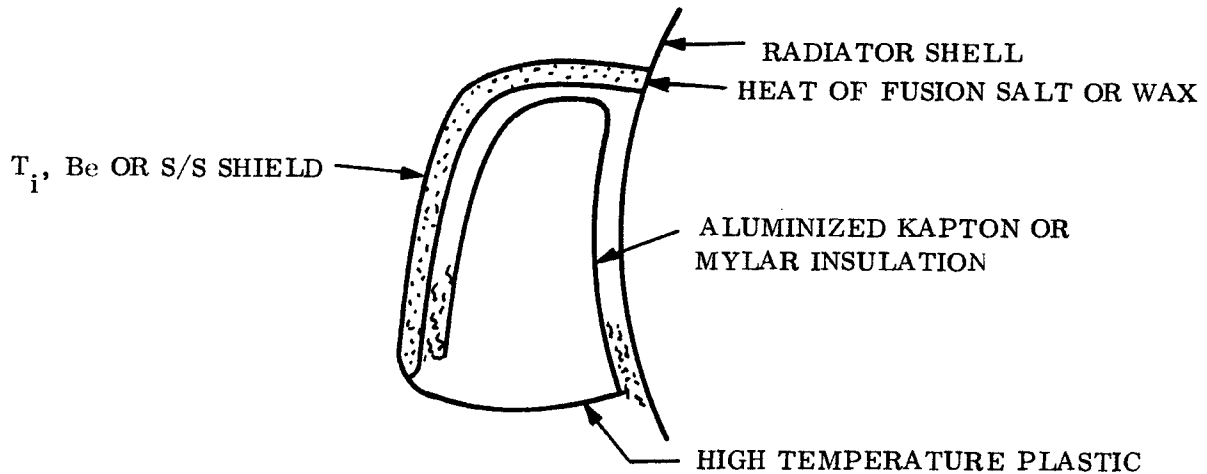
Advantages:

1.   Maintains constant temperature during plume impingement.

2.   Highly predictable performance analytically.

Disadvantages:

1.   High weight penalty. Most potential heat of fusion materials have latent heat of fusions on the order of 100 - 150 BTU/lb. This system might represent as much as a 30 lb weight penalty per system.

2.   Significant development work required.

d. Shadow shield

ACTS

Be, S/S OR T_i SHADOW SHIELD
(GOLD PLATED BACK FACE)

PRESENT
CONFIGURA-
TION
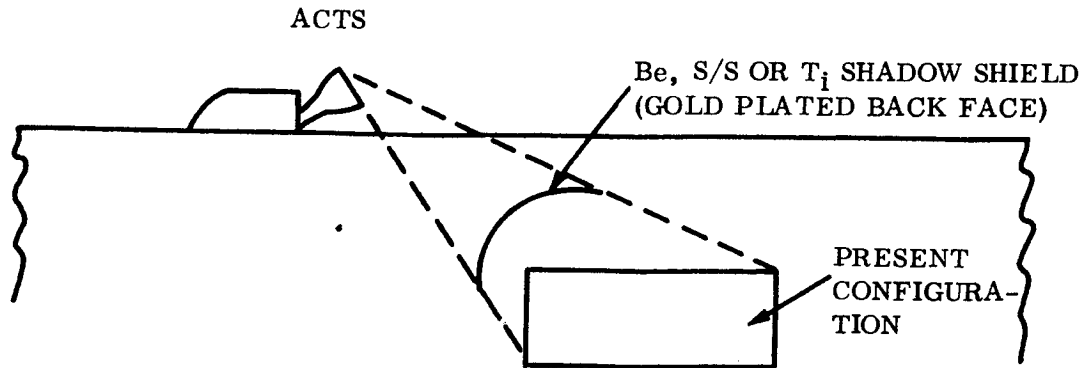
Advantages:

1. Minimizes direct heating problem.

2. Minimizes import of plume impingement problem on system design.

Disadvantages:

1. Creates very difficult interface problems on account of weight penalty
    plus impact on DACO radiator design.

The proposed approach is a combination of concepts a and b. This concept would consists of

a high-temperature shroud with a composite insulation blanket. Covering a portion of this

shroud would be a partial shield which would provide a degree of protection from the

peak heating effects of the orbit adjust thruster firing. This configuration is shown in

Figure 2.4-1.

COMPOSITE INSULATION
OUTER LAYERS - S/S OR
AL FOIL
INNER LAYERS - ALUMINIZED
MYLAR

INSULATION
STAND-OFF
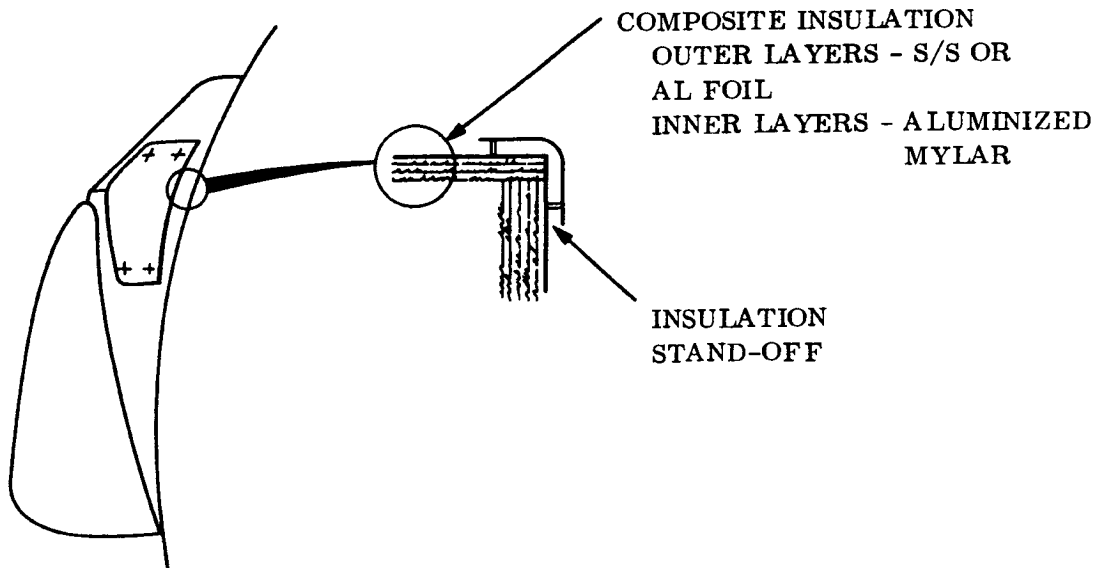
Figure 2.4-1. Proposed Shroud Configuration

All of the interior surfaces of the shroud are insulated with the exception of the lower earth-facing surface. This lower earth-facing surface constitutes the basic temperature control surface for the externally mounted system. The coating pattern on this control surface is adjusted to minimize the temperature variation over a given orbit and to limit the temperature variation over the entire orbit mission. The lower earth-facing surface was chosen for this purpose since it is exposed to the smallest solar heating input. Hence, the variation this surface is subject to in heat input is minimized. Also, this surface is relatively isolated from the effects of the orbit adjust thruster firing.

2.4.1.2 Temperature Constraints

Table 2.4-1 gives a summary of allowable temperature variations for the external components, both for operational and non-operational modes.

TABLE 2.4-1. ALLOWABLE TEMPERATURE VARIATIONS FOR
ACQUISITION TRACKING SYSTEM

	MINIMUM TEMPERATURE	MAXIMUM TEMPERATURE
Roll and Pitch Gyro (Mounting surface)	0°F	+100°F
Pitch and Roll Motor	-65°F	+160°F
Pitch and Roll Encoders	- 5°F	+160°F
Roll and Pitch Amplifiers	-65°F	+160°F
Mirrors	-10°F	+140°F

2.4.1.3 Environment

2.4.1.3.1 Orbit Envelope

Figure 2.4-2 shows the mission orbit envelope. Five cases have been analyzed to bracket the expected range of external heat inputs.

2.4.1.3.2 Orbital Heat Rates

Table 2.4-2 summarizes the range of orbital heating rates predicted for the mission as presently defined.

~~SECRET~~ **SPECIAL HANDLING**
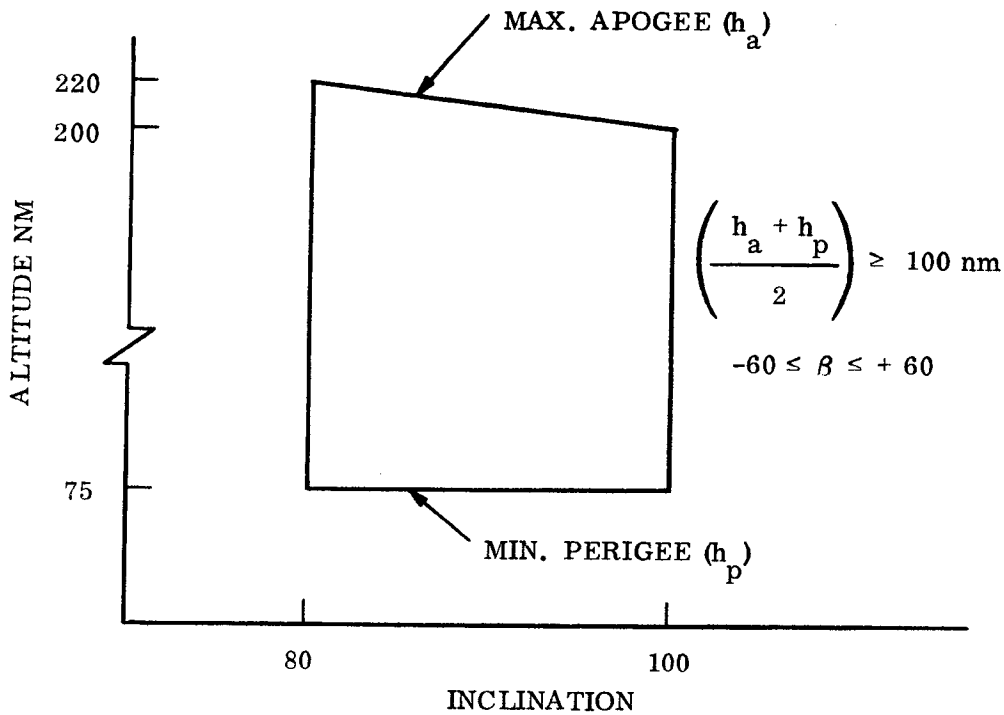
Figure 2.4-2. Mission Orbit Envelope

TABLE 2.4-2. TABULATED VALUE OF NOMINAL VALUES OF SOLAR (S), ALBEDO (A), EARTH (E), AND MOLECULAR HEAT FLUXES (Q_{MOL}) ON THE ON-ORBIT SHROUD

CASE NO.	β	DAY	PERIGEE	APOGEE	$\overline{E}$ Btu/hr-ft^2	$\overline{S+A}$ Btu/hr-ft^2	$\overline{Q}_{MOL}$ Btu/hr-ft^2
1	-60°	2	75 nm	125 nm	27.5	114.0	71.4
2	0°	2	75 nm	125 nm	26.6	88.7	71.1
3	0°	82	80 nm	180 nm	26.6	83.9	28.6
4	$+60^{\circ}$	182	220 nm	220 nm	24.0	51.2	0
5	-60°	2	100 nm	100 nm	27.5	114.0	35.1

Note: (1) The average molecular heat flux cited is for the forward face only since the flux level on the remaining surfaces is negligible.

(2) β = Angle between earth-sun line and orbital plane.

~~SECRET~~ **SPECIAL HANDLING**

SECRET SPECIAL HANDLING

2.4.1.3.3 Free Molecular Heating

The predicted molecular heating curves for the above cases are shown in Figure 2.4-3.

2.4.1.4 External System Temperature Behavior

2.4.1.4.1 Ascent Heating

The on-orbit shroud is covered at liftoff, as previously described, by an external shroud, the function of which is to protect the on-orbit shroud from excessive temperatures and pressure loading during ascent. It also serves the auxiliary function of limiting the system temperature during the prelaunch period when it is exposed to an extended period of solar heating. Figure 2.4-4 shows the ejectable shroud peak temperature time behavior. The integrated average temperature-time behavior is considerably less than this. The period between ejection of the ascent fairing and orbit injection has not been evaluated in detail since the time of fairing ejection has just recently been defined. Figure 2.4-5 shows the expected on-orbit shroud temperature-time behavior during ascent, based on the assumption that ejection of the aerodynamic fairing will not occur before 290 seconds after launch.

2.4.1.4.2 Normal Orbit Characteristics

The first 90-minute portion of Figures 2.4-6 and 2.4-7 shows the shroud temperature-time behavior for the hot orbit condition. Both the tracking mirror and the fixed fold assembly are maintained at virtually a constant 70^OF over the entire orbit during a non-operational mode. The tracking mirror varies less than 2^OF over the orbit. Since in an operational mode the mounting surface for the roll gyro is approximately 30^OF hotter than the temperature of the shroud control surface, the choice of coatings was dictated by the requirement of maintaining the average temperature of the control surface on the shroud to within $0-70^O$F overall normal orbit conditions. The actual estimated operating range for the tracking mirror is 55 ± 15^OF, and for the folding mirror, the predicted variation is 53 ± 17^OF.

~~SECRET~~ **SPECIAL HANDLING**
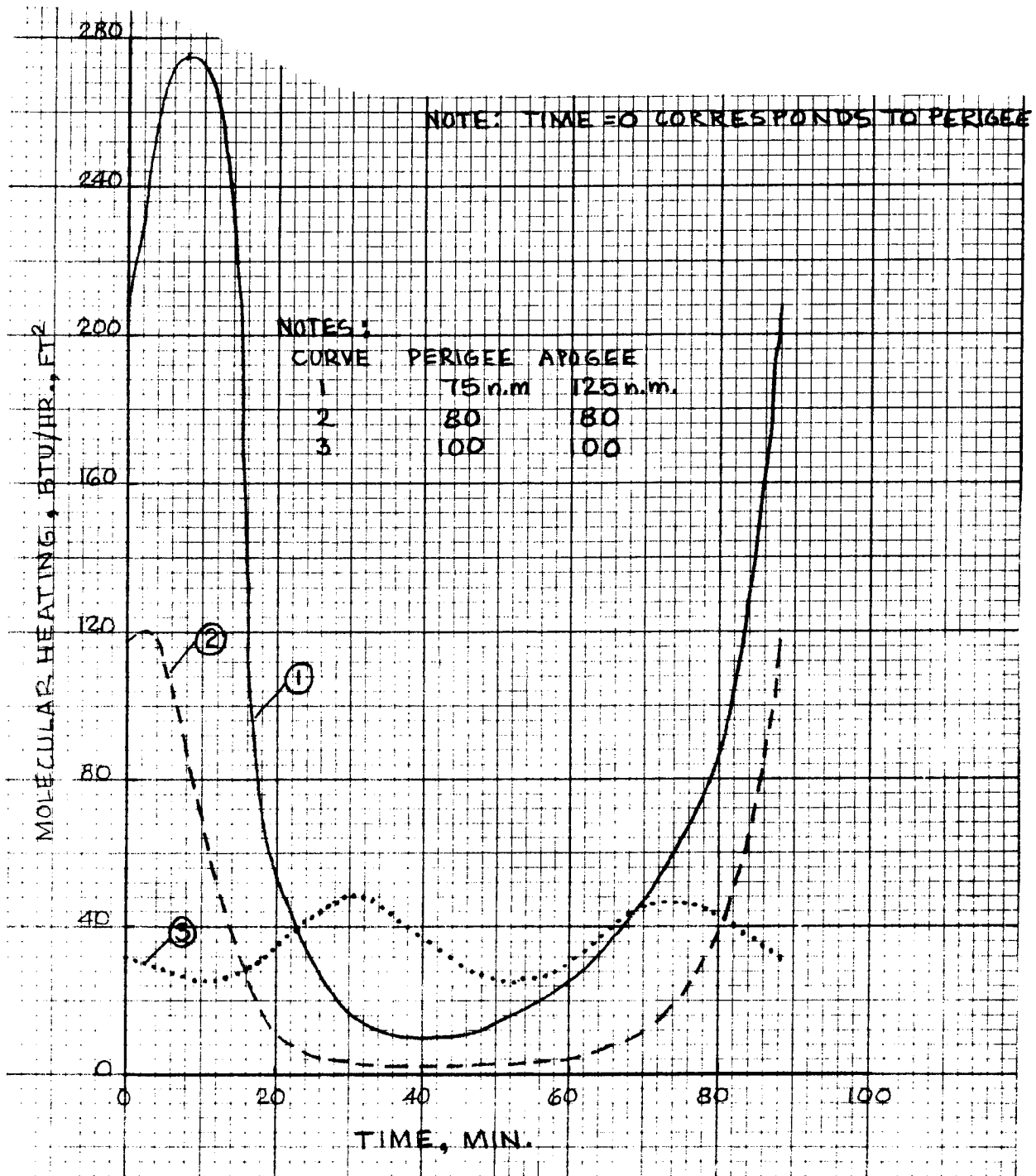
Figure 2.4-3. Free Molecular Heating Rate on Forward
Face of On-Orbit Shroud

~~SECRET~~ **SPECIAL HANDLING**

~~SECRET~~ SPECIAL HANDLING
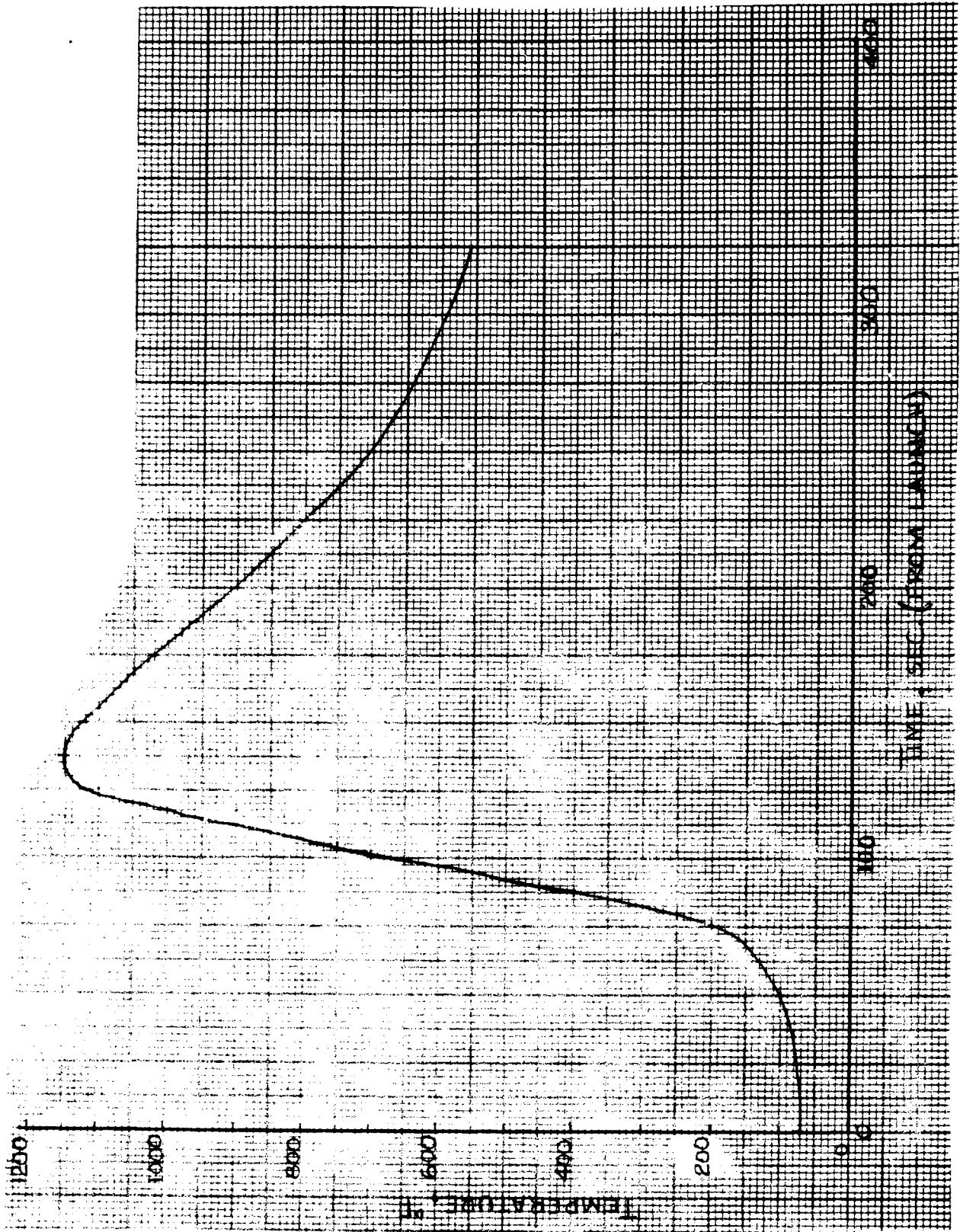
Figure 2.4-4. Peak Temperature – Time Curve for Ejectable Shroud

~~SECRET~~ SPECIAL HANDLING

~~SECRET~~ **SPECIAL HANDLING**
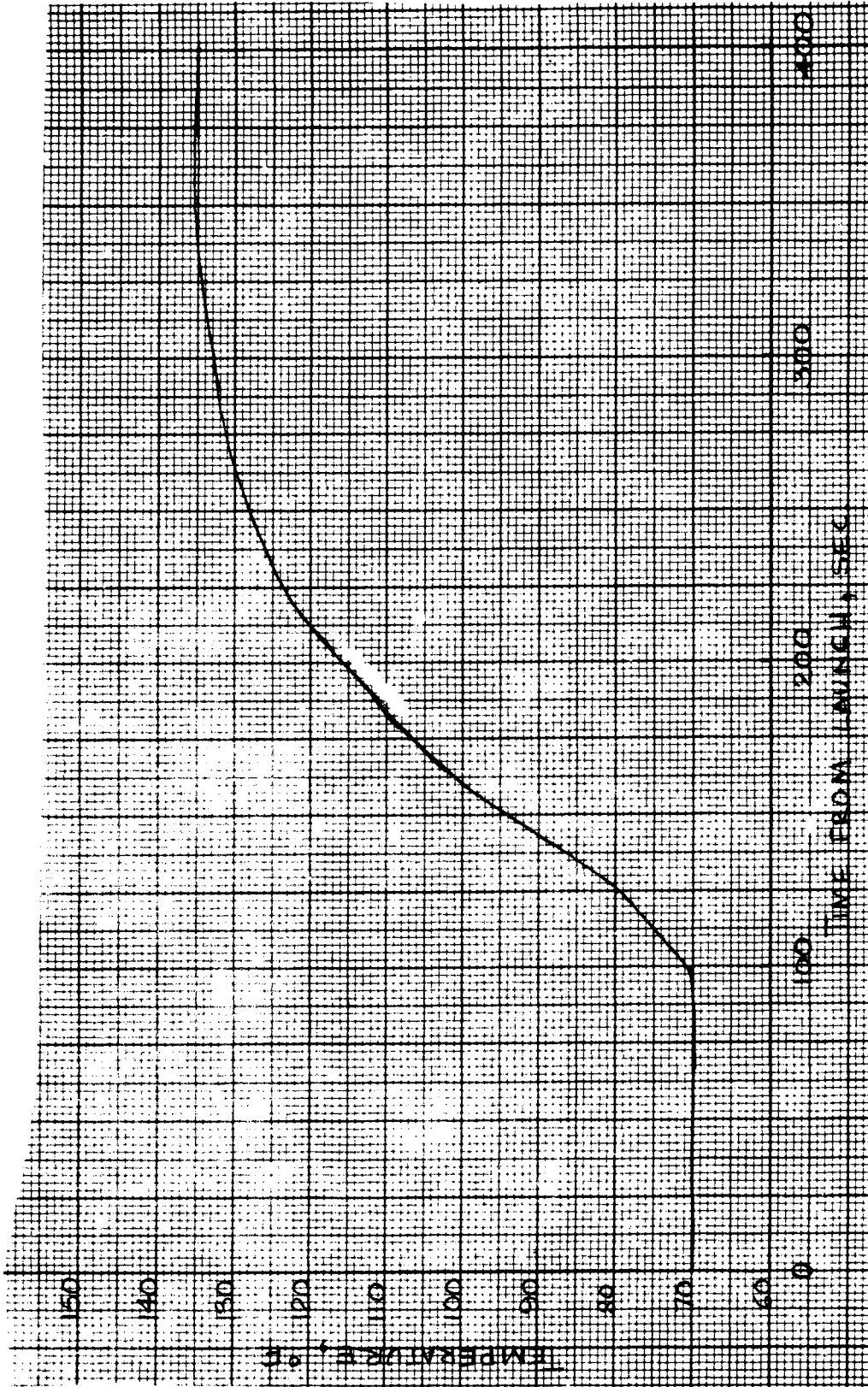
Figure 2. 4-5.   Maximum On–Orbit Shroud Temperature Versus Time During Ascent

~~SECRET~~ **SPECIAL HANDLING**

~~SECRET~~ **SPECIAL HANDLING**
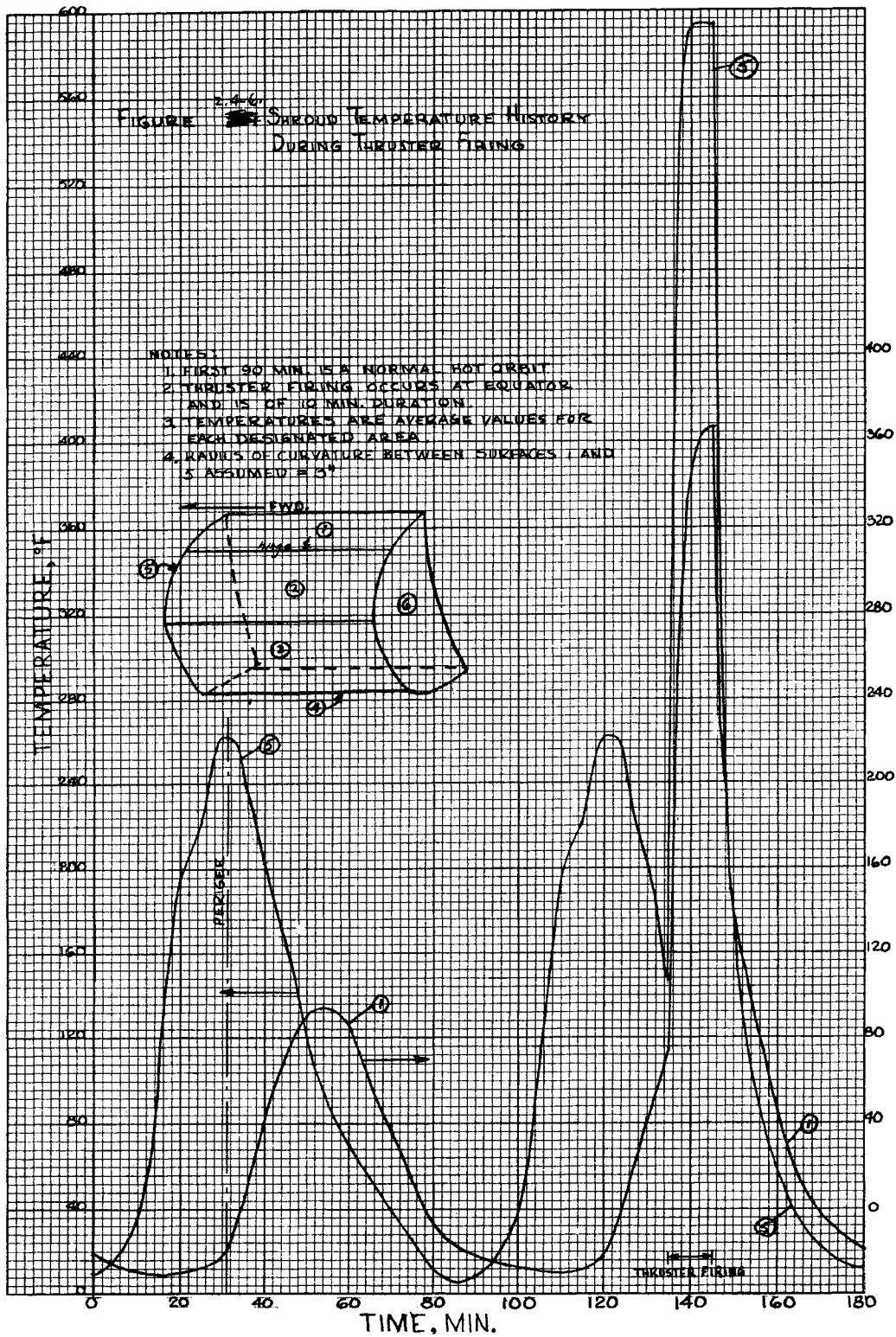
Figure 2.4-6. Shroud Temperature History During Thruster Firing

~~SECRET~~ **SPECIAL HANDLING**
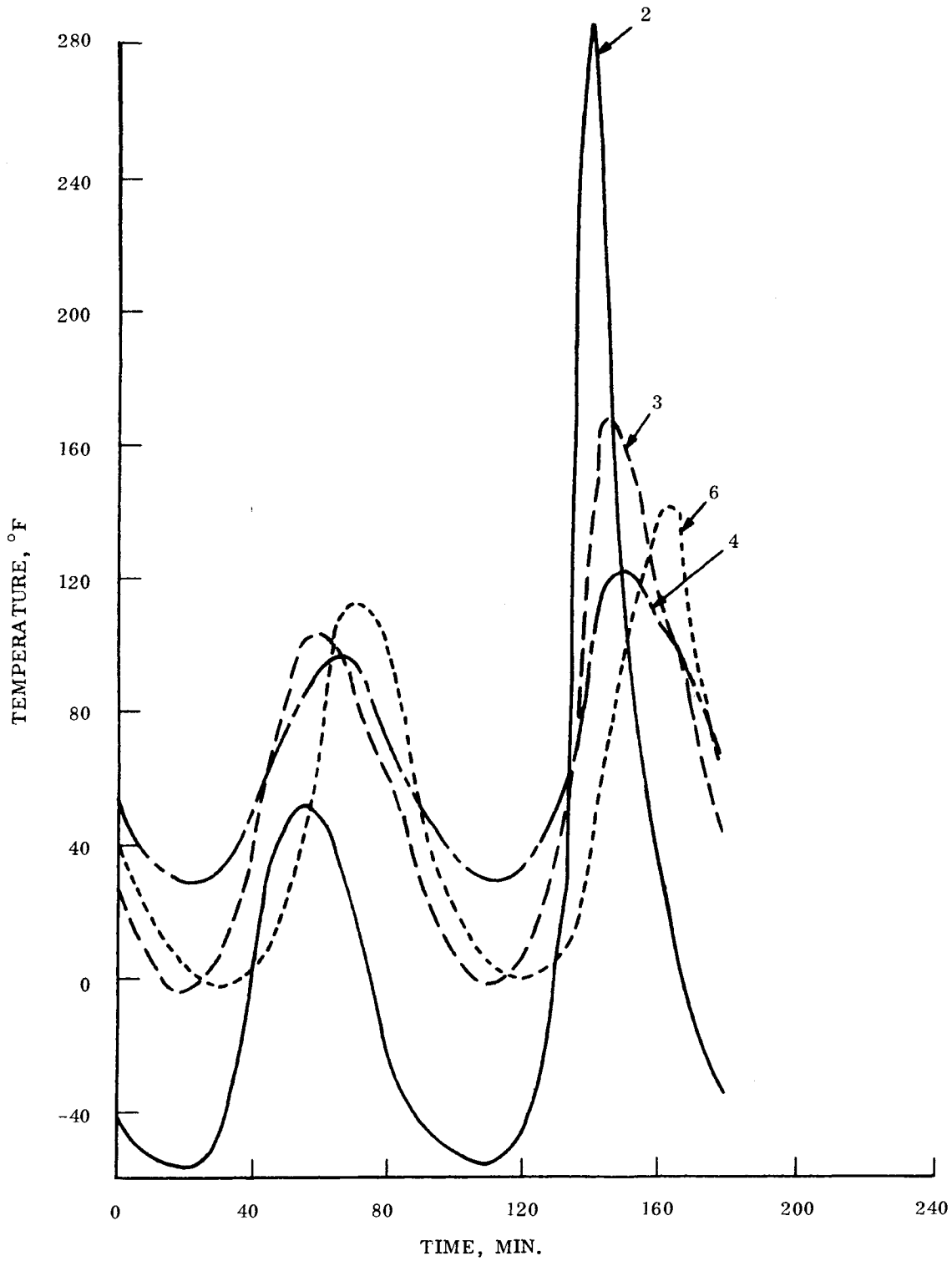
Figure 2.4-7. Shroud Temperature History During Thruster Firing

~~SECRET~~ **SPECIAL HANDLING**

Table 2.4-3 gives a summary of the assumed coating pattern for the on-orbit shroud.

TABLE 2.4-3. SUMMARY OF COATING PROPERTIES
ASSUMED FOR ON-ORBIT SHROUD

SURFACE	EMITTANCE	SOLAR ABSORPTANCE
1	0.75	0.3
2	0.75	0.3
3	0.10	0.35
4	0.16	0.14
5	0.75	0.3
6	0.2	0.12

2.4.1.4.3 Operational Mode - Gyro Warmup

The effect of the warmup period for the gyro on the tracking mirror has been analyzed on the following basis:

a. Cold case (sink temperature = 0^OF)

b. 60-watt coarse heater energized in gyro when gyro temperature is in the temperature range $\leq 159^O$F.

c. A 10-watt fine control heater is utilized to maintain the gyro at 160 ± 5^OF.

d. Vehicle pressure shell maintained at 70 ± 5^OF.

The following temperatures have been predicted for the end of a twenty minute operational period:

Roll motor   = 55^OF   Bezel   = 17^OF

Yoke   = 30^OF   Tracking Mirror = 11^OF

Belly band   = 40^OF

~~SECRET~~ **SPECIAL HANDLING**

2.4.1.4.4 Orbit Thruster Heating

A. <u>Orbit Adjust Maneuvers</u> - The following is a description of the expected modes of operation:

Orbit adjustments are made every three days to reinitialize the orbit starting with revolution No. 44 and every 48 revolutions thereafter.

Mode: Non-intersecting initial and decayed orbits

    a.   Two-burn procedure 180° apart

    b.   Both thrusts forward

    c.   Firings occur at equator ±5°

    d.   First burn of 4 minutes' duration occurs when vehicle is proceeding from north to south (sunlit side of earth)

    e.   Second burn is of 0.4 minute duration occurring when vehicle is proceeding from south to north (earth's umbra)

Mode: Intersecting initial and decayed orbits. Two procedures are currently being considered to reinitialize the orbit.

    a.   Two-burn procedure

        1.   First thrust vector forward

        2.   Second thrust aft

        3.   First burn occurs when vehicle is proceeding from north to south and is of 4 minutes' duration.

4. Second burn is of 0.4 minute duration occurring when vehicle is proceeding from south to north

5. Firings occur at equator $\pm 5^{\circ}$

b. Single-burn procedure

1. Thrust vector forward

2. Single burn would occur at the equator $\pm 5^{\circ}$ in the descending mode, i.e., vehicle is proceeding north to south

3. The firing cycle would be four 4-minute burns each separated by a 3-day period followed by a 3-day interval and then a 10-minute burn

The two-burn technique is currently the baseline design, although the single-burn technique is under consideration. The single-burn technique would not fully correct for perigee drift so that the one-burn technique might be alternated with a two-burn technique. In the two-burn technique described for an intersecting degraded and initial orbit, the vehicle is turned around the yaw axis. This maneuver takes approximately one minute.

B. <u>Plume Characteristics</u> – The plume characteristics supplied to us by DACO have been reproduced in the accompanying figures (Figures 2.4-8 and 2.4-9) and in Tables 2.4-4 and 2.4-5.

Figure 2.4-10 shows the relative position of one of the Y-axis thrusters and the on-orbit shroud. For purposes of analysis, the shroud has been divided into a number of nodes for which the heat flux distribution has been calculated. Figure 2.4-11 shows the shroud surface identification.

The plume characteristics supplied to us by DACO essentially assume that the flow before impinging on the shroud is that of a free jet. This neglects the interaction of the boundary

~~SECRET~~ SPECIAL HANDLING
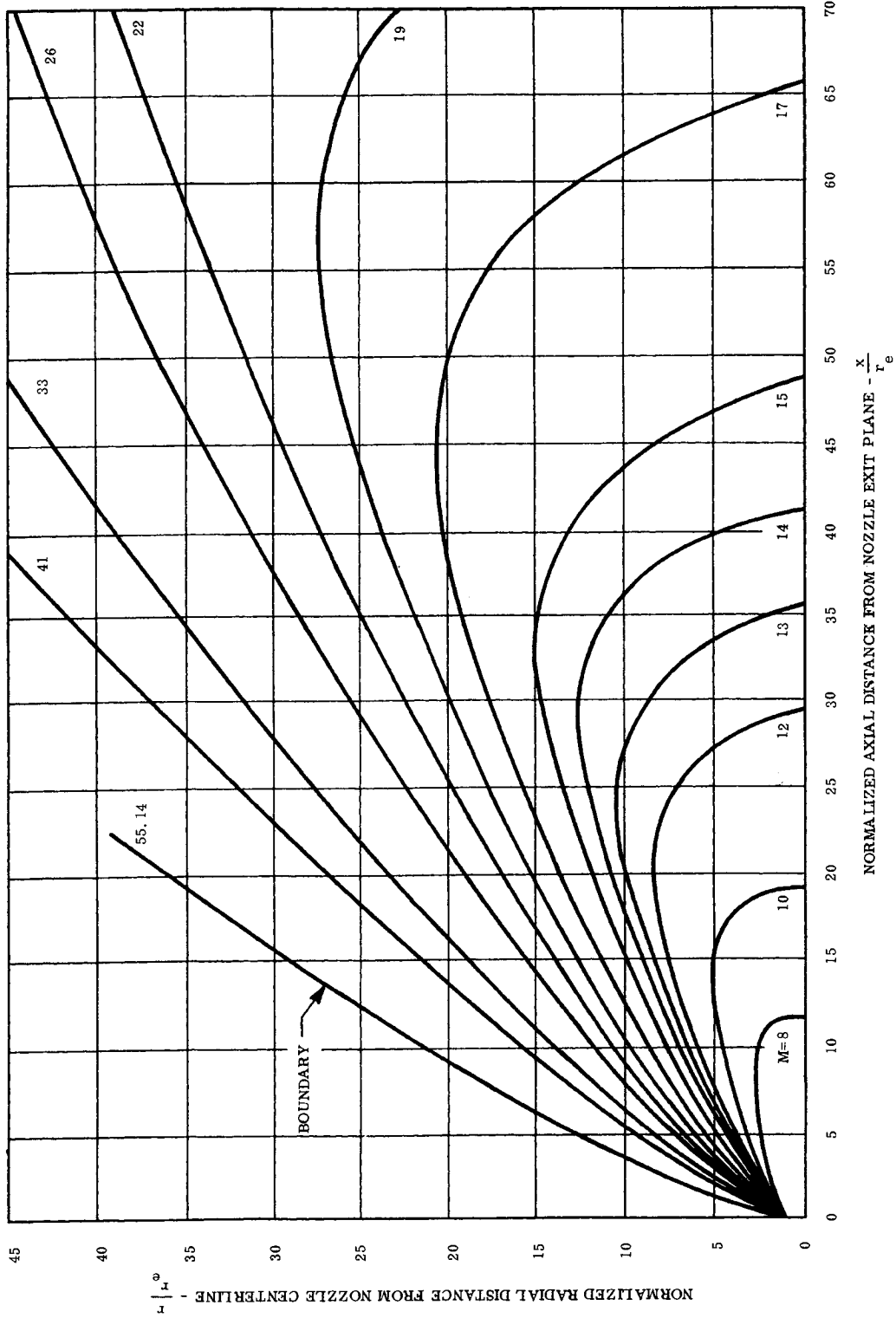
Figure 2.4-8. Mach Number Distribution in the Exhaust Plume

~~SECRET~~ SPECIAL HANDLING

~~SECRET~~ **SPECIAL HANDLING**
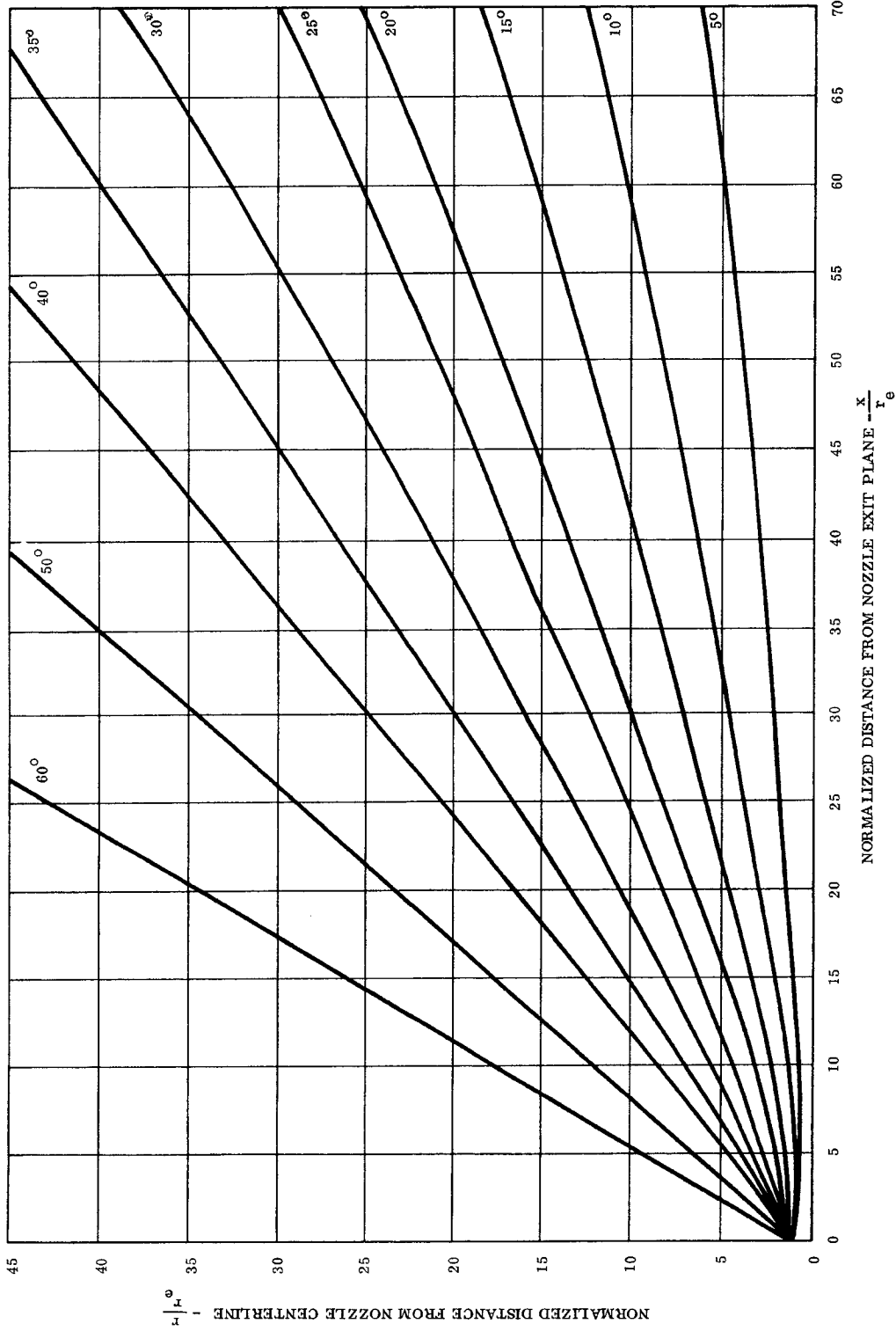
Figure 2. 4-9. Flow Angle Distribution in the Exhaust Plume

layer and the shock on the cylindrical lab module with the shroud. The oblique shock (Figure 2.4-12) is estimated to lie about 2° above the radiator skin; thus the majority of the shroud extends above such viscous effects. Also neglected is the effect on the plume properties of the constriction of the plume by the radiator. The effect of the radiator on the inviscid flow field near the radiator is to increase the density and hence the heat flux. On the other hand, the viscous effects on the lab module radiator tends to reduce heat transfer to the body since the gas in the boundary layer is cooled. Also the adverse pressure gradient caused by the shroud in the boundary layer might cause the boundary layer to

TABLE 2.4-4. MOL FRACTION OF CHEMICAL
SPECIE IN THRUSTER PLUME

SPECIE	MOLECULAR FRACTION
CO	0.1287
CO_2	0.0401
H	0.0179
H_2	0.1576
H_2O	0.3343
N_2	0.3075
NO	0.0013
O	0.0008
OH	0.0111
O_2	0.0007

2-242

TABLE 2.4-5. FLOW PROPERTIES FOR ORBIT ADJUST PLUME

MACH NUMBER	DENSITY LB/FT^3	TEMP $^\circ$R	VELOCITY FT/SEC	GAMMA
5.0	0.1423×10^{-3}	1259	9,445	1.327
6.0	0.5586×10^{-4}	916	9,757	1.349
7.0	0.2544×10^{-4}	692	9,942	1.362
7.5	0.1791×10^{-4}	609	10,009	1.366
8.0	0.1290×10^{-4}	540	10,064	1.370
8.5	0.9486×10^{-5}	482	10,110	1.373
9.0	0.7096×10^{-5}	432	10,148	1.375
9.5	0.5392×10^{-5}	390	10,181	1.377
10.0	0.4161×10^{-5}	353	10,209	1.379
10.5	0.3244×10^{-5}	322	10,233	1.381
11.0	0.2559×10^{-5}	294	10,254	1.382
11.5	0.2042×10^{-5}	269	10,272	1.384
11.75	0.1830×10^{-5}	258	10,280	1.385
12.0	0.1645×10^{-5}	248	10,289	1.385
12.5	0.1338×10^{-5}	229	10,303	1.386
13.0	0.1097×10^{-5}	212	10,315	1.383
13.5	0.9062×10^{-6}	197	10,326	1.389
14.0	0.7543×10^{-6}	183	10,336	1.389
14.5	0.6327×10^{-6}	171	10,345	1.389
15.0	0.5337×10^{-6}	160	10,353	1.389
15.5	0.4527×10^{-6}	150	10,361	1.389
16.0	0.3859×10^{-6}	141	10,367	1.389
17.0	0.2842×10^{-6}	125	10,379	1.389
18.0	0.2129×10^{-6}	112	10,389	1.389
19.0	0.1620×10^{-6}	101	10,397	1.389
20.0	0.1249×10^{-6}	91	10,404	1.389
27.5	0.2471×10^{-6}	48	10,435	1.389

~~SECRET~~ SPECIAL HANDLING
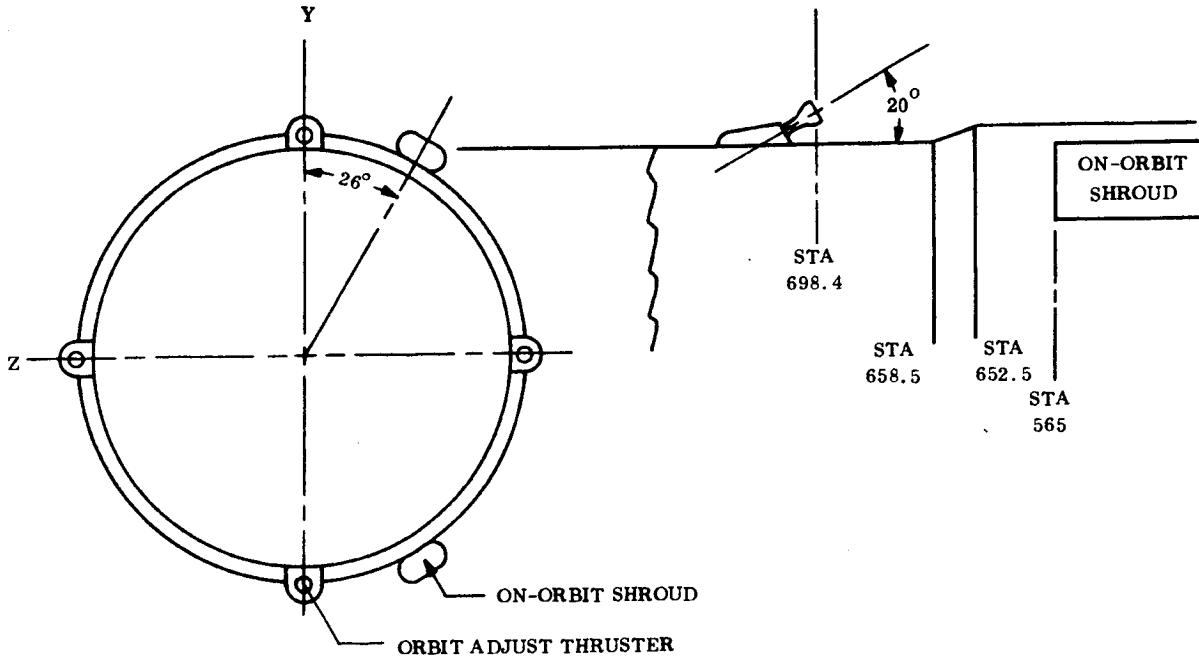
Figure 2.4-10. Relative Position of Orbit Adjust Thrusters
and the On-Orbit Shroud
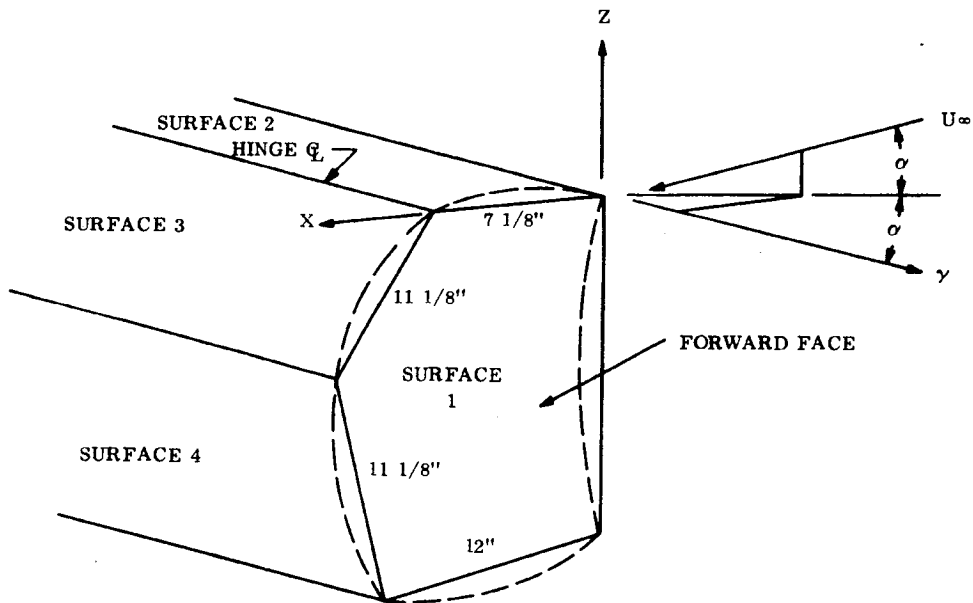
NOTE: AXES SHOWN DO **NOT** CORRESPOND TO VEHICLE AXES

Figure 2.4-11. Velocity Coordinates and Shroud Surface Identification

~~SECRET~~ SPECIAL HANDLING

separate from the lab module somewhere in front of the on-orbit shroud. As a result, there would be a dead region at the base of the shroud with a resultant reduction in heat transfer. As a conservative analysis, we have evaluated the increased density ρ_∞ in the inviscid flow to evaluate the heat transfer.

Several other simplifying assumptions have been made:

a. There is no X component of the flow (see Figure 2.4-11). The flow vector is radial from the nozzle and impinges with angles of $\alpha = -1.7^\circ$ and $\gamma = 13.75^\circ$.

b. Boundary layer theory can predict the heat transfer even though Reynold's number is low.

c. Radiation from the gas behind the normal shock is negligible compared with the convective flux.

The heat transfer to the stagnation point of the cylindrical corner between surfaces 1 and 2 is given by:

$$q_o = 0.57 \, Pr_2^{-0.6} \sqrt{\beta \rho_2 \mu_2} \; Cp \, (T_{aw} - T)^{(1)}$$

where:

Subscript 2 denotes conditions behind the normal shock formed in front of the cylinder

T_{aw} = adiabatic wall temperature = $T_{stagnation} \sqrt{Pr}$

β = velocity gradient at the stagnation point

$\quad = 0.3 \; U_\infty / R_o$

---

[1]Truitt, R.W., "Fundamentals of Aerodynamic Heating," New York, Ronald Press Co., 1960.

$$\rho_2 = 6\rho_\infty$$

ρ = density

The calculated values of these constants are:

$M = 19$

$\rho_\infty = 0.162 \times 10^{-6}$ lb/ft^3

$U_\infty = 10,379$ ft/sec

$T_{stagnation} = 7550^\circ R$

$C_p = 0.285$ Btu/lb, $^\circ R$ $(= 1/2\ U_\infty^2/T_{stag\ notion})$

$Pr = 0.7$

$\mu = 5 \times 10^{-5}$ lb/ft, sec

Hence for those parts of the shroud which protrude above the oblique shock (X coordinate ≥ 7 in) the heat transfer is:

$$q_o = \frac{0.779 \times 10^{-4}}{R_o}(6310 - T_w)\ \frac{Btu}{ft^2, sec}$$

The first order effect of the interaction between the plume and the cylinder will be a region (inviscid) of increased density along the surface of the cylinder. This flow, imping-ing on a normal surface, will result in higher heat transfer than that due to impingement of the jet without interaction. The increased density will lie behind an oblique shock which lies close to the cylinder. Thus, only a part of the on-orbit shroud will be affected.

The flow along a line to the on-orbit shroud is considered. Local mach number and flow angle β determines a local shock angle α shown in Figure 2.4-12. The abscissa is the

~~SECRET~~ **SPECIAL HANDLING**
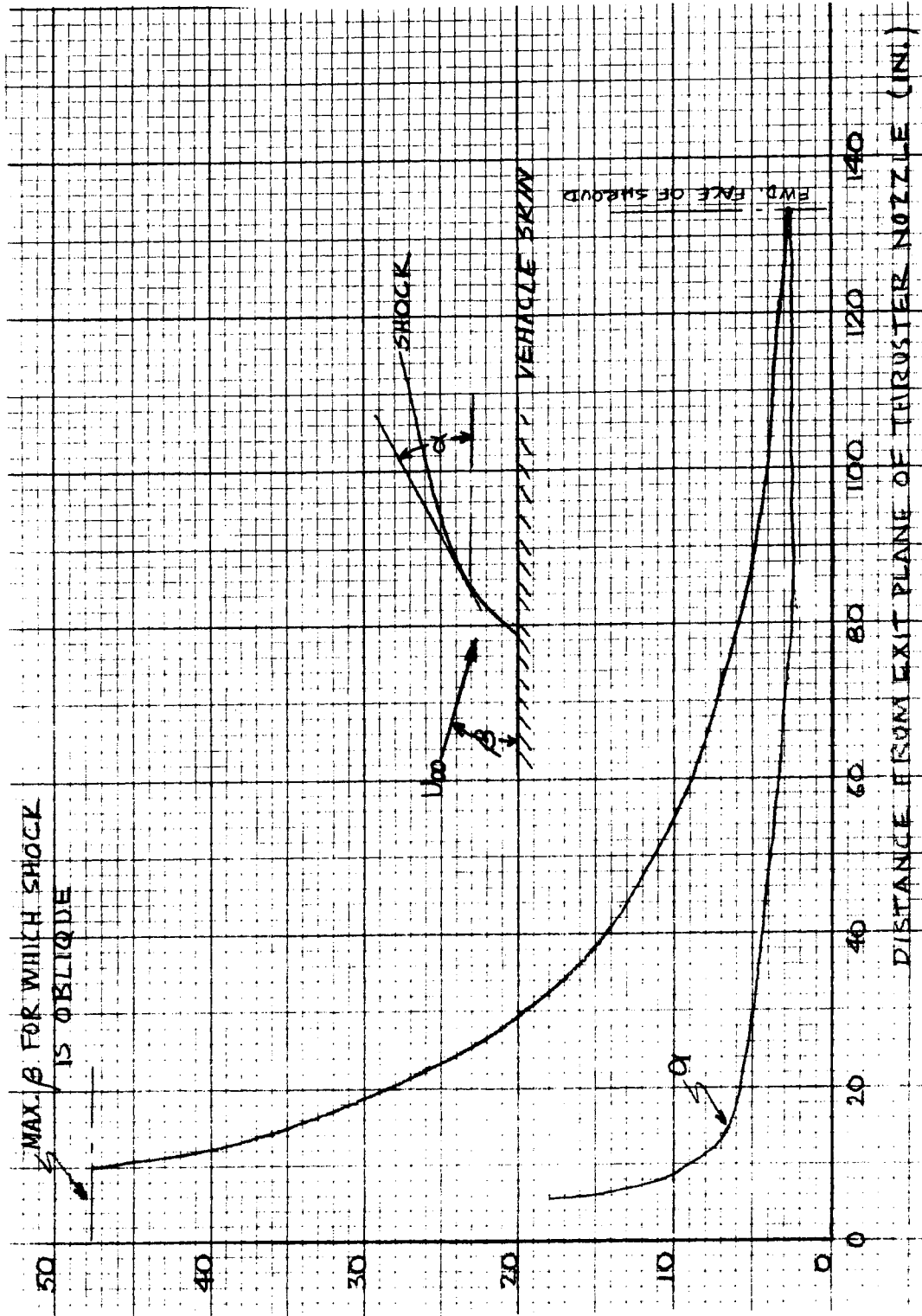
Figure 2.4-12. Oblique Shock Angles

~~SECRET~~ **SPECIAL HANDLING**

station number; thus, at station 568, the local conditions are evaluated at 26° radial position from the nozzle. The shock shape is plotted to scale in Figure 2.4-13 using local α to determine the intersection of the shock with the shroud. The ramp at station 558.5 would produce a shock and an expansion fan, but these have been neglected since the ramp width (6 in.) is small. About 7 in. of the on-orbit shroud are below the shock. Figure 2.4-14 shows the flow conditions behind the oblique shock evaluated using local angles and mach numbers. Note that the density is increased by a factor of 1.8 over ρ_{∞}. The flow between the cylinder and the shock is supersonic and produces a normal shock in front of the shroud with a further increase in density by a factor of about 6. The analysis is valid with ρ_{∞} replaced by 1.8 ρ_{∞}.

Those parts of the shroud which do not protrude above the oblique shock (i. e., X coordinate less than 7 in.) have heat transfer increased by a factor of $\sqrt{1.8}$; i. e.,

$$q_o = \frac{1.035 \times 10^{-4}}{\sqrt{R_o}} (6310 - T_w) \frac{Btu}{ft^2, sec}$$

There are two other significant errors. One of these is due to the unknown composition and the thermodynamic properties behind the shock. The composition in the free jet, approximately

$$
\begin{aligned}
CO &= 0.1387 \\
H_2 &= 0.167 \\
H_2O &= 0.360 \\
H_2 &= 0.3343
\end{aligned}
$$

~~SECRET~~ **SPECIAL HANDLING**
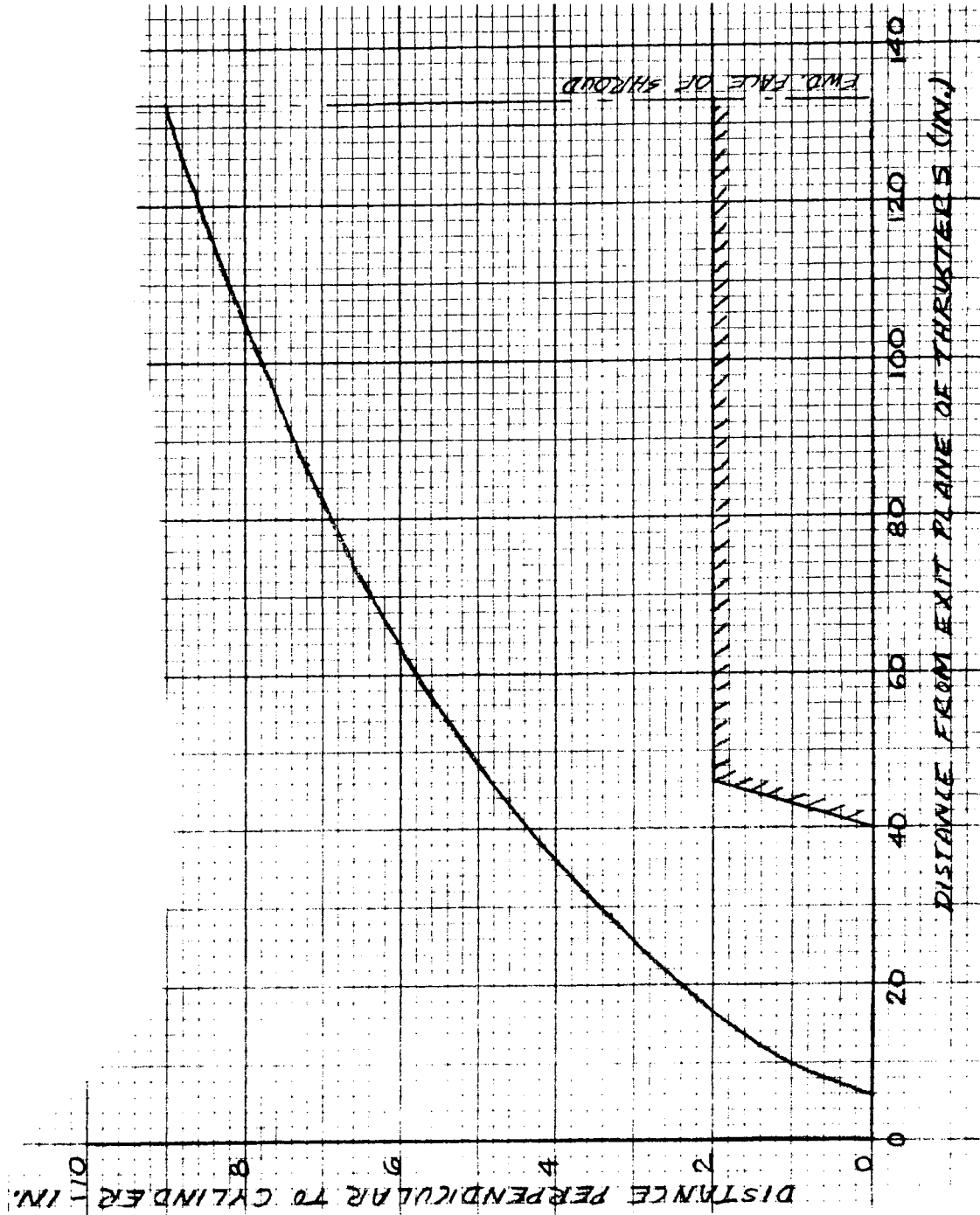
Figure 2.4-13. Shock Shape on Vehicle Skin (Neglecting Interaction with Boundary Layer)

~~SECRET~~ **SPECIAL HANDLING**

~~SECRET~~ **SPECIAL HANDLING**
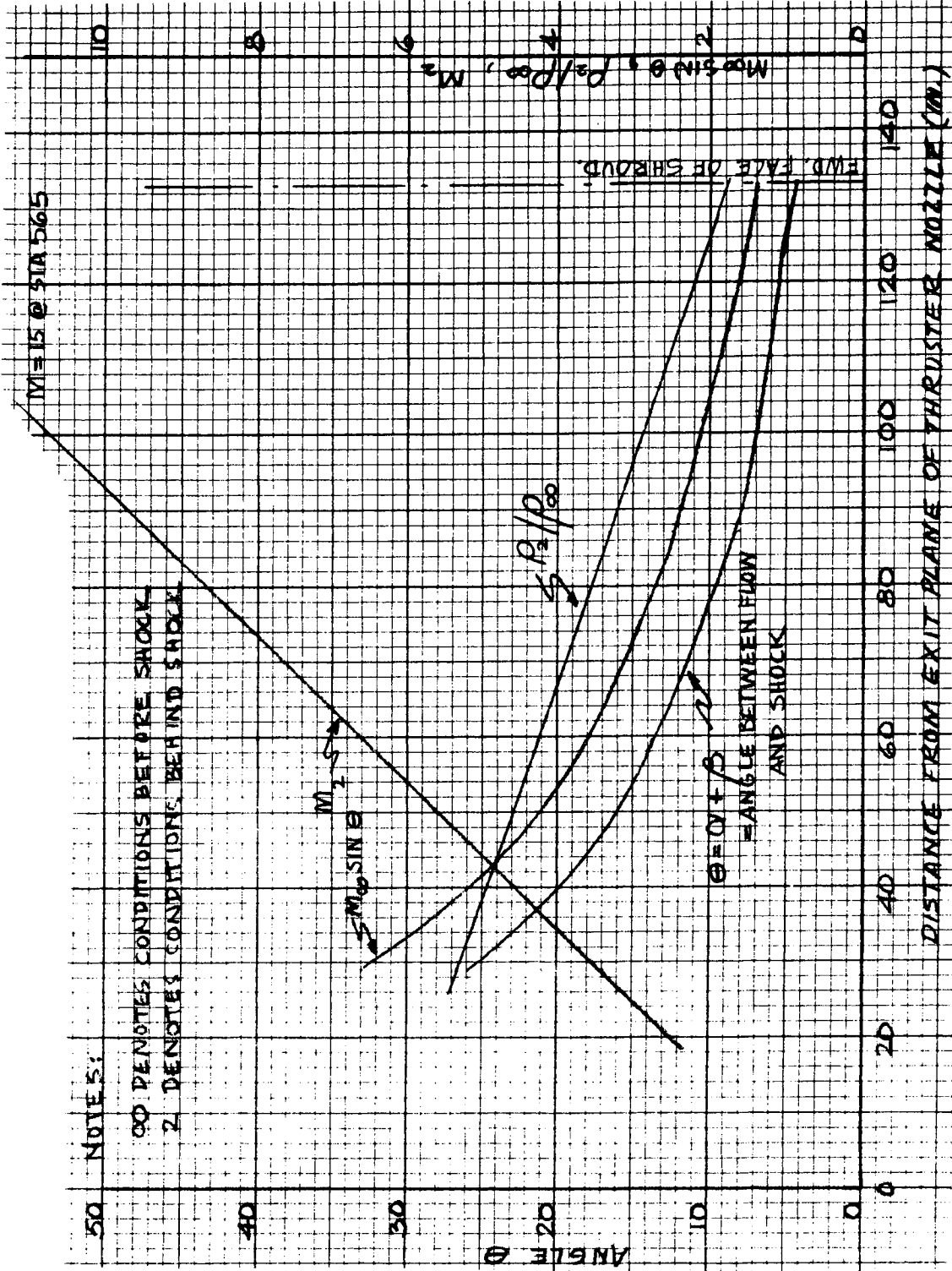
Figure 2.4-14. Properties Behind Shock on Vehicle Shell

~~SECRET~~ **SPECIAL HANDLING**

by mole fraction, gives (based on R. H. Kohrs Advanced Aerospace Phys. Tech. Memo No. 30)

$$Pr = 0.815$$

$$\mu_2 = 5.26 \times 10^{-5}$$

$$OR \quad q = \frac{0.99 \times 10^{-4}}{\sqrt{R_o}} (6810 - Tw)$$

approximately 4 percent lower than the previous formula.

Another inaccuracy is due to the assumption of two-dimensional flow around the cylinder. This assumption is valid if $\frac{R_o}{L} << 1$ where L is the cylinder length (length of edge between 1 and 2). For $\frac{R_o}{L} > 1$, the curved nature of the cylinder would make the flow tend toward that of an axisymmetric stagnation point which would have heat transfer given by $\sqrt{2}$ times the q_o given previously.

Figure 2.4-15 shows the calculated heat flux distribution along surfaces 1 and 2 as a function of distance from the stagnation point. The heat flux to surface 3 is the same as surface 2 along their common edge and the same as surface 1 along their common edge. The two-dimensional distribution within surface 3 is assumed to be the product of the two distributions in perpendicular directions. The other surfaces receive no convective flux.
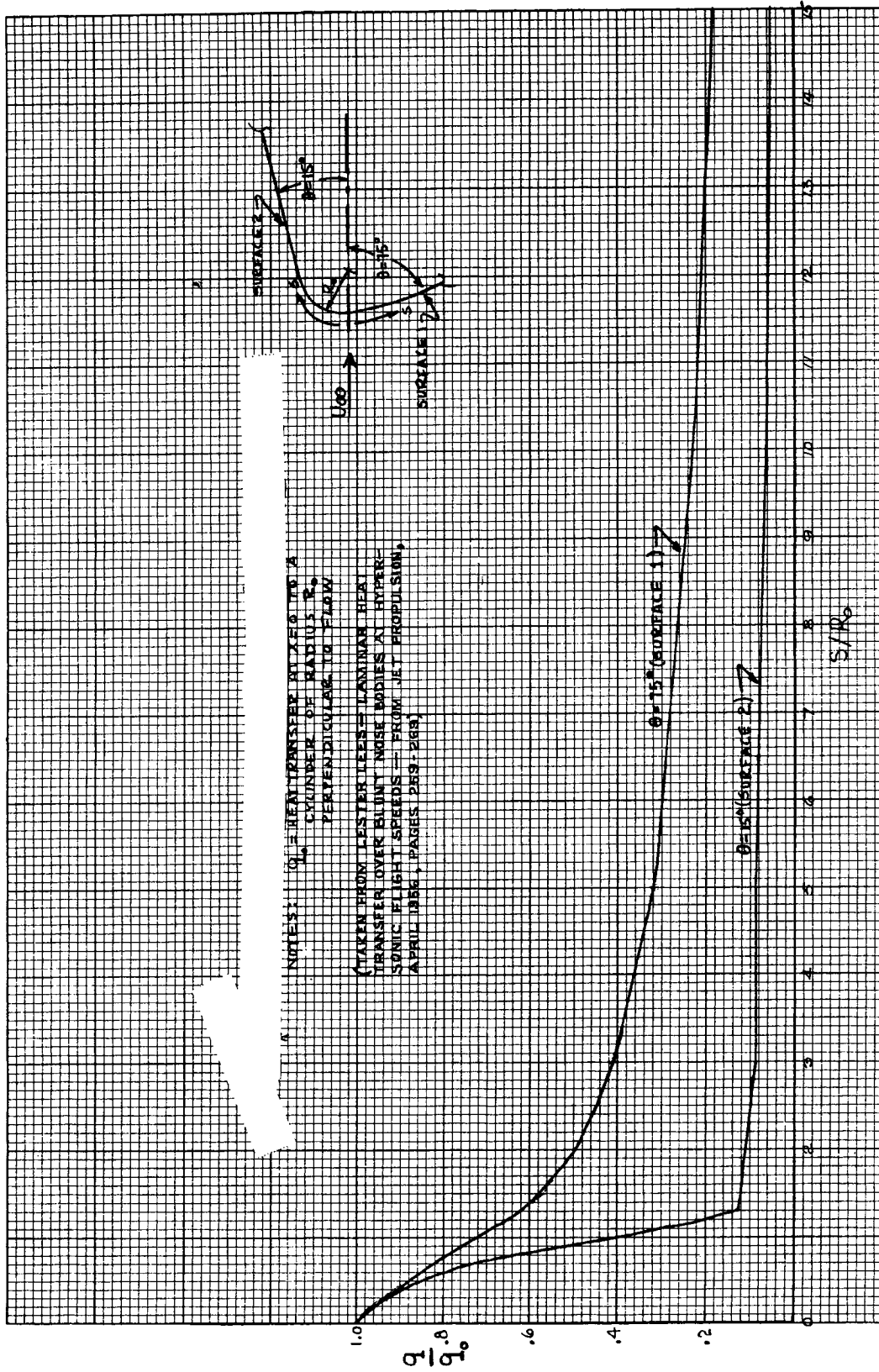
Figure 2.4-15.   Heat Transfer Distribution (from Lester Lees)

C. **Shroud Temperature Behavior During Thruster Firing** - One condition has been analyzed to date. For the purpose of evaluating the average temperature behavior of the shroud, a 3-inch radius was assumed for the edge common to the forward face of the shroud and the top sector of the shroud. The maximum temperature on the forward face of the on-orbit shroud is estimated to be about $800^{\circ}F$ based on (1) neglecting condction effects; and (2) using the relationship

$$\left(\frac{T_{max}}{T_{avg}}\right)^4 = \left(\frac{Q_{max}}{Q_{avg}}\right)$$

where

$$Q = \text{heating rate}$$

$$T = \text{absolute temperature}$$

The average temperature peaks out at about $600^{\circ}F$. Figures 2.4-6 and 2.4-7 shows the impact of the thruster firing for the one typical case cited. The first 90-minute period is typical of a hot-orbit case as previously cited. The thruster firing is assumed to occur at the equator on the sunlit side of the earth.

The temperature of the external optics rose approximately $2^{\circ}F$ during the thruster firing transient. Figures 2.4-6 and 2.4-7 also indicate that the system will essentially recover from the thruster firing transient within two orbits. The insulation was represented, for the purposes of this analysis, as a material with an effective emittance of 0.03. Most of the data accumulated to date on typical carefully installed multi-layer insulation blankets shows a range of 0.01 - 0.03 for the effective emittance at temperatures closer to room temperature. As the average blanket temperature increases, the effective emittance actually decreases so that a value of 0.03 is a highly conservative value. As discussed in section 2.4.1.6, the insulation can, under normal orbital conditions, have a greater effective thermal conductivity by a factor of almost 10 without deleterious effects.

2.4.1.4.5 Gyro Response Characteristics

In order to maximize the gyro reliability, the gyro is activated just prior to an activity mode and then deenergized following the activity mode. Temperature control is achieved by means of two thermostatically regulated heaters. These heaters consist of a 50-watt coarse control heater for rapid heat-up plus a 10-watt heater for fine control. The 50-watt heater is activated when the gyro temperature is more than $5^{\circ}F$ below the set point. The gyro set point is $160 \pm 5^{\circ}F$. The fine control heater is activated when the gyro temperature is less then the set point. Figure 2.4-16 shows a typical gyro temperature-time curve for a $0^{\circ}F$ sink temperature. In order to analyze the heatup and cooldown transient, it was assumed that the gyro case itself was maintained at $0^{\circ}F$. This assumption results in predicting a longer heatup period than will actually occur. Also, this tends to predict a lower temperature after cooldown than will actually occur during a series of active orbits.

2.4.1.5 Coating Selection

The function of the coatings employed on the on-orbit shroud is twofold:

a. Prevent spurious light reflections from entering the optical system

b. Control the shroud temperature and, concurrently, the temperature of the optical elements within the defined limits.

The first objective is accomplished by coating all of the non-optical surfaces internal to the on-orbit shroud with a thermodynamically black coating. The second objective is achieved by means of an array of coatings. The method for selecting the coating array is as follows:

a. The shroud is divided into several discrete zones.

b. The variation in the orbital average environmental heat fluxes can be calculated for each zone.

c. For those zones which are subject to any significant heating from the orbit adjust thruster firing, a coating with a low solar absorptance and high emittance will
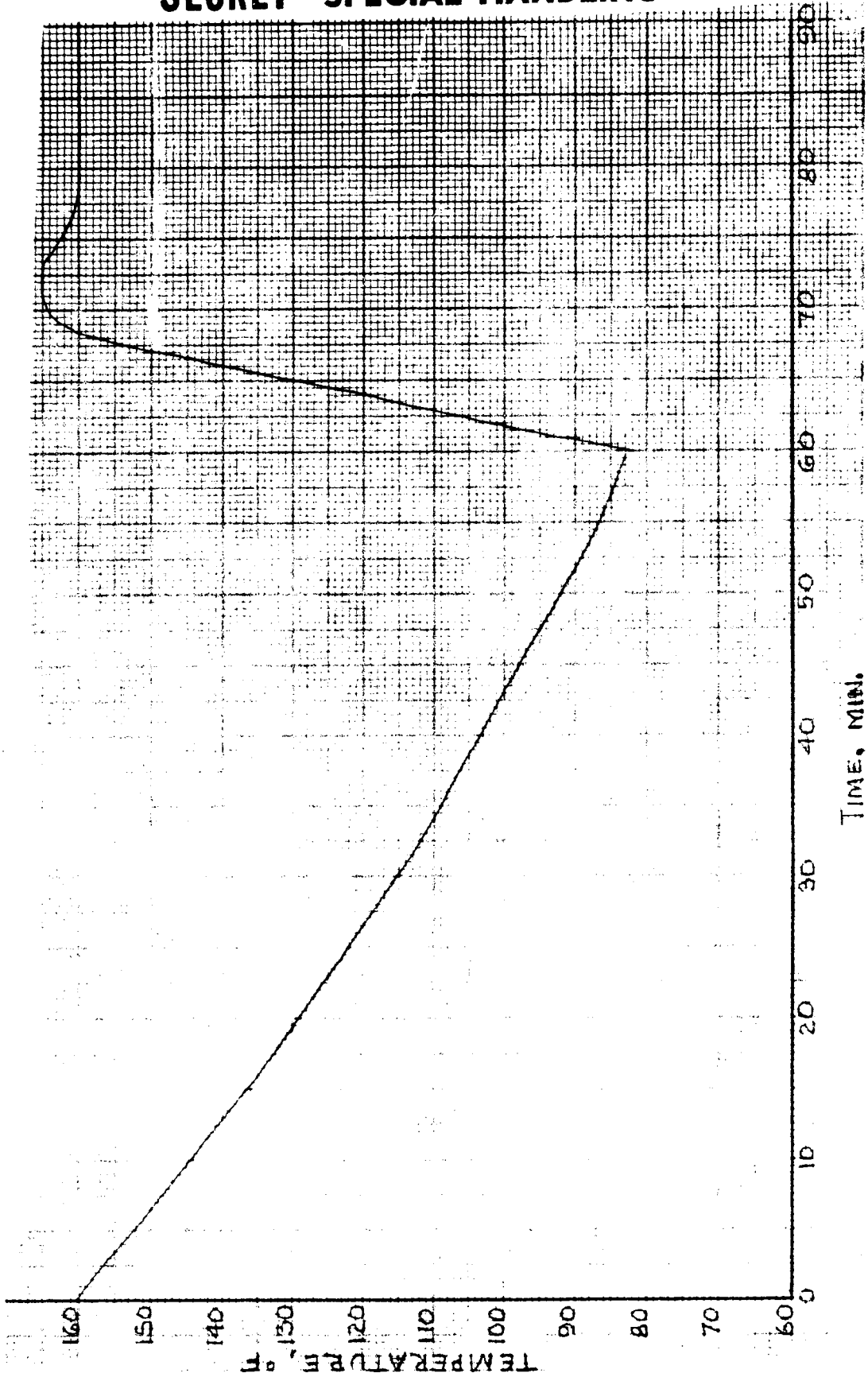
Figure 2.4-16. Typical Gyro Temperature Cycle (0 Degree Fahrenheit Sink)

2-255

be used to limit the peak temperature which these surfaces will be subject to during the aforementioned short-term transient.

d. For the remaining zones, a coating pattern will be chosen with two characteristics: (1) Lowest emittance coating available compatible with the required solar absorptance. This tends to minimize the temperature variation of the skin over the course of an orbit; (2) Choose coatings which, under the condition of peak environmental heating (exclusive of the thruster firing temperature) and peak internal heat generation, will limit the average skin temperature to less than 70°F. This is compatible with maintaining the internal equipment within the temperature range of 0 - 100°F. Coatings have not yet been specified in detail. The above philosophy will be followed in selecting specific materials.

2.4.1.6 Insulation Materials

Two insulation blanket configurations are being proposed. These two assemblies are shown in Figure 2.4-17. Table 2.4-6 shows some of the materials currently being reviewed for this application.

VEHICLE
SKIN

VEHICLE
SKIN

HIGH TEMPERATURE
BLANKET

LOW TEMPERATURE
BLANKET

(a) HIGH TEMPERATURE
BLANKET

(b) COMPOSITE BLANKET
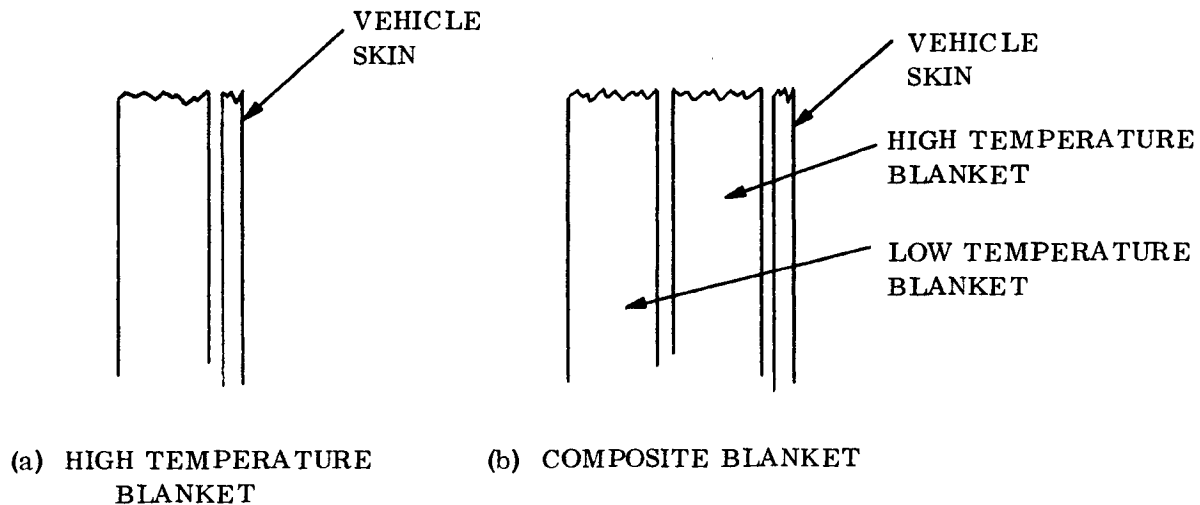
Figure 2.4-17. Insulation Assemblies

TABLE 2.4-6. INSULATION MATERIALS

HIGH-TEMPERATURE MATERIALS	
Shields	Spacers
Aluminum Foil Stainless Steel Foil Copper Foil Nickel Foil Molybdenum Foil Tantalum Foil	Borosilicate Glass Fiber Paper Refrasil Carbon Cloth Zirconia Paper
LOWER TEMPERATURE MATERIALS	
Aluminized Mylar Aluminized Kapton ("H" Film)	

The reason for choosing a composite blanket over a single material is to minimize weight. The major disadvantage of a composite blanket is the difficulty of predicting analytically the optimum number of layers for each of the two materials.

2.4.1.7 Areas Requiring Additional Analysis

The remaining tasks essential to completion of the external system thermal analysis are summarized below:

a. Coating evaluation

1. Selection of materials

2. Evaluating of tolerances of property values resulting from application plus environmental degradation

b. Effect of door cycling on tracking mirror and fixed fold assembly gradients

    c.   Insulation evaluation

        1.   Material evaluation

        2.   Configuration optimization

        3.   Design of mounting method

        4.   Tolerance evaluation

    d.   Failure modes

        1.   Open door

        2.   Failed fixed fold assembly mount heater

    e.   Ascent heating analysis

        1.   Evaluate impact of new shroud design

        2.   Evaluate time period following shroud ejection and prior to orbit injection

        3.   Evaluate impact of orbit injection maneuver

    f.   Orbit Adjust Thruster Firing

        1.   Analysis of several potential shroud configurations

        2.   Evaluation of system recovery time

2.4.2 TELESCOPE ASSEMBLY

2.4.2.1 Design Philosophy

The Optical performance of the Acquisition Tracking System is sensitive to optical distortion caused by thermal gradients in the optical elements. The design philosophy developed to minimize temperature-induced distortions is:

a. Thermally decouple tube from external environment by means of a highly reflective finish on the tube exterior

b. Minimize contact area between optical elements and their mounts

c. Use of low thermal conductivity materials, where structurally feasible, to mount the various optical elements in place.

In addition to the above considerations, the absence of a gravitational field precludes any significant convection heat path resulting from the presence of a gas. The analyses performed to date indicate that an active control system is not required and that a judicious selection of the exterior surface finish plus isolation mounting of the individual optical elements constitutes an acceptable design solution.

2.4.2.2 Temperature Constraints

Precise temperature constraints have not yet been generated although the optimum temperature is around 70°F, the temperature at which the elements are fabricated. Having the elements operate at temperatures slightly higher than this results in relative movement of the elements with an accompanying defocusing.

2.4.2.3 Environment Description

The telescope passes through three widely differing environments:

a. One section of the component extends into the living crew area where the temperatures are maintained between 66° and 80°F by an active air flow system. The forced convection essentially maintains the portion of the telescope in this area between the temperature levels previously cited.

b. The major portion of the telescope assembly passes through two consoles (either consoles 2 and 3 or 7 and 8) containing electronic dissipating components and cold plate heat exchanges in a stagnant gaseous environment of approximately 5 psia.

c. In the area between the birdcage structure and the pressure shell, an annulus exists where living crew area air is recooled and moisture is condensed in an air-to-liquid heat exchanger. This annulus acts as an airflow duct, and a forced convective environment exists.

2.4.2.3.1 Console Temperature Envelope

The temperature envelope developed for the telescope is shown in Figures 2.4-18 through 2.4-22. The concept of a cylindrical envelope on which the boundary temperatures could be specified was developed in order to minimize the amount of reanalysis required, prompted by relocations of black boxes. The most extreme temperatures expected on these boundaries have been specified.

2.4.2.3.2 Atmosphere Characteristics

Table 2.4-7 shows the nominal design properties for either a 100 percent O_2 atmosphere at 5 psia or a 70 percent O_2/30 percent He atmosphere. The 70 percent O_2/30 percent He atmosphere is the baseline design condition.

2.4.2.4 Temperature Profiles

2.4.2.4.1 Outer Section (Window and Objective Elements)

The temperature gradients across the window and the objective elements are critical in evaluating the optical degradation of the telescope system. As previously stated, the design objective of minimal temperature gradients can be met basically by virtue of the fact that gaseous conduction is low and that radiation coupling to the environment can be minimized by means of a low emittance surface finish on the exterior of the tube. These three elements have been analyzed along with a 25-inch-long section of tube. An adiabatic boundary was assumed at the end of the tube. Each element was axially trisected to form three disks. Each disk was in turn divided radially into 25 areas. The window housing was represented

~~SECRET~~ **SPECIAL HANDLING**
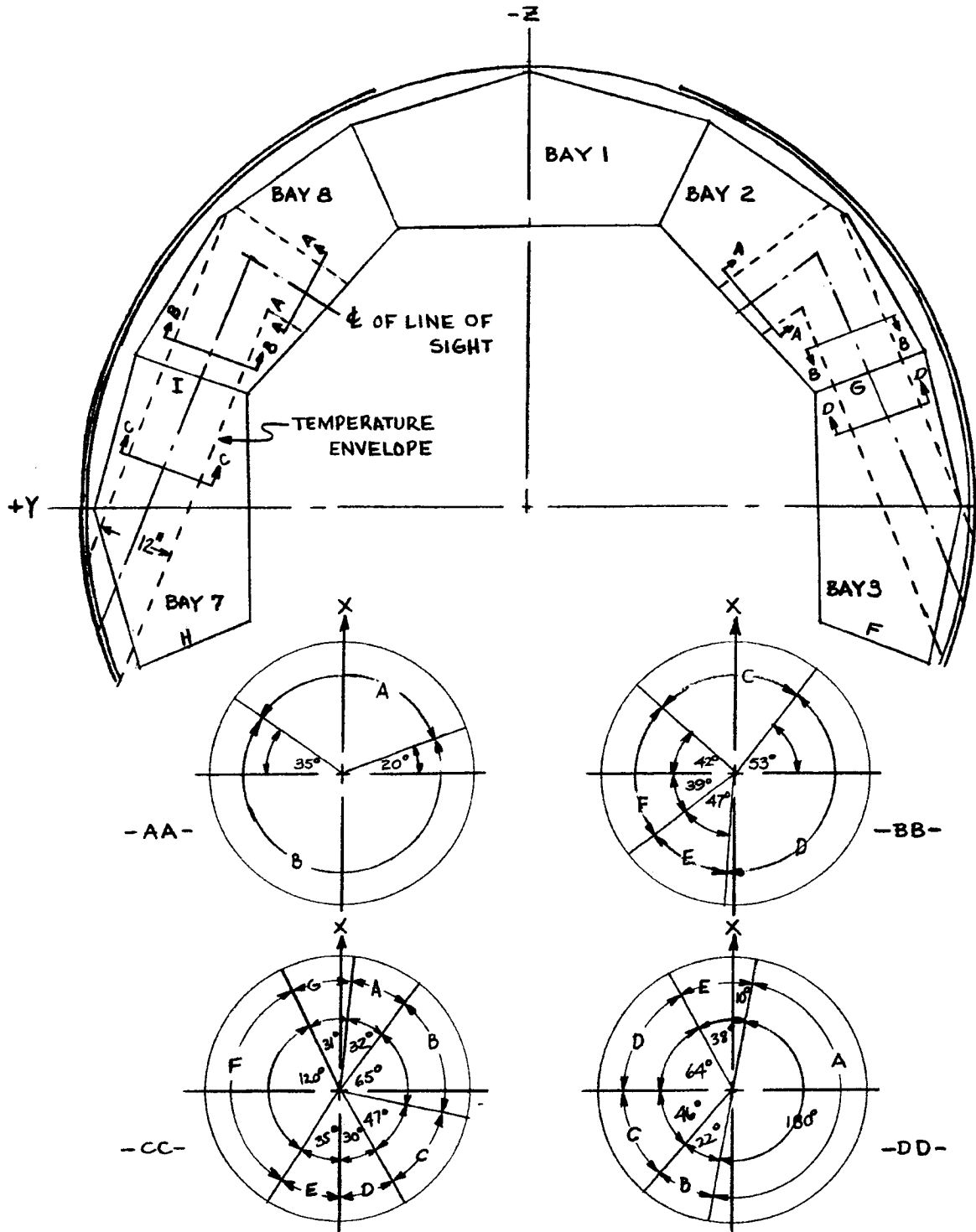
Figure 2.4-18. Effective Temperature Zones for
Telescope Temperature Envelope

~~SECRET~~ **SPECIAL HANDLING**
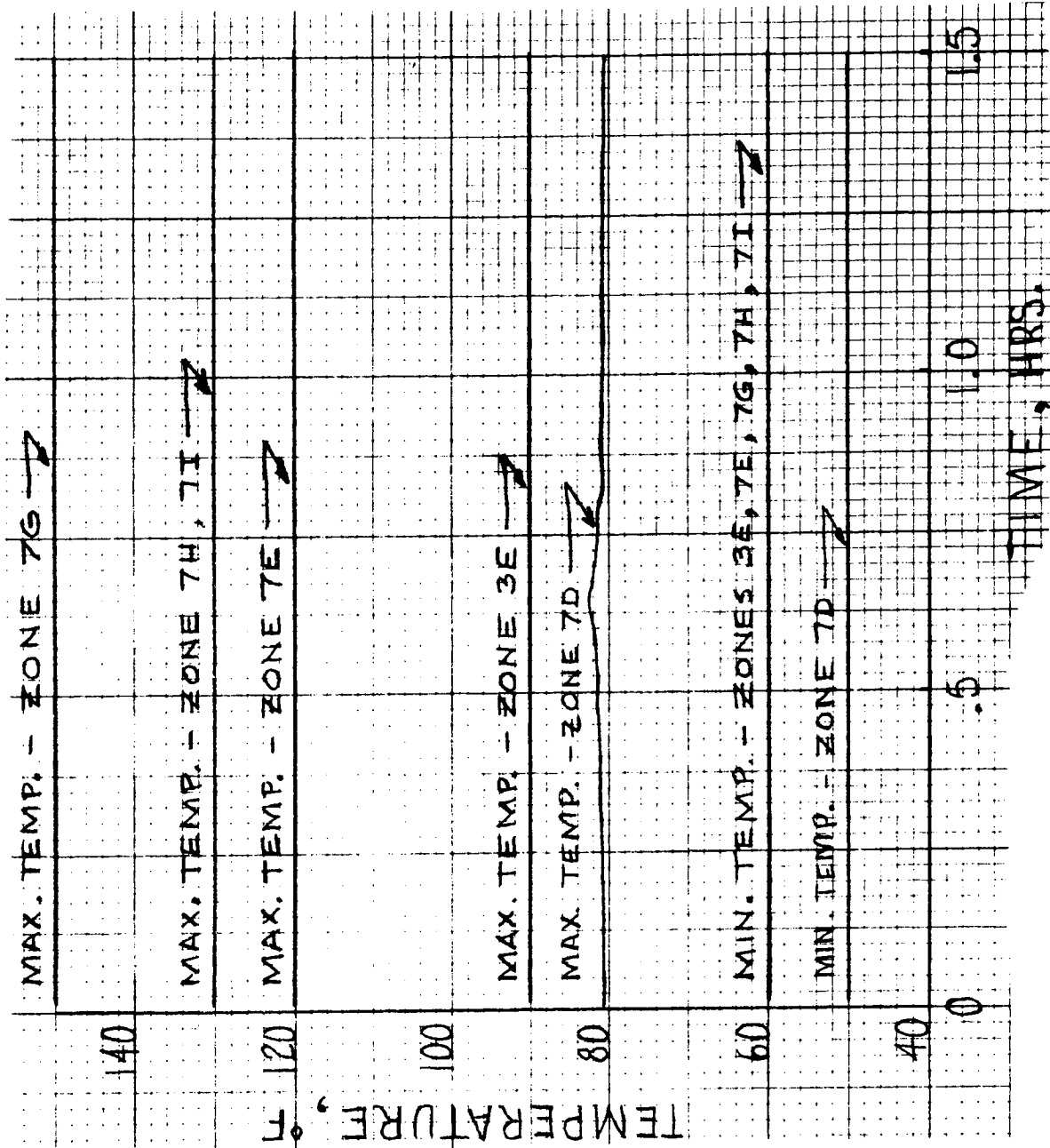
Figure 2.4-19. Transient Temperature of Bays 3 and 7

The chart plots TEMPERATURE, °F (vertical axis, from 40 to 140) against TIME, HRS. (horizontal axis, from 0 to 1.5), showing curves labeled:

- MAX. TEMP. – ZONE 7G
- MAX. TEMP. – ZONE 7H, 7I
- MAX. TEMP. – ZONE 7E
- MAX. TEMP. – ZONE 3E
- MAX. TEMP. – ZONE 7D
- MIN. TEMP. – ZONES 3E, 7E, 7G, 7H, 7I
- MIN. TEMP. – ZONE 7D

~~SECRET~~ **SPECIAL HANDLING**

Figure 2. 4-20. Transient Temperature of Bays 3 and 7

~~SECRET~~ **SPECIAL HANDLING**
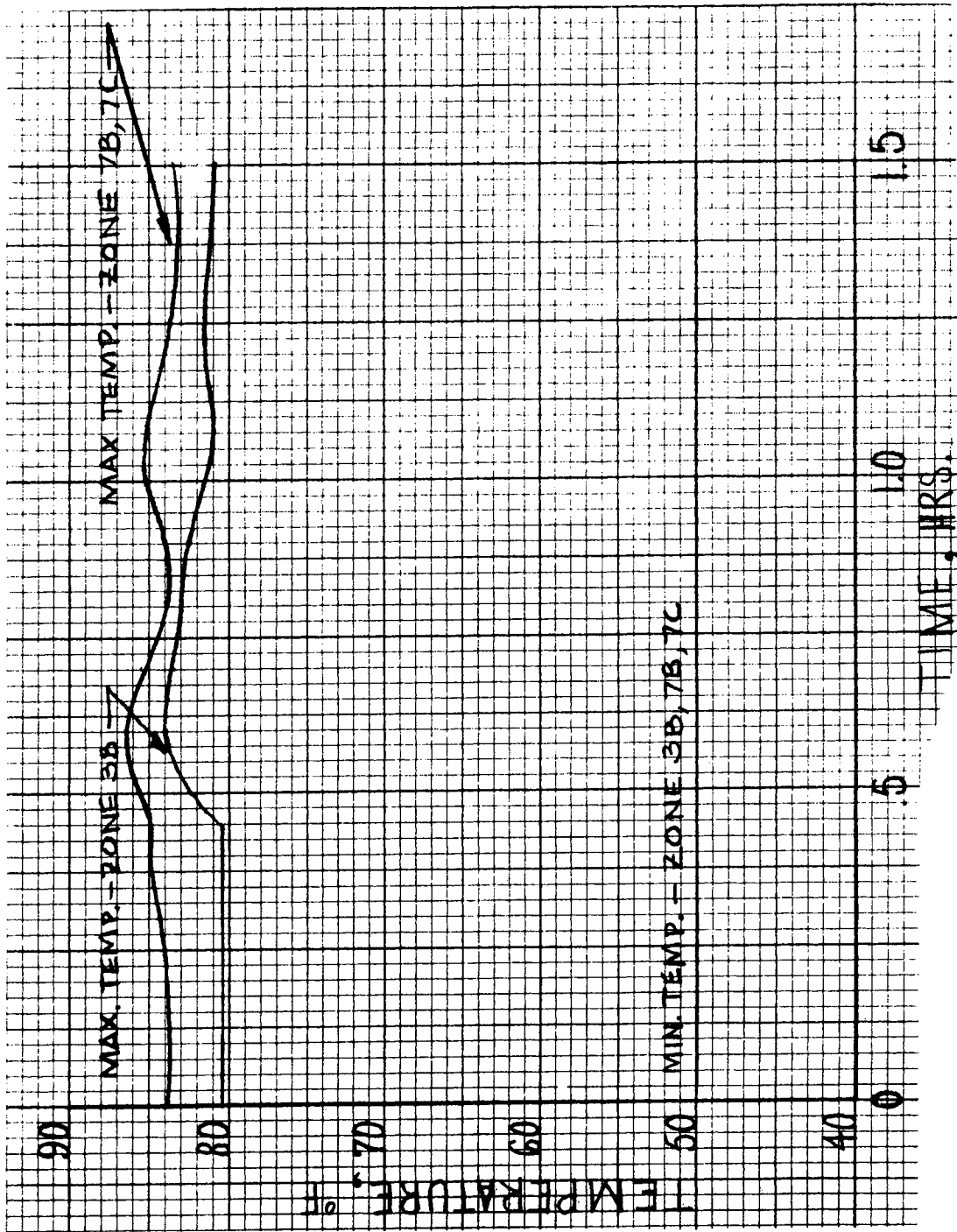
Figure 2.4-21. Transient Temperature of Bays 3 and 7

2-264

~~SECRET~~ **SPECIAL HANDLING**

~~SECRET~~ SPECIAL HANDLING
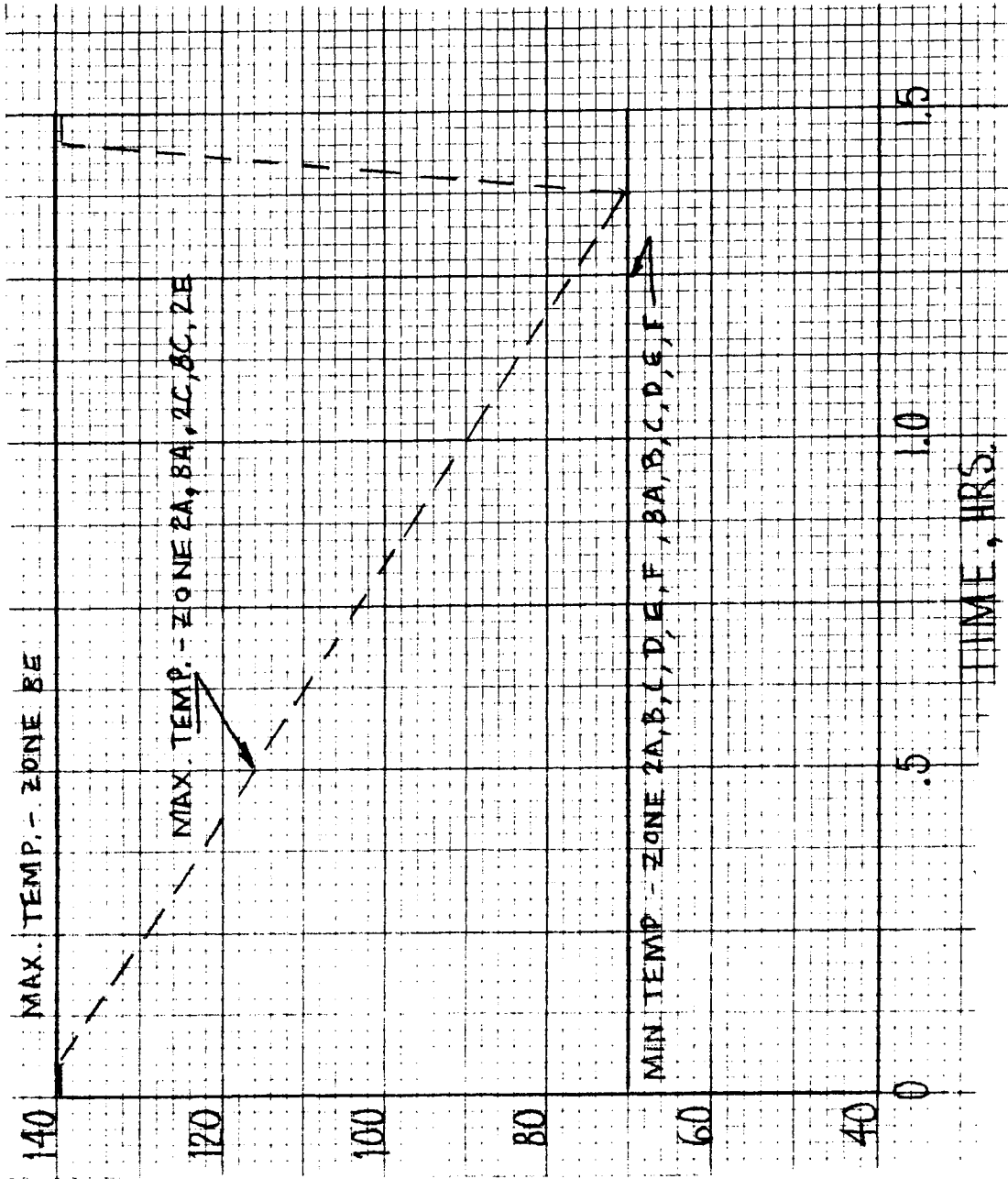
Figure 2.4-22. Transient Temperature of Bays 2 and 8

TABLE 2.4-7. NOMINAL DESIGN PROPERTIES

	HELIUM/O_2	PURE O_2
Partial Pressure O_2	3.5 psia	5.0 psia
Partial Pressure CO_2	5.0 mm Hg	5.0 mm Hg
Partial Pressure H_2O	7.5 mm Hg	7.5 mm Hg
Partial Pressure He	65.0 mm Hg	--
Molecular Weight	24.75	31.93
Gas Const (R)	$62.43 \frac{lb\text{-}ft}{lb\text{-}^{\circ}R}$	$48.4 \frac{lb\text{-}ft}{lb\text{-}^{\circ}R}$
Density	0.0216 lb/ft^3	0.0278 lb/ft^3
C_p	0.2675 Btu/lb-$^{\circ}$R	0.2240 Btu/lb $^{\circ}$R
C_v	0.1868 Btu/lb-$^{\circ}$R	0.1614 Btu/lb $^{\circ}$R
k	0.0253 Btu/hr ft $^{\circ}$F	0.0151 Btu/hr ft $^{\circ}$F
μ	0.0487 lb-in./ft-hr	0.0485 lb/ft-ft

by an additional five modes, and the retaining rings were likewise broken up into five modes each. The boundary condition assumed was a 4° radial gradient imposed on the outermost window disk. A 70°F boundary temperature was assumed. Figure 2.4-23 shows the nodal breakdown used in the analysis. Table 2.4-8 gives a summary of the results of this analysis.

TABLE 2.4-8. SUMMARY OF OBJECTIVE LENS ELEMENT
TEMPERATURE GRADIENTS

ELEMENT NO. 1	MAXIMUM TEMPERATURE (°F)	MINIMUM TEMPERATURE (°F)	MAXIMUM GRADIENT (°F)
Disc 1	71.587	69.243	2.344
2	71.436	69.371	2.065
3	71.296	69.492	1.804
ELEMENT NO. 2			
Disc 1	71.274	69.579	1.695
2	71.193	69.602	1.591
3	71.104	69.664	1.440

It should be emphasize that DACO is required to maintain the peripheral temperature gradient around the window to ± 1°F.

2.4.2.4.2 Elbow Region

A steady state analysis has been made on the elbow region to determine gross steady state temperature levels of individual elements and to indicate temperature problem areas to be examined in a transient analysis. The assumed environment was an O_2/He environment. Two cases were analyzed:
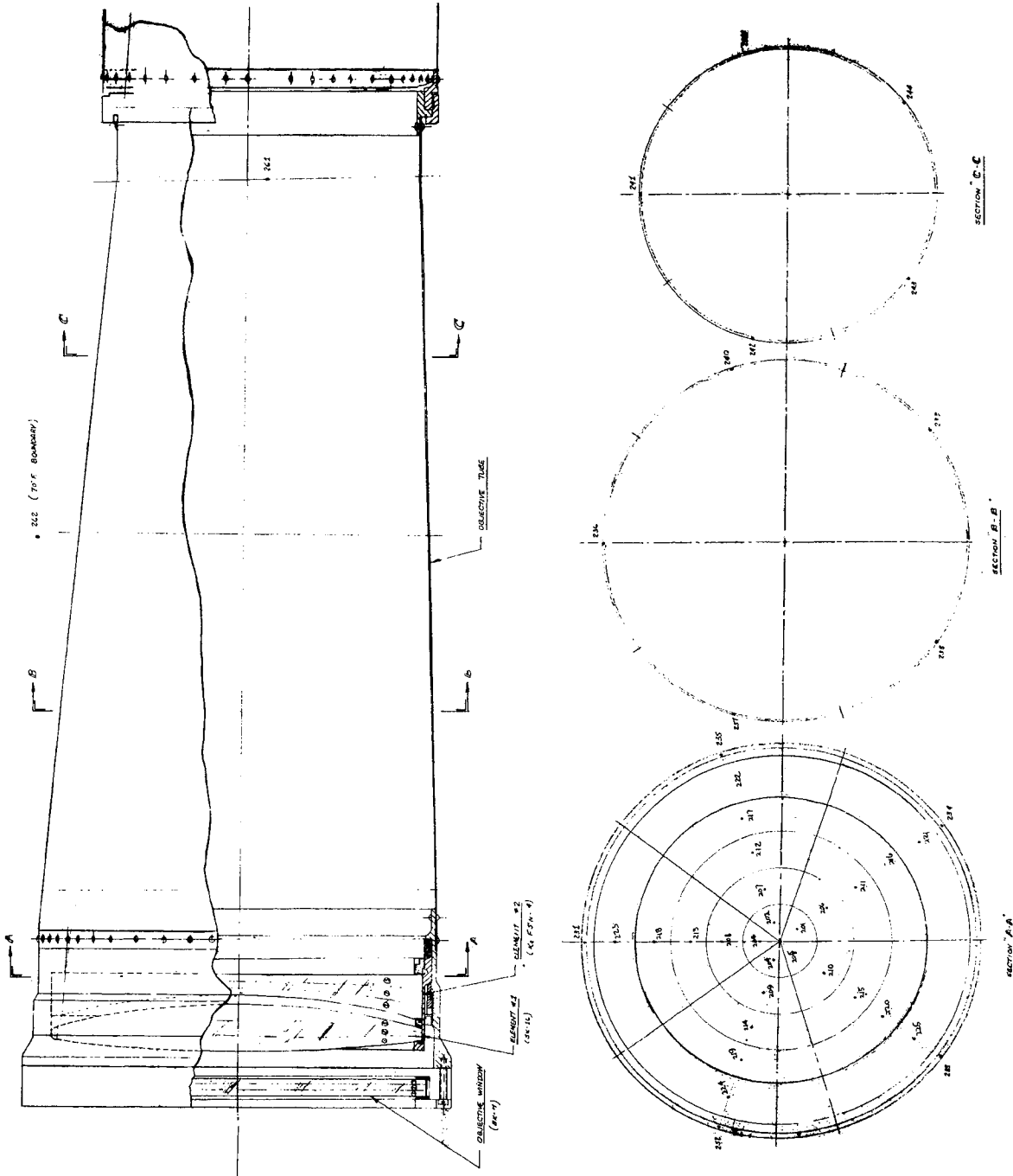
Figure 2. 4-23. Nodal Network of Outer Elements

Case 1.   Fold mirror back face plus inner surface of mirror cover with an emittance = 1.0

Case 2.   Fold mirror back face plus inner surface of mirror cover with an emittance = 0.1

A summary of the temperature pattern obtained is shown in Table 2.4-9. The nodal identification of the elbow region is shown in Figure 2.4-24.

An analysis is currently in progress to determine a more detailed temperature distribution through the low power group.

2.4.2.4.3 Pechan Prism

A detailed steady state analysis of the Pechan prism has been completed based on a 70°F to 140°F boundary temperature. A schematic of the nodal arrangement is shown in Figure 2.4-25. The average heat dissipation from the Pechan drive motor is 0.24 Btu/hr. An adiabatic boundary was assumed at either end of the Pechan structure. A summary of the results is presented in Table 2.4-10.

As is evident from Table 2.4-10, the Pechan prism is essentially an isothermal mass, with a nominal temperature of 98.6°F. The maximum radial gradient is on the order of 0.01°F. This corresponds to a negligible optical path difference (OPD). The field flattener has a nominal temperature of 98.5^{O}F with a maximum radial gradient of 0.15^{O}F. The OPD for the field flattener is 1/20 λ for a temperature gradient of 0.15^{O}F. This by itself will not significantly affect the image quality. However, if all of the elements were to produce wavefront patterns which were to add up in phase, then some noticeable degradation would occur.

2.4.2.4.3 Zoom Assembly

The zoom assembly is also exposed to unsymmetric boundary temperatures. In addition, the eyepiece contains a heat source, namely the peripheral display. Table 2.4-9 shows a temperature gradient of 1.58^{O}F in the zoom structure. The temperature gradients in the individual elements have not yet been determined.

Figure 2. 4-24. Node Designations of Elbow
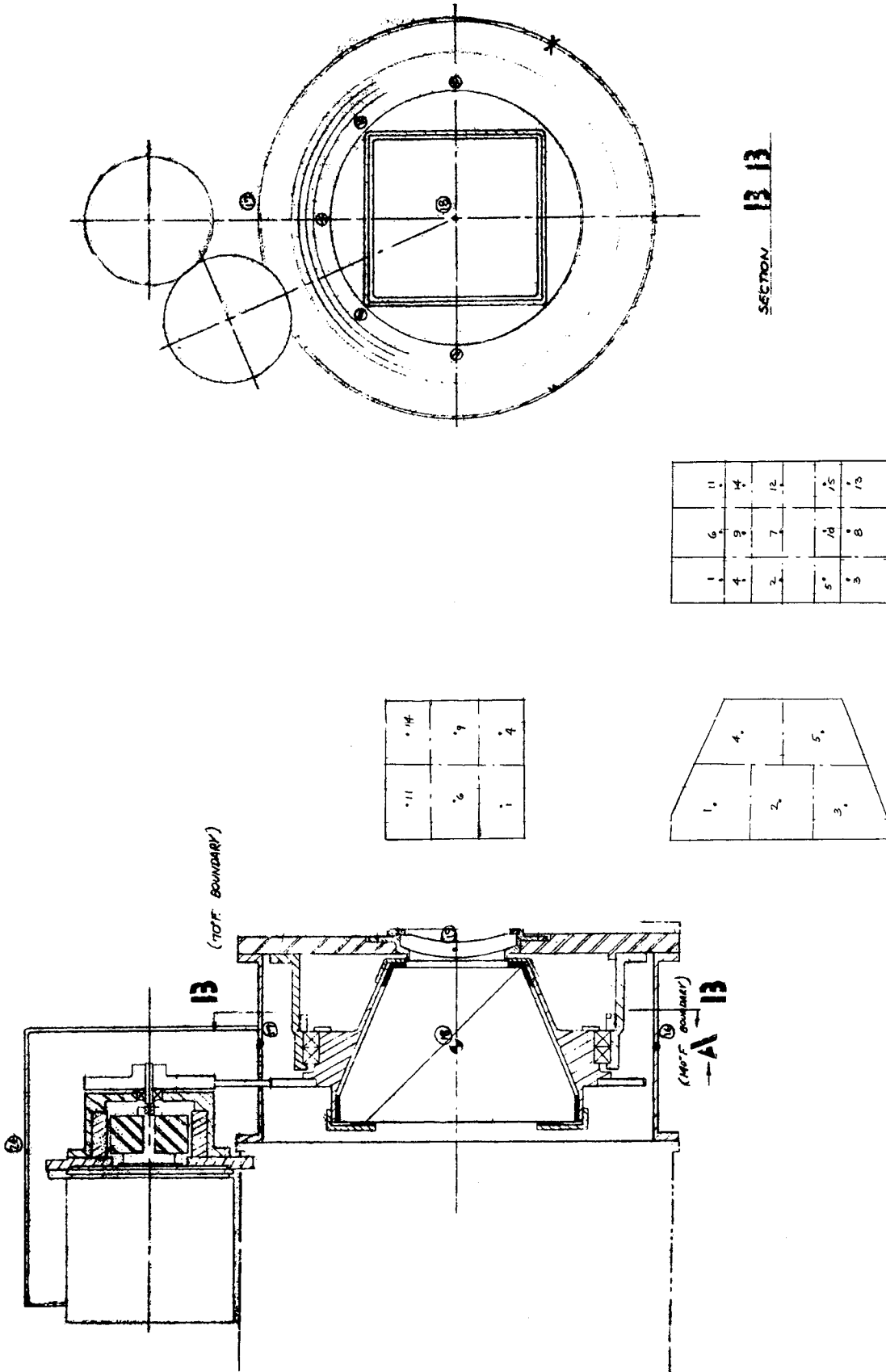
Figure 2.4-25. Node Designations for Pechan and Structure

2-271

~~SECRET~~ **SPECIAL HANDLING**

TABLE 2.4-9. TEMPERATURE DISTRIBUTION IN ELBOW REGION

NODE	DESIGNATION	CASE 1	CASE 2
1	Tube	100.0	100.5
2		96.2	96.7
3		99.1	99.6
4		99.3	99.8
5	Elbow	98.7	99.2
6		97.4	98.6
7		97.4	98.6
8		95.8	97.0
9	Zoom Structure	99.9	98.8
10	Elbow	98.4	96.8
11		96.0	96.8
12		98.1	98.5
13		95.0	97.3
14	Low Power Elements	97.4	98.2
15	Fold Mirror	96.6	97.6
16	Pechan Structure	98.5	98.6
17		97.6	97.7
18	Pechan	98.3	98.1
19	Field Flattener	98.6	98.2
21	Zoom Element	98.4	97.8
22	Pechan Drive	97.6	97.7
23	Zoom Elements	98.6	98.0
24	Cover	81.4	81.3
25	Mirror Cover	97.2	97.7
26		98.0	98.4

~~SECRET~~ **SPECIAL HANDLING**

~~SECRET~~ **SPECIAL HANDLING**

TABLE 2.4-10. TEMPERATURE DISTRIBUTION IN PECHAN PRISM

PECHAN PRISM		FIELD FLATTENER	
NODE NO.	TEMPERATURE (^{O}F)	NODE NO.	TEMPERATURE (^{O}F)
1	98.65	21	98.55
2	98.65	22	98.47
3		23	98.40
4	98.64	24	98.55
5	98.65	25	98.47
6		26	98.41
7			
8			
9	98.64		
10	98.65		
11			
12			
13			
14			
15			

2.4.2.5 <u>Conclusions</u>

The analysis completed to date has indicated no serious optical distortion resulting from temperature gradients imposed on the various optical elements.

2.4.2.6 <u>Additional Analysis Required</u>

Following is a summary of work remaining to be completed:

a.   Couple models of individual sections together to evaluate total system.

b.   Evaluate transient effects

c.   Examine gradients in all of the critical elements.

2.4.3 THERMAL DEVELOPMENT TEST PLANS

2.4.3.1 General

Optical system characteristics can be superimposed on one another. For this reason, the acquisition optics testing will be done on two distinct component assemblies. The optical system can be divided into two distinct zones: the portion of the system external to the pressure shell and that portion of the system internal to the pressure shell, with the window being common to both regions. Testing, consequently, will be done in two distinct phases: The development model of the tracking mirror, fixed fold assembly, and window will be mounted in a simulated shroud and subjected to a simulated space environment; a development model of the telescope assembly will likewise be tested, subjected to a simulated environment representative of the interior of the pressure shell.

2.4.3.2 Externally Mounted Equipment

A. Environmental Simulation

B. Earth and Albedo and Simulation – No precise techniques for the simulation of the combined effects of albedo and Earth emission. Several schemes have been investigated for potential means to provide a simulated environment. These are listed below along with a brief description of some of their inherent advantages and disadvantages.

    a. High-Pressure Xenon Arc Lamp

       Advantages: Best source of those considered for solar simulation.

       1. Poor spectral match. High proportion of energy emitted in narrow wavelength band $(0.8-1\mu)$.

       2. This type of lamp currently not adaptable to use in a vacuum chamber.

b. Iodine Quartzline Lamp

Advantages:

1. Provides closest approximation to the combined spectrum of earth emission and albedo flux.

2. Rapid response time; can be cycled to represent variations in incident irradiation.

3. This type of lamp has seen considerable vacuum service.

4. Simple controls.

5. Lower operating pressure – 1–2 atmospheres compared to 20 atmospheres for Xenon lamp.

Disadvantages:

1. Difficult to achieve uniform flux; array has to be folded in order to give proper field of view between the several optical surfaces and the simulated earth.

2. Relatively high cost compared to I/R heater panel.

c. I/R Heater Panel

Advantages:

1. Relatively inexpensive

2. Requires no elaborate calibration

Disadvantages:

1. Poor overall spectrum match

2. Relatively slow response time

Figure 2.4–26 shows the mean spectral distribution of albedo radiation. Plotted on the same figure is the spectral distribution of a 3250°K black body characteristic of the effective color temperature of the iodine quartzline lamp at full power. The latter

~~SECRET~~ **SPECIAL HANDLING**
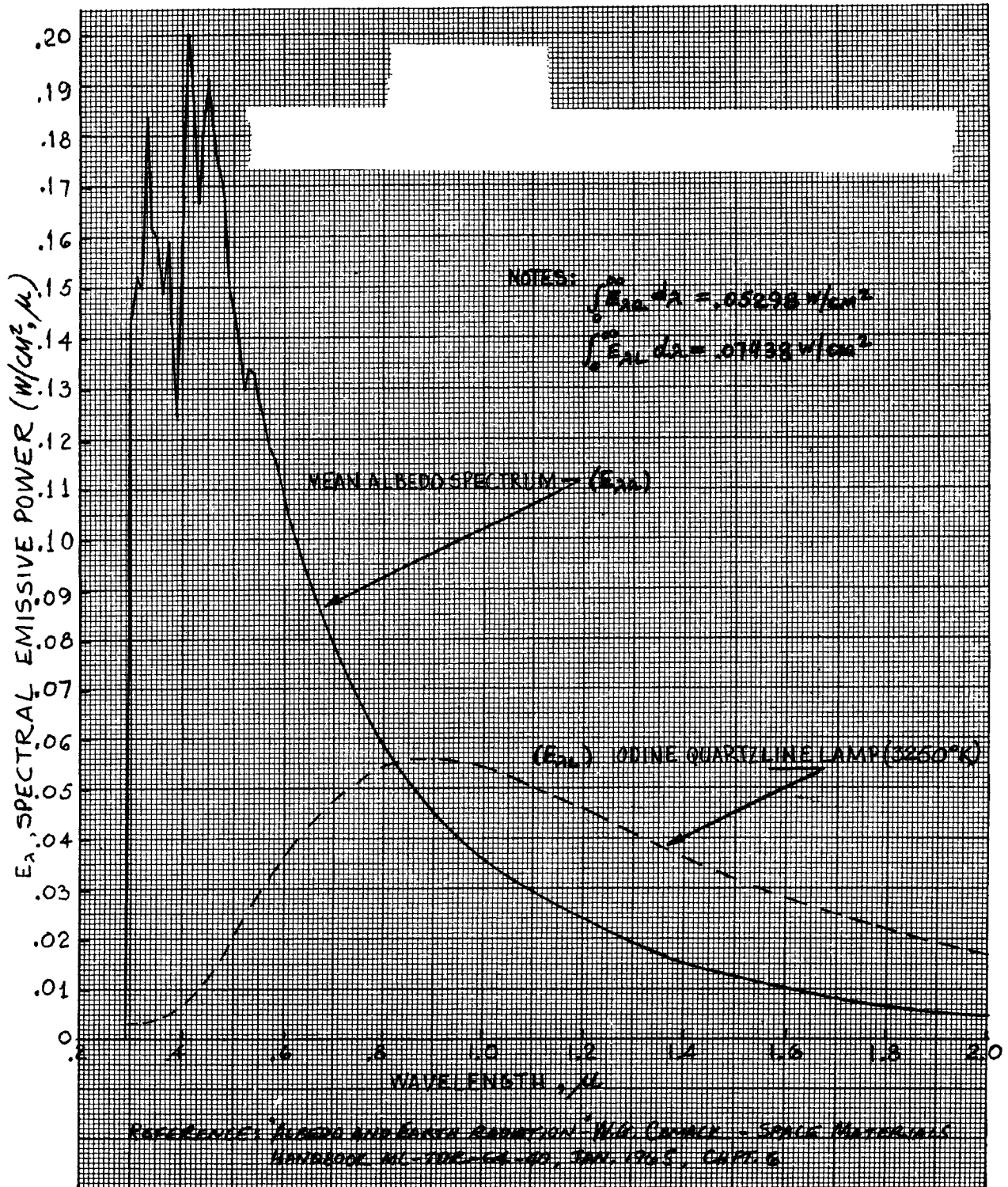
Figure 2.4-26.   Mean Spectral Distribution of Albedo Radiation

~~SECRET~~ **SPECIAL HANDLING**

curve has been normalized such that the integrated value gives an emissive power equal to the combined emissive power of the earth emission plus albedo. Figure 2.4-27 gives a plot of the spectral distribution of the approximate earth emission. The effective absorptance for an aluminized surface typical of the tracking mirror front surface and for a thermodynamically black surface (typical of the remainder of the enclosed system) for several energy sources is tabulated below:

As is evident from Table 2.4-11, there is a very significant difference in the effective absorptance of an aluminized surface from an I/R source as compared with the actual combined earth and albedo flux. The present test scheme calls for the use of an array of iodine quartzline heaters to provide a simulated earth and albedo. Solar, molecular heating and ascent effects can be acceptably simulated by affixing a series of thin heater blankets to the remaining surfaces of the on-orbit shroud.

C. <u>Pressure and Temperature Simulation</u> – The Itek vacuum chamber facility in which these tests will be conducted is capable of providing a vacuum of 1×10^{-5} mmHg, a pressure more than adequate to represent the vacuum of outer space. Temperature simulation of outer space is accomplished by means of a LN_2 cooled inner shroud.

D. <u>Transient Testing</u> – A series of tests will be run under the condition of a simulated environment. There are three major tests planned:

    a.   <u>Static Thermal Test</u> – This test would be for the express purpose of measuring temperature patterns within the external system for a non-operational mode under simulated orbital heat fluxes.

    b.   <u>Optical Test</u> – This test would be a purely optical test in which interferometric measurements would be made on the external optical assembly.

    c.   <u>Operational Test</u> – This test would be used to generate data on power consumption, tracking stability of the tracking mirror.

Various orbital parameters will be varied along with investigating viewing periods of varying duration.

2-278

~~SECRET~~ SPECIAL HANDLING

Figure Deleted

Figure 2.4-27. Approximate Spectral Distribution of Earth Radiation

TABLE 2.4-11. COMPARISON OF CHARACTERISTICS OF DIFFERENT
EARTH AND ALBEDO EMISSION SOURCES

SOURCE	EFFECTIVE ABSORPTANCE	
	ALUMINIZED SURFACE	BLACK PAINT
Actual Albedo plus Earth	0.106	0.95
Solar Flux	0.153	0.95
Earth Flux	0.131	0.96
Iodine Quartzline Lamp	0.093	0.94
I/R Source	0.049	0.96
Xenon Arc Lamp	0.186	0.95

E. Steady State Soak Tests – The external assembly will be maintained at various uniform temperature levels in the range of 0-100°F. Interferometric measurements will be made to determine the distortions resulting from the system operating over this wide range of temperatures.

2.4.3.3 Internal Mounted Equipment

A. Simulation of Zero-Gravity Effects – The absence of a gravitational field eliminates one very major heat transfer mode; viz, natural convection. Any accurate thermal testing of the telescope must correct for the presence of natural convection effects. Two concepts have been explored to simulate a zero-gravity field:

a. Wrap the exterior surface of the telescope with a lightweight foam.

b. Test the telescope assembly in a reduced-pressure atmosphere (≈ 2.5 cmHg.)

These techniques will be discussed further in order:

B. <u>Foam Enclosure</u> - Low density freon-blown polyurethane foams are available having thermal conductivity comparable to either the O_2 or O_2/He atmospheres previously described. These foams would simulate the conductance of the actual gaseous environment. The major disadvantages of foams are two: (a) eliminates radiation coupling between elements internal to telescope and externally between the tube and the simulated environment; (b) will not simulate the transient characteristics of either the O_2 or He/O_2 atmospheres.

C. <u>Reduced Pressure Testing</u> - At Grashof numbers ≤ 2000, convection is suppressed in an enclosed gas space. At 2.5 cmHg pressure, thermal conductivity of the enclosing gaseous atmosphere is reduced by 5-7% from that at atmospheric pressure. For a test condition at atmospheric pressure, the temperature differential measured on the telescope tube could be as much as 25% lower than that compared with a zero-gravity O_2/He atmosphere and upwards of 47% lower than that predicted for a zero-gravity O_2 atmosphere. This very obviously establishes the need for this kind of testing.

D. <u>Individual Element Testing</u> - Individual elements will be tested while subject to a simulated environment. These elements will be selected on the basis of analysis having shown these elements to be potential problem areas.

E. <u>Telescope Assembly Vacuum Testing</u> - A model of the telescope assembly will be tested in a simulated environment in a vacuum chamber maintained at reduced pressure to determine temperature gradients in the various optical elements. A series of heaters will be mounted on a framework enclosing the telescope to program the expected temperature behavior of the telescope environment.

2.5 ATS STRUCTURES ANALYSIS

The following section of this report shows the structural analysis performed by GE on the ATS portion of the acquisition subsystem. The purpose of the analysis was to verify the structural integrity of the subcontractor's design. The analysis indicates that the subcontractor's design is adequate from the structural standpoint. It also indicates that the subcontractor's design is not optimized thus making a saving in weight probable. It should be stated again that all the structural analysis shown in the report was performed by GE using subcontractor drawings as a basis. The report also determines the possible system misalignments due to factors such as 1g load relief and mechanical joint slippage. A discussion is also included on the area of dynamic analysis. The complete system dynamic analysis planned by GE with subcontractor assistance is discussed in detail. The status of the subcontractor's weight is also discussed in detail.

The ATS structures analysis section is broken down into the following subsections:

2.5.1   Structural Analysis of Telescope Under Powered Flight Loads

2.5.2   Structural Analysis of Tracking Pedestal Under Powered Flight Loads

2.5.3   Structural Analysis of the Protective Shroud Under Powered Flight Loads and On-Orbit Operating Loads

2.5.4   Deflection Analysis of Telescope and Tracking Pedestal Due to 1G Load Relief

2.5.5   Determination of Optical Path Misalignments Due to Mechanical Joint Slippage

2.5.6   Determination of Misalignments Due to Shell Pressurization and "Hot-Dogging"

2.5.7   Dynamic Analysis and Loads Determination

2.5.8   ATS Weight Analysis

2.5.1 STRUCTURAL ANALYSIS OF THE TELESCOPE UNDER POWERED FLIGHT LOADS

Introduction

The structural analysis of the telescope which follows is intended to verify the basic structural integrity of the design and to determine the validity of the subcontractor's weight estimate by determining the degree of optimization of the telescope structure. Also, recommendations will be made concerning areas and methods of potential weight reductions.

Conclusions

The analysis indicates that the subcontractor's structure is able to withstand the loads due to powered flight accelerations with an adequate margin of safety. It also shows that the structure is over-designed, thus indicating the possibility of a reduction in structural weight.

Description of Structure

The telescope structure is a tubular structure made of aluminum. In the analysis, beryllium was considered for certain portions of the structure. The purpose of this was to demonstrate the feasibility of using beryllium in the structure. The walls of the tubular portion of the telescope (between shear fitting and penetration fitting) are currently 0.040-inch thick. The elbow which has to carry the weight of the Pechan prism and the zoom/eye piece by a combined bending and torsion is made of aluminum and has a heavier gage wall. This is necessitated by higher loading. The structural housing for the Pechan prism and the zoom/eye piece are also of a heavier gage wall. This is necessitated by high local loads primarily due to drives. The structure is mounted to the Lab Module pressure shell at two places. The objective end of the telescope is mounted to the DACO shell penetration fitting. This joint was originally planned to be designed so that there would be no capability of transmitting a torque. This concept is reflected in the analysis. A torque transmitting joint is currently being studied. Such a joint would allow a better seal and may be easier to fabricate. The other joint is the shear-tie between the telescope shell and the vehicle shell. This joint is located at the field joint between the elbow and the constant diameter portion of the

telescope. The shear-tie is so designed that it will carry loads due to telescope twisting and also vehicle longitudinal (X direction) loads. The shear-tie is designed to transmit a minimum amount of load in the telescope logitudinal direction. This was also reflected in the analysis.

BY MJP
CK.
DATE 6-14-67 REV.

SPECIAL SUB-SYSTEM TELESCOPE PRELIMINARY STRESS ANALYSI

THE FOLLOWING IS A PRELIMINARY STRESS ANALYSIS OF THE
SPECIAL SUB-SYSTEM TELESCOPE. THE ANALYSIS IS INTENDED
TO DETERMINE WHETHER THE SUBCONTRACTORS DESIGN IS
OPTIMIZED AND IF NOT TO RECOMMEND AREAS THAT CAN
BE OPTIMIZED FROM THE STRESS STANDPOINT, THUSLY
ALLOWING FOR DECREASES IN SUB-SYSTEM WEIGHT.

THE SPECIAL SUB-SYSTEM TELESCOPE IS A TUBULAR STRUCTURE
THAT IS MOUNTED TO THE VEHICLE SHELL AT TWO POINTS.
THIS IS SHOWN IN THE FOLLOWING SKETCH:

MOUNTING POINT - "B"

MOUTING POINT "A"
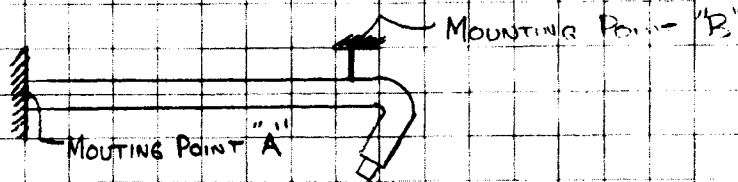
NOTE: MOUNT "A" IS NOT DESIGNED TO CARRY A TORSION LOAD.

THE LOAD FACTORS USED IN THIS ANALYSIS WILL BE THE SAME AS THE
STEADY-STATE ACCELERATIONS WHICH WERE GIVEN TO THE SUB-CONTRACTOR
FOR DESIGN PURPOSES (REF: PIR 7223-278). THESE LOAD FACTORS
WERE OBTAINED FROM THE "MARTIN 2ND LOAD CYCLE" MODIFIED
TO SHOW TRENDS FROM THE 3A LOAD CYCLE. THE FOLLOWING ARE
THE DESIGN LOAD FACTORS:

	X DIRECTION (g's)	Y DIRECTION (g's)	Z DIRECTION (g's)
MAX. X LOAD	± 10.0	± 0.72	± 0.72
MAX. Y LOAD	+3.0 / -1.0	± 1.8	± 0.72
MAX. Z LOAD	+3.0	± 0.72	± 1.8

FORM 1-8136 B (9-58)

NRO APPROVED FOR
RELEASE 1 JULY 2015

SECRET SPECIAL HANDLING

GENERAL ● ELECTRIC

PAGE 2 OF 19
MODEL
REPORT

BY *MJP*

CK.

DATE 6-14-67 REV.

THE LOADS GIVEN ARE LIMIT LOADS. IN ORDER TO OBTAIN
ULTIMATE LOADS USE THE FOLLOWING RELATION: (ULT = 1.4 × LIMIT)

THE SIGN CONVENTION IS SHOWN IN THE FOLLOWING SKETCH:

20°

THE +X AXIS PETS INTO THE PAPER

+Y

+Z
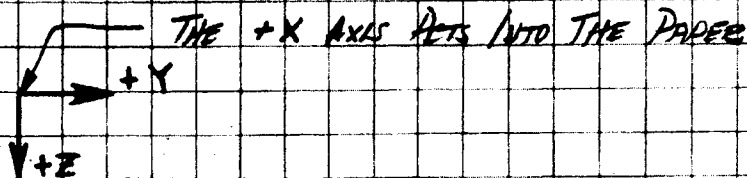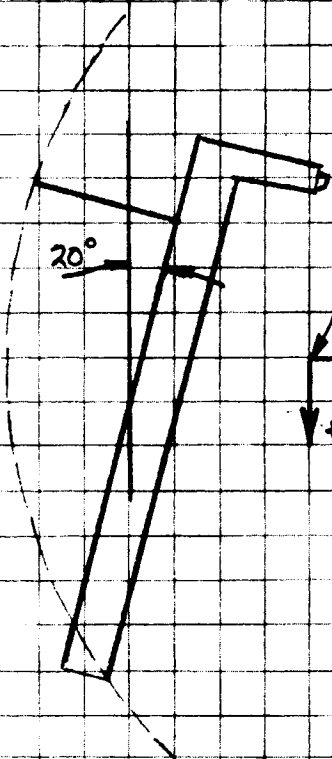
THE TELESCOPE WILL BE ANALYZED USING
THE "MASS" PROGRAM (MECHANICAL ANALYSIS
OF SPACE STRUCTURE) ON THE IBM 7094
COMPUTER. THE STRUCTURE HAS TO BE
MODELED FOR ADAPTATION TO THE
PROGRAM. THE FOLLOWING SHOWS THE
ACTUAL TELESCOPE CONFIGURATION AND
THE JOINTS USED IN THE MODEL.
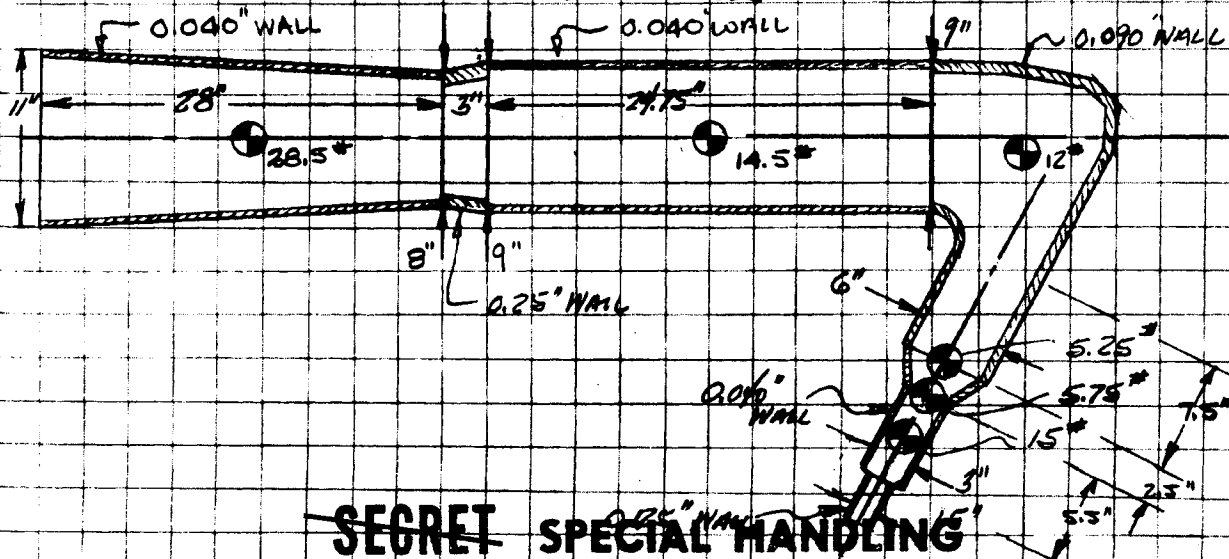
0.040" WALL   0.040" WALL   9"   ~0.090" WALL

11"   28"   3"   24.75"

28.5#   14.5#   12#

8"   9"

0.25" WALL

6"

0.040"
WALL   5.25#

5.75#   1.5"

15#

3"   2.5"

5.3"

FORM 1-6136 B (9-58)

2-288

BY MJP

CK.

DATE 6-15-67 REV.

MODEL

REPORT

THE COMPUTER MODEL WILL BE THE FOLLOWING:

REF. JT. 8001

REF. JT. 8002

12.0 #

14.5 #

28.5 #

5.25 #

5.75 #

15.0 #

40

2" SPACING BETWEEN POINTS

3" SPACING BETWEEN POINTS EXCEPT 1" BETWEEN 26-27 & 3/4" BETWEEN 27-28 AND 29-30

3"
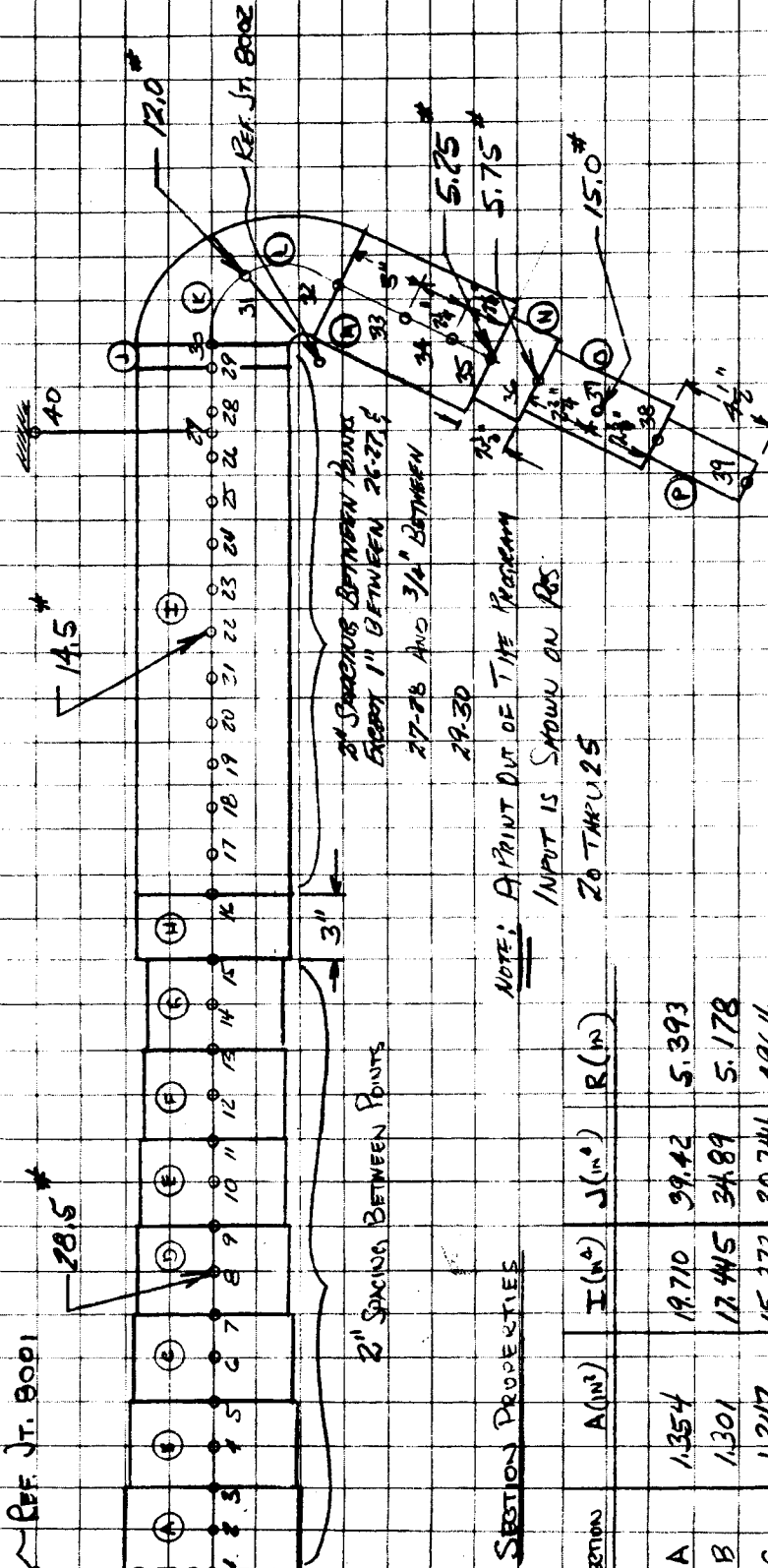
NOTE: A PRINT OUT OF THE PROGRAM INPUT IS SHOWN ON PGS 26 THRU 25

NOTE: JT. 1 WAS NOT GIVEN THE CAPABILITY TO CARRY A TORQUE THUSLY SIMULATING THE ACTUAL SITUATION

SECTION PROPERTIES

SECTION	A(in²)	I(in⁴)	J(in⁴)	R(in)
A	1.354	18.710	39.42	5.393
B	1.301	17.445	34.89	5.178
C	1.247	15.372	30.744	4.964
D	1.194	13.458	26.916	4.749
E	1.140	11.721	23.442	4.535
F	1.087	10.138	20.276	4.321
G	1.030	8.705	17.140	4.107
H	0.975	6.0916	1.91.53	4.25
I	1.131	11.4451	22.702	4.5

BY MJP	PAGE 4 OF 19
CK.	MODEL
DATE 6-15-67 REV.	REPORT

SECTION PROPERTIES (CONT.)

SECTION	A (in²)	I (in⁴)	J (in⁴)	R (in)
J	2.545	25.764	51.528	4.5
K	2.332	21.281	42.562	4.125
L	1.908	12.166	24.332	3.375
M	1.696	7.634	15.268	3.0
N	1.272	4.294	8.588	2.25
O	0.377	0.424	0.848	1.5
P	0.785	0.393	0.786	0.75

THE FOLLOWING ARE THE LOADS THAT WERE USED IN THE ANALYSIS:

JOINT NO.	F_x	F_y	F_z
	$(F_x = W \times 10 G\text{'s})$	$(F_y = W \times \sqrt{0.77^2 + 0.12^2})$	$(F_z = W \times \sqrt{0.72^2 + 0.2^2})$
8	285#	29.0#	29.0#
22	145#	15.0#	45.0#
31	120#	12.0#	12.0#
35	52.5#	5.5#	5.5#
36	57.5#	6.0#	6.0#
37	150.0#	15.0#	15.0#

THE TABLE ON THE FOLLOWING PAGE GIVES THE INTERNAL
LOADS (FORCES & MOMENTS) AT EACH POINT IN THE STRUCTURE
CONSIDERED ON PG. 3. THE INTERNAL LOADS CAN THEN BE
USED TO DETERMINE THE STRESSES.

THE INTERNAL LOADS ARE IN A NORMALIZED SIGN
CONVENTION. THIS CONVENTION IS SHOWN IN THE FOLLOWING
SKETCH.

BY				PAGE 5 OF 19
CK.		GENERAL ⚛ ELECTRIC		MODEL
DATE 6-15-67 REV.				REPORT

~ Ref. Jt. 8091
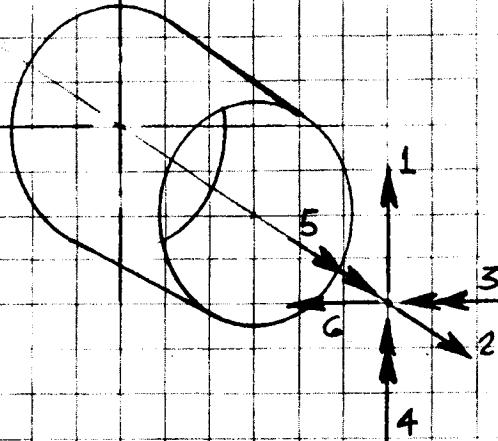
Note: Loads were obtained from computer program print-out

The internal loads will be:

Jt. No.	F_1 (#)	F_2 (#)	M_3 (in-#)	M_4 (in-#)	M_5 (in-#)	F_6 (#)
1	-13.122	82.474	28.840	2864.1	0.0	260.4
2	-13.122	82.474	2.5959	2343.3	0.0	260.4
3	-13.122	82.474	-23.648	1822.5	0.0	260.4
4	-13.122	82.474	-49.893	1301.8	0.0	260.39
5	-13.122	82.474	-76.137	780.97	0.0	260.4
6	-13.122	82.474	-102.38	260.18	0.0	260.39
7	-13.122	82.474	-128.63	-260.61	0.0	260.39
8	15.878	53.474	-154.87	-781.39	0.0	-24.605
9	15.878	53.474	-123.11	-732.17	0.0	-24.609
10	15.878	53.474	-91.358	-682.94	0.0	-24.609
11	15.878	53.474	-59.602	-633.71	0.0	-24.613
12	15.878	53.474	-27.846	-584.48	0.0	-24.613
13	15.878	53.474	3.9099	-535.25	0.0	-24.609
14	15.878	53.474	35.665	-486.02	0.0	-24.615
15	15.877	53.474	67.419	-436.77	0.0	-24.621
16	15.877	53.474	115.05	-362.91	0.0	-24.625
17	15.876	53.474	146.80	-313.65	0.0	-24.627
18	15.876	53.474	178.56	-264.38	0.0	-24.627
	15.876	53.474	210.31	215.13	0.0	-24.623

SECRET SPECIAL HANDLING

BY *MJP*

CK.

DATE 6-15-67 REV.

GENERAL ● ELECTRIC

INTERNAL LOADS (CONT.)

Jt. No	F₁	F₂	M₃	M₄	M₅	F₆
20	15.876	53.474	242.06	-165.87	0.0	-24.631
21	15.875	53.474	273.81	-116.60	0.0	-24.629
22	30.876	38.474	305.56	-67.334	0.0	-169.62
23	30.875	38.474	367.31	271.93	0.0	-169.62
24	30.875	38.474	429.06	611.19	0.0	-169.62
25	30.875	38.474	490.81	950.46	0.0	-169.63
26	30.875	38.474	552.56	1289.7	0.0	-169.64
27	-38.498	38.505	383.39	1459.4	-4292.6	380.09
28	-38.445	38.505	544.89	1079.4	-4292.6	380.05
29	-38.505	38.505	467.90	319.30	-4292.6	380.11
30	38.498	38.505	-439.03	-34.249	-4292.6	-380.04
31	36.159	-9.8563	-226.89	-2419.0	-3868.9	-260.04
32	9.7167	-36.197	-120.87	-2796.2	123.04	-260.04
33	9.7158	-36.197	-91.707	-2015.7	123.04	-260.06
34	9.3052	-36.305	-69.838	-1428.8	139.20	-260.07
35	7.6870	-28.687	-49.291	-856.08	129.80	-207.52
36	12.483	-17.152	-30.077	-361.42	0.0	-150.01
37	12.483	17.152	0.0	0.0	0.0	-150.0
38	0.0	0.0	0.0	0.0	0.0	0.0
39	0.0	0.0	0.0	0.0	0.0	0.0

THE FOLLOWING MATERIALS WERE USED IN THE ANALYSIS

MEMBERS 1-2 THRU 28-29 : BERYLLIUM $\begin{cases} E = 42 \times 10^6 \text{ PSI} \\ G = 20 \times 10^6 \text{ PSI} \end{cases}$

MEMBERS 29-30 THRU 32-33 : ALUMINUM $\begin{cases} E = 10 \times 10^6 \text{ PSI} \\ G = 4 \times 10^6 \text{ PSI} \end{cases}$

MEMBERS 33-34 THRU 38-39 : BERYLLIUM $\begin{cases} E = 42 \times 10^6 \text{ PSI} \\ G = 20 \times 10^6 \text{ PSI} \end{cases}$

MEMBER 27- SECRET BERYLLIUM $\begin{cases} E = 42 \times 10^6 \text{ PSI} \end{cases}$

SECRET SPECIAL HANDLING

NRO APPROVED FOR
RELEASE 1 JULY 2015

~SECRET~ SPECIAL HANDLING
GENERAL ● ELECTRIC

PAGE 7 OF 19
MODEL
REPORT

BY MJP
CK.
DATE 6-15-67 REV.

THE BENDING MOMENT DIAGRAMS ARE SHOWN ON PGS. 8 & 9.

THE STRESSES WILL NOW BE CALCULATED:

THE BENDING STRESS @ JT. 1

$$M_3 = 28.84 \text{ IN-\#}$$
$$M_4 = 2864.1 \text{ IN-\#}$$

$$Z_1 = (19.710/5.393) = 3.65 \text{ IN}^3$$

$$\therefore \quad \sigma = \frac{28.84}{3.65} + \frac{2864.1}{3.65} = 8.0 + 785.0 = 793 \text{ PSI}$$

THE MATERIAL IS BERYLLIUM HOT-PRESSED BLOCK WITH THE
FOLLOWING PROPERTIES:

REF: MIL-HDBK-5A
TABLE 9.2.1.1
MARL: AMS 7901 Be (2% BeO MAX)

$$F_{ty} = 27000 \text{ PSI}$$
$$F_{tu} = 40000 \text{ PSI}$$
$$F_{su} = 33000 \text{ PSI}$$

THE DIRECT TENSILE STRESS WILL BE:

$$\sigma = 82.474/1.354 = 61 \text{ PSI}$$

$$\therefore \quad \sigma_{COMB} = 793 + 61 = 854 \text{ PSI (LIMIT)}$$

$$M.S = \frac{27000}{854} - 1 = + \text{ LARGE (LIMIT)}$$

THE SHEAR STRESSES WILL BE:
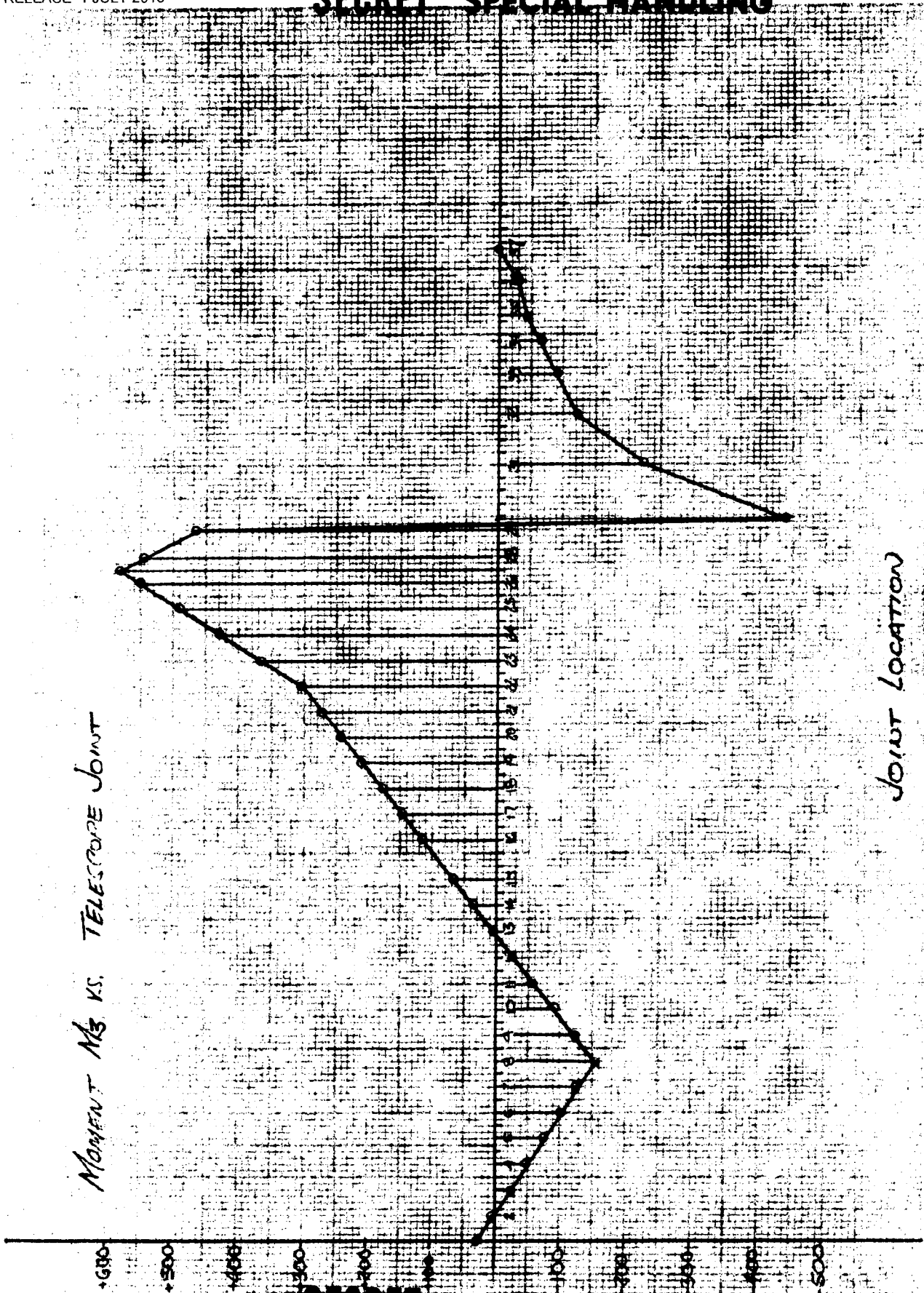
MOMENT M3 VS. TELESCOPE JOINT

JOINT LOCATION

MOMENT M_4 VS. TELESCOPE JOINT

JOINT LOCATION

2-295

NRO APPROVED FOR
RELEASE 1 JULY 2015
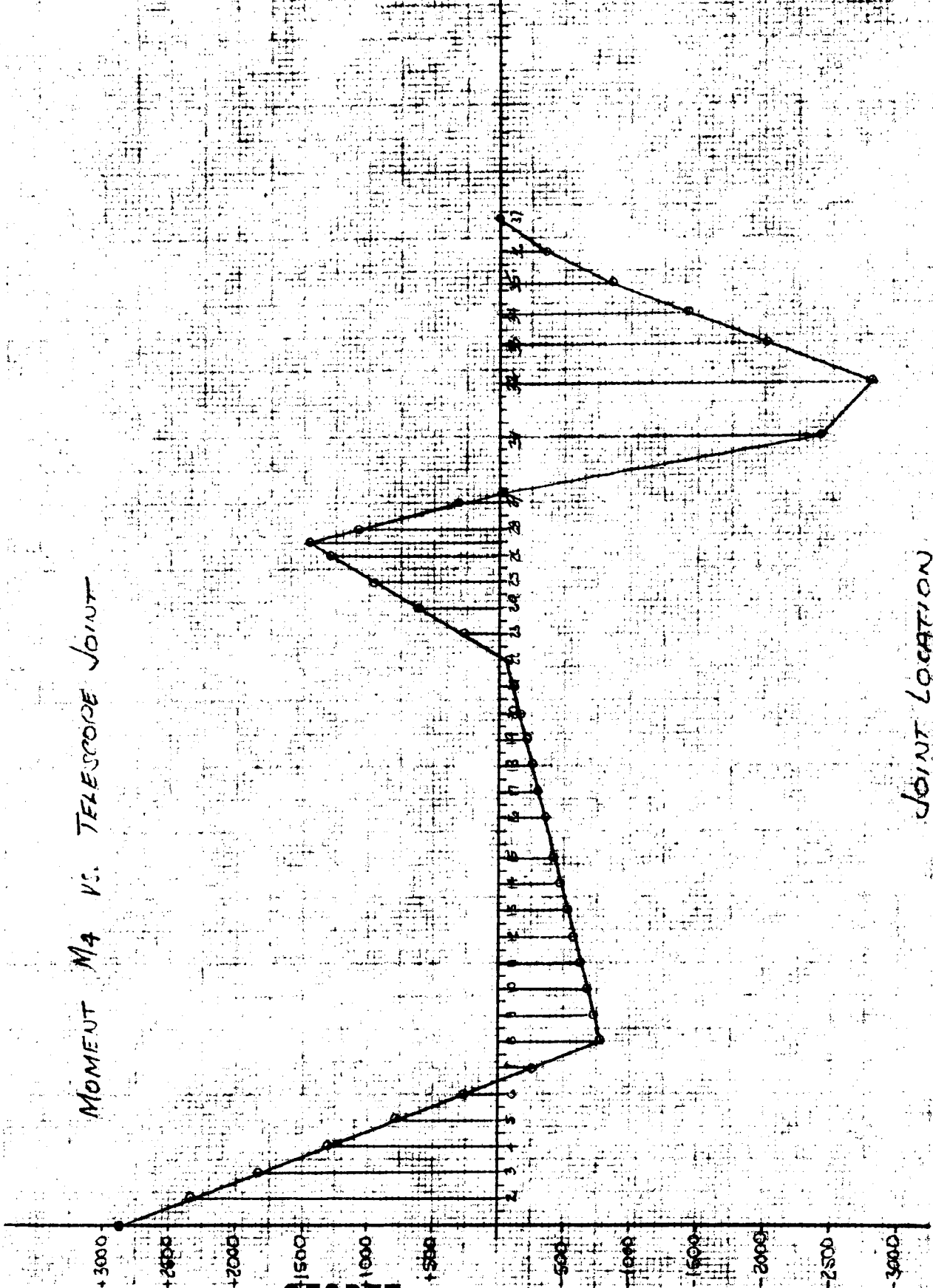
BY MJP

CK.

DATE 6-15-67 REV.

SECRET SPECIAL HANDLING
GENERAL ELECTRIC

PAGE 10 OF 19

MODEL

REPORT

$$Q = \Sigma A \bar{y}$$

$$\text{WHERE}: \quad \bar{y} = \frac{0.424(R_0^3 - R_1^3)}{(R_0^2 - R_1^2)} = \frac{(0.424)(5.393^3 - 5.353^3)}{(5.393^2 - 5.353^2)}$$

$$\bar{y} = \frac{0.424(3.46)}{(0.430)} = 3.412 \text{ in.}$$

$$Q = \Sigma A \bar{y} = \frac{1.354(3.412)}{2.0} = 2.305 \text{ in}^3$$

$$\tau = \frac{VQ}{I b} = \frac{(260.4)(2.305)}{(19.710)(0.046)} + \frac{(13.122)(2.305)}{(19.710)(0.040)}$$

$$\tau = 760 + 40 = 800 \text{ PSI. (LIMIT)}$$
$$\tau = 1.4 \times 800 \text{ PSI} = 1120 \text{ PSI (ULT)}$$

$$M.S. = \frac{33000}{1120} - 1 = + \text{LARGE (ULT)}$$

THE STRESSES @ STA. 27 WILL NOW BE CALCULATED:

THE BENDING MOMENTS ARE: $M_3 = 583.39$ IN-#
$$M_4 = 1459.4 \text{ IN-#}$$

$$Z_{cr} = 11.451/4.5 = 2.545 \text{ in}^3$$

$$\sigma_b = \frac{583.39}{2.545} + \frac{1459.4}{2.545} = 230 + 574 = 804 \text{ PSI}$$

THE DIRECT TENSILE STRESS IS:

$$\sigma = 38.498/1.131 = 34 \text{ PSI}$$

BY *MJP*	SPECIAL HANDLING	PAGE *11 OF 19*
CK.	GENERAL ● ELECTRIC	MODEL
DATE *6-15-67* REV.		REPORT

$\therefore \ \sigma_{COMBINED} = 804 + 34 = 838 \ PSI$

DETERMINE SHEAR DUE TO TORSION:

$T = 4292.6 \ IN\text{-}\#$

$\tau = \dfrac{Tr}{J} = \dfrac{(4292.6)(4.5)}{22.902} = 844 \ PSI$

COMBINING BENDING & TORSIONAL SHEAR BY MOHR'S CIRCLE:

$\sigma_N = 419 + \sqrt{419^2 + 844^2} = 419 + \sqrt{175500 + 711000}$

$\sigma_N = 419 + 940 = 1359 \ PSI. \ (LIMIT)$

$M.S. = \dfrac{27000}{1359} - 1 = + LARGE \ (LIMIT)$

THE VERTICAL SHEAR WILL BE:

$V_1 = 38.505^{\#} \ \& \ V_6 = 380.09^{\#}$

$Q = \Sigma A \bar{y} \quad WHERE: \ \bar{y} = 0.424 \dfrac{(R_0^3 - R_1^3)}{(R_0^2 - R_1^2)}$

$\bar{y} = \dfrac{0.424 (4.5^3 - 4.46^3)}{4.5^2 - 4.46^2}$

$\bar{y} = \dfrac{(0.424)(2.407)}{(0.358)} = 2.850 \ IN.$

$Q = \Sigma A \bar{y} = 0.565 (2.850) = 1.610$

$\tau = \dfrac{VQ}{Ib} = \dfrac{(38.505)(1.610)}{(1.451)(0.040)} + \dfrac{(380.09)(1.610)}{(1.451)(0.040)}$

$\tau = 1350 + 1340.0 = 1475.0 \ PSI.$

BY MJP

CK.

DATE 6-15-67 REV.

MODEL

REPORT

COMBINING SHEAR STRESSES :

$$\tau = 844 + 1475.0 = 2319 \text{ PSI.} \quad (\text{LIMIT})$$
$$\tau = 1.4 (2319) = 3240 \text{ PSI} \quad (\text{ULT})$$

$$M.S. = \frac{32000}{3240} - 1 = + \text{LARGE} \quad (\text{ULT})$$

CHECK STRESSES @ JT. 32

THE BENDING MOMENTS ARE : $M_3 = 120.87$
$M_4 = 2796.2$

$$Z_{32} = 7.634/3.0 = 2.545$$

$$\sigma_b = \frac{120.87}{2.545} + \frac{2796.2}{2.545} = 48 + 1100 = 1148 \text{ PSI}$$

THE AXIAL STRESS IS :

$$\sigma = \frac{36.197}{1.696} = 21 \text{ PSI.}$$

$$\therefore \quad \sigma_{COMBINED} = 1148 + 21 = 1169 \text{ PSI}$$

THE SHEAR DUE TO TORSION WILL BE :

$$\tau = \frac{Tr}{J} = \frac{(123.04)(3.0)}{15.268} = 24 \text{ PSI}$$

THE COMBINED STRESS WILL BE SLIGHTLY GREATER THAN
THE COMBINED BENDING & TENSION.

$$M.S. = \frac{27000}{1169} - 1 = + \text{LARGE} \quad (\text{LIMIT})$$

SECRET SPECIAL HANDLING

GENERAL ⊕ ELECTRIC

BY MJP

CK.

DATE G15-67 REV.

PAGE 13 OF 19

MODEL

REPORT

THE SHEAR STRESSES WILL BE:

$$Q = \Sigma A \bar{y} \qquad WHERE: \quad \bar{y} = 0.424 \frac{(R_0^3 - R_i^3)}{(R_0^2 - R_i^2)}$$

$$\bar{y} = 0.424 \frac{(3.0^3 - 2.91^3)}{(3.0^2 - 2.91^2)}$$

$$\bar{y} = 0.424 \left(\frac{2.358}{0.532}\right) = 1.879 \text{ IN.}$$

$$Q = \Sigma A y = 0.848(1.879) = 1.590 \text{ IN}^3$$

$$\tau = \frac{VQ}{Ib} = \frac{(9.7167)(1.590)}{(7.634)(0.090)} + \frac{(260.04)(1.590)}{(7.634)(0.090)}$$

$$\tau = 23 + 602 = 625 \text{ PSI}$$

COMBINING WITH TORSIONAL SHEAR:

$$\tau = 625 + 24 = 649 \text{ PSI (LIMIT)}$$
$$\tau = 1.4(649) = 910 \text{ PSI (ULT)}$$

$$M.S. = \frac{32000}{910} - 1 = + \text{LARGE (ULT)}$$

THE FOLLOWING TABLE SUMMARIZE THE STRESS DATA
OBTAINED:

JT. No.	COMBINED BENDING, TENSION & SHEAR	COMBINED SHEARS	MIN. M.S.
1	854 PSI	1120 PSI	+ LARGE (ULT)
27	1359 PSI	3240 PSI	+ LARGE (ULT)
32	1169 PSI	910 PSI	+ LARGE (LIMIT)

SECRET SPECIAL HANDLING

~~SECRET~~ SPECIAL HANDLING

GENERAL ● ELECTRIC

BY MJP	
CK.	MODEL
DATE 6-15-67 REV.	REPORT

CHECK SHEAR - TIE :

THE SHEAR-TIE USED IN THE ANALYSIS IS A FLAT-SHEET 0.125 IN THICK WITH THE FOLLOWING DIMENSIONS:

LOADS @ 40 END.

$M_{X-X} = 7591.3$ IN-#
$M_{YY} = 0.1315$ IN-#
$M_T = 549.78$ IN-#
$P_{AXIAL} = 69.372$
SHEARS ARE SMALL

$$I_{X-X} = \frac{0.125(14)^3}{12} = 28.6 \text{ IN}^4$$

$$Z_{X-X} = 28.6/7.0 = 4.086 \text{ IN}^3$$

$$I_{XY} = \frac{14(0.125)^3}{12} = 2.28 \times 10^{-3} \text{ IN}^4$$

$$Z_{XY} = \frac{2.28 \times 10^{-3}}{0.125} = 1.825 \times 10^{-2} \text{ IN}^3$$

$$A = 14(0.125) = 1.75 \text{ IN}^2$$

$$K = 0.333 (14)(0.125)^3$$
$$K = 10.6 \times 10^{-3} = 1.06 \times 10^{-2}$$

∴ COMBINED BENDING & TENSION :

$$f_{COMB} = \frac{7591.3}{4.086} + \frac{0.1315 \times 10^2}{1.825} + \frac{69.372}{1.75}$$

~~SECRET~~ SPECIAL HANDLING

FORM 1-8136 B (2-86)

2-300

BY MJP ~~SECRET~~ SPECIAL HANDLING

GENERAL ELECTRIC

CK.

DATE 6-15-67 REV.

$$\sigma_{comb} = 860 + 7 + 40 = 1907 \text{ PSI}$$

TORSIONAL SHEAR STRESS:

$$\tau = \frac{TZ}{K} = \frac{(549.78)(0.125) \times 10^{+2}}{1.06} = 6500 \text{ PSI}$$

COMBINED BENDING & TORSION:

$$\sigma_N = 954 + \sqrt{954^2 + 6500^2}$$

$$\sigma_N = 954 + 6560 = 7514 \text{ PSI}$$

$$M.S. = \frac{27000}{7514} - 1 = +2.6 \text{ (LIMIT)}$$

$$\tau = 6500 \text{ (LIMIT)}$$
$$\tau = 1.4 \times 6500 = 9100 \text{ PSI (ULT)}$$

$$M.S. = \frac{31000}{9100} - 1 = +2.5 \text{ (ULT)}$$

BY MJP	GENERAL ● ELECTRIC	PAGE 16 OF 19
CK.		MODEL
DATE 6-16-67 **REV.**		REPORT

THE TELESCOPE STRUCTURE WILL NOW BE CHECKED FOR CRIPPLING AND PRESSURE EFFECTS.

DETERMINE THE CRITICAL CRIPPLING PRESSURE FOR AN EXTERNAL PRESSURE (WINDOW RUPTURES IN ORBIT)

CONSIDER CASE 31 (PG. 318) FROM ROARK

$$P_{CRIT} = 0.807 \frac{Et^2}{Lr} \sqrt[4]{\left(\frac{1}{1-\nu^2}\right)^3 \left(\frac{t^2}{r^2}\right)}$$

CONSIDER THE PORTION BETWEEN THE VEHICLE SHELL AND THE SHEAR TIE.

$$\therefore \quad L = 52$$
$$r = 5.5$$
$$t = 0.04$$
$$E = 42 \times 10^6$$
$$\nu = 0.012$$

$$P_{CRIT} = \frac{(0.807)(42 \times 10^6)(0.04)^2}{(52)(5.5)} \sqrt[4]{(1)\frac{0.040^2}{5.5^2}}$$

$$P_{CRIT} = \frac{(190)(0.2)}{2.34} = 16.25 \text{ PSI}$$

THE PRESSURE IN THE LM ON ORBIT IS 5 PSI. THEREFORE P_{CRIT} IS FAR IN EXCESS OF THE ACTUAL PRESSURE.

CHECK STRESSES DUE TO A 5 PSI ΔP.

$$\sigma_{HE} = \frac{PR}{t} = \frac{(5.0)(5.5)}{(0.04)} = 690 \text{ PSI}$$

THIS STRESS WILL NOT BE ADDITIVE TO THE STRESSES PREVIOUSLY CALCULATED, BECAUSE THEY WILL NOT OCCUR AT THE SAME TIME.

NRO APPROVED FOR
RELEASE 1 JULY 2018 BY *MJP*

CK.

DATE 6-16-67 REV.

~~SECRET SPECIAL HANDLING~~

PAGE *17 OF 19*

MODEL

REPORT

$$\therefore M.S. = \frac{27,000}{670} - 1 = + \text{LARGE (LIMIT)}$$

CHECK THE CRITICAL CRIPPLING STRESSES DURING THE POWERED FLIGHT PHASE.

THE PORTION OF THE TELESCOPE BETWEEN STS. 1 & 27 DOES NOT SEE A TORQUE THEREFORE IT WILL BE CHECKED FOR COMPRESSION & BENDING ONLY.

COMPRESSION CHECK (REF. CASE 25 PG. 316 ROARK)

$$S' = \frac{1}{\sqrt{3}} \frac{E}{\sqrt{1-v^2}} \frac{t}{r}$$

FOR OUR CASE $1-v^2 \approx 1.0$

$$\therefore S' = \frac{42 \times 10^6}{\sqrt{3}} \left(\frac{0.040}{5.5} \right) = 0.1765 \times 10^{+6} \text{ PSI}$$

$$\therefore S' = 176500 \text{ PSI} \gg \text{ACTUAL COMPRESSIVE STRESS}$$

BENDING CHECK (REF. CASE 26 PG. 316 ROARK)

$$M' = K \frac{E}{1-v^2} r t^2 \qquad \text{WHERE } K \text{ CAN VARY FROM 0.72 TO 1.14, THE CONSERVATIVE VALUE OF 0.72 WILL BE USED.}$$

$$M' = \frac{(0.72)(42 \times 10^6)(1.0)(0.04)^2}{1.0}$$

$$M' = (6400)(0.72)(42) = 193,500 \text{ IN-# } \gg \text{ACTUAL BENDING MOMENT}$$

BY *MJP*

CK.

DATE 6-16-67 REV.

MODEL

REPORT

CHECK THE TUBE FOR CRIPPLING DUE TO TORSIONAL SHEAR:
(REF. CASE 27 (PG. 317 ROARK)

$$S_s' = \frac{E}{1-v^2}\left(\frac{t}{L}\right)^2 \left[2.8 + \sqrt{2.6 + 0.494\,H^{3/2}}\right]$$

WHERE: $H = \sqrt{1-v^2}\ \dfrac{L^2}{tr}$

THE ELBOW IS MADE OF ALUMINUM THEREFORE USE PROPERTIES
FOR ALUMINUM:

LET $L = 52"$ (DISTANCE BETWEEN JS. 1 & 27) & LET
$t = 0.040$ IN. BOTH OF THESE ASSUMPTION ARE VERY CONSERVATIVE
SINCE THEY ASSUME THAT THE BUILT-IN END CARRIES
TORQUE & THE SHEAR TIE IS NON-EXISTANT.

$$\therefore\ H = \sqrt{0.91}\left(\frac{52^2}{0.040 \times 5.5}\right) = \frac{(0.952)(2704)}{0.22}$$

$$H = 11700$$

$$\therefore\ S_s' = \frac{10 \times 10^6}{0.91}\left(\frac{0.040}{52.0}\right)^2 (791)$$

$$S_s' = \frac{(11.0)(1600)(791)}{2704} = 17600\,(0.292) = 5140.0\ PSI$$

$$\therefore\ S_s' = 5140\ PSI \gg ACTUAL\ SHEAR\ STRESSES.$$

~~SECRET~~ SPECIAL HANDLING

GENERAL ⬤ ELECTRIC

BY MJP

CK.

DATE 6-16-67 REV.

CHECK CRIPPLING OF THE SHEAR TIE

CONSIDER CASE 1 Pa. 312 OF ROARK.

$$S' = K \frac{E}{1 - v^2} \left(\frac{t}{b} \right)^2$$

USE K FOR $a/b = \infty$ ∴ K = 3.29 & b = 14

$$S' = \frac{(3.29)(42 \times 10^6)}{1.0} \left(\frac{0.125^2}{14^2} \right)$$

$$S' = \frac{138 \times 10^6}{196} (0.015625) = 11000 \text{ PSI} > \sigma_{ACTUAL}$$

FROM THE STRESS LEVELS SHOWN IN THE ANALYSIS IT
CAN BE SEEN THAT IN ALL CASES THE LEVELS ARE QUITE
LOW. THE ANALYSIS DOES NOT CONSIDER THE DETAILED
AREAS WHICH BECAUSE OF EQUIPMENT MOUNTING ETC.
MAY CAUSE SOME HIGHER LOCAL STRESSES. THESE HAVE
NOT BEEN ACCOUNTED FOR BECAUSE OF LACK OF INFORMATION
OR LACK OF A FIRM DESIGN. THE SAME HOLDS
TRUE FOR THERMAL EFFECTS WHICH SHOULD NOT BE
OF ANY CONSEQUENCE STRESS-WISE.

THIS ANALYSIS IN NO WAY INTENDS TO SERVE AS A
COMPLETE STRESS ANALYSIS BUT DOES GIVE A GOOD
INDICATION AS TO WHAT STRESS LEVELS CAN BE
EXPECTED AND WHAT AREAS ARE OVERDESIGNED. IT
ALSO INDICATES THAT ON THE WHOLE THE STRUCTURE
IS NOT OPTIMIZED AND WEIGHT SAVINGS ARE FEASIBLE

~~SECRET~~ SPECIAL HANDLING

2.5.2 STRUCTURAL ANALYSIS OF TRACKING A PEDESTAL UNDER POWERED FLIGHT LOADS

Introduction

The structural analysis of the tracking pedestal is intended to verify the structural integrity of the subcontractor's design and to determine the validity of the subcontractor's weight estimate. This is done by determining how optimized the structure is and making recommendations as to areas of potential weight savings.

Conclusions

The analysis shows that the structure is capable of carrying the loads imposed by powered flight accelerations. The high margins of safety calculated indicate that the structure has not been optimized. This means weight reductions may be feasible.

Description of Structure

The tracking pedestal structure is a beryllium structure which will be machined from hot pressed beryllium block. The structure is made of four basic pieces; the pedestal, the motor-encoder housing, the yoke, and the mirror bezel. This analysis does not include the mirror bezel; the other portions are included. The pedestal is a short cylinder with a three-point gusseted mounting plate. The connection to the vehicle shell is accomplished by using three DACO provided mounting studs. The connection between the motor housing and the pedestal is made by using mechanical fasteners. The motor-encoder housing houses the roll motor and encoder. The pitch gyro electronics will be mounted externally on the housing but this is not reflected in the analysis presented since at the time this analysis was performed the electronics was mounted to the mirror bezel. The roll shaft runs the full length of the housing and is supported by double row bearings at the forward and aft end. The roll shaft is attached to the yoke by means of mechanical fasteners. The yoke is a fabricated box structure which supports the mirror and bezel, the roll gyro and electronics, the pitch gyro, and the pitch motor and encoder. The pitch motor and encoder are mounted

on opposite sides of the yoke and are attached to the ends of the yoke arms by means of mechanical fasteners. The roll gyro and electronics are mounted to the yoke close to the roll shaft. The pitch gyro is mounted to the mirror bezel. The bezel is a beryllium pan into which the mirror is potted. The bezel has fittings to which shafts are attached which form the pitch shaft of the mirror. In the analysis, the mirror and bezel are considered to be a lumped mass with a rigid member forming the pitch shaft.

BY *MJP*

CK.

DATE *7/22/67* REV.

~~SECRET~~ **SPECIAL HANDLING**
GENERAL ● ELECTRIC

PAGE 1 OF

MODEL

REPORT

PRELIMINARY STRESS ANALYSIS OF THE SPECIAL SUB/SYSTEM PEDESTAL

THE PEDESTAL CONSISTS OF THE SUPPORT STRUCTURE, HOUSINGS AND COMPONENTS THAT MAKE UP THE TRACKING MIRROR ASSEMBLY. THE PEDESTAL IS ATTACHED TO THE D/RO LAB MODULE SHELL AT 3 POINTS BY MEANS OF STUDS WHICH ARE INTEGRAL PARTS OF THE SHELL. THE FOLLOWING SKETCH SHOWS THE BASIC CONFIGURATION OF THE PEDESTAL.
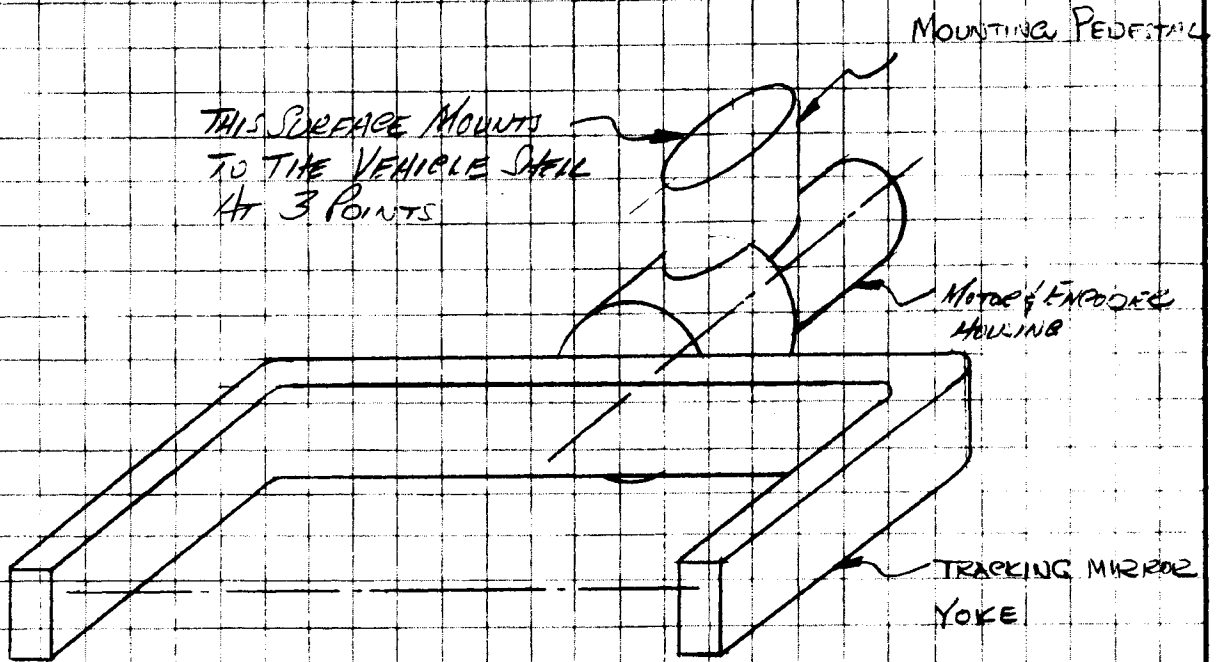
MOUNTING PEDESTAL

THIS SURFACE MOUNTS TO THE VEHICLE SHELL AT 3 POINTS

MOTOR & ENCODER HOUSING

TRACKING MIRROR YOKE

THE LOAD FACTORS USED IN THIS ANALYSIS WILL BE THE SAME AS THE STEADY-STATE ACCELERATIONS WHICH WERE GIVEN TO THE SUB-CONTRACTOR FOR DESIGN PURPOSES (REF: PIR 7223-278). THESE LOAD FACTORS WERE OBTAINED FROM THE "MARTIN 2ND LOAD CYCLE" MODIFIED TO SHOW TRENDS FROM THE 3A LOAD CYCLE. THE FOLLOWING ARE THE DESIGN LOAD FACTORS.

(SEE NEXT PAGE)

~~SECRET~~ **SPECIAL HANDLING**

BY MJP				MODEL
CK.				REPORT
DATE	REV.			

	X DIRECTION	Y DIRECTION	Z DIRECTION
MAX. X LOAD	±10.0	±0.72	±0.72
MAX. Y LOAD	+3.0 / -1.0	±1.8	±0.72
MAX. Z LOAD	+3.0 / -1.0	±0.72	±1.8

THE LOADS GIVEN ARE LIMIT LOADS. IN ORDER TO OBTAIN
ULTIMATE LOADS USE THE FOLLOWING RELATION (ULT= 1.4 × LIMIT)

THE INTERNAL LOADS ANALYSIS WAS PERFORMED USING
THE MASS PROGRAM (MECHANICAL ANALYSIS OF SPACE
STRUCTURES) ON THE IBM 7074 COMPUTER. THE OUTPUT
GIVES THE INTERNAL FORCES AND MOMENTS AT PREVIOUSLY
SPECIFIED POINTS. THE MODEL USED IS THE FOLLOWING:
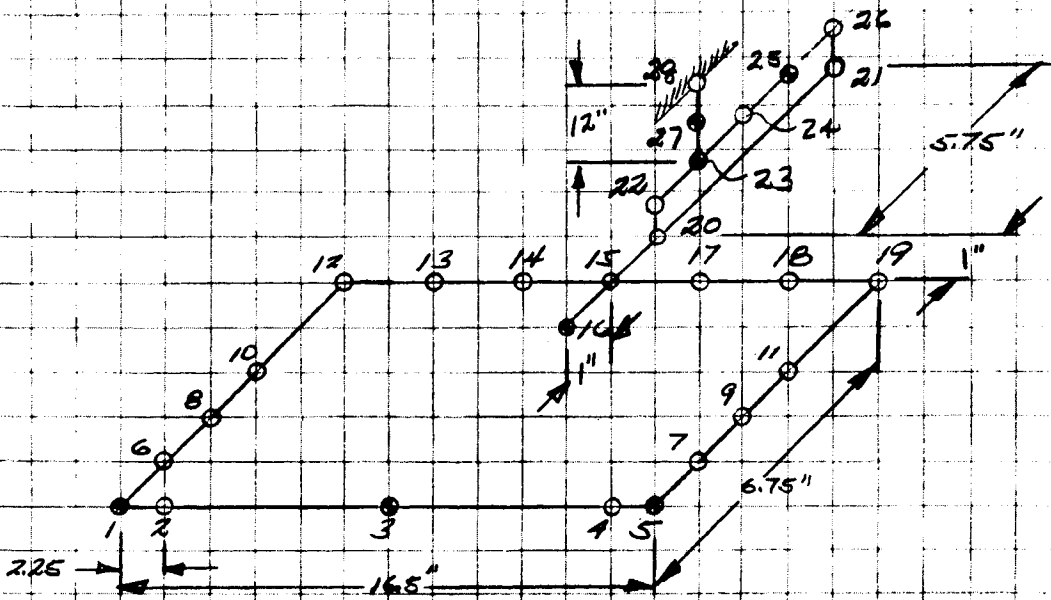
~~SECRET~~ SPECIAL HANDLING

GENERAL ● ELECTRIC

BY MJP		
CK.		
DATE	REV.	

MASSES ARE CONCENTRATED AT THE FOLLOWING POINTS:

Point.	Concentrated Mass
1	3.75 #
3	36.00 #
5	5.25 #
16	5.5 #
23	7.25 #
25	8.50 #
27	5.00 #

Section Properties of Structural Members

Member	Description	A	I_{1-1}	I_{2-2}	J
1-6	3x1.5x0.1 Rect. Tube	0.86	1.000	0.3315	0.7675
4-8	3x1.5x0.1 Rect. Tube	0.86	1.00	0.3315	0.7675
8-10	3x1.5x0.1 Rect. Tube	0.86	1.00	0.3315	0.7675
10-12	3x1.5x0.1 Rect. Tube	0.86	1.00	0.3315	0.7675
5-7	3x1.5x0.1 Rect. Tube	0.86	1.00	0.3315	0.7675
7-9	3x1.5x0.1 Rect. Tube	0.86	1.00	0.3315	0.7675
9-11	3x1.5x0.1 Rect. Tube	0.86	1.00	0.3315	0.7675
11-19	3x1.5x0.1 Rect. Tube	0.86	1.00	0.3315	0.7675
12-13	3x3x0.1 Square Tube	1.16	1.63	1.63	2.44
13-14	3x3x0.1 Square Tube	1.16	1.63	1.63	2.44
14-15	3x3x0.1 Square Tube	1.16	1.63	1.63	2.44
15-16	1" Dia. Circ. Shaft	0.785	0.049	0.049	0.098
15-17	3x3x0.1 Square Tube	1.16	1.63	1.63	2.44
17-18	3x3x0.1 Square Tube	1.16	1.63	1.63	2.44
18-19	3x3x0.1 Square Tube	1.16	1.63	1.63	2.44
15-20	1" Dia. Circ. Shaft	0.785	0.049	0.049	0.098
20-21	1" Dia. Circ. Shaft	0.785	0.049	0.049	0.098
22-23	8.5" OD 0.125" t	3.335	29.50	29.50	59.00
23-24	8.5" OD 0.125" t	3.335	29.50	29.50	59.00

~~SECRET~~ SPECIAL HANDLING

	BY MJP			PAGE 4 of
	CK.			MODEL
	DATE	REV.		REPORT

MEMBER	DESCRIPTION		A	I_{1-1}	I_{2-2}	J
24-25	6.4" OD	0.125 t	2.435	12.05	12.05	24.10
25-26	6.4" OD	0.125 t	2.435	12.05	12.05	24.10
23-27	7.5" OD	0.1875 t	4.307	28.81	28.81	57.62
27-28	7.5" OD	0.1875 t	4.307	28.81	28.81	57.62

THE MATERIAL FOR THE ENTIRE STRUCTURE IS
BERYLLIUM. THE PROPERTIES FOR 2% BeO HOT
PRESSED BLOCK WILL BE USED:

REF: MIL-HDBK-5A $F_{cy} = 28,700$ PSI
     TABLE 9.2.1.1 $F_{tu} = 40,000$ PSI
     AMS 7901 Be $F_{su} = 33,000$ PSI

THE LOADS ARE ACTING IN THE FOLLOWING MANNER:

BY *MJP*		GENERAL ⬤ ELECTRIC	PAGE 5 OF
CK.			MODEL
DATE	REV.		REPORT

LOADS ACTING ON 3 x 1.5 x 0.1 MEMBERS
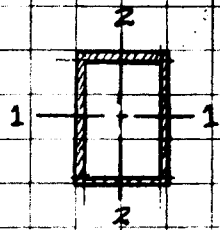
JOINT	M_{1-1} ②	M_{2-2} ①	M_T ②	V_{1-1} ④	V_{2-2} ①	V_a ②
1	0.452	181.56	2.8752	5.1841	28.242	211.94
5	0.4299	190.75	2.2383	7.1462	15.935	233.06
6	9.1685	229.22	2.8752	5.1841	28.242	211.94
7	11.625	217.64	2.2383	7.1462	15.935	233.06
8	17.888	276.87	2.8752	5.1841	28.242	211.94
9	23.693	244.53	2.2383	7.1462	15.935	233.06
10	26.579	324.53	2.8752	5.1841	28.242	211.94
11	35.765	271.43	2.2383	7.1462	15.935	233.06
12	35.320	372.19	2.8752	5.1841	28.242	211.94
19	47.827	398.32	2.2383	7.1462	15.935	233.06

CHECK STRESSES @ Jt. 12

$I_{11} = 1.00$; $Z_{11} = 0.667$
$I_{22} = 0.3315$; $Z_{22} = 0.4425$
$A = 0.86$
$J = 0.7675$

$$\sigma = \frac{M_{11}}{Z_{11}} + \frac{M_{22}}{Z_{22}} + \frac{V_a}{A} = \frac{35.32}{0.667} + \frac{372.19}{0.4425} + \frac{211.94}{0.86}$$

$$\sigma = 53 + 840 + 246 = 1139 \text{ PSI}$$

SHEAR STRESSES WILL BE NEGLIGIBLE

BY MJP		SECRET SPECIAL HANDLING GENERAL ELECTRIC	PAGE 6 OF
CK.			MODEL
DATE	REV.		REPORT

$$\therefore \quad M.S. = \frac{27000}{1139} - 1 = +LARGE \ (LIMIT)$$

LOADS ACTING ON 3×3×0.1 MEMBER

JOINT	M_{1-1} ④	M_{2-2} ③	M_T ⑤	V_{1-1} ⑥	V_{2-2} ⑪	V_A ⑥
12	2.8701	372.19	35.315	5.1543	211.94	28.242
13	11.300	210.06	35.315	5.1543	211.94	28.242
14	25.476	793.50	35.315	5.1543	211.94	28.242
15	39.676	1376.3	35.315	5.1543	211.94	28.242
15	56.85	1624.5	47.827	7.1606	233.06	15.937
17	37.162	983.53	47.827	7.1606	233.06	15.937
18	17.457	342.61	47.827	7.1606	233.06	15.937
17	2.2476	298.33	47.827	7.1606	233.06	15.937

CHECK STRESSES @ JT. 15

$$I_{11} = 1.63 \ ; \ Z_{11} = 1.075$$
$$I_{22} = 1.63 \ ; \ Z_{22} = 1.075$$
$$A = 1.16$$
$$J = 2.44$$

$$\sigma = \frac{M_{11}}{Z_{11}} + \frac{M_{22}}{Z_{22}} + \frac{P}{A} = \frac{56.85}{1.075} + \frac{1624.5}{1.075} + \frac{15.937}{1.16}$$

$$\sigma = 53 + 1510 + 14 = 1577 \ PSI$$

SHEAR STRESSES WILL BE NEGLIGIBLE :

$$M.S. = \frac{27000}{1577} - 1 = +LARGE \ (LIMIT)$$

BY MJD		PAGE 70F
CK.		MODEL
DATE	REV.	REPORT

LOADS ACTING ON 1" DIA. SHAFT

JOINT	M_{1-1} ④	M_{2-2} ⑤	M_T ⑤	V_{1-1} ⑥	V_{2-2} ①	V_A ③
15	85.930	250.91	17.179	17.901	17.885	500.01
20	103.83	268.79	17.179	17.901	17.885	500.01
21	15.974	0.7345	17.179	17.901	17.885	500.01

CHECK STRESSES @ JT. 20

$$I_{11} = 0.049 \quad ; \quad Z_1 = 0.098$$
$$I_{22} = 0.049 \quad ; \quad Z_{22} = 0.098$$
$$A = 0.785$$
$$J = 0.098$$

$$\sigma = \frac{M_{11}}{Z_{11}} + \frac{M_{22}}{Z_{22}} + \frac{P}{A} = \frac{103.83}{0.098} + \frac{268.79}{0.098} + \frac{500.01}{0.785}$$

$$\sigma = 1060 + 2740 + 636 = 4436 \ PSI$$

TORSIONAL SHEAR:

$$\tau = \frac{TK}{J} = \frac{(17.179)(0.5)}{0.098} = 90 \ PSI$$

VERTICAL SHEAR:

$$\tau = \frac{4V}{3A} + \frac{4V}{3A} = \frac{(17.901)(4)}{(3)(0.785)} + \frac{(17.885)(4)}{(3)(0.785)}$$

$$\tau = 30 + 30 = 60 \ PSI$$

$$\tau = 90 + 60 = 150 \ PSI.$$

NRO APPROVED FOR
RELEASE 1 JULY 2015

SECRET SPECIAL HANDLING

GENERAL ⬤ ELECTRIC

PAGE 8 OF

MODEL

REPORT

BY MJP

CK.

DATE   REV.

BENDING IS CRITICAL:

$$M.S. = \frac{27000}{4436} - 1 = +LARGE \; (LIMIT)$$

LOADS ACTING IN MOTOR & ENCODER HOUSING:

JOINT	M_{1-1} ④	M_{2-2} ③	M_T ⑤	V_{1-1} ⑥	V_{2-2} ①	V_A ②
22	29.779	0.9234	15.660	26.30	65.094	324.89
23	12.963	106.70	15.660	26.30	65.093	324.89
23	4.7805	166.57	4.8719	0.3687	37.975	260.12
24	5.3927	104.86	4.8719	0.3687	37.975	260.12
25	5.8353	57.393	4.8719	0.3687	37.975	260.12
26	16.852	1.1174	4.8719	8.8157	46.808	175.12

CHECK STRESSES AT JT. 24 (MIN. CROSS SECTION)

$$I_{11} = 12.05 \; ; \; Z_{11} = 3.76$$
$$I_{22} = 12.05 \quad Z_{22} = 3.76$$
$$A = 2.435$$
$$J = 24.1$$

$$\sigma = \frac{M_{11}}{Z_{11}} + \frac{M_{22}}{Z_{22}} + \frac{V_A}{A} = \frac{5.3927}{3.76} + \frac{104.86}{3.76} + \frac{260.12}{2.435}$$

$$\sigma = 2 + 38 + 107 = 147 \; PSI$$

SHEAR STRESSES WILL BE NEGLIGIBLE

$$M.S. = \frac{27000}{147} - 1 = +LARGE \; (LIMIT)$$

LOADS AT PEAK

JOINT	M_{1-1} ①	M_{2-2} ②	M_T ③	V_{1-1} ④	V_{2-2} ⑤	V_A ⑥
23	20.57	10.374		1.822	657.51	33.817
	22	6907	273.01	1.837	657.51	33.817
28	457	8175.8	273.01	18.467	707.51	38.977

CHECK STRESSES

$T_r = 38.21$ $t_A = 7.68$

$A = 4.307$

$J = 57.62$

$$f = \frac{M_{1-1}}{?} + \frac{M_{2-2}}{?} + \frac{V_A}{A} = 457.00 + 8175.8 + \frac{38.977}{4.307}$$

$$f = 60 + 1065 + 9 = 1134 \ PSI$$

SHEAR STRESSES

$$\tau = \frac{4V_{1-1}}{3A} + \frac{4V_{2-2}}{3A} + \frac{M_T r}{J} = \frac{(4)(707.51)}{(3)(4.307)} + \frac{(4)(38.977)}{(3)(4.307)}$$

$$+ \frac{(273.01)(3.75)}{57.62}$$

$$\tau = 219 + 12 + 18 = 249 \ PSI$$

COMBINED BENDING & TORSION STRESS WILL BE
APPROXIMATELY EQUAL TO BENDING & STRESS
WILL NOT BE CRITICAL

$$\therefore M.S. = \frac{27000}{1134} - 1 = HIGH \ (LIMIT)$$

NRO APPROVED FOR
RELEASE 1 JULY 2010

SECRET SPECIAL HANDLING

PAGE 10 OF

CK.

DATE   REV.

MODEL

REPORT

GENERAL ELECTRIC

IT IS EVIDENT FROM THE PREVIOUS CALCULATIONS THAT THE TRACKING PEDESTAL IS FAR FROM BEING OPTIMIZED. ADDITIONAL WORK WILL BE DONE IN ORDER TO DETERMINE THE OPTIMUM SIZES & RATES.

2.5.3 STRUCTURAL ANALYSIS OF THE PROTECTIVE SHROUD UNDER POWERED FLIGHT LOADS AND ON-ORBIT OPERATING LOADS

Introduction

The structural analysis performed on the protective shroud was intended to demonstrate to the subcontractor that a much lighter weight shroud is attainable with the use of lighter materials and some design changes to make the design more efficient. The shroud design proposed by the subcontractor was not analyzed due to the fact that the design weight of 23.5 pounds was unacceptable. An effort was made to derive a minimum weight preliminary design for transmission to the subcontractor. The results of this analysis show that it may be possible to design a shroud weighing approximately 14 pounds. The weight could possibly increase slightly due to thermal problems but hopefully the design could be further optimized toward the 14-pound weight. The shroud was checked for powered flight loads as well as a worst case on-orbit load due to attempted operation with a motor seizure.

Description of Structure

The shroud design analyzed is a basic beryllium framework with beaded fiberglass skins to give additional rigidity to the structure. The end plates are shown as fiberglass but could be made of beryllium if thermal problems dictate this. The envelope is the same as the subcontractor and the deflections incurred are no worse than the subcontractor's design, the reason for this being the sizeable increase in stiffness due to the beryllium framework and beaded skin versus the subcontractor's aluminum structure (e. g., E for beryllium = 42×10^6 psi versus E for aluminum = 10×10^6 psi).

Design Loads

Shell acceleration from the Martin Second Load Cycle will be used. The conditions considered will be for the maximum axial load condition and for the maximum lateral load condition.

2-319

-SECRET- SPECIAL HANDLING

Maximum axial load condition:

Axial g's: +5.6
             -2.7   } Stage II Ignition

Lateral g's: Negligible }

Maximum lateral load condition:

Axial g's: +2.8
               +0.59

Yaw g's: +0.41   } Launch
               -0.24

Pitch g's: +0.80
               -0.44

Note: All accelerations are limit and ultimate = 1.4 x limit.

The basic configuration of the proposed shroud is shown in Figure 2.5-1. For the purpose of analysis the weight of the shroud structure will be assumed to be 10 pounds.
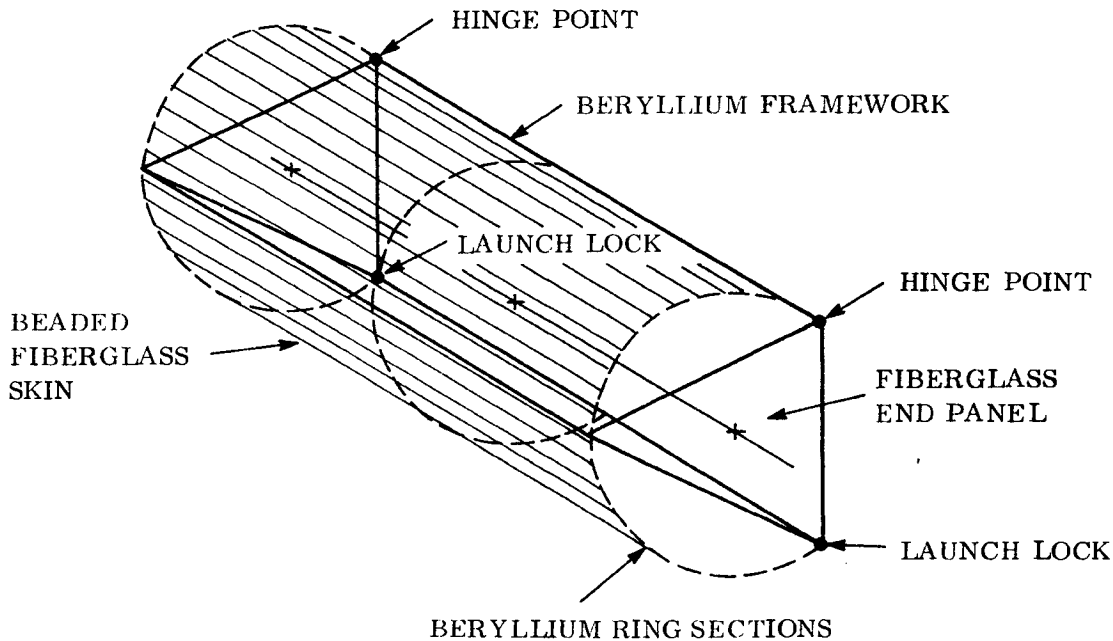
Figure 2.5-1. Basic Configuration of Proposed Shroud

-SECRET- SPECIAL HANDLING

~~SECRET~~ SPECIAL HANDLING

TABLE 2.5-1. MATERIAL COMPARISONS

MATERIAL	F_{tu} @ R.T. psi	F_{tu} @ 400°F 1/2 hr soak psi	F_{ty} @ R.T. psi	F_{ty} @ 400°F 1/2 hr soak psi	F_{cy} @ R.T. psi	F_{cy} @ 400°F 1/2 hr soak psi	F_{su} @ R.T. psi	F_{su} @ 400°F 1/2 hr soak psi	E @ R.T. 10^6 psi	E @ 400°F 1/2 hr soak 10^6 psi	G @ R.T. 10^6 psi	ρ #/in.^{3}
2024-T42 Aluminum (Flat Sheet and Plate)	62000	46500	38000	29600	38000	-	37000	-	10.5	9.45	4.0	0.100
2024-T4 Aluminum (Extrusions)	57000	40500	42000	34850	38000	-	30000	-	10.5	9.45	4.0	0.100
HK31A-H24 Magnesium (Sheet and Plate)	34000	20750	26000	17925	20000	18000	23000	-	6.5	5.78	2.4	0.0647
HM31A-T5 Magnesium (Extrusions)	37000	19250	26000	14550	19000	15600	-	-	6.5	5.85	2.4	0.0651
AMS 7901 Beryllium (Shapes)	40000	32800	27000	22950	27000	-	33000	26400	42.5	41.2	20.0	0.067

Note: All of the above values were obtained from MIL-HDBK-5A.

2-321

~~SECRET~~ SPECIAL HANDLING

Analyze the beryllium framework:
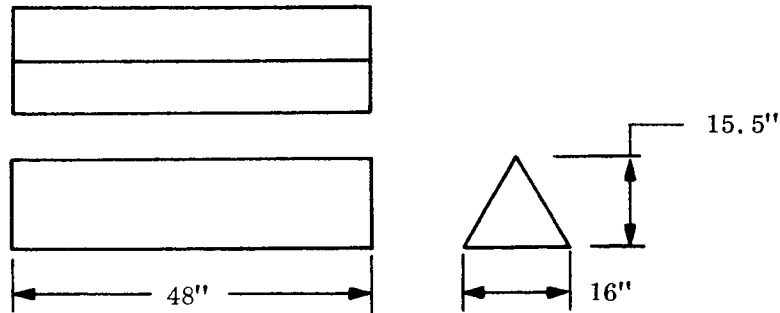
Consider the following loading case:

The loading applies to an axial acceleration. Consider the load to be taken out at each of the three corners of the rectangular framework.
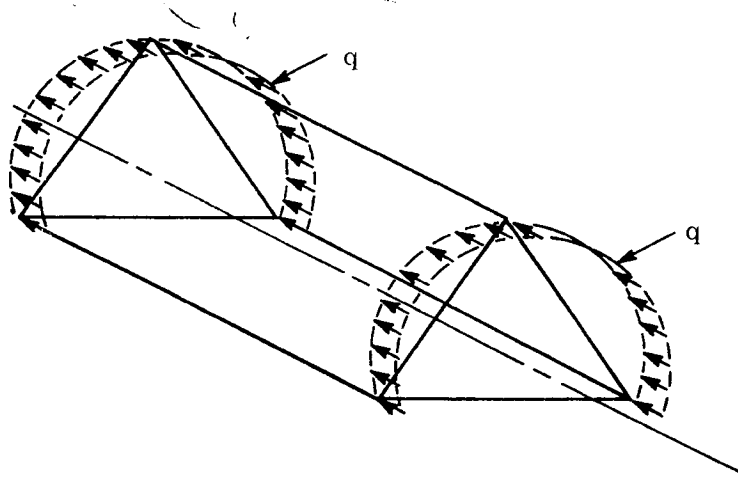
To determine the load distribution consider the curved beams to be continuous straight beams on three supports with a uniform load.

2-322

$$R_1 = \frac{3}{16} qL$$

$$R_2 = \frac{10}{16} qL$$
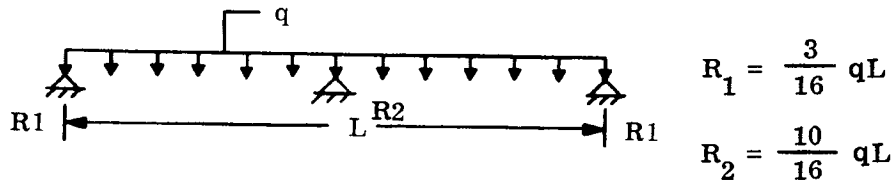
∴ We have the following:

∴ $R_2 = 5/8$ (5 pounds) = 3.125 pounds

$R_1 = 0.9375$ pound
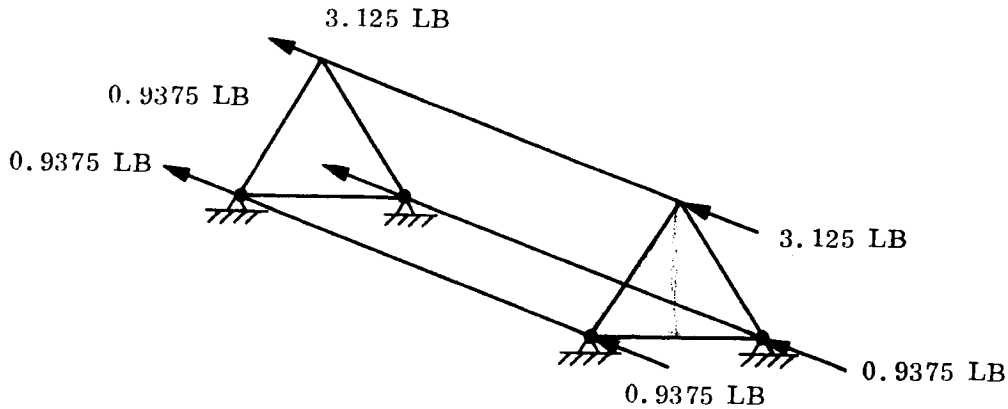
Consider the following:
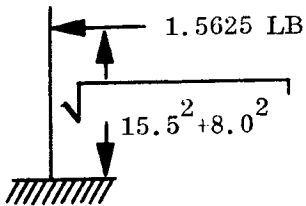
$$M_{MAX} = 1.5625 \sqrt{15.5^2 + 8.0^2}$$

$$= 1.5625 \sqrt{304}$$

$$= 1.5625 (17.4)$$

$$= 27.2 \text{ in. -lbs}$$

2-323

Determine Z_{req} for an angle made of AMS 7901 beryllium

F_{ty} @ $400°F = 22950$ psi

$$\therefore \quad 22950 = \frac{27.2 \ (5.6 \ \text{g's})}{Z_{REQ}} = \frac{152.5}{Z_{REQ}}$$

$$Z_{REQ} = \frac{152.5}{229.5} \times 10^{-2} = 6.65 \times 10^{-3}$$

Try using a 7/8 inch by 7/8 inch by 0.040-inch thick angle

Section properties: $A = 0.066$ in.^{2}

$$I_{xx} = I_{yy} = 0.0051 \ \text{in.}^4$$

$$Z = I/C = 0.051/(0.875 - 0.249)$$
$$Z = 0.0051/0.626 = 0.0081 \ \text{in.}^3$$

$$\therefore \quad \sigma_b = M/Z = 152.5/0.0081 = 18850 \ \text{psi}$$

$$\text{M.S.} = \frac{22950}{18850} - 1 = +0.22 \ (\text{LIMIT})$$

Limit will be critical condition $\dfrac{F_{tu}}{F_{ty}} = 1.43 > 1.4$

Determine deflection:

$$\delta = \frac{PL^3}{3EI} = \frac{1.5625 \ (5.6) \ (17.4)^3}{(3) \ (42 \times 10^6)(0.0051)}$$

$$\delta = \frac{(1.5625)(5.6)(1.74)^2(17.4)}{126 \ (51)} = 0.072 \ \text{inch}$$

2-324

Check Column Action of Longitudinal Member

Consider Case 7 (page 305) in Roark:

$$P_{CRIT} \quad L = \frac{\pi^2 EI}{(1.122)^2} \qquad \text{Where} \qquad L = 48 \text{ inches}$$
$$I = 0.0051$$

$$P_{CRIT}(48) = \frac{(9.85)(42 \times 10^6)(0.0051)}{2900} = (0.875)(1.76)(9.85)$$

$$P_{CRIT} = 15.2 \text{ lb/in. where } P_{ACTUAL} = \frac{6.25}{48} = 0.13 \text{ lb/in. } \times 5.6 = 0.73 \text{ lb/in.}$$

Check lower longitudinal angles for the following condition:
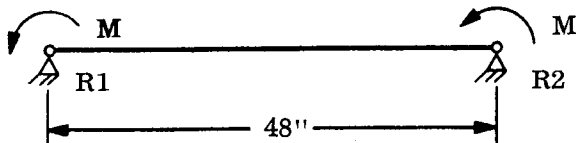
$$M = 15.5(3.125)$$
$$M = 48.5 \text{ in.-lb}$$

$$Z = 2(0.0081) = 0.0162$$

$$\therefore \quad \sigma_b = \frac{M}{Z} = \frac{48.5}{0.0162} = 3000 \text{ psi}$$

Check shear:

$$Q = \Sigma A_y = 0.626(0.04)(0.313) = 0.00785$$

$$\tau = \frac{VQ}{I_b} = \frac{(1.5625)(5.6)(1.54)}{(0.040)} = 338 \text{ psi (LIMIT)}$$

$$\tau_{ULT} = 1.4 \times 338 = 473 \text{ psi}$$

$$M.S. = \frac{26400}{473} - 1 = +\text{LARGE (ULT)}$$

Check crippling of angle:

$$\sigma_{CRIT} = K \frac{E}{1 - v^2} \left(\frac{t}{b}\right)^2 \quad \text{for Be } 1 - v^2 \approx 1.0$$

$$\therefore \sigma_{CRIT} = KE \left(\frac{t}{b}\right)^2 = 3.29(42 \times 10^6) \left(\frac{0.04}{0.626}\right)^2$$

$$\sigma_{CRIT} = (3.29)(42)(0.41) \times 10^4 = 56.6 \times 10^4 \text{ psi}$$

$$\tau_{CRIT} = K \frac{E}{1 - v^2} \left(\frac{t}{b}\right)^2 > \sigma_{CRIT} \quad \text{for K} = 4.40$$

$\therefore$ Crippling will not be critical.

Applying the maximum axial load factor of 5.6:

$$\sigma_b = 5.6 \times 3000 = 16800 \text{ psi}$$

$$\therefore \text{M.S.} = \frac{22950}{16800} - 1 = +0.36 \text{ (LIMIT)}$$

There will also be a stress component due to the axial load which will be negligible and also a beam-column effect which will not be considered at this time.

Consider the Case of Launch Acceleration Where We Have a Lateral Load

Determine magnitude of lateral accelerations:
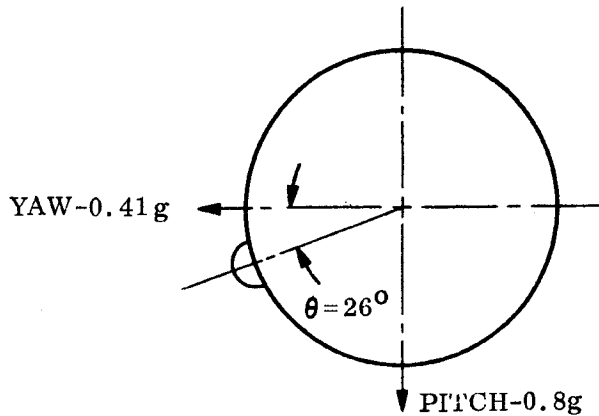
Acceleration acting at shroud

$$G_R = 0.41 \cos 26^O + 0.8 \cos 64^O$$

$$G_R = 0.41(0.898) + 0.8(0.438)$$

$$G_R = 0.368 + 0.35 = 0.718 \text{ g}$$

$$G_T = 0.41 \sin 26^O - 0.8 \sin 64^O$$

$$G_T = 0.41(0.438) - 0.8(0.898)$$

$$G_T = 0.1795 - 0.71 \text{ g}$$

$$G_T = 0.539 \text{ g}$$

YAW-0.41g

$\theta = 26^O$

PITCH-0.8g

We will get the following loading condition:

(Launch Accelerations)

(The accelerations are applied to the loads shown.)

8.75 LB

2.625 LB

2.625 LB

$q_1 = 0.15$ LB/IN.

$q_2 = 0.112$ LB/IN.

8.75 LB

2.625 LB   2.625 LB

2-327
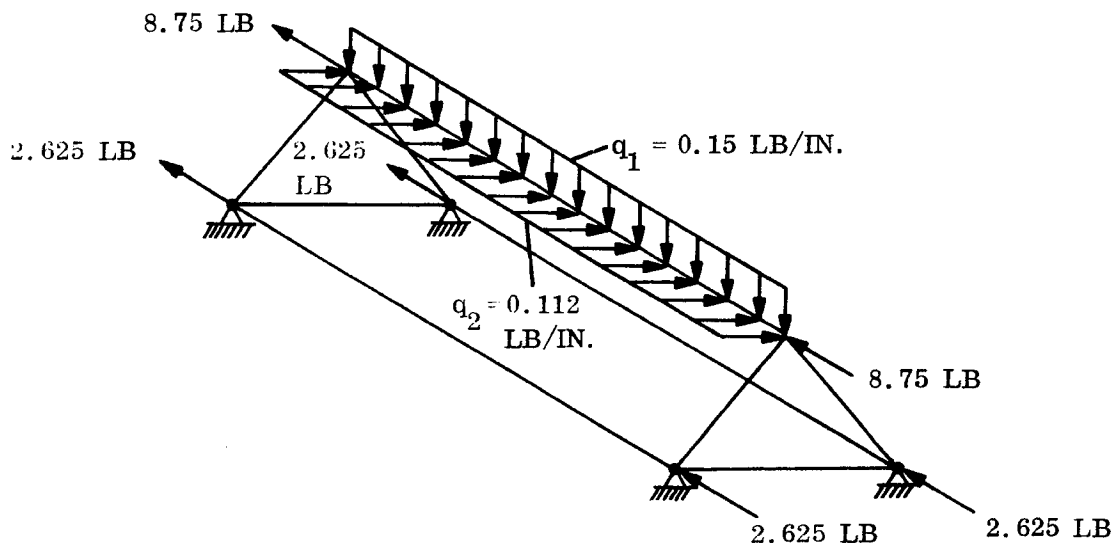
Determine Bending Stresses in the Longitudinal Beam

$$Z = 0.0081 \text{ in.}^3$$

$$A = 0.066 \text{ in.}^2$$

$$M_{q_1} = \frac{qL^2}{8} = \frac{(0.15)(48)^2}{8} + \frac{(0.112)(48)^2}{8} = 43.2 + 32.3 = 75.5 \text{ in./lb}$$

$$\therefore \; \sigma = \frac{M}{Z} + \frac{P}{A} = \frac{75.5}{0.0081} + \frac{8.75}{0.066} = 9330 + 133 = 9463 \text{ psi}$$

$$M.S. = \frac{22950}{9463} - 1 = +1.42 \text{ (LIMIT)}$$

Shear will not be critical.

Check Bending in Members Forming End Triangle

Loading:

Section properties of angles

$$A = 0.066 \text{ in.}^2$$

$$J_{xx} = I_{yy} = 0.0051 \text{ in.}^4$$

$$Z = 0.0081 \text{ in.}^2$$
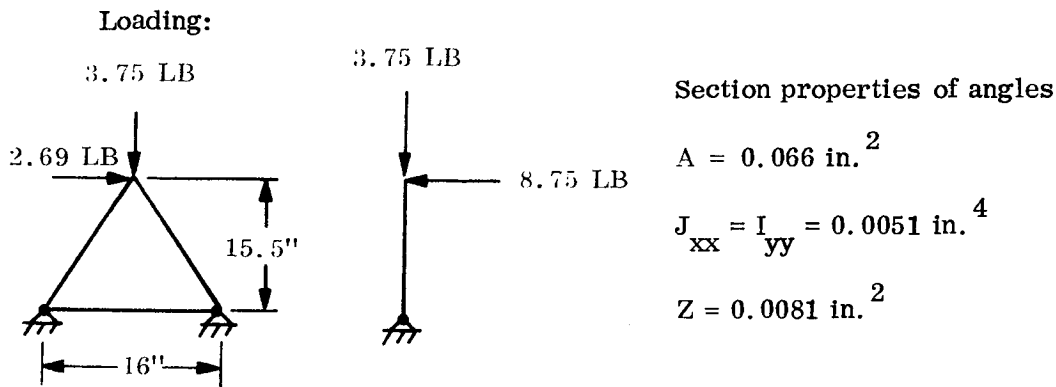
M due to 8.75-pound load $= 4.375 \sqrt{15.5^2 + 8.0^2} = 4.375(17.4)$

$$M = 76.1 \text{ in./lb}$$

M due to 3.75-pound load $= 3.75(8) = 30 \text{ in./lb}$

M due to 2.69-pound load $= 41.7 \text{ in./lb}$

$$\therefore \quad M_{TOTAL} = 147.8 \text{ in. /lb}$$

$$\therefore \quad \sigma_b = \frac{M}{Z} = \frac{14780}{0.81(2)} = 9150 \text{ psi}$$

Determine Tensile Loads and Stresses

Consider components to be additive (they may not be so):

$$P = \frac{15.5}{17.4}(3.75) + \frac{8}{17.4}(2.69) = 3.34 + 1.24 = 4.58 \text{ pounds}$$

$$\therefore \quad \sigma_t = P/A = 4.58/0.066(2) = 35 \text{ psi}$$

$$\therefore \quad \sigma = 9200 \text{ psi} \qquad\qquad M.S. = \frac{22950}{9200} - 1 = +1.40 \text{ (LIMIT)}$$

Determine Weight of Framework

$$L = 4(17.4) + 2(16) + 3(48) = 70 + 32 + 144 = 246 \text{ inches}$$

$$\therefore \quad V = LA = 246(0.066) = 16.2 \text{ in.}^3$$

$$W = \rho V = 0.067(16.2) = 1.10 \text{ pounds}$$

Determine effect of a 100 in. /lb torque applied at one end of the shroud and the other end
is locked (no launch locks).

LOCKED END
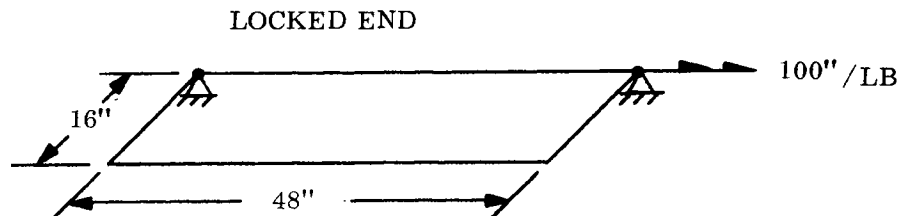
Compare Torsional Rigidity of Members to Bending Rigidity

Consider the 7/8 inch by 7/8 inch by 0.040-inch thick angles:

Developed length - 1.65

$$\therefore \quad K = \beta bt^3 = 0.333(1.65)(0.04)^3 = 8.8 \times 10^{-4}$$

Consider the following:
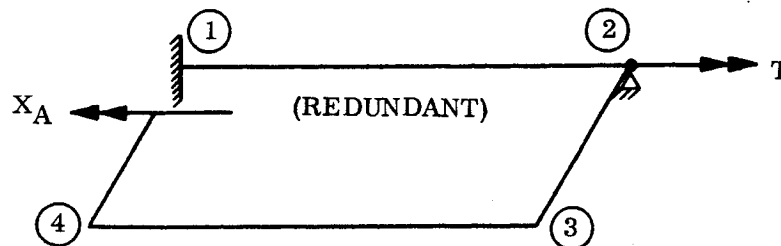
where: $X_A = - \dfrac{\delta ao}{\delta aa}$ (Ref: Peery page 457)

δ ao = Deflection due to applied loads

δ aa = Deflection due to unit redundant

$$\delta ao = \frac{TL}{KG} = \frac{(5)(48)}{(8.8)} \times 10^{-2} = 0.273 \text{ inch}$$

$$\delta aa = 2\left(\frac{ML}{EI}\right) + 2\left(\frac{TL}{KG}\right)$$

$$\delta aa = \frac{(2)(16)}{(42)(0.0051)} \times 10^{-6} + \frac{(2)(48)}{(8.8)(20)} \times 10^{-2}$$

$$\delta aa = \frac{32 \times 10^{-2}}{(42)(51)} + \frac{48}{88} \times 10^{-2} = (0.015 + 0.545) \times 10^{-2}$$

$$\delta aa = 0.56 \times 10^{-2}$$

$$\therefore XA = -\frac{0.273}{0.56} \times 10^2 = 48.75 \approx 49 \text{ in./lb}$$

$\therefore$ The twisting in 1-2 is 51 in./lb.

Determine the Torsional Capability of the Shell (Shroud Skin)

Assume the skin to be made of 181-Volana Glass Fabrk (Ref: page 79 to 81, MIL-HDBK-17):

Mechanical Properties: (@ 400°F/one-half hour soak)

Flexural strength - 48000 psi

Tensile strength - 35000 psi

Modulus of elasticity - 2.9×10^6 psi

Assume shear strength to be 60 percent of tensile strength:

$$\therefore F_{S_U} = 21000 \text{ psi}$$

Also assume μ (Poisson's ratio) = 0.12

$$\therefore G = \frac{E}{2(1+0)} = \frac{2.9 \times 10^6}{2.24} = 1.3 \times 10^6$$

Consider the following skin cross-section:
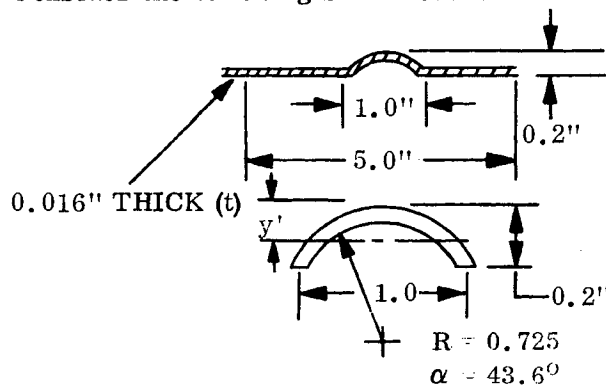
Determine section properties:
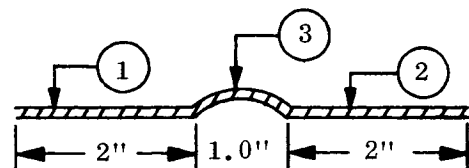
Determine Io and y for bead:

$$I = R^3 t \left(\alpha + \sin\alpha \cos\alpha - \frac{2 \sin^2 \alpha}{\alpha} \right)$$

$$I = (0.725)^3 (0.016) \left[\frac{43.6}{57.3} + \sin 43.6^\circ \cos 43.6^\circ - \frac{2 (\sin 43.6)^2}{43.6/57.3} \right]$$

$$I = 0.38(0.016) \left[0.764 + 0.5 - 1.25 \right]$$

$$I = 0.006(0.014) = 84 \times 10^{-6} \text{ in.}^4$$

$$y_1 = R \left(1 - \frac{\sin\alpha}{\alpha} \right) = 0.725 \left(1 - \frac{0.69}{0.764} \right) = 0.725 (1 - 0.904)$$

$$y_1 = 0.725(0.096) = 0.069 \text{ in.}$$

$$A = 2\alpha Rt = \frac{87.2(0.725)(0.016)}{57.3} = 0.01765 \text{ in.}^2$$

Determine total section properties:

	A	y	A_y	I_o	d	Ad^2
1	0.032	0.008	2.56^{1-4}	0.6825^{1-6}	0.0264	22.4^{1-6}
2	0.032	0.008	2.56^{1-4}	0.6825^{1-6}	0.0264	22.4^{1-6}
3	0.018	0.131	23.4^{1-4}	84.0^{1-6}	0.097	169.0^{1-6}
	0.082		28.52^{1-4}	85.365^{1-6}		213.8^{1-6}

$$\bar{y} = \frac{28.52}{8.2} \times 10^{-2} = 3.44 \times 10^{-2}$$

$$\therefore \text{ INA} = 299 \times 10^{-6} \text{ in.}^4$$

Determine equivalent flat section:

$$I = 299 \times 10^6 = \frac{5t^3}{12}$$

$$t^3 = 716 \times 10^{-6}$$

$$t_{equiv} = 8.9 \times 10^{-2} = 0.089 \text{ inch}$$
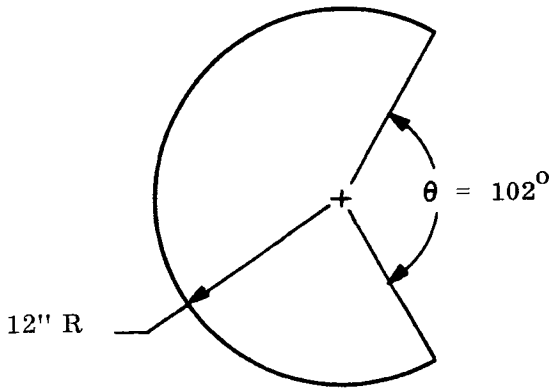
ANGLE OF TWIST:

$$\theta = \frac{TL}{\beta bt^3 G} \qquad b = \frac{258}{57.3}(12) = 54 \text{ inches}$$

$$\theta = \frac{(1.0)(48)}{(0.333)(54)(0.089^3)(20 \times 10^6)}$$

$$\theta = \frac{144}{(54)(20)(705)}$$

$$\theta = 1.89 \times 10^{-4} \text{ rad/lb}$$

$\theta = 102^{\circ}$

12" R

Angle of twist for Be framework:

$$\theta = \frac{TL}{KG} = \frac{(0.51)(2.4)}{(8.8)} \times 10^{-2} = 0.139 \times 10^{-2} \text{ rad/lb}$$

$$\frac{TL}{\beta bt^3 G} = \frac{TL}{KG}$$

$$1.89 \times 10^{-4} \ T_S = 0.139 \times 10^{-2} \ T_F$$
$$T_S = 0.0735 \times 10^2 \ T_F = 7.35 \ T_F$$
$$T_S + T_F = 100 \qquad \therefore \quad 8.35 \ T_F = 100$$
$$T_F = 12 \text{ in./lb}$$

$\therefore$ Determine torsional shear stress in the framework:

$$\tau = \frac{T}{\alpha \, bt^2} = \frac{6.1(3)}{1.65(0.04)^2} = \frac{18.3}{26.4} \times 10^4$$

$\tau = 6950$ psi (LIMIT)

$\tau = 1.4 \times 6950 = 9725$ psi (ULT)

$$\therefore \ \ M.S. = \frac{26400}{9725} - 1 = +1.71 \ (ULT)$$

Determine torsional shear stress in the shell:

$$\tau = \frac{T}{\alpha \, bt^2} = \frac{264}{42.6 \times 10^{-2}} = 6.2 \times 10^2$$

$\tau = 620$ psi (LIMIT)

$\tau = 1.4 \times 620 = 870$ psi (ULT)

$$\therefore \ \ M.S. = \frac{21000}{870} - 1 = +LARGE \ (ULT)$$

Check shear crippling:

Shell:

$$\tau_{CRIT} = 0.1E \frac{t}{\gamma} + 5E \left(\frac{t}{b} \right)^2$$

$$\tau_{CRIT} = (0.1)(2.9) \left(\frac{0.016}{12.0} \right)^{1+6} + (5)(2.9) \left(\frac{256}{25} \right)$$

$$\tau_{CRIT} = \frac{(2.9)(16)}{0.12} + (2.9)(51.2) = 387 + 148 = 535 \ psi$$

A crippling problem exists. Consider increasing the thickness to 0.020 inch.

$$\therefore \ \tau_{CRIT} = \frac{(2.9)(20)}{0.12} + (2.9)(80) = 484 + 232 = 716 \text{ psi}$$

Due to the beef-up the shell will take more load thus for brevity consider the shell to carry the full 100 lb/in.

$$\therefore \ \tau = 620 \left(\frac{100}{88}\right) = 705 \text{ psi (does not reflect increase in } t_{equiv})$$

$$\therefore \ \text{Increase wall to 0.020 inch}$$

Determine weight of shell:

BEADED AREA

54"

48"

Unbeaded area = 39 x 43 = 1675 in.^{2}

$V = 1675(0.02) = 33.5$ in.^{3}

$WT = 0.068(33.5)$

$WT = 2.280$ pounds
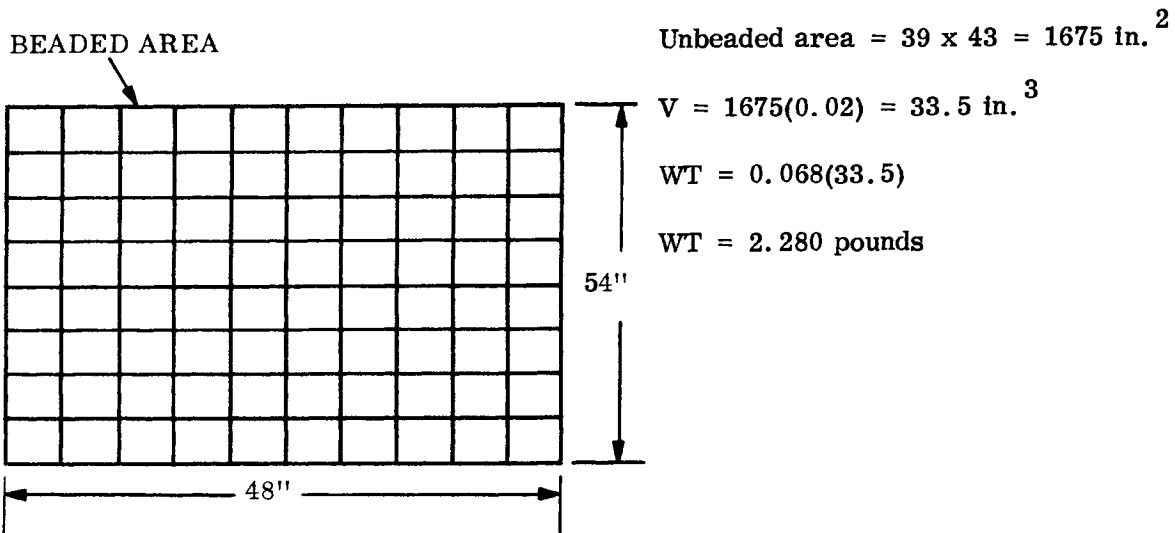
Weight of Beads:

$L = 54(9) + 48(11) = 486 + 528 = 1014$ in.

$V = AL = 0.018(1014) = 18.25$ in.^{3}

$WT = 0.068(18.25) = 1.25$ pounds

$\therefore \ \text{Weight of skin} = 3.53$ pounds

Determine weight of rings. (Consider them to be the same as stiffeners.):

$A = 0.066$ in.^{2}

$L - 54(4) = 216$ in. (assume 4 rings)

$\therefore V = 14.25$ in.^{3}

$WT = 0.067(14.25) = 0.96$ pound ≈ 1.0 pound

Weight of ends (assume double end):

$A = \pi R^2 = \pi(144) = 452$ in.^{2} x 4 = 1808 in.^{2}

$V = 1808(0.016) = 29.0$ in.^{3}

$WT = 0.068(29) \approx 2.0$ pounds

$\therefore$ Total weight $= 1.1 + 3.5 + 1.0 + 2.0 = 7.6$ pounds

Assume additional structural weight to bring total to 9.0 pounds.

Consider drive to weigh 3.0 pounds and insulation and coatings to weigh 2.0 pounds.

$\therefore$ Shroud weight is 14.0 pounds

2.5.4 DEFLECTION ANALYSIS OF TELESCOPE AND TRACKING PEDESTAL DUE TO 1G LOAD RELIEF

Introduction

A deflection analysis of the telescope and tracking pedestal was performed to determine the effects of optical path alignment due to 1g load relief. The results of this analysis are shown on the following pages.

BY		PAGE 1 OF
CK.		MODEL
DATE	REV.	REPORT

PRELIMINARY DEFLECTION ANALYSIS OF TELESCOPE DUE TO 1G LOAD RELIEF.

WHEN THE TELESCOPE IS INSTALLED THERE WILL BE SOME DEFLECTION DUE TO THE WEIGHT OF THE TELESCOPE ITSELF. WHEN IN-ORBIT AND IN A "0G" FIELD THE TELESCOPE DEFLECTION WILL BE RELIEVED. THIS WILL CAUSE A MISALIGNMENT OF THE LINE OF SIGHT. THE PURPOSE OF THIS ANALYSIS IS TO EVALUATE THE MAGNITUDE OF THIS MISALIGNMENT.

THE MODEL USED FOR THE STRESS ANALYSIS OF THE TELESCOPE WILL BE USED TO GENERATE THE REQUIRED DEFLECTIONS:
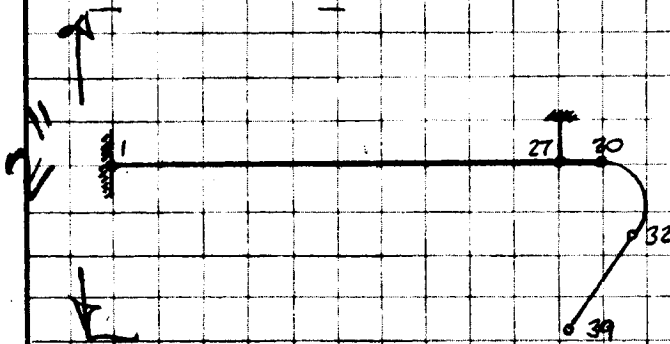
WHEN INSTALLED IN THE VEHICLE IN AN UPRIGHT POSITION. THE TELESCOPE WILL BE IN SUCH A POSITION THAT THE TELESCOPE WILL LIE IN A STATION PLANE.

1) DETERMINE DEFLECTIONS OF TELESCOPE UNDER A 1G FIELD (DEFLECTIONS IN LONGITUDINAL DIRECTION)

Pt.	δ_G	Pt.	δ_G	Pt.	δ_G	Pt.	δ_G
1	0.0	9	2.3705^{1-5}	17	3.1600^{1-5}	25	2.3494^{1-5}
2	6.5003^{1-7}	10	2.6519^{1-5}	18	3.0934^{1-5}	26	2.3704^{1-5}
3	2.4323^{1-6}	11	2.8777^{1-5}	19	3.0048^{1-5}	27	2.4193^{1-5}
4	5.1470^{1-6}	12	3.0481^{1-5}	20	2.8983^{1-5}	28	2.4966^{1-5}
5	8.5724^{1-6}	13	3.1636^{1-5}	21	2.7780^{1-5}	29	2.7108^{1-5}
6	1.2446^{1-5}	14	3.2244^{1-5}	22	2.6481^{1-5}	30	2.8025^{1-5}
7	1.6482^{1-5}	15	3.2329^{1-5}	23	2.5165^{1-5}	31	6.7062^{1-5}
8	2.0336^{1-5}	16	3.2006^{1-5}	24	2.4075^{1-5}	32	1.7726^{1-4}

BY			
CK.			
DATE		REV.	

Pt.	S_a
33	$2.8549^{1.4}$
34	$3.7817^{1.4}$
35	$4.7100^{1.4}$
36	$5.7189^{1.4}$
37	$6.8936^{1.4}$
38	$8.1478^{1.4}$
39	$1.0234^{1.3}$

THE DEFLECTIONS WERE OBTAINED FROM THE COMPUTER PROGRAM OUTPUT USED IN THE STRESS ANALYSIS OF THE TELESCOPE. THE DEFLECTED SHAPE OF THE TELESCOPE IS SHOWN ON PAGES 3 and 4.

THE DEFLECTION OF THE EYEPIECE WITH RESPECT TO THE OBJECTIVE LENS IS THE FOLLOWING.

DEFLECTION OF EYE PIECE (Pt. 39) = 1.0234×10^{-3} inches
DEFLECTION OF OBJECTIVE LENS (Pt. 1) = 0.0

$$\therefore \Delta S = 1.0234 \times 10^{-3} \text{ IN.}$$

ANGULAR CHANGE.
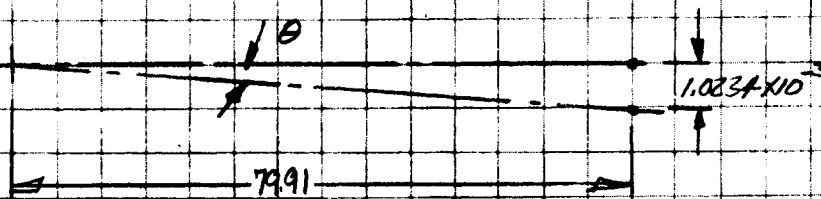
$$TAN \theta = \frac{1.0234 \times 10^{-3}}{79.91} = 0.01284 \times 10^{-3}$$

$$\theta = TAN^{-1} (1.284 \times 10^{-5})$$

$$\theta = 2.65 \text{ SEC}$$

P8.3 OF

DEFLECTION - IN X 10⁻⁵

3.0   2.0   1.0
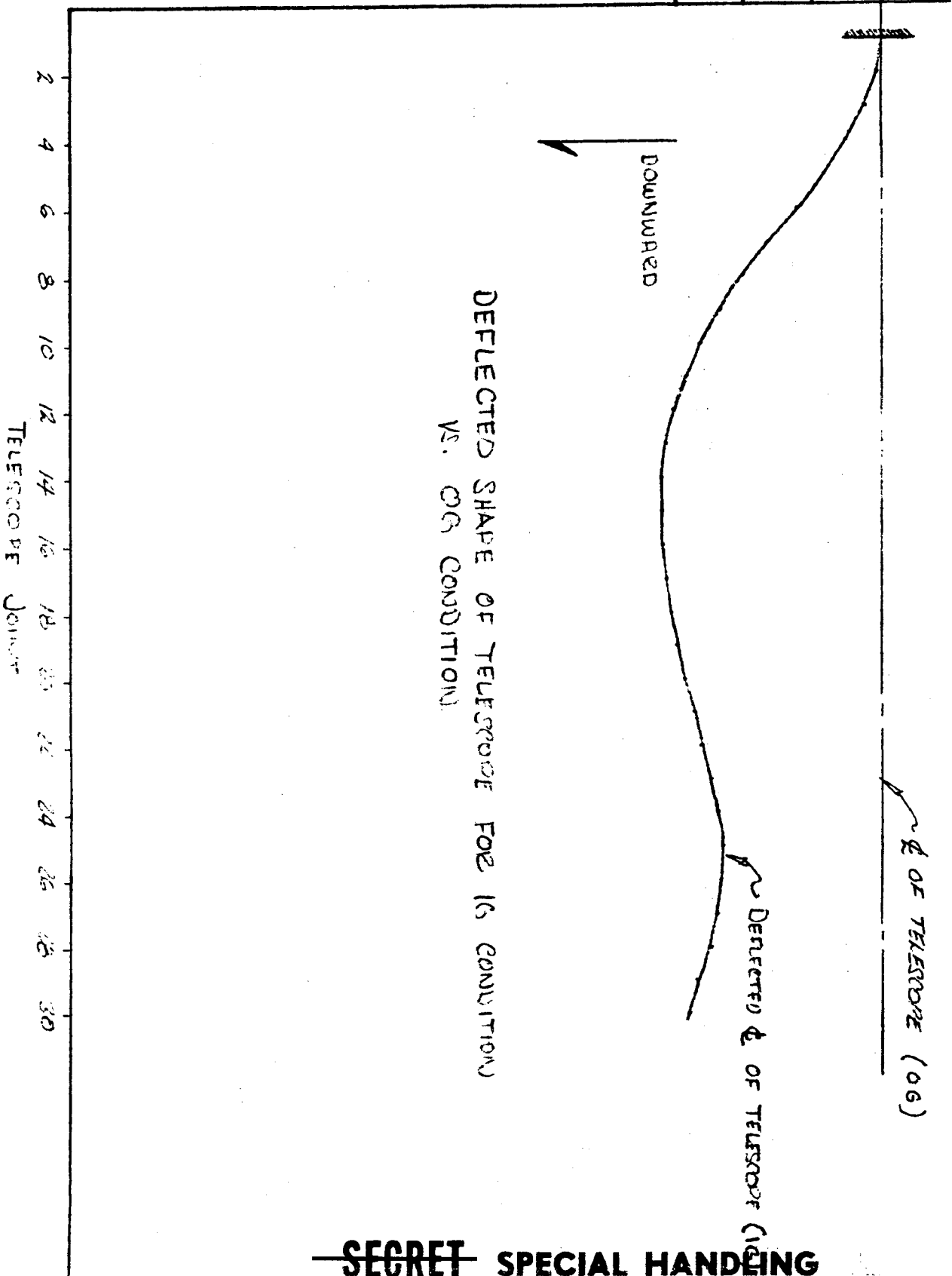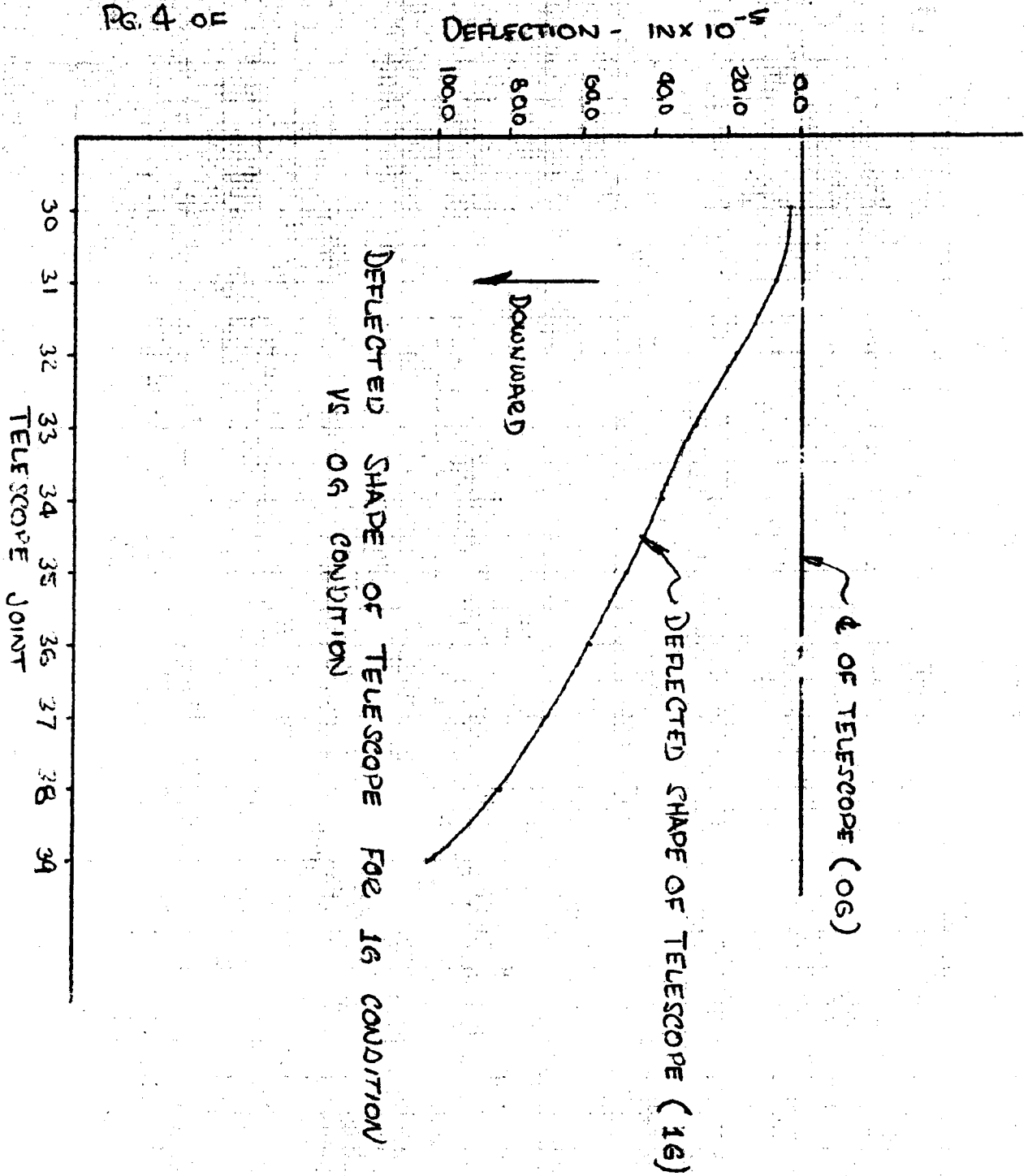
DOWNWARD

DEFLECTED SHAPE OF TELESCOPE FOR 1G CONDITION
VS. OG CONDITION

TELESCOPE JOINT

2 4 6 8 10 12 14 16 18 20 22 24 26 28 30

℄ OF TELESCOPE (OG)

DEFLECTED ℄ OF TELESCOPE (1G)

2-340

Pg. 4 of

DEFLECTION - IN X 10⁻⁵

DEFLECTED SHAPE OF TELESCOPE VS OG CONDITION

DOWNWARD

DEFLECTED SHAPE OF TELESCOPE FOR 1G CONDITION

DEFLECTED SHAPE OF TELESCOPE (1G)

¢ OF TELESCOPE (OG)

TELESCOPE JOINT

SECRET SPECIAL HANDLING

BY		GENERAL ⬤ ELECTRIC	PAGE 5 OF
CK.			MODEL
DATE	REV.		REPORT

THIS INDICATES THAT THE CHANCE IN THE
LINE OF SIGHT DUE TO THE 1G LOAD RELIEF
IS MINIMAL

SECRET SPECIAL HANDLING

FORM 1-8136 B (9-58)

2-342

NRO APPROVED FOR
RELEASE 1 JULY 2015

SECRET SPECIAL HANDLING
GENERAL ELECTRIC

BY			PAGE 1 OF
CK.			MODEL
DATE	REV.		REPORT

PRELIMINARY DEFLECTION ANALYSIS OF TRACKING
PEDESTAL DUE TO 1 B LOAD RELIEF

WHEN THE TRACKING PEDESTAL IS INSTALLED ON THE
VEHICLE THERE WILL BE SOME DEFLECTION OF THE
TRACKING PEDESTAL DUE TO ITS OWN WEIGHT. WHEN
IN-ORBIT AND IN A "O" B FIELD THE TRACKING PEDESTAL
DEFLECTION WILL BE RELIEVED. THIS WILL CAUSE
A MIS-ALIGNMENT BETWEEN THE LINE OF SIGHT
AND THE TRACKING MIRROR. THE PURPOSE OF THIS
ANALYSIS IS TO EVALUATE THE MAGNITUDE OF
THIS MIS-ALIGNMENT.

THE POINT OF PRIME CONCERN WILL BE THE CENTER
OF THE TRACKING MIRROR.

WE HAVE THE FOLLOWING CONFIGURATION WITH THE
COORDINATE SYSTEM:
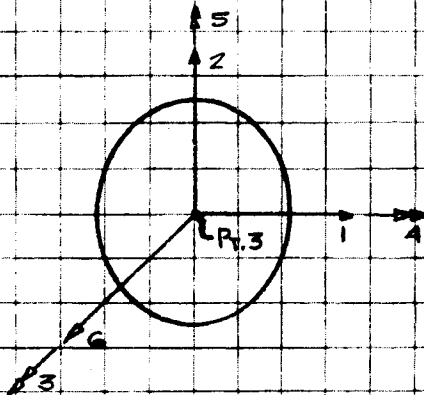
FROM THE COMPUTER PRINT-OUT.

THE DEFLECTIONS & ROTATIONS AT
PT. 3 (CENTER OF TRACKING
MIRROR) ARE:

$$\delta_1 = 1.8482 \times 10^{-4} \quad IN.$$
$$\delta_2 = -5.3370 \times 10^{-5} \quad IN.$$
$$\theta_3 = 3.8015 \times 10^{-7} \quad RAD$$
$$\theta_4 = -6.0068 \times 10^{-6} \quad RAD$$
$$\theta_5 = -2.4123 \times 10^{-5} \quad RAD$$
$$\delta_6 = 1.2585 \times 10^{-4} \quad IN.$$

NRO APPROVED FOR
RELEASE 1 JULY 2015

~~SECRET~~ SPECIAL HANDLING

GENERAL ● ELECTRIC

BY		PAGE 2 OF
CK.		MODEL
DATE	REV.	REPORT

THE RESULTANT ANGULAR ROTATION OF THE MIRROR WILL BE:

$$\Theta_R = \sqrt{\Theta_3{}^2 + \Theta_4{}^2 + \Theta_5{}^2}$$

$$\Theta_R = \sqrt{0.3805^2 + 6.0068^2 + 24.123^2} \times 10^{-6}$$

$$\Theta_R = \sqrt{0.145 + 36.0 + 582.0} \,(10^{-6})$$

$$\Theta_R = 24.8 \times 10^{-6} \text{ RAD.}$$

$$\Theta_R = 0.085 \text{ MIN} = 5.1 \text{ SEC}$$

THE RESULTANT TRANSLATIONAL MOVEMENT OF THE

$$\delta_R = \sqrt{\delta_1{}^2 + \delta_2{}^2 + \delta_6{}^2}$$

$$\delta_R = \sqrt{1.8482^2 + 0.5337^2 + 1.2585^2} \times 10^{-4}$$

$$\delta_R = \sqrt{3.41 + 0.284 + 1.58} \times 10^{-4}$$

$$\delta_R = 2.29 \times 10^{-4} \text{ IN.}$$

$$\therefore \quad \delta_R = 0.000229 \text{ IN.}$$

2.5.5 DETERMINATION OF OPTICAL PATH MISALIGNMENTS DUE TO MECHANICAL JOINT SLIPPAGE

Introduction

The amount of mechanical joint slippage has been determined and how this joint slippage will affect the optical path. On the tracking mirror a misalignment between the center of the mirror and the pressure bulkhead has been determined. For the telescope the misalignment between the eye-piece and objective lens has been determined along with the optical path misalignment between the eye piece and tracking mirror. It should be noted that the amount of mechanical joint slippage is a maximum worst case value. It assumes worst tolerances, single fastener joints, and total movement in an adverse direction. It is strictly a hypothetical number and should not be used for design purposes.

BY			
CK.			MODEL
DATE	REV.		REPORT

MISALIGNMENTS DUE TO MECHANICAL JOINT SLIPPAGE

TRACKING PEDESTAL

THE TRACKING PEDESTAL MISALIGNMENT WILL BE DETERMINED USING THE CENTER OF THE LAB MODULE PRESSURE BULKHEAD AT STATION 500 AND THE CENTER OF THE TRACKING MIRROR AT STATION 537.5 AS THE REFERENCE POINTS.

THE MECHANICAL JOINTS BETWEEN THESE TWO POINTS ARE THE FOLLOWING:

1) JOINT BETWEEN THE LAB MODULE SHELL AND THE BULKHEAD
2) JOINT BETWEEN THE PEDESTAL AND THE LAB MODULE SHELL
3) JOINT BETWEEN THE PEDESTAL AND THE ROLL HOUSING
4) JOINT BETWEEN THE ROLL SHAFT AND THE YOKE
5) JOINT BETWEEN THE YOKE AND TRUNNION
6) JOINT BETWEEN THE TRACKING MIRROR BEZEL AND THE TRUNNION.

THE HOLE AND BOLT TOLERANCES USED WILL BE FOR A CLOSE FIT PER GE PRACTICE.

FIT	BOLT SIZE	BOLT TOLERANCE	HOLE TOLERANCE
CLOSE	#10-32	$0.189 \begin{array}{c} +0.000 \\ -0.003 \end{array}$	$0.191 \begin{array}{c} +0.006 \\ -0.000 \end{array}$
CLOSE	¼"	$0.249 \begin{array}{c} +0.000 \\ -0.003 \end{array}$	$0.250 \begin{array}{c} +0.006 \\ -0.000 \end{array}$

NRO APPROVED FOR
RELEASE 1 JULY 2015

~~SECRET~~ SPECIAL HANDLING
GENERAL ELECTRIC

PAGE 2 OF

MODEL

REPORT

BY

CK.

DATE   REV.

CONSIDER JTS. 1 & 2 TO BE ¼" AND JTS 3 THRU 6 TO BE #10's.

ASSUME MAXIMUM HOLE SIZE AND MINIMUM BOLT SIZE

FOR NO. 10's $\left. \begin{array}{l} BOLT = 0.186 \\ HOLE = 0.197 \end{array} \right\}$ $\Delta = 0.011"$

FOR ¼'s $\left. \begin{array}{l} BOLT = 0.246 \\ HOLE = 0.256 \end{array} \right\}$ $\Delta = 0.010"$

$$\therefore \Delta_{TOTAL} = 2(0.011) + 4(0.010)$$

$$\Delta_{TOTAL} = 0.062 \text{ IN.}$$

DETERMINE ANGULAR CHANGE:

$$\theta = TAN^{-1} \frac{\Delta}{L} = TAN^{-1} \frac{0.062}{37.5} = TAN^{-1} 1.655^{1\cdot3}$$

$$\therefore \theta = 5.68 \text{ min} \quad (\text{ANGULAR MISALIGNMENT BETWEEN TRACKING MIRROR AND BULKHEAD})$$

TELESCOPE

THE MISALIGNMENT OF THE TELESCOPE DUE TO MECHANICAL JOINT SLIPPAGE WILL BE DETERMINED BY USING THE OBJECTIVE LENS AND THE EYE-PIECE AS REFERENCE POINTS. THE MISALIGNMENT WILL ALSO BE CALCULATED FOR THE OPTICAL PATH BETWEEN THE EYE-PIECE AND THE CENTER OF THE TRACKING MIRROR.

BY		PAGE 3 OF
CK.		MODEL
DATE	REV.	REPORT

THE MECHANICAL JOINTS BETWEEN THE EYE-PIECE AND THE OBJECTIVE LENS ARE THE FOLLOWING:

1) JOINT BETWEEN TELESCOPE AND THE PRESSURE FITTING
2) JOINT BETWEEN OBJECTIVE END AND 1ST LOW POWER GROUP HOUSING
3) JOINT BETWEEN 1ST LOW POWER GROUP HOUSING AND THE ELBOW
4) JOINT BETWEEN THE ELBOW AND THE PECHAN PRISM HOUSING.
5) JOINT BETWEEN THE PECHAN PRISM HOUSING AND THE ZOOM HOUSING.
6) JOINT BETWEEN THE ZOOM HOUSING AND THE EYE PIECE

THE TOLERANCES ON PAGE 1 ALSO HOLD FOR THIS CASE.

ASSUME ALL JOINTS TO BE # 10's.

$$\therefore \quad \begin{array}{c} BOLT = 0.186 \\ HOLE = 0.197 \end{array} \Bigg\} \ \Delta = 0.011 \ IN.$$

$$\Delta_{TOTAL} = 6(0.011) = 0.066 \ IN.$$

THE LENGTH OF THE OPTICAL PATH BETWEEN THE EYE PIECE AND THE OBJECTIVE LENS IS 79.91 IN. (NOTE: THIS CAN BE OBTAINED FROM SECT. 1.0)

$$\therefore \quad \theta = TAN^{-1} \frac{\Delta}{L} = TAN^{-1} \frac{0.066}{79.91} = TAN^{-1} (0.826 \times 10^{-3})$$

$$\theta = 2.84 \ MIN \quad \begin{array}{l} (ANGULAR \ MISALIGNMENT \\ BETWEEN \ EYE \ PIECE \ AND \\ OBJECTIVE \ LENS) \end{array}$$

SECRET SPECIAL HANDLING
GENERAL ● ELECTRIC

BY		PAGE 40E
CK.		MODEL
DATE	REV.	REPORT

THE MAXIMUM POSSIBLE CHANGE IN LINE OF SIGHT
BETWEEN THE EYE PIECE AND THE TRACKING
MIRROR WILL BE THE SUM OF THE PREVIOUSLY
CALCULATED MISALIGNMENTS:

$$\therefore \quad \Theta = 5.68 + 2.84 = 8.52 \text{ MIN}$$

(ANGULAR MISALIGNMENT
BETWEEN EYE PIECE AND
TRACKING MIRROR)

SECRET SPECIAL HANDLING

2.5.6 DETERMINATION OF MISALIGNMENTS DUE TO SHELL PRESSURIZATION AND "HOT-DOGGING"

Introduction

The effects of shell pressurization on system misalignments has been investigated. The results of this analysis are presented in this section.

The value of angular misalignment between the tracking mirror and the external fixed-fold mirror was determined using the computer program used to determine the shell stiffness matrix discussed in Section 2.5.7. Considerable additional analysis is required in this area to support error analysis.

Preliminary analysis has also been performed to determine the effect of vehicle thermal bending or "hot-dogging" on system alignment. Results-to-date indicate that "hot-dogging" may not have a significant effect.

A possible reason for this is the fact that the micrometeoroid shield acts as a buffer. Therefore, any thermal distortions are felt by the shield only and very negligible distortions are seen by the pressure shell itself.

2-351

SECRET SPECIAL HANDLING PAGE 1 OF 2

GENERAL ● ELECTRIC

BY		MODEL
CK.		REPORT
DATE	REV.	

DETERMINATION OF LINE OF SIGHT ANGULAR MIS-ALIGNMENTS DUE TO SHELL PRESSURIZATION (5 PSI ON-ORBIT ΔP VS. O PSI INSTALLATION ΔP)

THE ANGULAR MIS-ALIGNMENT OF THE LINE OF SIGHT BETWEEN THE TRACKING MIRROR AND THE EXTERNAL FIXED-FOLD MIRROR DUE TO ON-ORBIT SHELL PRESSURIZATION HAS BEEN DETERMINED. AT THE TIME OF HARDWARE INSTALLATION THE ANGULAR MIS-ALIGNMENT BETWEEN THE TWO MIRRORS WAS CONSIDERED TO BE 0° AND A ΔP≠O ACROSS THE SHELL WAS CONSIDERED. THE SHELL WAS THEN CONSIDERED TO BE PRESSURIZED SO THAT A ΔP=5 PSI EXISTED ACROSS THE SHELL WALL. THE MIS-ALIGNMENT INFORMATION WAS OBTAINED USING THE VEHICLE LAB MODULE SHELL MODEL USED TO DETERMINE THE SYSTEM MOUNTING POINTS INFLUENCE COEFFICIENTS. A UNIFORM RADIAL LOADING OF 5 PSI WAS USED TO SIMULATE A 5 PSI INTERNAL PRESSURE. THE MIS-ALIGNMENT BETWEEN THE TRACKING MIRROR AND THE EXTERNAL FIXED-FOLD MIRROR WAS THEN OBTAINED USING THE ROTATIONS AT THE AFT FOOT OF THE TRACKING PEDESTAL AND THE ROTATION OF THE SHELL PENETRATION FITTING WHICH SUPPORTS THE EXTERNAL FIXED-FOLD MIRROR. THE DIFFERENCE OF THESE TWO ROTATIONS GIVES US THE ANGULAR MIS-ALIGNMENT. THE LAB MODULE PRESSURE CAN BE CYCLED BETWEEN 4.8 PSI AND 5.2 PSI. THE MIS-ALIGNMENTS AT THESE TWO PRESSURE VALUES WERE ALSO DETERMINED.

SECRET SPECIAL HANDLING

BY		GENERAL ● ELECTRIC	MODEL
CK.			REPORT
DATE	REV.		

THE ANGULAR MIS-ALIGNMENT DUE TO A PITCHING ACTION IS :
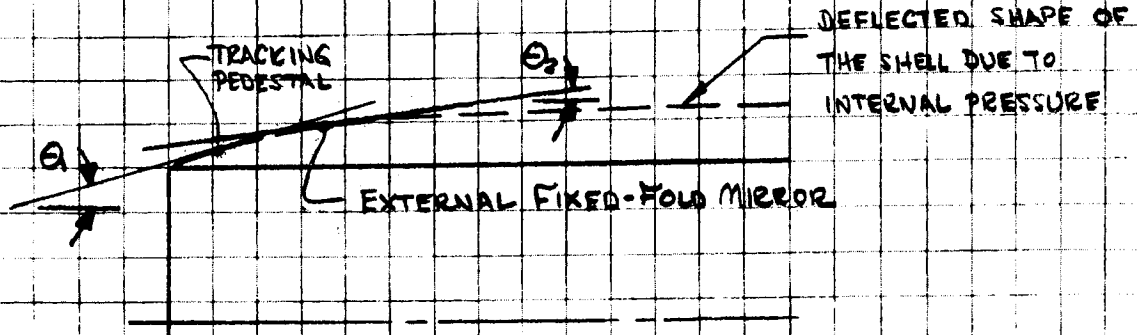
FROM THE COMPUTER PRINT-OUT :

Θ_1 (@ PEDESTAL) = 16.44651 E-4 RADIANS

Θ_2 (@ FIXED-FOLD) = 9.60326 E-4 RADIANS

$\therefore$ Θ_{TOTAL} = $|\Theta_1 - \Theta_2|$ = 6.84325 E-4 RAD.

IN TERMS OF DEGREES AND/OR MINUTES OF ARC.

Θ = 0.0392° = 2.35 MIN

THE PRESSURE IN THE LAB MODULE CAN VARY FROM 4.8 PSI TO 5.2 PSI. USING THE SAME METHODS THE ANGULAR MIS-ALIGNMENTS WERE ALSO OBTAINED. THEY ARE :

Θ = 0.0376° = 2.26 MIN @ ΔP = 4.8 PSI

Θ = 0.0408° = 2.45 MIN @ ΔP = 5.2 PSI

2.5.7 DYNAMIC ANALYSIS AND LOADS DETERMINATION

Introduction

Structural dynamic analysis of the ATS portion of the acquisition subsystem will be performed by GE. The analysis will utilize the models of system components provided by the subcontractor along with a GE generated model of the Lab Module pressure shell. This analysis will be used to determine overall systems response due to various disturbances along with the determination of loads due to these disturbances.

Discussion

The structural dynamic analysis performed by the subcontractor has been reviewed in detail by GE. It is felt that, considering the stage of the design effort, the subcontractor's analysis meets his requirements. However, considerably more dynamic analysis is required in order to verify total system performance. The subcontractor does not have the capability or the required inputs to perform such an extensive analysis. Therefore, GE will perform the analysis with certain information obtained from the subcontractor. This information will be in the form of detailed models of the telescope, fixed-fold mirror, and tracking pedestal. These models will have node points at each of the major pieces of glass or groups of glass so that the effects of disturbances on system performance can be monitored and evaluated. Stiffness matrices for each of these components will be generated by the subcontractor and then incorporated into an overall system matrix, which will include the coupling effects of the vehicle shell. The vehicle shell will be represented by a 36 x 36 stiffness matrix which represents six degrees of freedom at the six system mounting points. This matrix was generated by GE because the associate contractor could not generate the needed information prior to June 1968. The information needed was the 36 x 36 matrix for this analysis along with the local shell flexibilities which were needed by the subcontractor for design purposes. The information was initially generated in the form of a 36 x 36 influence coefficient matrix and then inverted to obtain the stiffness matrix. The influence coefficient matrix was obtained by modeling the DACO Lab Module pressure shell.

The model represented an 80-inch long portion of the Lab Module shell. The pressure bulkhead at Station 517 was represented by a series of radial springs which represented the bulkhead flexibility. The forward end of the shell was considered to be simply supported. The matrix was generated using structural analysis programs on the GE 635 computer. The disturbance mentioned previously will come from many sources. Among the more important ones will be: tracking and slewing of both the acquisition and main optics tracking mirrors; ACTS firings; opening and closing of the thermal cover and protective shroud, and activation of the acquisition system controls in order to change power, etc.

The system model will also be used to evaluate the response to pyrotechnic shock and random vibration so that realistic design loads can be used. At the onset of the design of this system the subcontractor had used a steady-state load of 35 g's in each direction to design the structure. This was obtained from DR1100 which stated that the system was to see a 35g shock pulse for 2.6 milliseconds. This was a very conservative, if not unrealistic approach, therefore it was felt that it was necessary to clarify the loading so that a realistic structure could be obtained. To accomplish this, powered flight accelerations were obtained using load factors from the Martin Second Cycle Loads Report modified to show trends obtained from the 3A load cycle. The "bird-cage" was used as a basis for determining these loads. The powered flight load factors are as follows:

<div align="center">Limit loads (ULT = 1.4 x LIMIT)</div>

	$\underline{X}$	$\underline{Y}$	$\underline{Z}$
Max. X load	±10.0	±0.72	±0.72
Max. Y load	+3.0 / -1.0	±1.8	±0.72
Max. Z load	+3.0 / -1.0	±0.72	±1.8

The X, Y, and Z directions are in the vehicle coordinate system.

The shock loading was also clarified by giving the subcontractor the shock curve (Figure 2.5-2). This curve was obtained from SAFSL 10003 and reflects a reduction of peak shock of 3.5. The curve was also modified by extending the curve past the 100 cps cut-off shown in SAFSL 10003.

The Lab Module shell stiffness and flexibility matrices are also included after the shock curve.

Figure 2.5-2. Shock Curve

BY			MODEL
CK.			
DATE	REV.		REPORT

THE STIFFNESS MATRIX FOR THE SUBSYSTEM ALPHA MOUNTING POINTS WAS OBTAINED BY MODELING THE LAB MODULE SHELL FROM DACo DRAWING 1872094 AND OBTAINING AN INFLUENCE COEFFICIENT MATRIX USING THIS MODEL. THE INFLUENCE COEFFICIENT MATRIX WAS OBTAINED BY USING THE GE 635 COMPUTER. UNIT FORCES AND MOMENTS WERE APPLIED TO THE MOUNTING POINTS IN A RADIAL, TANGENTIAL, AND LONGITUDINAL DIRECTIONS THUSLY YIELDING A 36 x 36 MATRIX. THE MATRIX WAS THEN INVERTED TO OBTAIN THE STIFFNESS MATRIX.

BY		PAGE
CK.		MODEL
DATE	REV.	REPORT

LOCATION OF MOUNTING POINTS

○ Pt. 5   ○ Pt. 6

31.416" ARC FROM
Y AXIS TOWARD
-Z AXIS

——————————————————— ± Y AXIS

26° FROM Y
AXIS TOWARD
+Z AXIS

11.870" CHORD
@ 60.0" R

○ Pt. 3

Pt. 4

○ Pt. 1   ○

○ Pt. 2

STA. 518.91   528.66   549.56 556.4 563.24

BY				MODEL
CK.				
DATE	REV.			REPORT

DIRECTION OF LOADINGS

M_T F_R

M_X

F_X IS APPLIED
PERPENDICULAR
TO THE PLANE
OF THE PAPER
($+$ INTO PAPER)

M_R F_T
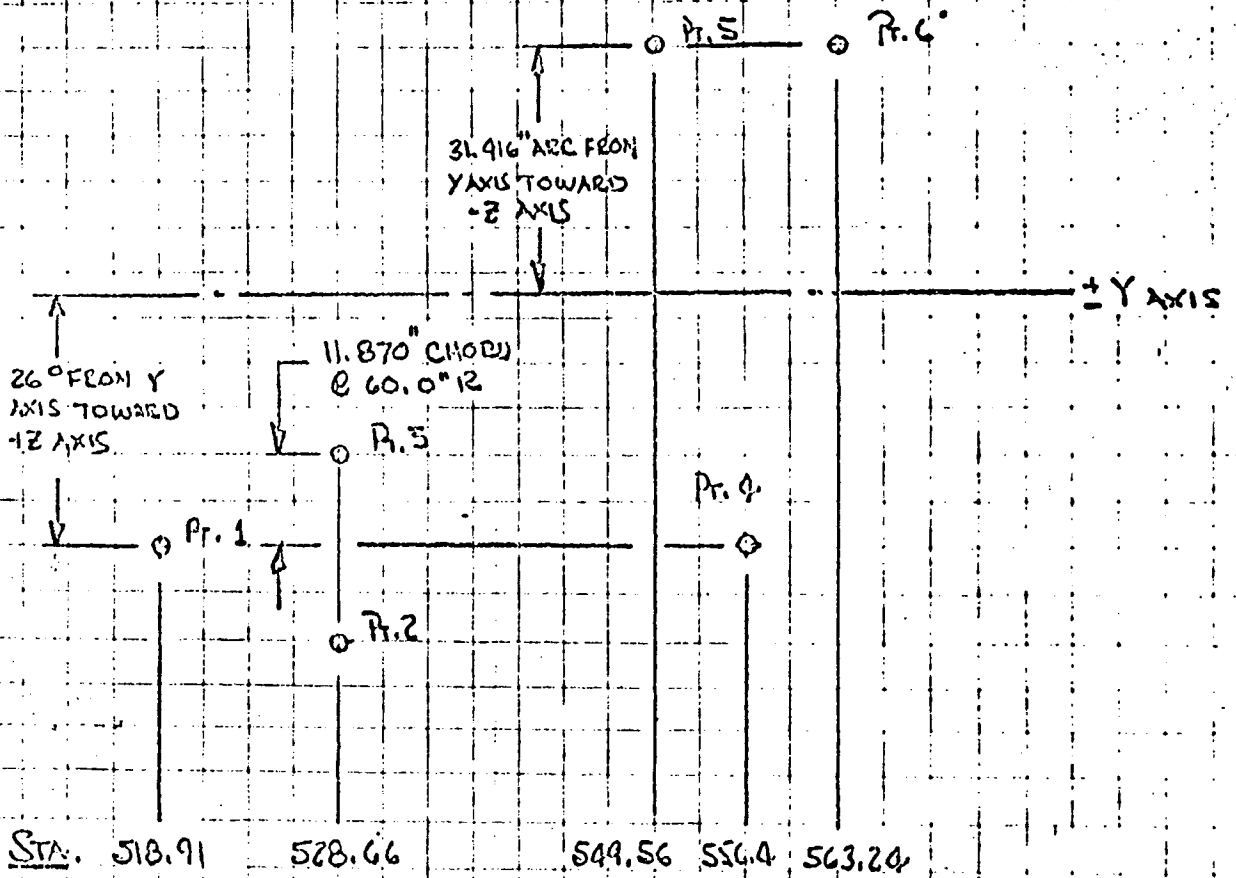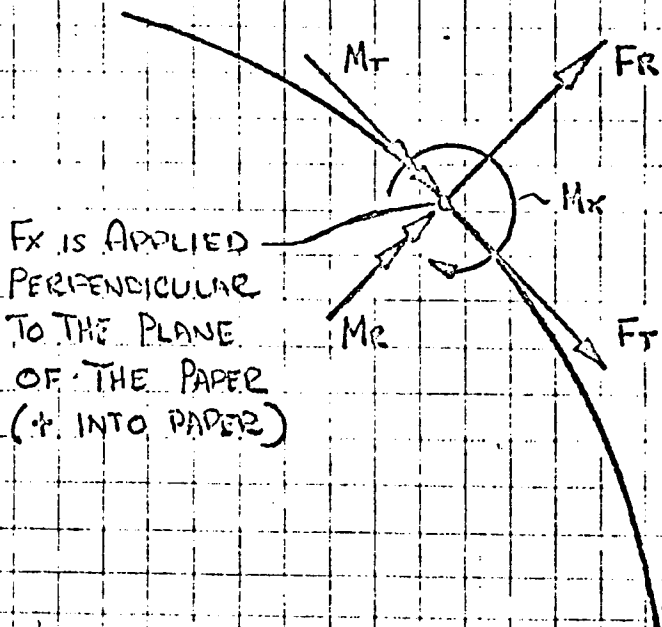
NOTE: ALL DIRECTIONS SHOWN ARE ($+$)

SECRET SPECIAL HANDLING PAGE 4

GENERAL ⊕ ELECTRIC

BY			
CK.			MODEL
DATE		REV.	REPORT

STIFFNESS MATRIX SET-UP

	δ_{1R}	δ_{1T}	δ_{1X}	θ_{1R}	θ_{1T}	θ_{1X}	δ_{2R}	δ_{2T}	δ_{2X}	θ_{2R}	θ_{2T}	θ_{2X}							δ_{6R}	δ_{6T}	δ_{6X}	θ_{6R}	θ_{6T}	θ_{6X}
F_{1R}	$a_{1,1}$	$a_{1,2}$	$a_{1,3}$	$a_{1,4}$	$a_{1,5}$																			$a_{1,36}$
F_{1T}	$a_{2,1}$	$a_{2,2}$																						
F_{1X}	$a_{3,1}$		$a_{3,3}$																					
M_{1R}	$a_{4,1}$			$a_{4,4}$																				
M_{1T}	$a_{5,1}$				$a_{5,5}$	$a_{5,6}$	$a_{5,7}$	$a_{5,8}$																$a_{5,36}$
M_{1X}	$a_{6,1}$					$a_{6,5}$																		
F_{2R}						$a_{7,5}$																		
F_{2T}						$a_{8,5}$																		
F_{2X}																								
M_{2R}																								
M_{2T}																								
M_{2X}																								
$\cdot$																								
$\cdot$																								
$\cdot$																								
$\cdot$																								
F_{6R}																								
F_{6T}																								
F_{6X}																								
M_{6R}																								
M_{6T}																								
M_{6X}	$a_{36,1}$			$a_{36,5}$																				$a_{36,36}$

SECRET SPECIAL HANDLING

BY		GENERAL ⊕ ELECTRIC	PAGE 5
CK.			MODEL
DATE	REV.		REPORT

RELATION OF COMPUTER OUTPUT TO MATRIX

STIFFNESS MATRIX

1

$$a_{11} \quad a_{12} \quad a_{13} \quad a_{14}$$
$$a_{15} \quad a_{16}$$
$$a_{1,36}$$

2

$$a_{21} \quad a_{22} \quad a_{23} \quad a_{24}$$
$$a_{25} \quad a_{26}$$
$$a_{2,36}$$

36

$$a_{36,1} \quad a_{36,2} \quad a_{36,3} \quad a_{36,4}$$
$$a_{36,5} \quad a_{36,6}$$
$$a_{36,36}$$

STIFFNESS MATRIX

1

3.91161353E+04	-2.29933176E+04	-3.89229463E+04	-2.27625337E+04
3.79223315E+04	2.00812130E+02	4.31131836E+02	-2.14956877E+02
-2.52589294E+04	5.15456586E+03	-2.76576425E+03	1.25953209E+06
3.28739201E+02	-2.87596295E+03	2.97615193E+04	-9.69928459E+03
6.79185444E+02	-2.90265877E+01	-1.19762494E+02	-4.82572490E+03
-7.79181653E+03	1.48410760E+03	-6.49540182E+02	2.60260026E+01
-1.28373763E+01	-1.44306292E+02	2.57304945E+01	2.99124062E+02
1.25023373E+01	-5.75244560E-01	4.27731332E+00	-6.17502580E+01
-7.94080078E+00	-1.14213322E+02	1.11620057E+01	-7.49403438E-01

2

-2.29933237E+04	3.60172072E+06	1.14779057E+05	-1.71586094E+05
-2.69854788E+04	-2.29429035E+04	4.13251282E+03	-5.04820632E+04
1.48786471E+04	-2.06113076E+04	1.33780667E+04	2.25957314E+02
1.61202467E+04	-7.45522129E+04	-3.36667360E+04	7.67359939E+04
-9.51753113E+03	7.94524162E+02	-3.96962959E+02	-1.03077360E+04
4.78250283E+04	-2.93847363E+03	1.58103447E+03	-7.20141554E+01
-8.96974316E+01	7.72369682E+02	-1.49480731E+02	-1.91452301E+03
-1.07980592E+02	3.42926767E+00	-5.69307628E+01	2.28911343E+02
2.11345034E+01	5.86616479E+02	-5.72669783E+01	3.45843170E+00

3

-3.89229409E+04	1.14779796E+05	4.36931694E+06	4.96945151E+04
-7.30522979E+04	-2.61147827E+03	-3.03316113E+03	1.35286840E+05
1.69741457E+05	-1.33233654E+05	5.99071831E+04	-1.49907449E+02
1.41793322E+03	-1.29537339E+04	-2.34079996E+05	2.40578560E+05
-4.81973563E+04	2.10993214E+02	-1.41933232E+03	5.35695444E+04
1.31559063E+05	-2.62225137E+04	9.11146387E+03	-4.24144184E+02
-2.31033175E+02	1.60736414E+03	-8.81455269E+02	-3.83722739E+03
-6.76182013E+01	-4.12523496E+00	-1.76161744E+02	1.73293634E+03
-9.18515297E+02	3.10813156E+03	-9.51894064E+01	-3.39248928E+00

4

-2.27625315E+04	-1.71586078E+05	4.96944951E+04	5.77406141E+05
-4.95395496E+04	1.06794934E+03	-7.75862763E+02	6.23611450E+03
3.74609653E+04	-1.90840338E+04	5.14321213E+03	5.54687706E+02
9.20186893E+02	-6.71229980E+03	-3.87903223E+04	1.13636917E+04
-9.90257186E+02	-2.70714725E+02	1.06508790E+02	3.10901175E+03
1.09839579E+04	-2.17525762E+03	1.01237084E+03	5.58703553E+01
-2.07021421E+01	2.29954921E+02	-3.87281308E+01	-4.39181112E+02
1.38285821E+02	-1.37827727E+01	-1.12082635E+00	7.58754139E-01
6.74306989E+00	5.09536910E+02	5.21563507E+01	-1.39032494E+01

5

8.06805508E+04	-2.07304457E+04	-7.30523165E+04	-4.95393511E+04
-5.00232451E+04	1.27412965E+04	-6.69174640E+03	3.35317945E+01
-1.58206799E+02	8.06060724E+03	6.08287646E+04	-1.50250361E+04
2.43402868E+02	-8.25383097E+01	-3.43380470E+02	-8.45901111E+03
-1.43553621E+04	3.21016675E+03	-1.42302692E+03	5.70823994E+01
2.14128726E+01	-2.86053736E+02	4.66960864E+01	5.85851372E+02
2.50613807E+01	-1.52709191E+00	4.79382402E+00	-1.07242736E+02
-9.21172476E+00	-1.91933661E+02	2.13065824E+01	-1.90405391E+00

6

2.05812136E+02	-2.09422963E+04	-2.61147772E+03	1.66794917E+03
2.75644203E+02	1.56943643E+03	5.30635152E+01	1.87601738E+02
-1.43232389E+02	3.68298360E+02	-1.66192343E+02	-2.27096032E-01
-7.91878679E+01	7.89915904E+02	7.97342697E+02	-2.65951649E+03
1.23670170E+02	-5.64696324E+00	2.04185539E+00	-1.71644211E+02
-1.16628542E+03	5.76844408E+01	-1.86221712E+01	2.21393515E+00
2.39262473E+00	-1.45177861E+01	8.31527245E+00	3.72965641E+01
1.12647359E+00	2.82396302E-02	1.76533552E+00	-1.16579932E+01
2.23586091E+00	-2.50660693E+01	1.07277787E+00	2.55430343E-02

7

4.31131741E+02	-9.13249854E+03	-3.03315616E+03	-7.75652969E+02
-6.24312380E+00	5.30635095E+01	2.63742907E+03	-3.61757363E+04
-1.29221138E+03	2.14370179E+03	-1.12770270E+03	-2.59721940E+01
7.63978483E+01	1.19729518E+03	1.37104280E+03	2.27109648E+02
-6.36451380E+01	6.59168142E+00	1.55536479E+01	-2.36486053E+03
-5.66349190E+02	-5.60327120E+01	8.30012560E+01	4.90198775E+00
-2.29265401E-03	1.24596895E+01	3.46022817E+00	-2.03518577E+01
-9.99592118E-01	7.63315467E-02	1.35832386E+00	-7.43448472E+00
2.14401040E+01	-1.41739024E+01	-1.45600187E+00	9.19006151E-02

8

-2.14957140E+02	-5.94382575E+04	1.35286988E+05	6.23611230E+03
-1.87456291E+01	1.87601311E+02	-3.61757363E+04	1.58301791E+06
1.16072604E+05	-9.55398826E+04	4.76260454E+04	-1.34126579E+03
-1.90289628E+02	4.07199640E+03	-9.98216494E+04	3.05102246E+04
-4.58955556E+03	1.41791840E+02	6.27326180E+02	-5.11832935E+03
8.14126787E+04	-8.41834755E+03	4.12823954E+03	-1.72105621E+02
-8.91997550E+01	4.14288456E+02	-1.44965790E+02	-9.01996330E+02
-2.13327515E+01	1.25739244E+00	-2.63218737E+01	2.25380350E+02
-5.63885567E+02	3.16450550E+02	-1.93055360E+01	1.80990310E+00

2-364

9

-2.52509297E+04	1.48735707E+04	1.09741364E+05	3.74699663E+04
-5.90232475E+04	-1.43200265E+02	-1.29221193E+03	1.10572563E+05
1.17721725E+05	-9.46872480F+04	4.25906147E+04	-1.02736280E+02
-7.04560607E+02	-2.29556667E+04	-1.26709353E+05	9.79197327E+03
2.23575757E+03	1.22297296E+02	2.33072159E+03	5.74871167E+04
-8.38344592E+03	-1.42751177E+04	7.28598053E+03	-2.53574240E+02
-2.96346090E+01	7.34059277E+01	-2.14139223E+02	-2.36054142E+02
-1.63724005E+01	2.32207513E+00	-2.94312444E+01	5.73007134E+01
-6.23430992E+02	1.14960735E+02	-1.77419931E+00	2.80716914E+00

10

5.15490470E+03	-2.66112915E+04	-1.33233650E+05	-1.20842354E+04
1.27412957E+04	3.60290290E+02	2.14376137E+03	-9.53390506E+04
-9.45075460E+04	1.01643247E+05	-1.31346700E+04	1.03771357E+02
5.09023617E+02	1.27622600E+04	8.52200040E+04	-2.37092053E+04
5.58991620E+03	-6.72361503E+01	-1.82162379E+02	-2.30226772E+04
-6.37736987E+04	4.06146411E+03	-1.95802248E+03	1.67504679E+02
3.19063770E+01	-1.73290796E+02	1.43225515E+02	4.63652670E+02
6.73064439E+00	1.78734120E-01	3.67360056E+01	-2.39894199E+02
6.17431671E+02	-3.91291701E+02	-2.11969456E+00	-2.32691586E-02

11

-2.76576407E+03	1.33789595E+04	5.99071036E+04	5.14381274E+03
-6.69174615E+03	-1.66192354E+02	-1.18779395E+03	4.76260415E+04
4.20006157E+04	-1.31346877E+04	9.53603520E+04	-4.69496751E+01
-1.49465137E+02	-5.80272205E+03	-3.94852060E+04	1.30227400E+04
-1.23760331E+03	3.06590930E+01	0.75169005E+01	1.05458639E+04
2.92003975E+04	-2.40255554E+03	3.82233906E+02	-7.65564117E+01
1.44206342E+01	8.17465540E+01	-6.66872416E+01	-2.13227541E+02
-3.00171280E+00	-5.54024000E-02	-1.65369017E-01	1.47329174E+02
-2.76114574E+02	2.19754751E+02	0.20262352E-01	3.74738420E-02

12

8.25970617E+00	2.25956516E+02	-1.50031076E+02	5.54687454E+02
-3.35300688E+01	-2.27093604E-01	-2.59721572E+01	-1.34125410E+03
-1.80755650E+02	1.03771472E+02	-4.68497409E+01	7.37885567E+02
-5.97503674E+04	1.31780857E+02	1.78900041E+02	-7.18052312E+01
1.25117540E+01	-1.63060609E+00	-6.29927043E+01	3.27472290E+00
-1.40566029E+02	-4.22690811E+01	1.57825027E+01	1.07621384E+00
5.27503730E-01	1.05523529E+00	1.99457267E+00	-9.34926463E-02
3.53639670E-01	-4.46467003E-02	1.27368501E-01	3.65272543E+00
-1.80260021E+00	3.77742354E+00	2.56232168E-01	-5.43985124E-02

13

3.28737942E+02	1.61262546E+04	1.41793626E+03	9.26179764E+02
-1.58206992E+02	-7.91860159E+01	7.63971748E+01	-1.96229494E+02
-7.64060852E+02	3.69003281E+02	-1.49265001E+02	-5.97502995E+00
2.22267376E+03	-1.42076644E+03	1.45033727E+03	2.34376746E+03
-4.92702976E+02	4.11467916E+00	-4.51943469E+01	2.00996899E+03
9.37749929E+02	-2.66391660E+01	-3.02469972E+01	3.24041254E-05
-2.39686687E+01	1.55048126E+02	-4.55190123E+00	-3.35065246E+02
-9.47878551E+00	-6.80922629E-01	-1.18995898E+01	1.15285470E+02
1.93605721E+01	2.16591879E+02	-1.44264439E+01	-4.26883373E-01

14

-2.87590598E+03	-7.45521494E+04	-1.29637795E+04	-8.71230054E+03
8.96060408E+03	7.28915930E+02	1.19729530E+03	4.67199925E+03
-2.29556653E+04	1.27621993E+04	-5.80072131E+03	1.31780083E+02
-1.48078638E+03	2.83619547E+05	4.04093647E+04	-1.97105439E+04
7.93231393E+02	-2.79697967E+02	-3.26672870E+03	-3.56520084E+04
-3.85809009E+04	5.03940200E+03	-1.44356722E+03	3.08508110E+02
-1.80620480E+02	-3.17225929E+02	8.06676697E+02	6.24910049E+02
8.26252956E+01	-2.10849836E+01	-2.76596527E+02	6.91573410E+02
-3.31867668E+02	2.39612689E+03	6.62848854E+01	-2.40525056E+01

15

2.97615181E+04	-3.36667651E+04	-2.34880242E+05	-3.87293311E+04
6.08287646E+04	7.98342674E+02	1.37104327E+03	-9.98816592E+04
-1.26709580E+05	8.56220918E+04	-3.94052619E+04	1.75999615E+02
1.45833752E+03	4.04693799E+04	8.44929727E+05	-7.75530234E+04
5.45207501E+03	-2.37967274E+02	-1.47302866E+03	-5.78948516E+04
-1.36134805E+05	2.87338152E+04	-1.24824974E+04	2.35939701E+02
2.58687954E+02	-2.37873944E+03	-7.64439117E+02	5.63797956E+03
9.54571743E+01	2.41141090E+00	1.80996025E+02	-1.22477637E+03
-7.55233543E+02	-3.27467487E+03	8.59080611E+01	2.14629263E+00

16

-9.69928442E+03	7.67358965E+04	2.40578543E+05	1.13638921E+04
-1.50250353E+04	-2.65951666E+03	2.27109440E+02	3.05102029E+04
9.09196277E+03	-2.37092026E+04	1.88227445E+04	-7.18015041E+01
2.34376682E+03	-1.97105400E+04	-7.75530039E+04	2.72930650E+05
-8.07377901E+03	1.38217369E+02	-2.59159737E+02	2.65964224E+04
1.79150209E+05	-5.19475038E+03	1.25996156E+03	-2.65773145E+02
-2.11956666E+02	1.29570771E+03	-2.01204505E+02	-3.05800416E-05
-5.67708921E+01	-6.76819759E+00	-1.77393237E+02	1.27256167E-05
-2.97643442E+00	2.60239951E+03	-6.80944412E+01	-6.53637626E+00

~~SECRET~~ **SPECIAL HANDLING**

17

6.79185455E+02	-9.51752478E+03	-4.81976597E+04	-9.92207590E+02
2.43402870E+02	1.23670002E+02	-6.30451263E+01	-4.58955530E+03
2.23575726E+03	3.58951665E+03	-1.23800336E+03	1.25115459E+01
-4.92702866E+02	7.93231527E+02	5.45287495E+03	-8.87370277E+03
4.86921491E+04	-1.54446520E+01	3.52213712E+01	-4.91146881E+03
-2.00914739E+04	5.64555397E+02	-1.93544118GE+02	4.63508012E+01
4.49656806E+01	-2.52769648E+02	-4.84053124E+01	6.15420802E+02
1.20671419E+01	1.76690024E+02	2.99306486E+01	-2.47246044E+02
-1.51931414E+02	-4.99469218E+02	2.03600234E+01	1.60596281E+00

18

-2.90260822E+01	7.94585506E+02	2.10493780E+02	-2.70714700E+02
-2.05384026E+01	-5.64696348E+00	6.59167939E+00	1.41701790E+00
1.82296905E+02	-5.72361498E+01	3.80596700E+01	-1.00060671E+00
4.11467465E+00	-8.79697212E+02	-2.37007232E+02	1.30217371E+02
-1.54446564E+01	7.30370769E+02	2.62826674E+01	1.15447653E+02
1.37473417E+02	-4.26657978E+00	8.39130806GE-01	-1.11013636E+00
9.13882107E-01	-1.27002697E+01	-1.31491695E+00	2.46362731E+01
7.36006834E-01	2.84431207E-02	3.65684611E-02	-3.12557685E+00
-2.73060951GE+00	-6.33069557E+00	7.24344060E-01	1.78723577E-02

19

-1.19708060E+02	-3.95973679E+02	-1.41951342E+03	1.06808927E+02
-3.43380096E+02	2.04189993E+00	1.86536449E+01	6.27287179E+02
2.33871658E+03	-1.82161715E+02	8.75184151E+01	-6.20927196E+01
-4.51943469E+01	-3.20672406E+03	-1.47323798E+03	-2.59138371E+02
3.52219989E+01	2.60320581E+01	1.97022600E+03	6.20726822E+02
1.40116205E+03	2.83905159E+03	-8.64044559E+02	-8.71003995E+01
-2.10890030E+00	-7.54737263E+01	-5.94634557E+01	5.54679670E+01
-4.63495684E+00	9.48763585E-01	-2.50554002E+00	-1.19030316E+02
7.37242994E+01	-1.29726680E+02	-4.87346917E+00	1.24384964E+00

20

-4.02572433E+03	-1.03078539E+04	5.35655303E+04	3.19901260E+03
-8.45901025E+03	-1.71644217E+02	-2.36406957E+03	-5.11703575E+03
5.74871230E+04	-2.30226770E+04	1.05450228E+04	3.27472533E+00
2.00996663E+03	-3.56520028E+04	-5.75948472E+04	2.65904231E+04
-4.91146257E+03	1.15447865E+02	6.20227379E+02	1.10026033E+02
2.52456272E+04	-2.82927711E+03	8.72673966E+02	-5.42947500E+02
6.94657880E+01	-1.03896312E+03	-1.80642098E+02	2.41372417E+03
-1.90788696E+01	2.67979383E+00	1.02386201E+02	-4.57074615E+02
-3.03452808E+02	-6.62114E+03	-3.25698771E+01	6.16483933E+00

~~SECRET~~ **SPECIAL HANDLING**

2-367

25

1.28373749E+01	-8.65973677E+01	-2.31033198E+02	-2.77091417E+01
0.14128650E+01	2.30222720E+00	-2.29220622E-03	-3.01207024E-01
-0.06446245E+01	3.19053089E+01	-1.44202374E+01	3.27537357E-01
-0.39657671E+01	-1.17020504E+02	2.58687922E+02	-2.61956659E+02
4.49656787E+01	0.13082054E-01	-8.10294692E+00	6.94637899E+01
-8.40204983E+01	-1.70879650E+01	7.14703447E+00	1.16584961E+20
1.84033620E+03	-2.32992601E+02	8.32769545E+02	-3.97916064E+03
-7.56359390E+02	4.69732670E+00	-6.29561100E+02	-1.39954477E+02
-3.21229419E+03	-1.74093702E+03	4.09613023E+01	3.61204390E+00

26

-1.44326303E+02	7.73362470E+02	1.62736343E+03	2.29954859E+02
-2.76653656E+02	-1.42177906E+01	1.24596899E+01	4.14228158E+02
7.34067049E+01	-1.73290792E+02	0.17466897E+01	1.63524906E+00
1.58043130E+02	-8.17226169E+02	-2.37873962E+03	1.29570262E+03
-2.52709665E+02	-1.27002721E+01	-7.54737463E+01	-1.03296327E+03
3.40636101E+02	-5.01412625E+01	1.63900113E+01	1.77744007E+00
-8.32992645E+02	2.26610908E+05	1.05020135E+03	2.24070910E+05
-1.41764915E+02	-5.90387573E+02	3.50496101E+02	-1.61469020E+05
1.06389044E+03	4.59981675E+05	-3.07242878E+02	1.74121158E+02

27

0.57304674E+01	-1.40491665E+02	-8.81456970E+02	-3.37281322E+01
4.66960789E+01	8.31526613E+00	3.46022364E+00	-1.44936008E+02
-0.14173050E+00	1.45025401E+02	-6.60374050E+01	1.09456565E+02
-0.59214133E+00	8.06673500E+02	-7.04460292E+02	-9.01266850E+02
-1.04059844E+01	-1.31491654E+00	-5.94635015E+01	-1.30648619E+02
-3.04368580E+02	-3.73142276E+01	-2.07771173E+01	1.63391957E+00
0.32862564E+02	1.05019990E+03	5.79571100E+05	3.86909928E+01
-4.56912150E+03	6.47150844E+00	3.03604751E+03	-4.12446365E+02
-2.75284580E+05	-3.04366617E+03	2.26483051E+03	2.20389748E+01

28

0.99123833E+02	-1.01451750E+03	-3.33722391E+03	-4.39180750E+02
0.85851126E+00	3.72966050E+01	-2.03516008E+01	-9.01995415E+02
-0.76052290E+02	4.63662261E+02	-2.13227533E+02	-9.05277227E+02
-3.35085644E+02	6.24910667E+02	5.63797797E+03	-3.25829242E+03
6.15419553E+02	2.40362674E+01	5.54677320E+01	2.41373101E+03
-7.43899727E+02	-1.97226761E+02	9.15112991E+01	6.13471943E+00
-3.97916144E+03	2.24070600E+05	3.26027981E+01	9.27532588E+06
0.18264160E+02	-8.98505471E+02	2.26641399E+02	-4.77614000E+05
-1.01733210E+03	-2.38740700E+05	-2.71151657E+03	-2.24272270E+02

29

1.26923342E+01	-1.87988725E+02	-6.78122747E+01	1.57875796E-02
7.55613643E+01	1.12647387E+20	-9.09521917E-01	-2.13327825E+01
-1.63723969E+01	6.73263254E+20	-3.20171443E+00	3.53632697E-01
-9.47278623E+00	8.26252677E+01	9.54571628E+01	-5.67708945E+01
-1.20671401E+01	7.36026980E-01	-4.63495976E+00	-1.90782727E+01
-2.90778530E+00	-2.13626750E+01	8.50276220E+00	5.58273591E-01
-7.56359436E+02	1.41764968E+02	-4.56912494E+03	8.18264122E+02
3.25188518E+04	-4.04385940E+00	9.19110031E+02	-8.53066635E+01
8.95013916E+03	3.37129504E+03	1.15470439E+03	-4.03309453E+00

30

-9.79244591E-01	3.42928457E+00	-4.12528878E+00	-1.37027757E+01
-1.53769925E+00	2.82396721E-02	7.83315506E-02	1.25739938E+00
2.34027161E+00	1.78733967E-01	-5.54294546E-02	-4.46467824E-02
-6.80900036E-01	-2.10249878E+01	2.41141191E+00	6.16869710E+00
1.76609826E+00	2.84431105E-02	9.48763035E-01	2.67978577E+00
-1.94528658E-01	-1.28172727E+00	-1.71072816E-02	6.47578053E-02
4.69732600E+00	-5.90687650E+02	6.47151542E+00	-8.98505768E+02
-1.04385972E+00	7.49292915E+02	-2.11166406E+00	1.79687006E+02
-1.40169353E+01	1.75277228E+02	6.50130045E+00	-1.50567868E+00

31

4.27781326E+00	-5.69311496E+01	-1.76861773E+02	-1.12081912E+00
4.79389777E+00	1.76533605E+00	1.35032469E+00	-2.03218744E+01
-2.94313959E+01	3.67366825E+01	-1.65369136E+01	1.27366573E-01
-1.10959967E+01	-2.76596501E+02	1.80956233E+02	-1.77393276E+02
8.99306490E+01	3.65064904E+02	-2.50354055E+00	1.02367612E+02
-1.63906941E+02	1.30320827E+01	-6.60585245E+00	7.55766009E-01
-6.29561226E+00	3.57496145E+02	3.03695135E+03	2.26642004E+02
-1.91100016E+02	-2.11166304E+00	1.81871898E+03	-6.78375168E+02
-1.24356315E+02	7.04608655E+02	-2.96195772E+02	-1.89889317E+00

32

-6.17502337E+01	2.28911428E+02	1.73293423E+03	7.58753042E+01
-1.07248720E+02	-1.16572069E+01	-7.43448651E+00	2.25379921E+02
8.73077121E+01	-2.30794171E+02	1.87329172E+02	3.65273892E+00
1.15085480E+02	6.91373757E+02	-1.22477629E+03	1.27256131E+03
-2.47046000E+02	-3.12557462E+00	-1.19930332E+02	-4.37074378E+02
9.44263135E+02	-2.40569977E+02	1.04690449E+02	6.99762335E+00
-1.39954420E+02	-1.61469020E+05	-4.12439732E+02	-4.27614082E+05
-8.53806433E+01	1.79586960E+02	-6.78375099E+02	2.25817727E+05
-7.16535016E+02	-2.50217865E+05	8.61367718E+02	-6.15823809E+02

33

-7.94276763E+00	2.11436844E+01	-9.18512512E+02	6.74264718E+02
-9.21172006E+00	2.25520036E+00	2.14431273E-01	-5.83326704E+02
-6.25431953E+02	6.17431625E+22	-2.79414062E-02	-1.07632741E+00
1.93605797E+01	-3.71867356E+02	-7.55252227E+02	-2.07643362E+02
-1.51931412E+02	-2.78060609E+00	7.57243423E+01	-3.03452839E+02
-7.29475990E+02	4.50216330E+02	-1.24009804E+02	2.25840343E+20
-5.21209404E+03	1.05329037E+03	-2.75224512E+05	-1.01733212E+23
2.95014035E+03	-1.49169354E+01	-8.24354019E+02	-8.16553804E+02
5.77611013E+05	2.75925012E+03	-5.03897552E+03	-1.28644761E+01

34

-1.14213371E+02	5.86594772E+02	3.10012411E+03	1.59536434E+02
-1.91933570E+02	-2.54663671E+01	-1.41740059E+01	3.16402563E+02
1.14507332E+02	-3.91801963E+02	2.19754316E-72	3.77743601E+00
2.16501757E+02	2.30612406E+03	-3.27467603E+03	2.68209862E+03
-1.99409921E+02	-6.35076040E+00	-1.29728735E+02	-1.21213254E+03
1.43251254E+03	-2.04389658E+02	1.00103034E+02	3.76670666E+00
-1.74093797E+03	4.59981863E+05	-3.04567307E+03	-2.22740606E+05
5.37129400E+03	1.73277309E+02	7.54208563E+02	-2.58217873E+05
2.75925046E+03	2.11328775E+06	2.08085547E+03	1.14529637E+02

35

1.11680011E+01	-5.72666060E+01	-9.51895256E+01	5.21593449E+01
3.13064926E+01	1.07277807E+00	-1.45800100E+00	-1.93055274E+01
-1.77414794E+00	-2.11970329E+00	6.24087567E-01	2.50231531E-01
-1.44264476E+01	6.62043804E-01	8.59600430E+01	-2.12044565E+01
5.03600215E+01	7.24344006E-01	-4.07546947E+20	-3.25693724E+01
5.96510164E+00	-3.07819417E+01	1.22981900E+01	2.72407242E-01
4.69812991E+01	-3.07242984E+02	2.26403823E+03	-2.71151710E+03
1.15470435E+03	6.50129992E+00	-2.96193722E+02	2.01367725E+02
-5.03607583E+03	2.02085541E+03	-5.21533403E+04	-3.85049667E+00

36

-7.49403410E-01	3.45841959E+00	-3.59243805E+00	-1.39032527E+01
-1.00405434E+00	2.55431514E-02	9.10045955E-02	1.82982385E+00
2.80716280E+00	-2.52689406E-02	5.74734607E-02	-5.43905958E-02
-1.26003243E-01	-2.40589306E+01	8.14029349E+00	-6.53037536E+00
1.60596250E+00	1.78723424E-02	1.24394996E+00	6.16437408E+00
-5.55320111E-01	7.00144435E-01	-3.93386011E-01	5.90034211E-02
3.61284345E+00	1.74121119E+02	2.20389607E+01	-2.24272497E+02
-1.03309447E+00	-1.50587897E+00	-1.89889368E+20	-6.15828172E+02
-1.28046694E+01	1.14929394E+02	-3.05049661E+00	7.62483204E+02

2-370

1

5.07640002E-05	1.17190000E-07	2.76420000E-08	-1.66180001E-08
-2.39850001E-05	8.14160002E-08	-1.76779999E-05	-6.82219998E-07
-5.22860000E-08	3.94099999E-07	-1.55950000E-07	-1.51200000E-06
-9.19330000E-06	1.34840000E-06	-1.09870000E-07	6.24119998E-07
-5.89250000E-07	9.21880002E-07	1.44089999E-06	4.70949999E-08
1.44710000E-07	-1.10300000E-07	8.08880003E-08	-1.91780000E-07
1.21670000E-07	2.27060000E-08	-2.27979999E-09	-1.90499999E-10
-9.87060000E-09	4.15620001E-08	2.31620000E-07	1.43280000E-08
9.43690001E-10	-9.83249995E-10	-4.28090002E-09	4.38769998E-08

2

1.17190000E-07	3.27110001E-07	-1.61360001E-11	1.10150000E-07
1.00620000E-07	4.40380001E-06	2.02699999E-06	6.79229997E-08
-2.94729999E-09	1.05920000E-07	-3.84669998E-08	-3.65030002E-08
-1.53830000E-06	7.30709999E-08	1.97659999E-09	-5.91710002E-08
4.78820001E-08	-2.08990000E-07	7.66320003E-08	1.86090000E-07
-1.62270000E-09	7.85850003E-10	-9.05590003E-09	1.10860000E-07
-2.30560000E-08	5.34360001E-09	-8.81350002E-11	1.39830000E-11
-1.49470001E-10	2.92100000E-09	-1.90120000E-08	5.02059999E-09
-2.05210000E-10	-7.17360000E-11	-6.32520002E-10	2.77070000E-09

3

2.76420000E-08	-1.61360001E-11	2.53410001E-07	7.64500000E-11
1.36830000E-07	-1.22920001E-10	1.21479999E-07	4.90320001E-09
1.70070000E-08	2.72350000E-07	-9.79330004E-08	1.21910000E-08
1.62770000E-08	-1.68150001E-08	1.61630000E-08	-1.89840000E-07
2.05819999E-07	-1.64339999E-08	1.21479999E-07	2.10050000E-11
2.80960000E-08	1.99520001E-08	-2.01899999E-08	1.47200000E-08
-9.10929998E-09	-4.14319998E-10	2.39600000E-10	-2.23629999E-11
8.56230000E-11	-1.48600000E-09	-9.99740002E-09	-5.03519997E-10
1.01670000E-10	1.07660000E-11	-1.54739999E-11	-1.80630000E-09

4

-1.66180001E-08	1.10150000E-07	7.64500000E-11	1.87510000E-06
1.18700000E-06	-1.15450000E-07	1.77130001E-06	5.90770002E-08
-5.70760000E-09	9.92029996E-08	-3.61320001E-08	-1.36580000E-06
-1.33910000E-06	5.28770001E-08	4.53490001E-09	-4.19649999E-08
4.97910002E-08	7.36879997E-07	5.03380000E-08	1.69090001E-07
-1.36210000E-09	1.46920000E-09	-8.69840000E-09	-1.32029999E-07
-2.34910000E-08	4.88599999E-09	-4.37519999E-11	1.01550000E-11
-8.76770001E-09	3.78979998E-08	-2.02979999E-08	4.61580002E-09
-1.65750001E-10	-6.50870000E-11	-4.03899999E-09	3.89880002E-08

5

-2.39850001E-05	1.00620000E-07	1.36830000E-07	1.18700000E-06
2.59500000E-05	-1.53769999E-08	1.22380000E-05	4.65260001E-07
8.71470000E-07	-1.97270001E-10	1.49530001E-07	2.76350001E-08
4.22009998E-06	-7.50170003E-07	-7.18759999E-07	-1.39580000E-08
5.57729997E-07	7.36879997E-07	5.03380000E-08	1.69890001E-07
-1.36210000E-09	1.46920000E-09	-8.69840000E-09	-1.32029999E-07
-2.34910000E-08	4.88599999E-09	-4.37519999E-11	1.01550000E-11
-8.76770001E-09	3.78979998E-08	-2.02979999E-08	4.61580002E-09
-1.65750001E-10	-6.50870000E-11	-4.03889999E-09	3.99880000E-08

6

8.14160002E-08	4.40380001E-06	-1.22920001E-10	-1.15450000E-07
-1.53769999E-08	7.11310000E-04	4.32930001E-07	-1.21950000E-08
-2.03530000E-08	2.25940000E-08	-8.29000002E-09	-4.38920001E-07
-1.01430000E-06	-2.77790001E-07	3.29710002E-08	5.69589997E-06
-9.45800005E-09	-7.52310001E-07	4.32930001E-07	1.23640000E-07
-1.36190000E-08	6.94329999E-09	-4.93340002E-09	1.09490000E-07
-7.05029999E-08	2.47990001E-09	6.10169998E-10	7.08080001E-11
1.71940000E-09	-6.11390000E-09	-8.37309999E-08	4.07739997E-09
-3.94610001E-10	1.17970000E-10	-6.53479999E-10	-5.66010000E-09

7

-1.76779999E-05	2.02699999E-06	1.21479999E-07	1.77130001E-06
1.22380000E-05	4.32930001E-07	5.87930001E-04	1.41180000E-05
-1.69220000E-06	1.00490000E-06	3.28930000E-07	4.14169999E-05
-3.89190000E-05	-1.71870001E-06	9.61669997E-07	-3.10700000E-06
2.95289999E-06	-1.11080000E-05	-1.52530000E-05	1.68560000E-05
-1.39100000E-06	1.69680000E-06	-1.97140000E-06	1.28350000E-05
-2.71270000E-06	2.42599999E-07	1.28350000E-08	-8.27180000E-11
4.58520000E-08	-6.14230000E-08	-3.19320000E-06	2.48549998E-07
-1.65890000E-08	-8.10290003E-11	-5.81740001E-09	-1.44280000E-07

8

-6.82219998E-07	6.79229997E-08	4.90320001E-09	5.90770002E-08
4.65260001E-07	-1.21950000E-08	1.41180000E-05	1.02360001E-06
-5.87920002E-08	6.37500001E-07	-2.52010000E-07	2.08469999E-06
-1.21159999E-06	-7.22360003E-08	3.46480000E-08	-1.02870000E-07
9.91069999E-08	-3.80189999E-07	-5.85469998E-07	6.20809999E-07
-5.29439999E-08	6.80159999E-08	-7.70930004E-08	4.81390003E-07
-9.84039996E-08	8.24799995E-09	4.95100003E-10	-6.07170000E-10
1.78710000E-09	-2.82970000E-09	-1.17700000E-07	8.51280002E-09
-5.97160002E-10	9.53600003E-12	-5.73969999E-11	-6.03419997E-09

9

-5.22860000E-08	-2.94729999E-09	1.70070000E-08	-5.70760000E-09
8.71470000E-07	-2.03530000E-08	-1.69220000E-06	-5.87920002E-08
1.52230000E-06	1.27490000E-06	-4.48590001E-07	-1.00490000E-07
6.44270003E-07	-1.23590000E-08	1.49079999E-08	7.20189998E-08
-1.08900000E-07	7.20489997E-08	-1.69220000E-06	-5.40860000E-07
2.37720000E-07	1.64090000E-07	-1.41590000E-07	-3.69770000E-07
5.35370002E-08	-7.72389996E-09	2.56229999E-10	2.08979999E-11
-8.28359999E-10	-2.22839999E-09	6.26009999E-08	-7.11609999E-09
7.02710001E-10	8.98379999E-11	9.07450001E-11	8.12299998E-10

10

3.94099999E-07	1.05920000E-07	2.72350000E-07	9.92029996E-08
-1.97270001E-10	2.25940000E-08	1.00490000E-06	6.37500001E-07
1.27490000E-06	1.37350000E-05	-1.77260000E-08	-2.93639999E-07
-3.74370001E-06	-6.20450002E-08	-7.50740000E-07	-6.07279999E-09
5.70010000E-09	9.12939999E-08	-2.33800000E-06	1.53850000E-06
1.21870001E-06	9.11919995E-09	-8.96249996E-09	-7.86400003E-08
-2.43430001E-07	2.00429999E-08	-6.70080003E-09	-1.33579999E-10
3.19580001E-09	1.47320001E-09	-2.77489999E-07	1.90539999E-08
-1.55280000E-08	-2.20960000E-10	-5.90970002E-10	-1.11900000E-09

11

-1.55950000E-07	-3.84669998E-08	-9.79330004E-08	-3.61320001E-08
1.49530001E-07	-8.29000002E-09	3.28930000E-07	-2.52010000E-07
-4.48590001E-07	-1.77260000E-08	1.12060000E-05	1.02980000E-07
1.41010000E-06	2.16489999E-08	2.79260000E-07	3.18580001E-09
-8.31609999E-08	-3.42230000E-08	8.59360000E-07	-5.74319998E-07
-4.54209999E-07	2.26129999E-08	1.10180000E-07	2.88390001E-08
9.09000004E-08	-7.56170004E-09	2.48080001E-09	4.92439999E-11
-1.18360000E-09	-5.46759998E-10	1.03510000E-07	-7.18950000E-09
5.70339997E-09	3.10449999E-11	2.48359999E-10	4.17850001E-10

12

-1.51200000E-06	-3.65030002E-08	1.21910000E-08	-1.36580000E-06
2.76350001E-08	-4.38920001E-07	4.14169999E-05	2.08469999E-06
-1.00490000E-07	-2.93639999E-07	1.02980000E-07	1.36510000E-03
3.49690001E-06	-3.52200001E-07	1.05300000E-08	4.90269998E-08
-5.31089999E-08	4.54019999E-08	4.14169999E-05	5.15259998E-07
-1.23210000E-07	-4.04880001E-08	3.63160000E-08	5.60010001E-07
-6.83270001E-08	-9.17200005E-09	9.94899996E-10	-6.91829996E-11
4.14040002E-09	-1.82369999E-08	-1.21779999E-07	-7.48020001E-09
-4.55350001E-10	3.28970001E-10	3.01930000E-09	-2.40480000E-08

13

-9.19330000E-06	-1.53830000E-06	1.62770000E-08	-1.33910000E-06
4.22009998E-06	-1.01430000E-06	-3.89190000E-05	-1.21159999E-06
6.44270003E-07	-3.74370001E-06	1.41910000E-06	3.49690001E-06
4.77300000E-04	1.08259999E-06	-1.55680000E-06	-3.09640001E-06
3.20949999E-06	1.28280000E-06	1.40180000E-05	-1.07110000E-05
-1.59710000E-07	1.56910000E-07	4.16990002E-07	-9.34660000E-06
8.73379997E-06	-1.10450000E-06	-4.25629998E-08	4.32879999E-09
1.27660000E-07	-2.36609999E-07	6.71440000E-06	-9.88400004E-07
1.98420000E-08	1.64039999E-08	2.41850000E-07	-2.56130001E-07

14

1.34840000E-06	7.30709999E-08	-1.68150001E-08	5.28770001E-08
-7.50170003E-07	-2.77790001E-07	-1.71870001E-06	-7.22360003E-08
-1.23590000E-08	-6.20450002E-08	2.16489999E-08	-3.52200001E-07
1.08259999E-06	3.85880003E-06	-4.79629998E-08	8.47369996E-08
1.27030001E-07	4.09450001E-06	6.23070002E-06	1.05660000E-06
1.74489999E-07	-2.88930000E-07	1.68230001E-07	-5.79789998E-08
6.89709999E-07	3.49359999E-08	-7.83139997E-09	-3.22950000E-10
-1.70329999E-08	1.20670000E-07	8.34200002E-07	1.64330001E-08
3.86920002E-09	-2.09129999E-09	3.00080000E-09	1.16000000E-07

15

-1.09870000E-07	1.97659999E-09	1.61630000E-08	4.53490001E-09
-7.18759999E-07	3.29710002E-08	9.61669997E-07	3.46480000E-08
1.49079999E-08	-7.50740000E-07	2.79260000E-07	1.05300000E-08
-1.55680000E-06	-4.79629998E-08	1.43250000E-06	1.60790000E-07
5.72470000E-08	6.18860003E-08	9.61669997E-07	4.41990000E-07
1.69370001E-07	-3.53139999E-07	2.63019999E-07	3.87690001E-07
-2.56029999E-07	4.07330001E-08	6.80079998E-09	-4.50470002E-10
-2.20240001E-09	1.43750000E-08	-2.27099999E-07	3.33050001E-08
5.05160003E-09	-6.56880002E-10	-4.53479998E-09	6.75540002E-09

16

6.24119998E-07	-3.91710002E-08	-1.89840000E-07	-4.19649999E-08
-1.39580000E-08	5.69589997E-06	-3.10700000E-06	-1.02870000E-07
7.20109998E-08	-6.07279999E-09	3.18580001E-09	4.90269998E-08
-3.09640001E-06	8.47369996E-08	1.60790000E-07	4.37030002E-06
6.90349999E-08	-2.69640001E-07	1.33210000E-06	-7.20019997E-07
-7.10659997E-07	3.09889998E-08	1.63389999E-08	1.30010001E-08
6.60890002E-07	-6.53879999E-08	5.13659998E-09	3.34059998E-10
2.99559999E-09	-1.74180000E-09	5.93739998E-07	-6.13260003E-08
8.05989997E-09	5.92440000E-10	1.35460000E-08	3.95400002E-09

~~SECRET~~ **SPECIAL HANDLING**

17
```
-9.89250000E-07    4.78820001E-08    2.05819999E-07    4.97910002E-08
 5.57729997E-07   -9.45800005E-09    2.95289999E-08    9.91069999E-08
-1.08900000E-07    5.70010000E-09   -8.31609999E-08   -5.31089999E-08
 3.20949999E-06    1.27030001E-07    5.72470000E-06    6.85349999E-08
 2.11810000E-05    2.64110000E-07   -4.56270001E-07    6.43720002E-07
 6.92470003E-07   -3.31779999E-08    4.44960002E-08   -2.58390000E-09
-5.92040003E-07    7.25489997E-08    1.07350000E-08   -3.32739999E-10
-4.84020002E-09    1.31430000E-09   -5.05730000E-07    6.64810003E-08
 8.17620005E-09   -8.66330001E-10   -1.38239999E-06   -3.12349999E-09
```

18
```
 9.21880002E-07   -2.08990000E-07   -1.64339999E-08    7.36879997E-07
 7.36879997E-07   -7.52310001E-07   -1.11080000E-05   -3.80189999E-07
 7.20489997E-08    9.12939999E-08   -3.42230000E-08    4.54019999E-08
 1.28280000E-06    4.09450001E-06    6.18860003E-08   -2.69640001E-07
 2.64110000E-07    1.36600000E-03   -1.11080000E-05   -2.11640000E-07
 1.58090000E-07   -1.48260000E-08    3.60930001E-10   -4.74560000E-07
-1.65359999E-07    2.03999999E-07   -3.47429999E-09   -2.89110000E-09
-6.81939998E-08    2.25899999E-07    5.62220002E-07    1.36350000E-07
 8.42579995E-09   -6.74369999E-09   -3.44550002E-08    2.11060000E-07
```

19
```
 1.44089999E-06    7.66320003E-08    1.21479999E-07    5.03380000E-08
 5.03380000E-08    4.32930001E-07   -1.52530000E-05   -5.85469998E-07
-1.69220000E-06   -2.33800000E-06    8.59360000E-07    4.14169999E-05
 1.40180000E-05    6.23070002E-06    9.61669997E-07    1.33210000E-06
-4.56270001E-07   -1.11080000E-05    5.40120003E-04   -1.14020000E-06
-1.39100000E-06   -1.29640000E-05    8.82510005E-06    1.28350000E-05
 4.47460002E-06    7.82430000E-07    1.28350000E-08    1.78160000E-08
 5.19880001E-08   -6.14230000E-08    3.65060001E-06    8.34790001E-07
-1.65890000E-08   -9.66239999E-09    8.29499998E-08   -1.44280000E-07
```

20
```
 4.70949999E-08    1.86090000E-07    2.10050000E-11    1.69090001E-07
 1.69090001E-07    1.23640000E-07    1.68560000E-05    6.28809999E-07
-5.40860000E-07    1.53850000E-06   -5.74319998E-07    5.15259998E-07
-1.07110000E-05    1.05660000E-06    4.41990000E-07   -7.20019997E-07
 8.43720002E-07   -2.11640000E-07   -1.14020000E-06    1.12360000E-05
-2.23790000E-08    1.94470000E-08    9.55320004E-10    9.19319996E-06
-9.95190007E-07    1.94609999E-07    8.30960001E-09   -1.71070000E-09
 5.72980002E-09    9.08539999E-08   -1.06120000E-06    1.60580001E-07
 1.53559999E-09   -3.45039999E-09   -6.62680000E-09    1.79549999E-08
```

2-375

~~SECRET~~ **SPECIAL HANDLING**

21

1.44710000E-07	-1.62270000E-09	2.80960000E-08	-1.36210000E-09
-1.36210000E-09	-1.36190000E-08	-1.39100000E-06	-5.29439999E-06
2.37720000E-07	1.21870001E-06	-4.54209999E-07	-1.23210000E-07
-1.59710000E-07	1.74489999E-07	1.69370001E-07	-7.10659997E-07
6.92470003E-07	1.58090000E-07	-1.39100000E-06	-2.23790000E-08
2.24589999E-06	3.98719999E-08	6.05329999E-08	1.38890000E-10
-2.77870000E-08	4.28680003E-09	3.57020000E-09	-4.96599997E-10
-3.70170000E-09	1.67630000E-09	2.24500001E-08	-1.84050000E-09
3.47140000E-09	-3.41220000E-10	-2.96010000E-09	-4.06900000E-10

22

-1.10300000E-07	7.85850003E-10	1.99500001E-08	1.46920000E-09
1.46920000E-09	6.94329999E-09	1.69680000E-06	6.80159999E-08
1.64090000E-07	9.11919995E-09	2.26129999E-08	-4.04880001E-08
1.56910000E-07	-2.88930000E-07	-3.53139999E-07	3.09889998E-08
-3.31779999E-08	-1.48260000E-08	-1.29640000E-05	1.94470000E-08
3.98719999E-08	1.16440000E-05	1.06460000E-07	-3.16440001E-07
4.74460000E-08	-8.80300000E-09	-4.57350002E-09	8.17140001E-10
1.14640000E-08	2.23650001E-08	-8.88000002E-08	-7.42839998E-10
-9.76199999E-09	4.48089999E-10	8.54670001E-09	1.84450000E-09

23

8.08880003E-08	-9.05590003E-09	-2.01899999E-08	-8.69840000E-09
-8.69840000E-09	-4.93340002E-09	-1.97140000E-06	-7.70930004E-08
-1.41590000E-07	-8.96249996E-09	1.10180000E-07	3.63160000E-08
4.16990002E-07	1.68230001E-07	2.63019999E-07	1.63389999E-08
4.44960002E-08	3.60930001E-10	8.82510005E-06	9.55320004E-10
6.05329999E-08	1.06460000E-07	1.89580001E-05	2.16960000E-07
-2.58720001E-08	5.68940001E-09	3.75850001E-09	-6.04940001E-10
-7.09249998E-09	-1.14750000E-09	6.60049997E-08	-7.14389999E-10
4.98000002E-09	-3.72469999E-10	-5.46390000E-09	-8.87109997E-10

24

-1.91780000E-07	1.10860000E-07	1.47200000E-08	-1.32029999E-07
-1.32029999E-07	1.09490000E-07	1.28350000E-05	4.81390003E-07
-3.69770000E-07	-7.86400003E-08	2.88390001E-08	5.60010001E-07
-9.34660000E-06	-5.79789998E-08	3.87690001E-07	1.30010001E-08
-2.50390000E-09	-4.74560000E-07	1.28350000E-05	9.19319996E-06
1.38890000E-10	-3.16440001E-07	2.16960000E-07	1.10379999E-03
-1.75869999E-06	8.18509998E-08	1.03959999E-08	-4.68840000E-09
-4.04630002E-09	-1.03500000E-07	-1.70040001E-06	3.76939999E-08
-7.81499998E-09	-2.05400000E-09	-1.68090000E-08	-1.88800000E-07

~~SECRET~~ **SPECIAL HANDLING**

25

```
 1.21670000E-07    -2.30560000E-08    -9.10929998E-09    -2.34910000E-08
-2.34910000E-08    -7.05029999E-08    -2.71270000E-06    -9.84039996E-08
 5.35370002E-08    -2.43430001E-07     9.09000004E-08    -6.83270001E-08
 8.73379997E-06     6.89709999E-07    -2.56029999E-07     6.60890002E-07
-5.92040003E-07    -1.65359999E-07     4.47460002E-06    -9.95190007E-07
-2.77870000E-08     4.74460000E-08    -2.58720001E-08    -1.75869999E-06
 6.29529997E-04     2.11950001E-06    -2.51700001E-07     3.72359999E-07
 8.04379999E-06    -1.88830001E-06     2.17979999E-04     3.37710000E-06
 3.66419999E-06     9.40620000E-08     1.49200000E-06     5.24380002E-08
```

26

```
 2.27060000E-08     5.34360001E-09    -4.14319998E-10     4.88599999E-09
 4.88599999E-09     2.47990001E-09     2.42599999E-07     8.24799995E-09
-7.72389996E-09     2.00429999E-08    -7.56170004E-09    -9.17200005E-09
-1.10450000E-06     3.49359999E-08     4.07330001E-08    -6.53879999E-08
 7.25489997E-08     2.03999999E-07     7.82430000E-07     1.94609999E-07
 4.28680003E-09    -8.80300000E-09     5.68940001E-09     8.18509998E-08
 2.11950001E-06     9.84819997E-06    -2.94089999E-08     7.19189996E-08
 4.24210000E-09     6.38069997E-06     1.55879999E-06     6.84600002E-06
-6.30350000E-09    -3.01170001E-07     7.42969997E-08     3.53700000E-06
```

27

```
-2.27979999E-09    -8.81350002E-11     2.39600000E-10    -4.37519999E-11
-4.37519999E-11     6.10169998E-10     1.28350000E-08     4.95100003E-10
 2.56229999E-10    -6.70080003E-09     2.48080001E-09     9.94899996E-10
-4.25629998E-08    -7.83139997E-09     6.80079998E-09     5.13659998E-09
 1.07350000E-08    -3.47429999E-09     1.28350000E-08     8.30960001E-09
 3.57020000E-09    -4.57350002E-09     3.75850001E-09     1.03959999E-08
-2.51700001E-07    -2.94089999E-08     2.27469999E-06    -2.62890001E-10
 3.18569999E-07    -2.51710000E-08    -3.58170001E-06    -2.27220001E-08
 1.07570000E-06     1.42500001E-09    -3.53100999E-08    -6.98219997E-08
```

28

```
-1.90480999E-10     1.30930000E-11    -2.27620999E-11     1.01550000E-11
 1.01550000E-11     7.00080001E-11    -8.27180000E-11    -6.07170000E-12
 2.08979999E-11    -1.33579999E-10     4.92439999E-11    -6.91829996E-11
 4.32870999E-09    -2.02950000E-10    -4.50470002E-10     3.34059998E-10
-3.32739999E-10    -2.89110000E-09     1.78160000E-08    -1.71070000E-09
-4.96599997E-10     8.17140001E-10    -6.04940001E-10    -4.68840000E-09
 3.72359999E-07     7.19189996E-08    -2.62890001E-10     1.19719999E-07
-1.19550000E-09     1.28929999E-07     2.09523000E-07     2.88190002E-07
 2.78820000E-09     7.50619999E-09     9.89729998E-09     2.63350000E-07
```

~~SECRET~~ **SPECIAL HANDLING**

~~SECRET~~ **SPECIAL HANDLING**

29

-9.87060000E-09	-1.49470001E-10	8.56230000E-11	-8.76770001E-09
-8.76770001E-09	1.71940000E-09	4.58520000E-08	1.78710000E-09
-8.28359999E-10	3.19580001E-09	-1.18360000E-09	4.14040002E-09
1.27660000E-07	-1.70329999E-08	-2.20240001E-09	2.99559999E-09
-4.84020002E-09	-6.81939998E-08	5.19880001E-08	5.72980002E-09
-3.70170000E-09	1.14640000E-08	-7.09249998E-09	-4.04630002E-09
8.04379999E-06	4.24210000E-09	3.18569999E-07	-1.19550000E-09
3.14220001E-05	1.00150000E-07	-1.38860000E-05	-3.29850001E-08
5.00199998E-09	-9.68049996E-09	-1.28470001E-06	5.34589999E-08

30

4.15620001E-08	2.92100000E-09	-1.48600000E-09	3.78979998E-08
3.78979998E-08	-6.11390000E-09	-6.14230000E-08	-2.82970000E-09
-2.22839999E-09	1.47320001E-09	-5.46759998E-10	-1.82369999E-08
-2.36609999E-07	1.20670000E-07	1.43750000E-08	-1.74180000E-09
1.31430000E-09	2.25899999E-07	-6.14230000E-08	9.08539999E-08
1.67630000E-09	2.23650001E-08	-1.14750000E-09	-1.03500000E-07
-1.88830001E-06	6.38069997E-06	-2.51710000E-08	1.28929999E-07
1.00150000E-07	1.33910000E-03	1.03590000E-06	3.47320000E-06
3.77909998E-09	-2.46470002E-07	-2.01010000E-07	4.30969999E-06

31

2.31620000E-07	-1.90120000E-08	-9.99740002E-09	-2.02979999E-08
-2.02979999E-08	-8.37309999E-08	-3.19320000E-06	-1.17700000E-07
6.26009999E-08	-2.77489999E-07	1.03510000E-07	-1.21779999E-07
6.71440000E-06	8.34200002E-07	-2.27099999E-07	5.93739998E-07
-5.05730000E-07	5.62220002E-07	3.65060001E-06	-1.06120000E-06
2.24500001E-08	-8.88800002E-08	6.60049997E-08	-1.70040001E-06
2.17979999E-04	1.55879999E-06	-3.58170001E-06	2.09523000E-07
-1.38860000E-05	1.03590000E-06	6.43020001E-04	3.57580001E-06
5.51600003E-07	1.55660000E-08	6.36879997E-06	3.45590001E-06

32

1.43280000E-08	5.02059999E-09	-5.03519997E-10	4.61580002E-09
4.61580002E-09	4.07739997E-09	2.48549998E-07	8.51280002E-09
-7.11609999E-09	1.90539999E-08	-7.18950000E-09	-7.48020001E-09
-9.88400004E-07	1.64330001E-08	3.33050001E-08	-6.13260003E-08
6.64810003E-08	1.36350000E-07	8.34790001E-07	1.60580001E-07
-1.84050000E-09	-7.42839998E-10	-7.14389999E-10	3.76939999E-08
3.37710000E-06	6.84600002E-06	-2.27220001E-08	2.88190002E-07
-3.29850001E-08	3.47320000E-06	3.57580001E-06	9.83150005E-06
1.57250000E-08	-5.96690004E-08	4.64270000E-08	6.82690001E-06

~~SECRET~~ **SPECIAL HANDLING**

$3.43602001E-10$	$-9.05217220E-10$	$1.01670000E-10$	$-1.65750001E-10$
		$-1.65302224E-08$	$-5.97160002E-10$
		$5.70539007E-09$	$-4.55350001E-10$
		$5.05160003E-09$	$8.05980007E-09$
		$-1.65790000E-08$	$1.53559999E-09$
$3.47140000E-09$	$-9.76190999E-09$	$4.90002002E-09$	$-7.81499999E-09$
$3.66419999E-06$		$1.07570000E-06$	$2.78820000E-09$
		$5.51600003E-07$	$1.57250000E-08$
		$2.70000002E-07$	$8.08330000E-09$

54

			$-6.50870000E-11$
$-6.50870000E-11$			$9.53600003E-12$
			$3.28070001E-10$
			$5.80440006E-10$
			$-3.45039999E-09$
		$-4.72000009E-10$	$-2.05400000E-09$
		$1.40500001E-09$	$7.50619999E-09$
		$1.00000000E-08$	$-5.96690004E-09$
			$3.40500000E-09$

$-4.28090002E-09$			$-4.03889999E-09$
		$-5.21740001E-09$	$-5.73969999E-11$
		$2.48359999E-10$	$3.01930000E-09$
	$5.00080000E-09$	$-4.53470998E-09$	$1.35460000E-08$
$-1.38239999E-08$	$-3.44550002E-08$	$8.29499999E-08$	$-6.62680000E-09$
$-2.96010000E-09$	$8.54670001E-09$	$-5.46390000E-09$	$-1.68090000E-08$
$1.49200000E-06$	$7.42969997E-08$	$-3.53109999E-08$	$9.89729998E-09$
$-1.28470001E-06$	$-2.01010000E-07$	$6.36879997E-06$	$4.64270000E-08$
$2.79720000E-07$	$-9.01789998E-09$	$3.12517001E-05$	$2.05030000E-07$

56

$4.38769998E-08$	$2.77070000E-09$	$-1.80630000E-09$	$3.99880000E-08$
$3.99880000E-08$	$-5.66010000E-09$	$-1.44280000E-07$	$-6.03419997E-09$
$8.12299998E-10$	$-1.11900000E-09$	$4.17850001E-10$	$-2.40480000E-08$
$-2.56130001E-07$	$1.16000000E-07$	$6.75540002E-09$	$3.95400002E-09$
$-3.12349999E-09$	$2.11060000E-07$	$-1.44280000E-07$	$1.79549999E-08$
$-4.06900000E-10$	$1.84450000E-09$	$-8.87109997E-10$	$-1.88800000E-07$
$5.24380002E-08$	$3.53700000E-06$	$-6.98219997E-08$	$2.63350000E-07$
$5.34589999E-08$	$4.30969999E-06$	$3.45590001E-06$	$6.82690001E-06$
$9.08330003E-09$	$3.40500000E-09$	$2.05030000E-07$	$1.38930000E-03$

2.5.8 ATS WEIGHT ANALYSIS (See Section 4.4 for total subsystem weight status)

2.5.8.1 The weight of the system has been under very close scrutiny because the system weight is currently well above the weight acceptable. Various steps are currently being taken to determine what a realistic system weight will be so that a final weight figure can be negotiated with the customer. The structural analysis in Sections 2.5.1 through 2.5.3 was performed with the identification of overweight areas in mind. The results of the analysis are being used to show the subcontractor where weight may be reduced and if necessary, how to reduce weight. Much of this increase can be attributed to misinterpretation of environmental information such as loads and temperatures. A concerted effort is being made to clarify this information so that a representative weight can be obtained. Currently, the most troublesome weight areas are the protective shroud, the gimbal inertias and sizeable weight increases in the telescope.

A. Protective Shroud

The latest subcontractor weight estimate of the protective shroud is 23.5 pounds. The shroud weight has doubled over an earlier estimate of 11 pounds. The reasons given by the subcontractor for the weight increase is that the thermal environment is such (350°F) that aluminum is the only lightweight material that can be used. This has caused the greatest increase since beryllium or magnesium were being considered before. It is felt that this is a poor solution, since at the temperatures quoted, beryllium has more than ample strength and the ductility of beryllium at this temperature is quite favorable along with the modulus of elasticity. Another reason given is that there is a requirement for redundant drives which necessitates an increase in drive weight. This requirement will cause some increases in weight but with a more efficient drive design the weight increase can be kept at a minimum. The other factor causing weight increases is the fact that a better definition of the design has been obtained. This is an unavoidable increase but should be able to be kept to a minimum. GE estimates that it may be possible to design a shroud

2-381

that will weigh a minimum of 14 pounds. This estimated weight considers the redundant drives and a better design definition. One other potential problem area on the shroud is the effects of the plume from the ACTS. The plume will impinge on the shroud and preliminary thermal analysis indicates that temperatures of $1000^{\circ}F$ are possible. One solution would be to install a shield over a portion of the front end of the shroud. This shield should weigh less than a pound and would reduce the temperatures to more acceptable levels.

B. Gimbal Inertias

Currently the inertias of the rolling and pitching masses are below specification values. Inertias below specification levels will cause a reduction in smoothness which would cause jitter when the mirror is moved. The logical means of increasing inertia is to add mass at some distance from the reference axis. The subcontractor has attempted to do this but has caused sizeable increases in system weight which are totally unacceptable. Therefore, the subcontractor has been directed to perform studies on repositioning gyros, etc, to reduce the amount of weight needed for bringing the inertias up to specification value. The studies performed have been reviewed with the subcontractor but they have not progressed to a definite conclusion. Work is also being performed to determine the lowest inertias that would be tolerable. Coupled with the inertia problem is the fact that the roll and pitch masses are not balanced. To alleviate this problem the subcontractor, under GE direction, will make provision for adding balancing weights during ground testing. The weights will then be removed and the system locked for powered flight. At the present time it appears that some additional weight will be required to raise the inertias to an acceptable value but the exact amount is unknown. A five-pound allowance for such a weight had been carried previously so the subcontractor is requesting an additional 28 pounds for inertia make-up. This number is part of the current weight estimate.

C. Increased Telescope Weight

The weight of the telescope has increased by seven pounds per side or 14 pounds for the total system. The reasons given by the subcontractor for this increase has been increased glass weight (a sufficient mounting edge had not been considered) and also by the addition of the Q-mirror and its related hardware along with better design definition. These increases cannot be discounted but it appears that it may be possible to reduce the weight of the telescope to a point where there will be a zero net increase or decrease. There are certain areas that may offer promising weight reductions. The telescope wall thickness is now 0.040 inch. It appears possible that this thickness can be reduced to 0.030 inch to 0.032 inch as indicated by structural analysis. The subcontractor is investigating this aspect. The reduced wall thickness can also be applied to the Pechan prism housing and the zoom/eye piece housing. Another area being considered is the substitution of beryllium for aluminum in the telescope structure. The subcontractor has been very hesitant to do this since he claims that the coefficient of thermal expansion of the aluminum compensates for changes in the index in refraction of the glass due to temperature gradients. However, the subcontractor has never backed up this statement analytically and has not investigated other materials. He was directed to perform these studies and to formally report these results to GE so that a material change can be initiated, if possible.

2.5.8.2 The current ATS weight estimate is 375 pounds. This weight includes the increased telescope weight, additional weight for inertia make-up, and the GE estimate for the shroud. It also includes weight for a sun-sensor which was not carried previously and a two-pound addition to the tracking pedestal harness due to DACO's refusal to relocate their harness penetration. In Table 2.5-2, a breakdown of the 375-pound weight is compared with that of the mutually agreed upon 323-pound weight in August 1967.

TABLE 2.5 -2. ATS WEIGHT BREAKDOWNS (Sheet 1 of 2)

DETAILED 323 LB AND 375 LB BREAKDOWNS		
ITEM	323 LB	375 LB
Telescope Objective End	52.50	58.00
Telescope Low Power Group	54.50	43.58
Telescope Elbow Assembly		14.80
Telescope Pechan Assembly	13.00	14.00
Telescope Shear Mount	2.50	3.58
Telescope Zoom Assembly		11.54
Telescope Eye Piece Assembly	27.00	6.00
Telescope Harness and Connectors		11.50
Telescope Total	149.5	163.00
External Fixed-Fold Mirror	30.5	30.5
Tracking Pedestal	108.0	110.0
Additional Weight for Inertias and Balancing	5.0	33.0
Tracking Pedestal Total	113.0	143.0
Inner Shroud	22.0	28.0
Pressure Window	8.0	8.5
Sun-Sensor	0.0	2.0
System Total	323.0	375.0

TABLE 2.5-2. ATS WEIGHT BREAKDOWNS (Sheet 2 of 2)

COMPARISON OF 323 LB, 329 LB, 344 LB, AND 375 LB BREAKDOWNS				
ITEM	323 LB	329 LB	344 LB	375 LB
Telescope	149.5	149.5	149.5	163
External Fixed-Fold Mirror	30.5	30.5	30.5	30.5
Tracking Pedestal	113.0	113.0	120	143
Inner Shroud	22	28	36	28
Pressure Window	8	8	8	8.5
Sun-Sensor	0	0	0	2

2.5.8.3 Potential Weight Reduction Areas Under Study

There are a number of weight reduction areas currently under study. These studies are being performed by both the subcontractor and GE. These items are listed along with a brief description.

a. Reduction of Shock Loading Due to Extension of DR 1100A Shock Curve Below 100 Hz - The subcontractor is currently cutting off the shock curve at 100 Hz which means that for any structural frequency below 100 Hz, the shock value for 100 Hz is being used. This is very conservative since the frequency of the structure is in the 30 to 40 Hz range. It has been determined by discussion with Aerospace Corp. engineers that the curve should be extended to 0 g's. This will cause a reduction in shock loading which should cause a reduction in structural weight.

b. Reduction of Telescope Wall Thickness to Possibly 0.030 Inch - This is covered in a previous portion of this section.

c. Reduction of Mirror Thickness From 1.0 inch to 0.75 inch - Studies are currently being made to reduce the fixed-fold and tracking mirror thicknesses to 0.75 inch. The biggest problem appears to be tolerances. The subcontractor claims that a reduction in mirror thickness will cause a tightening of tolerances to the point where it may be impossible to fabricate. Another mirror study is being made on the possibility of going to an egg-crate mirror which would cause sizeable decreases in weight. It should be noted that the weight savings may not be applicable to the tracking mirror since this may aggravate the inertia problem.

d. Usage of Beryllium in the Telescope Structure - This is covered in a previous portion of this section.

e. Design Optimization - This can be accomplished by performing detail structural analysis to determine overdesigned areas and then taking the necessary steps to reduce the weight and eliminate the overdesign. This process will evolve as more details of the design are defined.

2.5.8.4 Potential Weight Increase Areas

There are currently some areas which will require close scrutiny due to their potential impact on the system weight. Some of these areas are near solution with a minimum weight increase while others are still pending.

a. Increased Shroud Weight Due to ACTS Plume Impingment - Covered previously in this section; may cause only a small increase in structure and insulation.

b. Out-of-Specification Inertias - Covered previously in this section; currently being studied with some increase likely.

c. Increased Structural Weight Due to Increased Structural Stiffness Necessitated by Dynamic Disturbances from ACTS Controls, etc. - This area is discussed in the dynamic analysis section but could cause serious problems.

2-387/2-388

~~SECRET~~ **SPECIAL HANDLING**

2.6 BORESIGHTING (See also 2.3.2)

The equations for the boresighting procedure are derived and a degraded mode of operation investigated. The material is broken down in Paragraphs 2.6.1 and 2.6.2.

2.6.1 NORMAL MODE EQUATIONS

To point the main optics by using the ATS, the alignment between the ATS optical system and the primary optical system must be known. This ATS/Primary optics alignment is found by on-orbit boresighting.

The form of the boresighting equations depends upon the types of errors that are considered in the ATS and primary optics.

Considering the ATS and the primary optics as two rigid boxes, the alignment error between them can be written as α_x, α_y, and α_z.

ATS "BOX"   PRIMARY OPTICS "BOX"

OPTICAL AXIS $(\alpha_x, \alpha_y, \alpha_z)$

TM   TM

OPTICAL AXIS

LOS

LOS

2-389
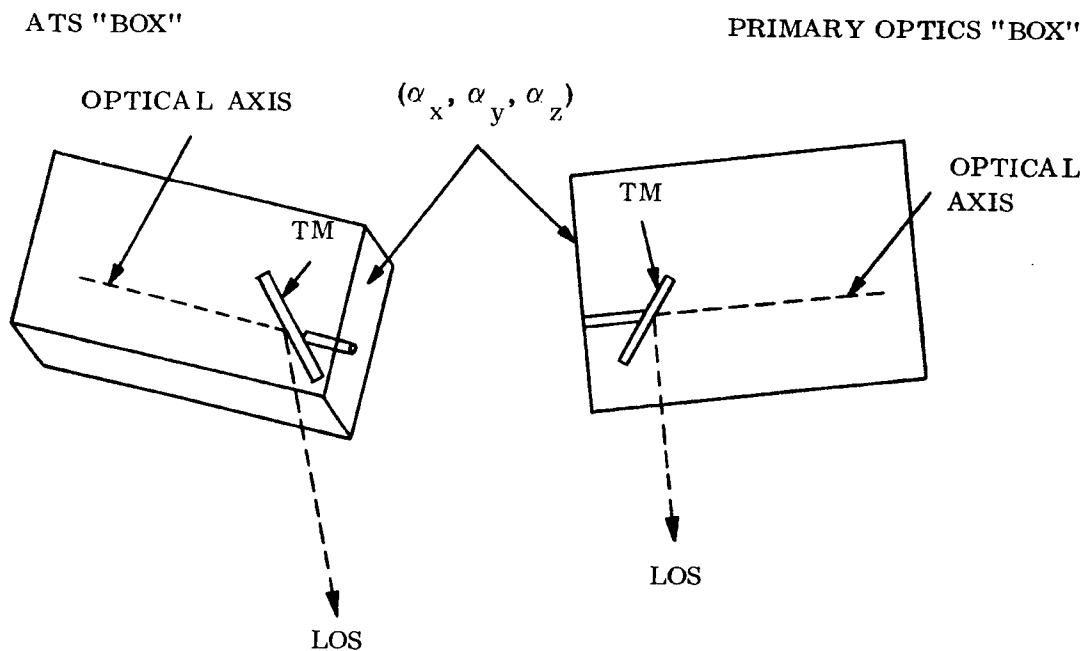
~~SECRET~~ **SPECIAL HANDLING**

If α_x, α_y, and α_z are the only major errors from the ATS system to the primary optics tracking mirror, the boresighting equations can be derived as follows:

If α_x, α_y, and α_z are misalignments between the ATS and the primary optical systems, the primary optics coordinates x_p, can be related to the ATS coordinates, x_a, by:

$$\begin{Bmatrix} x_a \\ y_a \\ z_a \end{Bmatrix} = \begin{bmatrix} 1 & \alpha_z & -\alpha_y \\ -\alpha_z & 1 & \alpha_x \\ \alpha_y & -\alpha_x & 1 \end{bmatrix} \begin{bmatrix} \theta_s \end{bmatrix} \begin{Bmatrix} x_p \\ y_p \\ z_p \end{Bmatrix} \qquad (9)$$

where

$$\begin{bmatrix} \theta_s \end{bmatrix} = \begin{bmatrix} \cos\theta_s & 0 & -\sin\theta_s \\ 0 & 1 & 0 \\ \sin\alpha_s & 0 & \cos\theta_s \end{bmatrix} \qquad (10)$$

If $\begin{Bmatrix} V_{in_a} \end{Bmatrix}$ and $\begin{Bmatrix} V_{in_p} \end{Bmatrix}$ are the line of sight vectors in terms of the ATS and primary optics coordinates, the "images" in both systems can be written as:

$$\begin{Bmatrix} V_{image_A} \end{Bmatrix} = \begin{bmatrix} \psi_g^T \end{bmatrix} \begin{bmatrix} M_a \end{bmatrix} \begin{bmatrix} \psi_g \end{bmatrix} \begin{Bmatrix} V_{in_a} \end{Bmatrix} \qquad (11)$$

and

$$\begin{Bmatrix} V_{image_P} \end{Bmatrix} = \begin{bmatrix} b^T \end{bmatrix} \begin{bmatrix} M_p \end{bmatrix} \begin{Bmatrix} V_{in_p} \end{Bmatrix} \qquad (12$$

2-390

~~SECRET~~ **SPECIAL HANDLING**

where

$$\left[\psi_s\right] = \begin{bmatrix} \text{Cos } \psi_g & \text{Sin } \psi_g & 0 \\ -\text{Sin } \psi_g & \text{Cos } \psi_g & 0 \\ 0 & 0 & 1 \end{bmatrix} \qquad (13)$$

(ψ_s is the ATS gimbal skew angle.)

$$\left[b\right] = \begin{bmatrix} 1 & bz & -by \\ -bz & 1 & 0 \\ by & 0 & 1 \end{bmatrix} \qquad (14)$$

(by and bz are the misalignments of the primary optical axis.)

M_a and M_p are matrices consisting of sines and cosines of the gimbal angles.

$$M_a = \begin{bmatrix} -s2\sigma_a & c2\sigma_a \, s\omega_a & -c2\sigma_a \, c\omega_a \\ c2\sigma_a \, s\omega_a & c^2\omega_a + s^2\omega_a \, s2\sigma_a & s\omega_a \, c\omega_a \, (1-s2\sigma_a) \\ -c2\sigma_a \, c\omega_a & s\omega_a \, c\omega_a \, (1-s2\sigma_a) & s^2\omega_a + c^2\omega_a \, s2\sigma_a \end{bmatrix} \quad (15)$$

$$M_p = \begin{bmatrix} s2\sigma_p & & & & & \\ -c2\sigma_p \, s\omega_p & \cdot & \cdot & \cdot & \cdot & \cdot \\ c2\sigma_p \, c\omega_p & & & & & \end{bmatrix} \qquad (16)$$

($s\xi$ and $c\xi$ are used for Sin ξ and Cos ξ)

2-391

~~SECRET~~ **SPECIAL HANDLING**

The "image" of the line of sight is a ray along the x axis.

$$\left\{ V_{image}{}_{a} \right\} = \left\{ \begin{matrix} -1 \\ 0 \\ 0 \end{matrix} \right\} \tag{17}$$

$$\left\{ V_{image}{}_{p} \right\} = \left\{ \begin{matrix} 1 \\ 0 \\ 0 \end{matrix} \right\} \tag{18}$$

Next, solve equations 11 and 12 to obtain the line of sight vector, and make the following substitution:

$$\left\{ \begin{matrix} A_a \\ B_a \\ C_a \end{matrix} \right\} = \left\{ V_{in}{}_a \right\} = \left[\psi_s{}^T \right] \left[-M_a \right] \left[\psi_s \right] \left\{ \begin{matrix} 1 \\ 0 \\ 0 \end{matrix} \right\} \tag{19}$$

and

$$\left\{ \begin{matrix} A_p \\ B_p \\ C_p \end{matrix} \right\} = (\theta_s) \left\{ V_{in}{}_p \right\} = (\theta_s)\,(M_p)\,(b) \left\{ \begin{matrix} 1 \\ 0 \\ 0 \end{matrix} \right\} \tag{20}$$

Equations 19 and 20 are related to each other by the transformation in equation one.

$$\left\{ \begin{matrix} A_a \\ B_a \\ C_a \end{matrix} \right\} = \begin{pmatrix} 1 & \alpha_z & -\alpha_y \\ -\alpha_z & 1 & \alpha_x \\ \alpha_y & -\alpha_x & 1 \end{pmatrix} \left\{ \begin{matrix} A_p \\ B_p \\ C_p \end{matrix} \right\} \tag{21}$$

or:

$$
\begin{bmatrix}
0 & -C_p & B_p \\
C_p & 0 & -A_p \\
-B_p & A_p & 0
\end{bmatrix}
\begin{Bmatrix}
\alpha_x \\
\alpha_y \\
\alpha_z
\end{Bmatrix}
=
\begin{Bmatrix}
A_a - A_p \\
B_A - B_p \\
C_A - C_p
\end{Bmatrix}
\tag{21}
$$

These equations can now be used with measured ATS and primary TM gimbal angles to determine the alignment between the ATS and main optics. (However, it should be mentioned that equation 21 represents only 2 independent equations. Thus, more than one set of measurements will be necessary to solve for α_x, α_y and α_z.

Let the subscript one refer to one set of measured gimbal angles and two refer to another set. Then:

$$
\begin{bmatrix}
0 & -C_{p1} & B_{p1} \\
C_{p1} & 0 & -A_{p1} \\
0 & -C_{p2} & B_{p2} \\
C_{p2} & 0 & -A_{p2}
\end{bmatrix}
\begin{Bmatrix}
\alpha_x \\
\alpha_y \\
\alpha_z
\end{Bmatrix}
=
\begin{Bmatrix}
A_{a1} - A_{p1} \\
B_{a1} - B_{p1} \\
A_{a2} - A_{p2} \\
B_{a2} - B_{p2}
\end{Bmatrix}
\tag{22}
$$

To solve this set of equations, two methods an available. One, drop one equation, and solve for α_x, α_y, and α_z by standard matrix inversion; and two, perform a maximum likelihood solution for α_x, α_y, and α_z. The second method will yield the best accuracy since the measured gimbal angles will contain some error, and hence this is the desired method of solving for α_x, α_y, and α_z.

This maximum likelihood solution for the ATS alignment is:

$$
\begin{Bmatrix} \alpha_x \\ \alpha_y \\ \alpha_z \end{Bmatrix} = \left[(K)^T K \right]^{-1} K^T \begin{Bmatrix} A_{a1} - A_{p1} \\ B_{A1} - B_{p1} \\ A_{a2} - A_{p2} \\ B_{A2} - B_{p2} \end{Bmatrix} \tag{23}
$$

where:

$$
(K) = \begin{bmatrix} 0 & -C_{p1} & B_{p1} \\ C_{p1} & 0 & -A_{p1} \\ 0 & -C_{p2} & B_{p2} \\ C_{p2} & 0 & -A_{p2} \end{bmatrix} \tag{24}
$$

The disadvantage of this second method is that the equations are more complex and there-fore will require more computer time for solution.

An error analysis performed on this boresighting procedure has shown an improvement of about 7 percent in the pointing accuracy of the main optics in the slave mode when the least squares solution is used for foresighting. Hence the least squares solution is the currently planned method of obtaining the ATS/Prime Optics boresighting.

The error analysis conducted for ATS boresighting has shown that with apportioned values of errors that were used, the prime optics can point within 6 minutes (slave mode) and the ATS can point within 8 minutes (automatic mode neglecting ephemeric and target location errors). However if the ATS on orbit misalignment exceeds the apportioned values, the pointing errors increase. This increase would then require an increase in the number of ATS alignment errors found by the boresighting procedure.

~~SECRET~~ **SPECIAL HANDLING**

2.6.2 FAILED PELLICLE MODE

This paragraph presents the procedure required for boresighting the ATS to the main optics in case of failure of the visual optics in the primary optical system. (Failed pellicle mode).

The standard procedure for boresighting each ATS to the main optics is to center a target simultaneously with both the main optics and ATS, and record the gimbal angles in both systems. When this has been done for two targets, the gimbal angle information can be used to determine the alignment between the ATS system and the primary optical system.

The procedure becomes more complicated for the failed pellicle mode. For this mode, the crew must:

a. Locate and center the target with the ATS that is being boresighted.

b. Command the main optics to point to the same target--assuming perfect alignment between the main optics and the ATS.

c. Photograph the target, and record the ATS and main optics gimbal angles at the time of photography.

d. Record the primary optical axis alignment.

e. Repeat the procedure for a second target.

f. Develop both photographs.

g. Inspect both photographs to determine the primary TM gimbal angles that would have caused the target image to appear on the center of the film format. Enter these angles into the computer via the keyboard.

If the target does not appear near the center of format on the pictures taken in step c, the accuracy obtained by this boresighting procedure may be degraded. This in turn, implies that the boresighting procedure may have to be repeated for each ATS to obtain sufficient accuracy.

~~SECRET~~ **SPECIAL HANDLING**

h. Insert the gimbal angles obtained in step g, the ATS gimbal angles from step c, and the optical axis alignment from step d into the computer program used for the standard boresighting procedure.

2.6.2.1 Nomenclature

by, bz – angular offset of the primary optical axis in the pitch and yaw direction (by and bz are obtained from on board alignment monitors)

σ – tracking mirror pitch gimbal angle

ω – tracking mirror roll gimbal angle

θ_S – pitch angle of the primary optical axis and tracking mirror (θ_S = 2 degrees nominally)

k – optical magnification

S( ) – used for sine ( )

C( ) – used for cosine ( )

2.6.2.2 Analysis

Assume that a photograph has been obtained and a well defined target appears on it. (Note that this assumes that the alignment between the ATS and primary optical system must be no worse than 30 arc min.   Since the MO semi field of view is approximately 32 arc min., a 30 arc min. alignment error between the ATS and primary optics would cause the target image to appear at the edge of the film format.) Also assume that the primary TM gimbal angles and optical axis alignment were recorded at the time the picture was taken. It is then desired to find the TM roll and pitch corrections that would cause the target image to appear on the center of the film format.

The photograph can be represented as shown in the following sketch. The axes y, z define the center of the film format.

~~SECRET~~ **SPECIAL HANDLING**
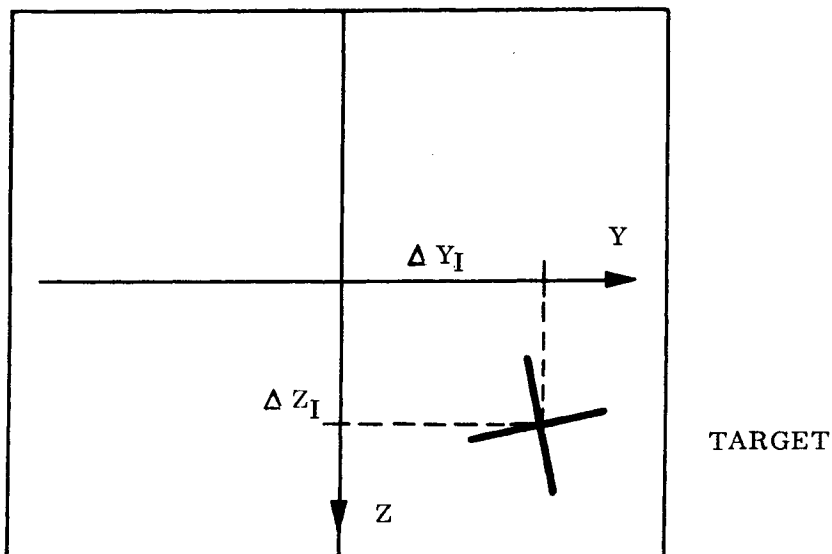
TARGET

Let Δy_I and Δz_I represent the displacement of the target image from the center of the film format.

Let $\vec{V}$ in represent a ray entering the primary optical system. The image of this ray is:

$$\vec{V} \text{ image} = (b)(M_p)(\theta_S) \vec{V} \text{ in} \tag{1}$$

where

$$(b) = \begin{pmatrix} 1 & b_z & -b_y \\ -b_z & 1 & 0 \\ b_y & 0 & 1 \end{pmatrix} \tag{2}$$

$$M_p = \begin{bmatrix} S2\sigma \\ -C2\sigma \, S\omega \\ C2\sigma \, C\omega \end{bmatrix} \tag{3}$$

2-397

$$\theta_S = \begin{bmatrix} \cos\theta_S & 0 & -\sin\theta_S \\ 0 & 1 & 0 \\ \sin\theta_S & 0 & \cos\theta_S \end{bmatrix} \tag{4}$$

If the optical system is pointed perfectly, and $\vec{V}$ in represents the line of sight, the image is a vector along the x axis. When errors are present, the image will have components along the y and z axes.

Then, one can write:

$$\vec{V} \text{ image (desired)} = (b)\,(M_p)_{\text{desired}}\,(\theta_S)\,\vec{V}_{LOS} = \begin{Bmatrix} 1 \\ 0 \\ 0 \end{Bmatrix} \tag{5}$$

and

$$\vec{V} \text{ image (actual)} = (b)\,(M_p)_{\text{actual}}\,(\theta_S)\,\vec{V}_{LOS} = \begin{Bmatrix} 1 \\ k\,\Delta Y \\ k\,\Delta Z \end{Bmatrix} \tag{6}$$

Equating $(\theta_S)\,\vec{V}_{LOS}$ from both equations given

$$(M_p)_{\text{desired}}\,(b)^T \begin{Bmatrix} 1 \\ 0 \\ 0 \end{Bmatrix} = (M_p)_{\text{actual}}\,(b)^T \begin{Bmatrix} 1 \\ k\,\Delta Y \\ k\,\Delta Z \end{Bmatrix} \tag{7}$$

Since (b) is obtained from the alignment monitor, (M_p) actual is derived from measured gimbal angles; and Δy, Δz are obtained from the photographs, equation (7) can be used to solve for the desired gimbal angles.

If b_y and b_z are assumed to be small, equation (7) can be approximated to:

$$
\left\{ \begin{array}{c} S2\sigma \\ -C2\sigma\, S\omega \\ C2\sigma\, C\omega \end{array} \right\}_{desired} \doteq (M_p)_{actual} \left[(b^T) \left\{ \begin{array}{c} 0 \\ k\,\Delta Y \\ k\,\Delta Z \end{array} \right\} + \left\{ \begin{array}{c} 1 \\ 0 \\ 0 \end{array} \right\} \right] \tag{8}
$$

From equation 8 the desired pitch and roll angle can be easily obtained.

2.7 IMAGE DEROTATION AND MANUAL CONTROL STICK RECOUPLING

The equations relating to derotation of the target image via the Pechan prism, and the decoupling of MCS signals, is presented in this section. The material is subdivided as follows;

2.7 IMAGE DEROTATION AND MANUAL CONTROL STICK DECOUPLING

2.7.1 INTRODUCTION

Image derotation is the alignment of the image such that it appears on the visual display the same as it would appear if it were observed in-track. The reason for image derotation is for visual adaptation.

Decoupling refers to coordinating the fore and aft motion of the control stick to vertical motion of the image on the visual display and right and left motion of the control stick to horizontal motion of the image on the visual display. The decoupling equations relate image motion at the center of the visual display to gimbal angle rates necessary to produce such image motion.

The image velocity sensor (IVS) measures how well the target is being tracked by sensing any motion of the image relative to the line-of-sight (LOS). The gimbal angle rate errors necessary to track the target are then given by the decoupling equations.

The equations for these functions are derived in this section.

2.7.2 NOTATION AND DEFINITIONS

LOS	Line-of-sight
Subscript a	Associated with ATS
Subscript p	Associated with primary optics
C	Cosine
S	Sine
$X_B Y_B Z_B$	Body reference system
$X_p Y_p Z_p$	Primary optics reference system (nominal)

2-403

X_a Y_a Z_a	ATS reference system
$X'_p Y'_p Z'_p$	Primary optics reference system (misaligned)
θ_s	Total cant angle (primary optics = 2 degrees)
x_g	Gimbal cant angle (ATS = 9 degrees)
σ , ω	Gimbal angles – Smith notation
θ , Ω	Gimbal angles – Balch notation
$[M]$	Mirror matrix (tracking mirror)
$\{P\}$	Object point
$\{P'\}$	Image point
$\{\dot{P}'\}$	Image velocity
γ	Derotation angle
γ IVS	Angle to IVS sensor orientation
b_y, b_z	Angular misalignments of primary optical axis
$\dot{\ell}_y$, $\dot{\ell}_z$	Components of measured (IVS) or desired (control stick) image velocity
$\Delta\dot{\sigma}$, $\Delta\dot{\omega}$	Gimbal angle rates corresponding to $\dot{\ell}_y$ and $\dot{\ell}_z$
K_o	Constant due to magnification, loop gains, etc.
$\{\hat{N}\}$	Unit normal to tracking mirror
$\{\hat{T}\}$	In-track unit vector

2-404

2.7.3 COORDINATE SYSTEMS

The coordinate systems in which the gimbal angles are measured for the ATS and primary optics are shown in Figures 2.7-1 and 2.7-2 respectively. Their relation to the body reference system is shown in Figure 2.7-3 in which it can be seen that:

$$\begin{Bmatrix} X_p \\ Y_p \\ Z_p \end{Bmatrix} = \begin{bmatrix} \theta_s \end{bmatrix} \begin{Bmatrix} X_B \\ Y_B \\ Z_B \end{Bmatrix}$$

where (1)

$$\begin{bmatrix} \theta_s \end{bmatrix} = \begin{bmatrix} C\theta_s & 0 & S\theta_s \\ 0 & 1 & 0 \\ -S\theta_s & 0 & C\theta_s \end{bmatrix}$$

and

$$\begin{Bmatrix} X_a \\ Y_a \\ Z_a \end{Bmatrix} = \begin{bmatrix} x_g \end{bmatrix} \begin{Bmatrix} X_B \\ Y_B \\ Z_B \end{Bmatrix}$$

where (2)

$$\begin{bmatrix} x_g \end{bmatrix} = \begin{bmatrix} Cx_g & Sx_g & 0 \\ -Sx_g & Cx_g & 0 \\ 0 & 0 & 1 \end{bmatrix}$$

2-405
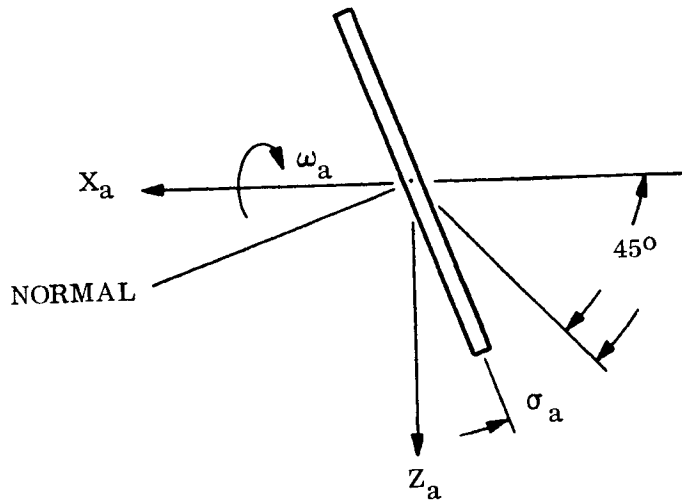
$$\{\widehat{N}_a\} = \sqrt{\frac{2}{2}} \begin{Bmatrix} (C\sigma_a + S\sigma_a) \\ -(C\sigma_a - S\sigma_a)\,S\omega_a \\ (C\sigma_a - S\sigma_a)\,C\omega_a \end{Bmatrix}$$

Figure 2.7-1
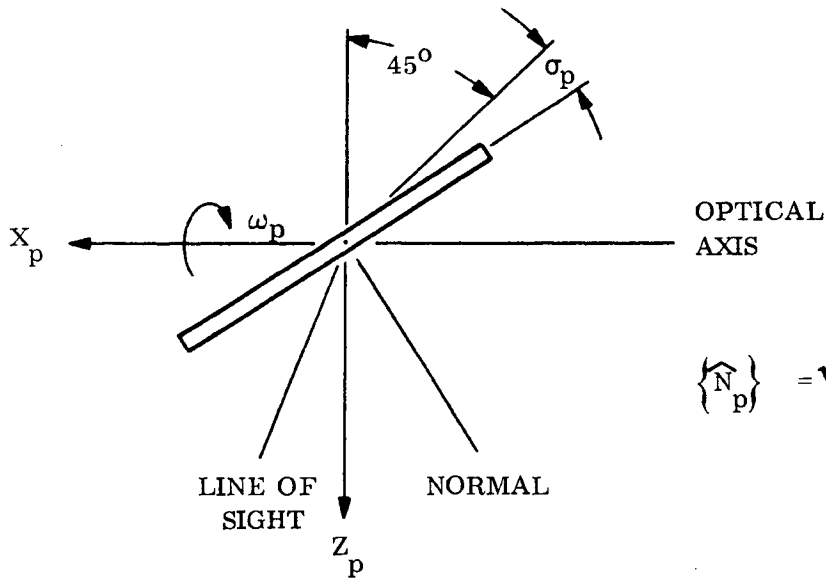
$$\{\widehat{N}_p\} = \sqrt{\frac{2}{2}} \begin{Bmatrix} -(C\sigma_p - S\sigma_p) \\ -(C\sigma_p + S\sigma_p)S\omega_p \\ (C\sigma_p + S\sigma_p)C\omega_p \end{Bmatrix}$$

Figure 2.7-2
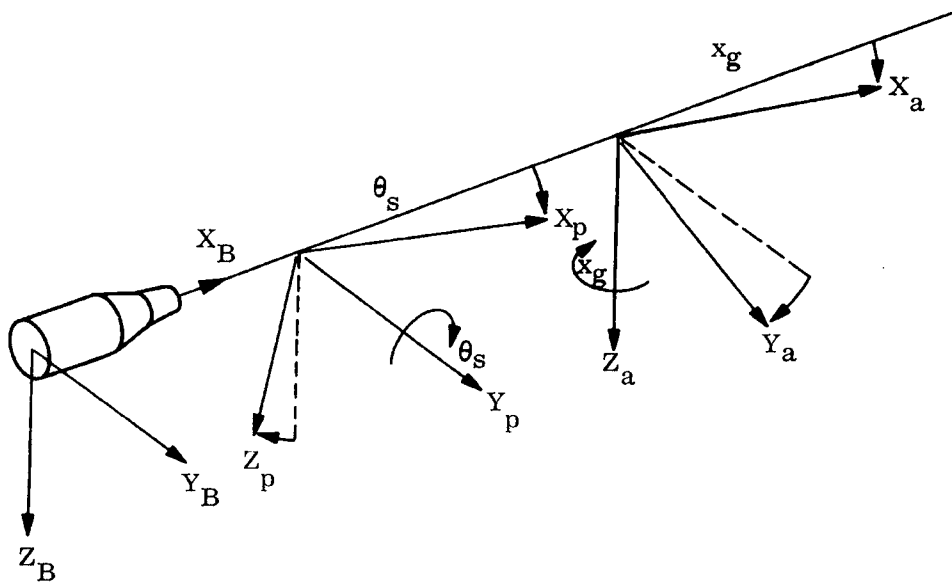
Figure 2.7-3

2.7.4 TRACKING MIRROR MATRIX

The mirror matrix which transforms object space into image space is a function of the direction cosines of the normal to the mirror. The normal to the mirrors are given in Figures 2.7-1 and 2.7-2. Therefore the mirror matrices,

for ATS are:

$$
\left[M_a \right] = \begin{bmatrix} -S2\sigma_a & S\omega_a C2\sigma_a & -C\omega_a C2\sigma_a \\ S\omega_a C2\sigma_a & C2\omega_a + S^2\omega_a S2\sigma_a & S\omega_a C\omega_a (1 - S2\sigma_a) \\ -C\omega_a C2\sigma_a & S\omega_a C\omega_a (1 - S2\sigma_a) & S2\omega_a + C2\omega_a S2\sigma_a \end{bmatrix} \tag{3}
$$

for primary optics are:

$$
\left[M_p \right] = \begin{bmatrix} S2\sigma_p & -C2\sigma_p S\omega_p & C2\sigma_p C\omega_p \\ -C2\sigma_p S\omega_p & C2\omega_p - S2\omega_p S2\sigma_p & S\omega_p C\omega_p (1 + S2\sigma_p) \\ C2\sigma_p C\omega_p & S\omega_p C\omega_p (1 + S2\sigma_p) & S2\omega_p - C2\omega_p S2\sigma_p \end{bmatrix} \tag{4}
$$

~~SECRET~~ **SPECIAL HANDLING**

2.7.5 IMAGE DEROTATION

The purpose of image derotation is to orient the image such that a vertical line in the image plane corresopnds to an in-track line in object space

For ATS:

Since the image plane is the $Y_B Z_B$ plane, the image points are given by

$$\{P'_a\} = \begin{bmatrix} x_g \end{bmatrix}^T \begin{bmatrix} M_a \end{bmatrix} \begin{bmatrix} x_g \end{bmatrix} \{P_a\} \tag{5}$$

The image of the in-track unit vector in the image plane is found from (5) to be (Figure 2.7-4).

$$\begin{Bmatrix} Y_B \\ Z_B \end{Bmatrix} = \begin{Bmatrix} S\omega_a C2\sigma_a C2x_g - Sx_g Cx_g (C^2\omega_a + S2\sigma_a(1+S^2\omega_a)) \\ -C\omega_a C2\sigma_a Cx_g - Sx_g S\omega_a C\omega_a (1-S2\sigma_a) \end{Bmatrix} \tag{6}$$
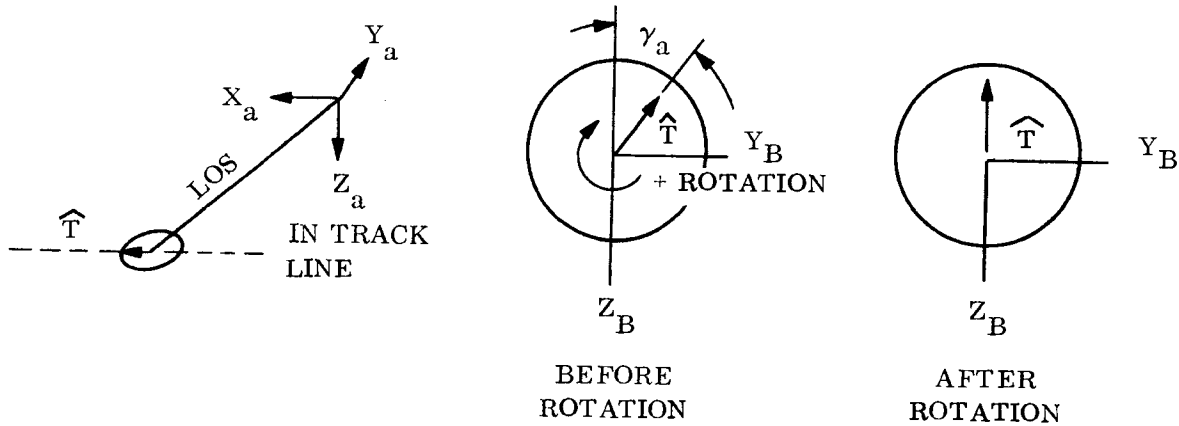
Figure 2.7-4

~~SECRET~~ **SPECIAL HANDLING**

Defining positive rotation of the image to be given by the right hand rule about the X_B axis, the image derotation angle for the ATS is given by:

$$\gamma_a = TAN^{-1} \left\{ \frac{S\omega_a \, C2\sigma_a \, C2x_g - Sx_g Cx_g \, (C^2\omega_a + S2\sigma_a \, (1 + S^2\omega_a))}{-C\omega_a \, C2\sigma_a \, Cx_g - Sx_g S\omega_a C\omega_a \, (1 - S2\sigma_a)} \right\} \quad (7)$$

where

$$-90^\circ \leq \gamma_a \leq 90^\circ$$

Since the actual image rotation is twice the derotation prism rotation, the command to the derotation prism would be $\gamma a/2$ to orient the image.

For primary optics:

There is an on-board alignment monitor associated with the primary optics that measures the angular offset of the optical axis about the Y_p and Z_p axes. These measurements, deonted by b_y and b_z, are used to construct a transformation matrix between the $X_p Y_p Z_p$ and $X'_p Y'_p Z'_p$ coordinate systems (Figure 2.7-5). Since the image plane is the $Y'_p Z'_p$ plane, the image points are given by

$$\{P'_p\} = [b] [M_p] [\theta_s] \{P_p\}$$

where   (8)

$$[b] = \begin{bmatrix} 1 & b_z & -b_y \\ -b_z & 1 & 0 \\ b_y & 0 & 1 \end{bmatrix}$$

2-412

The image of the in-track unit vector in the image plane is found from (8) to be (Figure 2.7-6).

$$\begin{Bmatrix} Y \\ Z \end{Bmatrix} = \begin{Bmatrix} -C2\sigma_p S\omega_p C\theta_s - S\omega_p C\omega_p S\theta_s (1 + S2\sigma_p) - b_z (S2\sigma_p C\theta_s - C2\sigma_p C\omega_p S\theta_s) \\ C2\sigma_p C\omega_p C\theta_s - S^2\omega_p S\theta_s + C^2\omega_p S2\sigma_p S\theta_s + b_y (S2\sigma_p C\theta - C2\sigma_p C\omega_p S\theta_s) \end{Bmatrix} \quad (9)$$

Defining positive rotation of the image to be given by the right hand rule about the X'_p axis, the image derotation angle for the primary optics is given by:

$$\gamma_p = TAN^{-1} \left\{ \frac{-C2\sigma_p S\omega_p C\theta_s - S\omega_p C\omega_p S\theta_s (1 + S2\sigma_p) - b_z (S2\sigma_p C\theta_s - C2\sigma_p S\theta_s C\omega_p)}{C2\sigma_p C\omega_p C\theta_s - S^2\omega_p S\theta_s + C^2\omega_p S2\sigma_p S\theta_s + b_y (S2\sigma_p C\theta_s - C2\sigma_p C\omega_p S\theta_s)} \right\} \quad (10)$$

$$\begin{Bmatrix} X'_p \\ Y'_p \\ Z'_p \end{Bmatrix} = \begin{bmatrix} 1 & b_z & -b_y \\ -b_z & 1 & 0 \\ b_y & 0 & 1 \end{bmatrix} \begin{Bmatrix} X_p \\ Y_p \\ Z_p \end{Bmatrix}$$

X'_p – ACTUAL OPTICAL AXIS

X_p – OPTICAL AXIS IF NO MISALIGNMENTS
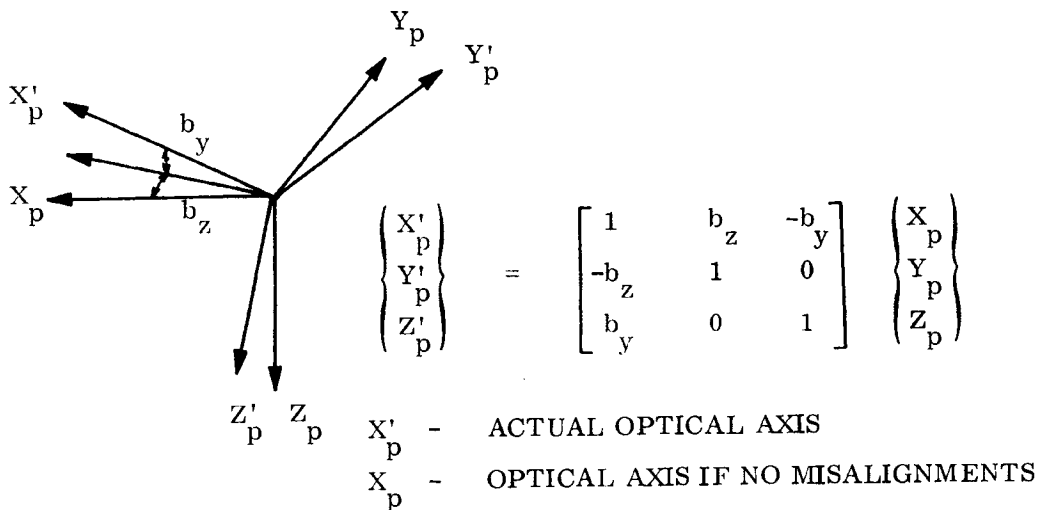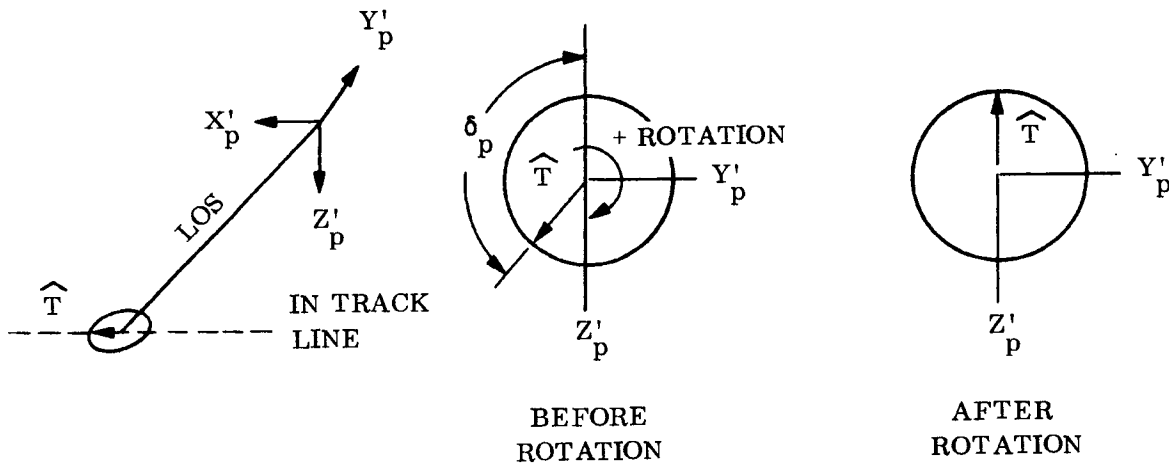
Figure 2.7-5

Figure 2. 7-6

Again the command to the derotation prism should be γ p/2 to orientate the image correctly.

Equations (7) and (10) are derived assuming the image of the tracking mirror is not inverted before reaching the visual display. Sould the image be inverted an odd number of times i. e., 1, 3, 5....., then the derotation angle is given by (180 – γ) where γ is given by (7) or (10).

~~SECRET~~ **SPECIAL HANDLING**

2.7.6 IMAGE MOTION DECOUPLING

The purpose of image motion decoupling is to relate vertical and horizontal image motion to changes in the gimbal angles. These equations give the gimbal angle rates necessary to correct for image motion detected by the IVS, and also provide the coordination between control stick motion and image motion on the ATS and primary optics visual display. Denoting the induced image motions by the control stick or the image motions detected by the IVS as $\dot{\ell}_y$ and $\dot{\ell}_z$, the decoupling equations are derived as follows. (See Figure 2.7-7.)

For ATS:

The position of the image is given by (5) and the velocity of the image is given by the chain rule as follows:

$$\left\{ \dot{P}'_a \right\} = \left[\frac{\partial \left\{ P'_a \right\}}{\partial \sigma_a} \quad \frac{\partial \left\{ P'_a \right\}}{\partial \omega_a} \right] \left\{ \begin{array}{c} \Delta \dot{\sigma}_a \\ \Delta \dot{\omega}_a \end{array} \right\} \tag{11}$$

ATS VISUAL DISPLAY	PRIMARY OPTICS VISUAL DISPLAY	IVS SENSOR DISPLAY

Figure 2.7-7

2-415
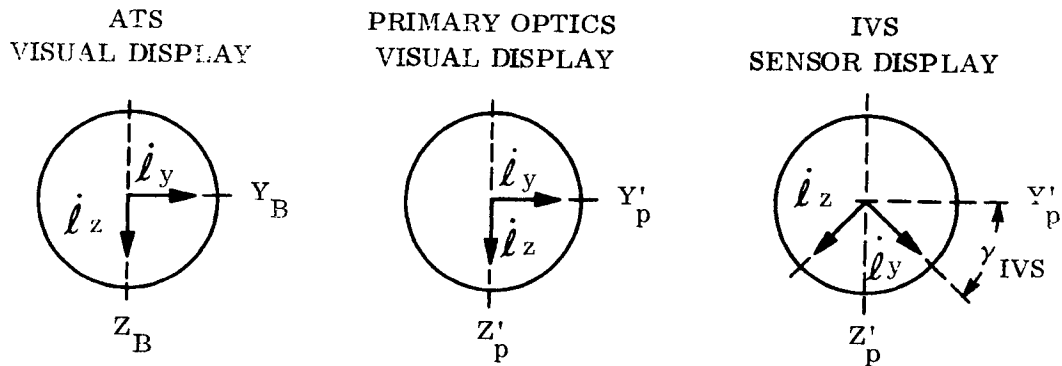
~~SECRET~~ **SPECIAL HANDLING**

Now it is assumed that $\dot{\ell}_y$ and $\dot{\ell}_z$ are the velocity components of the image of the optical axis; that is the image point at the center of the visual display. If any other point were chosen for decoupling, the off-axis image velocities would have to be considered in the decoupling equations. Since the mirror matrix is involutory ($[M] = [M]^{-1}$), the object whose image is along the optical axis is given by:

$$\left\{ P_a \right\} = \left[x_g \right]^T \left[M_a \right] \left[x_g \right] \left\{ \begin{array}{c} -1 \\ 0 \\ 0 \end{array} \right\} \tag{12}$$

Taking the partials indicated in (11) and substituting (12) for $\left\{ P_a \right\}$ yields:

$$\frac{\partial \left\{ P_a \right\}'}{\partial \sigma_a} = \left[x_g \right]^T \frac{\partial \left[M_a \right]}{\partial \sigma_a} \left[M_a \right] \left[x_g \right] \left\{ \begin{array}{c} -1 \\ 0 \\ 0 \end{array} \right\} \tag{13}$$

$$\frac{\partial \left\{ P_a \right\}'}{\partial \omega_a} = \left[x_g \right]^T \frac{\partial \left[M_a \right]}{\partial \omega_a} \left[M_a \right] \left[x_g \right] \left\{ \begin{array}{c} -1 \\ 0 \\ 0 \end{array} \right\}$$

The products of the partial derivative of the mirror matrix and the mirror matrix are given by:

$$\frac{\partial \left[M_a \right]}{\partial \sigma_a} \left[M_a \right] = 2 \begin{bmatrix} 0 & -S\omega_a & C\omega_a \\ S\omega_a & 0 & 0 \\ -C\omega_a & 0 & 0 \end{bmatrix} \tag{14}$$

$$\frac{\partial \left[M_a \right]}{\partial \omega_a} \left[M_a \right] = 2 \begin{bmatrix} 0 & C\omega_a C2\sigma_a & S\omega_a C2\sigma_a \\ -C\omega_a C2\sigma_a & 0 & -(1-S2\sigma_a) \\ -S\omega_a C2\sigma_a & (1-S2\sigma_a) & 0 \end{bmatrix} \tag{15}$$

2-416

Now evaluating the partials in (13) and substituting them into (11) yields:

$$\left\{\begin{array}{c} \dot{\ell}_x \\ \dot{\ell}_y \\ \dot{\ell}_z \end{array}\right\} \equiv \left\{\dot{P}'_a\right\} = \left[\left\{\begin{array}{c} 0 \\ -2S\omega_a \\ 2C\omega_a Cx_g \end{array}\right\} \quad \left\{\begin{array}{c} 0 \\ C2\sigma_a C\omega_a \\ S\omega_a C2\sigma_a Cx_g + Sx_g (1-S2\sigma_a) \end{array}\right\}\right] \left\{\begin{array}{c} \Delta\dot{\sigma}_a \\ \Delta\dot{\omega}_a \end{array}\right\} \qquad (16)$$

Since $\dot{\ell}_y$ and $\dot{\ell}_z$ are the only components under consideration (16) reduces to

$$\left\{\begin{array}{c} \dot{\ell}_y \\ \dot{\ell}_z \end{array}\right\} = \left[\begin{array}{cc} -2S\omega_a & C2\sigma_a C\omega_a \\ 2C\omega_a Cx_g & S\omega_a C2\sigma_a Cx_g + Sx_g (1 - S2\sigma_a) \end{array}\right] \left\{\begin{array}{c} \Delta\dot{\sigma}_a \\ \Delta\dot{\omega}_a \end{array}\right\} \qquad (17)$$

The inverse of Equation (17) is actually the desired expression since the gimbal angle rate commands are to be derived from $\dot{\ell}_y$ and $\dot{\ell}_z$ which correspond to control stick position. Also image derotation has to be considered in the final equation which is:

$$\left\{\begin{array}{c} \Delta\dot{\sigma}_a \\ \Delta\dot{\omega}_a \end{array}\right\} = \frac{K_o}{D} \left[\begin{array}{cc} K_4 & -K_3 \\ -K_2 & K_1 \end{array}\right] \left[\begin{array}{cc} C\gamma_a & S\gamma_a \\ -S\gamma_a & C\gamma_a \end{array}\right] \left\{\begin{array}{c} \dot{\ell}_Y \\ \dot{\ell}_z \end{array}\right\}$$

where

$$
\begin{aligned}
K_1 &= -2S\omega_a \\
K_2 &= 2C\omega_a Cx_g \\
K_3 &= C2\sigma_a C\omega_a \\
K_4 &= S\omega_a C2\sigma_a Cx_g + Sx_g (1 - S2\sigma_a) \\
D &= K_1 K_4 - K_2 K_3 \\
K_o &= \text{Constant depending upon optical magnification, loop gains....} \\
\gamma_a &= \text{Image derotation angle}
\end{aligned}
\qquad (18)$$

2-417

For primary optics:

The analysis for decoupling in the primary optics follows the same logic as for decoupling in the ATS.   Equation (11) becomes:

$$\left\{\dot{P}_p'\right\} = \left[\frac{\partial \left\{P_p'\right\}}{\partial \sigma_p} \quad \frac{\partial \left\{P_p'\right\}}{\partial \omega_p}\right] \left\{\begin{array}{c} \Delta\dot{\sigma}_p \\ \Delta\dot{\omega}_p \end{array}\right\} \tag{19}$$

The object whose image is along the optical axis is given by:

$$\left\{P_p\right\} = \left[\theta_s\right]^T \left[M_p\right] \left[b\right]^T \left\{\begin{array}{c} 1 \\ 0 \\ 0 \end{array}\right\} \tag{20}$$

Taking the partials indicated in (19) and substituting (20) for $\left\{P_p\right\}$ yields:

$$\frac{\partial \left\{P_p\right\}'}{\partial \sigma_p} = \left[b\right] \frac{\partial \left[M_p\right]}{\partial \sigma_p} \left[M_p\right] \left[b\right]^T \left\{\begin{array}{c} 1 \\ 0 \\ 0 \end{array}\right\}$$

$$\tag{21}$$

$$\frac{\partial \left\{P_p'\right\}}{\partial \omega_p} = \left[b\right] \frac{\partial \left\{M_p\right\}}{\partial \omega_p} \left[M_p\right] \left[b\right]^T \left\{\begin{array}{c} 1 \\ 0 \\ 0 \end{array}\right\}$$

Where the products of the partials of the mirror matrix and the mirror matrix are given by:

$$\frac{\partial \left[M_p\right]}{\partial \sigma_p} \left[M_p\right] = 2 \begin{bmatrix} 0 & -S\omega_p & C\omega_p \\ S\omega_p & 0 & 0 \\ -C\omega_p & 0 & 0 \end{bmatrix} \tag{22}$$

$$\frac{\partial \left[M_p\right]}{\partial \omega_p} \left[M_p\right] = \begin{bmatrix} 0 & -C2\sigma_p C\omega_p & -C2\sigma_p S\omega_p \\ C\omega_p C2\sigma_p & 0 & -(1 + S2\sigma_p) \\ C2\sigma_p S\omega_p & (1 + S2\sigma_p) & 0 \end{bmatrix} \tag{23}$$

2-418

Now evaluating the partials in (21) and substituting in (19) yields the desired velocity components:

$$
\begin{Bmatrix} \dot{\ell}_y \\ \dot{\ell}_z \end{Bmatrix} = \begin{bmatrix} 2S\omega_p & C\omega_p C2\sigma_p + b_y(1 + S2\sigma_p) \\ -2C\omega_p & S\omega_p C2\sigma_p + b_z(1 + S2\sigma_p) \end{bmatrix} \begin{Bmatrix} \Delta\dot{\sigma}_p \\ \Delta\dot{\omega}_p \end{Bmatrix} \tag{24}
$$

As before, the inverse of (24) is actually desired since the gimbal angle rate commands are to be computed from $\dot{\ell}_y$ and $\dot{\ell}_z$, that is:

$$
\begin{Bmatrix} \Delta\dot{\sigma}_p \\ \Delta\dot{\omega}_p \end{Bmatrix} = \frac{K_0}{D} \begin{bmatrix} K_4 & -K_3 \\ -K_2 & K_1 \end{bmatrix} \begin{bmatrix} \gamma \end{bmatrix} \begin{Bmatrix} \dot{\ell}_y \\ \dot{\ell}_z \end{Bmatrix}
$$

where (25)

$$
\begin{aligned}
K_1 &= 2S\omega_p \\
K_2 &= -2C\omega_p \\
K_3 &= C\omega_p C2\sigma_p + b_y(1 + S2\sigma_p) \\
K_4 &= S\omega_p C2\sigma_p + b_z(1 + S2\sigma_p) \\
\begin{bmatrix} \gamma \end{bmatrix} &= \text{is a rotation matrix to be discussed}
\end{aligned}
$$

For the primary optics visual display which has been derotated by the angle given in Equation (10), the rotation matrix is:

$$
\begin{bmatrix} \gamma \end{bmatrix}_{\substack{\text{Visual} \\ \text{Display}}} = \begin{bmatrix} C\gamma_p & S\gamma_p \\ -S\gamma_p & C\gamma_p \end{bmatrix} \tag{26}
$$

~~SECRET~~ **SPECIAL HANDLING**

For the IVS, if the coordinate system in which the image velocities are measured is rotated about the X'_p axes (right hand rule defining positive) by an angle γ_{IVS} from the Y'_p Z'_p axes then the rotation matrix in (25) is given by:

$$\left[\gamma\right]_{IVS} = \begin{bmatrix} c\gamma_{IVS} & -s\gamma_{IVS} \\ s\gamma_{IVS} & c\gamma_{IVS} \end{bmatrix} \tag{27}$$

Notice that the IVS senses $\dot{l}_y$ and $\dot{l}_z$ which are due to $\Delta\dot{\sigma}_p$ and $\Delta\dot{\omega}_p$. The gimbal rate command to correct the image motion is then the negative of these or $-\Delta\dot{\sigma}_p$ and $-\Delta\dot{\omega}_p$.

~~SECRET~~ **SPECIAL HANDLING**

2.7.7 APPROXIMATIONS TO THE DEROTATION EQUATIONS

Since the reason for derotating the image is for ease in visual adaptation by the crew, the question arises about the accuracy with which the image need be orientated. Neglecting gimbal cant in the case of the ATS and total cant and misalignments in the case of the primary optics equations (7) and (10) reduce to:

$$\gamma_a \approx -\omega_a \tag{28}$$

$$\gamma_p \approx \pi - \omega_p \tag{29}$$

Investigating the range of gimbal angles, these equations introduce maximum errors of 15 degrees in the ATS derotation and 2 degrees in the primary optics derotation. Therefore equation (28) is not recommended for approximating the ATS derotation angle.

The obliquity angle is a good approximation to the ATS derotation angle. However, this quantity would have to be computed first since it is not available in the computer.

2.7.8 STANDARDIZED EQUATIONS

Early work done by several groups resulted in several definitions of gimbal angles. The extensive work done by E. Balch has resulted in his notation being chosen to be the standard notation. The transformation between the notation used in this report and the standard notation is given by:

$$\sigma_a = \theta_a - 45^{\circ} \qquad \sigma_p = 45^{\circ} - \theta_p$$
$$\omega_a = \Omega_a \qquad \omega_p = -\Omega_p$$

(30)

2-423/2-424

~~SECRET~~ **SPECIAL HANDLING**

2.7.9 IMAGE DEROTATION

ATS:

$$\gamma_a = \mathrm{TAN}^{-1} \left\{ \frac{S\Omega_a S2\theta_a C2x_g - Sx_g Cx_g (C^2\Omega_a - C2\theta_a (1 + S^2\Omega_a))}{-C\Omega_a S2\theta_a Cx_g - Sx_g S\Omega_a C\Omega_a (1 + C2\theta_a)} \right\}$$

$$-90^{\circ} \leq \gamma_p \leq 90^{\circ}$$

Primary Optics:

$$\gamma_p = \mathrm{TAN}^{-1} \left\{ \frac{+S2\theta_p S\Omega_p C\theta_s + S\Omega_p C\Omega_p S\theta_s (1 + C2\theta_p) - b_z (C2\theta_p C\theta_s - S2\theta_p C\Omega_p S\theta_s)}{S2\theta_p C\Omega_p C\theta_s - S^2\Omega_p S\theta_s + C^2\Omega_p C2\theta_p S\theta_s + b_y (C2\theta_p C\theta_s - S2\theta_p C\Omega_p S\theta_s)} \right\} \quad (32)$$

or

$$\gamma_p \approx \pi + \Omega_p \quad (\text{within } 2^{\circ}) \qquad 90^{\circ} \leq \gamma_p \leq 270^{\circ}$$

2.7.10 IMAGE MOTION DECOUPLING

ATS: Equation (18)

$$K_1 = -2S\Omega_a$$

$$K_2 = 2C\Omega_a Cx_g$$

$$K_3 = S2\theta_a C\Omega_a$$

$$K_4 = S\Omega_a S2\theta_a Cx_g + Sx_g(1 + C2\theta_a)$$

(33)

Primary Optics: Equation (25)

$$K_1 = -2S\Omega_p$$

$$K_2 = -2C\Omega_p$$

$$K_3 = C\Omega_p S2\theta_p + b_y(1 + C2\theta_p)$$

$$K_4 = -S\Omega_p S2\theta_p + b_z(1 + C2\theta_p)$$

(34)

Also:

$$\dot{\sigma}_a = \dot{\theta}_a \qquad\qquad \dot{\sigma}_p = -\dot{\theta}_p$$

$$\dot{\omega}_a = \dot{\Omega}_a \qquad\qquad \dot{\omega}_p = -\dot{\Omega}_p$$

(35)

~~SECRET~~ **SPECIAL HANDLING**

SECTION 3.0

CUE SYSTEM ANALYSIS

The material in this section is subdivided as follows;

~~SECRET~~ **SPECIAL HANDLING**

3.1 INTRODUCTION

A full PDR report by Lear Sigler was submitted to the Air Force. This report provided analysis of the optics and controls and described the projector design in detail. This report presents the results of an independent GE optical analysis of the VDP and reviews Lear's comments concerning compliance with the GE component spec.

3-3/3-4

3.2 VDP OPTICAL ANALYSIS

An analysis of the projection optics has been performed. The active elements which were included in the analysis are the film base, the right-angle prism, and the lens which is a Cooke triplet operating at F/3.55. The purpose of the analysis is to determine if the system is capable of meeting the required performance level and to evaluate the assigned manufacturing tolerance values.

The on-axis modulation transfer function, MTF, is shown in Figure 3.2-1. For comparison, the MTF of an aberration-free, diffraction-limited system is also shown which represents an upper limit to the performance of a real system of the same numerical aperture. The abscissa of Figure 3.2-1 is the spatial frequency in line pairs per mm of the aerial image (which appears immediately behind the rear projection screen) and is related to the film spatial frequency through the magnification, m, of the system; i.e.,

film frequency = m x (screen frequency).

The ordinate is the modulation transfer function which represents the ratio of the image contrast to the object contrast; i.e.,

$$\text{MTF (2)} = \frac{C_i\,(U)}{C_o\,(mU)}$$

where

$C_i\,(U)$ = image contrast at image frequency 2,

$C_o\,(mU)$ = object contrast at object frequency m2,

and

$$C = \frac{B\,max - B\,min}{B\,max + B\,min}$$

IDEAL DIFRACTION LIMITED (MTF)
PROJECTION SYSTEM MTF NOT
INCLUDING SCREEN.

FOCAL LENGTH = 2.90276 CM
MAGNIFICATION = 13.0
IMAGE SPACE CUTOFF = 35.4 LP/MM
OBJECT SPACE CUTOFF = 487 LP/MM
$f^\# = \frac{1}{2NA} = 3.69$
SPECTRUM = 0.76P, 0.16S, 0.08T
FOCAL SHIFT = 0.495 CM

DIFFRACTION LIMIT

228 LP/MM
ON FILM

PROJECTION
SYSTEM LESS
SCREEN

128 LP/MM
ON FILM

MTF →
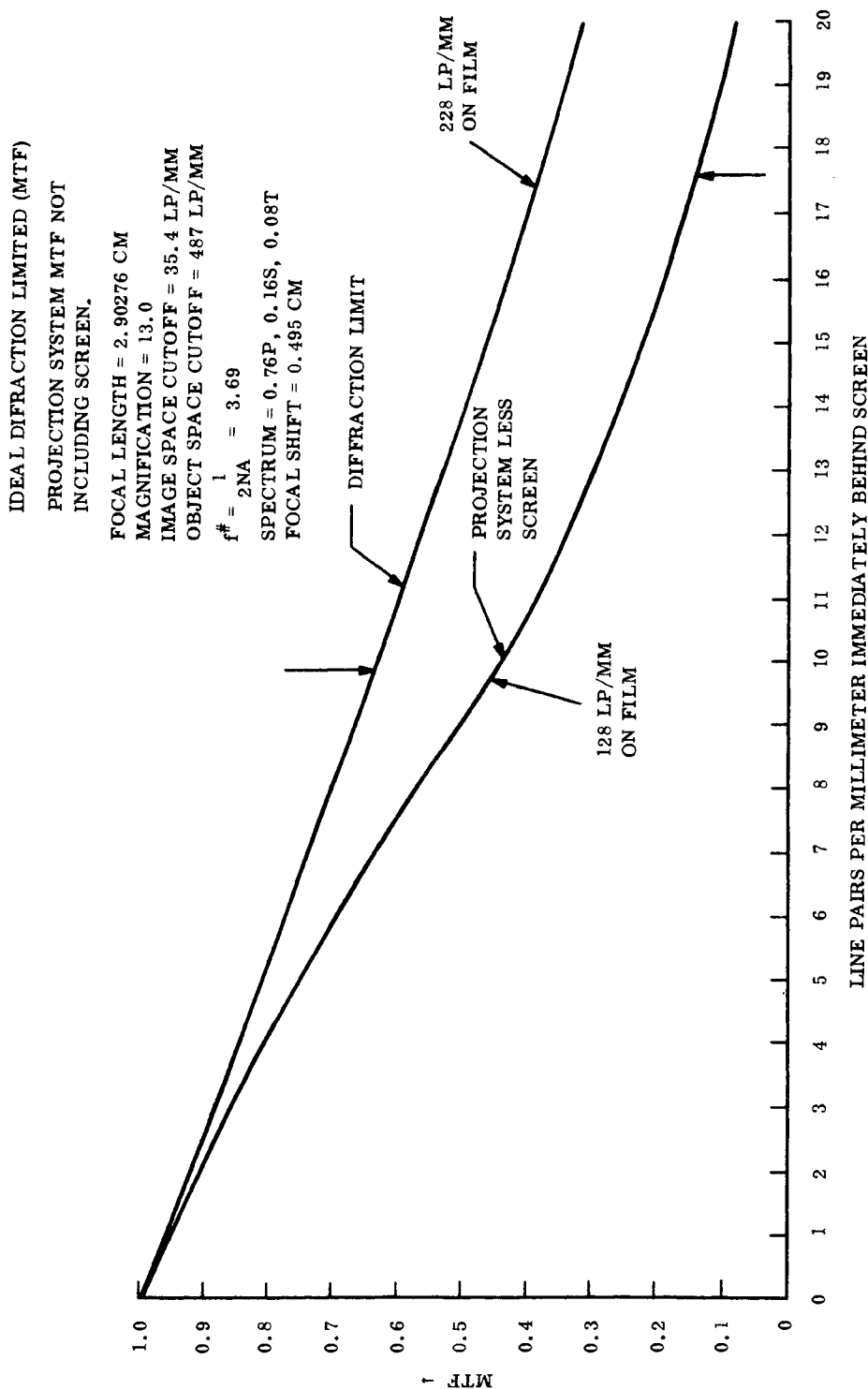
LINE PAIRS PER MILLIMETER IMMEDIATELY BEHIND SCREEN

Figure 3.2-1. On-Axis Modulation Transfer Function, Film-to-Screen Image

3-7

It is seen from Figure 3.2-1 that at 9.8 lp/mm the MTF value for an aerial image is approximately 0.45 and at 17.6 lp/mm the MTF value is 0.14. The two frequencies correspond to the film frequencies of 128 lp/mm and 228 lp/mm, respectively for a system magnification of 13.0.

To include the effects of the screen on the overall system, the MTF of the projection optics must be multiplied by the MTF of the rear projection screen. Figure 3.2-2 shows both MTF curves and their product curve which represents the overall MTF of the system.

Evaluation of the system must be made in terms of the minimum perceptible contrast which is first discernible by the eye. Measurements of this quantity by DePalma and Lowry, JOSA 52, 328 (1962), are presented in Figure 3.2-3. From the figure, it is clear that frequencies near 10 lp/mm cannot be perceived by a normal population observer with this system, since contrast values approaching unity would be required. On the other hand, a 10x magnifier having an MTF as low as 1/2 would require contrast values exceeding a contrast of only 0.005. This value corresponds to an average brightness of 20 ft-lamberts viewed at a distance of 10 inches.

Working the problem in reverse, we will calculate the minimum film contrast necessary at 128 lp/mm on the film to yield a perceptible contrast on the screen using a 10x magnifier with an MTF equal to 0.50. The equation to use is:

$$C_{film} = \frac{C \text{ min. percept.}}{(MTF)_{mag.} \times (MTF)_{screen} \times (MTF)_{proj.}}$$

3-8

~~SECRET~~ SPECIAL HANDLING
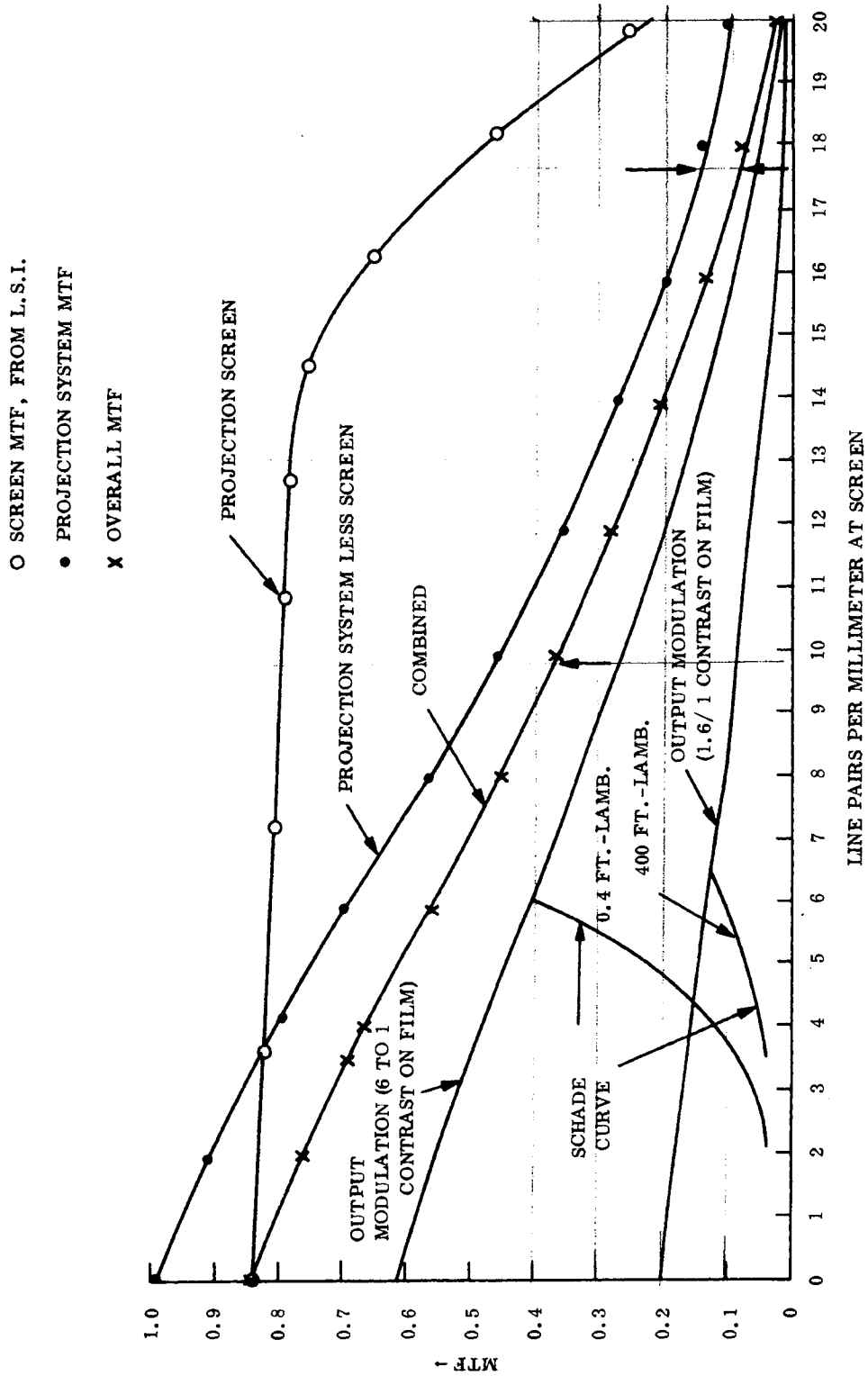
Figure 3.2-2. On-Axis Modulation Transfer Function, Film-to-Screen Image

3-9

~~SECRET~~ SPECIAL HANDLING
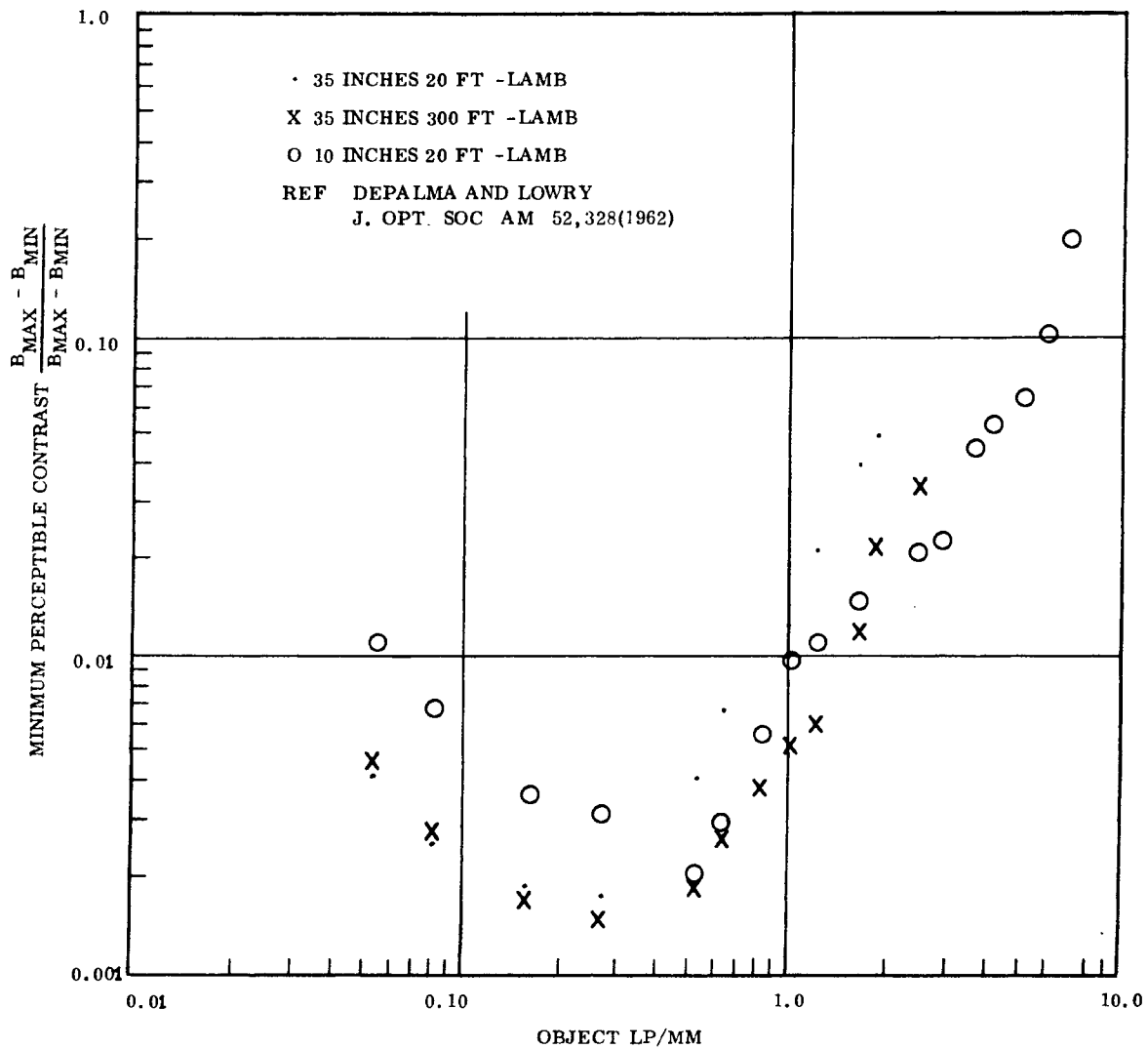
Figure 3.2-3. Contrast Sensitivity for Sine Wave Test Objects as a Function of Object Spatial Frequency for Several Viewing Distances and Brightnesses

~~SECRET~~ **SPECIAL HANDLING**

where

$$(MTF)\ mag. = 0.50$$

$$(MTF)\ screen = 0.80$$

$$\left.\right\} \quad Product = 0.195$$

$$(MTF)\ proj. = 0.49$$

Thus

$$C_{film} = \frac{0.005}{0.195}$$

$$= 0.025$$

which corresponds to a relative contrast of 1.05/1.0 at 128 lp/mm on the film.

For 228 lp/mm on the film, the MTF values become:

$$(MTF)\ mag. = 0.50$$

$$(MTF)\ screen = 0.66$$

$$\left.\right\} \quad Product = 0.0595$$

$$(MTF)\ proj. = 0.18$$

$$C\ min.\ percept. = 0.012$$

$$C_{film} = \frac{0.012}{0.0595} = 0.202.$$

This corresponds to a relative contrast of 1.5/1 at 228 lp/mm on the film.

An analysis of the tolerance values assigned to the component separations and lens thicknesses has been performed by use of a statistical approach. Referring to Figure 3.2-4, the lens thicknesses considered are of lenses I, II, and III and of the prism. The separation considered is the distances between the surfaces of lenses I-II, II-II, and between III

~~SECRET~~ **SPECIAL HANDLING**

~~SECRET~~ **SPECIAL HANDLING**
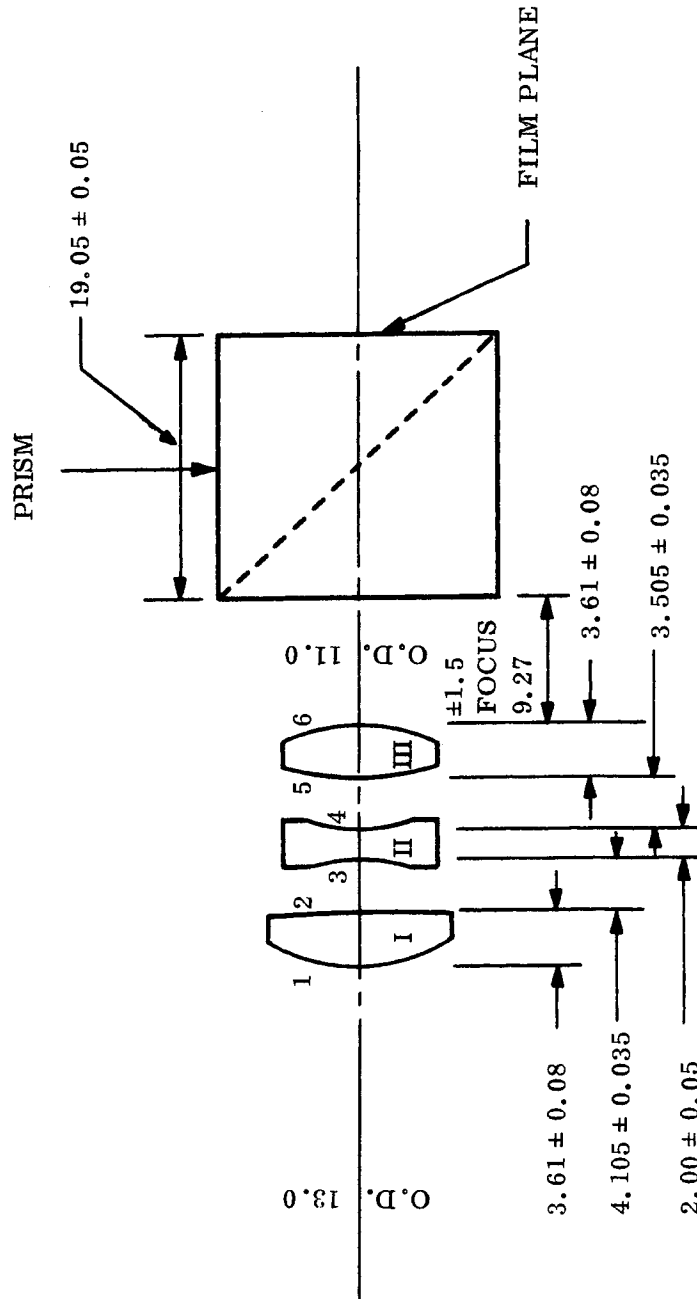
Figure 3.2-4. Visual Display Projector Projection Lens and Deviating Prism

~~SECRET~~ **SPECIAL HANDLING**

and the prism. The tolerances shown in the figure were used in this analysis. If it can be assumed that the assigned tolerance value represents one standard deviation, then the propagation of errors for a system of several parameters, each with an assigned standard deviation, results in a system standard deviation which can be computed by the relationship

$$\sigma^2 = \sum_{n=1}^{n} \left(\frac{\partial F}{\partial X_n}\right)^2 \sigma_n^2$$

where X_n is the nth parameter, σ_n is the standard deviation of the nth parameter, σ is the standard deviation of F, and n is the total number of parameters.

This calculation has been carried out, and the results are indicated in Figure 3.2-5. Also shown for comparison is the nominal MTF curve as calculated by LSI. It is seen to fall within the calculated standard deviation.

The interpretation of the curve of Figure 3.2-5 is that if the tolerance values assigned to different parameters represents one standard deviation, then the system standard deviation at any frequency represents the range in which there is a 63 percent chance that the MTF value will fall. Also the chance that the MTF value will be more than one standard deviation below the nominal value is 19 percent.

Shown on Figure 3.2-3 is the minimum perceptible contrast as determined from the Schade curve and the screen contrast resulting from film contrasts of both 6 to 1 and 1.6 to 1. The intersection of the output modulation curves and the Schade curve represents the visual cutoff of the system for the specified input contrast. Using a display brightness of 400 ft-lamberts, the visual cutoff for a 1.6-to-1 contrast input occurs at 6.5 line pairs per mm on the screen or 84.5 line pairs/mm on the film.
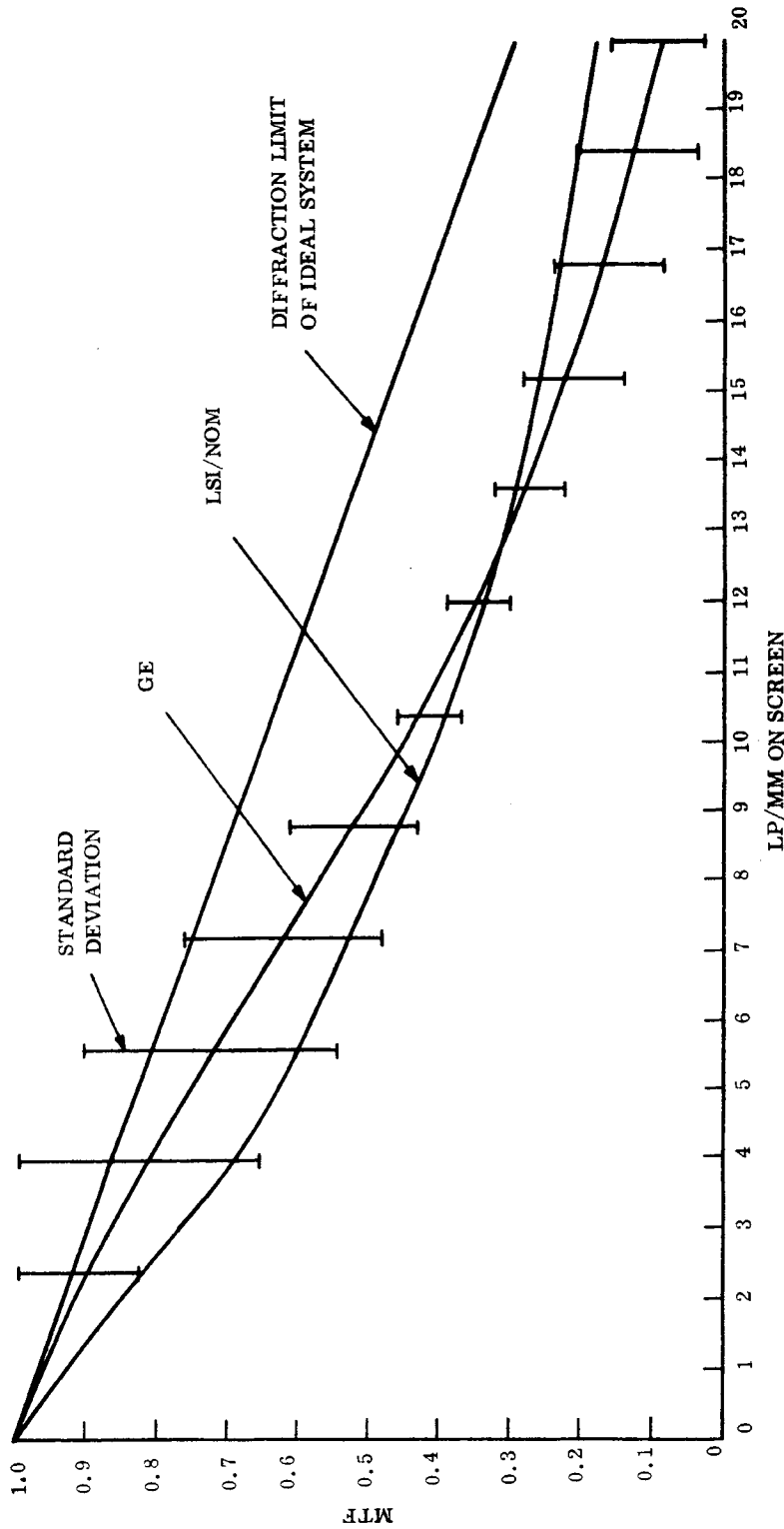
Figure 3.2-5. Tolerance Evaluation

It is unlikely that the average unaided eye will be able to resolve the screen image pro-
duced by 228 lp/mm on the film, regardless of the film input contrast.

From inspection of Figure 3.2-2, it is possible to determine the minimum magnification
necessary to resolve 17.6 lp/mm on the screen (228 lp/mm on the film at 6 to 1 contrast).
At 17.6 lp/mm, the screen contrast is seen to be 0.05, allowing for a magnifier MTF of
0.9, the resulting contrast becomes 0.045. The Schade curve (0.40 ft-lamberts) has a
value of 0.045 at 2.6 lp/mm. The necessary magnification is therefore 17.6/2.6 = 6.7.
A similar calculation indicates that for a display brightness of 400 ft-lamberts a minimum
magnification of 17.6/4.0 = 4.4 is necessary.

3.3 SUBCONTRACTOR COMPLIANCE COMMENTS

The following is a listing of the Visual Display Projector requirements set forth in the Component Specification. A brief summary of the estimated system performance and the method of analysis used to determine this estimate are also included. This material was submitted by Lear Siegler, Inc. in their VDP Design Review Report in November 1967.

3.3.1 ACCESS TIME (SINGLE FRAME OPERATION)

Requirement - The time to step one frame in either direction shall not exceed 0.35 second.

Analysis Method - Digital and Analog computer studies.

Estimated Performance - 0.30 second or less.

Variances - None

3.3.2 OPERATING TIMES

Requirement

    b. Projection lamp turn-off and Binary Code comparison shall be accomplished in 0.05 second after receipt of external command.

    c. Frame search rate shall be 100 frames per second.

    d. Acceleration, deceleration and fine positioning within a screen image accuracy of ±0.125 inch shall be accomplished within 0.35 second.

    e. Frames shall be searched, positioned, and displayed within
$$0.35 + \frac{\text{number of frames}}{100} \text{ second.}$$

    f. Switching to standby mode shall be accomplished within 0.05 second after external command is removed.

    g. Warm-up time shall be less than 10.0 seconds.

Analysis Method

    Paragraphs b., f., and g., - Theoretical circuit analysis.

    Paragraphs d. and e. - Digital and Analog computer studies.

    Paragraph c. - Breadboard tests.

Estimated Performance

b.   The propagation time for the VDP circuits is less than 1 millisec. However, a delay circuit must be incorporated at the input dependent upon the maximum "zero" time of the updating external command. If this max. zero time is less than 45 millisec, the requirement can be met.

c.   100 frames per second minimum.

d, e.   0.35 second maximum except as noted below.

f.   Switching time will be 1 millisec plus max. "zero" time of updating external command. It is assumed that the projector is displaying a frame at the time external command is removed.

g.   Less than 1.0 second.

Variances

d, e.   When there are less than three consecutively numbered frames prior to the commanded frame, up to 0.10 second additional time may be required.

3.3.3 DISPLAY SCREEN BRIGHTNESS

Requirement - Brightness shall be adjustable from 0 to 15 foot-lamberts.

Analysis Method - Theoretical based on published data.

Estimated Performance - 0 to 15 foot-lamberts on optical axis.

Variance - None

3.3.4 DISPLAY RESOLUTION (PROTECTOR)

Requirement – A viewer with a 10x (max.) magnifier will be able to resolve up to and including 228 lp/mm at 6 to 1 contrast on the film (corresponds to 17.6 lp/mm on the screen).

Analysis Method – LSI and subcontractor theoretical and computer analysis, also breadboard test data.

Estimated Performance – Resolution of 228 lp/mm (on film) at 6 to 1 contrast ratio is possible with a 7x magnifier.

3.3.5 ALPHA-NUMERIC DISPLAY TIME

Requirement – The alpha numeric display shall be accomplished within 0.3 second after receipt of external command.

Analysis Method – Theoretical analysis of circuit.

Estimated Performance – Time to display will be less than 0.1 second. Since the standby control monitors only the projector external command lines, the alpha-numeric display can only be used when the VDP is out of standby mode. Therefore, the time required to go from standby to full power need not be considered.

3.3.6 SEARCH AND FINE POSITIONING POWER

Requirement – Maximum power to be 31 watts, limited to 1.0 amp.

Analysis Method – Theoretical power analysis from circuit schematics.

Estimated Performance – Maximum power during high speed search will be 26 watts. Input current will be 1.2 amp. at 22V input and 0.84 amp. at 31V. Pulse power (less than 1 sec) will be 41.4 watts during acceleration for a period of 0.2 second. This is 1.88 amp at an input voltage of 22V or 1.34 amp at 31V.

<u>Variance</u> - Maximum power is not exceeded during search but maximum current is exceeded by 0.2 amp. at 22V input. If maximum current is to be limited to 1.0 amp. even at 22V, then the power limitation is 22 watts, not 31 watts. General Electric Action Item D-12 is to clarify this requirement as well as to establish a pulse power requirement.

3.3.7 SCREEN ILLUMINATION POWER

<u>Requirement</u> - Maximum total power during screen illumination shall not exceed 30 watts, current limited at 1 amp.

<u>Analysis Method</u> - Theoretical power analysis from circuit schematics.

<u>Estimated Performance</u> - Maximum power during screen illumination will be 22 watts. Input current will be 1.0 amp. at 22V or 0.71 amp. at 31V input.

<u>Variance</u> - None

3.3.8 ALPHA NUMERIC DISPLAY POWER

<u>Requirement</u> - Maximum power shall not exceed 5 watts.

<u>Analysis Method</u> - Theoretical power analysis from schematics.

<u>Estimated Performance</u> - Maximum power drawn from the input line when only the alpha-numeric display is used will be 6.0 watts at maximum brightness.

<u>Variance</u> - Maximum power is exceeded by 1.0 watts. The actual load for the display is less than 5 watts, but power supply efficiency is low when only the display is used. Therefore, during projection mode the additional power required for the alpha numerics will be less than 5 watts.

3.3.9 STANDBY POWER

<u>Requirement</u> - Maximum standby power shall not exceed 0.03 watt.

<u>Analysis Method</u> - Theoretical analysis of circuit.

Estimated Performance - Maximum standby power will be less than 0.03 watt.

Variance - None

3.3.10 POWER INTERRUPT

Requirements - The VDP shall withstand voltages from 0 to 20 volts for periods up to one second and return to specified performance within 10 seconds.

Analysis Method - Theoretical analysis of system schematics.

Estimated Performance - This requirement is met.

Variance - None

3.4 CONTROLS AND STRUCTURE

Discussion and supporting analysis of VDP controls is presented in detail in the LSI Visual Display Projector Design Review Report (LSI-TD-755-1167-ID) dated November 1967. A description of VDP controls (panel) is also contained in this report in Section 5.

SECTION 4.0

SUBSYSTEM DESIGN INFORMATION

The material in this section is subdivided as follows:

4.1   Drive K Electronics

4.2   Control Sticks

4.3   Gyro Selection

4.4   Weight and Power Status

4.1 DRIVE K ELECTRONICS

4.1.1 INTRODUCTION

The Drive K Electronics has been subdivided into seven subfunctions designated K-0, K-1, K-2, ---- K-7. This portion of the engineering analysis report outlines the functional requirements of each circuit function, briefly describes the circuit approach for each including preliminary schematics, and includes the engineering laboratory data which has been taken on these circuit functions.

4.1.2 K-0 ELECTRONICS

In its primary function, the K-0 electronics provides the digital circuitry for the precise positioning of both the inner and outer axes of Drive K by means of a position servo system. It will accept information in digital form for both axes from the MDAU and integrate it to develop digital commanded position information. It will process digital signals received from position encoding devices in each axis to develop actual position information. A digital position error word for each axis will be derived in the K-0 electronics from a comparison of commanded and actual positions and sent to digital-to-analog converters in the K-1 electronics. That component will provide the analog drive signal for the position servo system. Actual position data will be supplied to the MDAU on request.

4.1.2.1 Functions (K-0)

The K-0 electronics portion of the DKE (Figure 4.1-1) shall be capable of performing the following functions:

a. Provide the input/output buffering required for the flow of data between the various functional areas of the DKE and components associated with but not part of the DKE package. The function of the buffer portion of the K-0 electronics is to provide the following capabilities:

    1. To accept the command rate data used for the control of a two-axis position servo referred to as the Main Drive.

    2. To accept and decode the position/rate signal (received as part of the command rate data input) used for control of the commanded scaling in the K-0 electronics and to provide inhibit signals to K-3, K-5, K-6B and Gyros as shown in Figure 4.1-1.

    3. To accept and distribute the position command data required by the K-3 electronics.

    4. To transmit position feedback data received from an associated component.

    5. To provide switching required to accept data from multiple sources.

    6. To transmit digital data to the telemetry subsystem.

4-5

~~SECRET~~ **SPECIAL HANDLING**
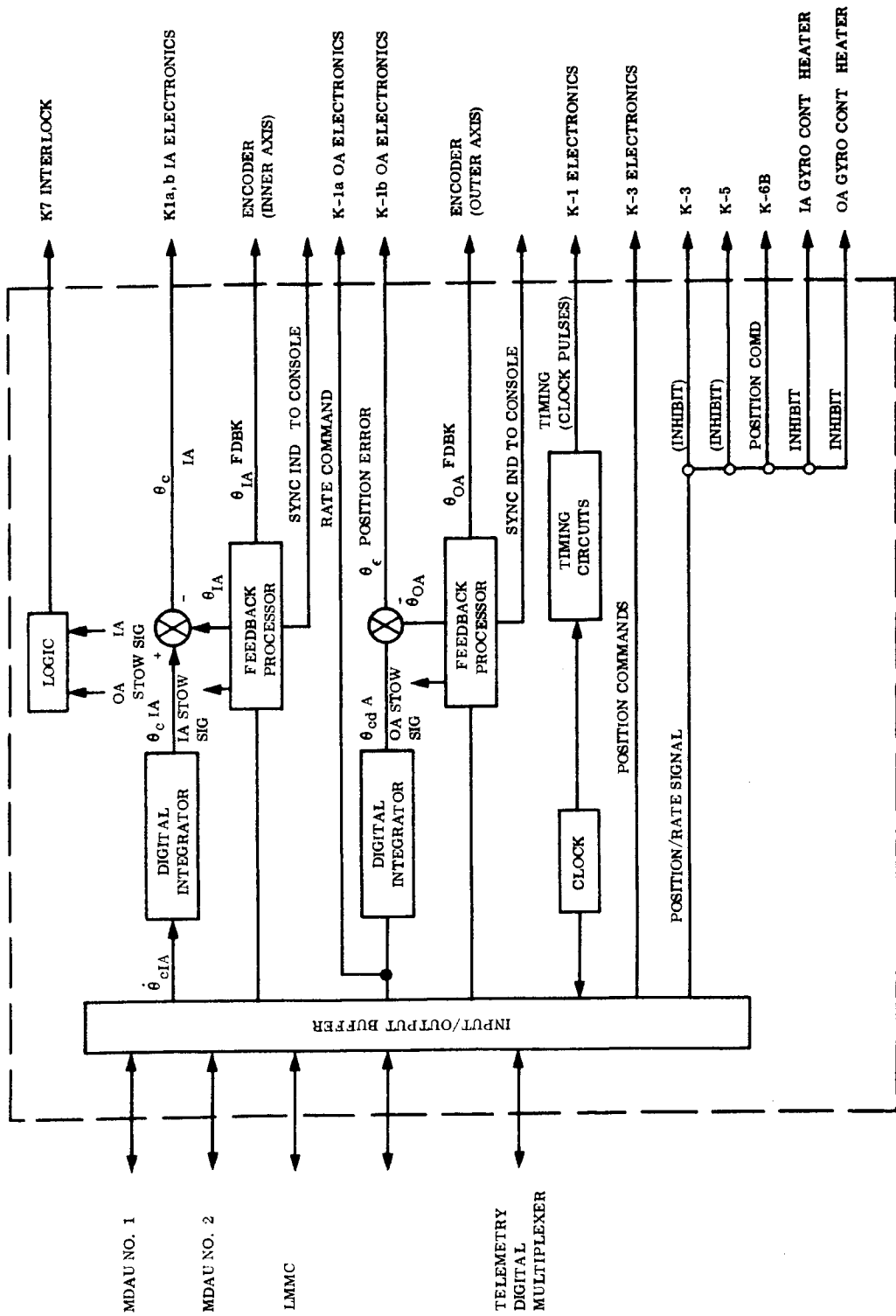
Figure 4.1-1. K-0 Electronics Block Diagram

~~SECRET~~ **SPECIAL HANDLING**

b.   Digitally integrate the rate command data received by the input/output buffer to generate a position command signal for servo control in two axis.

c.   Process the feedback data from two associated, incremental encoders and to generate a binary digital word which is representative of this data.

d.   To digitally combine position command data inputs and encoder feedback inputs and to generate from these binary-coded position error signals which are transmitted to the K-1 electronics.

e.   To generate an interlock signal for K-7 from signals received from the associated incremental encoders.

f.   To accept primary and back-up stow commands and generate required stow signals.

g.   To accept and respond to a back-up sync command.

4.1.2.2 Performance Characteristics (K-0)

4.1.2.2.1 Input/Output Buffering (K-0)

A.   Digital Rate Command - The θ input buffer receives 32 bits of rate command information from either of two identical components (MDAU 1 and MDAU 2) at the rate of 100 times per second. The data is strobed serially into the register by means of 32 shift pulses on a separate line originating in the same component as the data. The first data bit contains no information and is always transmitted as a logic "0". Bits 2 through 16 are 14 data bits plus sign (15 bits total) representing the inner axis rate command. Bit 17 indicates the position mode or rate mode scale factor to be used in the arithmetic operations. Bits 18 through 32 are 14 data bits plus sign representing the outer axis rate command. The data is transmitted least significant bits (LSB) first. Within (TBD) μ sec following reception of the last bit, the K-0 electronics will be sent an execute pulse originating in the same component as the data. The K-0 electronics will use this pulse to set the scale factor command into the control logic and to alert the logic to the fact that rate command data will be shifted from the input buffer to the respective inner axis and outer axis 0 shift registers during the next timing cycle. The scaling for this command is as indicated in Table 4.1-1.

TABLE 4.1-1. RATE COMMAND SCALING

PARAMETER	POSITION MODE (HIGH RATE RANGE)	Iθ RATE MODE (LOW RATE RANGE)	OA RATE MODE (LOW RATE RANGE)
$\dot{\theta}_c$ MSB	26.7796 deg/second	6.6959 deg/second	1.6737 deg/second
$\dot{\theta}_c$ LSB	3.269×10^{-3} deg/sec	8.1725×10^{-4} deg/sec	2.043×10^{-4} deg/sec
N	14 bits + sign bit	14 bits + sign bit	14 bits + sign bit

B. <u>Stow Command</u> - Means shall be provided to accept a manually initiated stow command to back up the automatic stow command received on the rate command line. The stow command shall cause a 5°/sec rate to be registered until stowing has been accomplished. The backup stow command will originate in the control console.

C. <u>K-3 Command</u> - The K-3 command is also a binary digital word received by the K-0 electronics. This command is received once per position mode selection, and has scale factors as indicated in Table 4.1-2.

TABLE 4.1-2. K-3 FUNCTION COMMAND SCALING

θ_{K3}	MSB (most significant bit)	22.5 deg
θ_{K3}	MSB (least significant bit)	0.045 deg
N_{K3}		10 bits + sign bit

D. <u>Position Readout</u> - The Drive K Electronics position readout from the encoders consists of two binary digital words transmitted from the K-0 electronics and having scale factors as indicated in Table 4.1-3. The encoder feedback words shall have a code bit in addition to the data bits to identify the specific load position being transmitted.

~~SECRET~~ **SPECIAL HANDLING**

TABLE 4.1-3. OA AND IA DKE POSITION READOUT SCALING

	θ MSB	45 deg
	θ LSB	2.75×10^{-3} deg
	N_θ	15 bits + sign bit
Encoder Scaling:	IA:	$\dfrac{360}{2^\theta}$ deg/count (2)
	OA	$\dfrac{360}{2^\theta}$ deg/count (2)
Encoder Pulse Rate, Max:	IÁ:	120 KHz
	OA:	150 KHz

a.   <u>Encoder Feedback Register Characteristics:</u> The feedback registers in which the OA and IA position words are accumulated shall be scaled as indicated in Table 4.1-4.

TABLE 4.1-4. OA AND IA FEEDBACK REGISTER SCALING

	IA AND OA
θ_{FDBK} MSB	45°
θ_{FDBK} LSB	1.25 arc sec
$N_{\theta_{FDBK}}$	18 bits ± sign bit

~~SECRET~~ **SPECIAL HANDLING**

~~SECRET~~ **SPECIAL HANDLING**

b. Synchronization - The feedback processor shall include means to synchronize the OA or IA feedback binary digital register word to the OA or IA load position whenever the OA or IA passes through a specific reference point referred to as the "sync" position. The sync positions are:

OA Sync: 0 degree

IA Sync: +11.25 degrees

Synchronization of the θ_{FDBK} registers shall take place automatically, without interrupting any other functions, whenever the load passes through the sync position in the position mode. Automatic sync will be inhibited during the rate mode.

c. Initialization - The feedback data processor shall generate signals which will cause the OA and IA to drive through the sync positions and to reset the rate command (θ_c) to zero and the position command register to the sync position within 10 milliseconds after power turn-on and the receipt of a K-7 load mechanism CW limit signal. In addition to the automatic initialization which shall take place whenever power is turned on, a redundant backup initialization path shall be provided which shall operate on a manually initiated signal originating on a control console.

4.1.2.3 Additional Buffering Requirements for K-0

a. The input/output buffer shall transmit a constant 625 kHz clock output signal.

b. The input/output buffer shall transmit digital telemetry signals to the telemetry subsystem.

c. Generate inhibit signals to K-3, K-5, K-6b, and gyro control heaters as a function of the position/rate mode.

d. The input/output buffer shall transmit an interlock signal to the K-7 electronics indicating that either the OA or IA stow limit is not present.

e. The input/output buffer shall generate a separate indication of OA and IA sync by supplying a one second logic level to the control console upon receipt of the following:

~~SECRET~~ **SPECIAL HANDLING**

1. A change in state (0 to 1 or 1 to 0) of the respective encoder sector line and,

2. An initialize gate indicating the main drive is in the process of being synchronized.

4.1.2.4 Digital Integrator (K-0)

The digital integrator includes a 15-bit rate command register (θ shift register), a 32-bit position accumulator shift register, and a full adder. The θ shift register is periodically updated with rate command information from the θ input buffer. The contents of the θ shift register are then repetitively added to the accumulator to derive commanded position information.

When the rate mode of operation is commanded, the contents of the θ shift register are serially added to the 15 LSBs of the accumulator register once every timing cycle. Information is restored in the θ shift register by an end around shift and the results of the addition are fed into the MSB end of the accumulator register. Note that there are only 15 bits of information in the θ shift register compared with the 32 bits in the accumulator register. Thus, if the θ information is positive, θ's continue to be added to the accumulator data following the MSB of θ data. If negative, 1's are added. This is in keeping with the signed 2's complement binary notation. The result in the accumulator is commanded position information at the end of the timing cycle.

Whenever the θ shift register is to be updated with new information, the end around shift is interrupted and new data is entered from the θ input buffer as the previous word in the θ shift register is being added to the contents of the accumulator register. Both inner axis and outer axis θ shift registers are updated simultaneously.

In the position mode, the operation is the same as before except that 0's are added to the 2 LSBs of the accumulator data and then the θ data is added to bits 3 through 17 of the accumulator data.

4-11

~~SECRET~~ **SPECIAL HANDLING**

The digital integration shall be performed at a rate of 19.5 kHz + 0.01 percent. The accumulator for the integrated rate command (θ command register) shall be scaled to accept the effect of the LSB in the rate command word. For each axis, the scaling is as shown in Table 4.1-5.

TABLE 4.1-5. POSITION COMMAND SCALING

θ_c MSB	45 deg
θ_c LSB	4.1910×10^{-8} deg
N_{θ_c}	31 bits + sign bit

4.1.2.5 Feedback Processor (K-0)

The feedback processor includes a five-bit up-down counter, a shift register buffer for the counter, a full adder, a 20-bit position feedback shift register (θ feedback), and inter-face logic.

Each encoder (IA and OA) provides data on two lines. One line carries pulses when the encoder travels in one direction, and the other line carries pulses when the encoder travels in the opposite direction. Pulses appearing on these lines are mutually exclusive. If the up-down counter is counting in the up direction corresponding to the positive direction of rotation of the encoder and the encoder changes direction, the interface logic will sense the first pulse appearing on the opposite line and switch the counter to count pulses on this line in the down direction. The contents of the counter in the down mode represent position changes in signed 2's complement binary notation.

The contents of the up-down counter are added to the θ feedback shift register once every timing cycle. This is accomplished by inhibiting the pulses on the encoder input lines for

~~SECRET~~ **SPECIAL HANDLING**

one 625 kHz clock period. During the inhibit time, the contents of the counter are trans-ferred to the shift register and then the counter is reset. The inhibit signal is released and the contents of the shift register are serially added to the contents of the θ feedback shift register. The results of the addition are returned to the θ feedback shift register via an end around shift. The encoder input lines are inhibited for less than 1/4 of the shortest encoder pulse cycle so that no count is lost.

When the encoder sync pulse is detected, the up-down counter is immediately reset and alerts the control logic that the θ feedback shift register is to be reset. This is to insure that the contents of the θ feedback shift register accurately represent the encoder position. The counter continues to count, from zero, the encoder pulses occurring after the sync until the next inhibit period. During the next inhibit period, the θ feedback register is preset and the contents of the counter are transferred as before to the associated shift register. Subsequent to the inhibit period, the shift register contents are added to the contents of the θ feedback shift register. The sync logic will be disabled during the rate mode of operation.

The K-0 electronics will detect and accept requests from an MDAU for position feedback data, and within 100 μ sec, will respond with a "ready" signal if data is ready. During the 100 μ sec period, the contents of the θ feedback shift register will be shifted non-destructively to an output buffer register. Between 1.6 and 3.2 μ sec after the appearance of the ready signal, the K-0 electronics will accept from the MDAU a series of 625 kHz pulses to send position feedback data from the buffer register to the MDAU. The 17 bits of data sent back will include a sign bit and a tag bit to indicate whether it is inner axis or outer axis data. The type of data will alternate with successive request signals.

4.1.2.6 Position Error Adder (K-0)

This unit digitally combines the output of the θ integrator-adder representing commanded position information and the contents of the θ feedback shift register once each timing

4-13

cycle. The control logic will select the appropriate thirteen bits plus sign of each word to be added during either the rate or position mode of operation. The scaling for position and rate modes is indicated in Table 4.1-6.

TABLE 4.1-6. OA AND IA ERROR WORD SCALING

θ_E MSB	0.41842 deg
θ_E LSB	1.02×10^{-4} deg
N_{θ_E}	13 bits + sign bit

This data (θ_E) shall then be transmitted to the two D/A converters of the K-1 electronics, so that $\theta_{E_{LSB}}$ is positioned in the LSB location of the K-1 D/A converter.

4.1.2.7 Timing and Control Circuitry

All the necessary clock signals required for operating the K-0 electronics in a synchronous manner are derived from this unit. The prime source is a stable 1.25 mHz oscillator. This unit will process the output of the 1.25 mHz oscillator to derive two 625 kHz (800 ns wide) clocks phase displaced by 90° from each other. From these clocks, four additional 625 kHz clocks are derived. Each is 400 ns wide and is displaced 400 ns from the preceding one. With this clock arrangement, time races in the control logic are avoided and reliable operation insured. These clocks are used in conjunction with the outputs of a 5-stage synchronous counter pulsed at a 625 kHz rate to provide control signals during each timing cycle. This logic circuitry will combine internal and external signals with signals from the timing generator to insure the proper sequence of operations of the K-0 electronics within the basic timing cycle. The timing cycle consists of 32 pulses of a continuous 625 kHz clock, and all operations are repetitive from cycle to cycle. The control logic will also furnish appropriate sequences of shift pulses to the registers in the various units to control the transfer of data. It will also supply logic and timing functions to the D/A converters in the K-1 electronics.

4.1.3 K-1 ELECTRONICS

4.1.3.1 Description

The K-1 electronics (see Figure 4.1-2) will operate in a primary mode or a backup mode. In the primary mode, the K-1 electronics will provide drive signals to the Inner Axis gyro (IA) and to the Outer Axis gyro (OA). The IA signals will be developed by a D/A conversion of position error (θ_E) data received from the K-0 electronics. The OA signals will be developed by a D/A conversion of rate (θ) command information received from the K-0 electronics. The output of the D/A ladder networks (IA and OA) provide the inputs for the buffer and compensation amplifiers. These amplifiers provide the power gain required to drive the gyro torquer coils (IA and OA). The amplifiers are identical in each axis.

The requirements on the amplifiers are very stringent, requiring low drift, low output noise, and high gain linearity. To meet these requirements, it was necessary to use discrete part amplifiers (see Figure 4.1-3) rather than microcircuit amplifiers. A description of the amplifier characteristics follows:

The amplifier has two stages of differential gain, a buffer stage to match impedances, and a class B output stage to provide the five watts of power required. The input differential stage uses a 2N2453A transistor consisting of two matched transistors on the same chip to obtain good parameter matching and excellent temperature tracking at the input stage. The second differential stage also uses matched transistors with similar characteristics. The amplifier uses current feedback to provide a high output impedance to the load and results in the transfer function of output current for input voltage required by the specification. The amplifier gain is 169 ma/volt in each axis. The drift at the output is less than 2.0 ma, 2σ and the linear range of operation is up to 200 ma into a 100-ohm torquer coil load.

~~SECRET~~ **SPECIAL HANDLING**
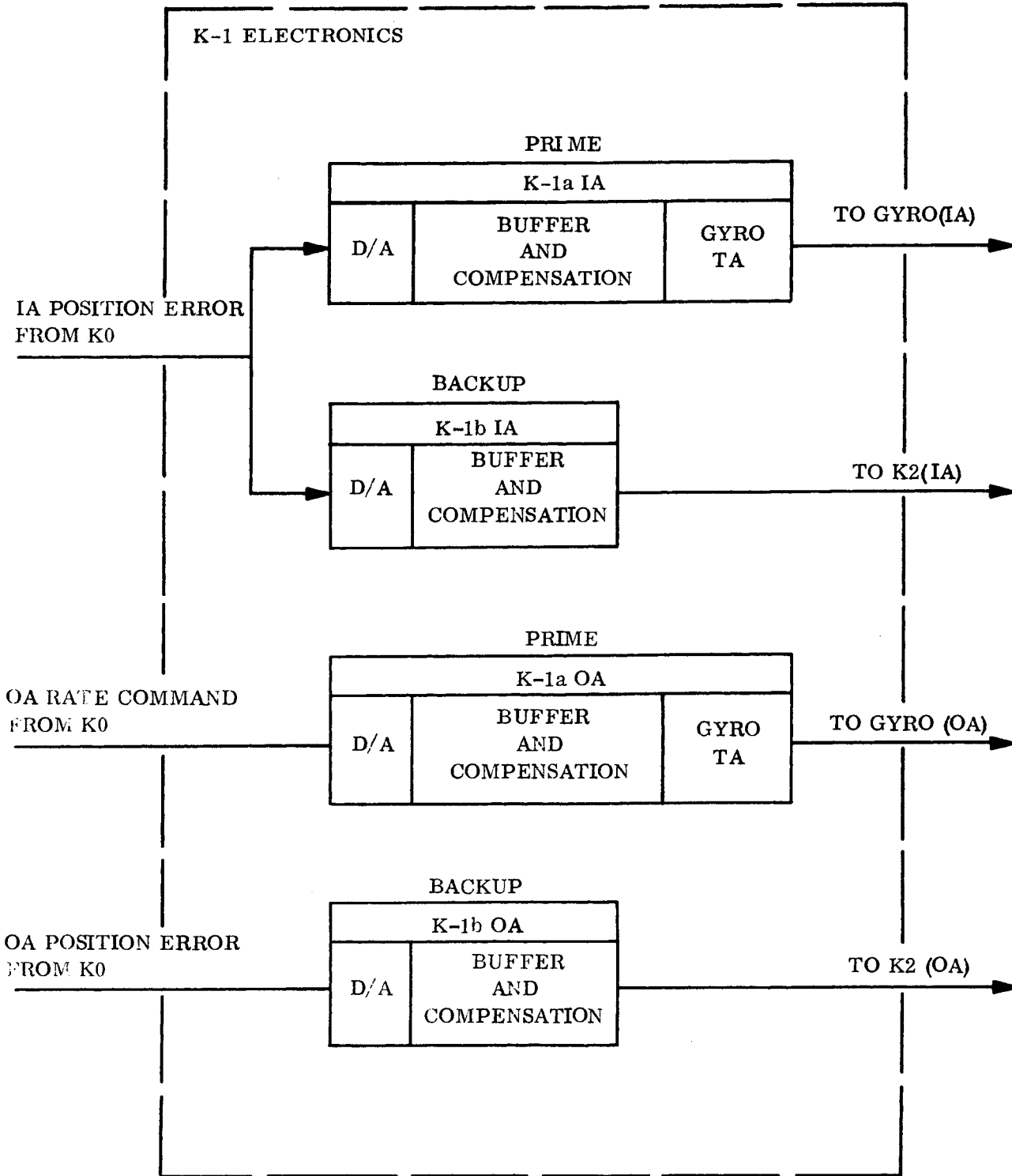
Figure 4.1-2. K-1 (IA and OA) Electronics Block Diagram

~~SECRET~~ **SPECIAL HANDLING**

~~SECRET~~ SPECIAL HANDLING
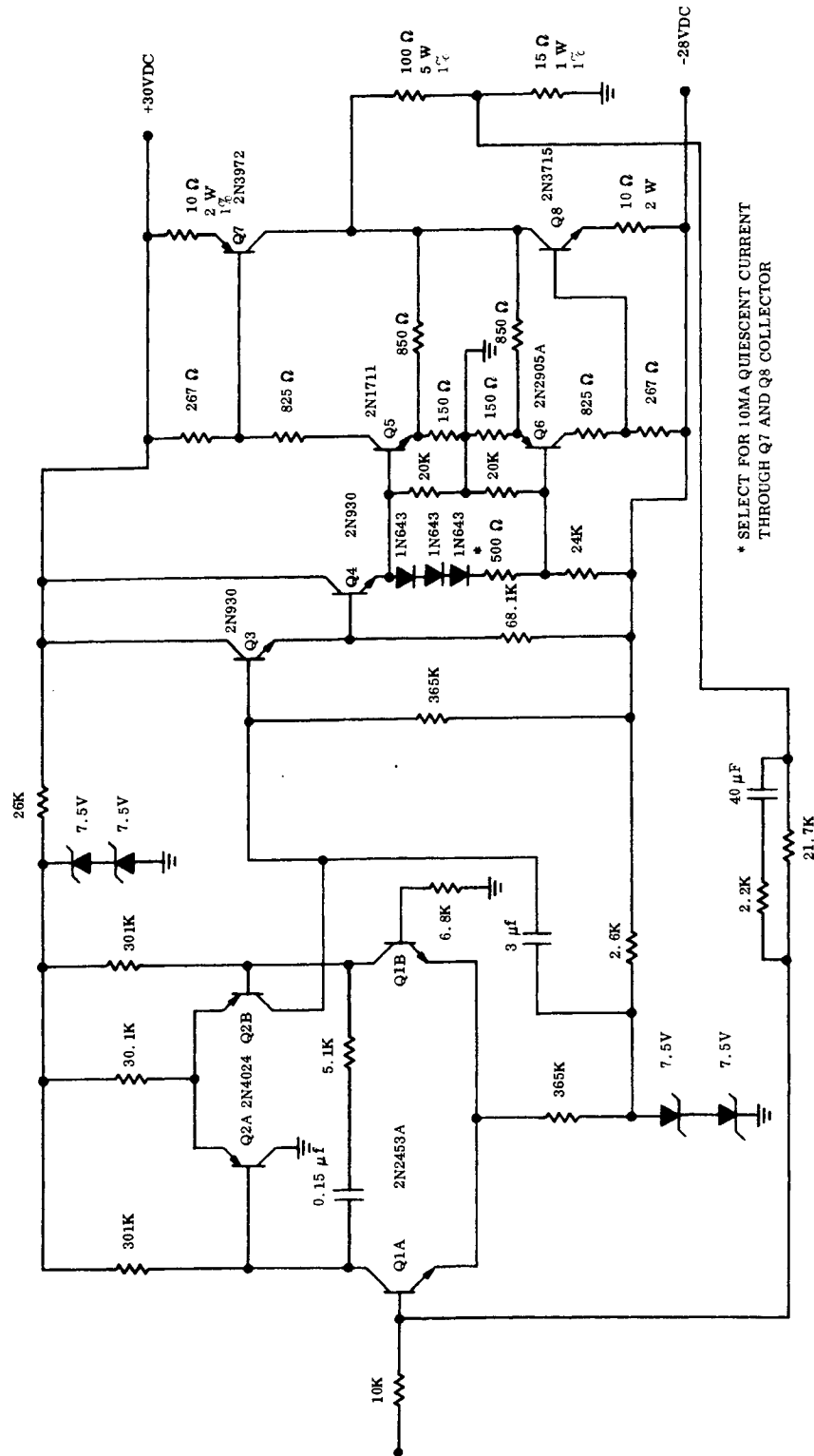
Figure 4.1-3. Drive K Buffer Amplifier, K-1a IA (K-1a OA)

~~SECRET~~ SPECIAL HANDLING

In the IA backup mode, the D/A conversion of IA, θ_E data from the K-0 electronics will result in signals to drive the K-1a IA, amplifier. In the OA backup mode, the D/A conversion of OA θ_E data from the K-0 electronics will result in signals to drive the K-1b OA amplifier. Mode selection will be determined by signals from the console.

The K-1b amplifier is shown in Figure 4.1-4. The amplifier shown has a closed loop voltage gain of 23.2. Breadboard tests of the output drift show a 19.2 mv change in the output over the range from -18°C to +70°C.

The plot of the open loop gain (GH) and phase margin is shown in Figure 4.1-5. The closed loop gain is $\frac{G}{1 + GH}$. If the minimum GH product is 800, a variation of the forward gain (G) from infinity to 18,800 (giving a GH of 800) will produce a total gain variation of 0.125 percent. The gain is therefore controlled primarily by the ±1 percent feedback resistor which maintains a 3.5 percent tolerance on the gain.

The stability of the amplifier was determined by using the ECAP computer program and worst case transistor parameters. The phase margin at the crossover, with all transistors at their worst case maximum value, is 40 degrees.

4.1.3.2 Requirements Summary (K-1)

The K-1 electronics shall perform the following functions:

a. Accept digital position error data or rate command data and timing signals from the K-0 electronics and convert these signals to analog voltages. Logical and timing functions of the D/A converter will be supplied by the K-0 electronics.

b. Provide the required transfer functions to generate gyro command and K-2 input signals.

c. Provide analog status signals of critical circuit parameters to K-9 electronics (telemetry conditioning and AGE).

4-18

~~SECRET~~ **SPECIAL HANDLING**
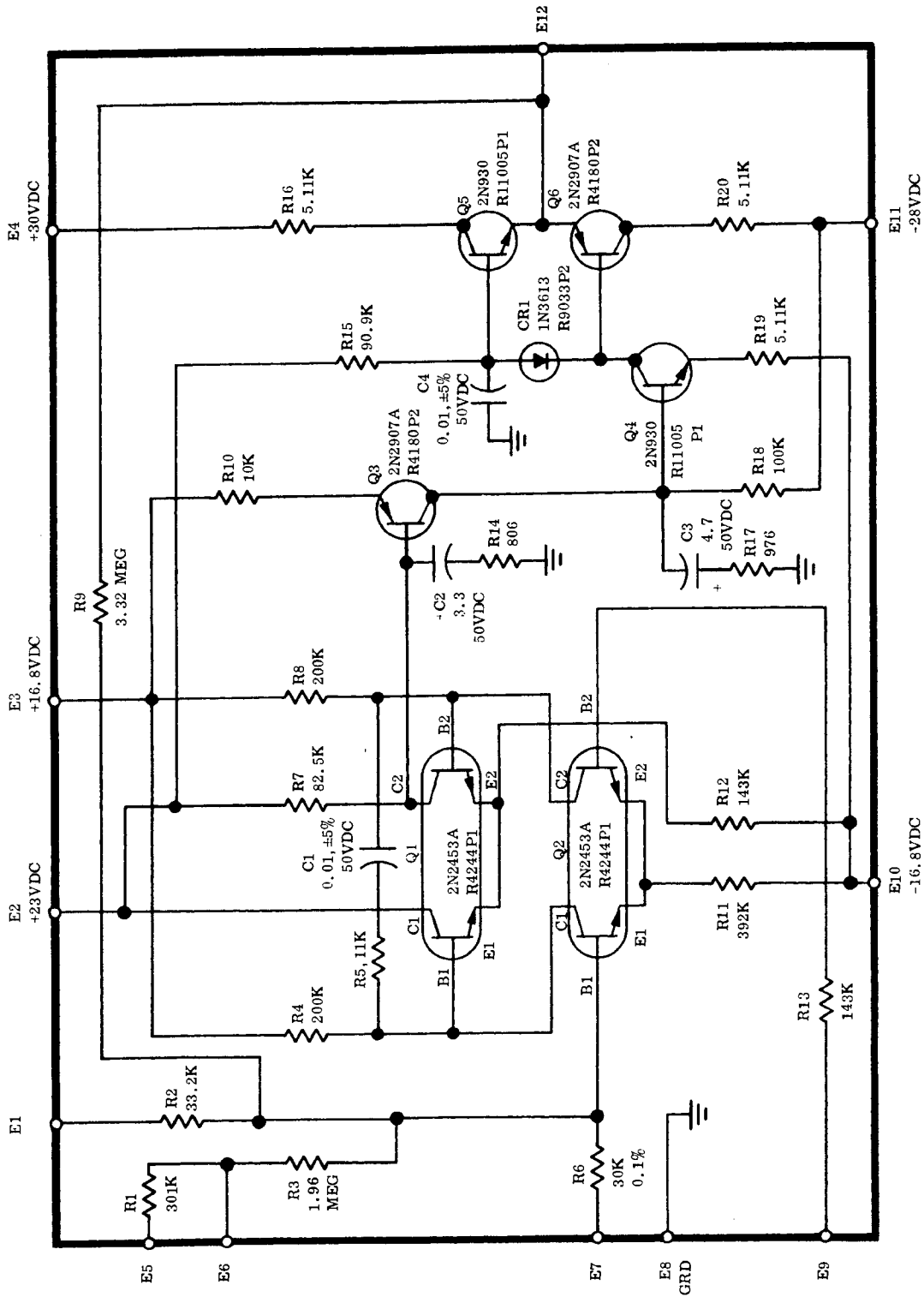
Figure 4.1-4. Drive K Amplifier K-1b OA (K-1a IA)

4-19

~~SECRET~~ **SPECIAL HANDLING**

~~SECRET~~ SPECIAL HANDLING
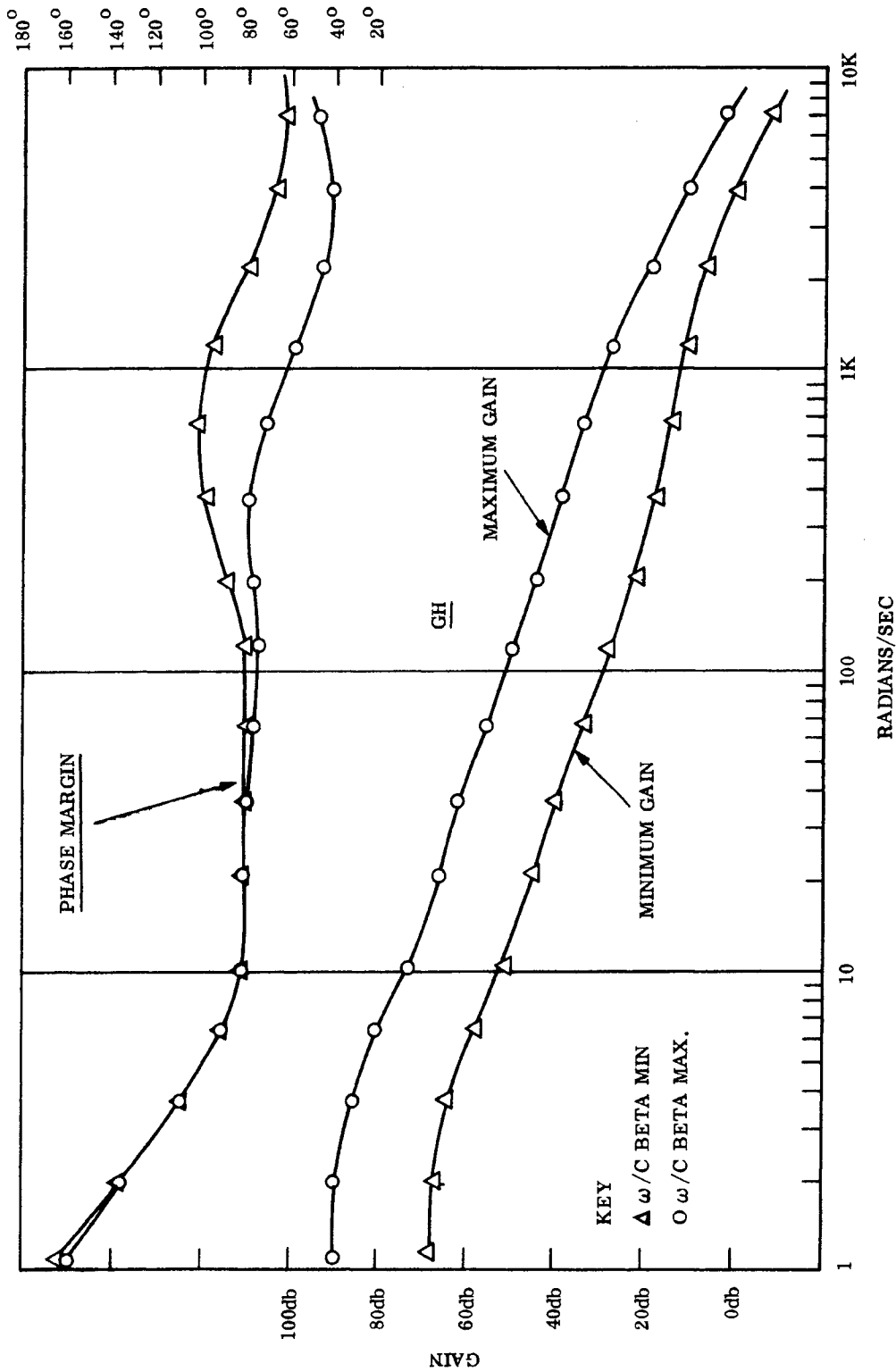
Figure 4.1-5. Inner Axis Compensation Amplifier

~~SECRET~~ SPECIAL HANDLING

4.1.3.3 Performance Characteristics (K-1)

a. <u>D/A Conversion</u> - The D/A converters of the K-1 electronics shall generate voltages proportional to the OA and IA position errors and OA rate command received from the corresponding channels of the K-0 electronics. Each converter shall have a constant scale factor gain (volts/quantum level) and shall be consistent with Table 4.1-6 for K-1a IA, K-1b IA, and K-1b OA; and Table 4.1-1 for K-1a OA. Timing signals for the D/A converters shall be derived from K0. Each converter shall be capable of processing word rates of 19.5 kHz. D/A conversion delay shall not exceed the inverse of word rate.

b. <u>Electronics Gain</u> - The following steady state gains shall be provided:

$$K-1_a \text{ IA} \qquad 72.5 \; \frac{\text{AMPS}}{\text{RAD}} \; \pm 5 \text{ percent}$$

$$K-1_b \text{ IA} \qquad 13,600 \; \frac{\text{VOLTS}}{\text{RAD}} \; \pm 5 \text{ percent}$$

$$K-1_a \text{ OA} \qquad 0.220 \; \frac{\text{AMPS-SEC}}{\text{RAD}} \; \pm 5 \text{ percent}$$

$$K-1_b \text{ OA} \qquad 1730 \; \frac{\text{VOLTS}}{\text{RAD}} \; \pm 6 \text{ percent}$$

These gains shall remain the same for position and rate modes. Compensating buffer amplifier gains shall be made to keep the gain constant for position and rate mode digital scaling. A maximum of 100 milliseconds between digital scale changes and analogue scale changes is allowed.

c. <u>Dynamic Response</u> - The following transfer functions shall be provided in K-1 electronics:

$$K-1a \text{ IA} \qquad \frac{S/10 + 1}{S + 1}$$

$$K-1b \text{ IA} \qquad \frac{S/20 + 1}{(S/200 + 1)(S/100 + 1)}$$

4-21

~~SECRET~~ **SPECIAL HANDLING**

K-1A OA $\dfrac{1}{S/30 + 1}$

K-1b OA $\dfrac{S/10 + 1}{(S/100 + 1)\,(S/1000 + 1)}$

The break frequencies shall be generated within a ±10 percent tolerance. Additional phase lag due to breaks above 30 rad/sec shall not contribute more than 6 degrees phase lag at 30 rad/sec.

d. **Linear Range and Saturation** - The gain specification given above shall apply within the following output ranges:

K-1a IA, K-1a OA: ±0.1 to 200 ma into a load of 100 ohms ±10 percent with a stability of better than 1 percent. In the region of 0.04 ma, the gain shall not be less than zero. The saturated output current shall not exceed 240 ma in magnitude. Recovery, to 90 percent of its saturated value, shall occur in less than 2 milliseconds when the input is switched to zero from a saturating level.

K-1b IA, K-1b OA: ±17.5 Volts. Saturation shall not exceed a value which will damage K-1b or the following stage, K-2. Recovery to 90 percent of saturation shall occur in less than 2 milliseconds when the input is switched to zero from a saturation level.

e. **D. C. Offset and Long Term Drift:**

K-1a IA   ±1 ma

K-1a OA   ±10 m amps

K-1b IA   ±380 mv

K-1b OA   ±57.3 mv

The long term drift applies to frequencies below 0.2 rad/sec.

f. **High Frequency Noise (W ≥ 0.2 rad/sec)** - TBD

~~SECRET~~ **SPECIAL HANDLING**

~~SECRET~~ **SPECIAL HANDLING**

4.1.3.4 Stability Analysis (K-1)

A stability analysis was performed on the K-1a buffer amplifier shown in Figure 4.1-3. The open loop gain of the amplifier varies from 10,000 V/V to 80,000 V/V when driving a 115-ohm load. The closed gain required for this amplifier is 16 V/V (145 ma/V). The open loop gain variation will cause only a 0.12 percent amplifier gain change. Most of the amplifier gain variation can be assigned to the input and output impedance variations.

A stability analysis was also performed on the K-1b backup amplifier shown in Figure 4.1-4. This amplifier is very similar to the K-1a amplifier discussed above and has an open loop gain of 18,000 V/V to 100,000 V/V. The closed loop gain required for this amplifier is 58.5 V/V for the inner axis and 5.05 V/V for the outer axis. The open loop gain variation will cause less than a 0.1 percent gain change for the closed loop operation of the inner axis amplifier. The gain change will be less for the outer axis amplifier. As in the case of the K-1 buffer amplifier, most of the gain variation can be assigned to the input and output impedance variations.

4.1.3.5 Test Results

The K-1a amplifier has been breadboarded and subjected to the following tests:

    a.   DC gain and linearity test

    b.   Drift test due to temperature

    c.   Noise rejection

    d.   Open loop frequency response

~~SECRET~~ **SPECIAL HANDLING**

~~SECRET~~ **SPECIAL HANDLING**

The DC gain and linearity test was made with the amplifier load equal to 115 ohms. The test was run at three different temperatures: $-20^{\circ}C$, $+25^{\circ}C$ and $+70^{\circ}C$. The test data is summarized below:

	$-20^{\circ}C$	$+25^{\circ}C$	$+70^{\circ}C$
Gain	16.496	16.486	16.471
Zero Offset	- 0.0555 volts	- 0.065 volts	- 0.070 volts

The DC gain obtained from this data is 1.655 V/V ±0.04 percent (144 ma ±0.04 percent) and meets the specification requirements.

The temperature drift obtained from this data is less than ±10 mv (± 90 μ A) for temperature variations from $-20^{\circ}C$ to $+70^{\circ}C$. Separate testing has not been performed on the K-1b amplifier. However, due to the close similarity of design, this amplifier can be expected to perform as well as the K-1a type.

A test was conducted to determine the effect of power supply line noise on the output noise of the amplifier. The following outputs were obtained when a 20 mv signal was introduced on the negative power supply lines:

f (cps)	E_o (mv)
20	0.2
60	0.4
100	0.6
200	1.4
300	1.1
400	1.0
500	1.0
600	1.0

A test was conducted to determine the open loop frequency response of the amplifier and the results are shown in Figure 4.1-6.

~~SECRET~~ **SPECIAL HANDLING**

~~SECRET~~ SPECIAL HANDLING
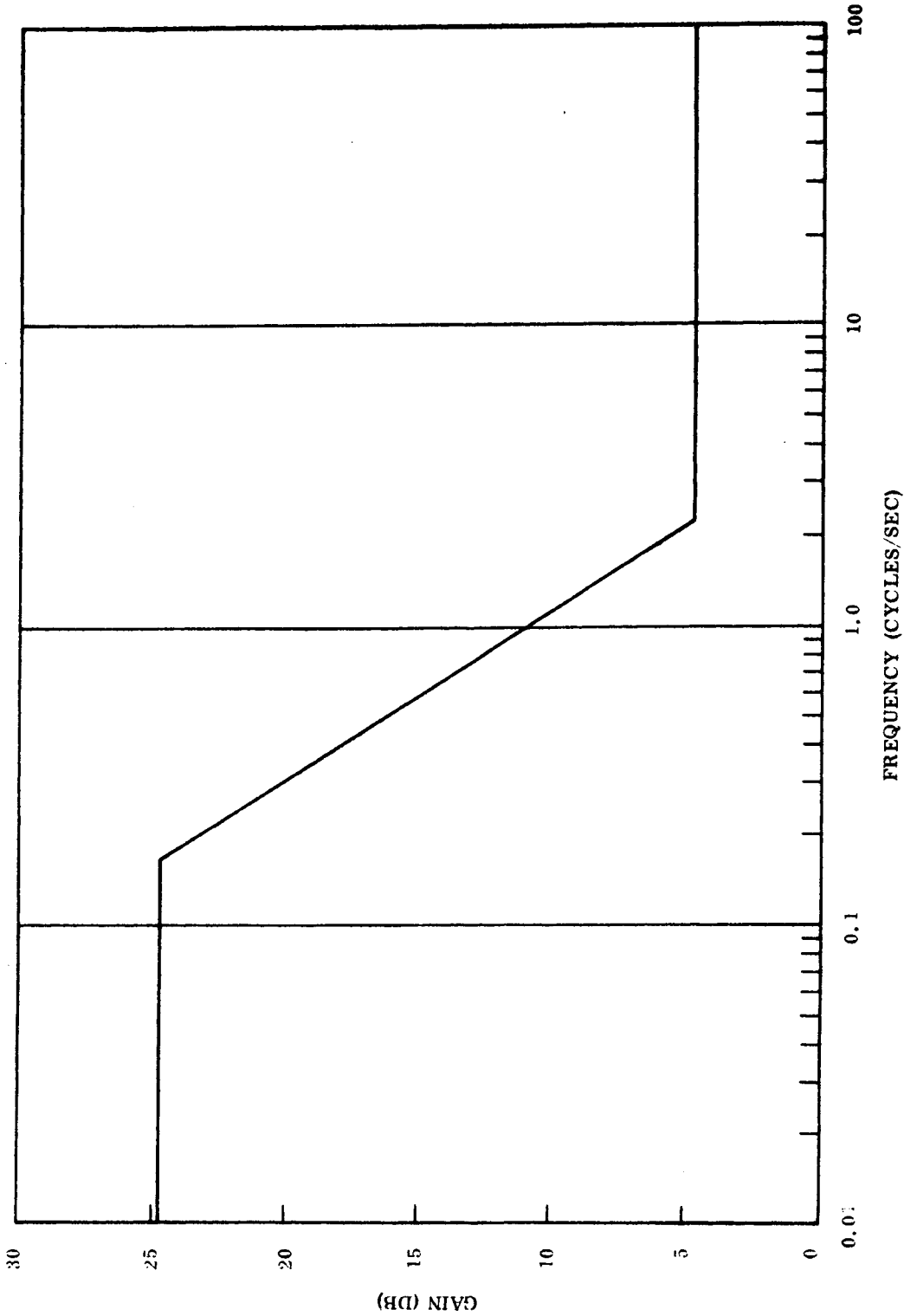
Figure 4.1-6. Frequency Response of Buffer Amplifier

4.1.4 K-2 ELECTRONICS

4.1.4.1 Description

The K-2 electronics shown in Figure 4.1-7 control the analog current needed to drive the torque motor stator windings of the main drive. This circuitry consists of a compensation amplifier and a power amplifier for each of the two drive axes. The inputs to the compensation amplifiers come from the K-1 electronics, and the power amplifiers are used to drive the torque motors.

The compensation amplifier is a 524AL microcircuit and the power amplifier uses discrete parts with a bridge circuit in the output stage. The load is 6.4 ohms for the outer axis and 19.4 ohms for the inner axis.

4.1.4.2 Performance Characteristics (K-2)

a. Gain - The following gains shall be provided in K-2 Electronics.

K2IA Comp. Amp.	28.6 V/V ±5 percent
K2IA Power Amp.	0.0281 amps/volt ±5 percent
K2OA Comp. Amp.	14.3 V/V ±5 percent
K2OA Power Amp.	0.132 amps/volt ±5 percent

b. Dynamics:

K2IA Comp. Amp. $\dfrac{(S/100 + 1)(S/40 + 1)}{(S/1000 + 1)(S/4 + 1)}$

K2IA Power Amp. $\dfrac{1}{(S/1000 + 1)}$

K2OA Comp. Amp. $\dfrac{(S/100 + 1)(S/40 + 1)}{(S/1000 + 1)(S/4 + 1)}$

K2OA Power Amp. $\dfrac{1}{(S/1000 + 1)}$
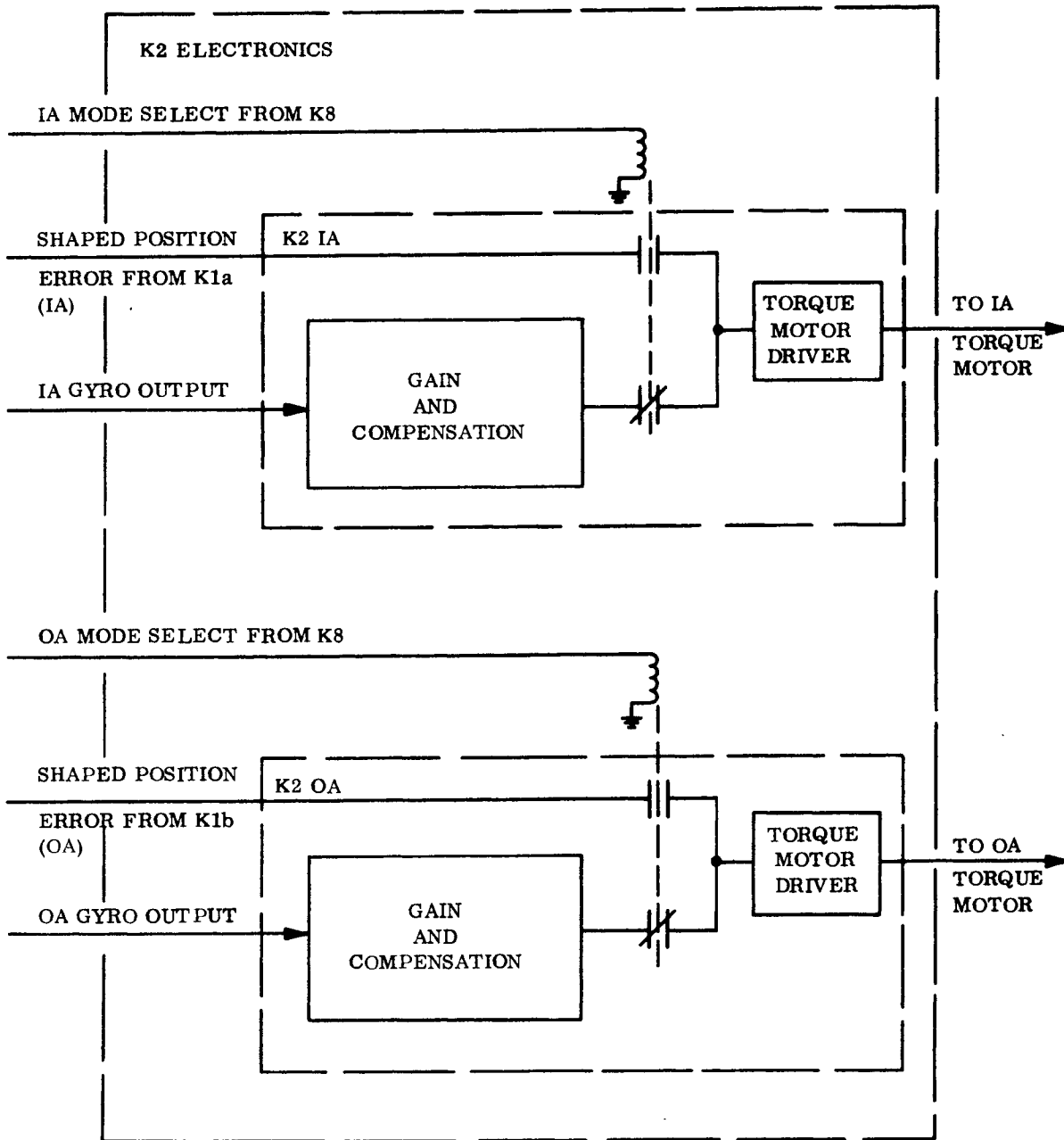
Figure 4.1-7. K-2 Electronics Block Diagram

~~SECRET~~ **SPECIAL HANDLING**

The critical frequencies shall be met within ±10 percent.

Additional critical frequencies shall not contribute more than 6° phase lag under 100 rad/sec for the compensation amplifier and 6° below 2000 rad/sec for the power amplifier.

c. Linear Range and Saturation - The gain and frequency values and tolerances stated in the above paragraphs shall be met within the range of operation indicated in the table below. In the power amplifier crossover region, the gain shall remain positive.

K2IA Comp Amp	±17.5 Volts
K2IA Power Amp	±(0.001 ± 0.228) Amp
K2OA Comp Amp	±17.5 Volts
K2OA Power Amp	±(0.01 ± 1.19) Amp

The load on the power amplifiers are:

K2IA Power Amp	36 ohms ±10 percent
K2OA Power Amp	7.6 ohms ±10 percent

For the compensation amplifiers, the saturation level shall be determined at a level that will not damage the following stages.

For the power amplifiers, the saturation levels shall be:

K2IA	0.565 ±15 percent Amp
K2OA	2.60 ±15 percent Amp

d. DC Offset and Long Term Drift

K2IA Comp Amp	500 mv
K2IA Power Amp	2 ma
K2OA Comp Amp	50 mv
K2OA Power Amp	4 ma

The long term drift applies to noise frequencies below 0.2 rad/sec.

~~SECRET~~ **SPECIAL HANDLING**

4.1.4.3 Stability Analysis (K-2)

A stability analysis was performed on the K-2 power amplifier (Figure 4.1-8). The open loop gain of the amplifiers varies from 200 V/V to 600 V/V when driving a 7.6-ohm load. The closed loop gain required for this amplifier is 1 V/V (0.32 A/V). The open loop gain variation will cause only a 0.35 percent amplifier gain change. Most of the amplifier gain variation can be assigned to the input and output impedance variations.

The K-2 compensation amplifier (Figure 4.1-9) consists of a 524AL microcircuit amplifier which has a specified open loop gain of 1200 V/V to 2000 V/V. The closed loop gain required is 28.6 V/V. The open loop gain variation will cause only 1.0 percent amplifier gain change. Most of the amplifier gain variation can be assigned to the input and output impedance variations.

4.1.4.4 Test Results on the K-2 Electronics

Breadboards were built for the compensation amplifier of Figure 4.1-9. The following tests were then conducted on the amplifier:

a. Frequency response test

b. Maximum output for 1 percent distortion

c. DC offset versus temperature

	-30°C	+25°C	+80°C
Output DC Offset (Input Grounded)	-3.7 mv	-2.2 mv	-0.6 mv

d. Linearity test (see Figure 4.1-10)

e. Rejection of power supply noise (see Figure 4.1-11)
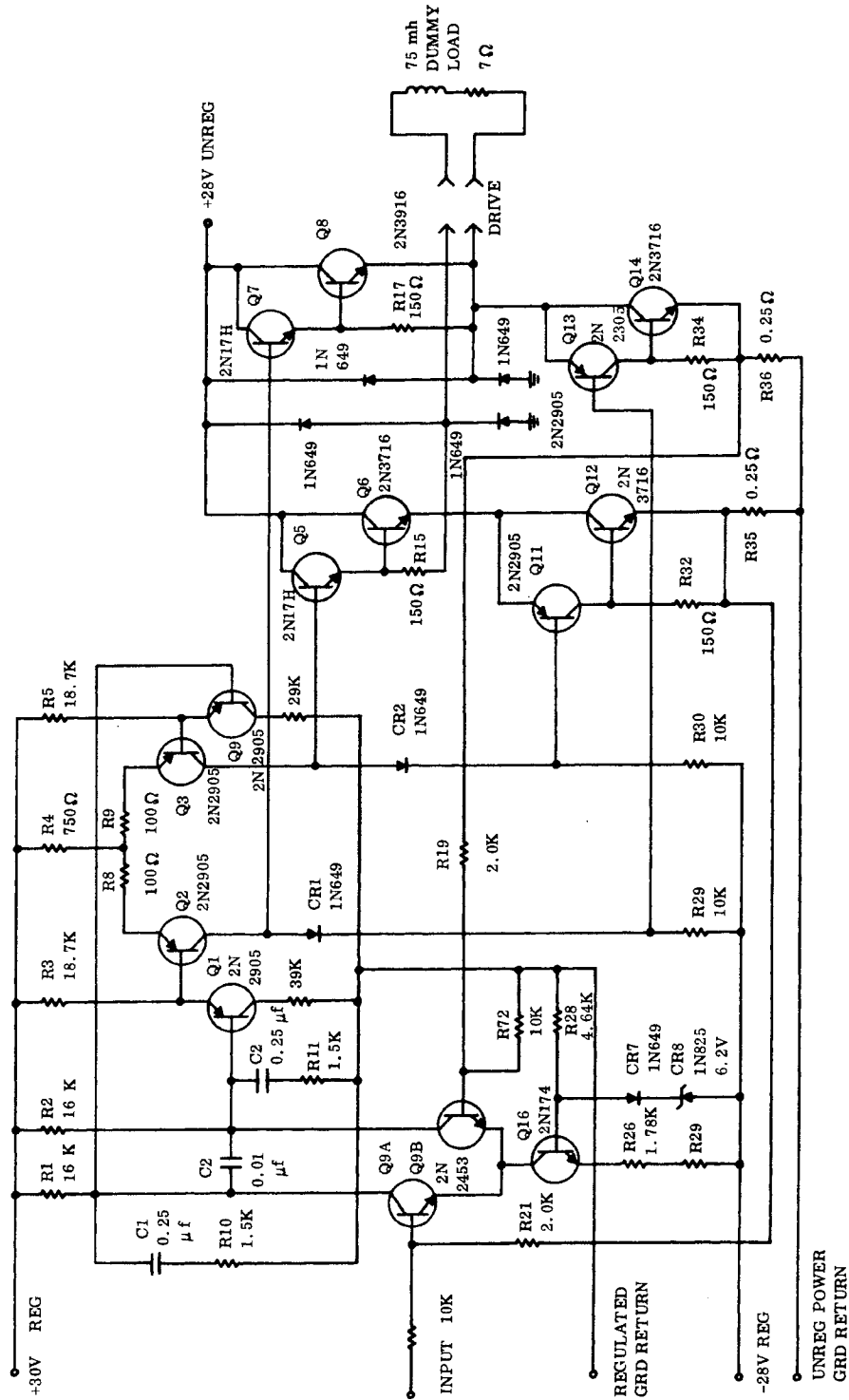
Figure 4.1-8. K-2 Power Amplifier
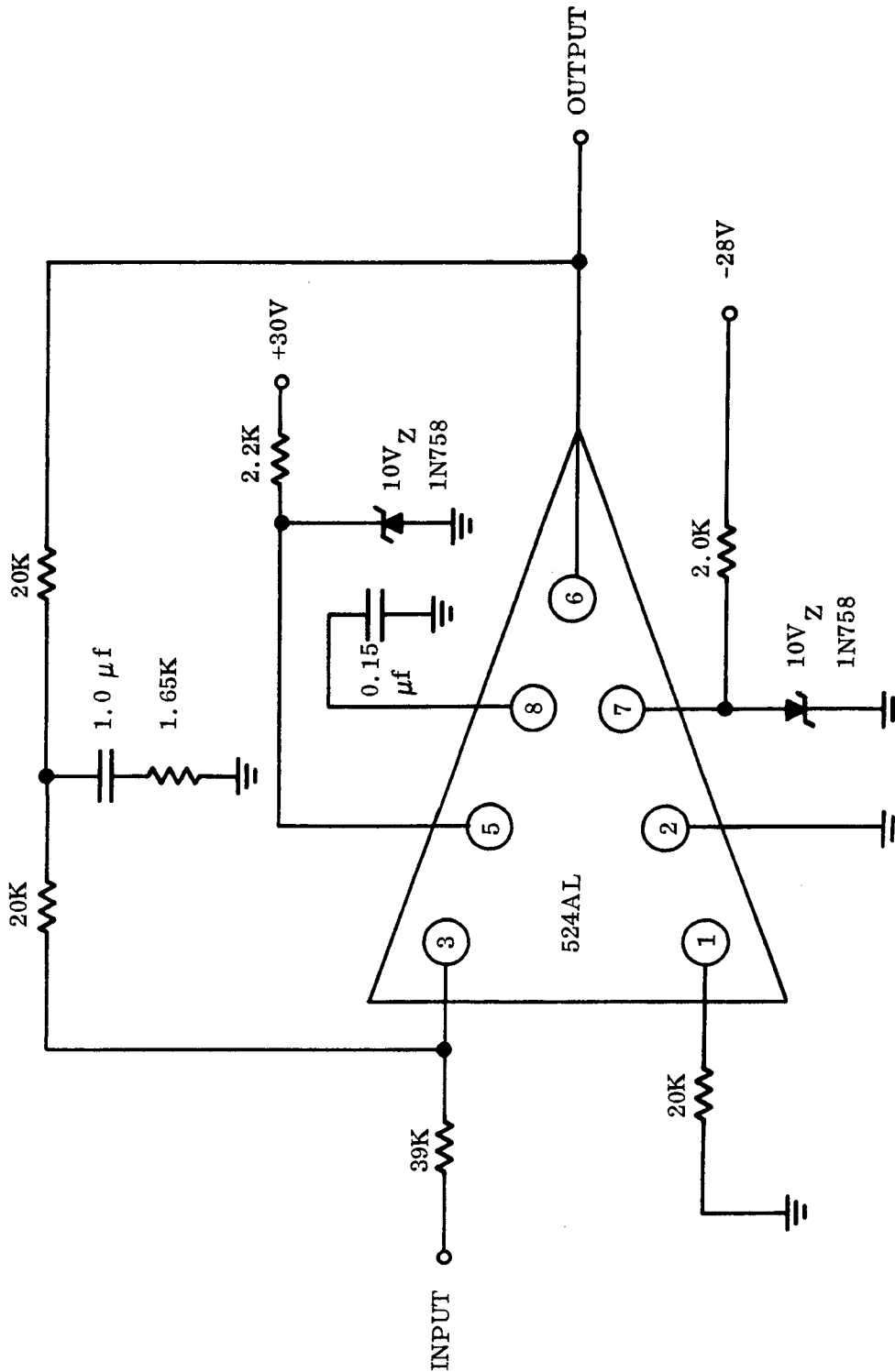
Figure 4.1-9. K-2 Compensation Amplifier

~~SECRET~~ **SPECIAL HANDLING**
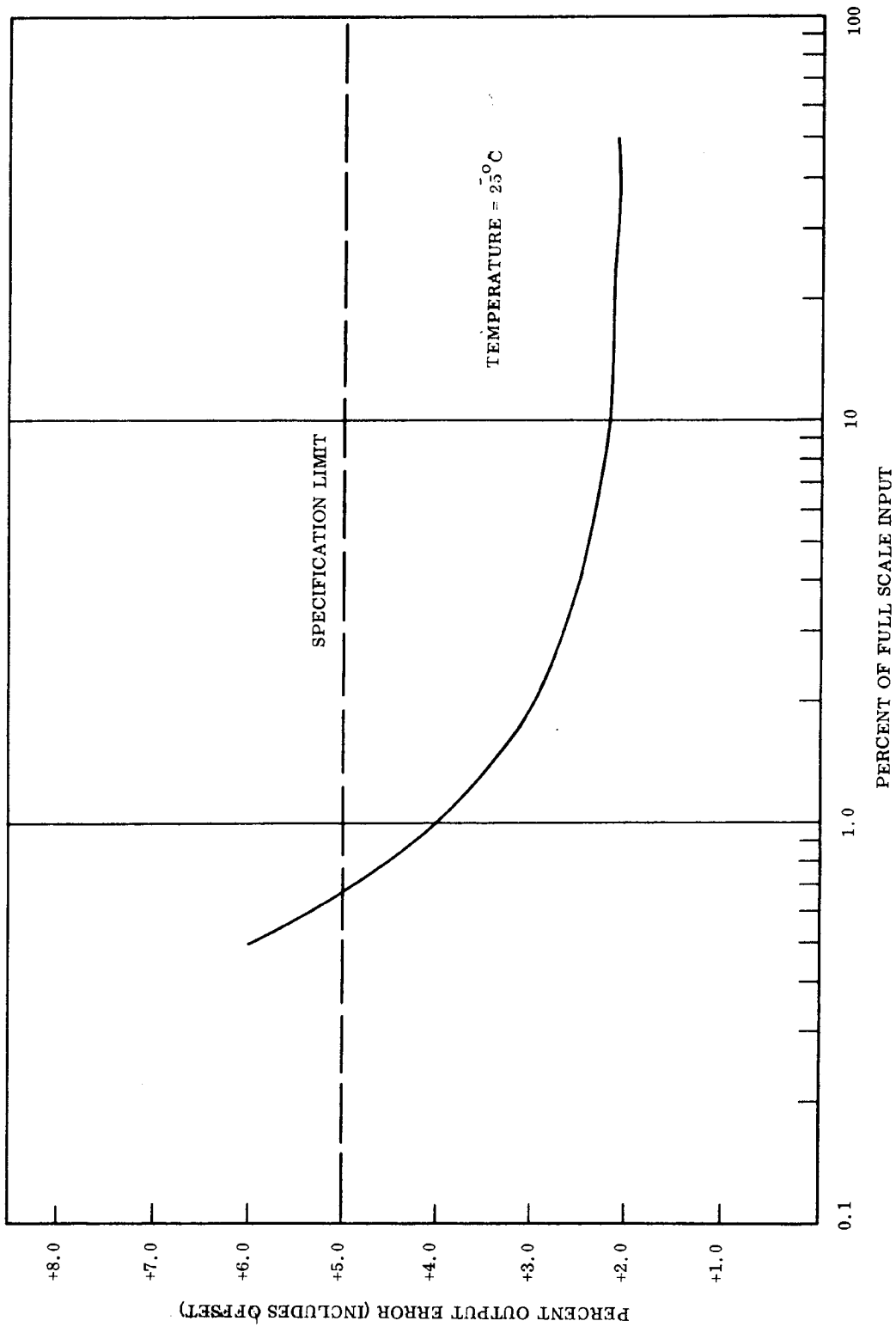
Figure 4.1-10. Linearity Check, K-2 Compensation Amplifier
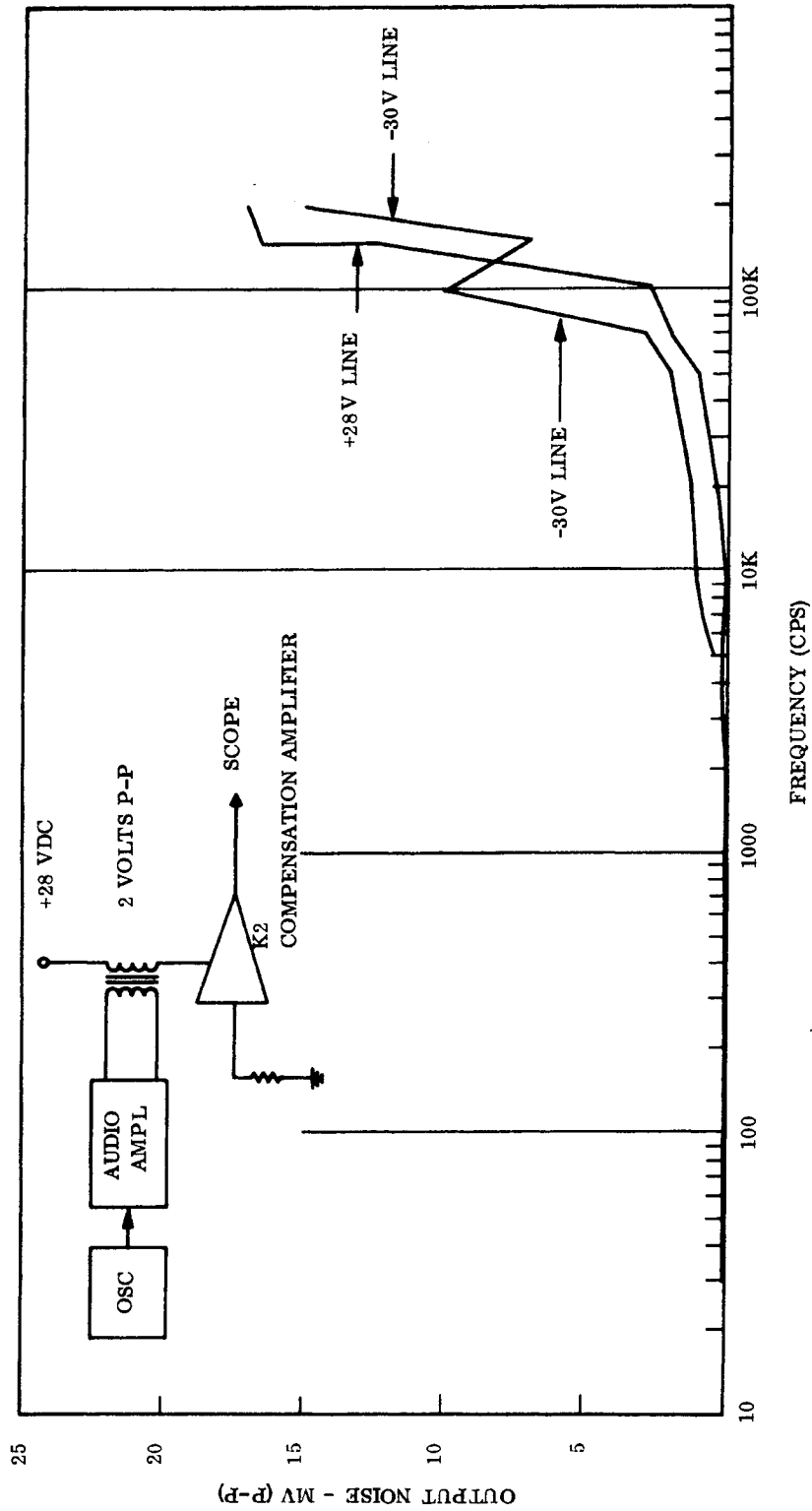
Figure 4.1-11. K-2 Compensation Amplifier – Susceptibility to Power Supply Ripple

A breadboard of the power amplifier (Figure 4.1-8) was constructed, and similar tests were conducted plus an additional test of the output noise. An output noise value of 0.5 ma was measured when the amplifier was connected to a 7-ohm resistive load.

Finally, the two amplifiers were mated and the following tests were conducted on the total K-2 electronics.

a. Linearity vs temperature

	$-15^{\circ}C$	$+25^{\circ}C$	$+70^{\circ}C$
Output DC Offset (Input Grounded)	+0.46 mv	+0.57 mv	+0.70 mv
Gain (ma/volt)	11.7	11.6	11.3

b. Rejection of power supply noise

c. Output Noise measurement

For this test, the combined amplifier was loaded by a 7-ohm resistor in series with a 75-millihenry inductor. The input was terminated in a 1000-ohm source. The output noise was measured on an oscilloscope as being less than 1 mv peak-to-peak. This is equivalent to approximately 150 microamperes at the output.

4.1.5 K-3 AND K-4 ELECTRONICS

Description

The K-3 and K-4 electronics (see Figure 4.1-12) provide control signal outputs to a dc torquer within the required gain, dynamic, and other performance characteristics outlined in the specification.

Each of the K-3 and K-4 electronics is comprised of a microcircuit compensation amplifier (see Figure 4.1-13) and a discrete part power amplifier (Figure 4.1-14). The compensation amplifier is a 524AL microcircuit and the power amplifier consists of two differential stages of gain followed by an output bridge which supplies current to a 51.3-ohm load. Feedback in the power amplifier is taken from the current sensing resistor to provide the high-source impedance required by a current amplifier.

The K-3 compensating amplifier has unity gain and drives the power amplifier which has a gain of 0.418 amp/volt.

The K-4 compensating amplifier also has a gain of unity and drives the power amplifier which has a gain of 0.0964 amp/volt.

~~SECRET~~ **SPECIAL HANDLING**

K3 INHIBIT FROM K0

K-3 POSITION
COMM'D
(DIGITAL)

K-3

D/A | COMM'D FILTER | SUMMER AND COMPEN | POWER AMPL

TO K3 MOTOR

POSITION FDBK (ANALOG)
TO MDAU NO. 1 AND NO. 2

POSITION FDBK
FROM K3 POSITION TRANSDUCER (ANALOG)

K-4 POSITION COMM'D
(ANALOG)

K-4

COMM'D FILTER | SUMMER AND COMPEN | POWER AMPL

TO K4 MOTOR

K4 HI/LO SIGNAL
TO MANUAL CONTROL
STICK ASSEMBLY

POSITION FDBK
FROM K4 POSITION TRANSDUCER
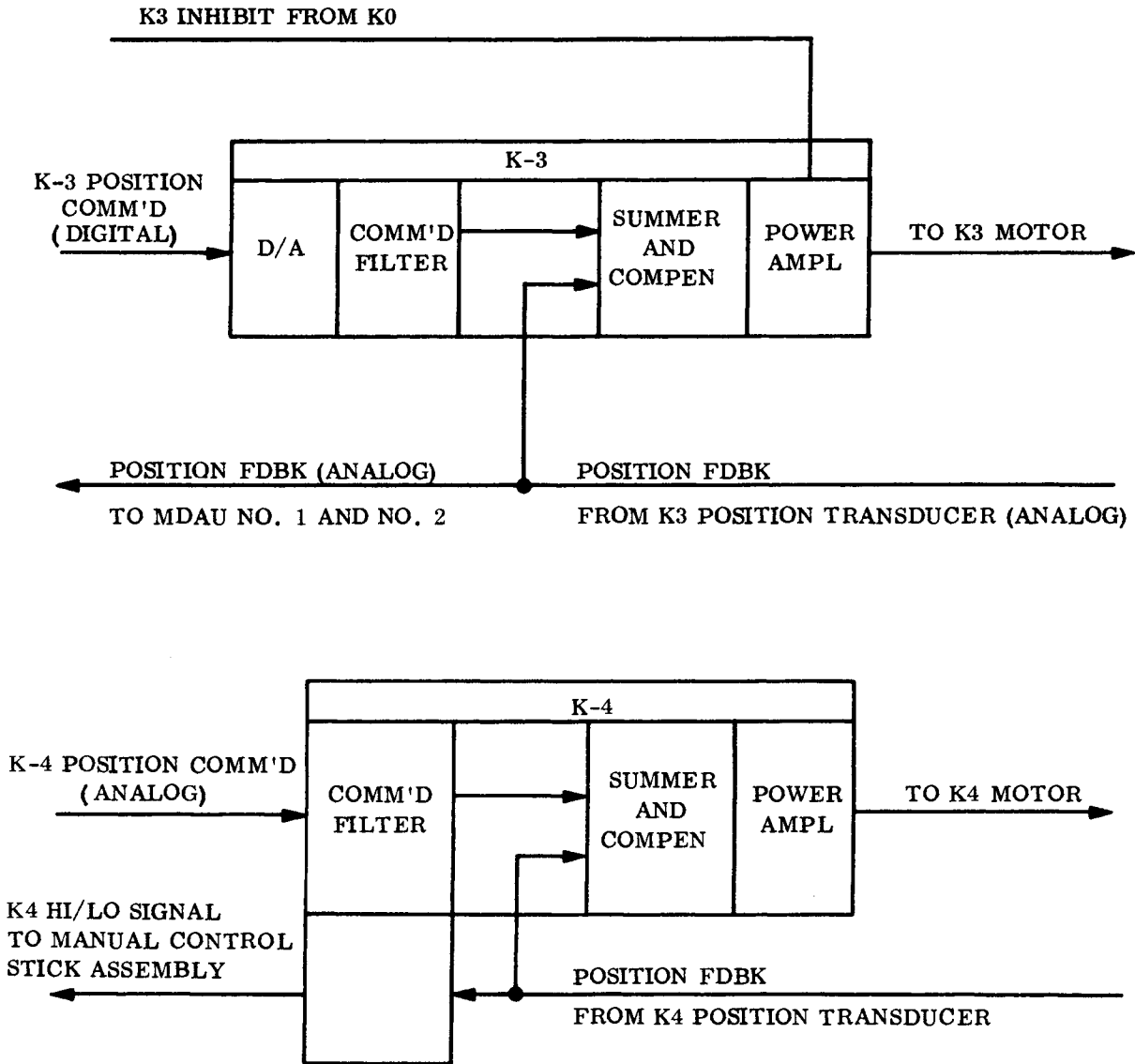
Figure 4.1-12. K-3 and K-4 Electronics Block Diagram

~~SECRET~~ **SPECIAL HANDLING**

~~SECRET~~ SPECIAL HANDLING
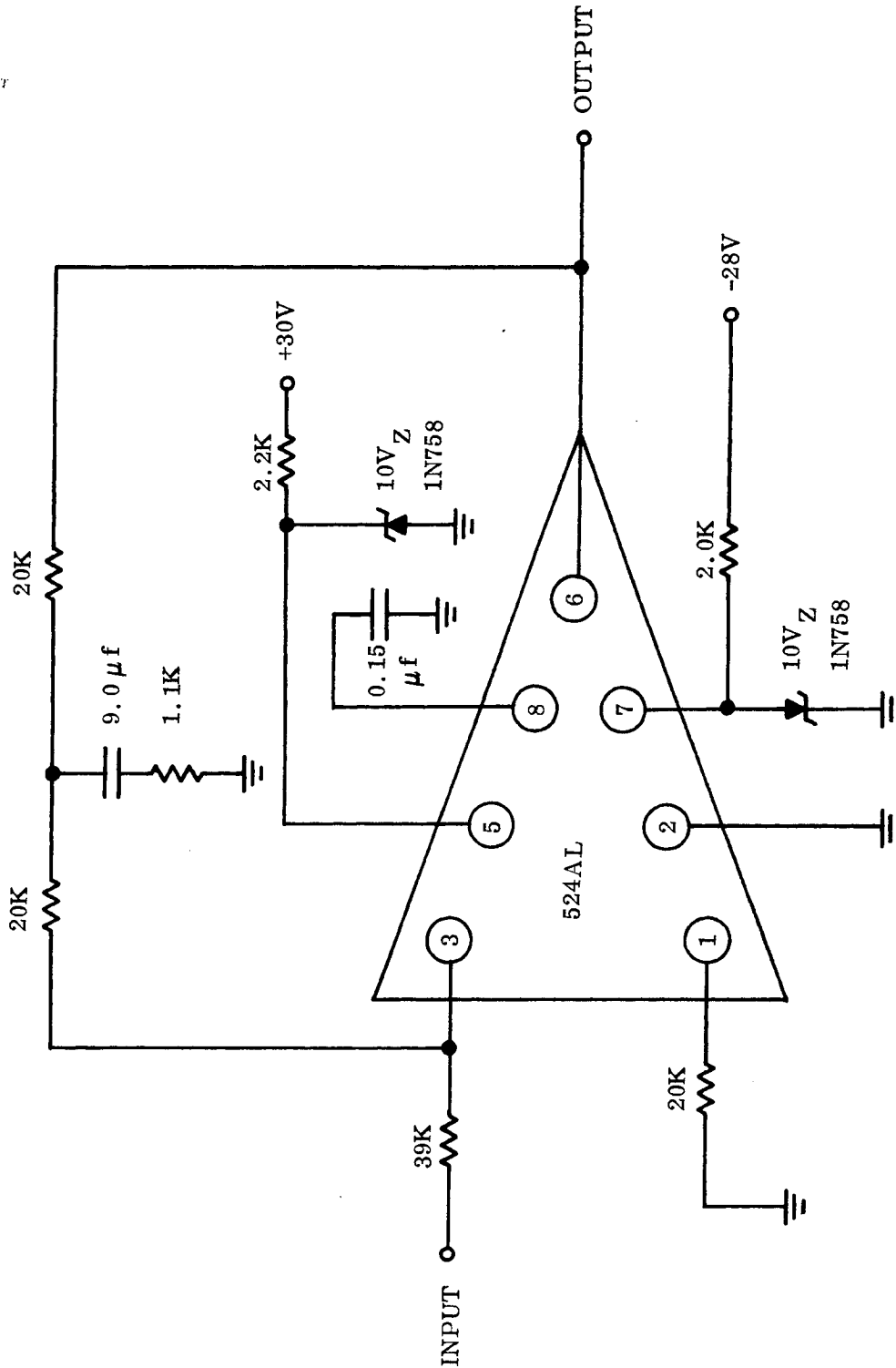
Figure 4.1-13. Compensation Amplifier

4-39

~~SECRET~~ **SPECIAL HANDLING**
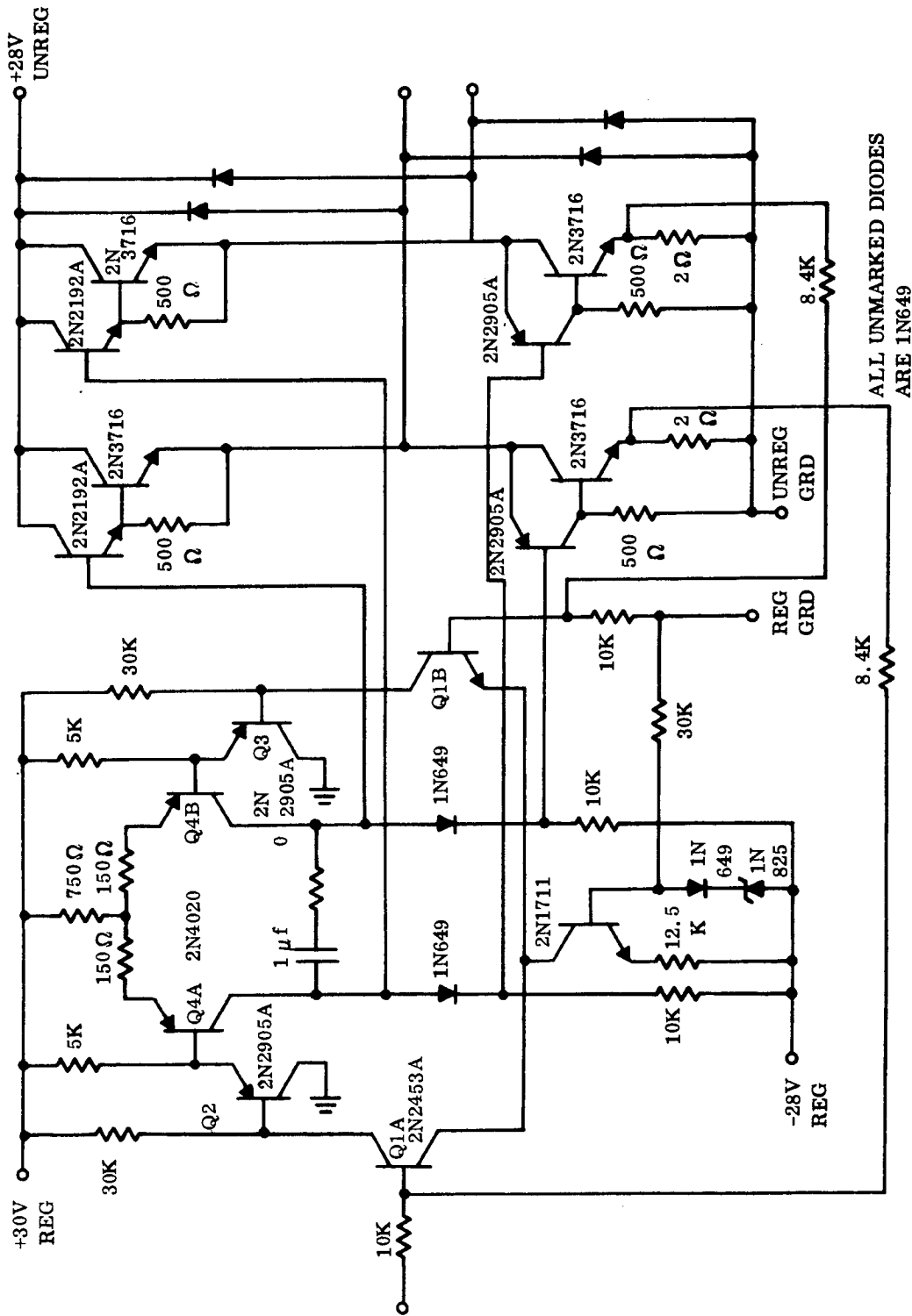
Figure 4.1-14. Power Amplifier

~~SECRET~~ **SPECIAL HANDLING**

~~SECRET~~ **SPECIAL HANDLING**

4.1.6 K-5, K-6 AND K-7 ELECTRONICS

Description

The K-5, K-6 and K-7 Electronics shown in block diagram fashion in Figures 4.1-15 and 4.1-16, are comprised of a number of logic controlled power switches. Some of these switches are bipolar and are used to drive motors bidirectionally. A circuit was designed (Figure 4.1-17) for bipolar power switch, and preliminary testing has been done on a breadboarded circuit.

4-41

~~SECRET~~ **SPECIAL HANDLING**

INHIBIT FROM K0

COMMANDS

K5 CW & CCW

K5	
LOGIC	POWER SWITCH

TO K5 MOTOR AND BRAKE RELEASE

FROM K5 CW & CCW LIMIT SWITCH

BIVALUED DISCRETE POSITION
INDICATION TO MCSA

TRIP COMM'DS {
FROM SUN SENSOR

FROM TEST SWITCH
ON CONSOLE

K6A	
TRIP LOGIC	TRIP POWER SWITCH

COMMAND TO K6A TRIP

TO K6A ALARM
(CONSOLE)
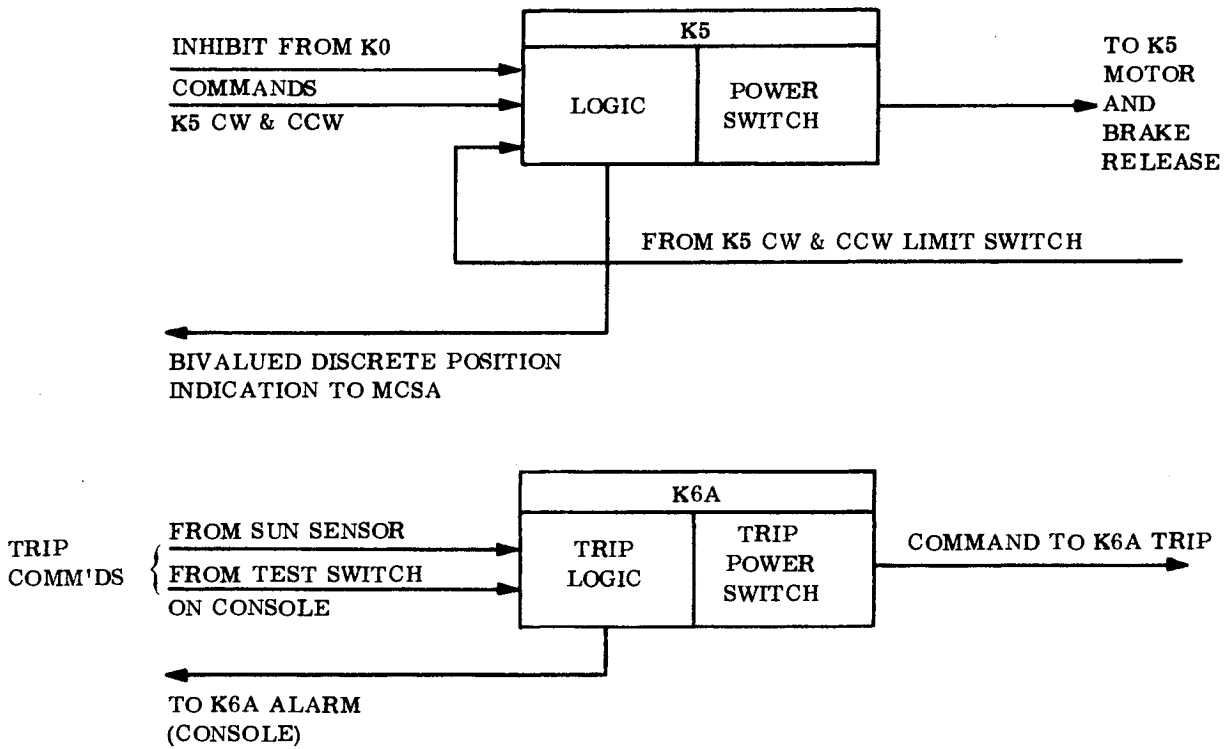
Figure 4.1-15.   K-5 and K-6A Electronics

~~SECRET~~ **SPECIAL HANDLING**

K6B

K6B POSITION
COMMAND
(FROM K0)

LOGIC | POWER SWITCH

TO K6B MOTOR

CW AND CCW LIMIT SWITCHES FROM K6B

K7 ELECTRONICS

PRI LAUNCH LOCK
RELEASE (FROM LMMC)
BU LAUNCH LOCK
RELEASE (FROM CONSOLE)
K7 RELEASE
COMMAND
K7 FWD DISCONNECT
COMMAND
K7 AFT DISCONNECT
COMMAND
PRI K7 COMMAND
(LMMC)
BU K7 COMMAND (CONSOLE)
K2 STOWED (FROM K0)

DRIVERS — K2 LAUNCH LOCKS
DRIVERS — K7 LAUNCH LOCKS
DRIVER — K7 RELEASE
DRIVER — K7 FWD DISCONNECT
DRIVER — K7 AFT DISCONNECT

LOGIC | FWD POWER SWITCH — K7 FWD MOTOR
AFT POWER SWITCH — K7 AFT MOTOR

FWD CW AND CCW LIMIT SWITCHES
AFT CW AND CCW LIMIT SWITCHES

K7 CLOSED
TO LMMC K2
POWER RELEASE

K7 ALARM TO CONSOLE

Figure 4.1-16. K-6B and K-7 Electronics

4-43

Figure 4.1-17. K-5 Switch Circuit

4.2 MAGNIFICATION CONTROLLER (See also Section 1.3.3.8)

Functional Characteristics

The Magnification Controller, commonly called the left hand control stick (LHCS), provides analog and discrete signals to control ATS high and low range magnification, ATS zoom, selection of main optics magnification levels, switch the MCS to control main optics, ATS finger-operated voting switches, and cue hold command.

Operation

Analog signals are generated by the LHCS to provide ATS zoom control. Movement of the stick through its range causes zoom operation. Upon reaching the midpoint of the ATS control range, a discrete signal commands ATS high range, and the zoom control resets to the lowest zoom position. Further movement of the stick causes ATS zoom to 127x.

Upon reaching ATS 127x, the stick can be moved to the left, generating a discrete which commands MCS main optics control. The stick can then be moved to one of four positions in detents, which command the four main optics magnification levels.

Finger-operated switches on the stick provide target reject, inactive, and active votes. Twisting the stick (20 degrees or less) generates a cue hold discrete command.

Status

The Magnification Controller system requirements have been defined. A preliminary design concept has been generated and a brassboard is being constructed for use in the R-38 simulation facility. Flight crew comments will be utilized in a redesign of the initial concept. This component is barely out of the paper design stage.

4.3 VENDOR SELECTION TRADE-OFFS AND CRITERIA FOR THE ATS RATE GYRO

The following factors influenced the selection of Honeywell as the gyro vendor:

a. The Drive A gyro had been under contract for about four months, and we wished to have as much commonality with it as possible to minimize costs.

b. The gyro transfer function and PSD envelope were specified by the N.G. & C. Requirements and Analysis Group, and were different from those of the A gyro.

c. The thermal environment was specified by the Systems-Thermal Analysis Group as 0 to 80°F (as opposed to 60 to 80°F for the A gyro).

d. The allowable space envelope was specified by the N.G. & C. Subsystems Engineering group.

Thus, the problem became one of trying to resolve items b, c, and d with item a. Item a dictated that the contract be placed with Honeywell and utilize the same basic instrument as specified for the A gyro. However, our previous fact-finding on the A gyro, completed in January, had shown that Honeywell was the only vendor who had a suitable "developed" gas bearing gyro, and was willing to accept the MOL requirements. Thus, there was really no other vendor to consider. (A gas bearing gyro is required because of noise and reliability considerations.)

Given the fact that space to mount a single package was not available, it was determined that two smaller packages could be made to fit the space available. A natural way to divide the component was to have the gyro in one package and the support electronics in another, connected with an interconnect cable.

With a much larger dynamic temperature environment (0 to 80°F) than that of the A gyro, a different thermal design was required. This took the form of raising the gyro temperature to the 160-170° range, the maximum desirable from reliability considerations. This higher operating temperature allows power savings over the Drive K environmental range compared with a design operating at a lower temperature.

The transfer function requirements being different, and the operating temperatures of the
A and K gyros having to be different because of their respective environments, if the same
fluid were used in both gyros, the gyros would require different damping gaps to achieve
the same damping coefficient. Alternately, different fluids could be used with the same
damping gap in each gyro. This was preferred from cost and commonality considerations,
and simplified the design of the gyro with respect to its transfer function. The noise re-
quirements were also different. Fortunately, in both cases, the gyros appear to be able
to meet the noise requirements, and work with Honeywell is underway to use a common
method of testing.

4.4 ALPHA SUBSYSTEM POWER REQUIREMENTS (See Also Section 2.5)

Figure 4.4-1 depicts the power flow within the alpha subsystem. The diagram shows the power flow for one manned station. Two identical stations are provided per subsystem. The diagram is drawn to highlight the power across contracted interfaces, namely Drive K Electronics, Itek (Sub A), Visual Display Projector and Gyroscopes. In each box is given the standby and peak power dissipated. The boxes in the Drive K Electronics signify major functional modules; the boxes in the Itek (Sub A) signify actuators, sensors, displays, or feedback transducers as defined by the legend. In the gyro, its mechanical elements, power conditioner (p.c.), electronics, heaters and heater controls are indicated; the Visual Display projector lists the power dissipated in several significant modes.

Table 4.4-1 tabulates the information from Figure 4.4-1 into four basic Alpha Subsystem Modes and mission average. The modes are Shroud Open, Slew, Track and Shroud Close modes. This represents a preliminary evaluation of the development status of the subsystem versus its allocated requirement not to exceed 480 watts peak or 70 watts average. The estimated figures from the table are 458.82 watts and 51.99 watts, respectively. The peak power allocation can be attained by selective inhibiting of the peripheral display, and gyro heaters during slew. Since the performance is expected to be within the allocation, no such recommendation is made at this time.

TABLE 4.4-1. ALPHA SUBSYSTEM PEAK AND AVERAGE POWER SUMMARY

	SHROUD OPEN	SLEW	TRACK	SHROUD CLOSE	MISSION AVERAGE
	←		WATTS		→
Torque Motor IA		13.0	1.3		0.42
Torque Motor OA		40.0	4.0		1.29
Prism Actuator		5.0			0.01
Zoom Actuator			5.0		0.01
Power Changer Actuator			22.1		0.03
Sun Shield Motor			11.0		0.70
Shroud Actuators	16.6			16.6	0.02
Encoders (2)		9.0	9.0		0.62
Prism F.B.		0.5	0.5		
Zoom F.B.		0.5	0.5		
Power Changer F.B.		0.01	0.01		
Sun Shield F.B.		0.01	0.01		
Peripheral Display		5.0	5.0		0.29
Sun Sensor		2.0	2.0		0.42
Gyro Warm Up Heater IA	61.5				3.12
Gyro Control Heater IA		8.5	8.5		0.83
Gyro Electronics IA	5.5	5.5	5.5		1.08
Gyro Spin Motor IA	2.5	2.5	2.5		
Gyro Torquer IA		4.0	4.0		
Gyro, Electronics, Heater OA	69.5	20.5	20.5		5.03
Drive K Electronics K0, K3, K4, K5, K6, K7, K9, K10		36.9	36.9		
DKE K2 Modules IA		1.7	1.7		
DKE IA Torquer Power Amplifier		1.7	1.7		
DKE K2 Module OA		1.7	1.7		
DKE OA Torquer Power Amplifier		17.3	5.4		3.69
DKE Power Amplifier, Prism		2.19			
DKE Power Amplifier, Zoom			2.19		
DKE Power Amplifier, Power Changer			2.1		
DKE Power Amplifier, Sun Shield Motor			1.0		
DKE Power Amplifier, Shroud	1.6			1.6	
DKE Power Amplifier, (2) gyro torquers		7.2	7.2		
Visual Display Projector		38.0	38.0		8.42
Totals, Peak per Crew Station	152.21	229.41	199.32	18.21	
Total, Average per Crew Station					25.99
Worst Case Peak per System		458.82			
Worst Case Peak Allocation		468.0			
System Average					51.99
System Average Allocation					70.0

~~SECRET~~ **SPECIAL HANDLING**

Figure 4.4-1. Alpha Subsystem Power Flow Chart (Two Sides Required)

~~SECRET~~ **SPECIAL HANDLING**

4.4.1 ALPHA WEIGHT STATUS

The weight bogies for the subsystem were negotiated in October with exception of the Acquisition Optics components.

These negotiated figures are shown in the table below along with the present status numbers. The Drive K electronics weight has grown significantly and may exceed 3.5 lbs. MDAU weight deltas are also not reflected in the following tabulation.

ALPHA WEIGHT DATA - FOR GE ITEMS ONLY - (2 SUBSYSTEMS)

	CURRENT	NEGO*
Gyros and Electronics	20.2	22
VDP (Excluding GFE Modules)	45.4	50
Control Sticks (Left Hand)	5.0	5
Harness	42.0	42
Headrest	5.0	5
Thermo Insulation	3.0	3
Support Structure	13.0	13
Console Signal Controller (Delta)	6.0	6
Power Controller (Delta)	5.0	5
Console Signal Controller - Per. Display	6.0	6
Peripheral Display Harness	4.0	4
Alpha Numeric Harness	4.0	4
Total (lbs.)	158.6	165
*Negotiated Weight as of October, 1967, except Drive K electronics		

SECTION 5.0

CONSOLES AND DISPLAYS

This section describes the present layout of the consoles and displays panels. The material is subdivided into two categories; Consoles and Displays Requirements and Panel Layout.

5.3 "B" Panel Controls and Displays

5.1 CONSOLES AND DISPLAYS REQUIREMENTS

The CEI requirements relevant to the consoles and displays subsystem and the aquisition subsystem are:

a.   Provide the controls, status indicators, and alarm initiating signals as required for proper operation, monitoring, and control of the GE AVE.

b.   Provide dual visual displays, cue displays, and controls on each reconnaissance console as required for proper operation of the acquisition group and the tracking mirror. (This requirement for dual visual displays has been changed to reflect the current acquisition subsystem design of a single telescope and pointing assembly at each console.)

5.2 PANEL LAYOUT - C & D Panels

Figure 5-1 depicts the current operational panel layout for the acquisition subsystem while Table 5-1 lists all the controls and displays on Panels 8C and 8D.

Those proposed controls and displays which are related to the operation of just the Alpha Subsystem and a description of their functions are as follows:

* 1.   ATS Track Light - Alerts the crew that the ATS is in a rate track mode and to begin ATS tasks.

* 2.   ATS Telescope - Provides for inspection of targets for weather coverage, activity status and optical feedback for manual steering control of the ATS telescope tracking mirror.

_____

*Indicates that this component is a direct part of the Acquisition Subsystem.

TABLE 5-1. LIST OF CONTROLS AND DISPLAYS

* 1.   ATS Track Light
* 2.   ATS Eyepiece Location
  3.   MO Track Light
  4.   MO Eyepiece Location
  5.   Zero Reset
  6.   Computer Update
  7.   Position Rate Control Stick
* 8.   Cue Display Screen
  9.   Rate Manual Switch
 10.   Exposure Adjust Switch
*11.   Cue Brightness
 12.   X Format Inhibit Light Switch
*13.   Cue Execute
*14.   Single Frame Step
 15.   Manual Shutter
*16.   Manual Cue Selector
 17.   Preferred Photo
 18.   Wrong Module
 19.   End of Reel – (Deleted)
*20.   Cue System Electrical Power Control (Mode Selector)
 21.   Cue Test – (Deleted)
*22.   ATS Hold Switch
*23.   Cue Focus
*24.   Cue Film Module Insert
*25.   Magnification Control Stick (Voting Switches and cue hold)
 26.   Position Mark
 27.   Shutter Mode
*28.   Peripheral Display Brightness Control
*29. α – N Display (Cue)
*30.   Track Path Switch
 31.   Camera Selection Switch
 32.   MO Brightness Control
 33.   IVS Saturate Light
 34.   Time to Next Group
*35.   Target Number
 36.   Timing Setting Control
 37.   Operate Switch
 38.   Numeric Display (Event Timer)
 39.   Mode Switch
 40.   Master Caution
 41.   Master Warning
 42. α–N Brightness Control

*Aquisition S/S related items.

~~SECRET~~ **SPECIAL HANDLING**
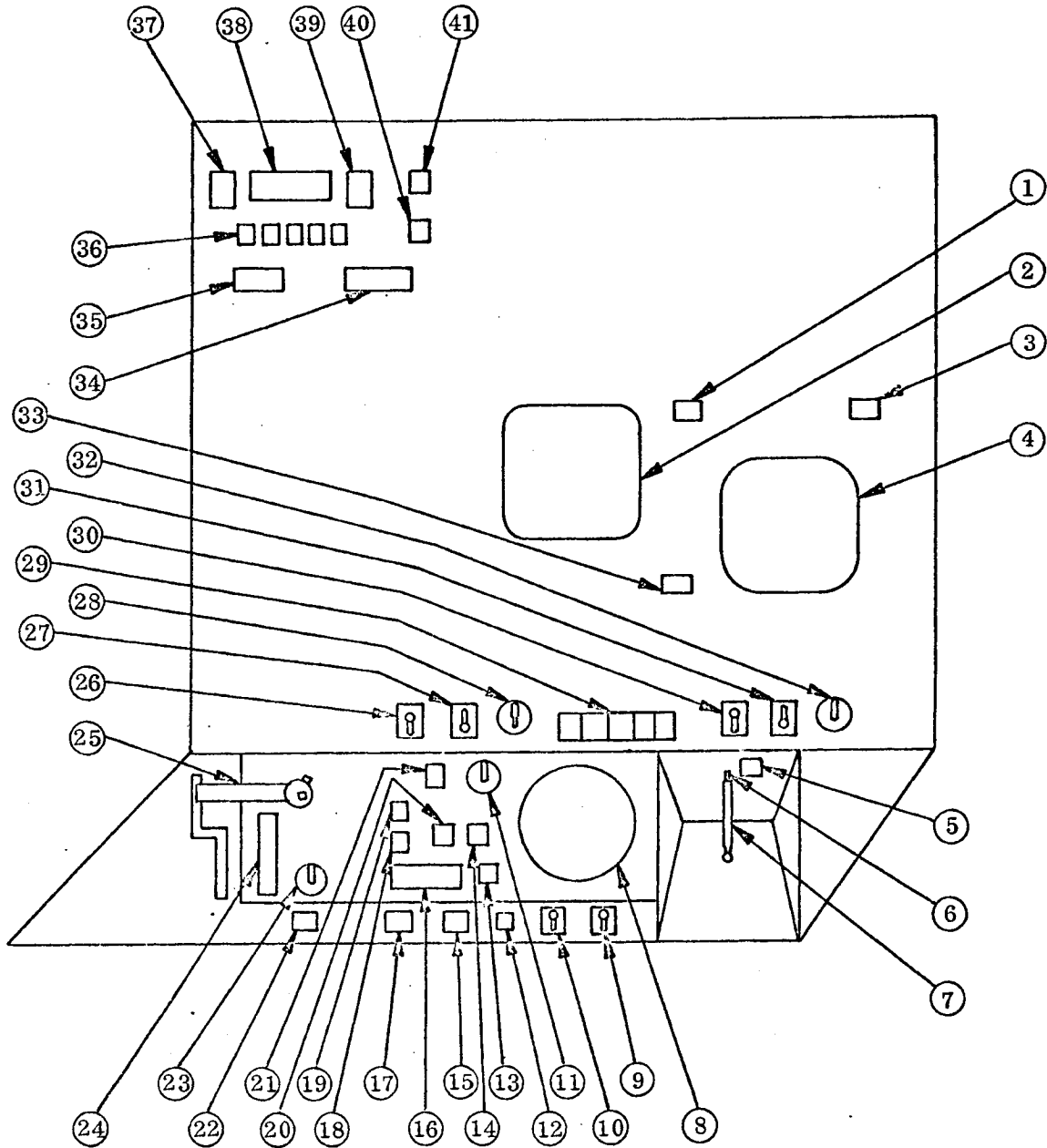
Figure 5-1. Panels 8C and 8D Component Configuration

5-5

~~SECRET~~ **SPECIAL HANDLING**

ATS Peripheral Display - Tentative Functions include:

a) An non-override light (Group 2 or 3) indicates the target being taken by the MO is a non-override target.

b) A primary light (Group 2 or 3) indicates the target in the ATS FOV is the primary target of the target group.

c) Groups 2 and 3 display coded patterns utilized for target identification and information.

d) A visual optics assigned light (Group 2 or 3) indicates the MO is assigned to this console and final target selection has been made and tracking has commenced.

e) A decision time wipeout indicates the time remaining to the end of decision time for the target group.

f) Lights in the decision time wipeout indicate the recommended dwell time for target viewing prior to slew to the next target.

7. Deleted

* 8. Cue Display Screen - Provides a projection surface for the cue display.

*11. Cue Brightness - Provides manual control of the image light intensity projected on the display screen.

*13. Cue Execute - Initiates the manual cue selection process.

*14. Single Frame Step - Allows individual frame stepping, in either direction, without resetting the manual cue selector.

*16. Manual Cue Selector - Provides a manual capability to select any desired cue.

*20. Cue System Electrical Power Control - Provides control of the cue display input power and selection of the VDP control mode.

*22. ATS Hold Switch - Provides a manual ATS target hold capability beyond the normal decision time and delays subsequent ATS slewing the next target group.

---

* Indicates that this component is a direct part of the Acquisition Subsystem.

*23. <u>Cue Focus</u> – Adjusts cue focus for maximum clarity.

*24. <u>Cue Film Module Insert</u> – Positions the cue film module in the VDP.

*25. <u>Magnification Control Stick</u>

    a) Provides Main Optics and ATS telescope magnification control.

    b) Provides a control stick gain signal proportional with telescope magnification of the ATS and the Main Optics in order to achieve a constant eyepiece scene rate throughout various powers of magnification.

    c) Provides three logic voting switches for computer analysis and final target decision.

    d) Provides a cue hold function.

*28. <u>Peripheral Display Brightness Control</u> – Provides manual light intensity control of the ATS peripheral displays.

*29. <u>Alphanumeric Display</u> – Displays information not provided by other convenient displays, which are pertinent to the target.

*30. <u>Track Path Select</u> – Provides a manual selection of the ATS track path for the respective console.

*35. <u>Target Number</u> – Provides a ready identification to the target presently displayed in the ATS FOV for crew reference and comment identification.

*42. <u>Alpha-Numeric Brightness Control</u> – Provides manual control of the α-N brightness.

As part of the operational controls associated with the ATS telescope eyepiece itself, a filter control is provided for image contrast enhancement. This filter wheel has four sections for neutral density or spectral filters and is controlled by a pointer knob on the side of the eyepiece.

In addition, the derotation mechanism, zoom lens, low power groups, and blanking shutter have backup override controls which minimize the possibility of a catastrophic failure mode.

_____

* Indicates that this component is a direct part of the Acquisition Subsystem.

These controls are behind the panel and have a requirement that they be operated with a pressurized gloved hand (Located behind 8C and 2C).

The derotation mechanism has a manual override and index which enables the astronaut to manually position the Pechan prism within plus or minus five degrees of the neutral or central position in the event of a control signal or drive motor failure. This is a 1-5/16 inch round knurled knob located behind the panel and must be turned several times to position the prism mounts (Located behind 8C and 2C).

The zoom lens has a manual override which enables the astronaut to manually change from low zoom to high zoom or vice versa in the event of a control signal or mechanism failure. The control itself is a two position pointer knob located behind the panel to rotate the gears which position the lens (Located behind 8C and 2C).

The magnification (power) change mechanism has a manual override capability which enables the astronaut to manually change from low power to high power and vice versa, in the event of a control signal or drive motor failure. The control is a key type of device which is turned to the desired position by turning a gear train which positions a cam controlling the lens position. Access to this control is from Douglas Console 3C and 7C because of its location in the system.

The blanking shutter has a manual override which enables the astronaut to manually remove the blanking devices from the optical path between the target scenes and eyepiece. This will be an operation in the event of a control signal or mechanism failure which prohibits display of the target image. The control is a round knob which is turned 90 degrees to reset the shutter and is located behind the panel (Located behind 8C and 2C).

The remaining control which has a direct astronaut interface is the launch locks which are accessible from Douglas' Console 3C and 7C. These launch locks hold the lens in a folded

position and must be released before the mission can be performed. There are also launch locks located outside the Lab Module and are activated by pyros. This may be initiated either by commands or manually.

5.3 "B" PANEL CONTROLS AND DISPLAYS

The following controls and displays have been identified for the Alpha subsystem on panels 8-B, and 2-B. These items are not required for normal ATS operations, but are made available for equipment checkout and contingency operations.

    1.   Controls to:

        a.   provide backup stow capability for acanners (each STS)

        b.   provide manual backup to drive scanners to sync position (each axis of each ATS)

        c.   select between redundant encoders (each ATS)

        d.   select between redundant control loops (each axis of each ATS)

        e.   enable/disable scanner amplifier power (each ATS)

        f.   enable/disable derotation drive power (each ATS)

        g.   enable/disable zoom drive power (each ATS)

        h.   enable/disable magnification drive power (each ATS)

        i.   test blanking shutter (each ATS)

        j.   enable/disable blanking shutter power (each ATS)

        k.   enable pyro circuits for door failure mode correction (each ATS)

        l.   fire pyro circuits for door failure mode correction

        m.   provide back-up control to drive door fully open or closed (each ATS)

        n.   mechanically disengage either/both door drive motors, an irreversible process (each ATS)

~~SECRET~~ **SPECIAL HANDLING**

    o.   electrically select/disable door drive motors (each motor)

    p.   actuate door spring-release mechanism to swing door free from scanner interference, irreversibly (each ATS)

2.   Display to indicate:

    a.   scanner is stowed, pitch and roll (each ATS)

    b.   analog position of door (one side): each ATS

    c.   door is fully open or closed, (each ATS)

    d.   scanner has achieved sync position (each axis of each ATS)

    e.   door is not operable (each ATS)

~~SECRET~~ **SPECIAL HANDLING**

SECTION 6.0

RELIABILITY, CONTAMINATION CONTROL AND MAINTAINABILITY

The material in this section is subdivided as follows:

6.1   Reliability Requirements and Evaluations

6.2   Contamination Control

6.3   Maintainability

6.4   Eye Hazard Analysis

6.1 REQUIREMENTS AND EVALUATIONS

6.1.1 SUMMARY

Based upon the Mission Reliability design criteria specified in Section 6.1.3, the following conclusions were reached:

a.   The system design concept appears adequate to meet the GE-AVE mission reliability requirements.

b.   The crew has been utilized to perform backup operations to the automatic equipment which is in agreement with the GE-AVE Reliability Policy. This should be pursued further to assure that this backup capability is optimized and that maintainability through repair or interchangeability of ATS-1 and ATS-2 components is possible.

c.   Additional studies appear necessary to assure that the design provides adequate crew protection for malfunctions in the sun blanking control functional assembly.

6.1.2 SYSTEM RELIABILITY REQUIREMENTS

The ATS system reliability requirements have been developed utilizing the SPDR (SS-MOL-1A) and the GE-AVE CEI (CP1000A1) as the guideline documents. Following is a summary of the pertinent system reliability statements:

a. SPDR, paragraph 3.3.4.3.3.11 states essentially that;

    1. The design shall be such that after any single failure, the navigation and control system shall be capable of supporting a productive mission.

    2. Redundancy shall be utilized and it shall be a design objective that this redundancy be achieved with minimum additional equipment configured so that failure may reduce capability but not abort the mission.

b. CEI – CP1000A1, paragraph 3.1.2.1 states:

    1. "The probability that the GE-AVE will meet the requirements of the mission shall be 0.97 (MA) ....."

    2. "Where practicable, the GE-AVE shall be designed so that after any single failure, the GE-AVE shall be capable of supporting a productive mission."

    3. Failure criteria for the evaluation of the system GE-AVE reliability are defined in terms of the primary mission objectives only; i.e. a failure to meet primary mission objectives is defined as:

        (a) Photographic mission terminated prior to 30 days

        (b) Less than 90 percent of the planned photographs obtained due to a GE-AVE malfunction

        (c) Degradation in the GE-AVE that causes a degradation in resolution greater than 10 percent on more than 10 percent of the ZI horizontal measurement

6.1.3 MISSION RELIABILITY DESIGN CRITERIA

Based upon these GE-AVE system level reliability requirements the following mission reliability design criteria have been established for the ATS subsystem:

a. The primary mission objectives are achievable with one of the two ATS subsystems performing in accordance with specification requirements. (Note: To minimize the MOL effectiveness degradation due to loss of a single ATS, it is desirable to be capable of putting all primary targets on high priority targets as one ATS system. This is the current plan.)

b. The probability that one of the two ATS systems is performing, within specification limits, shall be at least 0.999.

c. A reliability requirement for each ATS system has been established as 0.980 for the mission. This appeared attainable in the early design stages without utilizing block redundancy. (Note: Each ATS could be degraded to a 0.968 reliability prediction and still meet the system requirements expressed in b. above.)

d. Block redundancy within each ATS subsystem should be eliminated to minimize weight if its only purpose is to achieve the 0.980 reliability requirement. Block and/or functional redundancy within each ATS shall be utilized as required to meet the system level requirement of 0.999.

e. In the M/A mode, a functionally redundant operating mode exists that can negate the effects of a complete loss in the ATS function, i.e. the Automatic Mode with or without the crew utilizing the main optics eyepiece. This functionally redundant mode will permit achievement of a large percentage of the MOL objectives; however switching to the Automatic Mode due to equipment failure causes is considered as a failure of the GE-AVE M/A system to meet its primary mission objectives.

f. The design shall be such that no single failure will cause the loss of both ATS subsystems.

g. Provisions shall be made to utilize the crew to perform backup control, perform maintenance (interchange similar hardware), and perform diagnostic analysis where system effectiveness is improved without undue utilization of the crew's time.

6.1.4 DESIGN EXCEPTIONS

The design meets all of the above requirements except the individual reliability apportion-ment of 0.980 to each of the ATS subsystems (predicted to be 0.975 without degradation and 0.988 utilizing manual backup capabilities). The reliability data presented in the next sec-tion, when summarized at the ATS system level, establishes that:

a. The probability of completing the mission with both ATS meeting specification requirements is 0.951.

b. The probability of at least one of the two ATS systems meeting specification re-quirements is 0.9993.

c. The probability of at least one of the two ATS systems operable with degraded performance, is approximately 0.9999.

6.1.5 ACQUISITION SYSTEM RELIABILITY ESTIMATE

The reliability apportionment to the Acquisition Subsystem is based upon satisfactory per-formance with one of the two sets operative and is 0.999. The analysis, as reflected in Table 6.1-1, presents the prediction for each set and that for operational redundancy.

The estimate for the Optical Assembly, as shown, reflects prime configuration operation without manual backup. With manual backup, the prediction is increased from 0.9960 to 0.9981. As presented in Table 6.1-1, the analysis does not reflect the planned capability of switching out and by-passing the gyro's in the event of failure. The gyro's and gyro electronics represent a significant portion of the failure risk, principally due to the longer operating time with a 12-minute warm-up period prior to each operating period.

The failure rate applied to the Drive K Electronics reflects an upward scaling related to the recent increase in failure rate for the Drive A Electronics. In the case of the gyro and gyro electronics, the failure rate applied is that provided in the subcontractor's preliminary RFMA. It is considered to be conservative.

~~SECRET~~ **SPECIAL HANDLING**

TABLE 6.1-1. RELIABILITY ESTIMATE ANALYSIS

ITEM NUMBER	ITEM	λ (ppmh/c)	t (hrs/cy)	λt	PREDICTION	APPORTIONMENT	REMARKS/CRITICAL PARTS
	Optical Assembly			0.003983	0.9960	0.9957	NOTES: 1) Provision for operation with gyro's switched out is being implemented which will reduce total risk per set to 0.0141, increasing prediction to 0.9859 for each set and 0.9998 for one of two.
	Scan Assembly	4.52	50	0.000226	0.999774		
	Solar Blanking	36.561	10	0.000365	0.999635		
	Low Power Changer	26.874	12	0.000322	0.999687		
	Prism Assembly	5.212	50	0.000261	0.999739		2) Optical assembly analysis was performed by subcontractor. The analysis reflecting a predicted reliability of 0.9960 is based upon prime configuration operation. With manual backup and degradation, the prediction becomes 0.9981 for the optical assembly manual backup and gyro backup result in a set prediction of 0.988.
	Zoom and Eyepiece Assembly	5.403	25	0.000135	0.999865		
	Peripheral Display	7.483	20	0.000148	0.999852		
	Shroud	73.684	25	0.001842	0.998158		
	Drive K Electronics	98	65	0.006370	0.993630		MTBF 17,900 hours without redundancy
	Gyro and Electronics (2)	46	131	0.012052	0.98802		MTBF 16,500 hours
	Visual Display Projector	16.3	230	0.003749	0.996251		MTBF requirement 16,500 hours
	Each Side			0.025054	0.974946	0.99	
	One of Two			0.00063	0.99937	0.999	

~~SECRET~~ **SPECIAL HANDLING**

The failure rate applied to the Visual Display Projector presents a more conservative figure, 16.3 failure per million hours, as compared to approximately 8 fpmh provided by Lear Siegler in their proposal in response to RFP No. 134A.

The predicted inherent reliability of the subsystem, even with the degree of conservation included, indicates that the subsystem apportionment will be met.

6.1.6 SYSTEM FAILURE MODE AND EFFECTS

6.1.6.1 Introduction

This section summarizes data that is pertinent to the system reliability of the Acquisition Tracking Function. The information is presented in subsections 6.1.6.2 through 6.1.6.4.

6.1.6.2 Description of Function

This subsystem consists of a pair of high performance telescopes; one for each astronaut, with a variable magnification range. The magnification is a minimum of 16X and a maximum of 127X. Each telescope has the capability for providing to the astronaut a scan of the ground before, behind and on both sides of the orbiting vehicle to enable him to enhance the performance of the main optics. Included in this subsystem are the control loops necessary to perform the following functions: slew to a programmed target control tracking of ATS optics, orient target image to align with vehicle velocity vector, control the magnification of the optical system, provide automatic sun blanking control for astronaut eye protection and control opening and closing of external door which protects scanner and folding mirror when not in use. Also included in the Subsystem is a Visual Display Projector which has the primary function of displaying, either automatically or upon astronaut command, stored cue information to assist the astronaut in locating and recognizing preselected targets.

~~SECRET~~ SPECIAL HANDLING

SPECIAL SUBSYSTEM - RELIABILITY BLOCK DIAGRAM

```
┌────────────┐   ┌────────────┐   ┌────────────┐   ┌────────────┐   ┌────────────┐
│ MECHANISM  │───│  DRIVE K   │───│ ROLL GYRO  │───│ PITCH GYRO │───│   VISUAL   │
│            │   │ELECTRONICS │   │ ASSEMBLY   │   │ ASSEMBLY   │   │  DISPLAY   │
│            │   │            │   │            │   │            │   │ PROJECTOR  │
└────────────┘   └────────────┘   └────────────┘   └────────────┘   └────────────┘
```
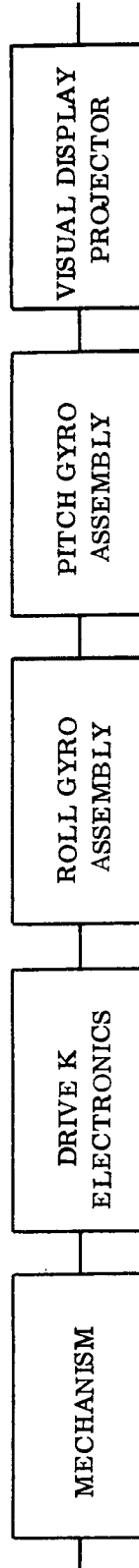
Figure 6.1-1. Reliability Block Diagram

~~SECRET~~ SPECIAL HANDLING

Figure 6.1-2 relates the interrelationships between the ATS, the astronauts and the other MPSS subsystems. It provides a pictorial presentation of the signals and commands between the subsystems.

6.1.6.3 System Reliability Block Diagram

Figure 6.1-3 presents the reliability logic of the ATS at the system level. It identifies the baseline operational paths to perform the ATS functions. Figure 6.1-4 presents the logic of one ATS system. In subsystem 6.1.6.4 more detailed logic diagrams are presented for each of the ATS functional assemblies.

6.1.6.4 System Failure Mode and Effects Analysis

Figures 6.1-5 through 6.1-16 in conjunction with Tables 6.1-2 through 6.1-10 provide a preliminary failure mode and effects analysis on a component input/output basis. The approach has been to analyze functional groupings of equipment regardless of where they appear in the subsystem component listings. The analysis is subdivided into the following functional assemblies:

Scanner Controls and Drives

Image Orientation

Zoom and Magnification Control

Sun Blanking

Shroud Door

Cue System

Scanner Passive Elements

Operational Interfaces

6-11

Figure 6.1-2. ATS Functional Interface Diagram

PATH	SYSTEM STATE
A	NOMINAL MODE
B	MINIMUM PERMISSIBLE TO MEET SYSTEM REQUIREMENTS
C	DEGRADED MPSS PERFORMANCE i.e., NETHER ATS OPERATING

*EACH ATS INCLUDES ALL EQUIPMENTS NECESSARY TO-PERFORM ACQUISITION FUNCTION
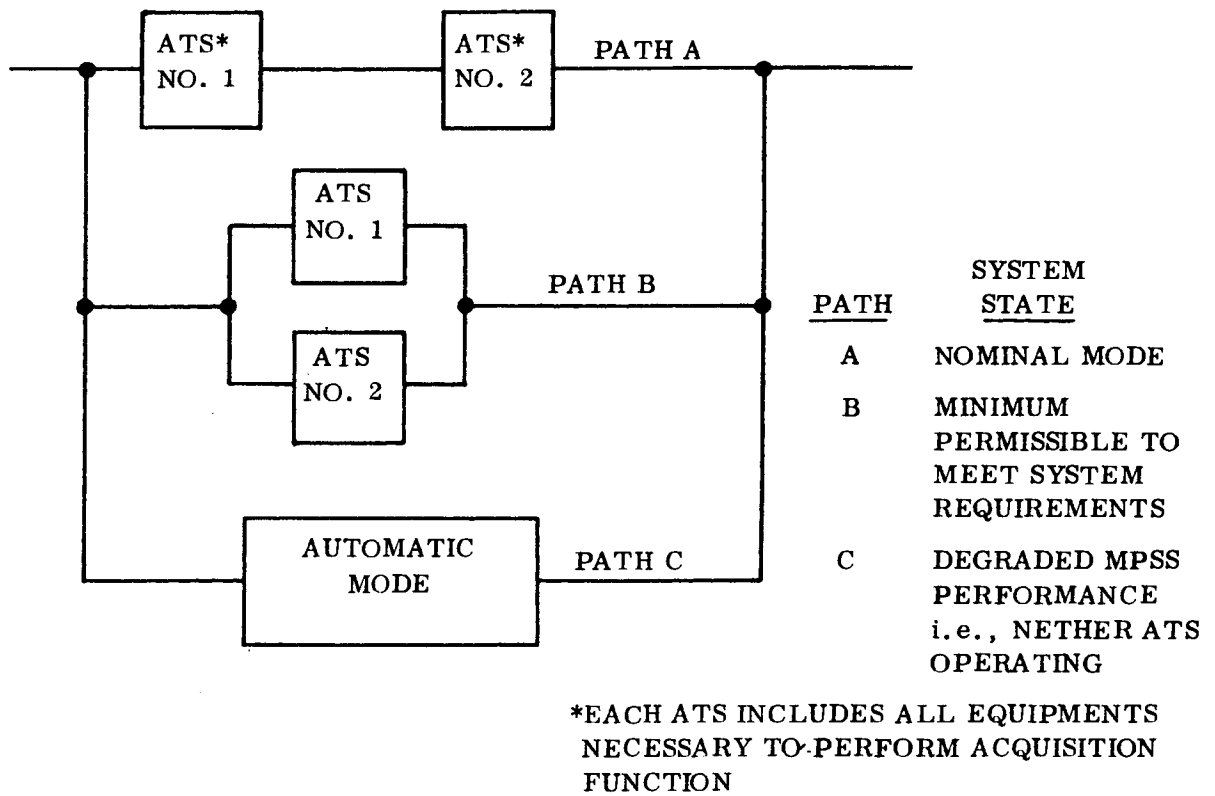
Figure 6.1-3. MPSS System Level Reliability Diagram

~~SECRET~~ **SPECIAL HANDLING**
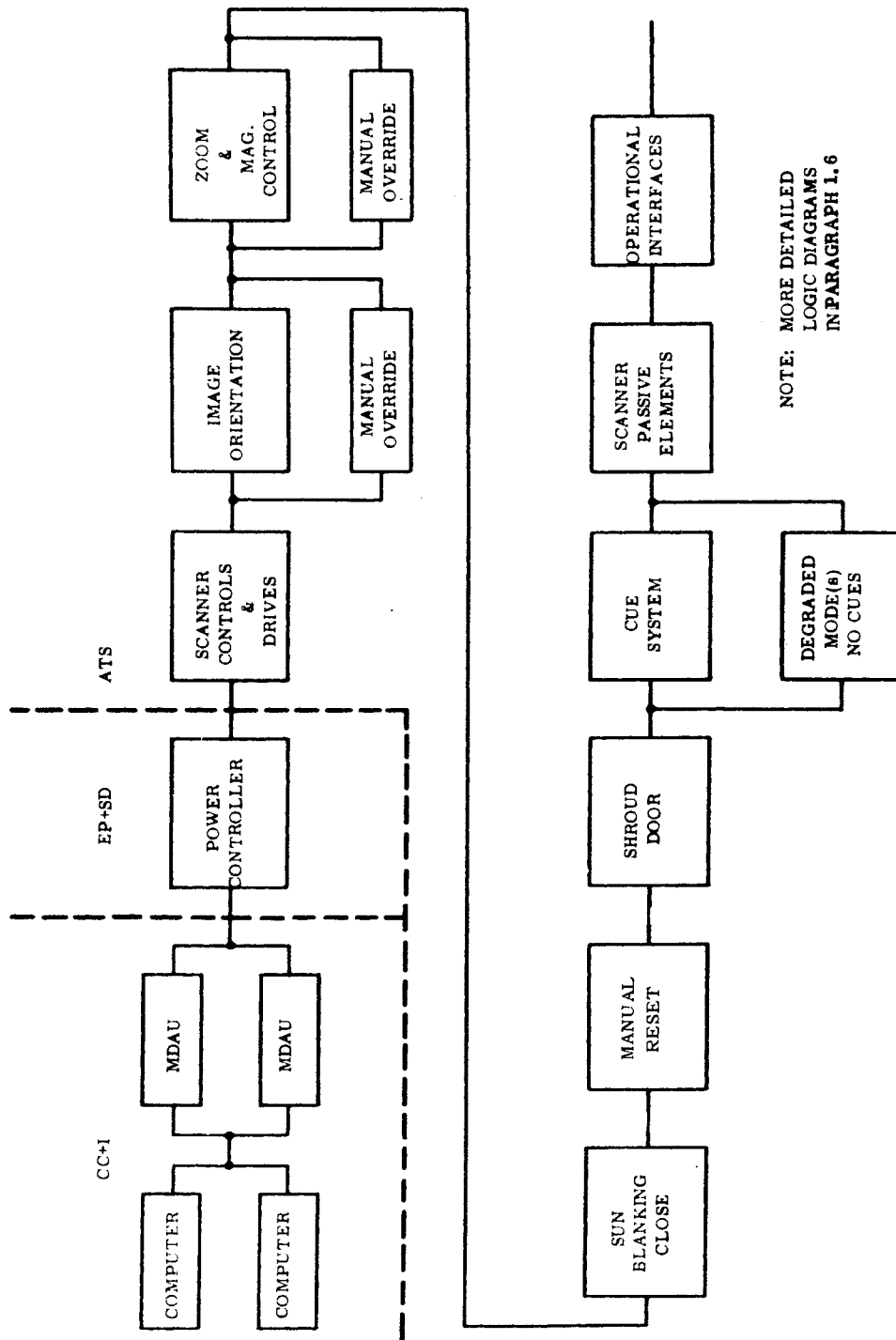
Figure 6.1-4. System Reliability Logic Diagram (Per ATS)

NOTE: MORE DETAILED
LOGIC DIAGRAMS
IN PARAGRAPH 1.6

6-14

~~SECRET~~ **SPECIAL HANDLING**

~~SECRET~~ SPECIAL HANDLING

Figure 6.1-5. Functional Assembly – Scanner Controls and Drives (Per ATS)

~~SECRET~~ SPECIAL HANDLING

Figure 6.1-6. Reliability Logic Diagram Scanner Controls and Drives (Per ATS)

~~SECRET~~ SPECIAL HANDLING

~~SECRET~~ SPECIAL HANDLING

Figure 6.1-7. Functional Assembly – Telescope–Image Orientation (Per ATS)

~~SECRET~~ SPECIAL HANDLING
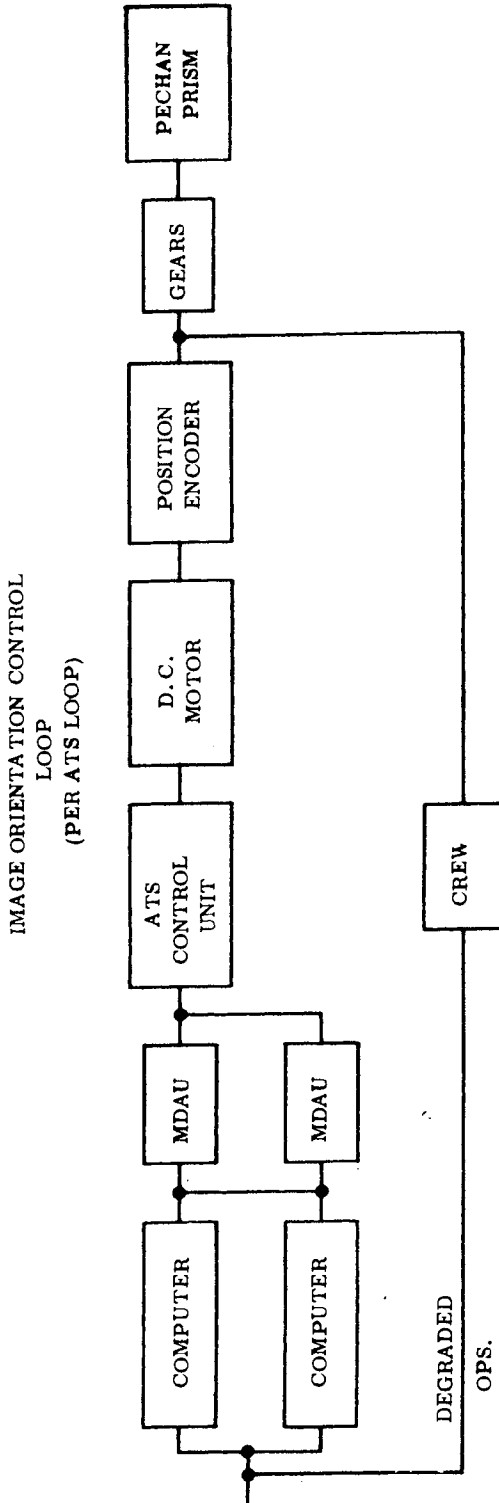
Figure 6.1-8. Reliability Logic Diagram – Image Orientation Control Loop (Per ATS Loop)

Figure 6.1-9. Functional Assembly – Zoom and Magnification Control (Per ATS)

SECRET SPECIAL HANDLING

Figure 6.1-10. Reliability Logic Diagram – Zoom and Magnification Control (Per ATS)

SECRET SPECIAL HANDLING

~~SECRET~~ **SPECIAL HANDLING**

SIGNAL SCHEMATIC

MANUAL (OPEN)

SHUTTER ASSEMBLY (SPRING CLOSE)

ATS CONTROL UNIT

BLANKING COMMAND

SUN SENSOR

CONTROL SCHEMATIC

SUN SENSOR

SHUTTER ASSEMBLY

ACQ. OPTICAL ASSEMBLY

M

R: 1

BLANKING LOGIC

ATS CONTROL UNIT

SUN SENSOR AMPLIFIER
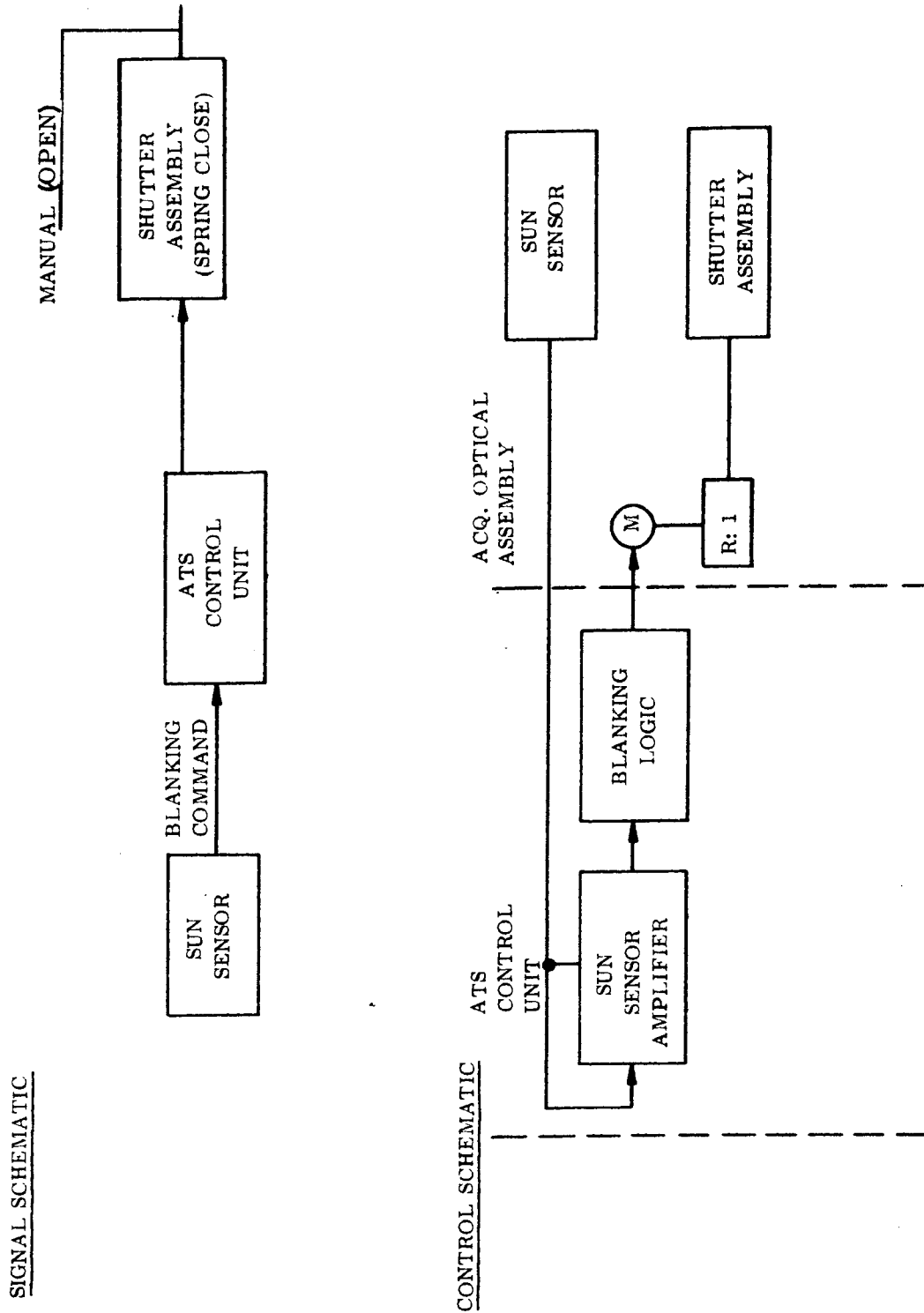
Figure 6.1-11. Functional Assembly – Blanking (Per ATS)

~~SECRET~~ **SPECIAL HANDLING**

~~SECRET~~ **SPECIAL HANDLING**

CLOSE

| SUN SENSOR | — | ATS CONTROL UNIT | — | SHUTTER | →
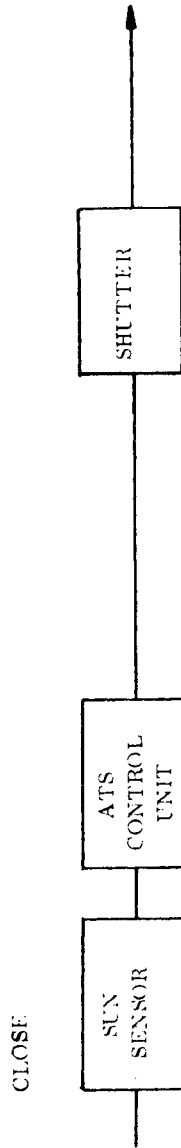
Figure 6.1-12. Reliability Logic Diagram – Blanking Assembly (Per ATS)

~~SECRET~~ **SPECIAL HANDLING**

~~SECRET~~ SPECIAL HANDLING
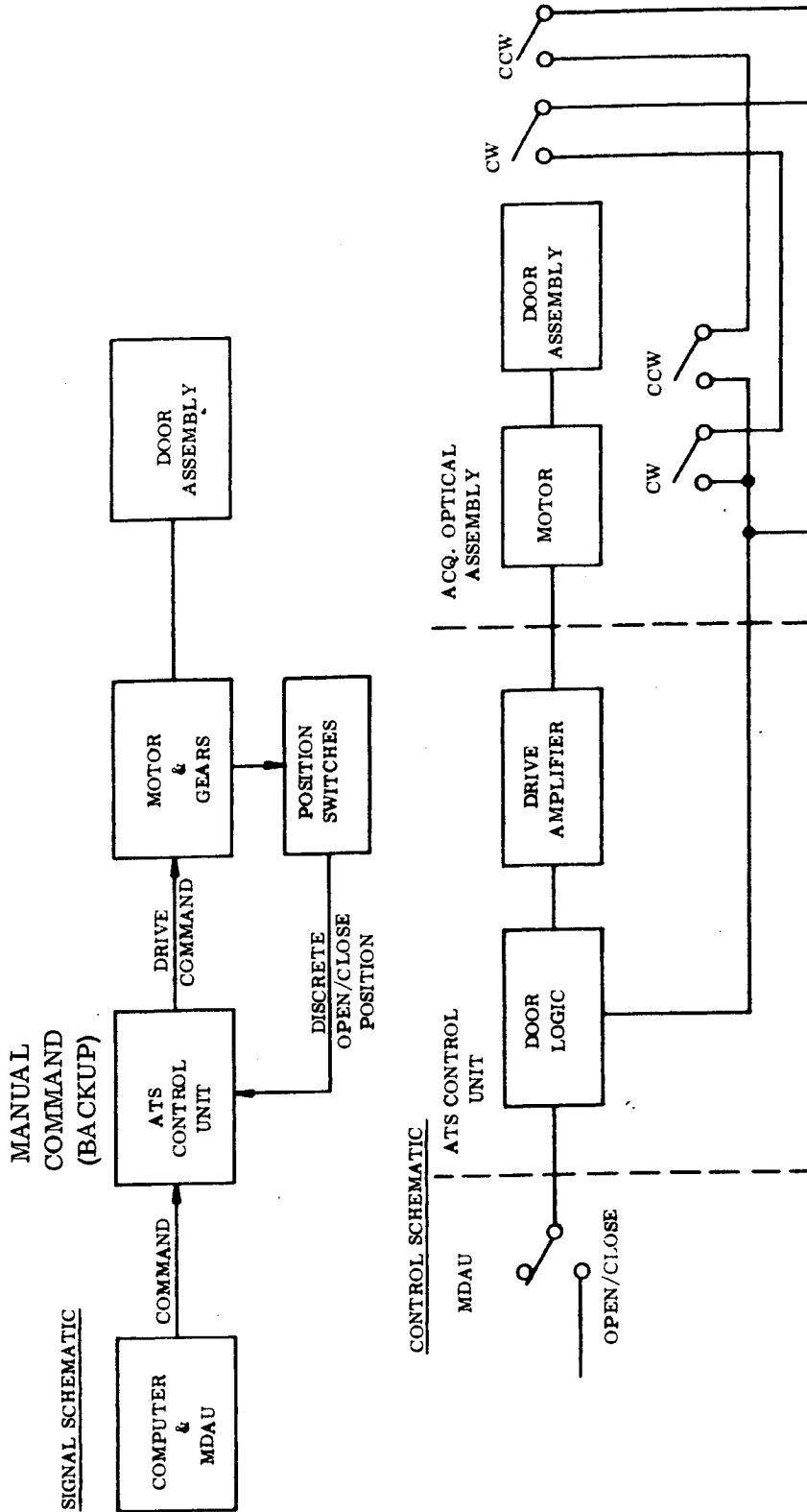
Figure 6.1-13. Functional Assembly, Shroud Door

~~SECRET~~ SPECIAL HANDLING

~~SECRET~~ SPECIAL HANDLING
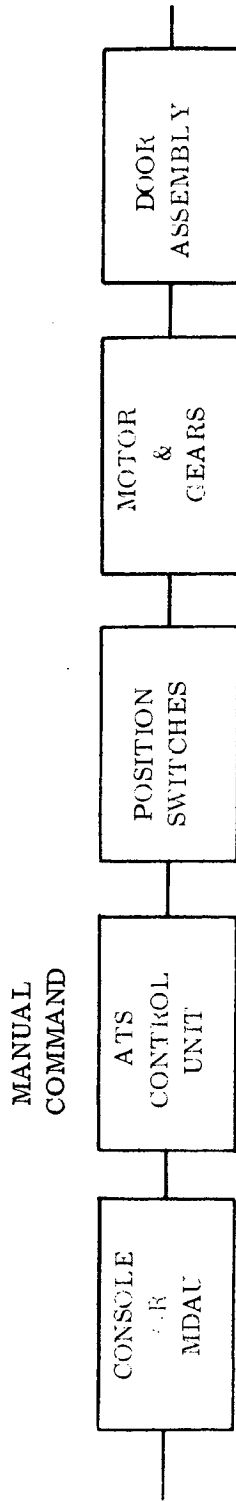
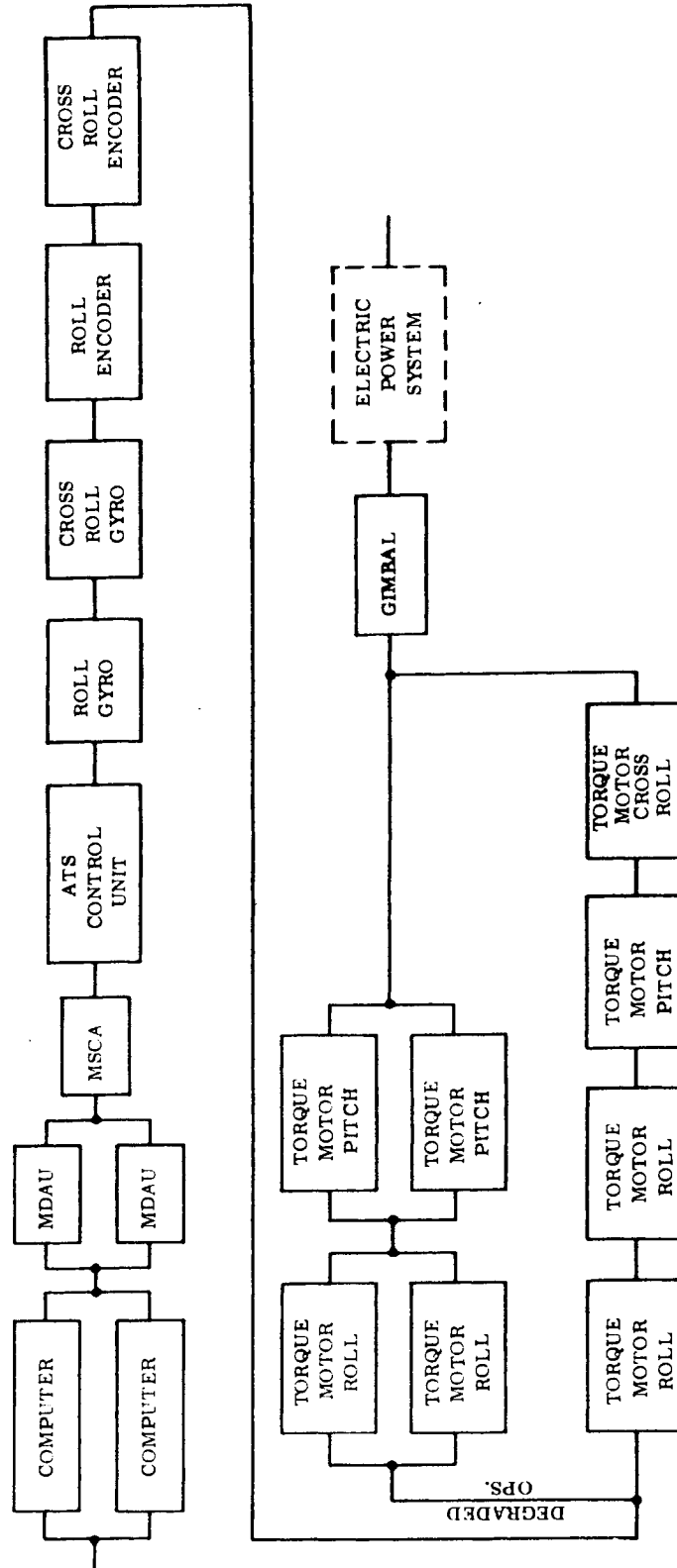Figure 6.1-14. Reliability Logic Diagram Shroud Door (Per ATS)

6-24

~~SECRET~~ SPECIAL HANDLING
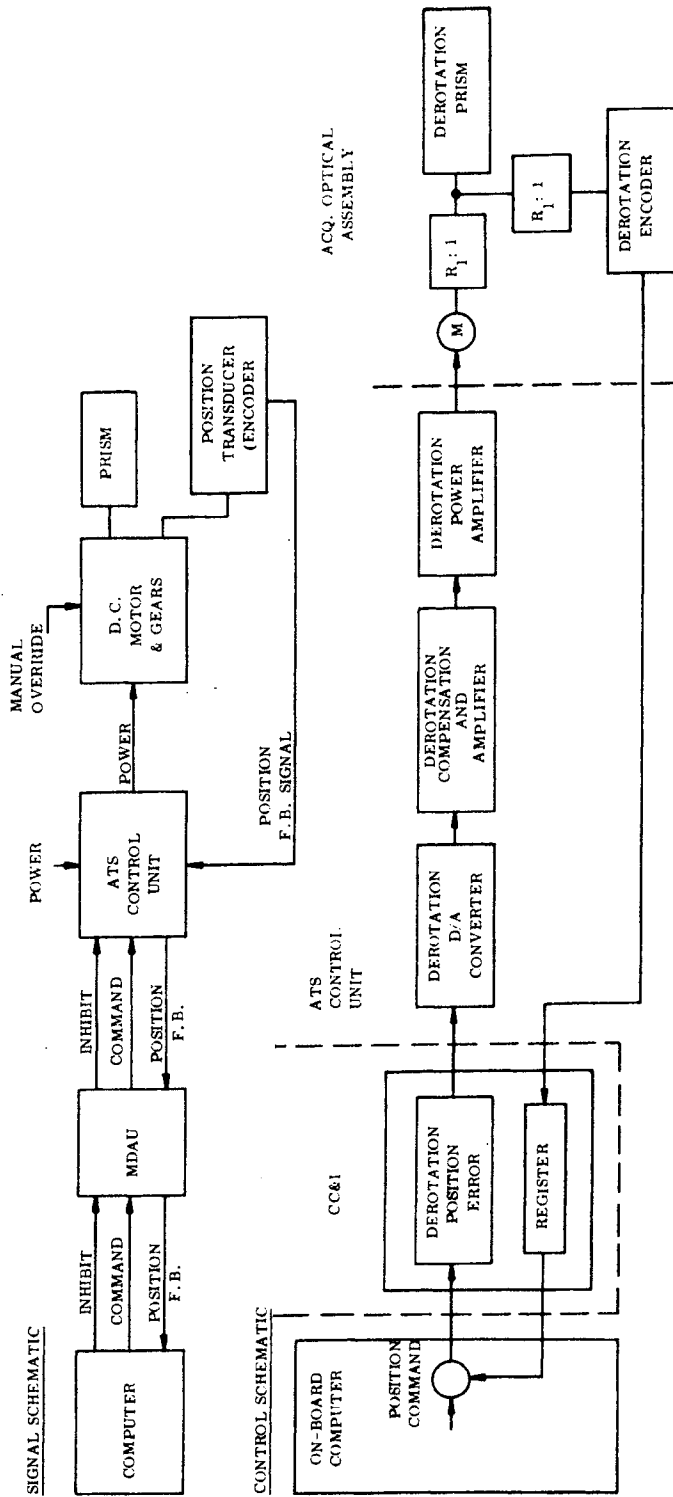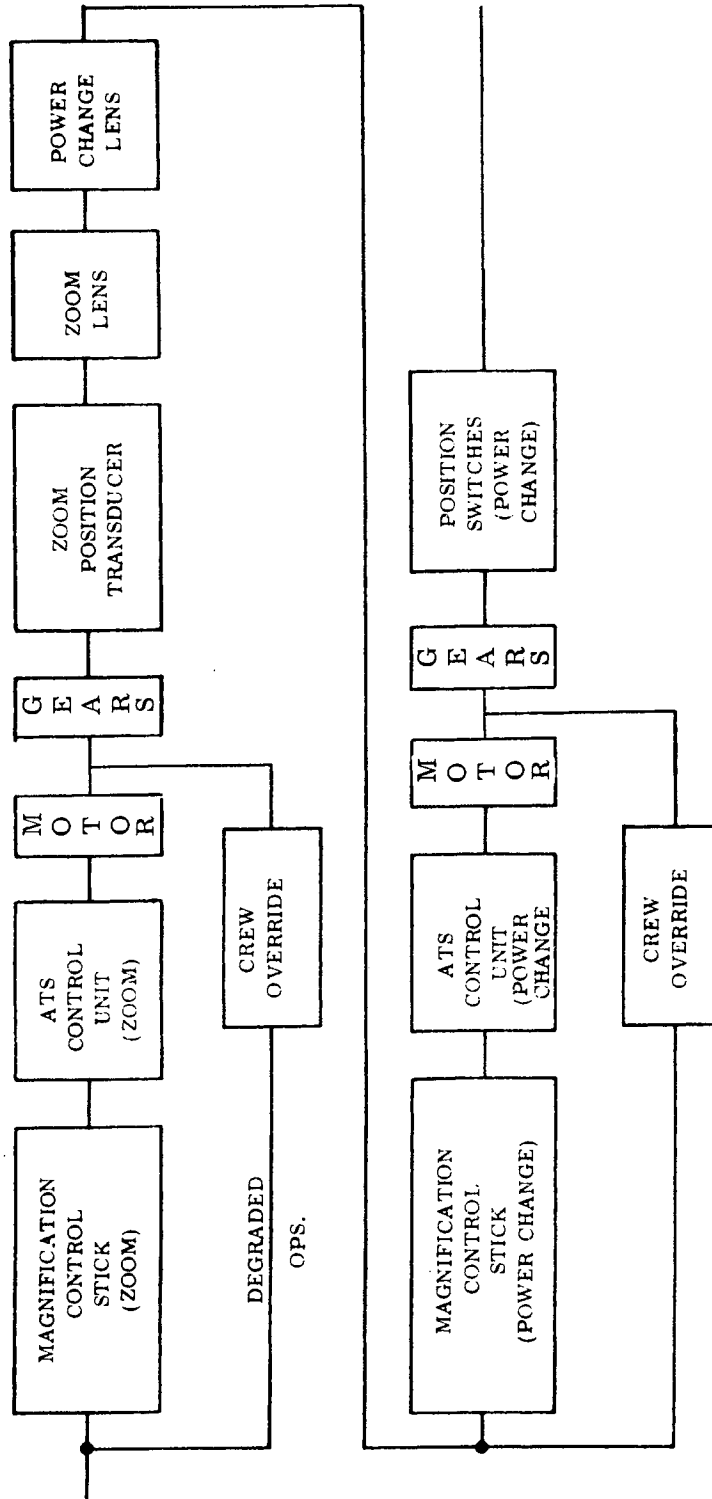
~~SECRET~~ **SPECIAL HANDLING**
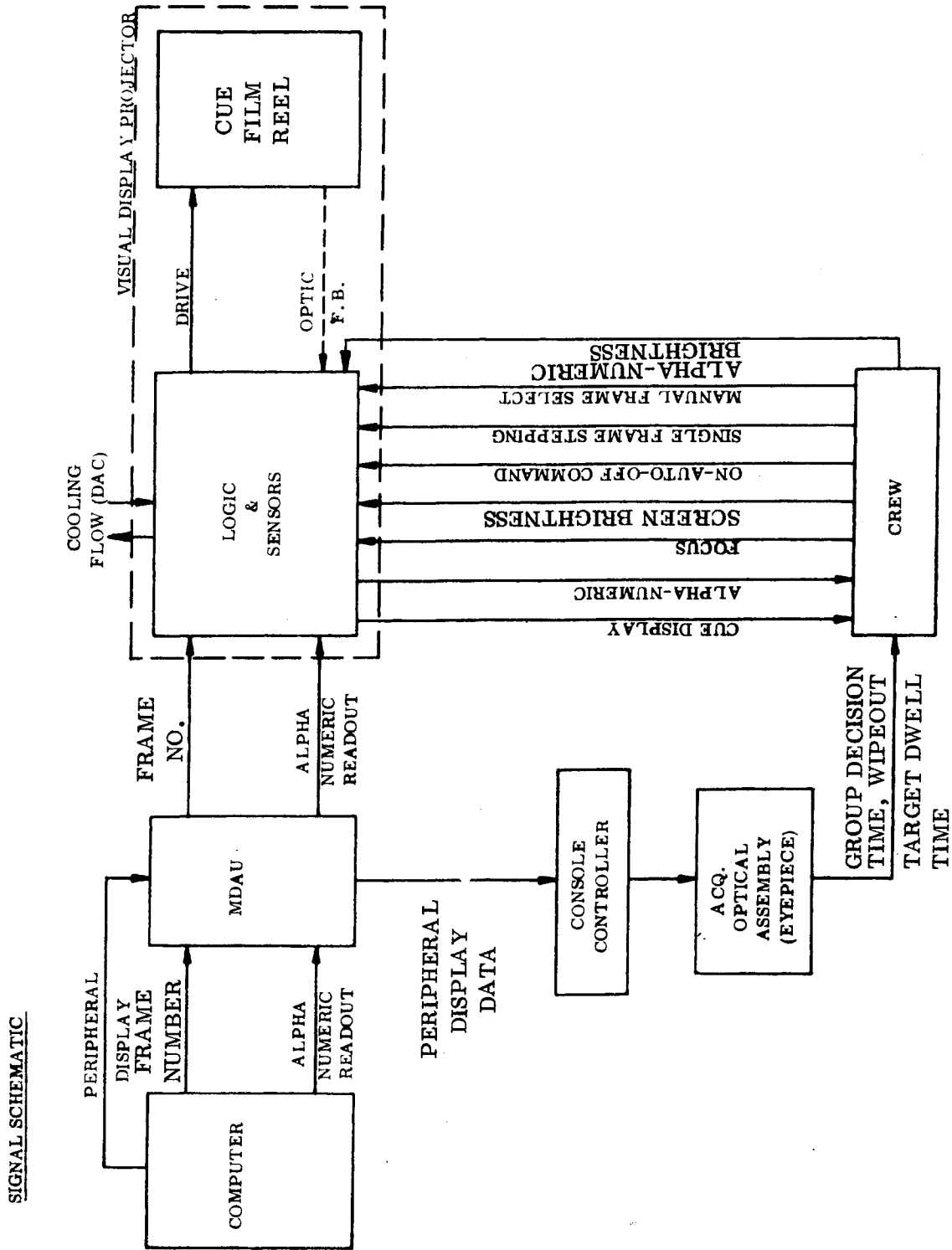
Figure 6.1-15. Functional Assembly Cue System and Peripheral Display

~~SECRET~~ **SPECIAL HANDLING**
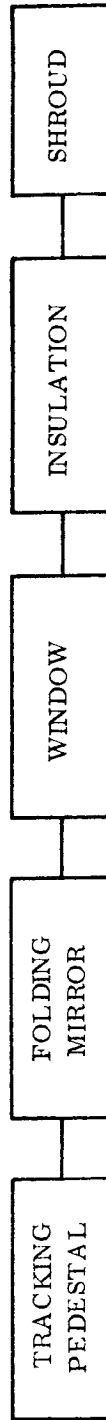
Figure 6.1-16. Functional Assembly Scanner Passive Elements Reliability Logic Diagram (Per ATS)

6-26

TABLE 6.1-2.   SCANNER CONTROLS AND DRIVES

Assembly Equipment Name	Failure Mode	Effect	Detection	
			TLM	MAS/Crew
1. MSCA	1.1 No output - Piece part failure - No power input from EP&SD - Stick pickoff failure	Lose capability to correct for pointing and tracking errors and to perform limited search mode		Degradation of intelligence gathering function. Elimination of updating no pointing or tracking equations
	1.2 Gain Change - Gain change logic failure	Scene rate will not be constant with magnification change		Image rate will change as magnification is changed on ATS
	- No input or partial input from magnification logic	(Same as above)		(Same as above)
2. Computer/ MDAU	2.1 No input to ATS Control Unit - Loss of MDAU or computer	ATS not commanded to slew or track		No useful scene in ATS eyepiece
	2.2 Command input timing errors	Failure to point and track planned targets		Scene will not correspond to cue briefing
	2.3 Error in scanner command - Computation error	Pointing error and rate error		For pointing error, scene irrelevant. For rate error, larger rate correction required by crew

~~SECRET~~ SPECIAL HANDLING

TABLE 6.1-2. SCANNER CONTROLS AND DRIVES (Cont)

Assembly Equipment Name	Failure Mode	Effect	Detection TLM	Detection MAS/Crew
2. Computer/ MDAU (cont)	- Loss of position feedback signal	Scanner will not acquire target.		Large stick inputs must be continually applied to maintain target pointing. Resolution will be degraded
	- Loss or error in decoupling computation	Efficiency of rate and position nulling by MCS will be reduced		Scene movement will not correspond to stick movement
	Refer to: DIN 50196-04-1 page 3-153			
3. ATS Control Unit	3.1 No output or constant output to gyro torquers - Piece part failure - Overtemperature - No power input	Failure to point ATS (Backup mode available using crew and position servo loop)		Non-useable scene in eyepiece
	3.2 Dynamic malfunction in torquer output - Gain change - Compensation change	Failure to acquire planned target		Non-planned scene or non-useable scene presented in eyepiece
	3.3 Error in torquer command output	Pointing and tracking error		(Same as above)

~~SECRET~~ SPECIAL HANDLING

~~SECRET~~ SPECIAL HANDLING

TABLE 6.1-2. SCANNER CONTROLS AND DRIVES (Cont)

Assembly Equipment Name	Failure Mode	Effect	Detection TLM	Detection MAS/Crew
3. ATS Control Unit (cont)	3.4 No output to one or more torque motors a) No output to all torque motors - Amplifier failure - Power failure	Failure to point ATS		No useable scene in eyepiece
	b) No output to both the roll or pitch set of torque motors - Amplifier failure	No scanner motion in one axis ∴ failure to acquire target		(Same as above)
	c) No output to one roll or pitch torque motor - Power amplifier failure	Increased time to acquire target		None (increased time order of second) after several slews malfunction might be noted
	3.5 Loss in feedback output to MDAU	Scanner will not acquire target		Effective loss of ATS.
	3.6 Error in feedback signal to MDAU	Pointing error in ATS		(Same as above) or less severe

~~SECRET~~ SPECIAL HANDLING

TABLE 6.1-2. SCANNER CONTROLS AND DRIVES (Cont)

Assembly Equipment Name	Failure Mode	Effect	Detection	
			TLM	MAS/Crew

4. Gyro	4.1 No output
	- Bearing, fluid seal, mech failure
	- Open winding torque motor
	- Open pickoff signal
	- Loss of power
	  • Internal
	  • EP&SD or mode controller
		ATS goes to a hardover roll or pitch position (Backup position loop available)		Later

	4.2 Error in output - Drift - Reduced gain - Thermal control failure	Random errors in target centering in FOV. Crew can compensate through MSCA		Increased effort using stick to maintain ATS pointing degraded resolution

SECRET SPECIAL HANDLING

TABLE 6.1-2. SCANNER CONTROLS AND DRIVES (Cont)

Assembly Equipment Name	Failure Mode	Effect	Detection	
			TLM	MAS/Crew
5. Torque Motor (Redundant windings)	5.1 No output - Open winding	Increased slew time		None immediately. After several slews, larger slew time might be noted. Could result in skipping of target
	5.2 Erratic output	Jitter on ATS optics in tracking mode		Degraded resolution
6. Gimbal	6.1 Bearing seizure	No scanner motion in one axis		Loss of ATS. Limited response to stick commands
	6.2 Bearing roughness	Jitter in ATS optics in tracking mode		Degraded resolution

7. Encoder (Assume re-dundant lamps and electronics)	7.1 No output
	  - Mechanical failure
	  - Loss of power input
		Pointing will wander		Effective loss of ATS. Large stick inputs necessary to maintain target pointing. Degraded resolution

	7.2 Output error	Pointing error		Same as above

SECRET SPECIAL HANDLING

~~SECRET~~ SPECIAL HANDLING

TABLE 6.1-3. TELESCOPE - IMAGE ORIENTATION

Assembly Equipment Name	Failure Mode	Effect	Detection	
			TLM	MAS/Crew
1. ATS Control Unit Electronics - Pechan drive	1.1 No output to torquer	Pechan prism assumes fixed position. In-track target vector component not aligned with display vertical.		Target directional reference will not correspond to cue briefing.
	1.2 Fixed output to torquer (failure to null)	Pechan prism assumes one of two extreme positions; image not aligned with vertical. Crew can manually reposition		Same as above
	1.3 Dynamic failure - Low gain	Increased time to reach steady state value. Final prism position will be in error		Deviation from target directional reference sensed after several target runs.
	- Erratic output	Possible increased errors in position of prism. No additional adverse effect during tracking due to inhibit during track mode		Same as above

~~SECRET~~ SPECIAL HANDLING

TABLE 6.1-3. TELESCOPE - IMAGE ORIENTATION (Cont)

Assembly Equipment Name	Failure Mode	Effect	Detection	
			TLM	MAS/Crew
1. ATS Control Unit Electronics (Cont)	1.4 Failure to inhibit during scanner tracking mode of operation.	Prism motor could contribute to scanner jitter. Degraded resolution.		Possible recognition of degraded resolution.
	1.5 No output feedback signal to MDAU	Manual control stick motions and image motions become coupled.		Scene movement will not correspond to stick movement-reduced efficiency in nulling rates and position
2. DC Torque Motor and Gears	2.1 No output – Open winding	Pechan prism assumes fixed position. Although crew can manually override, directional reference is lost.		Target directional reference will not correspond to cue briefing
	– Mechanical failure	Pechan prism assumes fixed position. Crew override may not be possible		Same as above
	2.2 High friction	Longer time to reach steady-state value or locked in fixed position		Scene rotation termination after scanner slew or loss of directional reference; scene orientation different from cue briefing.

~~SECRET~~ **SPECIAL HANDLING**

TABLE 6.1-3. TELESCOPE - IMAGE ORIENTATION (Cont)

Assembly Equipment Name	Failure Mode	Effect	Detection TLM	Detection MAS/Crew
3. Pechan Prism	3.1 Prism fracture or chipping	Loss of light or distortion to complete loss of ATS		Decreased intensity of scene to total loss of resolution
4. Position Transducer (Encoder)	4.1 No output – Open circuit – Mechanical failure – Loss of power	Stick and image become coupled		Scene movement will not correspond to stick movement. Reduced rate and position will effect.
	4.2 Output error	Partial coupling of stick and image		Same as above but to lesser extent.
5. Computer/ MDAU	5.1 No output command – Loss of MDAU or computer	Pechan prism stays in last commanded position. Loss of directional reference.		Target directional reference will not correspond to cue briefing. Time to detection will depend on fixed position of prism.
	5.2 Loss of inhibit signal	Possible contribution to jitter on ATS optics. Degraded resolution.		Degraded resolution.
	5.3 Output command error – Computational error	Error in positioning prism. Loss of directional reference		Target directional reference will not correspond to cue briefing.
	– Loss of feedback signal	Will operate open-loop. Stick and image become decoupled.		Scene movement will not correspond to stick movement.

~~SECRET~~ **SPECIAL HANDLING**

~~SECRET~~ SPECIAL HANDLING

TABLE 6.1-4. POWER CHANGE CONTROL

Assembly Equipment Name	Failure Mode	Effect	Detection	
			TLM	MAS/Crew
Magnification Control Stick	No output or false output	Fixes zoom in last commanded (high or low) range. Crew can manually over-ride--No power change capability.		Magnification range will not change as magnification control stick passes detent.
ATS Control Unit	No input from magnification control stick or no output to power change motor	(Same as above)		(Same as above)
Torque Motor	Cannot accept input command or does not give output	Fixed zoom range crew can override		Constant magnification. No stick response
Mag Sensing Position Switches	No output to computer	Loss of gain change if in other magnification range.		None - if desired zoom operating in corresponding range. If zoom in other range then scene rate function of magnification

~~SECRET~~ SPECIAL HANDLING

~~SECRET~~ **SPECIAL HANDLING**

TABLE 6.1-5. ZOOM CONTROL

Assembly Equipment Name	Failure Mode	Effect	Detection	
			TLM	MAS/Crew
Magnification Control Stick	No stick output	Fixed magnification, (crew can override manually)		No response to stick movement
	Locked in fixed position	(Same as above)		Cannot move stick
ATS Control Unit	No command to torquer	(Same as above)		No response to stick movement
	Cannot accept magnification feedback signal	Loss of gain control		Scene rate will be function of commanded magnification
Torque Motor	No output	Fixed magnification, crew can override manually		No response to magnification stick movement
Position Transducer	No output	Loss of gain change		Scene rate will be function of commanded magnification
Computer	No input from position transducer	(Same as above)		(Same as above)

~~SECRET~~ **SPECIAL HANDLING**

~~SECRET~~ **SPECIAL HANDLING**

TABLE 6.1-6. BLANKING (PER ATS)

Assembly Equipment Name	Failure Mode	Effect	Detection	
			TLM	MAS/Crew
1. Sun Sensor	1.1 Signal – Open	Shutter remains in closed position. crew can reposition.		No scene in eyepiece. Manually open shutter
	1.2 Signal – Ground	Shutter remains open. May cause <u>a crew safety prob-lem</u> if light level becomes high		Later
	1.3 Error in light level			
	– Low setting	Shutter closes when not required		No scene – can override
	– High setting	Shutter fails to open at high light level. <u>Potential safety problem</u>		Later
2. ATS Control Unit	2.1 No output in closed command – Drive failure – Open/ground in CCW feedback	Will not respond to sun sensor signals. Potential crew safety problem		Later

~~SECRET~~ **SPECIAL HANDLING**

~~SECRET~~ SPECIAL HANDLING

TABLE 6.1-6. BLANKING (PER ATS) (Cont)

Assembly Equipment Name	Failure Mode	Effect	Detection		
			TLM	MAS/Crew	
3. Spring	3.1 Jammed – Open winding – Mechanical failure	Shutter remains closed Shutter remains closed		No scene. Open shutter manually Same as 2.1	

~~SECRET~~ SPECIAL HANDLING

TABLE 6.1-7. SHROUD DOOR

Assembly Equipment Name	Failure Mode	Effect	Detection	
			TLM	MAS/Crew
1. Computer/ MDAU	1.1 Command signal – Open	Door remains in last commanded position. If closed lose ATS. If open thermal and contamination problems with mirror effecting resolution.		No scene if closed. If open detect light thru eyepiece when door should be commanded closed.
	1.2 Command signal – Ground	Door remains open		Detect light thru eyepiece when door should be commanded closed
	1.3 Timing error in command	Varied, minor to loss of resolution to loss of ATS		Similar to 1.1
2. ATS Control Unit	2.1 No output in open command – Driver failure – Open/ground in CW feedback	Door will not open upon command. Loss of ATS		No scene
	2.2 No output in closed command – Driver failure – Open/ground in CCW feedback	Door remains open. Potential thermal and contamination problems with mirror effecting resolution		Detect same as 1.2

TABLE 6.1-7. SHROUD DOOR (Cont)

Assembly Equipment Name	Failure Mode	Effect	Detection TLM	Detection MAS/Crew
3. Motor and Gears	3.1 No output - Open winding - Mechanical failure	Door remains in last commanded position (same as 1.1)		Same as 1.1
4. Position Switches	4.1 Open CW position SW	Door will not re-open after a closure		No scene
	4.2 Ground CW position SW	Open command to door motor, does not shut off		TBD
	4.3 Open CCW position SW	Once opened door remains opened		Same as 1.2
	4.4 Ground CCW position SW	Same as 4.3		Same as 1.2

TABLE 6.1-8. CUE SYSTEM

Assembly Equipment Name	Failure Mode	Effect	TLM	MAS/Crew
			Detection	
1. Visual Display Projector	1.1 Loss of screen display - Projection lamp failure - Lens fracture - Loose electrical cables	Loss of cue to one console. Projection lamps can be replaced. Prepass briefing can be achieved on other projector. No briefing available during target pass		
	1.2 Loss of alphanumeric	Loss of information to crew during target pass		
	1.3 Loss of focus adjust	Reduced resolution in cues		
	1.4 Loss of brightness adjust	Maintain one brightness level.		
	1.5 Loss on-auto-off command capability - No "on" mode	Loss of flexibility in prepass briefing		
	- No "auto" mode	Loss of cue system during target pass		
	- No "on-auto"	Similar to 1.1		
	- No "off" mode	Reduced life		

~~SECRET~~ **SPECIAL HANDLING**

TABLE 6.1-8. CUE SYSTEM (Cont)

Assembly Equipment Name	Failure Mode	Effect	Detection	
			TLM	MAS/Crew
1. Visual Display Projector (Cont)	1.6 Loss – single frame stepping	Reduced flexibility. Inability to step one frame in either direction		
	1.7 Loss – manual frame select	Inability to manually call up cue.		
	1.8 Failure film to advance			
	– Motor drive failure	Loss of cue for one console		
	– Sensor logic	Loss of cue for one console		
	– Jammed film	Lose all cues in one film module		
	1.9 No cue			
	– Broken film	Lose all cues in one film module		
	1.10 Erroneous cue selection	Loss of cue system during target passes		
	– Search logic and sensors			
	1.11 Increased time frame-to-frame	Degradation of effectiveness during target pass		

~~SECRET~~ **SPECIAL HANDLING**

~~SECRET~~ SPECIAL HANDLING

TABLE 6.1-8. CUE SYSTEM (Cont)

Assembly Equipment Name	Failure Mode	Effect	Detection	
			TLM	MA8/Crew
2. Computer/ MDAU	2.1 Failure in cue film command	Loss of auto mode of operation. Effective loss of cue system during target pass. De-graded pretarget pass briefing		
	2.2 Failure in alpha numeric command	Loss of infor-mation to crew during target pass		
	2.3 Failure in peripheral display	Reduced effective-ness of crew to perform real time target selection		
3. Acquisition Optical As-sembly (Eye-piece)	3.1 Loss or error in - Decision time - Time wipeout - Priority	Same as 2.3 above		

~~SECRET~~ **SPECIAL HANDLING**

TABLE 6.1-9. SCANNER PASSIVE ELEMENTS

Assembly Equipment Name	Failure Mode	Effect	Detection TLM	Detection MAS/Crew
1. Tracking Pedestal	1.1 Deformation or fracture - Attachment to LM	Varied, ranging from loss of pointing accuracy to complete loss of ATS		
	- Pedestal structure	Same as above		
	- Gimbal structure	Same as above plus loss of tracking smoothness		
	1.2 Opens or shorts electrical cabling	Varied, ranging from loss of instrumentation to loss of ATS		
	1.3 Mirror distortion, fracture, galling, etc	Varied, from barely detectable loss of resolution to loss of ATS		
2. Folding Mirror	2.1 Deformation or fracture - Attachment to LM	Varied, ranging from loss of pointing accuracy or minor vignetting to loss of ATS		
	2.2 Mirror distortion, fracture, galling, etc	Varied, ranging from barely detectable loss of resolution to loss of ATS		

~~SECRET~~ **SPECIAL HANDLING**

~~SECRET~~ SPECIAL HANDLING

TABLE 6.1-9. SCANNER PASSIVE ELEMENTS (Cont)

Assembly Equipment Name	Failure Mode	Effect	Detection		
			TLM	MAS/Crew	
3. Window	3.1 Structural failure of window or attachment to LM (the ATS objective lens provides a backup for windoe).				
4. Insulation	Failure in attachment to LM	Varied, ranging from vignetting of target scene to complete obscuration of target scene or loss of resolution due to thermal gradients			
5. Shroud	Deformation or fracture - Attachment to radiator	Varied, ranging to loss of ATS due to thermal gradients			
	- Insulation attachment to shroud	Same as 4 above			

~~SECRET~~ SPECIAL HANDLING

TABLE 6.1-10. OPERATIONAL INTERFACES

Assembly Equipment Name	Failure Mode	Effect	Detection		
			TLM	MAS/Crew	
1. Inputs Command System	1.1 Loss target reject switch	Crewman cannot reject potential target from computer priority voting.			
	1.2 Loss target active switch	Lose ability to inform computer of cloud free active target for priority voting			
	1.3 Loss target inactive switch	Same as 1.2 except for inactive targets			
	1.4 Loss ATS hold signal	Crewman can not hold target past decision time point			
	1.5 Loss of computer update signal for main optics pointing and tracking	Reduced pointing and tracking accuracy on main optics			
	1.6 Failure ATS/main optics slave commands	TBD			
2. EP&SD Interface	2.1 No power to components - single ATS (Electronics, roll gyro, cross-roll gyro)	Loss of one ATS system			

~~SECRET~~ SPECIAL HANDLING

~~SECRET~~ **SPECIAL HANDLING**

TABLE 6.1-10. OPERATIONAL INTERFACES (Cont)

Assembly Equipment Name	Failure Mode	Effect	TLM	Detection MAS/Crew
2. EP&SD Interface (Cont)	- Power controller switches	Switch to alternate power controller relays		
	- Mode controller switches	TBD		
	- MDAU switch commands (Type II)	Switch to backup MDAU		
	2.2 No power to both ATS			
	- MDAU command decoder failure	Switch to backup MDAU		

~~SECRET~~ **SPECIAL HANDLING**

6.2 CONTAMINATION CONTROL

6.2.1 PHILOSOPHY

Performance characteristics of optical systems such as the Visual Display Projector and the Acquisition Tracking System are specified in terms of resolution, obscuration, etc. To meet the specified performance requirements it is necessary to fabricate and assemble the equipment under conditions that control the contaminants which affect the final optical properties, to package the assembled item in such a way that contamination of critical surfaces can be controlled when the assembled unit is exposed to an uncontrolled environment, and to provide for local cleaning and area environmental control when it is necessary to open an assembly for maintenance or installation.

General Electric's philosophy is to define the performance requirements to the vendor, work with him in establishing facilities and procedures necessary to meet the requirements, and to provide in-house equipment and procedures to assure that contamination control requirements defined during manufactur will be maintained.

6.2.2 VISUAL DISPLAY PROJECTOR (VDP)

Contamination Control of the VDP has been specified for critical assembly areas to be supplied with air that meets FED STD 209A, Class 10,000, that the unit be capable of being externally cleaned so that it may be opened for maintenance work. Normal use of the VDP will be in an uncontrolled environment. Therefore, breathing ports are provided with filters the control entrance of contaminants while dust covers are required to protect the eye piece when it is not in use.

Packaging of the VDP for shipment will include use of plastic bags for contamination control. The same procedure will be employed during storage of the unit.

A review of all contamination control procedures for the VDP from factory-to-launch will be conducted by the Contamination Control Board to assure that consistent, integrated level of control is maintained.

6.2.3 ACQUISITION TRACKING SCOPE (ATS)

The Acquisition Tracking Scope (ATS) presents its own problem for contamination control in as much as the unit must be subjected to partial disassembly for installation into the Laboratory Module (LM) and the external mirror will be exposed to the room environment during testing and alignment at DACO.

To obtain the performance required for the ATS System GE is working with the manufacturer to utilize his experience in obtaining the necessary clean room environments, now estimated to be FED STD 209, Class 100,000, and operating procedures. Packaging requirements for shipment will be developed which will maintain the clean condition of the unit from the manufacturer to the point of equipment installation into the LM. Installation of the ATS into the LM will be accomplished at DACO in an Environmentally Controlled Sheltered Area supplied with air that meets FED STD 209A, Class 100,000 as defined by SAFSL 10003 with oils and volatiles uncontrolled. It is planned that a portable clean tent that has a FED STD 209A, Class 10,000 air supply with oils and volatiles reduced to:

NO_2	0.03 ppm
SO_2	0.01 ppm
Oxidents	0.01 ppm
Hydrocarbon	0.03 ppm

will be available at DACO and VAFB. Acetylene, Entane, Ethylene and Methane are not controlled.

An Environmental Conditioning Blower unit, normally used to supply class 10,000 air with oil and volatiles controlled to the Mission Module (MM), will be available to supply clean air to local areas if needed.

For extended test periods at DACO that require the external optics to be exposed to the class 100,000 room local plastic covers may be used to protect the mirror from excessive contamination during these periods. At other times the external cover will be kept in place to provide maximum protection of the mirror.

Contamination Control at VAFB is maintained by: (1) having FED STD 209A, Class 100,000 air with oils and volatiles uncontrolled supplied to the MOL Environmental Shelter which encloses the LV; (2) having a portable class 10,000 clean tent with oils and volatiles controlled available for use, and; (3) by keeping the system covered when not being tested.

6.3 MAINTAINABILITY

6.3.1 CONCEPT

6.3.1.1 Ground

All of the subsystem components will be maintained on pad in the event of a failure with the exception of the optical assembly, the folding mirror and the support structure. Mainten- ance of the first two components require the use of the alignment facilities not presently planned for at VAFB. If either of these components fail, the present maintainability con- cept calls for shipment of the LM back to the factory for repair. Provisions for maintain- ing the support structure at VAFB will not be made since the probability of failure and the probability of failure detection are extremely low. Since the predicted failure rate for this component is 0.0001, non-detection of potential failure at the launch pad is not con- sidered a serious problem. All other components will be repaired by removing the faulty one and replacing it with a good component. The faulty component will then be shipped, in most cases, to the factory for repair and then be cycled back as a spare.

6.3.1.2 On-Orbit

On-orbit maintenance is currently limited to switching to redundant equipment. The possibility of including provisions for some minor replacement of alpha subassemblies is under study.

6.3.2 ANALYSIS

In this analysis, detection of a failure is, in some cases, limited to those periods of time where a ground crew member has visual access to the particular component or when TLM is being received by the CITE. In cases where there is not TLM or visual access, such as some hidden structure, no failure detection is normally possible.

6-53

Repair times given are the total times required to correct a failure. Time includes obtaining spares, AGE and test equipment, removing the faulty component, installing and validating the good one, and restoring the system to its original state.

a. The two VDPs, located in console Nos. 2 and 8, can be replaced on pad. The exact operations to be performed depend upon details not yet firmed up. Consideration is being given to operations associated with disconnection of cold plate plumbing installed in the VDPs. This problem area will have to be resolved before a complete analysis of VDP removal can be made. Assuming a minimal amount of this type of operation, the VDPs can be removed, replaced and revalidated in 6 to 11 hours depending upon where in the launch cycle the failure occurs. Detection of a failure is limited to prior to T-120 minutes.

b. The harness penetration set, a high reliability item (0.9999) may be repaired in 8 to 16 hours. Detection of a failure is possible till T-10 minutes.

c. The Drive K electronics contained in the consoles may be repaired in 6.5 to 18 hours. Detection of a failure is possible until T-10 minutes.

d. The shroud door and drive are replaced as a unit. Detection of a failure is possible prior to T-120 minutes. Maintenance times range from 10.6 to 14.7 hours.

e. The headrest on the console is highly reliable (0.9999). Detection of a failure is limited to prior to T-120 minutes. Repair can be accomplished in 5 to 10 hours.

f. The magnification control stick may be removed and replaced if repair is required. Detection of a failure however is limited to prior to T-270 minutes. Maintenance time required is seven hours.

6.3.3 EFFECTS OF MAINTAINABILITY ON OTHER SUBSYSTEMS

At present, it appears that the design and procedure associated with the Alpha subsystem does not degrade the maintainability of other subsystems. A study is under way to insure that the lack of ability to remove the optical assembly does not prohibit maintenance of other subsystems.

~~SECRET~~ **SPECIAL HANDLING**

6.3.4 SUMMARY

With the exception of the optical assembly and the folding mirror, ground maintenance activities can be performed with a minimum of problems and delay in time on the components of the Alpha Subsystem.

The optical assembly has a high enough failure rate (0.9957) such that methods of repairing it on pad will be studied in order to increase the probability of meeting the launch window. The folding mirror is a highly reliable item (0.9999) and should present little problem. The same holds true for the structural members.

TABLE 6.3-1. CHARACTERISTICS AFFECTING MAINTAINABILITY FOR ALPHA SUBSYSTEM COMPONENTS MAINTAINED ON PAD

COMPONENTS	APPROX. SIZE (INCHES)	WEIGHT (POUNDS)	QUANTITY	ACCESS
Support Structure	N/A	N/A	N/A	
VDP	18 x 8.5 x 8	25	2	Console Nos. 2 and 8
Harness	N/A	N/A	(later)	(later)
Drive K Electronics	9 x 17 x 5	17.5	2	Console Nos. 2 and 8
Shroud Door and Drive	36 x 48 x 12	(later)	2	LM Exterior
Headrest	6 x 7 x 2	3	2	Console Nos. 2 and 8
Magnification Control Stick	7 x 7 x 10	6	2	Console Nos. 2 and 8

6.4 EYE HAZARD ANALYSIS

A "ball-park" analysis has been performed to approximate the level of irradiance produced on the cornea and retina of the eye when viewing the sun spectral reflection of the sun, and certain other objects. It was the purpose of this analysis to determine if a sun-blanking device was required for the ATS for protection against direct solar viewing, and also to attempt to determine if specular reflections of the sun from surface water presented a hazard.

The direct viewing of the sun with the ATS was found to produce extremely high irradiance of the cornea of the eye which would certainly inflict damage. However, the nature of the MOL orbit and the hardware restraints on the scan field of the ATS make it virtually impossible to view the sun if the OV is earth stabilized. An automatic blanking shutter is thus required generally only as a backup for those cases where the OV is not earth-stabilized and when the ATS is commanded to point away from the earth.

The effect of viewing specular reflections of the sun from surface water was not so conclusively determined. The specular reflectance of water is very much dependent on the angle of incidence and the surface roughness of the water. Using a very conservative (high) value for surface reflectance (five percent) the irradiance level on the cornea was computed to be 0.2 watt/cm^2. The effect of such an irradiance level on the cornea has not been determined.

To meaningfully assess the hazard presented by specular reflection from surface water, better data is needed to (a) determine the damage threshold of the eye in terms of irradiance levels and exposure times, and (b) to determine reasonable reflectance values for large bodies of surface water.

6.4.1 SUMMARY OF CONCLUSIONS

a. The most damaging concentration of energy when viewing the sun, or a specular reflection of the sun, will occur on the <u>cornea</u> of the eye, not the retina. Retinal irradiance will be <u>lower</u> through the AO than when the sun is viewed with the naked eye from the earth. The irradiance of the cornea, however, will be much greater with the AO.

b. The concentration of energy on the cornea is such that even specular reflection of ground water may present a hazard. Direct viewing of the sun will inflict a serious burn on the cornea! Corneal irradiance is most severe at high power.

c. Since retinal irradiance is not high when viewing a specular reflection, the crew may be able to stare at a specular reflection without realizing cornea damage is occurring.

d. While a sun sensor actuated shutter can prevent the sun from entering the field of view (FOV), it will probably not be possible to prevent specular reflections from briefly entering the field before the shutter closes.

e. Diffuse reflecting clouds etc. will not damage the eye when viewed through the AO.

6.4.2 DISCUSSION

The severity of the eye damage problem can be evaluated by analyzing the irradiance of the cornea and retina produced when viewing various sources such as the sun, specular solar reflections, clouds, etc. "Ball park" calculations of this nature follow and are summarized in Table 6.4-1. Since the eye damage thresholds have not yet been determined, the corneal and retinal irradiances produced when viewing the sun with the naked eye are included to provide a familiar reference. For the same reason figures are included for the viewing of a specular reflection off of a lake with the naked eye.

It may be surprising to note that irradiance level on the retina is less when viewing the sun through the high power AO, than when viewing the sun from the earth with the naked eye. It happens that the large aperture provided by the AO is more than offset by the magnification of the ATS which spreads the increased amount of light energy over a larger portion of the retina, and by the low transmission of the AO relative to that of the atmosphere.

6-59

TABLE 6.4-1. SUMMARY OF CORNEAL AND RETINAL IRRADIANCE LEVELS
FOR VARIOUS LIGHT SOURCES

SOURCE	IRRADIANCE OF RETINA	IRRADIANCE OF CORNEA	TOTAL FLUX AT CORNEA (WATTS)
1) Sun viewed with naked eye through one atmosphere (ground observer)	$0.3 \frac{watts}{mm^2}$	$0.0009 \frac{watts}{mm^2}$	0.018 (assumes 4mm pupil)
2) Specular Reflection of sun from water as seen with naked eye through one atmosphere (ground/aircraft observer)	$0.02 \frac{watts}{mm^2}$	$0.000045 \frac{watts}{mm^2}$	0.0009
3) Sun viewed through AO at high power (127X) (zero atmosphere)	$0.04 \frac{watts}{mm^2}$	$8 \frac{watts}{mm^2}$	25
4) Sun viewed through AO at low power (16X) (zero atmosphere)	$0.04 \frac{watts}{mm^2}$	$0.5 \frac{watts}{mm^2}$	1.5
5) Specular Reflection from surface water as seen through AO (at high power) (2 atmospheres)	$0.001 \frac{watts}{mm^2}$	$0.21 \frac{watts}{mm^2}$	0.8
6) Diffusely reflecting cloud through AO (at high power) (2 atmospheres)	$0.033 \times 10^{-4} \frac{watts}{mm^2}$	$1.4 \times 10^{-4} \frac{watts}{mm^2}$	4.35×10^{-4}
7) Diffusely reflecting cloud through AO (at low power)(2 atmospheres)	2.7×10^{-4}	$6.5 \times 10^{-4} \frac{watts}{mm^2}$	20.4×10^{-4}

It is less comforting to note that the irradiance levels at the cornea are extremely high when viewing the sun in either the high or low power case, and <u>may</u> be significant even when viewing a specular reflection from a smooth body of water. This fact becomes palatable if it is recognized that the energy collected in the large aperture is concentrated to pass a 2 mm exit pupil near the eye, and spreads to a much larger area on the retina.

The most disturbing possible source of eye damage is the specular reflections from the earth. It will be possible to prevent the sun from entering the FOV with either a sun sensor or computer actuated shutter. Specular reflections, however, will appear instantaneously in the FOV as the spacecraft moves into beams of reflected light from lakes, etc. These reflections will appear bigger, but no brighter, in the eyepiece than do similar reflections when viewed from airplane with the naked eye, but they will concentrate more than two orders of magnitude more energy on the cornea.

It should be noted that the assumptions on which these calculations are based on are very conservative. The assumptions which may introduce the most error in the specular reflection irradiances are:

a. The reflectivity of the water is taken as 0.05 which is probably not too far off for a perfectly smooth body of water. Any rippling, however, will reduce the specular reflectance as the diffusely scattered energy increases. A better estimate of the reflectivity could be obtained by measuring the reflectance of local lakes on a calm day as a function of incidence angles.

b. The transmission of the optics was taken as 35 percent*, the current Itek estimate. This figure should really be applied solely to the visible region of the spectrum. Since glass blocks nearly of the ultra violet which comprises about 10 percent of the solar spectrum, and some of the infrared (IR), a somewhat lower transmittance may be more realistic.

c. The transmittance of the atmosphere was taken as 0.65. The transmittance is a function of the angle of observation, weather conditions, etc. The chosen figure is believed to be realistic.

---

*More recent Itek shows 29 percent to be a more exact figure for transmission.

6-61

d. The transmittance of the eye was taken as 0.5. It is believed that the actual trans-
    mittance ranges between 0.05 and 0.7 as a function of wavelength. Since the same
    figure was used for the case of the naked eye viewing the sun the comparisons
    between the retinal irradiances of Table 6.4-1 are valid. Corneal irradiance
    values are not affected by this assumption.

e. No attempt was made to consider the spectral content of the energy incident on
    the eye in the analysis.

6.4.3 CALCULATIONS

The calculations which yielded the data in Table 6.4-1 are presented on the following pages.

a. <u>Sun viewed with naked eye through 1 atmosphere</u>

   -   Assume an atmospheric transmission of <u>65</u> percent = ρ_A

   -   Assume the eye focal length to be <u>17</u> mm

   -   Let S = the solar irradiance level = <u>140</u> MW/CM^2

   -   Let θ_s = the 1/2 cone collimation of the sun = 1/2 degree

   -   Let the pupil diameter of the eye = <u>4</u> mm

   -   Let T, the transmissibility of the eye = 0.5

The irradiance at the cornea is then,

$$I_c = \rho_A S = (0.65)(140 \text{ MW/CM}^2)$$

$$= \underline{0.0009 \text{ W/MM}^2}$$

The diameter of the image on the retina is

$$dr = 2f\theta_s = 2 \times 17 \times 0.0099 \quad (\theta_s = 49^O = 0.0044 \text{ rad})$$

$$= 0.150 \text{ MM}$$

The flux collected through a 4mm pupil is

$$F_c = \pi \frac{(a, y)^2}{4} \times 140 \text{ mw/cm}^2 (0.65)$$

$$= \underline{\underline{11.6 \text{ mw}}}$$

The irradiance on the retina is then,

$$I_R = \frac{T F_c}{\pi \, dr^2/4} = \frac{4 \times 11.60 \text{ mw} \times 0.5}{\pi (0.150)^2}$$

$$= \underline{\underline{0.27 \text{ w/mm}^2}}$$

b. **Sun as viewed through AO in orbit - high power case**

The flux collected is,

$$F = \rho \, \epsilon \, \frac{\pi \, s^2}{4} \qquad\qquad \begin{array}{l} \rho = \text{AO transmission} = 0.35 \\ a = \text{aperture diam.} = 10 \text{ inches} \end{array}$$

$$= (0.35)(0.00140) \left[\frac{10^2 \, \pi \, 25.4^2}{4} \right]$$

$$= \underline{\underline{25.00 \text{ w}}}$$

The irradiance level on the cornea is then, assuming a 2 mm exit pupil on the cornea

$$I_c = \frac{F_c}{\pi (2)^2/4} = \frac{25}{\pi (4.9)/4} = \underline{\underline{8 \text{ w/mm}^2}}$$

The image size on the retina is

$$d = 2m \, \theta_s f = 2 \times 17 \times 0.0044 \times 127 \qquad\qquad (f = 17 \text{ mm})$$

$$= \underline{\underline{19 \text{ mm}}}$$

The irradiance of the level is then approximately

$$IR = \frac{TF_c}{\pi d^2/4} = \frac{(0.5)(2.5)(4)}{\pi (19)^2}$$

$$= \underline{\underline{0.04 \text{ w/mm}^2}}$$

c. Sun through AO - Low Power Case - In the low power case the irradiance on the retina remains the same as in the high power case since the decreased effective aperture (2.5 inches) is compensated for by a reduction in magnification.

The irradiance of the cornea is reduced, however, the flux delivered to the cornea by the AO is reduced by the square of the aperture reduction $\left(\frac{2.5^2}{10^2}\right)$

$$I_c = \frac{6.25}{100} \times 8 = \underline{\underline{0.5 \text{ w/mm}^2}}$$

d. Specular Reflections of the sun from surface water as seen through the AO (High Power Case) - While a good figure for the reflectivity of smooth water was not available at this writing, it is certainly below 0.05. Assuming 0.05 and an atmospheric transmission of 0.65 the irradiance of the cornea and retina can be calculated from the similar values for direct viewing the sun with the AO

$$I_c = (0.65)^2 (0.05) (8)$$

$$= \underline{\underline{0.21 \text{ w/mm}^2}}$$

$$I_r = (0.65)^2 (0.05) (0.04)$$

$$= \underline{\underline{0.001 \text{ w/mm}^2}}$$

e. Diffusely reflecting cloud through AO (High Power Case) - The radiance of a diffusely reflecting cloud with a reflectivity of 0.9 is

$$B = \frac{(0.9) S}{\pi} = \frac{(0.9) (0.140) \text{ mw}}{\pi \text{ cm}^2} = 4 \times 10^{-4} \quad \frac{\text{w}}{\text{mm}^2 - \text{ster}}$$

6-64

The flux collected in the 1/2 degree AO field of view is, neglecting atmospheric losses,

$$F = \rho \pi B a \sin^2 1/4^o$$

$$= (0.35) \pi (4.4 \times 10^{-3}) \left(\frac{10^2 \pi}{4} \right) (25.4)^2$$

$$= \underline{\underline{4.35 \times 10^{-4} \text{ watts}}}$$

The irradiance of the cornea is then,

$$I_c = \frac{4.35 \times 10^{-4} \text{ w}}{\pi 2^2/4 \text{ mm}^2}$$

$$= \underline{\underline{1.4 \times 10^{-4} \text{ w/mm}^2}}$$

The diameter of the retina illuminated is the same as in b. above, d = 19 mm. The retinal irradiance is then,

$$I_R = \frac{TF}{\pi d^2/4} = \frac{(0.5)(4.35 \times 10^{-4})}{\pi (19)^2} \times 4$$

$$= \underline{\underline{0.033 \times 10^{-4} \text{ w/mm}^2}}$$

f. **Diffusely Reflecting Cloud – Low Power** – At low power the energy collected is increased by the larger FOV (4 degrees) and decreased by the reduction in aperture size

$$F_c = \rho \pi B a \sin^2 2^o$$

$$= (0.35)(\pi) \left(4 \times 10^{-4} \frac{w}{mm^2} \right) (3.9 \times 10^{-2})^2 \pi \left(\frac{2.5^2 \times 25.4^2}{4} \right)$$

$$= 204 \times 10^{-5}$$

$$= \underline{\underline{20.4 \times 10^{-4} \text{ w}}}$$

I_c is thus larger for the low power case by the ratio of the collected fluxes at low power and high power

$$I_c = \frac{20.4}{4.35} \times 1.4 \times 10^{-4} = 6.5 \times 10^{-4} \text{ w/mm}^2$$

The retinal irradiance is increased by the ratio of the collected fluxes and the decreased magnification squared.

$$I_R = \left(\frac{20.4}{4.35}\right) \left(\frac{127}{30}\right)^2 (0.033 \times 10^{-4} \text{ w/mm}^2)$$

$$= 27 \times 10^{-4} \text{ w/mm}^2$$

g. Specular reflection of sun aft of water as viewed through naked eye. The irradiance produced in this case are reduced from the values derived for viewing the sun directly by the reflectivity of the water.

$$I_c = (0.05)(0.4) = 0.02 \text{ w/mm}^2$$

$$I_R = (0.0009)(0.005) = 0.000045 \text{ w/mm}^2$$

$$F = (0.05)(0.018)$$

$$= 0.0009 \text{ w}$$

6-66